Digitized by the Internet Archive
in 2023 with funding from
Kahle/Austin Foundation

https://archive.org/details/contributionsfro0014unse

Carnegie Institution of Washington

UNIVERSITY OF ARIZONA
STEWARD
OBSERVATORY
TUCSON, ARIZONA

# CONTRIBUTIONS

FROM THE

# MOUNT WILSON OBSERVATORY

VOLUME XIV

NOS. 304-326

WITH SEVENTEEN PLATES

SEPTEMBER, 1925—SEPTEMBER, 1926

UNIVERSITY OF ARIZONA
C F
LIBRARY

C28
v.14

# CONTENTS

NO. PAGE

304. N.G.C. 6822, A Remote Stellar System. *Edwin Hubble* . . . 1

305. Reduction of Thirty-Nine Astrographic Zones to the International Photographic Scale. *Frederick H. Seares* and *Mary C. Joyner* . . . . . . . . . . . . . 27

306. Notes on Lines in the Spectra of Red Stars. *Paul W. Merrill* . 45

307. An Attempt to Detect Water-Vapor and Oxygen Lines in the Spectrum of Mars with the Registering Microphotometer. *Walter S. Adams* and *Charles E. St. John* . . . 53

308. Internal Motions of Messier 33. *Knut Lundmark* . . . 59

309. On the Origin of Bright Lines in Stellar Spectra. *Svein Rosseland* . . . . . . . . . . . . . . 65

310. A Spiral Nebula as a Stellar System: Messier 33. *Edwin Hubble* . . . . . . . . . . . . . . . . 83

311. A Spectrographic Study of Mira Ceti. *Alfred H. Joy* . . . 123

312. Solar Hydrodynamics. *V. Bjerknes* . . . . . . . . 185

313. On the Transmission of Radiation through an Absorbing Medium in Motion, with Applications to the Theory of Sun-Spots and Solar Rotation. *Svein Rosseland* . . . 215

314. On the Theory of the Continuous Spectrum of the Corona. *Edison Pettit* and *Seth B. Nicholson* . . . . . . . 241

315. Remarks on Various Statistical Properties of Galactic Cepheids Having Periods Longer than One Day. *J. Schilt* 247

316. Two New Variable Stars of the Type of W Ursae Majoris. *J. Schilt* . . . . . . . . . . . . . 265

317. On the Orbits of Four Spectroscopic Binaries. *R. F. Sanford* . 275

318. Multiplets in the Spark Spectrum of Iron. *Henry Norris Russell* 297

319. The Absolute Magnitudes and Parallaxes of 410 Stars of Type M. *Walter S. Adams*, *Alfred H. Joy*, and *M. L. Humason* 307

320. The Dwarf Companion to Castor as a Spectroscopic Binary and Eclipsing Variable. *Alfred H. Joy* and *R. F. Sanford* . 325

321. The Photographic Determination of Stellar Parallaxes with the 60- and 100-Inch Reflectors: Ninth Series. *Adriaan van Maanen*. . . . . . . . . . . . . 333

322. Provisional Elements and Dimensions of S Antliae Considered as an Eclipsing Binary. *Alfred H. Joy* . . . 351

## *CONTENTS*

NO. PAGE

323. General Characteristics of Electrically Exploded Wires. *J. A. Anderson* and *Sinclair Smith* . . . . . . . . . 359

324. Extra-Galactic Nebulae. *Edwin Hubble* . . . . . . . 379

325. Stellar Spectra of Class S: II. Changes in Spectra of Long-Period Variable Stars. *Paul W. Merrill* . . . . . . 429

326. The Electric-Furnace Spectra of Yttrium, Zirconium, and Lanthanum. *Arthur S. King* and *Edna Carter* . . . . . 457

# LIST OF PLATES

| NO | | FACING PAGE |
|---|---|---|
| I. | N.G.C. 6822, Photographed with the 100-Inch Telescope | 1 |
| II. | N.G.C. 6822; Negative Print of Plate I | 4 |
| III. | Internal Motions in Messier 33 | 60 |
| IV. | Messier 33, Photographed with the 60-Inch Reflector; Exposure, 8.5 Hours | 88 |
| V. | Messier 33, Photographed with the 100-Inch Reflector; Exposure, 90 Minutes | 88 |
| VI. | Messier 33, Photographed with the 100-Inch Reflector; Exposure, 30 Minutes | 88 |
| VII. | Light-Changes of Variables in Messier 33 | 88 |
| VIII. | Spectrograms of Mira Illustrating Spectral Variation with Magnitude and Phase | 133 |
| IX. | Spectrograms of Mira Illustrating the Behavior of the Hydrogen Emission Lines during a Cycle | 144 |
| X. | Spectrograms of Mira and Its Companion | 170 |
| XI. | Spectrograms of the Companion to Castor | 330 |
| XII. | Photographs of Iron Wire Explosions | 365 |
| XIII. | Photographs of Wire Explosions | 372 |
| XIV. | Elliptical and Irregular Nebulae: N.G.C. 3379, N.G.C. 221, N.G.C. 4621, N.G.C. 3115, N.G.C. 3034, N.G.C. 4449 | 383 |
| XV. | Normal and Barred Spirals: N.G.C. 4594, N.G.C. 8859, N.G.C. 2841, N.G.C. 5850, N.G.C. 5457, N.G.C. 7479 | 384 |
| XVI. | Irregular Nebula N.G.C. 4214 | 386 |
| XVII. | Spectra of S-Type Variable Stars | 430 |

PLATE I

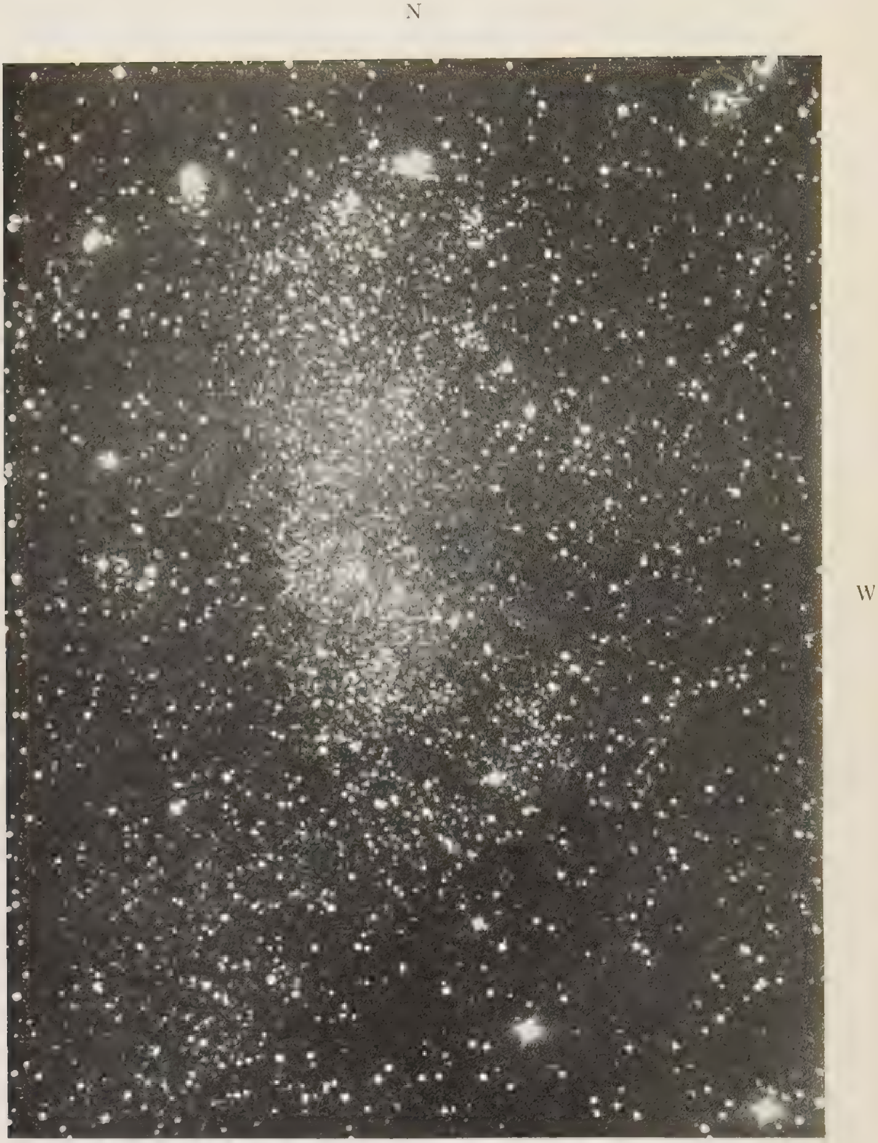

N.G.C. 6822

Photographed at the 42-foot focus of the 100-inch Hooker telescope on July 10, 1923. Exposure $3^h30^m$ on a Seed 30 plate. Enlargement 2.5 times original negative.

Contributions from the Mount Wilson Observatory, No. 304
Reprinted from the *Astrophysical Journal*, Vol. LXII, pp. 409–433, 1925

# N.G.C. 6822, A REMOTE STELLAR SYSTEM

By EDWIN HUBBLE

## ABSTRACT

*A study of N.G.C. 6822.*—The object is a very faint cluster of stars and nebulae, about $20' \times 10'$, resembling the Magellanic Clouds. Detailed investigations confirm the similarity and show that it extends to many structural features of these systems. Familiar relations such as those connecting periods and luminosities of Cepheids, luminosities of brightest stars involved in diffuse nebulae, and frequencies of the most luminous stars in the systems are consistent when applied to N.G.C. 6822, the first object definitely assigned to a region outside the galactic system.

*Variable stars.*—Eleven of the fifteen variables found in the cluster are Cepheids. A system of photographic magnitudes has been established from comparisons with the two nearest Selected Areas; and periods, light-curves, and magnitudes have been determined for the Cepheids. The periods range from 12 to 64 days and the magnitudes at maximum, from 17.45 to 19.05. The period-luminosity relation is conspicuous, and a comparison with Shapley's general curve in *Harvard Circular*, No. 280, indicates a distance for N.G.C. 6822 of 214,000 parsecs. $m-M=21.65$.

*Nebulae.*—Five diffuse nebulae are involved in the cluster. The four brightest show emission spectra similar to those of the diffuse galactic nebulae. A radial velocity of +25 km/sec., uncorrected for solar motion, has been derived from one slit spectrogram of the brightest nebula. The mean diameter of the diffuse nebulae, about 40 parsecs, is comparable with those of the largest nebulae in other systems. In addition to the diffuse nebulae, several small objects are present which are probably non-galactic nebulae whose images are superposed on that of the cluster.

*Star counts.*—The distribution of apparent photographic magnitudes has been determined down to 19.4, corresponding to absolute magnitude $-2.25$. The brightest stars in the system are of absolute magnitude about $-5.8$. When a mean color-index of $+1.35$ is assigned to the cluster stars, their frequencies are very similar to those of the absolute visual magnitudes in the vicinity of the sun.

*Luminosity and space density.*—The surface brightness of the central core is about 22.1 photographic magnitudes per square second of arc. This value leads to a total absolute magnitude of $-12.0$ for the core, or $-12.7$ for the entire system, and to a space density of about 6.1 absolute magnitudes per cubic parsec for the core, or 8.8 for the entire system.

*Cepheid criterion of distance.*—Since the Cepheid criterion appears to function normally in N.G.C. 6822, its value as a means of exploring extra-galactic space is considerably enhanced.

*Influence of instruments on observations of nebulae.*—A summary of the early observations of N.G.C. 6822 illustrates the confusion which may arise from disregarding the limitations of various types of instrument and emphasizes the caution required in discussing observations of nebulae.

N.G.C. 6822 is a faint irregular cluster of stars with several small nebulae involved. The position for 1925 is $\alpha = 19^{h}\,40.7^{m}$, $\delta = -15^{\circ}$, galactic latitude $-20^{\circ}$. The general appearance is shown on Plate I, enlarged from an exposure of three hours and a half with the 100-inch reflector. The total area covered by the cluster is about $20' \times 10'$, but the most conspicuous feature is a core about $8' \times 3'$ in which the star images are densely crowded. The photographs show a striking resemblance to the Magellanic Clouds, and detailed investigations have abundantly confirmed this first impression. Cepheid variables, diffuse nebulae, dimensions, density, and distribution of stellar luminosities agree in defining the system as a curiously faithful copy of the clouds, but removed to a vastly greater distance. N.G.C. 6822 lies far outside the limits of the galactic system, even as outlined by the globular clusters, and hence may serve as a stepping-stone for speculations concerning the habitants of space beyond.

### EARLY OBSERVATIONS

The early observations are confused, as is usual for faint complex objects. In the case of N.G.C. 6822 the confusion is clearly the result of disregarding the limitations of the various instruments employed. A short history will justify this statement and emphasize the caution required in discussing observations of nebulae. Barnard discovered[1] the object, apparently with his own 5-inch refractor. He described it as very faint and stated that some time later, when he determined its position with a 6-inch equatorial, it was seen with difficulty. The next year, however, he examined it with the 6-inch and a comet eyepiece. It was fairly conspicuous, large and round, about 10′ or 15′ in diameter, rather dense and even in its light. Barnard remarked:

> It certainly seems much larger and much denser than last year and I certainly think it has increased in density and size since that time. . . . If it had always been as large and bright as now, I cannot conceive how it could have been missed by observers when examining G.C. 4510 (the bright planetary N.G.C. 6818, which is about 40′ north preceding). Probably this is a variable nebula.[2]

The comet eyepiece accounts for these discrepancies. The 5-inch, it seems, was not equipped with this accessory, nor would one be used in determining positions with the 6-inch. So large and faint a cluster is best seen with a low power and a wide field. It will not stand magnification. At Mount Wilson, for instance, N.G.C. 6822 is fairly conspicuous in a short 4-inch finder with a low-power eyepiece, but is barely discernible at the primary focus of the 100-

---

[1] *The Sidereal Messenger*, **3**, 254, 1884.

[2] *Ibid.*, **5**, 31, 1886.

inch. The latter, however, shows the small bright details which are invisible in the finder. This factor is apparent in the later observations.

Barnard's remarks obviously refer to the cluster as a whole and furnish the description in the *N.G.C.*—"vF, L, E, dif." During the next year, 1887, the region was examined[1] with the 26-inch refractor at the Leander McCormick Observatory. The relatively high magnification and restricted field conspired to render the cluster inconspicuous. It was missed entirely by the observer. The two brightest of the small involved nebulae, however, were seen and measured. Curiously enough, they were both attributed to Barnard and the discrepancy with the *N.G.C.* description was overlooked. When the *First Index Catalogue* was compiled, the brighter of these two objects was assumed to be N.G.C. 6822, although the description in the *N.G.C.* was not amended, and the fainter object was listed as a new nebula, "I.C. 1308, eF, eS, lE, gbM, 6822 p $12^s$." H. A. Howe,[2] with a 20-inch refractor, found only the brighter of these two small nebulae and remarked that N.G.C. 6822 was "very small" instead of "large" as described by Barnard. Bigourdan[3] with a 12-inch could see neither of the small nebulae, nor, of course, the cluster. His instrument was in the blind zone, too large for the cluster and too small for the involved nebulae.

The first photographs were made in 1906 and 1907 by Wolf[4] at Heidelberg with the 16-inch Bruce camera and the 28.5-inch Walz reflector. He identified the two small nebulae as N.G.C. 6822 and I.C. 1308, and announced the cluster, Barnard's original discovery, as a new object which was duly listed in the *Second Index Catalogue* as "I.C. 4895, group of neb., 25′ diam." Wolf described the cluster as an exceptionally dense *Nebelfleckhaufen*, or cluster of small nebulae, similar to those more open clusters to whose study he has contributed so largely. This remarkable interpretation existed for fifteen years unchallenged and apparently unnoticed.

Finally in 1922, Perrine[5] published a fair description from a plate made with the 30-inch reflector at Córdoba. He properly identified the entire system as Barnard's nebula, N.G.C. 6822, and described it as a cluster of stars and nebulosity resembling the Magellanic Clouds.

---

[1] *Publications of the Leander McCormick Observatory*, **1**, Part 6.

[2] *Monthly Notices*, **60**, 137, 1900.

[3] *Observations des Nebuleuses*, **5**.

[4] *Astronomische Nachrichten*, **176**, 109, 1907.

[5] *Monthly Notices*, **82**, 489, 1922.

Meanwhile, the object had been photographed at Mount Wilson with the 10-inch camera, and the anomalous character of its image[1] had led to its being placed on the program for further study with the large reflectors. In July, 1921, Duncan[1] obtained two plates with the 100-inch reflector, on which the resemblance to the Magellanic Clouds was very striking. Detailed investigation was undertaken in July, 1923. The object was followed carefully through the two seasons of 1923 and 1924, and some plates are available for the seasons of 1921 and 1925. More than fifty direct exposures and several spectrograms have been made with the large reflectors.

## CEPHEID VARIABLES

A survey of the plates with a blink-comparator has led to the discovery of fifteen variable stars within the area covered by the system. These are marked on Plate II, and are identified by Arabic numerals. No variables have been found on the plates outside the limits of the cluster, hence those within the limits must be considered as actual members of the system. Eleven of the variables are clearly Cepheids, and a few of the remaining four may ultimately prove to be of the same type. Periods, normal curves, and photographic magnitudes have been determined for the Cepheids, the periods ranging from 12 to 64 days and the magnitudes, at maximum, from 17.45 to 19.05. The familiar period-luminosity relation is conspicuously present and the curve is parallel to Shapley's general curve expressing the corresponding relation among previously known Cepheids. The displacement in magnitudes between these two curves leads to a value of $m-M=21.65$, corresponding to a distance of 214,000 parsecs.

The system of magnitudes is based on nine Seed 30 plates taken with the 100-inch reflector. The zero-point and scale were determined from four 30-minute comparisons with the neighboring Selected Area 136 and two 20-minute comparisons with Selected

---

[1] *Mt. Wilson Contr.*, No. 256; *Astrophysical Journal*, **57**, 137, 1923. The plates are mentioned earlier in the *Mt. Wilson Annual Report for 1921.*

PLATE II

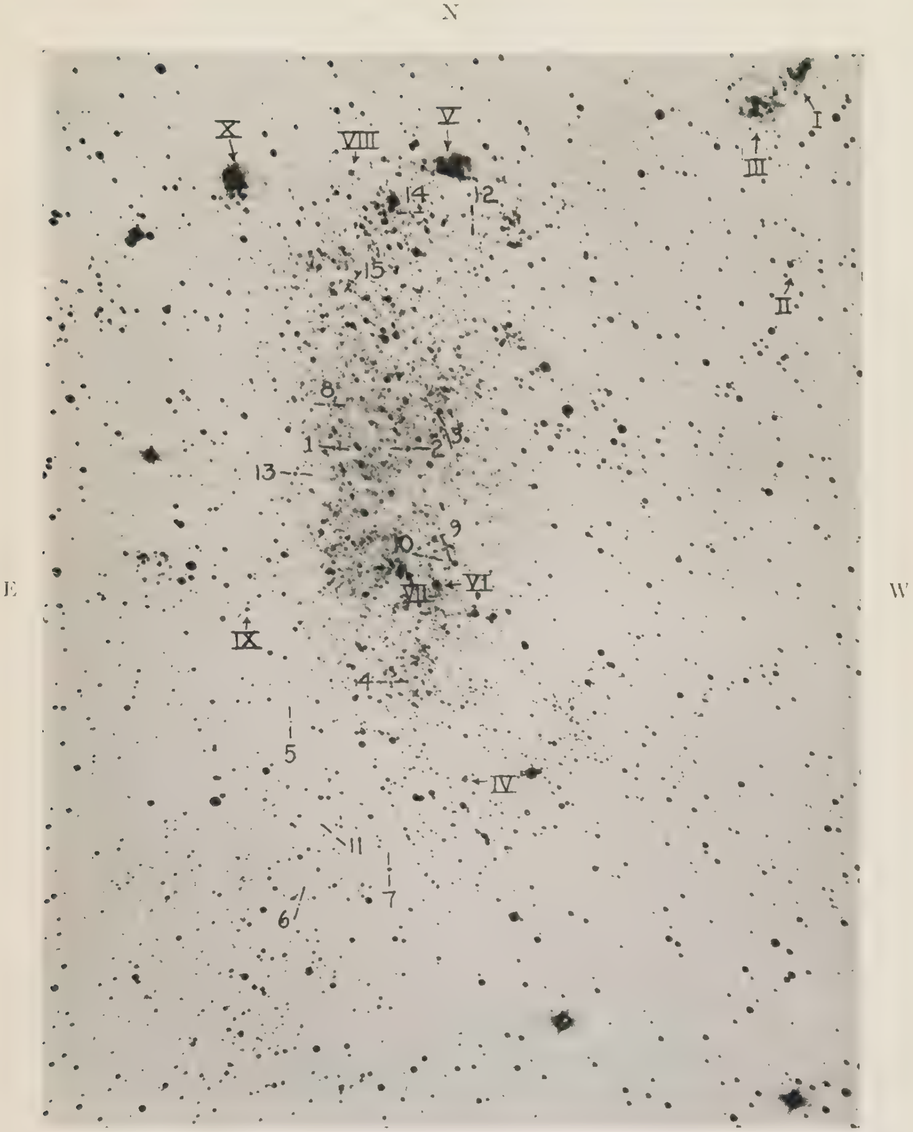

N.G.C. 6822

Negative print of Plate I. Variable stars are designated by Arabic figures; nebulae involved in or superposed on the cluster by Roman numerals.

Area 135. The plates were centered on three regions of the cluster —the center and points 3′ north and south, respectively—in order to reduce the effect of the distance correction. These comparisons gave magnitudes comparable with those of the Selected Areas down to the limits of the Mount Wilson measures[1] of the latter, about 18.0, and by a legitimate extrapolation, to a fraction of a magnitude fainter. The system was extended by means of three longer exposures, two of one hour each, and one of three hours and a half.

The internal agreement of the measures is very satisfactory down to about 19.1. Average deviations of individual plates from the mean are less than 0.1 mag. and the maximum range for an individual star on all the plates is 0.4 mag. Extrapolations beyond 18.0 depend upon the reliability of the faintest magnitude and a half of the scales in the two Selected Areas. If these are free from systematic errors, as is hoped, the extrapolation can be trusted for at least a magnitude. Distance corrections have never been thoroughly investigated for the field of the 100-inch, but the present measures were confined to the immediate vicinity of the optical axis, and approximate values of the corrections were derived from the measures themselves.

There is, however, a troublesome source of systematic error which has not been eliminated. Under ordinary observing conditions, long exposures at low altitudes with the 100-inch give images of appreciable dimensions. This is due to atmospheric refraction and changing seeing, focus, and figure. The result is that the faintest images are irregular and vary in density rather than in size. Above a certain limiting magnitude the effect is inappreciable, but as measures are carried down to fainter stars, the photometry of approximately point sources merges into photometry of surfaces. When the measuring is done with an ordinary scale-plate, the resulting magnitudes for the fainter stars become increasingly too bright. In the present measures, this effect becomes noticeable beyond about 19.1. Magnitudes fainter than this are increasingly unreliable, while those brighter are probably correct within 0.2.

A series of comparison stars was established for each variable in

---

[1] These measures on the international scale are unpublished but were available through the kindness of Mr. Seares.

## TABLE I

### Photographic Magnitudes of Variable Stars in N.G.C. 6822

| J.D.† | Q | Cepheid Variables | | | | | | | | | | | Other Variables | | | |
|---|---|---|---|---|---|---|---|---|---|---|---|---|---|---|---|---|
| | | 1 | 2 | 3 | 4 | 5 | 6 | 7 | 8 | 9 | 10 | 11 | 12 | 13 | 14 | 15 |
| 2875.44 | P | 18.85 | 18.5 | ...... | ...... | 18.85 | ...... | 18.2 | ...... | 18.8 | ...... | ...... | 18.65 | 18.1 | 18.5 | 18.85 |
| 2876.46 | G | 18.9 | 18.6 | 19.0 | 18.95 | 18.95 | 19.1 | 18.15 | 18.8 | 18.8 | 18.95 | 19.15 | 18.65 | 18.2 | 18.5 | 18.75 |
| 3611.50 | E | 18.2 | 18.3 | 19.0 | 18.35 | 18.9 | 18.75 | 17.45 | 18.85 | 19.2 | 19.3 | 19.2 | 18.85 | 18.2 | 18.75 | 18.75 |
| 3616.50 | G | 18.1 | 18.4 | 18.3 | 18.75 | 19.05 | 19.05 | 17.55 | 18.85 | 19.1 | 19.2 | 19.15 | 18.8 | 18.1 | 18.8 | 18.85 |
| 3619.53 | E | 18.4 | 18.6 | 18.45 | 19.0 | 19.15 | 19.25 | 17.55 | 18.95 | 18.85 | 19.25 | 19.3 | 19.05 | 18.2 | 18.8 | 18.7 |
| 3619.55 | G | 18.4 | 18.6 | 18.55 | 18.95 | 19.15 | 19.2* | 17.65 | 18.95 | 18.85 | 19.2 | 19.3 | 19.0 | 18.25 | 18.75 | 18.65 |
| 3638.37 | P | 18.85 | 18.0 | 18.95 | 19.0 | 18.95 | 19.1 | 18.0 | ...... | ...... | ...... | ...... | 18.8 | 17.9 | 18.85 | ...... |
| 3638.51 | F | 18.75 | 18.0 | 19.05 | 19.0 | 19.05 | 19.1 | 18.0 | 19.0 | ...... | 19.1 | 19.0 | 18.85 | 17.95 | 18.75 | 18.85 |
| 3639.40 | F | 18.85 | 17.9 | 19.0* | 19.15 | 18.9 | 19.2 | 18.05 | 18.85 | 18.9 | 19.2 | 19.05 | 18.75 | 17.95 | 18.7 | 18.85 |
| 3640.48 | P | 18.6 | 18.0 | 18.9* | ...... | 19.0 | ...... | 18.05 | ...... | ...... | ...... | 19.15 | 18.7 | 17.9 | 18.8 | 18.85 |
| 3641.50 | E | 18.55 | 18.05 | 19.0 | 18.95 | 18.9 | 19.15 | 18.15 | 18.6 | 19.1 | 19.2 | 19.2 | 18.85 | 17.85 | 18.8 | 18.85 |
| 3647.35 | F | 18.05 | 18.1 | 18.4 | 18.6 | 19.15 | 18.45 | 18.1 | 19.0 | 19.1 | 19.3 | 19.2 | 18.7 | 17.75 | 18.9 | 18.7 |
| 3678.38 | G | 18.1 | 17.85 | 18.45 | 18.95 | 19.05 | 19.15 | 17.5 | 18.95 | 19.3 | 19.2 | 19.1 | 18.75 | 17.9 | 18.7 | 18.75 |
| 3697.31 | F | 19.0 | 18.6 | 19.0* | 18.7 | 19.05 | 19.1 | 18.05 | 19.0 | 19.1 | 19.2* | 19.3 | 18.75 | 18.1 | 18.7 | 18.75 |
| 3698.33 | G | 19.05 | 18.65 | 19.05 | 18.45 | 18.95 | 19.2 | 17.9 | 18.95 | 19.1 | 19.3 | 19.0 | 18.8 | 18.05 | 18.75 | 18.7 |
| 3969.52 | G | 19.0 | 18.9 | 18.5 | 18.9* | 19.0 | 18.75 | 18.1 | 18.8 | 19.2 | 19.0 | 19.15 | 18.2 | 18.1 | 18.7 | 18.45 |
| 3971.51 | F | 18.9 | 18.8 | 18.5 | 18.9 | 18.9 | 18.9 | 18.15 | 18.7 | 18.75 | 18.85 | 19.15 | 18.3 | 18.1 | 18.8 | 18.4 |
| 3972.51 | P | 18.9 | ...... | ...... | ...... | 19.0 | 19.1 | 18.1 | ...... | ...... | ...... | 19.15 | ...... | 18.2 | 18.75 | 18.4 |
| 3990.45 | G | 18.8 | 18.3 | 19.05 | 18.85 | 19.1 | 18.75 | 17.8 | 18.9 | 19.0 | 18.8 | 19.2 | 18.05 | 18.3 | 18.4 | 18.45 |
| 3994.45 | F | 18.9 | 18.4 | 18.35 | 18.6 | 19.1 | 19.05 | 17.55 | 18.65 | 19.2 | 19.1 | 19.05 | 18.15 | 18.1 | 18.7 | 18.4 |
| 3995.45 | G | 19.0 | 18.45 | 18.4 | 18.75 | 19.15 | 19.1 | 17.65 | 18.75 | 19.05 | 18.9 | 19.2 | 18.2 | 18.1 | 18.65 | 18.5 |
| 3996.40 | E | 18.9 | 18.7 | 18.4 | 18.8 | 19.15 | 19.2 | 17.5 | 18.65 | 18.95 | 19.0 | 19.3 | 18.1 | 18.1 | 18.5 | 18.5 |
| 3997.40 | G | 19.0 | 18.5 | 18.4 | 18.9 | 18.95 | 19.1 | 17.55 | 18.85 | 19.1 | 19.1 | 19.3 | 18.2 | 18.2 | 18.6 | 18.4 |
| 3998.44 | E | 18.9 | 18.6 | 18.4 | 18.85 | 18.8 | 19.2 | 17.55 | 18.85 | 19.3 | 18.95 | 19.25 | 18.1 | 18.1 | 18.6 | 18.45 |
| 4002.37 | E | 19.05 | 18.7 | 18.65 | 19.0 | 19.15 | 19.25 | 17.65 | 18.9 | 19.15 | 18.95 | 19.35 | 18.0 | 17.95 | 18.4 | 18.45 |
| 4003.37 | G | 19.0 | 18.9 | 18.8 | 18.9 | 19.15 | 19.25 | 17.65 | 18.85 | 19.0 | 18.9 | 19.05 | 18.1 | 17.9 | 18.6 | 18.4 |
| 4004.37 | E | 18.9 | 19.0 | 18.7 | 18.95 | 19.1 | 19.1 | 17.6 | 19.0 | 18.8 | 18.8 | 19.05 | 18.05 | 18.05 | 18.5 | 18.5 |

| | | | | | | | | | | | | | | | | |
|---|---|---|---|---|---|---|---|---|---|---|---|---|---|---|---|---|
| 4024.34......... | P | 19.05 | 18.25 | 18.4 | 18.9 | 19.0 | 19.2 | 17.9 | 19.0 | 18.9 | 18.85 | ...... | 18.2 | 17.8 | 18.55 | 18.45 |
| 4025.34......... | F | 19.0 | 18.3 | 18.45 | 18.8 | 18.95 | 19.1 | 18.0 | 19.0 | 18.8 | 18.8 | 19.15 | 18.25 | 17.75 | 18.5 | 18.5 |
| 4026.40......... | P | 18.85 | 18.4 | 18.5 | 18.75 | 18.85 | 18.55 | 17.9 | 18.85 | 18.9 | 19.1 | 19.05 | 18.35 | 17.75 | 18.7 | 18.4 |
| 4031.33......... | E | 19.0 | 18.7 | 18.8 | 18.85 | 19.15 | 18.8 | 18.05 | 18.85 | 19.3 | 18.9 | 19.25 | 18.25 | 17.8 | 18.5 | 18.4 |
| 4032.33......... | G | 18.95 | 18.8 | 18.7 | 18.9 | 19.05 | 18.8 | 17.95 | 18.85 | 19.1 | 18.9 | 19.25 | 18.25 | 17.8 | 18.6 | 18.5 |
| 4049.35......... | P | 18.45 | 18.2 | 18.9* | 18.8 | ...... | 18.55 | 18.1 | ...... | ...... | ...... | ...... | 18.4 | 17.95 | 18.5 | 18.5 |
| 4050.35......... | F | 18.6 | 17.9 | 19.1 | 18.9 | 19.1 | 18.7 | 18.1 | 18.8 | 19.2 | 18.9 | 19.2 | 18.4 | 18.0 | 18.55 | 18.5 |
| 4054.32......... | P | 18.65 | 18.1 | 18.4 | 19.1 | 18.75 | 19.05 | 17.95 | 18.8 | 19.0 | 19.0 | 19.15 | 18.2 | 17.95 | 18.55 | 18.55 |
| 4056.32......... | G | 18.75 | 18.15 | 18.3 | 18.95 | 18.95 | 19.0 | 17.75 | 18.6 | 18.85 | 18.8 | 19.2 | 18.2 | 17.9 | 18.6 | 18.4 |
| 4057.32......... | F | 18.8 | 18.1 | 18.55 | 18.9 | 19.05 | 19.2 | 17.65 | 18.8 | 18.8 | 18.8 | ...... | 18.3 | 17.9 | 18.6 | 18.5 |
| 4058.32......... | E | 18.8 | 18.4 | 18.45 | 19.05 | 19.1 | 19.1 | 17.5 | 18.65 | 18.8 | 18.85 | 19.1§ | 18.35 | 18.0 | 18.55 | 18.45 |
| 4059.32......... | F | 18.9 | 18.4 | 18.6 | 18.8 | 19.1 | 19.1* | 17.5 | 18.8 | 18.85 | 19.0 | ...... | 18.3 | 18.05 | 18.6 | 18.55 |
| 4085.30......... | P | 19.0 | 18.1 | 18.3 | 18.85 | 19.0 | 19.2 | 17.85 | 18.8 | 19.1 | 18.8 | 19.3 | 18.3 | 18.3 | 18.5 | 18.5 |
| 4090.30......... | P | 19.0 | 17.9 | 19.0 | 18.95 | ...... | 18.6 | 17.9 | ...... | 18.8 | 18.8 | ...... | 18.2 | 18.25 | 18.5 | 18.6 |
| 4298.6.......... | F | 18.7 | 18.7 | 19.0 | 19.1 | 19.15 | 19.2 | 18.1 | ...... | 19.2 | 19.3 | ...... | 18.8 | 18.1 | 18.5 | 18.7 |
| 4319.6.......... | G | 18.3 | 18.0 | 18.4 | 18.9 | 18.85 | 19.15 | 17.55 | 19.0 | 19.3 | ...... | ...... | 18.9 | 18.2 | 18.6 | 18.8 |

* Limiting magnitude of the plate; variable invisible.

† Figures in this column are to be added to 2,420,000.0. The decimals represent Pacific mean time.

§ Discordant observation.

the manner described above, with successive steps averaging about 0.2 mag. These furnished easy and accurate means of following the variables. The data for the latter from the separate plates are collected in Table I. The first column gives the Julian Day representing Pacific mean time; the second, the quality of the plates, the letters "E," "G," "F," "P" and "vP" having their usual significance of "excellent," "good," "fair," "poor," and "very poor"; the remaining columns give the photographic magnitudes of the variables, which are designated by the numbers used on Plate II. The exposures were usually from 60 to 75 minutes on Seed 30 plates.

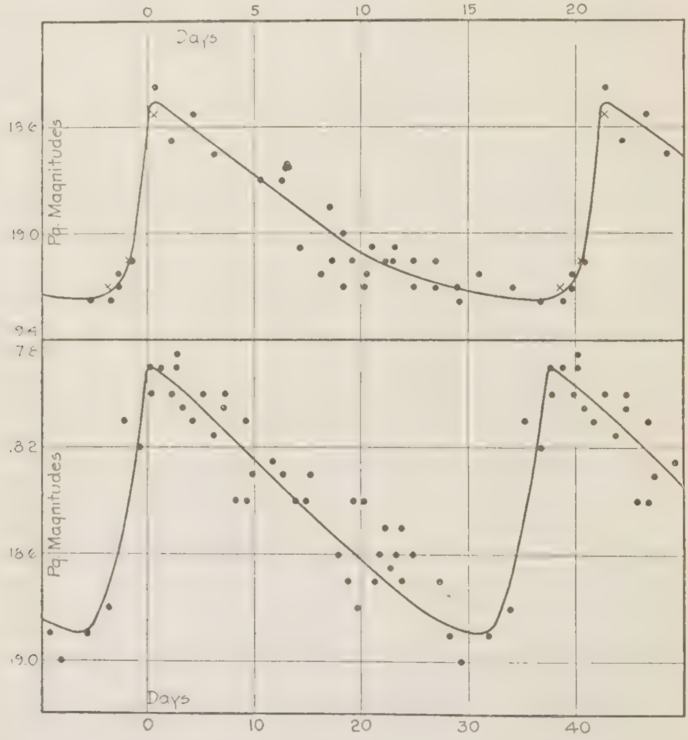

FIG. 1.—Light curves for two Cepheids in N.G.C. 6822. Upper curve, variable No. 6. Period 21.06 days; range 18.5–19.25. Lower curve, variable No. 2. Period 37.45 days; range 17.9–18.9. The three crosses on the rising slope of the upper curve represent observations on successive days and illustrate the rapid brightening of the variables.

The elements of the light-curves derived from these data for the eleven Cepheids are given in Table II. The small amplitudes found for the fainter stars are probably due, in part at least, to the systematic error previously mentioned. In order to emphasize their Cepheid characteristics two of the light-curves are illustrated in Figure 1. The other curves can easily be constructed from the data in Tables I and II.

The period-luminosity relation is shown in Figure 2, in which the logarithms of the periods in days are plotted against the photographic magnitudes at maxima. This departure from the customary usage of median magnitudes is required by the uncertainties in the fainter magnitudes, including most of those at minima. The full-line curve is the linear relation

$$m(\text{max.}) = 21.401 - 2.193 \log P \, ,$$

derived by a least-squares solution. The residuals are of the order of accuracy of the measures, averaging ±0.06 mag., with a maximum value of 0.20. This dispersion is surprisingly small and, in a measure, justifies the use of maximum rather than of median magnitudes. Furthermore, it excludes the possibility that the apparent magnitudes of the Cepheids might be sensibly affected by local absorption in the system.

TABLE II

NORMAL CURVES FOR CEPHEIDS

| Var. No. | Epoch J.D. | Period in Days | log *P* | Max. | Min. |
|---|---|---|---|---|---|
| 7......... | 2423994.0 | 64.0 | 1.806 | 17.45 | 18.15 |
| 2......... | 4050.0 | 37.45 | 1.574 | 17.9 | 18.9 |
| 1......... | 3678.0 | 30.55 | 1.485 | 18.1 | 19.0 |
| 3......... | 3994.0 | 29.2 | 1.47 | 18.35 | 19.1 |
| 6......... | 3647.0 | 21.06 | 1.325 | 18.5 | 19.25 |
| 8......... | 3972.0 | 20.72 | 1.315 | 18.6 | 19.0 |
| 4......... | 3992.0 | 17.31 | 1.238 | 18.5 | 19.1 |
| 9......... | 3971.0 | 16.86 | 1.225 | 18.75 | 19.25 |
| 10*........ | .......... | 16.5± | 1.22± | 18.8 | 19.2 |
| 5......... | 3699.0 | 13.87 | 1.142 | 18.8 | 19.2 |
| 11......... | 4003.0 | 11.77 | 1.071 | 19.05 | 19.35 |

* Observations uncertain but Cepheid characteristics are pronounced. Rejection would not affect the period-luminosity curve appreciably.

Magnitudes fainter than 19.0 are probably systematically too bright, the effect increasing with the numerical value of the magnitudes.

The determination of the distance of N.G.C. 6822 is based on

Shapley's latest revision[1] of the photographic period-luminosity curve. The form of this curve depends on more than a hundred Cepheids in the small Magellanic Cloud and should be definitive except in the region of very long periods. The zero-point[2] was derived from galactic Cepheids of intermediate periods.

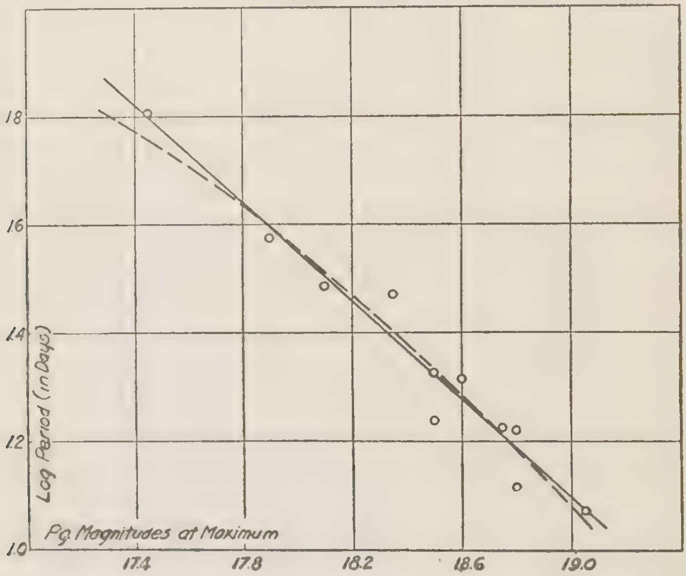

FIG. 2.—Period-luminosity relation among Cepheids in N.G.C. 6822. The continuous line represents the correlation curve, $m(\text{max}) = 21.40 - 2.19 \log P$. The broken curve indicates the corresponding portion of Shapley's general period-luminosity curve reduced to the scale of photographic magnitudes.

In Figure 2, Shapley's curve is represented by the dotted-line curve adjusted to fit the data for N.G.C. 6822 by shifting it along the magnitude axis. The uncorrected modulus is

$$m\ (\text{max.}) - M\ (\text{median}) = 21.26 \pm 0.02.$$

The maximum residual is 0.20 mag., and the mean ±0.11 mag.

---

[1] *Harvard Circular*, No. 280.

[2] Recent results by Strömberg for the solar motion referred to the galactic Cepheids indicate the possibility of a substantial correction to the zero-point (*Mt. Wilson Contr.*, No. 293; *Astrophysical Journal*, 61, 363, 1925). But until the question can be discussed in a definitive manner it seems best to use Shapley's value, with a full realization, however, of the possible necessity of a subsequent revision of all distances derived from the Cepheid criterion.

Since Shapley's curve is based on median magnitudes, the value of the modulus must be increased by half the mean range of the Cepheids in N.G.C. 6822. This quantity is somewhat uncertain, owing to the systematic error affecting the fainter magnitudes at minimum. The mean for all the Cepheids as listed in Table II is 0.67 mag., while for those brighter than 19.1 at minimum, the mean is 0.73 mag. Even this latter value appears to be low, judged by the apparent systematic decrease in range with decreasing luminosity and the ranges of Cepheids in other systems.[1] A value around 0.8 mag. would probably be nearer the truth. That actually used was 0.78 mag. The resulting values of the modulus and the distance are

$$\begin{aligned} m-M &= 21.65 \\ \pi &= 0''.00000468 \\ \text{Distance} &= 214{,}000 \text{ parsecs} \\ &= 700{,}000 \text{ light-years} \end{aligned}$$

On the assumption of the universal validity of the period-luminosity relation, the principal source of uncertainty in this result arises from that affecting the zero-point of Shapley's general relation. In addition there is the uncertainty in the extrapolated magnitude scales for the Cepheids in N.G.C. 6822. This is difficult to estimate, but probably does not exceed 0.2 mag. The error arising from accidental sources is insignificant, probably less than 0.05 mag. in the modulus, or 2.5 per cent in the distance.

As for the general validity of the period-luminosity relation, this formula has hitherto led invariably to estimates of distances which are consistent with other characteristics of the systems to which it has been applied. In the case of N.G.C. 6822 such a relation certainly exists, and, within the limits of observational error, its form, as shown by Figure 1, is the same as that observed elsewhere. The only questionable feature is the zero-point, and even here corroborative evidence is not lacking. This is presented in detail later, but reference may be made at this point to Shapley's estimate of the distance of N.G.C. 6822.

---

[1] A frequency curve for ranges of galactic Cepheids, based on data derived from Shapley (*Mt. Wilson Contr.*, No. 153; *Astrophysical Journal*, **48**, 279, 1918; and from the table compiled by the Committee on Variable Stars of the Astronomische Gesellschaft, *Vierteljahrsschrift der A. G.*, **59**, 298, 1924), shows a well-marked maximum at 0.8 mag. The data, however, are not homogeneous and, for the most part, are visual. Moreover, the relation between period and range has never been satisfactorily investigated.

He boldly assumed an analogy with the Magellanic Clouds, and, comparing angular dimensions, size, and luminosity of the diffuse nebulae, and estimated magnitudes of the brightest stars involved, arrived at a distance "on the order of a million light-years." This figure is comparable with that derived from the Cepheids and represents a brilliant application of the general principle of the uniformity of nature.

## VARIABLES OTHER THAN CEPHEIDS

For completeness, the observational data for the four other variables found in the system have been included in Table I. Concerning three of them, nothing is known beyond the fact that they vary through small ranges and apparently in an irregular manner. The remaining variable (No. 12) ranges from about 18.1 to 18.9 or more. In July, 1922, it was moderately faint; in 1923, July to October, it was faint and slowly rising; in 1924, July to November, it was bright and may have passed through a maximum about the beginning of August; in 1925, June to July, it was again faint. The period, if such exists, must be longer than five months.

## NEBULAE INVOLVED IN N.G.C. 6822

The only individual objects, other than the variables, which can be definitely identified as members of the system are five diffuse nebulae and the stars with which they are associated. Several other minute nebulous images lie within the limits of the cluster, which may be small, unresolved globular clusters belonging to the system, or, more probably, non-galactic nebulae whose images are superposed on N.G.C. 6822. The diffuse nebulae and the more conspicuous of the supposedly non-galactic nebulae are listed in Table III, under the Roman numerals by which they are designated on Plate II. The second and third columns give the co-ordinates in millimeters measured from the upper right (north preceding) corner of Plate II, and the remaining columns the class, diffuse or non-galactic; the general character of the spectrum when known, *E* denoting emission and *C*, continuous; and short descriptions with angular dimensions as measured on the three-and-a-half-hour exposure with the 100-inch reflector. The linear dimensions are given by the relation 1″=1.04 parsecs or 3.4 light-years. Number V is the object which Wolf and others identified as N.G.C. 6822, and Number X, that catalogued as I.C. 1308.

TABLE III

NEBULAE INVOLVED IN OR SUPERPOSED ON N.G.C. 6822

| NEBULA | CO-ORDINATES* |  | CLASS | SPECTRUM | DESCRIPTION |
|---|---|---|---|---|---|
|  | Horizontal | Vertical |  |  |  |
|  | mm | mm |  |  |  |
| I | 8.0 | 2.5 | Dif. | E | 32″×48″ several stars involved |
| II | 9.5 | 27.5 | Dif. | ........ | 20″ diam. Incomplete ring around star |
| III | 14.0 | 6.0 | Dif. | E | 52″ diam. Ring around several stars |
| IV | 52.5 | 95.5 | N.-G. | ........ | 5″ diam. Round, star 2″ n.p. center |
| V | 55.0 | 15.0 | Dif. | E | 20″×32″ cometic. Stars involved |
| VI | 56.0 | 70.0 | N.-G. | C | 8″ diam. Round |
| VII | 60.5 | 67.5 | N.-G. | C | 8″ diam. Round |
| VIII | 67.0 | 15.5 | N.-G. | ........ | 6″ diam. Round |
| IX | 81.0 | 73.0 | N.-G. | ........ | 5″ diam. Round |
| X | 83.0 | 16.0 | Dif. | E | 22″ diam. Ring around star, fainter extensions to 30″ s.p. star |

* Co-ordinates are measured from the upper right (north preceding) corner of Plate XV.

### DIFFUSE NEBULAE

The spectral characteristics of several of the nebulae were obtained from slitless spectrograms made at the primary focus of the 60-inch reflector with two prisms and an *f* 1.9 lens of 3-inch focus. Number V, the brightest of all the nebulae, registered eight definite images with others suspected. The wave-lengths and relative intensities are $N_1$ (10), $N_2$ (3), $H\beta$ (5), λ 4471 (1), $H\gamma$ (4), $H\delta$ (2), $H\epsilon$ (1), λ 3727 (1). Number X, the next brightest, registered five images which, with relative intensities, are $N_1$ (10), $N_2$ (3), $H\beta$ (5), $H\gamma$ (3), $H\delta$ (1). Numbers I and III registered one faint image each, probably the combination of $N_1$, $N_2$ and $H\beta$. The relative intensities of the characteristic lines $N_1$, $N_2$ and $H\beta$ in Numbers V and X are those of the diffuse nebulae in the galactic system and in the Magellanic Clouds.

The mean diameter of the five diffuse nebulae is about 37″, or 41 parsecs, which is comparable with the dimensions of the great loop of nebulosity in the constellation of Orion. The largest nebula, Number III, is a ring about 60 parsecs in diameter. This equals the diameter of N.G.C. 604 in Messier 33 and is of the order of size of the largest known diffuse nebula—N.G.C. 2070 in the large Magellanic Cloud—for which Shapley[1] gives a diameter of 80 parsecs.

A single slit spectrogram of Number V has been obtained under difficult observing conditions, using one prism and a 3-inch camera at the Cassegrain focus of the 100-inch. An exposure on August 16, 1923, registered faint images of $N_1$ and $N_2$. Independent measures by Dr. Sanford and the writer gave velocities, uncorrected for solar motion, of +16 and +34 km/sec., respectively. The mean, +25 km/sec., not only gives the order of velocity of nebula Number V but also, judged from the small peculiar motions of diffuse nebulae in general, represents the order of the motion of N.G.C. 6822 as a whole.

The emission character of the diffuse nebulae indicates that the spectral types of the brightest stars involved are very probably B0 or earlier.[2] Such stars are highly luminous, and it is not surprising to find them among the brightest contained in the cluster. Their faint apparent magnitudes combined with the considerable galactic latitude are strong evidence of their association with the extra-galactic system. Their presence alone would indicate an enormous distance for N.G.C. 6822.

The photographic magnitudes of the brightest stars involved in the individual nebulae are listed below. The measures required a very uncertain distance correction, and the resulting values may be more accurately described as estimates.

| Number | Apparent | Absolute |
|---|---|---|
| I. | 18.0 | −3.65 |
| II. | 18.0 | −3.65 |
| III. | 16.9 | −4.75 |
| IV. | 16.8 | −4.85 |
| V. | 16.8 | −4.85 |

---

[1] *Harvard Bulletin*, No. 816.

[2] *Mt. Wilson Contr.*, No. 241; *Astrophysical Journal*, **56**, 162, 1922.

The absolute magnitudes as computed from the modulus $m-M=21.65$, derived from the Cepheids, are comparable with those of the brightest Bo- and O-type stars in the galactic system. The large range among the latter, and the effects of selection on those in N.G.C. 6822, prevent the use of the data as an accurate criterion, but the comparison confirms the general order of the distance derived from the Cepheids, with evidence of an independent nature. This very materially supports the assumption that the period-luminosity relation functions normally in extra-galactic space.

### NON-GALACTIC NEBULAE

The objects in Table III which are classed as "N.G." (non-galactic) are small, round, blurry images whose diameters are functions of the exposure times. The two brightest (Nos. VI and VII) have registered faint continuous streaks on the slitless spectrograms, with no evidence of emission. A dozen or more small non-galactic nebulae are scattered over the reflector field outside the limits of N.G.C. 6822, and it is reasonable to expect that some may be found within the limits, especially as this is the region of best definition. Since, however, normal globular clusters are found in the Magellanic Clouds, there is a possibility that some of the objects in Table III may be the central regions of such clusters actually involved in N.G.C. 6822.

Shapley's[1] value for the average absolute photographic magnitude of globular clusters is about $-8.2\pm0.6$. At the distance of N.G.C. 6822, $m-M=21.65$, the apparent photographic magnitude for such a cluster as a whole would be about 13.5 or possibly 14.0 for the denser central portion. The brightest of the objects in N.G.C. 6822, however, is certainly fainter than 16.0, and the mean of the five listed in Table III is considerably more than a magnitude fainter than this. The discrepancy between them and normal globular clusters is almost conclusive.

Shapley reports seven globular clusters in the large Magellanic Cloud,[2] with apparent photographic magnitudes ranging from 7.2 to 12.0, the mean being 9.2. At the distance of N.G.C. 6822, these values would be increased about four magnitudes. Hence only the faintest, whose real nature is doubtful,[1] would be comparable with even the brightest of the objects in N.G.C. 6822.

---

[1] *Mt. Wilson Contr.*, No. 152; *Astrophysical Journal*, 48, 154, 1918.

[2] *Harvard Circular*, No. 271.

The angular diameters of the clusters in the large cloud range from $1'.1$ to $2'.6$ with a mean value of $1'.8$. At the distance of N.G.C. 6822, these quantities would be $11''$ to $25''$ with a mean of $17''$. A glance at Table III shows the diameters of the objects in N.G.C. 6822 ranging from $5''$ to $8''$ with a mean of about $6''.4$. Here again the discrepancy is almost impossibly large.

If a normal globular cluster were associated with N.G.C. 6822, the mean apparent photographic magnitude[2] of the twenty-five brightest stars would be about 20.2. In view of the dense crowding, the unresolved background, and the low observing altitude, it is improbable that such a cluster could be resolved by the 100-inch reflector. The discrepancies in size and brightness between normal globular clusters and the objects photographed with N.G.C. 6822, however, are sufficient to differentiate them, and the latter must be considered as ordinary small non-galactic nebulae whose images are superposed on that of N.G.C. 6822.

## DISTRIBUTION OF STELLAR LUMINOSITIES IN N.G.C. 6822

A preliminary attempt has been made to determine the distribution of the brighter absolute photographic magnitudes in N.G.C. 6822 by counting the stars within successive limits of apparent photographic magnitude over the central region, including the core. The area investigated is about $8'$ in declination and $4'$ in right ascension; more accurately it contains 33.75 square minutes of arc, and, to the limit of the counts, is estimated to cover about one-half of the stars in the entire system. This limit was set at 19.4 and approximate corrections for the systematic error affecting the fainter stars have been derived from minimum magnitudes of the Cepheids, the slope of the period-luminosity curve, and extrapolations of the luminosity function itself. These corrections have little weight, but they are confined to a single interval in which stars were counted and cannot seriously affect the final results.

[1] *Harvard Circular*, No. 271.

[2] *Mt. Wilson Contr.*, No. 152; *Astrophysical Journal*, **48**, 154, 1918.

The counts were made on the blink-comparator carrying a scale-plate on one side and a plate of N.G.C. 6822, covered by a reseau, on the other. The scale was calibrated from the series of comparison stars established for the variables, and the field stars were eliminated by means of the new distribution tables for different photographic magnitudes and galactic latitudes recently published by Seares and van Rhijn.[1]

TABLE IV

LUMINOSITY FUNCTION FOR THE BRIGHTER STARS IN N.G.C. 6822

| Pg. Mag. | Stars Counted | Normal No. | N.G.C. 6822 | | Kapteyn* | | |
|---|---|---|---|---|---|---|---|
| | | Gal. Lat. −20° | $\phi(m)$ | log $\phi(m)$ | $\phi(M)$ | log $\phi(M)$ | $M$ (vis.) |
| 19.4−19.1...... | 394 | 13.5 | 380.5 | 2.580 | 379 | 2.579 | −3.75 |
| 19.1−18.8...... | 230 | 11.6 | 218.4 | 2.339 | 219 | 2.340 | 4.05 |
| 18.8−18.5...... | 134 | 9.8 | 124.2 | 2.094 | 124 | 2.093 | 4.35 |
| 18.5−18.2...... | 78 | 8.3 | 69.7 | 1.843 | 69.2 | 1.840 | 4.65 |
| 18.2−17.9...... | 27 | 7.0 | 20.0 | 1.301 | 38.2 | 1.582 | 4.95 |
| 17.9−17.6...... | 25 | 5.9 | 19.1 | 1.281 | 20.7 | 1.317 | 5.25 |
| 17.6−17.3...... | 16 | 4.9 | 11.1 | 1.045 | 11.1 | 1.045 | 5.55 |
| 17.3−17.0...... | 11 | 4.1 | 6.9 | 0.84 | 5.9 | 0.77 | 5.85 |
| 17.0−16.7...... | 9 | 3.3 | 5.7 | .76 | 3.1 | .49 | 6.15 |
| 16.7−16.4...... | 9 | 2.7 | 6.3 | .80 | 1.6 | 0.20 | 6.45 |
| 16.4−16.1...... | 5 | 2.2 | 2.8 | .45 | 0.8 | 9.89 | 6.75 |
| 16.1−15.8...... | 5 | 1.8 | 3.2 | 0.51 | .4 | 9.59 | 7.05 |
| 15.8−15.5...... | 0 | 1.4 | − 1.4 | ........ | 0.2 | 9.29 | −7.35 |
| 15.5−15.2...... | 1 | 1.1 | − 0.1 | ........ | ........ | ........ | ........ |
| 15.2−14.9...... | 0 | 0.9 | − .9 | ........ | ........ | ........ | ........ |
| 14.9−14.6...... | 1 | .7 | − .3 | ........ | ........ | ........ | ........ |
| 14.6−14.3...... | 0 | 0.6 | − 0.6 | ........ | ........ | ........ | ........ |

* The last three columns give the numbers of stars (visual magnitudes) in a volume of $5.22\times10^8$ cubic parsecs, in which the distribution is in accordance with Kapteyn's luminosity function for stars in the vicinity of the sun. A comparison with the distribution of stars in N.G.C. 6822 indicates a mean color-index for the latter stars of +1.35 mag.

Results of the counts are given in Table IV. The first three columns represent the number of stars counted in the corresponding intervals of apparent magnitude and the normal number for an equal area in the galactic latitude of the cluster. The fourth and fifth columns give the numbers of stars, $\phi(m)$, with their logarithms, which can be attributed to the cluster. For the brightest stars the results are of low weight because of the small area involved. The remaining columns will be explained later.

The upper limit for the stars in N.G.C. 6822 is about 15.8, corresponding to the absolute photographic magnitude $-5.85$. This appears to be quite normal for the great isolated systems. The brightest star known in the local cluster is $-5.5$ ($\beta$ Orionis).[1] The limit for the small Magellanic Cloud[2] has been placed between $-4$ and $-7$; for the large cloud,[3] it is brighter than $-8$; for the globular clusters,[4] fainter than $-4$.

---

[1] *Proceedings of the National Academy of Sciences*, **11**, 358, 1925.

The smoothness of the luminosity function for N.G.C. 6822 invites a comparison with the corresponding function in the neighborhood of the sun. The latter has been derived by Kapteyn[5] from data based on visual magnitudes. Little is known concerning the distribution of color among the very luminous stars but, as a first approximation, the mean color-index may be assumed to be constant over the short range of magnitudes involved in the present counts. Successive numerical values of the color-index were tried, the two functions being shifted into approximate coincidence by adjusting the volume coefficient[6] for Kapteyn's function.

By this method of trial and error, the best fit was obtained with a mean color-index of $+1.35$ mag., and a volume coefficient of $5.22 \times 10^8$ cubic parsecs. The small range of the counts restricts the sensitiveness of the method, but on the assumption that the functions are comparable, the probable error of the color-index, assumed to be constant, is of the order of 0.3 mag. The numbers of stars, $\phi(M)$, and their logarithms, as calculated from Kapteyn's function with the foregoing assumptions, are listed in the sixth and seventh columns of Table IV. The eighth column gives the median absolute visual magnitudes of the stars in the two preceding columns. These magnitudes, corrected by $+1.35$, represent the photographic magnitudes of the stars counted in N.G.C. 6822, using the modulus $m-M=21.65$.

Figure 3 represents the two functions in a graphical form. The full broken line represents the counts in N.G.C. 6822; and the dotted curve, Kapteyn's luminosity function. The agreement, especially in the upper and more reliable portions, is remarkably close; but the comparison involves several assumptions and can scarcely be

---

[1] *Mt. Wilson Contr.*, No. 147; *Astrophysical Journal*, **47**, 280, 1918.

[2] *Harvard Circular*, No. 260.

[3] *Ibid.*, No. 271.

[4] *Proceedings National Academy of Sciences*, **6**, 293, 1920.

[5] *Mt. Wilson Contr.*, No. 229; *Astrophysical Journal*, **55**, 242, 1922.

[6] The volume coefficient represents the space throughout which stars must be distributed according to Kapteyn's function in order that the number of stars in a given interval of absolute magnitude may equal the number actually counted in the cluster

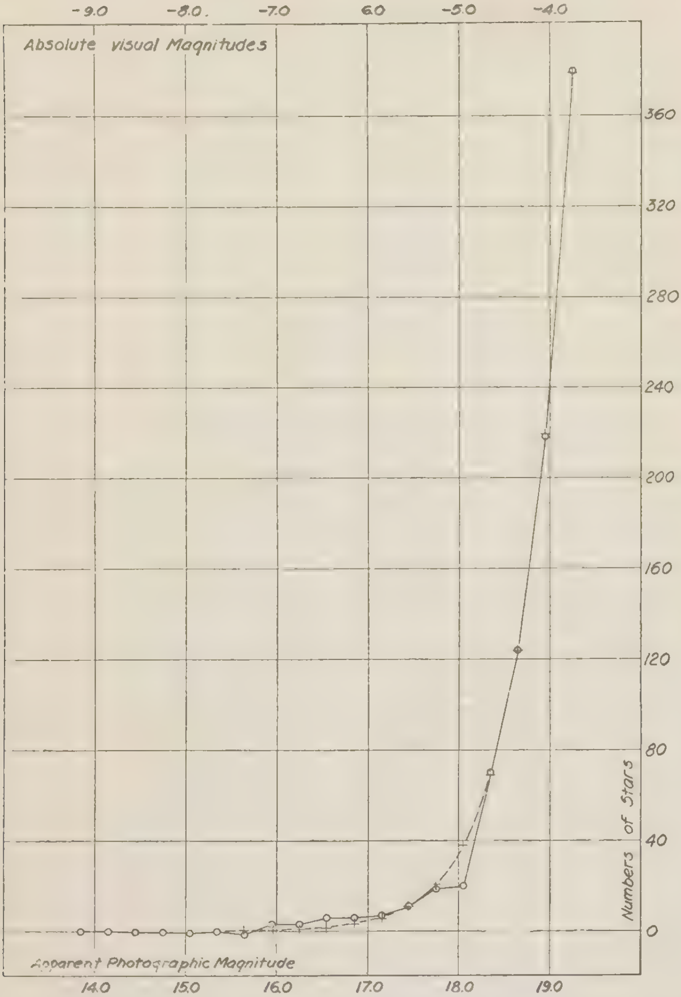

FIG. 3.—Comparison of the luminosity function for N.G.C. 6822 (circles) with Kapteyn's luminosity function (crosses) for stars in the vicinity of the sun. The best fit has been obtained by using a mean color-index of +1.35 mag. for the cluster stars and a volume coefficient of $5.22 \times 10^8$ cubic parsecs for Kapteyn's function.

considered as definitive. There is, however, a general similarity between the two functions, and the value of the color-index, judged by the incomplete data available for other systems, seems to be quite reasonable.

The color-index, indeed, appears to confirm the order of the absolute magnitudes assigned to the cluster stars and, consequently, the zero-point of Shapley's general period-luminosity curve for the Cepheids. If the distance assigned the cluster were too great, the color-index as derived from the counts would be too small, and vice versa. An error of 50 per cent in the distance corresponds to an error of about 0.9 mag. in the color-index. There seems to be no reason for supposing that the color-index actually determined from the present data is in error by this amount.

## TOTAL MAGNITUDE OF N.G.C. 6822

An approximation to the total photographic magnitude of N.G.C. 6822 has been obtained from short exposures with the 10-inch astrographic camera. The scale of these plates (1 mm = 3′) is so small that the cluster is unresolved and presents an amorphous surface. The brightest portion is the central core, which just registers in an exposure of 30 minutes on a Seed 30 plate. The corresponding surface brightness can be calculated from the value of 18.8±0.3 photographic magnitudes per square second of arc, which Seares[1] has derived for the limiting surface brightness registering in an exposure of 1 minute on a Seed 30 plate at the Newtonian focus of a reflector with a focal ratio of 1 to 5. For an exposure of 30 minutes the limiting surface brightness will be[2]

$$S.B. = 18.8 + 2.0 \log 30 = 21.8$$

This can be reduced to the system for a camera of focal ratio 1:4.5 by applying a correction[3] of +0.3, so that the final value is

$$S.B. = 22.1 \text{ per sq. sec. arc.}$$

---

[1] *Mt. Wilson Contr.*, No. 191; *Astrophysical Journal*, **52**, 162, 1920.

[2] The coefficient of log exposure time is 2.5 $p$, where $p$, the exponent in Schwarzschild's expression for the reciprocity law, is given the usual value of 0.8.

[3] This correction has been applied habitually in deriving surface brightness from limiting exposures with the 10-inch. For an example see *Mt. Wilson Contr.*, No. 250; *Astrophysical Journal*, **56**, 400, 1922.

The area covered by the central core is about $8' \times 3'$, hence the total apparent magnitude is

$$m = 22.1 - 2.5 \log (8 \times 3 \times 3600) = 9.7.$$

It is estimated that the core contributes about one-half the total luminosity of the nebula, hence the total apparent magnitude of the entire system is about 9.0. The corresponding absolute photographic magnitude is $-12.7$. The absolute visual magnitude is probably of the order of $-13.7$.

These quantities furnish an indication as to the space density. As a first approximation, the core can be considered as an ellipsoid whose maximum and minimum diameters are those of the projected image and whose third diameter, in the line of sight, is the mean of the other two. Since the linear scale is $1'' = 1.04$ parsecs, the diameters of the hypothetical ellipsoid are about $500 \times 190 \times 340$ parsecs. The volume is $1.7 \times 10^7$ cubic parsecs. The absolute photographic magnitude is $9.7 - 21.65 = -11.95$, hence the density is $2.5 \log (1.7 \times 10^7) - 11.95 = 6.1$ absolute photographic magnitudes per cubic parsec. By a similar computation the mean density of the entire system is found to be about 8.8. This is comparable with the density in the neighborhood of the sun,[1] when reasonable assumptions as to color-indices are introduced. The density of the core alone, however, appears to be from twenty to thirty times that near the sun.

A comparison of the total magnitude of the core, derived from the surface brightness, with that derived from the integration of the luminosity function, extrapolated beyond the limits of the star counts previously discussed, furnishes an independent check on the assumption that the latter is comparable with Kapteyn's function for the stars in the vicinity of the sun. The direct comparison of the two luminosity functions was restricted to some three magnitudes at the extreme bright ends of the curves. The excellent agreement over this small region suggests that the two functions are comparable throughout their entire range. In this case, the total luminosity of the portion of the cluster represented by the counts can be computed by integrating Kapteyn's function over a space equal to the volume coefficient, $5.22\times10^8$ cubic parsecs, derived in the restricted comparison. The total luminosity per cubic parsec, from Kapteyn's function, is 8.16 in absolute visual magnitudes.[1] The total magnitude of the cluster is, therefore,

---

[1] The space density near the sun is about 8.16 absolute visual magnitudes per cubic parsecs. Seares, *Mt. Wilson Contr.*, No. 191, *Astrophysical Journal*, **52**, 162, 1920.

$$2.5 \log (5.22\times10^8)-8.15=-13.64.$$

The core of N.G.C. 6822 covers an area about 25 per cent less than that over which the counts were made, but, as it is much denser than the rest of the cluster, the correction for reducing the volume coefficient to correspond to the core alone can be taken as half this amount. The total magnitude for the core alone is then about $-13.5$.

This visual luminosity is to be compared with the photographic absolute magnitude, $-12.0$, derived from the surface brightness and the angular area. The difference of 1.5 mag. represents the combined effect of the mean color-index of the core, errors in the various quantities involved, and any real difference there may be between the two luminosity functions themselves. A large part of the discrepancy can safely be attributed to color-index alone. The comparison of the luminosity functions indicated a mean color-index of $+1.35$ for the brighter stars. This value would probably require some reduction for the fainter stars, but the integrated effect of the factor cannot be accurately stated. The probable error in the surface brightness alone is of the order of $\pm0.4$ mag., and errors from other sources, although smaller, would add materially to the total.

The discrepancy in the two results, when the color-index is considered, appears to be within the probable errors of the determinations. Nothing remains which can be attributed with certainty to differences in the luminosity functions. As far as one can determine, the stars in N.G.C. 6822 appear to be the same sort of objects, distributed in much the same fashion, as those in the vicinity of the sun.

## COMPARISONS OF N.G.C. 6822 WITH THE MAGELLANIC CLOUDS

Comparisons between N.G.C. 6822 and the Magellanic Clouds are of special interest and significance because the distances of all three objects are based primarily on the Cepheid criterion. The appearance of the photographic images is remarkably alike. Shapley[1] has previously noted that "the dominating feature in both [the clouds] is an elongated patch of densely crowded stars similar to N.G.C. 6822." In the present paper, this feature is termed the core. Other points of similarity, which have already been discussed, are the presence of Cepheid variables and of diffuse nebulae, and the magnitudes and the luminosity function of the brightest stars.

---

[1] Seares, *Mt. Wilson Contr.*, No. 191; *Astrophysical Journal*, **52**, 162, 1920.

TABLE V

COMPARISON OF N.G.C. 6822 WITH THE MAGELLANIC CLOUDS

| | MAGELLANIC CLOUDS | | N.G.C. 6822 |
|---|---|---|---|
| | Large | Small | |
| Angular dimensions: | | | |
| Total | 7°.2×7°.2* | 3°.6×3°.6† | 20′×10′ |
| Core | 3°.6×1°.2 | 1°.8×0°.9 | 8′×3′ |
| Apparent luminosity: | | | |
| Total | 1.2 | 2.0‡ | 9.0 |
| Core | 1.9 | 2.7 | 9.7 |
| Surface brightness: | | | |
| Core | 21.0 | 21.0 | 22.1 |
| Distance | 34,500* | 31,600† | 214,000 |
| Linear dimensions: | | | |
| Total | 4300§ | 2000† | 1250×625 |
| Core | 2150×715 | 1100×500† | 500×190 |
| Volume: | | | |
| Total | $4.2\times10^{10}$ | $4.2\times10^{9}$ | $3.8\times10^{8}$ |
| Core | $9.2\times10^{8}$ | $2.3\times10^{8}$ | $1.7\times10^{7}$ |
| Absolute luminosity: | | | |
| Total | −16.5§ | −15.5 | −12.7 |
| Core | −15.8 | −14.8 | −12.0 |
| Mean density: | | | |
| Total | 10.0 | 8.5 | 8.8 |
| Core | 6.6 | 6.1 | 6.1 |

* *H.C.O. Circular*, No. 268. † *H.C.O. Circular*, No. 255. ‡ *H.C.O. Circular*, No. 260.

§ *H.C.O. Bulletin*, No. 816.

Luminosities are expressed in photographic magnitudes; surface brightness, in magnitudes per square second of arc; distances, linear dimensions, and volumes, in parsecs and cubic parsecs; densities, in absolute magnitudes per cubic parsec.

A more detailed comparison of dimensions, densities, and total luminosities is given in Table V, both for the cores and for the entire systems. Many of the data depend upon mere estimates which cannot claim any high accuracy, but even the orders of magnitude of the quantities are useful as a first approximation. Distances, dimensions, and luminosities for the two clouds, when given, have been taken from Shapley's papers.[1] The angular dimensions of the core of the larger cloud have been measured on the Franklin-Adams chart; the cores of both the clouds have been assumed to contribute one-half the total luminosity of the systems; the true figures of the two clouds are assumed to be globular, since their images are approximately circular; the figures of N.G.C. 6822 and of the cores of all three objects are assumed to be ellipsoids whose maximum and minimum diameters are those of the projected images and whose third diameters are the means of the other two. This last assumption is quite arbitrary, but can serve as a basis for comparison.

---

[1] *Harvard Bulletin*, No. 795.

## CONCLUSION

The present investigation identifies N.G.C. 6822 as an isolated system of stars and nebulae of the same type as the Magellanic Clouds, although somewhat smaller and much more distant. A consistent structure is thus reared on the foundation of the Cepheid criterion, in which the dimensions, luminosities, and densities, both of the system as a whole and of its separate members, are of orders of magnitude which are thoroughly familiar. The distance is the only quantity of a new order.

The principle of the uniformity of nature thus seems to rule undisturbed in this remote region of space. This principle is the fundamental assumption in all extrapolations beyond the limits of known and observable data, and speculations which follow its guide are legitimate until they become self-contradictory. It is therefore a matter of considerable importance that familiar relations are found to be consistent when applied to the first system definitely assigned to the regions outside the galactic system.

Of especial importance is the conclusion that the Cepheid criterion functions normally at this great distance. Cepheid variables have recently been found in the two largest of the spiral nebulae, and the period-luminosity relation places them at distances even more remote than N.G.C. 6822. This criterion seems to offer the means of exploring extra-galactic space; N.G.C. 6822 furnishes a critical test of its value for so ambitious an undertaking and the results are definitely in its favor.

---

[1] *Harvard Bulletin*, No. 816; *Harvard Circulars*, Nos. 255, 260, 268.

## ADDENDUM

A pair of Cramer Iso plates, exposed through a visual color filter at the primary focus of the 100-inch, have recently been obtained of N.G.C. 6822. The exposures were one and three hours, respectively. It has not yet been possible to calibrate accurately the plates, but preliminary comparisons have been made with short, unfiltered exposures obtained at the same time.

Cepheids 1, 2, 3, 4, and 5 were identified and gave indications of moderately large color-indices. The non-Cepheid variables appear to have larger color-indices; 12, 13, and 14 being estimated as red. The diffuse nebulae are clearly blue, and the stars associated with them have color-indices as small as, or smaller than, any others seen on the plates. The colors of the non-galactic nebulae were estimated to fall between those of the Cepheid and the non-Cepheid variables.

The general order of these results probably will not be materially changed when accurate measures are possible. They are thoroughly consistent with the conclusions reached in the previous discussion and furnish additional support to the view that the stars in N.G.C. 6822 are comparable with those in other systems.

Mount Wilson Observatory
September 1925

Contributions from the Mount Wilson Observatory, No. 305
Preprinted from the *Astrophysical Journal*

# REDUCTION OF THIRTY-NINE ASTROGRAPHIC ZONES TO THE INTERNATIONAL PHOTOGRAPHIC SCALE

By FREDERICK H. SEARES and MARY C. JOYNER

## ABSTRACT

*Calibration of magnitude scales of thirty-nine astrographic zones.*—Photographic magnitudes on the international scale corresponding to the values of log $N_m$ ($N_m$ = number of stars per square degree brighter than $m$) given for thirty-three zones in Table XV, *Mt. Wilson Contr.* No. 301, were interpolated from Table XVII of that paper. Together with the equivalent scale-readings or provisional magnitudes used to express the brightness of the stars, the interpolated magnitudes provide a calibration for from three to five points on the scales of the individual zones. The calibration was extended to other scale-readings for which counts are available by comparing mean densities for entire zones to successive limits of scale-reading with the adopted mean distribution of stars for all latitudes together. *Final results* are in Table IV, which also includes data for six Oxford zones for which counts have recently been published. Although the calibrations refer to zones as a whole, the residuals in limiting magnitude for different galactic latitudes given in Table I indicate that in many cases the calibrations are directly applicable to small parts of a zone. These residuals are not, however, a final test of consistency in the scales, because both errors of reduction and irregularities in stellar distribution contribute to their progressive character.

The determination of stellar distribution given in *Contribution* No. 301[1] was based in part on counts of thirty-three zones of the *Astrographic Catalogue*, collected and published mostly by Turner.[2] These data were referred to the international photographic scale by comparing values of log $N_m$ ($N_m$ = number of stars per square degree brighter than $m$) derived from the counts in each zone with van Rhijn's distribution table[3] which had already been reduced to the international scale by comparison with the *Mount Wilson Catalogue*. Mean densities (log $N_m$) for galactic latitudes 0°, 10°, 20° . . . . corresponding to several limiting values of the scale-reading[4] in each zone, and the means of the equivalent magnitudes interpolated from van Rhijn's table, may be found in Table XV of *Contribution* No. 301.

---

[1] *Astrophysical Journal*, **62**, 320, 1925.

[2] *Ibid.*, Table XIII gives references to the published data.

[3] *Groningen Publication*, No. 27, Table IV, 1917.

[4] The term "scale-reading" is used to indicate the brightness of stars as expressed in the zones, irrespective of whether the quantities given are actual scale-readings, estimates of brightness, or provisional magnitudes.

The mean magnitudes and the corresponding scale-readings, which were not given in Table XV, provide a calibration of the scales of the astrographic zones in terms of the international photographic scale, although not the best possible because of the influence of residual errors in van Rhijn's table. As remarked in *Contribution* No. 301, the precision can be increased by a reinterpolation of the magnitudes from the adopted distribution table. The details of this revision are shown in Table I of this article, arranged according to the declination of the zones. These results are later subjected to a process which minimizes the influence of certain accidental errors, and, finally, extended to scale-readings for which corresponding magnitudes have not yet been calculated. The adopted calibration is in Table IV, which gives the mean photographic magnitude on the international scale for practically all scale-readings for which counts are available. The omissions relate to bright stars in a few zones which are not numerous enough to give reliable values of the magnitudes.

The results of the reinterpolation are in the second and third lines from the end of each division of Table I. Thus for the Vatican zones,[1] +62°, scale-readings 40, 30, . . . . 0 correspond, respectively, to revised magnitudes 8.87, 10.08, . . . . 12.98. The provisional magnitudes from Table XV, *Contribution* No. 301, which head the columns of Table I, identify the mean densities used for the reinterpolation. For example, the densities corresponding to scale-reading 40 in the Vatican zones stand opposite provisional magnitude 8.81 in the fourth line of Table XV, *Contribution* No. 301. With the aid of Table XVII of that paper these densities give the revised magnitudes 9.26, 9.14, . . . . 8.62, which deviate from their mean of 8.87 by the amounts shown in Table I opposite the latitudes to which they refer. Occasionally the same provisional magnitude is associated with more than one series of densities; the declination of the zone, which also appears in Table XV, then removes the ambiguity.

---

[1] The published counts are the means for the three zones in declinations +64°, +62°, and +60°.

## TABLE I

### Provisional Magnitudes and Deviations

| Lat. | Vatican +62° | | | | | Oxford +31° | | | | |
|---|---|---|---|---|---|---|---|---|---|---|
| | 8.81 | 10.04 | 11.10 | 12.32 | 12.97 | ....... | ....... | ....... | ....... | ....... |
| 0° | −39 | −13 | − 4 | 0 | + 1 | +20 | +18 | +18 | +35 | +34 |
| 10 | −27 | −11 | − 1 | 0 | − 1 | +15 | +13 | +10 | +22 | +22 |
| 20 | −10 | − 5 | −11 | −14 | −10 | + 8 | + 6 | + 4 | +14 | +13 |
| 30 | +12 | + 6 | − 3 | −10 | − 3 | + 7 | + 8 | + 5 | +15 | +14 |
| 40 | +17 | + 4 | − 2 | − 1 | + 4 | 0 | + 4 | + 8 | + 9 | +10 |
| 50 | +21 | + 7 | + 6 | +10 | + 6 | − 6 | − 2 | + 4 | 0 | + 7 |
| 60 | +25 | +10 | +12 | +12 | + 3 | − 7 | −10 | − 4 | −15 | −13 |
| 70 | ....... | ....... | ....... | ....... | ....... | −10 | −15 | −13 | −28 | −25 |
| 80 | ....... | ....... | ....... | ....... | ....... | − 9 | −14 | −19 | −26 | −30 |
| 90 | ....... | ....... | ....... | ....... | ....... | −14 | −13 | −15 | −26 | −31 |
| Rev. *m* | 8.87 | 10.08 | 11.15 | 12.35 | 12.98 | 9.59 | 10.72 | 11.89 | 12.89 | 13.48 |
| Sc.R. | 40 | 30 | 20 | 10 | 0 | 35 | 26 | 18 | 12 | All |
| *m*−*m*′ | −0.39 | −0.23 | −0.22 | −0.22 | −0.22 | +0.01 | +0.12 | +0.09 | +0.10 | +0.10 |

| Lat. | Oxford +30° | | | | | Oxford +29° | | | | |
|---|---|---|---|---|---|---|---|---|---|---|
| | ....... | ....... | ....... | ....... | ....... | ....... | ....... | ....... | ....... | ....... |
| 0° | +28 | +22 | +22 | +36 | +20 | +29 | +34 | +33 | +41 | +29 |
| 10 | +17 | + 9 | + 6 | +18 | + 9 | +17 | +23 | +24 | +30 | +14 |
| 20 | +11 | − 5 | − 5 | + 2 | − 2 | + 4 | + 6 | + 9 | +15 | +10 |
| 30 | + 8 | − 6 | − 3 | − 1 | + 3 | − 2 | 0 | + 2 | + 7 | +10 |
| 40 | + 1 | − 7 | + 2 | − 2 | + 3 | −11 | −10 | − 8 | + 2 | + 5 |
| 50 | − 3 | − 6 | + 3 | − 3 | + 2 | − 5 | − 8 | −13 | − 3 | − 1 |
| 60 | − 7 | − 5 | 0 | − 9 | − 4 | − 8 | −10 | −18 | −11 | −10 |
| 70 | −15 | − 2 | −10 | −13 | − 9 | −10 | −12 | −13 | −20 | −18 |
| 80 | −18 | − 1 | − 8 | −14 | −11 | −10 | −12 | −12 | −26 | −16 |
| 90 | −22 | 0 | − 7 | −14 | −12 | − 9 | −14 | − 9 | −30 | −20 |
| Rev. *m* | 9.76 | 10.85 | 12.09 | 12.92 | 13.70 | 9.36 | 10.28 | 11.50 | 12.52 | 13.55 |
| Sc.R. | 35 | 26 | 18 | 12 | All | 35 | 26 | 18 | 12 | All |
| *m*−*m*′ | −0.03 | +0.03 | +0.13 | +0.07 | +0.10 | −0.01 | 0.00 | +0.07 | +0.18 | +0.19 |

| Lat. | Oxford +28° | | | Oxford +27° | | | | |
|---|---|---|---|---|---|---|---|---|
| | 10.05 | 12.43 | 13.68 | ....... | ....... | ....... | ....... | ....... |
| 0° | +17 | +12 | + 9 | + 8 | +23 | +25 | +24 | +26 |
| 10 | +16 | 0 | − 2 | + 6 | +11 | +19 | +15 | +12 |
| 20 | − 2 | + 5 | + 1 | − 1 | − 1 | + 9 | + 3 | − 1 |
| 30 | + 5 | +19 | +23 | + 3 | + 3 | + 9 | + 3 | 0 |
| 40 | 0 | +10 | +12 | + 6 | + 5 | + 7 | + 5 | + 9 |
| 50 | − 2 | − 3 | 0 | + 3 | + 6 | − 2 | + 5 | +13 |
| 60 | − 6 | −14 | −15 | − 2 | + 2 | − 8 | − 1 | 0 |
| 70 | −15 | −28 | −30 | − 6 | − 7 | −19 | −15 | −14 |
| 80 | ....... | ....... | ....... | −11 | −18 | −22 | −20 | −21 |
| 90 | ....... | ....... | ....... | −10 | −23 | −21 | −23 | −25 |
| Rev. *m* | 10.04 | 12.44 | 13.62 | 9.20 | 10.12 | 11.35 | 12.25 | 13.28 |
| Sc.R. | 30 | 12 | All | 35 | 26 | 18 | 12 | All |
| *m*−*m*′ | +0.15 | +0.24 | +0.22 | +0.07 | +0.07 | +0.12 | +0.17 | +0.15 |

| Lat. | Oxford +26° | | | | | Oxford +25° | | | | |
|---|---|---|---|---|---|---|---|---|---|---|
| | ....... | ....... | ....... | ....... | ....... | ....... | ....... | ....... | ....... | ....... |
| 0° | + 4 | + 9 | +13 | +17 | +29 | +32 | +23 | +29 | +19 | +24 |
| 10 | + 3 | + 2 | + 6 | + 5 | + 9 | +20 | +16 | +14 | + 4 | + 7 |
| 20 | 0 | − 6 | 0 | + 5 | − 8 | + 7 | +10 | − 2 | −10 | − 5 |
| 30 | + 2 | + 5 | +10 | +11 | − 2 | + 4 | +11 | − 6 | − 4 | + 3 |
| 40 | + 1 | +12 | +18 | +18 | +10 | + 2 | +10 | + 3 | + 9 | +12 |
| 50 | + 7 | +12 | +10 | +15 | + 7 | − 4 | + 2 | + 5 | +15 | + 9 |
| 60 | + 5 | + 5 | − 4 | − 4 | − 7 | −10 | − 9 | − 3 | + 4 | − 5 |
| 70 | − 1 | − 4 | −13 | −18 | − 6 | −16 | −19 | − 9 | − 8 | −14 |
| 80 | − 7 | −15 | −21 | −21 | −14 | −18 | −23 | −15 | −14 | −15 |
| 90 | −12 | −20 | −24 | −28 | −18 | −17 | −22 | −11 | −12 | −13 |
| Rev. *m* | 9.31 | 10.33 | 11.58 | 12.54 | 13.48 | 9.58 | 10.63 | 11.90 | 12.73 | 13.53 |
| Sc.R. | 35 | 26 | 18 | 12 | All | 35 | 26 | 18 | 12 | All |
| *m*−*m*′ | +0.07 | +0.08 | +0.18 | +0.18 | +0.16 | +0.15 | +0.13 | +0.18 | +0.08 | +0.17 |

TABLE I—*Continued*

| LAT. | PARIS +23° | | | | | PARIS +22° | | | | |
|---|---|---|---|---|---|---|---|---|---|---|
| | 9.20 | 10.45 | 11.74 | 12.82 | 13.25 | 9.26 | 10.38 | 11.71 | 12.79 | 13.34 |
| 0° | +25 | +32 | +40 | +32 | −14 | +25 | +20 | +26 | +14 | − 7 |
| 10 | +21 | +25 | +20 | +14 | −25 | +20 | +15 | +21 | + 8 | −12 |
| 20 | +11 | +10 | 0 | − 7 | −29 | +10 | +10 | + 8 | + 5 | − 8 |
| 30 | + 5 | + 9 | − 9 | −17 | −21 | + 3 | + 4 | + 7 | + 8 | −11 |
| 40 | − 2 | − 3 | − 9 | −10 | − 3 | − 3 | + 4 | + 5 | + 8 | − 2 |
| 50 | − 7 | −11 | −10 | + 3 | +21 | − 6 | − 2 | + 2 | + 5 | + 4 |
| 60 | − 9 | −14 | − 7 | 0 | +23 | − 9 | − 9 | − 9 | − 7 | + 6 |
| 70 | −15 | −16 | − 7 | − 3 | +19 | −14 | −16 | −15 | −13 | + 8 |
| 80 | −14 | −17 | − 7 | − 6 | +15 | −15 | −14 | −21 | −13 | +10 |
| 90 | −13 | −16 | − 7 | − 4 | +12 | −15 | −11 | −20 | −14 | +12 |
| Rev. *m* | 9.17 | 10.42 | 11.75 | 12.81 | 13.27 | 9.23 | 10.37 | 11.73 | 12.80 | 13.34 |
| Sc.R. | 8.0 | 9.0 | 10.0 | 11.0 | All | 8.0 | 9.0 | 10.0 | 11.0 | All |
| *m*−*m′* | +0.13 | +0.17 | +0.19 | +0.16 | 0.00 | +0.21 | +0.21 | +0.27 | +0.23 | +0.04 |

| LAT. | BORDEAUX +17° | | | BORDEAUX +16° | | | | |
|---|---|---|---|---|---|---|---|---|
| | 10.76 | 12.35 | 13.18 | 8.66 | 10.06 | 11.46 | 12.24 | 12.75 |
| 0° | +32 | +21 | +14 | +20 | +13 | + 5 | + 4 | −2 |
| 10 | +17 | + 9 | + 5 | +16 | + 9 | +10 | + 5 | 0 |
| 20 | − 1 | − 5 | 0 | + 9 | + 7 | + 9 | + 3 | +6 |
| 30 | − 5 | + 2 | + 4 | + 8 | + 8 | + 9 | + 8 | +6 |
| 40 | − 8 | 0 | +11 | − 6 | − 2 | + 2 | + 7 | +6 |
| 50 | − 7 | + 1 | + 4 | −10 | − 6 | − 3 | + 2 | +3 |
| 60 | − 8 | − 6 | − 6 | −12 | − 8 | − 7 | − 5 | −3 |
| 70 | −10 | − 8 | −13 | −14 | −12 | −10 | −10 | −6 |
| 80 | − 9 | −11 | −21 | −15 | −12 | −12 | −13 | −6 |
| Rev. *m* | 10.74 | 12.34 | 13.16 | 8.62 | 10.05 | 11.50 | 12.27 | 12.78 |
| Sc.R. | 8.5 | 10.0 | 12.0 | 7.5 | 8.5 | 9.5 | 10.5 | 12.5 |
| *m*−*m′* | +0.29 | +0.28 | +0.28 | +0.08 | +0.05 | +0.13 | +0.10 | +0.14 |

| LAT. | BORDEAUX +15° | | | | BORDEAUX +14° | | | |
|---|---|---|---|---|---|---|---|---|
| | 9.66 | 11.23 | 12.15 | 12.66 | 9.99 | 11.43 | 12.43 | 12.92 |
| 0° | +2 | 0 | +5 | +8 | −1 | −21 | −26 | −42 |
| 10 | +5 | +2 | +3 | −1 | −8 | −17 | −23 | −30 |
| 20 | −2 | 0 | +1 | −1 | −4 | −12 | − 6 | −12 |
| 30 | −2 | +5 | +1 | −6 | +3 | + 4 | + 9 | + 9 |
| 40 | −5 | −2 | −2 | −3 | +1 | + 5 | +10 | +13 |
| 50 | −1 | −6 | +1 | −1 | +1 | + 5 | + 7 | +15 |
| 60 | 0 | −4 | −2 | 0 | +2 | + 7 | + 6 | +12 |
| 70 | +2 | −1 | −4 | 0 | +2 | +12 | + 9 | +15 |
| 80 | +3 | +3 | −1 | 0 | +2 | +18 | +15 | +17 |
| Rev. *m* | 9.66 | 11.26 | 12.18 | 12.66 | 10.00 | 11.50 | 12.49 | 12.99 |
| Sc.R. | 8.5 | 9.5 | 10.5 | 12.5 | 8.5 | 9.5 | 10.5 | 12.5 |
| *m*−*m′* | +0.03 | +0.09 | +0.10 | +0.12 | +0.08 | +0.02 | +0.05 | +0.03 |

| LAT. | TOULOUSE +9° | | | | ALGIERS −1° | | |
|---|---|---|---|---|---|---|---|
| | 8.92 | 10.28 | 11.38 | 12.55 | 9.21 | 11.39 | 12.94 |
| 0° | −49 | −37 | −26 | −16 | + 4 | −11 | −21 |
| 10 | −41 | −31 | −15 | −17 | − 1 | −14 | −23 |
| 20 | −15 | − 7 | − 8 | −11 | − 7 | −10 | −16 |
| 30 | + 5 | + 9 | + 6 | − 5 | − 6 | − 1 | + 2 |
| 40 | +17 | +19 | + 9 | + 1 | − 4 | + 7 | +12 |
| 50 | +27 | +19 | +12 | +12 | + 5 | +13 | +23 |
| 60 | +27 | +17 | +12 | +19 | +10 | +15 | +20 |
| 70 | +29 | +13 | +12 | +17 | ......... | ......... | ......... |
| Rev. *m* | 8.99 | 10.35 | 11.47 | 12.59 | 9.20 | 11.45 | 12.98 |
| Sc.R. | 8.5 | 9.5 | 11.0 | 12.3 | 7.9 | 9.9 | 11.9 |
| *m*−*m′* | −0.20 | −0.01 | +0.04 | +0.08 | +0.20 | +0.21 | +0.31 |

## TABLE I—*Continued*

| LAT. | SAN FERNANDO −3° | | | | SAN FERNANDO −4° | | | |
|---|---|---|---|---|---|---|---|---|
| | 10.16 | 11.62 | 12.74 | 13.27 | 10.00 | 11.43 | 12.59 | 13.04 |
| 0° | +17 | +27 | +15 | +6 | +22 | +21 | +8 | 0 |
| 10 | +5 | +10 | +6 | −1 | +11 | +17 | +11 | +5 |
| 20 | −7 | −3 | +3 | −4 | −3 | +4 | +16 | +11 |
| 30 | −6 | +1 | +4 | +5 | −11 | −3 | +15 | +8 |
| 40 | −9 | −6 | −1 | +6 | −11 | −8 | +7 | +13 |
| 50 | −1 | −4 | −2 | +1 | −1 | −5 | −7 | +4 |
| 60 | 0 | −11 | −8 | −3 | −2 | −9 | −18 | −15 |
| 70 | −2 | −18 | −17 | −8 | −8 | −18 | −30 | −25 |
| Rev. *m* | 10.15 | 11.62 | 12.73 | 13.25 | 9.98 | 11.45 | 12.60 | 13.04 |
| Sc.R. | 8.5 | 9.5 | 10.5 | All | 8.5 | 9.5 | 10.5 | All |
| *m*−*m′* | +0.16 | +0.25 | +0.24 | +0.24 | +0.25 | +0.22 | +0.29 | +0.37 |

| LAT. | SAN FERNANDO −5° | | | | SAN FERNANDO −6° | | | |
|---|---|---|---|---|---|---|---|---|
| | 10.02 | 11.41 | 12.51 | 13.06 | 10.04 | 11.33 | 12.28 | 12.87 |
| 0° | +26 | +25 | +19 | +1 | +19 | +10 | +9 | +1 |
| 10 | +12 | +14 | +18 | −6 | +8 | +10 | +14 | +7 |
| 20 | −2 | +1 | +11 | −3 | −4 | +8 | +15 | +11 |
| 30 | −10 | −4 | +5 | −2 | +2 | +5 | +10 | +6 |
| 40 | −8 | −11 | 0 | +3 | +2 | −2 | −2 | 0 |
| 50 | −2 | −8 | −8 | +7 | −5 | −7 | −10 | −1 |
| 60 | −6 | −10 | −19 | +1 | −9 | −10 | −17 | −7 |
| 70 | −13 | −10 | −28 | −3 | −13 | −10 | −22 | −17 |
| Rev. *m* | 9.99 | 11.42 | 12.50 | 13.05 | 10.04 | 11.36 | 12.29 | 12.88 |
| Sc.R. | 8.5 | 9.5 | 10.5 | All | 8.5 | 9.5 | 10.5 | All |
| *m*−*m′* | +0.22 | +0.25 | +0.28 | +0.25 | +0.25 | +0.30 | +0.28 | +0.26 |

| LAT. | TACUBAYA −15° | | | | TACUBAYA −16° | | | |
|---|---|---|---|---|---|---|---|---|
| | 10.03 | 11.27 | 12.47 | 13.27 | 9.94 | 11.29 | 12.45 | 13.23 |
| 0° | +22 | +16 | +13 | −4 | +37 | +26 | −6 | −38 |
| 10 | +15 | +12 | +11 | −8 | +27 | +20 | −1 | −9 |
| 20 | +1 | 0 | +6 | −6 | +17 | +13 | +4 | +3 |
| 30 | 0 | +2 | +3 | 0 | +7 | +11 | +13 | +15 |
| 40 | −5 | 0 | +1 | +4 | −2 | +1 | +17 | +22 |
| 50 | −7 | −2 | −2 | +11 | −11 | −3 | +15 | +15 |
| 60 | −11 | −10 | −10 | +4 | −20 | −11 | −1 | +5 |
| 70 | −15 | −18 | −18 | −3 | −27 | −23 | −15 | −6 |
| 80 | ........ | ........ | ........ | ........ | −32 | −31 | −24 | −10 |
| Rev. *m* | 10.02 | 11.28 | 12.48 | 13.26 | 9.90 | 11.29 | 12.48 | 13.27 |
| Sc.R. | 8.5 | 9.5 | 10.5 | 11.5 | 8.5 | 9.5 | 10.5 | 11.5 |
| *m*−*m′* | +0.14 | +0.13 | +0.09 | +0.10 | +0.22 | +0.24 | +0.15 | +0.13 |

| LAT. | HYDERABAD −17° | | | HYDERABAD −18° | | | | |
|---|---|---|---|---|---|---|---|---|
| | 9.53 | 12.16 | 13.38 | 9.57 | 11.48 | 12.18 | 12.84 | 13.38 |
| 0° | +13 | +13 | +3 | +24 | +53 | +30 | +35 | +8 |
| 10 | +8 | +17 | +13 | +28 | +44 | +45 | +39 | +28 |
| 20 | +1 | +15 | +18 | +19 | +28 | +45 | +39 | +34 |
| 30 | +4 | +11 | +11 | +4 | +11 | +23 | +20 | +17 |
| 40 | 0 | +2 | +4 | −5 | −6 | −1 | −2 | +1 |
| 50 | −1 | −3 | −1 | −13 | −17 | −20 | −17 | −13 |
| 60 | −4 | −9 | −9 | −16 | −29 | −32 | −29 | −21 |
| 70 | −6 | −17 | −14 | −20 | −38 | −40 | −39 | −26 |
| 80 | −11 | −26 | −21 | −20 | −44 | −46 | −43 | −31 |
| Rev. *m* | 9.52 | 12.17 | 13.34 | 9.54 | 11.44 | 12.17 | 12.81 | 13.34 |
| Sc.R. | 50 | 20 | 8 | 50 | 30 | 20 | 12 | 8 |
| *m*−*m′* | +0.11 | +0.30 | +0.19 | +0.09 | +0.26 | +0.28 | +0.30 | +0.25 |

TABLE I—*Continued*

| Lat. | Hyderabad −19° | | | | | Cordoba −25° | | | | |
|---|---|---|---|---|---|---|---|---|---|---|
| | 9.39 | 10.19 | 11.35 | 12.19 | 13.30 | 8.74 | 9.95 | 11.33 | 12.88 | 13.36 |
| 0° | +36 | +23 | +38 | +23 | +12 | +14 | −14 | −13 | +14 | +21 |
| 10 | +24 | +16 | +27 | +19 | + 7 | + 6 | −12 | −18 | 0 | +11 |
| 20 | + 3 | + 4 | +13 | +19 | +12 | − 6 | −10 | −16 | − 1 | + 5 |
| 30 | − 4 | + 3 | + 6 | +10 | +16 | − 8 | − 4 | − 4 | + 4 | + 4 |
| 40 | − 8 | − 2 | − 4 | + 1 | + 6 | − 8 | − 1 | + 6 | − 2 | − 1 |
| 50 | − 9 | − 4 | −11 | − 3 | + 1 | − 5 | + 2 | + 7 | − 3 | − 1 |
| 60 | −12 | − 7 | −18 | −16 | − 9 | − 2 | +10 | + 9 | − 3 | − 8 |
| 70 | −14 | −15 | −23 | −23 | −17 | + 2 | + 9 | + 9 | − 4 | −10 |
| 80 | −19 | −19 | −26 | −26 | −24 | + 2 | + 9 | + 7 | − 4 | −14 |
| 90 | ...... | ...... | ...... | ...... | ...... | + 4 | +10 | +13 | − 5 | − 8 |
| Rev. $m$ | 9.34 | 10.19 | 11.34 | 12.19 | 13.28 | 8.72 | 9.98 | 11.39 | 12.89 | 13.32 |
| Sc.R. | 50 | 40 | 30 | 20 | 8 | 41 | 31 | 21 | 11 | 1 |
| $m-m'$ | +0.17 | +0.17 | +0.16 | +0.22 | +0.22 | +0.05 | −0.02 | 0.00 | +0.05 | +0.08 |

| Lat. | Cordoba −27° | | | | | Cordoba −29° | | | |
|---|---|---|---|---|---|---|---|---|---|
| | 8.62 | 10.04 | 11.38 | 12.79 | 13.03 | 9.25 | 10.70 | 12.48 | 12.96 |
| 0° | 0 | −12 | −12 | − 9 | −10 | −21 | −29 | −6 | −8 |
| 10 | − 9 | −19 | −15 | −13 | −18 | −18 | −21 | +1 | −7 |
| 20 | −17 | −13 | − 2 | + 3 | + 3 | −10 | − 8 | −2 | −4 |
| 30 | 0 | +10 | +23 | +11 | +16 | − 9 | − 7 | −3 | +1 |
| 40 | + 3 | +10 | +16 | +11 | +18 | − 9 | − 6 | −5 | 0 |
| 50 | + 6 | +11 | +12 | +16 | +14 | + 3 | − 2 | −3 | +4 |
| 60 | + 9 | +12 | + 1 | + 5 | + 5 | +12 | + 7 | +4 | +7 |
| 70 | + 6 | + 5 | − 5 | − 4 | − 5 | +18 | +16 | +5 | +3 |
| 80 | + 2 | + 1 | − 7 | −10 | −12 | +19 | +22 | +1 | +3 |
| 90 | + 1 | − 2 | − 9 | −14 | −12 | +19 | +24 | +5 | +2 |
| Rev. $m$ | 8.62 | 10.07 | 11.44 | 12.83 | 13.06 | 9.27 | 10.74 | 12.50 | 12.99 |
| Sc.R. | 41 | 31 | 21 | 11 | 1 | 31 | 21 | 11 | 1 |
| $m-m'$ | −0.01 | −0.02 | +0.03 | +0.06 | +0.08 | −0.10 | −0.11 | −0.01 | −0.01 |

| Lat. | Cordoba −31° | | | | Perth −32° | | |
|---|---|---|---|---|---|---|---|
| | 9.15 | 10.58 | 12.51 | 13.21 | 10.35 | 11.88 | 13.11 |
| 0° | −35 | −32 | −23 | − 8 | − 8 | −24 | −24 |
| 10 | −22 | − 5 | − 7 | −14 | − 9 | −14 | −15 |
| 20 | + 4 | + 8 | + 2 | −18 | − 8 | −11 | − 5 |
| 30 | +26 | +17 | +12 | + 2 | + 6 | + 7 | + 7 |
| 40 | +22 | +16 | +21 | +17 | +17 | +17 | +15 |
| 50 | +15 | +15 | +15 | +22 | +15 | +22 | +22 |
| 60 | + 8 | + 5 | + 5 | +12 | + 5 | +14 | +13 |
| 70 | − 1 | − 2 | − 6 | − 1 | − 6 | + 2 | 0 |
| 80 | − 8 | − 9 | − 9 | − 8 | −15 | − 9 | −10 |
| 90 | −12 | −11 | −12 | − 9 | ......... | ......... | ......... |
| Rev. $m$ | 9.18 | 10.61 | 12.57 | 13.22 | 10.36 | 11.96 | 13.14 |
| Sc.R. | 31 | 21 | 11 | 1 | D | G | M |
| $m-m'$ | −0.06 | −0.18 | −0.11 | −0.02 | −0.05 | −0.11 | −0.10 |

| Lat. | Perth −34° | | | | | Perth −36° | | | | |
|---|---|---|---|---|---|---|---|---|---|---|
| | 8.84 | 10.12 | 11.38 | 12.51 | 13.19 | 9.38 | 10.62 | 11.76 | 12.76 | 13.53 |
| 0° | −41 | −28 | −28 | −26 | −32 | − 6 | − 4 | 0 | +15 | − 1 |
| 10 | −30 | −18 | −14 | −13 | −13 | + 7 | − 2 | +16 | +27 | +23 |
| 20 | −17 | −13 | − 5 | + 1 | + 4 | +12 | +15 | +18 | +24 | +20 |
| 30 | −12 | − 2 | − 3 | + 3 | − 3 | +16 | +22 | +17 | +18 | +21 |
| 40 | − 2 | + 2 | − 3 | − 2 | − 1 | + 8 | + 9 | + 9 | + 2 | +11 |
| 50 | + 9 | +10 | + 2 | + 1 | + 5 | + 2 | + 1 | − 2 | − 8 | − 1 |
| 60 | +15 | +11 | + 7 | + 4 | + 4 | − 6 | − 8 | −13 | −19 | −16 |
| 70 | +21 | +10 | +10 | + 5 | + 6 | −13 | −15 | −19 | −26 | −24 |
| 80 | +27 | +12 | +16 | +11 | +14 | −18 | −19 | −25 | −30 | −29 |
| 90 | +33 | +18 | +22 | +14 | +20 | ...... | ...... | ...... | ...... | ...... |
| Rev. $m$ | 8.89 | 10.16 | 11.45 | 12.56 | 13.23 | 9.38 | 10.64 | 11.80 | 12.76 | 13.52 |
| Sc.R. | B | D | F | H | M | B | D | F | H | M |
| $m-m'$ | −0.21 | −0.10 | −0.09 | −0.05 | −0.07 | +0.01 | +0.06 | +0.09 | +0.10 | +0.12 |

TABLE I—*Continued*

| LAT. | PERTH-EDINBURGH −38° | | | | | CAPE −41° | | | |
|---|---|---|---|---|---|---|---|---|---|
| | 9.32 | 10.04 | 11.33 | 12.89 | 13.56 | 10.75 | 11.66 | 12.85 | 13.48 |
| 0° | −10 | − 7 | − 5 | + 9 | + 2 | +13 | − 6 | − 9 | −11 |
| 10 | − 3 | + 4 | +11 | + 8 | +11 | +12 | − 2 | −11 | − 9 |
| 20 | + 6 | + 9 | +16 | + 6 | + 7 | +11 | − 5 | −10 | − 9 |
| 30 | +17 | +17 | +14 | +12 | + 7 | +12 | + 4 | − 2 | + 2 |
| 40 | + 6 | + 7 | + 2 | + 9 | + 2 | + 4 | +11 | + 8 | +11 |
| 50 | 0 | + 1 | − 3 | + 3 | + 2 | − 2 | +11 | +21 | +14 |
| 60 | − 2 | − 6 | − 6 | − 9 | − 6 | − 8 | + 4 | +13 | +10 |
| 70 | − 5 | −12 | −12 | −16 | −12 | −18 | − 5 | − 2 | − 1 |
| 80 | − 9 | −15 | −17 | −20 | −16 | −25 | −10 | −12 | − 8 |
| Rev. *m* | 9.32 | 10.07 | 11.37 | 12.89 | 13.52 | 10.74 | 11.72 | 12.88 | 13.47 |
| Sc.R. | 40 | 30 | 20 | 10 | All | 130 | 100 | −3 | −5 |
| *m*−*m*′ | −0.05 | −0.02 | +0.07 | +0.03 | +0.03 | −0.06 | −0.17 | −0.13 | −0.07 |

| LAT. | CAPE −42° | | | | CAPE −43° | | | |
|---|---|---|---|---|---|---|---|---|
| | 9.49 | 11.80 | 12.49 | 13.57 | 9.57 | 11.76 | 12.45 | 13.54 |
| 0° | + 6 | 0 | + 2 | + 5 | − 1 | 0 | − 6 | − 2 |
| 10 | − 1 | −13 | − 6 | −11 | − 4 | − 8 | −16 | −10 |
| 20 | − 5 | −22 | −21 | −30 | −11 | −20 | −24 | −23 |
| 30 | −16 | −19 | −21 | −25 | − 5 | −16 | −16 | −22 |
| 40 | − 8 | − 7 | −13 | −11 | 0 | − 7 | − 5 | − 8 |
| 50 | + 2 | + 6 | + 4 | + 9 | + 6 | +11 | +11 | +13 |
| 60 | + 7 | +14 | +11 | +13 | + 6 | +12 | +19 | +20 |
| 70 | + 9 | +17 | +17 | +24 | + 5 | +14 | +20 | +15 |
| 80 | + 7 | +23 | +26 | +23 | + 6 | +12 | +20 | +17 |
| Rev. *m* | 9.48 | 11.85 | 12.51 | 13.53 | 9.59 | 11.80 | 12.48 | 13.51 |
| Sc.R. | 200 | 100 | 60 | −5 | 200 | 100 | 60 | −5 |
| *m*−*m*′ | −0.11 | −0.06 | −0.08 | −0.20 | −0.07 | −0.07 | −0.03 | −0.07 |

| LAT. | MELBOURNE −65° | | | | | |
|---|---|---|---|---|---|---|
| | ............ | ............ | ............ | 11.00 | ............ | 13.02 |
| 0° | −10 | −17 | − 1 | −20 | − 7 | −18 |
| 10 | −13 | −19 | −15 | −20 | −11 | −25 |
| 20 | −12 | −15 | − 8 | − 6 | − 6 | −23 |
| 30 | − 3 | − 8 | − 3 | + 5 | + 3 | − 1 |
| 40 | + 4 | + 7 | + 2 | +14 | + 3 | +18 |
| 50 | +15 | +23 | +11 | +15 | +11 | +28 |
| 60 | +18 | +26 | +15 | +13 | + 5 | +22 |
| Rev. *m* | 8.97 | 9.47 | 9.90 | 11.06 | 12.29 | 13.06 |
| Sc.R. | 31 | 26 | 21 | 16 | 11 | All |
| *m*−*m*′ | −0.30 | −0.27 | −0.32 | −0.16 | −0.21 | −0.30 |

## NOTES TO TABLE I

*Oxford:* Published limits for scale-readings of zones +31° to +29° and +27° to +25° increased one unit. *Monthly Notices*, **85**, 473.

*Toulouse:* For $0^h-6^h$ a scale of quarter-magnitudes was used, the record being to the nearest tenth; for $7^h-23^h$, a scale of tenths, extending to 13.3. *Ibid.*, **76**, 149. Scale-readings below 12.3 have not been used. For the same scale-reading values of log $N_m$ in the first quadrant are systematically lower than elsewhere by about 0.15. The corresponding values of *m* are about 0.35 mag. less than the tabulated limits, which refer to the interval $7^h-23^h$.

*Algiers:* Published limits reduced 0.1. *Ibid.*, **72**, 701.

*Cordoba:* The diameters of 58 stars at −25° have not been measured, being too faint or too large. *Ibid.*, **78**, 58. The inference from the text is that these stars are not included in the totals. If so, the value of *m* for Sc.R. 51 (See Table IV) is appreciably affected—the other magnitude limits to a much less extent. For zones −27°, −29°, −31°, the published limits for scale-readings have been increased by one unit (*ibid.*, **81**, 528) and "All" is assumed to correspond to Sc.R. 1, as for −25°.

*Cape:* Scale-readings for zones −42° and −43° assigned in accordance with the identification in *ibid.*, **79**, 567.

*Melbourne:* Published limits for scale-reading increased by one unit. *Ibid.*, **77**, 39.

Values of log $N_m$ for latitude 0° were not used in deriving provisional magnitudes because of the relatively large uncertainty affecting van Rhijn's distribution table in low latitudes. This objection does not hold in the case of the revised distribution table—at least not for the interval of brightness covered by the astrographic zones—and all available densities have accordingly been used. In general, the results of the reinterpolation are in close agreement with the provisional values found from van Rhijn's table. The largest difference is 0.09 mag.; the average, without regard to sign, 0.027; and the systematic difference, 0.01 mag.

Counts for six of the seven Oxford zones were published[1] after the reductions for *Contribution* No. 301 had been finished. Mean densities for these zones are collected in Table II, which also gives densities corresponding to four additional scale-readings of the Melbourne zone, −65°, necessary to complete the calibration. Provisional magnitudes were not derived, and the values in Table II are based on the revised distribution table.

The scale-readings in Table I, and indeed throughout the present discussion, are inclusive limiting values; the corresponding densities depend on counts which include all stars having a brightness equal to and greater than that represented by the scale-reading in question. This accounts for certain modifications of published values of the limits of the original counts referred to in the notes to Table I. The magnitudes therefore correspond to the faintest stars to which the respective scale-readings are assigned. Since the interval of brightness covered by the smallest step in scale-reading is sometimes half a magnitude or more, this point must be borne in mind in using the adopted calibration in Table IV.

The residuals in Table I are generally systematic, usually most noticeably so in the case of the brighter stars. This indicates a systematic departure, depending on latitude, of the mean zone-densities from the mean distribution for the whole sky. An extreme case is presented by Hyderabad, −18°; other zones, such as Bordeaux, +15°, are singularly free from such deviations, and systematic differences must be confined to relatively small areas within the zones.

---

[1] Complete references to the data used in the present discussion are given in Table XIII, *Contribution* No. 301.

The reliability and usefulness of the magnitudes is obviously greatest for those cases in which the residuals are small; but, even where there is a marked progression in the residuals, the mean magnitude is still a useful result, in spite of the fact that the uncertainty attached to the brightness of individual stars is correspondingly increased. Moreover, the systematic uncertainty may be less than would be inferred from the run in the residuals. It is assumed that within any zone a given scale-reading corresponds always to the same magnitude; but there are many departures from this ideal state of affairs. Differences in plates, development, and atmospheric conditions; seasonal fluctuations and subjective errors of measurement—all enter as disturbing factors, some of them accidentally, others systematically. Results from individual plates may be seriously

### TABLE II

SUPPLEMENTARY VALUES OF LOG $N_m$

| $m$ | Zone | 0° | 10° | 20° | 30° | 40° | 50° | 60° | 70° | 80° | 90° |
|---|---|---|---|---|---|---|---|---|---|---|---|
| 9.59.... | +31° | 0.62 | 0.55 | 0.44 | 0.34 | 0.28 | 0.25 | 0.21 | 0.18 | 0.15 | 0.15 |
| 10.72.... | +31 | 1.12 | 1.04 | 0.92 | 0.81 | 0.73 | 0.69 | 0.67 | 0.64 | 0.60 | 0.58 |
| 11.89.... | +31 | 1.62 | 1.54 | 1.41 | 1.29 | 1.18 | 1.12 | 1.08 | 1.06 | 1.04 | 1.01 |
| 12.89.... | +31 | 1.97 | 1.90 | 1.77 | 1.64 | 1.55 | 1.50 | 1.47 | 1.45 | 1.40 | 1.38 |
| 13.48.... | +31 | 2.22 | 2.14 | 2.00 | 1.86 | 1.76 | 1.68 | 1.66 | 1.63 | 1.60 | 1.58 |
| 9.76.... | +30 | 0.66 | 0.61 | 0.50 | 0.41 | 0.35 | 0.31 | 0.28 | 0.27 | 0.25 | 0.25 |
| 10.85.... | +30 | 1.16 | 1.11 | 1.02 | 0.92 | 0.83 | 0.76 | 0.70 | 0.64 | 0.60 | 0.58 |
| 12.09.... | +30 | 1.69 | 1.64 | 1.53 | 1.40 | 1.28 | 1.20 | 1.14 | 1.12 | 1.07 | 1.05 |
| 12.92.... | +30 | 1.98 | 1.93 | 1.83 | 1.71 | 1.60 | 1.52 | 1.46 | 1.41 | 1.37 | 1.35 |
| 13.70.... | +30 | 2.37 | 2.28 | 2.14 | 1.98 | 1.86 | 1.77 | 1.70 | 1.65 | 1.61 | 1.59 |
| 9.36.... | +29 | 0.48 | 0.44 | 0.36 | 0.28 | 0.23 | 0.15 | 0.12 | 0.09 | 0.06 | 0.04 |
| 10.28.... | +29 | 0.86 | 0.81 | 0.74 | 0.66 | 0.61 | 0.54 | 0.50 | 0.46 | 0.43 | 0.42 |
| 11.50.... | +29 | 1.39 | 1.32 | 1.23 | 1.15 | 1.09 | 1.04 | 0.99 | 0.92 | 0.88 | 0.85 |
| 12.52.... | +29 | 1.79 | 1.72 | 1.62 | 1.53 | 1.44 | 1.38 | 1.33 | 1.30 | 1.28 | 1.27 |
| 13.55.... | +29 | 2.27 | 2.20 | 2.04 | 1.90 | 1.80 | 1.73 | 1.67 | 1.63 | 1.58 | 1.57 |
| 9.20.... | +27 | 0.50 | 0.42 | 0.31 | 0.19 | 0.09 | 0.05 | 0.03 | 0.01 | 0.00 | 9.98 |
| 10.12.... | +27 | 0.84 | 0.79 | 0.70 | 0.58 | 0.48 | 0.42 | 0.39 | 0.38 | 0.39 | 0.39 |
| 11.35.... | +27 | 1.36 | 1.28 | 1.17 | 1.06 | 0.97 | 0.94 | 0.90 | 0.89 | 0.86 | 0.84 |
| 12.25.... | +27 | 1.75 | 1.67 | 1.56 | 1.44 | 1.33 | 1.25 | 1.20 | 1.19 | 1.17 | 1.16 |
| 13.28.... | +27 | 2.17 | 2.10 | 1.98 | 1.84 | 1.69 | 1.59 | 1.55 | 1.53 | 1.51 | 1.50 |
| 9.31.... | +26 | 0.57 | 0.48 | 0.35 | 0.24 | 0.16 | 0.08 | 0.05 | 0.03 | 0.03 | 0.03 |
| 10.33.... | +26 | 0.99 | 0.92 | 0.81 | 0.66 | 0.54 | 0.48 | 0.46 | 0.45 | 0.46 | 0.46 |
| 11.58.... | +26 | 1.51 | 1.43 | 1.30 | 1.15 | 1.02 | 0.98 | 0.97 | 0.95 | 0.94 | 0.93 |
| 12.54.... | +26 | 1.90 | 1.83 | 1.67 | 1.52 | 1.39 | 1.32 | 1.31 | 1.30 | 1.27 | 1.27 |
| 13.48.... | +26 | 2.24 | 2.19 | 2.08 | 1.92 | 1.76 | 1.68 | 1.64 | 1.57 | 1.55 | 1.54 |
| 9.58.... | +25 | 0.56 | 0.52 | 0.44 | 0.35 | 0.27 | 0.24 | 0.22 | 0.20 | 0.18 | 0.16 |
| 10.63.... | +25 | 1.06 | 0.99 | 0.87 | 0.76 | 0.67 | 0.64 | 0.63 | 0.62 | 0.60 | 0.58 |
| 11.90.... | +25 | 1.58 | 1.53 | 1.44 | 1.34 | 1.20 | 1.12 | 1.08 | 1.05 | 1.03 | 1.00 |
| 12.73.... | +25 | 1.97 | 1.91 | 1.80 | 1.65 | 1.49 | 1.39 | 1.35 | 1.33 | 1.31 | 1.28 |
| 13.53.... | +25 | 2.28 | 2.22 | 2.09 | 1.92 | 1.77 | 1.69 | 1.65 | 1.61 | 1.57 | 1.54 |
| 8.97.... | −65 | 0.48 | 0.40 | 0.26 | 0.12 | 0.00 | 9.90 | 9.85 | ....... | ....... | ....... |
| 9.47.... | −65 | 0.73 | 0.64 | 0.49 | 0.35 | 0.20 | 0.09 | 0.03 | ....... | ....... | ....... |
| 9.90.... | −65 | 0.85 | 0.81 | 0.64 | 0.51 | 0.40 | 0.31 | 0.25 | ....... | ....... | ....... |
| 12.29.... | −65 | 1.90 | 1.79 | 1.61 | 1.46 | 1.35 | 1.25 | 1.19 | ....... | ....... | ....... |

affected; but the formation of means for groups of several plates per hour of right ascension (one hour is the unit interval for grouping the counts) eliminates, or at least minimizes, many of the deviations. Seasonal effects and subjective factors of measurement may remain, however, as persistent systematic disturbances affecting the constancy of the magnitude associated with a given scale-reading; and it is natural to attribute to these sources much of the progression shown by the residuals of Table I.

But it must be noted that at least two other circumstances may contribute to the progression in the residuals: large-scale irregularities in the distribution of the stars and errors in drawing the curves which define log $N_m$ as a function of galactic latitude. The co-ordinates of the centers of the unit areas used for grouping the counts are functions of galactic longitude as well as of latitude. The average effect of galactic concentration has been removed by comparing the observed densities with the mean distribution table; but any systematic deviation in longitude remains in the residuals and may produce an important progressive effect. Further, any tilt of the curve of mean density (as a function of latitude) from its true position operates in the same way. Neither of these, however, affects the adopted relation between scale-reading and magnitude except as it appears in the mean magnitude for the whole zone, where both disturbances are at least partially compensated.

In certain cases the determination of the curve of mean density against latitude presented exceptional difficulty.[1] Thus in the Oxford zones, $+25°$ to $+31°$, the interval $3^h$ to $6^h$ of right ascension includes the extensive obscured area in Taurus;[2] the observed densities in this region for each magnitude of every zone are abnormally low, and the systematic effect can be traced through the Paris zones, $+23°$ and $+22°$, down into those of Bordeaux, $+17°$ to $+14°$. Again, the Algiers and San Fernando zones, $-1°$ to $-6°$, show approximately constant densities between $12^h$ and $18^h$ of right ascension, although the range in galactic latitude is $50°$ or more. The contrast with the other quadrants of right ascension, which extend over similar intervals in latitude, is striking, and there seems little doubt that the abnormal distribution here is also real. As far as possible, regions of known obscuration were ignored in drawing the mean curves, on the assumption that the removal of the obscuring clouds would reveal a normal distribution of stars. Several instances of this kind are mentioned in the notes following Table XIII of *Contribution* No. 301. It will be the purpose of a later contribution to attempt a separation of these and other real deviations from systematic irregularities which are observational in origin.

---

[1] For an illustration of typical curves, see Fig. 1, *Contribution* No. 135, *Astrophysical Journal*, **46**, 117, 1917. The curve for the Algiers zone and several others used for *Contribution* No. 135 were redrawn in deriving the mean distribution table in *Contribution* No. 301.

[2] Dyson and Melotte, *Monthly Notices*, **80**, 3, 1919.

The results in Table I include only part of the scale-readings for which counts are available. The calibration could have been completed by the method already used; but a shorter way, which has also the advantage of providing a means of reducing the accidental errors affecting the values already found, is to compare mean densities for entire zones to successive limits of scale-reading with the fifth column of Table XVIII in *Contribution* No. 301, which gives the adopted mean distribution for all latitudes together. Magnitudes found in this way require, however, a small correction because, to a given limit of brightness, the mean density of the stars within a narrow zone in declination is not the same as the mean for the whole sky. The correction, which varies with the declination of the zone, is easily calculated by deriving magnitudes as just suggested for the scale-readings already used and comparing the results with the revised values given in Table I. The quantities $m-m'$ in the last line of this table are the differences in question for these scale-readings.

The procedure is illustrated by the details for the Vatican zones shown in Table III. The total number of stars in the zone to each limiting value of the scale-reading, given in the line opposite $N$, is taken from the bottom of Table I, *Monthly Notices*, **75**, 602. The number of plates is ten per hour,[1] each having a field of $4\times169/144$ square degrees. To reduce the totals to stars per square degree, we have, therefore, the relation.

$$\log N_m = \log N - 3.0518.$$

---

[1] *Loc. cit.*, p. 603; or, more conveniently, see Table XIII, *Contribution* No. 301.

The values of the density thus found were used to interpolate the approximate magnitudes $m'$ from the fifth column of Table XVIII, *Contribution* No. 301. These differ systematically from the values of $m$ given in Table I by the quantities $m-m'$, which are the basis for the correction of $m'$.

The mean values of $m-m'$ vary with the declination and with other circumstances peculiar to the individual zones, such, for example, as the fact that, although regions of known obscuration were ignored in drawing the density-latitude curves used in deriving the values of $m$, the deficiency of stars in these regions, by affecting the totals $N$, enters directly into $m'$. Consequently, the corrections to $m'$ for any zone must be based primarily on the mean $m-m'$ for that zone.

TABLE III

Final Reduction for Vatican Zones

| Sc.R. | 50 | 40 | 30 | 20 | 10 | 0 |
|---|---|---|---|---|---|---|
| $N$ | 887 | 2201 | 6139 | 16750 | 50283 | 88782 |
| log $N_m$ | 9.896 | 0.291 | 0.736 | 1.172 | 1.650 | 1.896 |
| $m'$ | 8.35 | 9.26 | 10.31 | 11.37 | 12.57 | 13.20 |
| $m$ | .......... | 8.87 | 10.08 | 11.15 | 12.35 | 12.98 |
| $m-m'$ | .......... | −0.39 | −0.23 | −0.22 | −0.22 | −0.22 |
| Corrections | −0.33 | −0.31 | −0.28 | −0.25 | −0.24 | −0.24 |
| Adopted $m$ | 8.02 | 8.91 | 10.06 | 11.14 | 12.34 | 12.97 |

Further, some variation in $m-m'$ with brightness is also to be expected. This was investigated by forming the deviations of the values of $m-m'$ given in Table I from the means for the separate zones and arranging the results according to brightness for groups of zones covering a moderate range in declination. Within the precision of the data, the variation in $m-m'$ thus found is independent of declination, and is represented by the following mean values:

| | | | | | | |
|---|---|---|---|---|---|---|
| $m'$ | 8 | 9 | 10 | 11 | 12 | 13 |
| Var. in $m-m'$ | −0.08 | −0.05 | $-0.02^{5}$ | 0.00 | +0.02 | +0.02 |

The adopted correction to any $m'$ has therefore the form

$$\text{Mean } m-m'+\text{Variation in } m-m' \, .$$

Thus for the Vatican zones, the mean $m-m'$ is −0.26. For scale-reading 50, $m'=8.35$, and from the foregoing tabulation the varia-

## TABLE IV

### International Photographic Magnitudes for Astrographic Zones

VATICAN

| Sc.R. | 50 | 40 | 30 | 20 | 10 | 0 |
|---|---|---|---|---|---|---|
| +62°........ | 8.02 | 8.91 | 10.06 | 11.14 | 12.34 | 12.97 |

OXFORD

| Sc.R. | 45 | 35 | 26 | 18 | 12 | All |
|---|---|---|---|---|---|---|
| +31°........ | 8.43 | 9.60 | 10.70 | 11.90 | 12.89 | 13.48 |
| +30........ | 8.66 | 9.79 | 10.86 | 12.06 | 12.92 | 13.69 |
| +29........ | 8.30 | 9.39 | 10.32 | 11.52 | 12.48 | 13.51 |
| +27........ | 8.24 | 9.20 | 10.13 | 11.35 | 12.24 | 13.28 |
| +26........ | 8.25 | 9.32 | 10.34 | 11.56 | 12.52 | 13.48 |
| +25........ | 8.49 | 9.56 | 10.63 | 11.89 | 12.77 | 13.52 |

| Sc.R. | 50 | 40 | 30 | 18 | 12 | 9 |
|---|---|---|---|---|---|---|
| +28°........ | 7.95 | 8.99 | 10.05 | 11.57 | 12.43 | 13.08 |

| Sc.R. | 7 | 5 | 3 | All | .......... | .......... |
|---|---|---|---|---|---|---|
| +28°........ | 13.31 | 13.49 | 13.55 | 13.62 | .......... | .......... |

PARIS

| Sc.R. | 8.0 | 8.5 | 9.0 | 9.5 | 10.0 | 10.5 |
|---|---|---|---|---|---|---|
| +23°........ | 9.14 | 9.72 | 10.39 | 11.05 | 11.72 | 12.30 |
| +22........ | 9.20 | 9.72 | 10.35 | 10.97 | 11.70 | 12.27 |

| Sc.R. | 11.0 | 11.5 | All | .......... | .......... | .......... |
|---|---|---|---|---|---|---|
| +23°........ | 12.80 | 13.14 | 13.34 | .......... | .......... | .......... |
| +22........ | 12.79 | 13.17 | 13.42 | .......... | .......... | .......... |

BORDEAUX

| Sc.R. | 6.5 | 7.0 | 7.5 | 8.0 | 8.5 | 9.0 |
|---|---|---|---|---|---|---|
| +17°........ | 8.05 | 8.73 | 9.35 | 10.07 | 10.72 | 11.41 |
| +16........ | 7.18 | .......... | 8.60 | .......... | 10.06 | .......... |
| +15........ | 6.43 | .......... | 7.78 | .......... | 9.66 | .......... |
| +14........ | 6.89 | .......... | 8.13 | .......... | 9.96 | .......... |

TABLE IV, BORDEAUX—*Continued*

| Sc.R. | 9.5 | 10.0 | 10.5 | 11.0 | 11.5 | 12.5 |
|---|---|---|---|---|---|---|
| +17°........ | 11.91 | 12.35 | 12.65 | 12.93 | 13.13 | 13.17* |
| +16........ | 11.49 | .......... | 12.28 | .......... | 12.70 | 12.77 |
| +15........ | 11.26 | .......... | 12.18 | .......... | 12.61 | 12.65 |
| +14........ | 11.52 | .......... | 12.50 | .......... | 12.99 | 13.00 |

* This value corresponds to Sc.R. 12.0.

TOULOUSE

| Sc.R. | 8.0 | 8.5 | 9.0 | 9.5 | 10.0 | 10.5 |
|---|---|---|---|---|---|---|
| +9°......... | 8.63 | 9.06 | 9.71 | 10.34 | 10.69 | 11.05 |

| Sc.R. | 11.0 | 11.5 | 12.0 | 12.3 | .......... | .......... |
|---|---|---|---|---|---|---|
| +9°......... | 11.44 | 11.81 | 12.19 | 12.55 | .......... | .......... |

ALGIERS

| Sc.R. | 6.9 | 7.9 | 8.9 | 9.9 | 10.9 | 11.9 |
|---|---|---|---|---|---|---|
| −1°......... | 8.12 | 9.20 | 10.92 | 11.47 | 12.37 | 12.96 |

SAN FERNANDO

| Sc.R. | 8.0 | 8.5 | 9.0 | 9.5 | 10.0 | 10.5 |
|---|---|---|---|---|---|---|
| −3°......... | 9.43 | 10.16 | 10.91 | 11.61 | 12.22 | 12.73 |
| −4......... | 9.14 | 9.98 | 10.76 | 11.48 | 12.16 | 12.60 |
| −5......... | 9.19 | 9.99 | 10.73 | 11.42 | 12.03 | 12.50 |
| −6......... | 9.30 | 10.04 | 10.70 | 11.34 | 11.87 | 12.30 |

| Sc.R. | 11.0 | 11.5 | All | .......... | .......... | .......... |
|---|---|---|---|---|---|---|
| −3°......... | 13.04 | 13.21 | 13.25 | .......... | .......... | .......... |
| −4......... | 12.84 | 12.96 | 13.00 | .......... | .......... | .......... |
| −5......... | 12.77 | 12.99 | 13.06 | .......... | .......... | .......... |
| −6......... | 12.60 | 12.83 | 12.90 | .......... | .......... | .......... |

TACUBAYA

| Sc.R. | 8.0 | 8.5 | 9.0 | 9.5 | 10.0 | 10.5 |
|---|---|---|---|---|---|---|
| −15°........ | 9.28 | 10.00 | 10.66 | 11.28 | 11.94 | 12.50 |
| −16........ | 9.11 | 9.86 | 10.51 | 11.26 | 11.88 | 12.50 |

## TABLE IV, TACUBAYA—*Continued*

| Sc.R. | 11.0 | 11.5 | .......... | .......... | .......... | .......... |
|---|---|---|---|---|---|---|
| −15°........ | 12.97 | 13.28 | .......... | .......... | .......... | .......... |
| −16........ | 13.06 | 13.30 | .......... | .......... | .......... | .......... |

HYDERABAD

| Sc.R. | 50 | 40 | 30 | 20 | 12 | 8 |
|---|---|---|---|---|---|---|
| −17°........ | 9.54 | .......... | 11.31 | 12.13 | 12.75 | 13.36 |
| −18........ | 9.60 | .......... | 11.43 | 12.16 | 12.79 | 13.34 |
| −19........ | 9.32 | 10.18 | 11.36 | 12.18 | 12.90 | 13.28 |

CORDOBA

| Sc.R. | 51 | 41 | 31 | 21 | 11 | 1 |
|---|---|---|---|---|---|---|
| −25°........ | 7.36 | 8.68 | 9.99 | 11.41 | 12.89 | 13.30 |
| −27........ | 7.43 | 8.61 | 10.08 | 11.44 | 12.82 | 13.04 |
| −29........ | 6.73 | 7.83 | 9.27 | 10.76 | 12.48 | 12.98 |
| −31........ | 6.53 | 7.58 | 9.14 | 10.65 | 12.59 | 13.20 |

PERTH

| Sc.R. | A | B | C | D | E | F |
|---|---|---|---|---|---|---|
| −32°........ | 8.63 | 9.20 | 9.83 | 10.33 | 10.89 | 11.46 |
| −34........ | 8.49 | 8.92 | 9.50 | 10.15 | 10.89 | 11.45 |
| −36........ | 8.92 | 9.40 | 10.03 | 10.64 | 11.31 | 11.80 |

| Sc.R. | G | H | J | K | L | M |
|---|---|---|---|---|---|---|
| −32°........ | 11.98 | 12.45 | 12.81 | 13.05 | 13.16 | 13.16 |
| −34........ | 12.06 | 12.54 | 12.87 | .......... | .......... | 13.22 |
| −36........ | 12.36 | 12.76 | 13.08 | .......... | .......... | 13.51 |

PERTH-EDINBURGH

| Sc.R. | 50 | 40 | 30 | 20 | 10 | All |
|---|---|---|---|---|---|---|
| −38°........ | 8.30 | 9.33 | 10.08 | 11.34 | 12.89 | 13.52 |

CAPE

| Sc.R. | 300 | 200 | 170 | 150 | 130 | 110 |
|---|---|---|---|---|---|---|
| −41°........ | .......... | 9.60 | 9.94 | 10.22 | 10.71 | 11.33 |
| −42........ | 7.88 | 9.46 | .......... | .......... | .......... | .......... |
| −43........ | 7.98 | 9.58 | .......... | .......... | .......... | .......... |

TABLE IV, CAPE—*Continued*

| Sc.R. | 100 | 80 | 60 | −1 | −2 | −5 |
|---|---|---|---|---|---|---|
| −41° | 11.76 | 12.14 | 12.38 | 12.52 | 12.69 | 13.46* |
| −42 | 11.84 | ... | 12.50 | ... | ... | 13.58 |
| −43 | 11.82 | ... | 12.48 | ... | ... | 13.52 |

* Additional values for −41°: −3, 12.90; −4, 13.16.

MELBOURNE

| Sc.R. | 41 | 36 | 31 | 26 | 21 | 16 |
|---|---|---|---|---|---|---|
| −65° | 7.90 | 8.50 | 8.96 | 9.46 | 9.92 | 11.01 |

| Sc.R. | 11 | All | ... | ... | ... | ... |
|---|---|---|---|---|---|---|
| −65° | 12.28 | 13.09 | ... | ... | ... | ... |

## NOTES TO TABLE IV

The magnitudes listed in Table IV refer to the faintest stars to which the respective scale-readings have been assigned. The average magnitude corresponding to any scale-reading is brighter than the tabular value by approximately one-half the magnitude interval covered by the step in scale-reading.

*Vatican:* Results are mean values for zones +64°, +62°, and +60°.

*Bordeaux:* Difference in scales especially noticeable for +17°. See *Monthly Notices*, **79**, 140.

*Toulouse:* See note to Table I.

*Algiers:* The large irregularity in the scale has been discussed by Turner, *ibid.*, **72**, 701.

*Melbourne:* The images were measured on three different machines, for one of which there is an important systematic difference. See *ibid.*, **77**, 36.

tion in $m-m'$ is −0.07, which gives a total correction of −0.33 and an adopted limiting magnitude of 8.02. For those cases in which a value of $m$ is available from Table I, the adopted magnitude is the mean of $m$ and the corrected $m'$. The agreement in the pairs of values thus found is excellent, the mean difference being ±0.04 mag. The use of means tends to smooth out accidental errors in $m$ arising from uncertainty in drawing the density-latitude curves, which may be systematically too high or too low. The final results in the last lines of Table III appear in Table IV along with those for the other zones, which were all treated by the method outlined.

In using Table IV it is important to bear in mind a point already mentioned, namely, that the magnitudes refer to the faintest stars included among those to which the corresponding scale-reading has been assigned. A more useful tabulation of results would have been one giving average values of the magnitude corresponding to the respective scale-readings. These differ from the values appearing in Table IV by approximately one-half the magnitude interval corresponding to the smallest interval of scale-reading used to express the brightness of the stars. The step in scale-reading differs from zone to zone, and since the actual values were not always available, the results are necessarily presented as in Table IV.

It is also to be noted that Table IV pretends to be nothing more than an average calibration of the respective scales. Nevertheless, the residuals in Table I show that in many instances this calibration is directly applicable to small parts of a zone. Further, it should be recalled that, even when the residuals of Table I are systematic, the average calibration may be better than the residuals indicate, for large-scale irregularities in stellar distribution and certain errors involved in the method of reduction contribute to the progressive character of the residuals. Magnitudes for individual stars derived with the aid of Table IV, for obvious reasons, will be subject to a relatively large uncertainty.

MOUNT WILSON OBSERVATORY
October 1925

Contributions from the Mount Wilson Observatory, No. 306
Reprinted from the *Astrophysical Journal*, Vol. LXIII, pp. 13–19, 1926
Printed in the U.S.A.

# NOTES ON LINES IN THE SPECTRA OF RED STARS

By PAUL W. MERRILL

## ABSTRACT

*Lines of various elements in stellar spectra of classes M, N, and S.*—The behavior of lines of *H*, *He*, *Li*, *Na*, *K*, *Mg*, *Ca*, *Sr*, *Ba*, *Al*, *Ti*, *Zr*, *V*, *Cr*, *Mn*, and *Fe* is described, especial attention being paid to the series classification of the lines and their relative intensities in the various spectral types.

The rising interest in the chemical and physical problems of stellar atmospheres makes desirable the compilation of detailed data concerning stellar spectra in a form adapted for convenient reference. Professor Russell has prepared the way for this by publishing a classified list of spectral lines of astrophysical interest.[1] The purpose of the present paper is to describe lines of various chemical elements in the spectra of stars near the low-temperature end of the stellar sequence. The data refer chiefly to giant variable stars of classes M, N, and S.

A few introductory remarks will aid in the interpretation of the data which follow. In the first place, it is to be remembered that the dispersion with which spectrograms of red stars have been obtained is very small compared to that used in laboratory and solar research. This means that very accurate determinations of wavelength cannot be made; that faint lines cannot be observed; and that difficulties caused by the blending of neighboring lines will be numerous and troublesome.

The spectral region which has been extensively observed is limited to a few hundred angstrom units. The region most adequately studied lies between λ 4100 and λ 4500. At shorter wave-lengths the rapid drop in the spectral intensity-curve results in underexposed spectrograms, which rarely extend to the calcium line K (λ 3933). At wave-lengths longer than λ 4500, and especially beyond λ 4900, the observations are not so numerous, the prismatic dispersion is decidedly smaller, and the strong bands greatly interfere with the recognition and identification of lines. In attempting the present compilation the writer has been much impressed by the incompleteness of the data, especially outside the spectral limits λ 4100 to λ 4900. This is caused partly by inherent difficulties and partly by lack of adequate observations. A comparison of our knowledge of lines in stellar spectra with Russell's lists and other laboratory data will suggest numerous definite problems, many of which would readily yield to systematic observation.

---

[1] *Mt. Wilson Contr.*, No. 286; *Astrophysical Journal*, 61, 223, 1925.

TABLE I

CHARACTERISTIC INTENSITIES OF BRIGHT HYDROGEN LINES IN VARIABLE STARS AT MAXIMUM LIGHT

| | Class M | Class S | Class N |
|---|---|---|---|
| $H\alpha$ 6563 | 2 | 15 | 10 |
| $H\beta$ 4861 | 2 | 12 | 10 |
| $H\gamma$ 4340 | 20 | 5 | 5 |
| $H\delta$ 4102 | 30 | 3 | 2 |
| $H\epsilon$ 3970 | 2 | ........... | ........... |
| $H\zeta$ 3889 | 15 | 1 | Trace |
| $H\eta$ 3835 | 8 | ........... | ........... |
| $H\theta$ 3798 | 5 | ........... | ........... |
| $H\iota$ 3771 | 7 | ........... | ........... |
| $H\kappa$ 3750 | 1 | ........... | ........... |

The very valuable discussions of lines in spectra of class N by Hale, Ellerman, and Parkhurst,[1] and by Shane,[2] have been freely used in preparing the present paper. Through the kindness of Mr. Joy, his extensive investigation of *o* Ceti has been available for reference prior to its publication.

*Hydrogen.*—The Balmer lines are bright in all long-period variables of classes M and S, and in a few variables of class N. In all these classes the bright hydrogen lines have their greatest intensities near the time of maximum light and are weak or absent near minimum. Typical intensities at maximum are given in Table I.[3]

The anomalously low intensities of bright $H\alpha$, $H\beta$, and $H\epsilon$ in Me stars are very striking and present important physical problems.[4]

---

[1] *Publications of the Yerkes Observatory*, **2**, 253, 1903.

[2] *Lick Observatory Bulletins*, **10**, 79, 1920.

[3] For more detailed data, see the following references: Class Me, *Mt. Wilson Contr.*, No. 200; *Astrophysical Journal*, **53**, 185, 1921. Class Se, *Mt. Wilson Contr.*, No. 252; *Astrophysical Journal*, **56**, 457, 1922. Class Ne, *Lick Observatory Bulletins*, **10**, 79, 1920.

[4] *Physical Review*, **25**, 717, 1925.

It appears to be true in general that, the cooler the star, the greater is the departure of the relative intensities of the Balmer lines from those ordinarily observed in the laboratory.

The Balmer lines are frequently present in absorption in irregular variables and non-variable red stars. They are fairly strong in S-type spectra and high-luminosity stars of classes Mo–M3. They are weak in advanced M-types and in all red dwarf stars. In class N, $H\gamma$ and $H\delta$ have been observed as dark lines,[1] but not $H\alpha$ and $H\beta$.[1, 2]

Lines of the secondary spectrum of hydrogen have not been observed in stellar spectra.

*Helium.*—Lines of helium are not ordinarily found in the spectra of red stars. They appear, however, in R Aquarii at minimum brightness, but the spectrum at this time strongly resembles that of a planetary nebula, and its physical relationship to the M7e spectrum of the variable star is not understood.

*Lithium.*—No lines have been identified with certainty. The strong lines are not in favorable portions of the spectrum, but the intensities cannot be high.

*Sodium.*—The dark D lines are strong in most red stars, being outstanding features in classes N and S. In class M, however, they are not nearly so strong; in the advanced types M6e–M8e they are, in fact, surprisingly inconspicuous. Thus, in the coolest stars, these lines have but a small fraction of the intensity they exhibit at somewhat higher temperatures. As they are ultimate lines of neutral sodium, this behavior is unexpected and suggests that at the lowest-known stellar temperatures the supply of free sodium atoms in the reversing layer becomes nearly exhausted, perhaps by the formation of compounds.

*Potassium.*—The pair λλ 4044, 4047, $1s^2-2p^2$, is weak in types Mo to M4, but strengthens rapidly toward the end of the M sequence. This behavior is to be expected of lines in the principal series, and is at variance with the anomalous weakness of the D lines of sodium in the coolest stars. The potassium pair merits further study as its region has not been adequately observed in N and S spectra. Among M-type spectra it appears not always to have the same intensity in stars of a given subdivision, and perhaps varies with the light-phase.

---

[1] Hale, Ellerman, and Parkhurst, *op. cit.*, p. 373, 1903.

[2] Shane, *Lick Observatory Bulletins*, 10, 81, 1920.

*Magnesium.*—The low-temperature line λ 4571.11, $1S-1p^3$, is present in absorption in long-period variables of classes M and S near maximum light, changing to emission toward minimum.[1] At minimum it may become the strongest feature in the blue-violet portion of the spectrum. It is present as a weak absorption line in N-type spectra.

The green triplet λλ 5183.67, 5172.70, 5167.38, $1p^3-1s^3$, is described as "prominent" in absorption in class N by Hale, Ellerman, and Parkhurst. It is probably present in class S. It is difficult to observe in class M, at least with low dispersion, on account of the strong titanium oxide band having its head at λ 5167, but has been measured in the spectrum of α Herculis.

The first member of the diffuse triplet series $1p^3-2d^3$ consists of lines at λλ 3838.29, 3832.31, and 3829.36. Faint emission lines were measured in these positions on a single-prism spectrogram of R Leonis taken at Mount Wilson on February 26, 1921, forty-seven days after maximum light. There was only a trace of bright λ 4571 at this time, but a month later it was strongly developed. Unfortunately nothing can be said as to the intensities of the ultra-violet triplet on the later date. When properly observed, the relative behavior of these magnesium lines should yield valuable information concerning temperatures in the atmospheres of these stars.

*Calcium.*—The ultimate singlet λ 4226.73 is very strong and broad in absorption in red stars, and, in contrast to the behavior of the D lines of sodium, seems to grow more intense with decreasing temperature. λ 6572.78, $1S-1p^3$, if present at all, is weak in all classes of red stars.

The group given by Russell under excitation potential 1.88 is well represented in advanced M-types and probably also in N- and S-types. All the class I lines in this group seem to be present in M-type variables, although they are not strong, and a few are doubtful because nearly coincident with low-temperature lines of other elements.

---

[1] *Mt. Wilson Contr.*, No. 200; *Astrophysical Journal*, **53**, 185, 1921. *Publications of the Astronomical Society of the Pacific*, **33**, 206, 1921.

The ionized lines, Fraunhofer H and K, lie so far in the violet that abnormally long exposures are required to show them in the spectra of red stars. They are conspicuous broad dark lines on spectrograms having the proper density in their region and are doubtless present in all or nearly all red stars. Although probably somewhat less intense than in class K0, they are nevertheless surprisingly strong even in the cooler red stars such as χ Cygni. More extensive observations of these lines are very desirable to indicate their intensities in different stellar types and, in variable stars, their changes with phase.

*Strontium*.—The strong low-temperature line λ 4607.34, $1S-1P$, is well marked in red stars. In class M it appears, in general, to grow stronger with advancing type. The line λ 4832.08 has been measured in α Herculis, class M5.

The ionized lines λλ 4077.71 and 4215.52 are strong in class N, very strong in class S, and have widely different intensities in various M-type stars. While there is a strong tendency for these lines to grow weaker from M3 to M8, absolute magnitude, or some other factor, introduces considerable variations. These lines are very much stronger in χ Cygni, for example, than in certain other stars of the same type. In a few Me variables they have been observed to grow less intense after maximum light.

*Barium*.—The strong low-temperature line λ 5535.53, $1S-1P$, is weak or absent in all three types of red stars.

The ionized line λ 4554.04 is weak in class M, strong in class N, and very strong in class S, being, in fact, one of the distinctive features of class S. Its behavior is followed by that of the weaker line λ 4934.10.

*Aluminum*.—The pair λλ 3944.03 and 3961.54, $1p^2-1s^2$, is strong in Me variables. Mr. Joy informs me that in *o* Ceti it strengthens markedly toward minimum. Its intensity in classes N and S is not known.

*Titanium*.—The lines λλ 3981.77, 3989.77, and 3998.65 of the 0.0 energy-level of the neutral atom are strong in all subdivisions of class M, probably increasing in intensity with advancing type. Several others of the stronger lines arising from the 0.0 level have also been observed. The lines near λ 4500 from the level 0.82 are fairly strong in the early subdivisions, but decrease toward M8. This group of lines is present in N and S spectra also.

*Zirconium.*—The following strong zirconium lines are present in class S:

4535.75 blend with *Ti*
4542.22?
4575.52
4633.99
4687.81 }
4688.45 }
4710.08
4772.33
4815.06 }
4815.62 }
4828.06

They appear to be absent or much weaker in class M. This probably applies to class N also.

*Vanadium.*—Numerous lines from the two lowest levels are present in classes M, S, and N, although many are of moderate intensity. In class Me, which has been more extensively observed, these lower-level lines are represented with remarkable completeness.

*Chromium.*—The well-known triplet λλ 4254, 4274, 4289, $1s^7-1p^7$, is strong in all classes of red stars. In class M it shows a marked increase of intensity with advancing type. The green triplet near λ 5206 is present in all three classes. In class M nearly all the stronger lines in the 0.94 and 0.98 levels which lie in accessible parts of the spectrum have been observed, and λ 5328.34, the strongest line in the 2.88 group, has been measured in $\alpha$ Herculis.

*Manganese.*—The well-known low-temperature triplet near λ 4030, $1s^6-1p^6$, is very strong in M-type stars, increasing in intensity with advancing type. It is present in class S with approximately the same intensity as in the earlier subdivisions of class M. In Me variables, λ 4030 has been observed in emission during the phase of decreasing light. It appears first as a bright edge on the violet side of the dark line.

The multiplet $1d^6-1d'^6$ is represented by weak lines in class Me. They appear not to strengthen with advancing type to the same extent as the λ 4030 triplet. This might be expected because the level to which they belong is 2.16 volts above that for the triplet.

The line λ 4823.52 has been measured in all three classes of red stars.

*Iron.*—Comparing the iron-arc spectrum with lines in class M, we find a fragmentary and irregular correspondence, but if we use instead a list of King's low-temperature lines, or the lines originating from the 0.0 and 0.94 levels as compiled by Russell, the agreement is quite complete and satisfactory. The strong lines of level 1.54 are present with relatively low intensities, and lines of higher levels appear to be absent. The lines of the 1.54 level grow weaker with advancing type. Classes N and S resemble class M, except that the lines of level 1.54 are relatively stronger. Toward minimum of long-period variables of class Me the extreme low-temperature lines appear in emission. At an earlier phase after maximum, strong emission lines appear in the positions of the iron lines λλ 4202 and 4308. These are believed by several observers to arise from iron atoms, but some doubt as to the identification will probably remain until these lines can be shown by laboratory experiments to be outstanding under certain conditions. It is possible, however, that continued observations of stellar spectra may settle the matter by showing the presence in emission of related iron lines.

A remarkable fact, but one which seems well attested, is the presence of a few of the strongest enhanced lines of iron in Se variables,[1] in *o* Ceti,[2] and in certain other M stars.[3]

Mount Wilson Observatory
September 1925

---

[1] *Mt. Wilson Contr.*, No. 252; *Astrophysical Journal*, 56, 457, 1922.

[2] Unpublished data by Mr. Joy.

[3] *Publications of the Astronomical Society of the Pacific*, 34, 175, 1922.

Contributions from the Mount Wilson Observatory, No. 307
Reprinted from the *Astrophysical Journal*, Vol. LXIII, pp. 133–137, 1926
Printed in the U.S.A.

# AN ATTEMPT TO DETECT WATER-VAPOR AND OXYGEN LINES IN THE SPECTRUM OF MARS WITH THE REGISTERING MICROPHOTOMETER

By WALTER S. ADAMS and CHARLES E. ST. JOHN

## ABSTRACT

*Observation of water-vapor and oxygen in the spectra of Mars and the sky.*—If these gases are present in the atmosphere of Mars, the motion of the planet with reference to the earth should produce a relative displacement of the lines due to these gases in the two spectra.

*Material.*—Spectrograms of Mars and the sky were made with a 6-prism spectrograph, the scale being 1 mm = 7.3 A at D; graphs were drawn by a registering microphotometer on a scale of 1 mm = 0.12 A.

*Method of measurement.*—The lines of water-vapor and oxygen in the graphs of the two spectra were superposed; the relative displacements of the solar lines were then read directly from the curves.

*Results.*—The water-vapor lines in the spectrum of Mars were displaced 0.03 ± 0.01 A, and the oxygen lines 0.09 ± 0.03 A to the red, with respect to their positions in the sky spectrum. On taking account of the Doppler displacement, the length of path in the two atmospheres, and the amounts of water-vapor and oxygen above Mount Wilson, the quantity of water-vapor in the atmosphere of Mars, area for area, was found to be approximately 3 per cent of that over Pasadena, and the quantity of oxygen two-thirds of that above Mount Everest.

Before red-sensitive photographic plates were available, observations of the oxygen and water-vapor lines in the spectrum of Mars were necessarily visual. The first spectrograms covering the B-band of oxygen and the *a*-band of water-vapor[1] were made by V. M. Slipher in 1908.

Professor Very made photometric measurements of the relative intensity of the bands on Slipher's spectrograms and concluded that the atmosphere of Mars contained 1.75 times as much water-vapor as the atmosphere of the earth above Flagstaff and that the *B*-band of oxygen was 15 per cent stronger than in the spectrum of the moon at the same altitude.[2]

Campbell, from the equality of the *a*-band in spectrograms of Mars and the moon taken on Mount Whitney, came to the conclusion that the quantity of water-vapor in the atmosphere of Mars at the time of his observations was too small to be detected by the spectroscopic methods then available.[1]

---

[1] *Astrophysical Journal*, **28**, 397, 1908.

[2] *Lowell Observatory Bulletins*, Nos. 36 and 41, 1909.

The Doppler-Fizeau principle was applied by Lowell and Slipher with low dispersion in an attempt to detect lines originating in the atmosphere of Mars from their displacement with respect to similar lines originating in the atmosphere of the earth. They concluded that their measures neither proved nor disproved a displacement due to the motion of Mars relative to the earth.[2]

Campbell and Albrecht employed much higher dispersion and found for water-vapor lines near D a displacement of 19.2 km/sec. and for the $\alpha$-band of oxygen 18.1 km/sec., the displacement due to relative motion being 19.1 km/sec. They concluded that the water-vapor in the atmosphere of Mars was less than one-fifth that above Mount Hamilton and that the quantity of oxygen was small compared to that in the earth's atmosphere.[3]

The primary purpose of our observations was to test the applicability of the Doppler-Fizeau principle to this problem by the use of a spectrograph of higher dispersion and the registering microphotometer. The spectrograms of Mars and of the sky were taken with a 6-prism wooden spectrograph placed on a pier in the constant temperature room at the coudé focus of the 60-inch reflector. The scale of the original spectrograms was 1 mm = 7.3 A at D and 11.4 A at λ 6300. The scale of the graphs drawn by the registering microphotometer was 1 mm = 0.12 A at D and 0.19 A at λ 6300. The spectrograms were made on February 2, 1925, at a time when the relative velocity of Mars and the earth was considerable.

| | | |
|---|---|---|
| Mars | $5^h\ 35^m$–$9^h\ 20^m$ P.S.T. | Exp. 225 min. |
| Sky | $3^h\ 10^m$ P.S.T. | Exp. 30 sec. |
| Slit width | | 0.075 mm |
| Length of path in atmosphere of Mars (sec $z$) | | 2.2 |
| Length of path in atmosphere of Earth (sec $z$) | | 1.4 |
| Relative velocity | | +17.80 km/sec. |
| Velocity displacement at D | | 0.35 A |
| Velocity displacement at λ 6300 | | 0.37 A |

---

[1] *Lick Observatory Bulletins*, No. 169, 1909.

[2] *Lowell Observatory Bulletins*, No. 17, 1905.

[3] *Lick Observatory Bulletins*, No. 180, 1909.

*Water-vapor.*—The measurements were made by superposing successively the 6 water-vapor lines

$$\left.\begin{matrix}\lambda\,5879.820\\5879.945\end{matrix}\right\}\qquad \lambda\,5886.193\qquad \left.\begin{matrix}\lambda\,5887.560\\5887.620\\5887.905\end{matrix}\right\}$$

$$\left.\begin{matrix}\lambda\,5887.445\\5887.880\end{matrix}\right\}\qquad \lambda\,5919.860\qquad \lambda\,5920.776$$

in graphs of the spectra of Mars and the sky over millimeter cross-section paper and reading with a magnifier the distances between the lines of solar origin, λλ 5884, 5893, 5905, 5914, and 5922, on the two graphs. The means of the two observers were $2.6\pm0.13$ mm and $2.7\pm0.10$ mm, respectively, the final weighted mean being $2.67\pm0.08$ mm, equivalent to $0.32\pm0.01$ A.

The displacement of 0.35 A, due to relative motion, *minus* the measured displacement 0.32 A, is 0.03 A and represents the displacement to the red of the water-vapor lines in the combined Mars-sky spectrum due to water-vapor in the atmosphere of Mars. When the displacement is small compared with the width of the lines, as was the case on these graphs, the approximate relation

$$\Delta\lambda=(1+K_1/K_2)\delta$$

is applicable, where $K_1$ and $K_2$ are the intensities of the lines in the atmospheres of the earth and Mars, respectively. When $\Delta\lambda$ is 0.35 A and $\delta$ is 0.03 A, $K_2$ is 0.09 $K_1$.

The component of the water-vapor lines due to Mars in the Mars-sky spectrum at the time of observation was 9 per cent as strong as the component due to the water-vapor in the earth's atmosphere. The precipitable water above Mount Wilson at 5 P.M. on the day of observation was 0.73 cu. cm, for the preceding day 0.74 cu. cm, and for the following 0.75 cu. cm, or one-half that over Pasadena at noon for the same days. Taking into consideration the paths traversed in the two atmospheres, we find that the quantity of water-vapor in the atmosphere of Mars, area for area, was 6 per cent of that over Mount Wilson and 3 per cent of that over Pasadena. This indicates extreme desert conditions over the greater portion of the Martian hemisphere toward us at the time, which was near the beginning of the Martian spring, or about 2.5 Martian months after the solstice.

*Oxygen.*—Similar measurements were made with the oxygen lines.

$$\left.\begin{matrix}\lambda\,6276.815\\ 6277.021\end{matrix}\right\}\qquad \left.\begin{matrix}\lambda\,6277.513\\ 6277.634\\ 6277.701\\ 6277.837\end{matrix}\right\}\qquad \left.\begin{matrix}\lambda\,6279.084\\ 6279.308\end{matrix}\right\}\qquad \begin{matrix}\lambda\,6295.389\\ 6296.170\\ 6310.101\end{matrix}$$

The mean displacement of the solar lines λλ 6265, 6270, 6298, 6301–2, 6322, and 6339, referred to the oxygen lines in the Mars-sky spectrum, was 1.46±0.17 mm, equivalent to 0.28±0.03 A. The displacement due to relative velocity was 0.37 A. Applying the formula as above, we find that the Martian component of the oxygen line in the Mars-sky spectrum was 33 per cent of the earth's component.

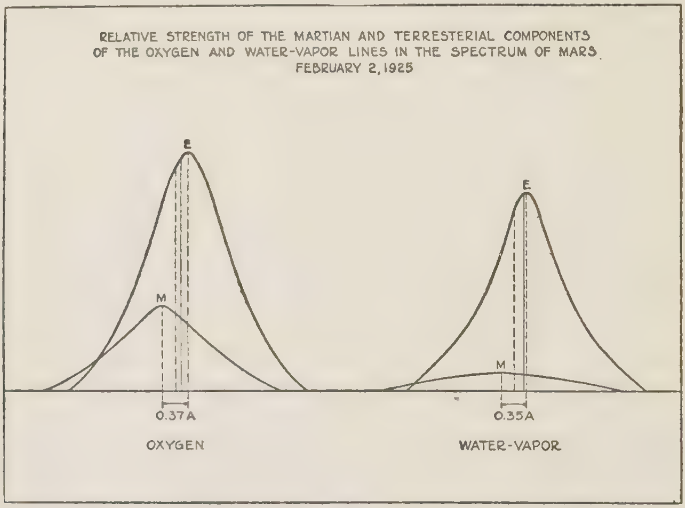

FIG. 1

On taking account of length of path and the elevation of the observing station, the oxygen in the atmosphere of Mars was found to be 16 per cent, area for area, of that over Mount Wilson, or about two-thirds of that in the earth's atmosphere above Mount Everest.

The heights of the curves *M* and *E* in Figure 1 indicate the relative intensities of the Martian and terrestrial components of the oxygen and water-vapor lines on the Mars-sky spectrogram. The Martian components are displaced to the red—to the left in the diagram—by the amount of the Doppler effect. For components of equal intensity the compound line in the spectrum of Mars would have been displaced by one-half the Doppler effect. The measured displacement, which is much less, is indicated by the position of the solid vertical line.

We wish to express our appreciation of the skill and experience of Miss Ware in the production, and her assistance in the measurements, of the microphotometer graphs.

Mount Wilson Observatory
November 1925

Contributions from the Mount Wilson Observatory, No. 308
Reprinted from the *Astrophysical Journal*, Vol. LXIII, pp. 67–71, 1926
Printed in the U.S.A.

# INTERNAL MOTIONS OF MESSIER 33

By KNUT LUNDMARK

## ABSTRACT

*Internal motions of Messier 33.*—The photographs measured and discussed by van Maanen, *Mt. Wilson Contr.* No. 260, were remeasured with the same measuring instrument and discussed by the same method. The same comparison stars and nebular points were selected for measurement. Any systematic difference in results is therefore of personal origin.

The values found for the *proper motion* are $\mu_\alpha=-0''.0015$, $\mu_\delta=-0''.0050$; van Maanen's results are $+0''.0034$ and $-0''.0044$, respectively. The annual *rotational components* can be represented by $-0''.00084+0''.00032\,\rho$, and $+0''.01063+0''.00119\,\rho$ (van Maanen), $\rho$ being the radial distance in minutes of arc. For the mean distance of the 399 nebular points, $\rho=7'.6$, these expressions for the rotational component become $+0''.00160$ (Lundmark) and $+0''.01969$ (van Maanen). The *correlation coefficients* between the rotational and radial components found by the two measures are $r_{\text{rot.}}=0.282\pm0.046$ (m.e.), $r_{\text{rad.}}=0.453\pm0.040$ (m.e.).

During a stay at the Mount Wilson Observatory in 1922–1923, at the suggestion of Director W. S. Adams and Dr. Adriaan van Maanen, I measured the well-known spiral nebula Messier 33 (N.G.C. 598) for internal motion. The plates used were the same as those measured by van Maanen,[1] and, for purpose of comparison, the same objects were selected for measurement. Thus four hundred nebular points, which as a rule are starlike objects, well distributed in the spiral arms and having a considerable range in brightness, were measured by both of us. The same instrument was used, the new large stereocomparator with a monocular arrangement, and the precautions suggested and described by van Maanen were observed throughout.[2] My measures were made at the same time as those of van Maanen, but the reduction was carried out after my return to Upsala.[3]

The plates were measured in six positions, three in each equatorial co-ordinate. For each set, the twelve plate constants were derived by a least-squares solution of the equations of condition yielded by the twenty-four comparison stars. The values of $\mu_\alpha$ and $\mu_\delta$ of the nebular objects were obtained with the aid of these plate constants, and the results from the different sets of measures were combined to form mean values. In discussing the measures, one point, No. 367, was omitted because its motion ($\mu = 0\overset{''}{.}112$ annually) is so large that it cannot well be a part of the nebula. By different methods, the motion of translation—the total proper motion of the nebula—was found to be

---

[1] *Mt. Wilson Contr.*, No. 260; *Astrophysical Journal*, **57**, 264, 1923.

[2] *Mt. Wilson Contr.*, No. 118; *Astrophysical Journal*, **44**, 210, 1916; *Mt. Wilson Comm.*, No. 72, 1921; *Proceedings of the National Academy of Sciences*, **7**, 1, 1921.

[3] Van Maanen, *Mt. Wilson Contr.*, No. 260; *Astrophysical Journal*, **57**, 264, 1923; *Mt. Wilson Annual Report*, 1923.

$$\mu_\alpha = -0\overset{''}{.}0015\ ;\quad \mu_\delta = -0\overset{''}{.}0050\ ,$$

which is in good agreement with the corresponding values of van Maanen, namely, $+0\overset{''}{.}0034$ and $-0\overset{''}{.}0044$, respectively.

Subtracting the translational motion from the values of $\mu_\alpha$ and $\mu_\delta$ for the nebular objects, we obtain the internal motions, which are illustrated in Plate III. These have been resolved into rotational and radial components. The positive sign is used for motions in the directions NESW and outward in the nebula.

The mean values of these components are

$$\mu_{\text{rot.}} = +0\overset{''}{.}0016\ ;\quad \mu_{\text{rad.}} = -0\overset{''}{.}0057\ .$$

The corresponding values from van Maanen's measures are $+0\overset{''}{.}0196$ and $+0\overset{''}{.}0029$, respectively. The standard deviations or dispersions around the means are

$$\sigma_{\text{rot.}} = \pm 0\overset{''}{.}0065\ ,\quad \sigma_{\text{rad.}} = \pm 0\overset{''}{.}0091 \text{ (Lundmark)}\ ;$$
$$\sigma_{\text{rot.}} = \pm 0\overset{''}{.}0080\ ,\quad \sigma_{\text{rad.}} = \pm 0\overset{''}{.}0096 \text{ (van Maanen)}\ .$$

The rotational motions found by me can be represented by the linear expression

$$\mu_{\text{rot.}} = -0\overset{''}{.}00084 + 0\overset{''}{.}00032\rho\ ,$$

where $\rho$ is the distance from the center of the nebula in minutes of arc.

A similar solution of van Maanen's components gave

$$\mu_{\text{rot.}} = +0\overset{''}{.}01063 + 0\overset{''}{.}00119\rho\ .$$

# PLATE III

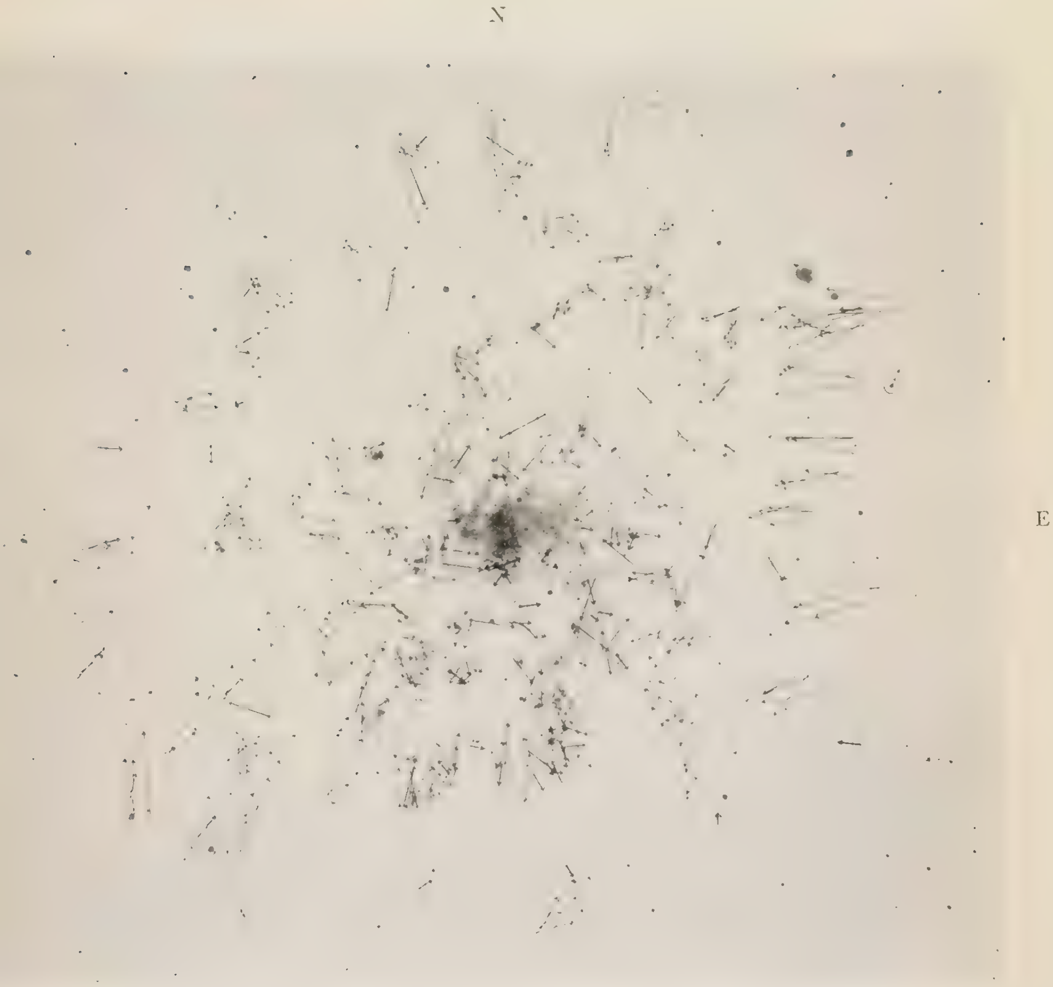

INTERNAL MOTIONS IN MESSIER 33

The arrows indicate the directions and magnitudes of the annual motions. The comparison stars are closed in circles. The scale of the nebula is 1 mm = 12″.4.

Since most of the nebular points are at some distance from the center, both series of measures give a general rotational motion of the nebula in the same direction. Further, both series show an increase in the rotation from the center outward of the same general order of magnitude. Using as variates the values of $\mu_{\text{rot.}}$ found by each measurer and computing the correlation coefficient $r$, we have

$$r=0.282\pm0.046 \text{ (m.e.)} ,$$

a value which, according to the rules used in statistics, should indicate a real correlation.

As the mean distance $\rho$ of the 399 objects is 7′61, the mean period of rotation will be $2.8\times10^6$ years according to my measures, and $0.23\times10^6$ according to the measures of van Maanen.

The correlation between the radial motions of the two measures is very definite. We have

$$r=+0.453\pm0.040 \text{ (m.e.)} .$$

When the radial motions were plotted against $\rho$, a rather definite relation was indicated. A least-squares solution was accordingly made, whereby it was found that the values of $\mu_{\text{rad.}}$ could be represented by the formula

$$\mu_{\text{rad.}}=-0\overset{''}{.}00117+0\overset{''}{.}00094\rho-0\overset{''}{.}00017\rho^2 .$$

The solution reduced the sum of the squares of the residuals from 45,845 (unit=0″001) to 25,623, or 44 per cent.

It does not seem very plausible that the change in $\mu_{\text{rad.}}$ with distance from the center should express any phenomenon arising from the actual internal motions of the nebula. It is perhaps more reasonable to assume its cause to be instrumental or optical, and the following explanation is tentatively suggested. The older plate, taken by Ritchey, is of unsurpassed quality and shows excellent definition over relatively a wide field. The later plate is very good, indeed, but does not quite match the older plate. Now it must be remembered that the comparison stars, as a rule, are brighter than the nebular objects, because the stars had to be so selected that there was little probability that they formed part of the nebula. Thus it is possible that a differential effect of coma has crept in and affected my measures in such a way as to introduce a spurious inward motion.

Since such an effect of coma would be radial, it leaves the foregoing conclusions regarding the rotation of the nebula unchanged; but it certainly must be of importance when analyzing the motion along and across the spiral arms.

The radial motions have been corrected for the general increase from center outward according to the foregoing formula. The corrected values of $\mu_{\text{rad.}}$ have been combined with the unchanged $\mu_{\text{rot.}}$. The resultant motion is thought to represent the combined effect of internal motion and unavoidable errors of measurement. This has been resolved into components along the spiral arms, $\mu_{\text{stream}}$, and perpendicular to the arms, $\mu_{\text{trans.}}$. The positive sign is used for motions from the center outward and for motions toward the left for an observer facing outward along the spiral arms.

The mean stream and transverse components are

$$\mu_{\text{stream}} = +0\overset{''}{.}0018\,,\quad \mu_{\text{trans.}} = -0\overset{''}{.}0004\,.$$

Van Maanen found the values $+0\overset{''}{.}0205$ and $-0\overset{''}{.}003$, respectively. The correlation between the two series of stream motions is expressed by

$$r = +0.330 \pm 0.047 \text{ (m.e.)}\,.$$

The stream motions derived by me show an increase with increasing distance from the center of more or less the same order of magnitude as that found by van Maanen.

Comparing van Maanen's results for the internal motions of seven spiral nebulae with the rotation of the spirals N.G.C. 224, 3031, and 4594, spectroscopically measured, we find, according to different assumptions, mean distances ranging between 10,000 and 40,000 light-years. The measures of Messier 33 made by me suggest somewhat larger distances, varying between 40,000 and 160,000 light-years. On account of the few cases investigated by spectroscopic methods, considerable uncertainty is involved in the application of the method.

The following formula[1] is easily deduced:

$$M = [3.71856]\mu^2_{\text{rot.}} d^3 \tan \rho \ ,$$

where $M$ is the mass within the distance $\rho$ from the center, expressed in minutes of arc, and $d$, the distance of the nebula from us, in parsecs. If we use the distance of 300,000 parsecs, as suggested by Hubble[2] from his investigations of Cepheids, the following values of $M$ are obtained:

$$1.6 \times 10^{14} \odot \text{ (van Maanen) ;}$$

$$1.1 \times 10^{12} \odot \text{ (Lundmark) .}$$

I wish to express my sincere thanks to Dr. Adams and Dr. van Maanen for the opportunity given me to measure the plates of Messier 33. My thanks are also given to them, as well as to other members of the staff, for the interest taken in my work and for valuable help and suggestions during the memorable time I had the privilege of working at the Mount Wilson Observatory.

UPSALA
August 1925

---

[1] *Publications of the Astronomical Society of the Pacific*, **34**, 108, 1922.

[2] *Observatory*, **48**, 139, 1925.

Contributions from the Mount Wilson Observatory, No. 309
Reprinted from the *Astrophysical Journal*, Vol. LXIII, pp. 218–235, 1926
Printed in the U.S.A.

# ON THE ORIGIN OF BRIGHT LINES IN STELLAR SPECTRA

By SVEIN ROSSELAND[1]

## ABSTRACT

*Origin of emission lines in stellar spectra.*—The discussion distinguishes four principal cases:

1. A star in hydrostatic and radiative equilibrium in which the emission of radiation from any small portion of matter corresponds to the case of true temperature equilibrium would show absorption lines over the main stellar disk, while the atmosphere projecting outside the disk would show emission lines.

2. Owing to general atomic properties, the thermal state of matter assumed in (1) can only be realized in nature, provided the pressure and temperature exceed certain limits. Below these limits, i.e., in the outer parts of the stellar atmospheres, fluorescence comes into play, manifesting itself all over the stellar disk, and it is suggested that bright line emission in early-type stars is due to such causes.

3. Any kind of penetrating radiation (i.e., in the nature of $\alpha$-, $\beta$-, or $\gamma$-rays) entering the atmosphere must produce bright-line radiation, as shown, for instance, in the case of the terrestrial aurora borealis.

4. If the hydrodynamic state of the atmosphere is far from a state of hydrostatic equilibrium, local regions of high temperature may be formed in the atmosphere, which necessarily must give rise to bright-line emission.

It is tentatively suggested that bright lines in late-type spectra owe their origin principally to such causes as are enumerated under (3), or possibly (4); the strong excitation of the gases concerned would seem to exclude (2), while (1) is excluded by the low density of the stars in question.

The radiation emitted from a star is generally resolvable into a continuous spectrum on which is superposed selective absorption in lines and bands. In a minor number of objects, however, bright lines are found to be superposed on the general continuous spectrum. The great scarcity of these objects shows that the conditions underlying the formation of bright lines are such as are not generally present in the atmosphere of an average star.

1. *Classification of bright-line stars.*—From the point of view of spectral classification, the objects showing bright lines fall essentially into two distinct classes, one at each end of the spectroscopic sequence. The first class contains stars of types O and B only. The early subdivisions of O-type stars show the Balmer series of hydrogen and the spectrum of ionized helium in pure emission. In the later subclasses the high frequency members of the Balmer series weaken and change into absorption. The resulting mixture of ab-

---

[1] Fellow of the International Education Board, 1924–26.

sorption and emission lines within the same spectral series is an essential characteristic for the class in question, as it is found among all bright-line B-stars hitherto observed.[1] To this class bright-line nebulae seem also to belong, since, with very few exceptions, they are all associated with B and O stars, with which they probably are physically connected.

At the other end of the spectral sequence we find bright-line objects very different from those considered above. With few exceptions they are all giant stars showing variability in light in long periods. The most notable exceptions[2] are some dwarf stars which show bright hydrogen lines, and vary little, if at all, in brightness. Although the spectra of long-period variables, as far as bright lines are concerned, are essentially characterized by the presence of hydrogen lines, other elements are represented by bright lines which sometimes are rather conspicuous. The wave-lengths of the bright lines show displacements to the violet, relative to the absorption lines, which vary in amount during the period of light variation and indicate that the radiating matter is constantly flowing out from the interior of the stars. The intensity distribution among the lines of the Balmer series is such that $H\delta$ is the strongest line, the intensities of the other lines decreasing to both sides, so that $H\gamma$ is fainter than $H\delta$ but stronger than $H\beta$, etc. It is significant, however, that in a small group of stars of very high luminosity, the intensity of the hydrogen lines decreases more or less regularly from $H\alpha$ to $H\beta$, etc. Bright lines are also essential characteristics of the spectra of variables of classes N, R, and S, and of irregular variables of late types. While hydrogen is still the dominating feature, other elements are invariably present, especially iron and titanium. The gap between these two classes is not complete, as bright lines are found occasionally in the spectra of Cepheids and irregular variables of spectral classes F, G, and K, the stars in question all being of exceptionally high luminosity.

---

[1] A complete survey of the bright-line B-stars is given by Merrill, Humason, and Burwell, *Contributions from Mount Wilson Observatory*, No. 294; *Astrophysical Journal*, **61**, 389, 1925.

[2] Adams and Joy: *Publications of the Astronomical Society of the Pacific*, **32**, 158, 1920; **34**, 174 and 175, 1922.

2. *General theoretical considerations.*—In order to give precision to the conceptions which will be used, it is convenient to recall briefly some definitions and formulae of the theory of radiative equilibrium.

Denote in a general way the radiation emitted per second from a certain volume element $\delta V$ (situated at the point $x$, $y$, $z$), directed within an element of solid angle $\delta w$ and contained in the frequency interval $d\nu$ by the expression

$$E_\nu \, d\nu \, \delta w \, \delta V ,$$

where $E_\nu$ is a function of $x$, $y$, $z$, $\nu$ and the direction cosines of the positive axis of $\delta w$. Denote by $I_\nu \, d\nu \, \delta w \, \delta\sigma$ the radiation in the frequency interval $d\nu$ which, per second, flows normally through the surface element $\delta\sigma$ and is contained in the solid angle $\delta w$. Considering the difference in flow in a distance $ds$ along the direction of $\delta w$, we see without difficulty that, if there is to be no change of state in the course of time, $I_\nu$ and $E_\nu$ must be connected through the differential relation[1]

$$\frac{\partial I_\nu}{\partial s} + x_\nu I_\nu = E_\nu \, . \tag{1}$$

The letter $x_\nu$ stands for the sum of the coefficients of absorption and scattering. We now introduce the notion of the optical thickness of a layer extending from a point $A$ to a point $B$ by the expression

$$(\tau_\nu)_{AB} = \int_A^B x_\nu \, ds \tag{2}$$

the integral being taken along the straight line joining the two points in question. The left-hand side of (1) may now be written in the form

$$e^{-\tau_\nu} \frac{\partial}{\partial s} (I_\nu e^{\tau_\nu})$$

---

[1] If the state of the system is variable in time $t$, an additional term $(1/c)(\partial I_\nu/\partial t)$ must be added to the left-hand side of (1), $c$ being the velocity of light.

where the point $A$ is assumed to be fixed, while $B$ is variable. Introducing $\tau_\nu$ as a variable, instead of $s$, and integrating from $A$ to $C$, we obtain from equation (1) the equivalent form

$$(I_\nu)_C=(I_\nu)_A\, e^{-(\tau_\nu)_{AC}}+\int_0^{(\tau_\nu)_{AC}}\frac{E_\nu}{x_\nu}e^{-z}dz\,;\quad z=(\tau_\nu)_{BC}\,. \tag{3}$$

The path of integration is in the direction opposite to the direction of $I_\nu$. As $E_\nu$ will, in general, depend on $I_\nu$, (3) is an integral equation for the determination of $I_\nu$, which, for special cases, will reduce to a linear integral equation of the Fredholm type.

The simplest case is met with when the function $E_\nu$ corresponds to true temperature equilibrium. We have then by Kirchoff's law that $4\pi E_\nu/c$ is equal to the product of the absorption coefficient and the energy density of black body radiation $B_\nu$. Thus

$$\frac{4\pi}{c}E_\nu=x_\nu\, B_\nu\,;\qquad B_\nu=\frac{8\pi h\nu^3}{c^3}\left(e^{\frac{h\nu}{kT}}-1\right)^{-1} \tag{4}$$

where $h$, $k$, $c$, and $T$ have their usual meaning. In this case we shall say that the system is in a quasi-thermal state, the difference from true temperature equilibrium consisting in the fact that the temperature $T$ may vary from point to point, as a consequence of which there will be a net flux of radiant energy at each point, and the energy density of radiation will not be equal to $B_\nu$. The conditions for the possible appearance of bright lines in the spectrum of the radiation emitted from a star in a quasi-thermal state are simple, as they depend solely upon the optical thickness of the star for general absorption, averaged in some way over the stellar disk. In order to see how this result emerges from the formula (3), we extend the integration from a point outside the star along a straight line so far into the star that the optical thickness of the intervening layer $\tau_\nu$ is very large compared with unity. The last term in (3) is then negligible, and, on using (4), the first term may be written in the form

$$I_\nu=\frac{c}{4\pi}B_\nu(1-e^{-\tau_\nu})\sim\frac{c}{4\pi}B_\nu \tag{5}$$

where $\bar{B}_\nu$ is the average value of $B_\nu$ along the path of integration, the weight function being $e^{-\tau_\nu}$. If the star is in a steady state, the temperature must of necessity increase on passing from the surface toward the interior, and, as $B_\nu$ increases rapidly with increasing temperature, it follows that the mean value of $B_\nu$ appearing in the foregoing formula will coincide approximately with the actual value of $B_\nu$ at the point below the surface where the optical thickness becomes comparable with unity.[1] The larger the absorption coefficient, the smaller is the distance below the surface at which a certain value of $\tau_\nu$ will be attained, and, by (5), the smaller the intensity of the emergent radiation. Thus the spectral lines will show up in absorption at this point on the stellar disk.

At the limb of the star it may happen, however, that the total optical thickness in the line of sight is not large compared to unity, as a consequence of which we obtain, instead of (5), the formula

$$I_\nu = \frac{c}{4\pi}\bar{B}_\nu(1-e^{-\tau_\nu}) \backsim \frac{c}{4\pi}\tau_\nu \bar{B}_\nu \, . \tag{6}$$

This just reverses the foregoing result, since $I_\nu$ now increases with increasing values of the absorption coefficient, and, in consequence, the spectral lines will be bright. Defining the atmosphere of a star as the boundary region, the optical thickness of which for the main spectral region is comparable to unity, we understand that the main stellar disk will show a continuous spectrum with absorption lines, while the atmosphere, as seen at the limb, will show a spectrum principally of emission lines. Hence the simple result that the condition for the appearance of emission lines in the integrated spectrum of the radiation emitted from a gaseous star in a quasi-thermal state is determined by the relative extension of its atmosphere. If this atmosphere outgrows its nuclear star completely, we have the limiting case of a quasi-thermal nebula showing a spectrum of emission lines.

The conditions necessary for the maintenance of a quasi-thermal state may be violated in three different ways: (1) The star in question may not be in a steady state: local variations in temperature may exist, producing, for instance, high temperature faculae and prominences. (2) The material may emit radiation at a rate which is independent of its temperature or of the intensity of the radiation sifting through the medium. Such is actually the case for the radiation emitted from radioactive substances. It does not matter much whether this radiation is ultimately corpuscular or electromagnetic in nature, as both would tend to set up a state of things which cannot be described by assigning to the substance any single temperature. (3) The radiation absorbed by the substance may not be changed into energy of true temperature radiation before being reradiated. When this is the case, the transformation of the radiation absorbed will depend essentially upon the scattering power of the substance. Such is the case for the phenomena of scattering, resonance, and fluorescent radiation. In any of these cases the conditions for the appearance of emission or absorption lines are different from those applying to the quasi-thermal case. We shall now discuss the third alternative more closely.

---

[1] The validity of this argument is limited by the implicit requirement that $B_\nu$ must increase at a slower rate than $e^{\tau_\nu}$, otherwise the integral would not converge, the intensity of emergent radiation being infinitely large.

3. *Fluorescence phenomena in stellar atmospheres.*—A little reflection will show that in the outer atmosphere of a star conditions will be such as to favor the formation of emission lines by fluorescence. In order to elucidate this point it is necessary to consider the physical processes underlying fluorescence phenomena in general. As we are dealing with gases only, and in most cases with monatomic gases, the question is much simplified, as it appears to be an established fact that, for a given temperature, the appearance of fluorescent radiation is a question of pressure only. The simplest instance of such processes is provided by mercury vapor, which, at pressures above a certain limit, absorbs radiation of wave-length 2536.7 A very strongly, the absorbed energy being converted directly into translational energy of temperature-motion of the atoms. For pressures below the critical limit, however, the absorbed radiation is largely re-emitted in all directions with unchanged wave-length. This influence of pressure on fluorescence phenomena is undoubtedly due to molecular collisions (of the so-called "second kind"). During the absorption process the atoms are transferred to some higher quantum state from which, after the lapse of some time, they return

to the normal state under emission of radiation. Collisions of such excited atoms with other atoms of the gas may have the result that the absorbed energy is, in the collision process, changed into energy of translation of the colliding atoms. The critical pressure must correspond to the case when the mean time between two successive collisions of an atom is of the same order of magnitude as the mean time interval in which the atom will remain in the quantum state from which (or in which) the emission process in question takes place.[1]

In the special case considered above the scattered radiation has the same wave-length as the incident radiation, because no free transition of the atom is possible except a reversion to the state from which it started. In the general case the scattered radiation will, by Stokes's law, be distributed over longer wave-lengths than the incident radiation, the law of distribution being determined by the energy distribution in the spectrum of the incident radiation and by the internal structure of the atoms in question, but not by the temperature of the substance as it may be calculated from the equation of state. In experiments on the extinction of resonance radiation in mercury the critical pressure has been found to be about one one-hundredth of an atmosphere, which indicates a mean life-period of the excited atom of about $10^{-7}$ to $10^{-8}$ seconds. This, again, is about what might be expected from theory.

Consider now the spectrum of the radiation received from a star by an observer situated at a distance $r$ from its center, $r$ being assumed to be larger than the radius of the star. Apart from the effect of darkening at the limb and the effect of absorption and emission lines, this spectrum, in the majority of cases, will show a fair resemblance to the spectrum of black body radiation, provided it is cut down by a factor $W$ which is the same for all wave-lengths. The quantity $4\pi W$ is equal to the solid angle subtended by the star as seen by the observer. The expression of the energy density of radiation in the frequency interval $\nu$ to $\nu+d\nu$ at the point in question is thus

$$\rho(\nu)d\nu = WB_\nu\, d\nu, \tag{7}$$

---

[1] For literature on this subject, cf. R. W. Wood, *Philosophical Magazine*, **23**, 689, 1912; J. Franck, *Zeitschrift für Physik*, **9**, 259, 1922; G. Cario, *ibid.*, **10**, 185, 1922; G. Cario and J. Franck, *ibid.*, **17**, 202, 1923.

the temperature involved in the expression for $B_\nu$ being the effective temperature of the star. The radiant field in question does not correspond to any kind of temperature radiation, as it has virtually a temperature associated with each infinitely small frequency interval. In the ultra-violet region ($h\nu$ large compared to $kT$) the energy density corresponds asymptotically to the temperature

$$T\left(1-\frac{kT}{h\nu}\log W\right)^{-1} \tag{8}$$

which for very large frequencies approaches indefinitely near to the effective temperature $T$ of the star. In the region of long wave-lengths ($h\nu$ small compared to $kT$) we may write asymptotically

$$\rho(\nu)=\frac{8\pi\nu^2}{c^3}kWT\ . \tag{9}$$

In this region the radiation has the virtual temperature $WT$, which is inversely proportional to the square of the distance from the center of the star, and for very large distances may, therefore, be only a minute fraction of the virtual temperature in the region of short wave-lengths.

A stratum of gaseous matter in radiative equilibrium with radiation from the star, placed at the point in question, will take up a temperature $t$ which satisfies the inequality $T>t>WT$, provided, of course, that the state of the gas is quasi-thermal.[1] This gas is, therefore, "cold" relative to the radiation of the region of short wave-lengths, and "warm" compared to that of the long waves. If the pressure of the gas falls considerably below the critical value, there seems to be no reason why the temperature (which now can be obtained only from the equation of state) should increase appreciably, although there is now no tendency for the gas to take up a quasi-thermal state, even approximately. The degree of departure from such a state will depend essentially on the distance of the stratum of gas from the photospheric layer of the star. In particular, the transformation of the radiation which is absorbed in a line spectrum will consist in the re-emission of another line spectrum, essentially of lower frequencies. There is apparently nothing in the trend of the foregoing argument which will be altered if the gas forms a part of the upper atmosphere of a star, and hence we are led to the following conclusion: In the atmosphere of a star, a closed surface may be drawn such that the matter outside this surface cannot be in a quasi-thermal state. In this part of the atmosphere emission of bright-line radiation will be likely to take place, the intensity depending, however, on a large number of different factors. In view of the rather large values of the critical pressure found in terrestrial experiments, it may further be concluded that the hypothetical bright-line emission from a quasi-thermal atmosphere or even from a nebula, as considered in section 2, is not realized in nature.

---

[1] C. Fabry, *Journal de Physique*, **6**, 207, 1916, and E. A. Milne, *Monthly Notices of the Royal Astronomical Society*, **82**, 368, 1922.

Let us now consider how far actually observed bright-line emission can be ascribed to fluorescence phenomena of the kind discussed above. It will then appear that the question is likely to be answered in the affirmative, as far as early-type stars are concerned. The most weighty argument in favor of such a hypothesis is afforded by the fact that in these stars the intensity of emission lines within the same spectral series is greatest for the members of long wavelength, while those of short wave-length most frequently show as absorption lines. This fact immediately reminds us of Stokes's fluorescence law. Moreover, the effective temperature of these stars is so large that the prominence of hydrogen and helium as fluorescent substances does not present any difficulty at all. The extension of the atmospheres which is necessary for the development of fluorescent radiation to the observed extent must probably be very great.

4. *Mathematical theory.*—The problem of determining the state of a fluorescent atmosphere in radiative equilibrium is beset with many difficulties, and only the outlines of the theory will be discussed, detailed applications being reserved for later papers. The equation of radiative transfer is still given by (1), provided $E_\nu$ is properly specified as a function of $I_\nu$ and the density of the gas. The function $E_\nu$ will be different for different kinds of emission processes. Consider the case of pure scattering. The scattering coefficient may be denoted by $\sigma_\nu$. The radiation scattered per unit time from a vol-

ume element $\delta V$ in the frequency interval $d\nu$ and within an elementary solid angle $\delta w$ is

$$S_\nu \delta w \delta V d\nu = \delta w \delta V d\nu \int \sigma'_\nu I'_\nu dw'$$

or

$$S_\nu = \int \sigma'_\nu I'_\nu dw' \; . \tag{10}$$

The integral in (10) is to be extended to $4\pi$ of solid angle. The quantity $S_\nu$ is the contribution to $E_\nu$ arising from pure scattering without change of wave-length. The coefficient $\sigma_\nu$ is, according to ordinary electromagnetic theory, proportional to $1+\cos^2 i$ where $i$ is the angle between the direction of the scattered radiation and the direction of the incident radiation. It is, moreover, a function of the state of excitation of the substance as, for instance, no selective scattering of the hydrogen Balmer lines will take place if all the atoms reside in the normal state. In the case of purely radiative equilibrium (collisions between atoms having a negligible effect on the state of excitation) the excitation will be effected by absorption of radiation only, and thus $\sigma_\nu$ will involve $I_\nu$ in some form or other.

Consider next the case of spontaneous emission. Let the frequency interval $\nu$ to $\nu+d\nu$ lie within the region of a spectral line of mean frequency $\nu_0$ corresponding to the free transition $i \rightarrow k$ of the atom. Let $a_{ik}$ be the probability of this particular transition and $n_i$ the number of atoms per unit volume in the $i$-state. The intensity of the spontaneous radiation must be equally distributed in all directions and the analogue of $S_\nu$ may be written directly in the form

$$R_\nu = \frac{h\nu}{4\pi} n_i a_{ik} f_{ik}(\nu) \tag{11}$$

The factor $f_{ik}$ has been introduced to account for the intensity distribution within the line. It must, according to Bohr's frequency relation, satisfy the equation

$$\int_0^\infty f_{ik}(\nu) h\nu d\nu = h\nu_0 \tag{12}$$

In view of the fact that $f_{ik}$ decreases very rapidly with increasing values of $|\nu-\nu_0|$, we must have, approximately,

$$\int_0^\infty f_{ik}(\nu) d\nu = 1$$

The processes discussed thus far give for $E_\nu$ the expression

$$E_\nu = \frac{h\nu}{4\pi} n_i a_{ik} f_{ik}(\nu) + \int \sigma'_\nu I'_\nu dw' \tag{13}$$

As the scattering coefficient $\sigma_\nu$ must be proportional to $n_i$ the functional form of $E_\nu$, as regards its dependence on $I_\nu$, is completely specified when $n_i$ is given as a function of $I_\nu$. The formal solution of this latter problem is very simple. In fact, in a steady state, the number of atoms leaving a particular stationary state $i$ in any given interval of time must be equal to the number of atoms entering this state in the same time interval. Thus we have

$$n_i(a_{i1} + a_{i2} + \;.\;.\;.\;.\; a_{ir}) = n_1 a_{1i} + n_2 a_{21} + \;.\;.\;.\;.\; n_r a_{ri}\,, \qquad i = 1.2\;.\;.\;.\;.\;r \tag{14}$$

No transition coefficient $a_{ii}$ occurs in this equation, and the introduction of one would have no meaning, as it would appear on both sides and drop out identically. We may, therefore, use the notation

$$a_{ii} = -\sum_{k=1}^{r} a_{ik}\,; \qquad k \gtrless i\,; \qquad i = 1.2\;.\;.\;.\;.\;r \tag{15}$$

and write (14) in the form

$$\sum_{i=1}^{r} n_i a_{ik} = 0\,; \qquad k = 1.2\;.\;.\;.\;.\;r \tag{16}$$

$r$ being the total number of physically distinct quantum states of the system. The determinant

$$A = |a_{ik}| \tag{17}$$

is zero in virtue of the relations (15).[1] Denoting the algebraic complement of $a_{ik}$ in the determinant (17) by $A_{ik}$, we find the general solution of (16) to be

$$n_i = \lambda_m A_{im}\,; \qquad i = 1.2\;.\;.\;.\;.\;r \tag{18}$$

where $\lambda_m$ is independent of the index $i$. The transition coefficients $a_{ik}$ are, according to the well-known theory of Einstein, linear functions of the energy density of the radiation field $\rho(\nu)$ for the frequency which corresponds to the transition in question. Now

---

[1] Pascal, *Determinanten* (Leipzig, 1900), p. 10.

$$\rho(\nu)=\frac{1}{c}\int I_\nu dw\ , \tag{19}$$

the integral being extended to $4\pi$ of solid angle. Thus $n_i$, by (18) and (19), becomes a function of the intensity of the radiation field for a large number of different frequency intervals distributed throughout the entire spectrum.

5. *Thermal equilibrium.*—The foregoing theory applies to any kind of radiative equilibrium. The equilibrium will be said to be "thermal" if there is an independent balance of transition processes between any two arbitrarily selected states, such that

$$n_i a_{ik}=n_k a_{ki} \tag{20}$$

The restrictions involved by these relations concerning the agencies underlying the transition processes are perhaps better elucidated by the statement: In thermal equilibrium the probability that an atom shall complete a closed route of transitions

$$i_1\rightarrow i_2\rightarrow \ .\ .\ .\ .\ i_n\rightarrow i_1$$

is equal to the probability that it shall complete the reverse route

$$i_1\rightarrow i_n\rightarrow \ .\ .\ .\ .\ \rightarrow i_2\rightarrow i_1$$

in the same time. As the transition probabilities are all independent, the statement in question takes the form

$$a_{i_1i_2}a_{i_2i_3}\ .\ .\ .\ .\ a_{i_ni_1}=a_{i_1i_n}\ a_{i_ni_{n-1}}\ .\ .\ .\ .\ a_{i_2i_1} \tag{21}$$

This statement may suitably be called the "principle of reversibility." Equation (21) follows from (20) by writing down the series of equations

$$n_{i_1}a_{i_1i_2}=n_{i_2}a_{i_2i_1}$$
$$n_{i_2}a_{i_2i_3}=n_{i_3}a_{i_3i_2}$$
$$\begin{matrix}\cdot & & \cdot\\ \cdot & & \cdot\end{matrix}$$
$$n_{i_n}a_{i_ni_1}=n_{i_1}a_{i_1i_n}$$

and multiplying the corresponding members. All the $n$'s drop out, and leave (21) as a result. Equations (21) are equivalent to (20).

If we knew the laws governing the transition processes, and thus the ratios of the different $a$'s, which by (18) determine the equilibrium state, it would be possible to specify the state of the system in thermal equilibrium on the basis of the foregoing theory. The principle of reversibility alone is not sufficient for this purpose, and additional hypotheses of a mechanical and electrodynamical kind are necessary.[1] In the present state of science it seems, however, more satisfactory to appeal to the general statistical theory of thermal equilibrium in which an explicit reference to the transition coefficients is avoided. Taking thus the ratios $n_i/n_k$ for granted, we find it possible, by (20), to determine new relations between the transition coefficients. The result of this procedure for the present case is well known. By Boltzmann's principle

$$n_i/n_k = p_i/p_k \, e^{-\frac{\chi_i - \chi_k}{kT}} \tag{22}$$

where $p_i$ is the weight and $\chi_i$ the energy of the $i$-state, and $p_k$, $\chi_k$ are the same quantities for the $k$-state. For transitions between quantized states the transition coefficients may be shown to satisfy the relations

$$a_{ik} = \alpha_{ik}(1 + \bar{\rho}_\nu) \; ; \qquad \chi_i > \chi_k \tag{23}$$

$$a_{ki} = \frac{p_i}{p_k} \alpha_{ik} \bar{\rho}_\nu \tag{24}$$

where $\alpha_{ik}$ is the probability of spontaneous transition $i \rightarrow k$, while $\bar{\rho}_\nu$ is the energy density of radiation for the frequency

$$\nu = (\chi_i - \chi_k)/h$$

---

[1] Cf. A. S. Eddington, *Philosophical Magazine*, 50, 803, 1925, where this question is discussed in detail. It appears that the distribution of energy with frequency (Planck's formula) may be obtained on the basis of the reversibility principle, provided Wien's displacement law, the $h\nu$-relation, and the linear relationship between the transition coefficients and the energy density of radiation for the particular frequency in question are taken for granted. Some approach toward a derivation of Boltzmann's formula for the distribution of atoms over the different quantum states can also be made on the same basis.

divided by $8\pi h\nu^3 c^{-3}$. The relations (23) and (24) are generally valid, whether the system is in thermal equilibrium or not.

6. *Equilibrium in reduced thermal radiation.*—A few simple applications of the foregoing theory for the case that the energy density of radiation is given by (7) will now be shown. The simplest case, which is not trivial, is offered by atoms possessing three possible states only, and this gives us a first idea about the nature of the distribution law in a fluorescent atmosphere. We assume the states to be enumerated in such a way that $\chi_1 < \chi_2 < \chi_3$. The sub-determinants entering (18) may be taken to be

$$A_{11} = a_{21}(a_{31} + a_{32}) + a_{23}\, a_{31} \tag{25}$$

$$A_{21} = a_{12}(a_{31} + a_{32}) + a_{13}\, a_{32} \tag{26}$$

$$A_{31} = a_{13}(a_{21} + a_{23}) + a_{12}\, a_{23} \tag{27}$$

From these expressions we obtain

$$-(a_{31}A_{31} - a_{13}A_{11}) = a_{32}A_{31} - a_{23}A_{21} = a_{21}A_{21} - a_{12}A_{11} = \Delta$$

where

$$\Delta = a_{13}\, a_{32}\, a_{21} - a_{12}\, a_{23}\, a_{31} \tag{28}$$

Using expressions (23), (24), and (7), we find

$$a_{12}a_{23}a_{31} = y\, a_{13}a_{32}a_{21}\ , \tag{29}$$

where

$$y = \frac{W^2 F_{31}}{F_{32}F_{21}}\ ; \qquad F_{ik} = 1 - (1 - W)e^{-\frac{\chi_i - \chi_k}{kT}}$$

When $W$ is less than unity the quantity $y$ is positive and less than unity, and equation (29) shows that it is easier for the atom to complete the circuit over all states in the direction 1→3→2→1 (one absorption-act and two emissions) than in the direction 1→2→3→1 (two absorptions and one emission). The effect of the atoms on the stream of radiation will, therefore, be to create one absorption line, corresponding to the transition 1→3, and two emission lines, corresponding to the transitions 3→2, 2→1. This result illustrates clearly the general process of generation of emission lines by fluorescence.

While the particular values of the spontaneous transition coefficients do not affect the law of distribution of atoms over the different quantum states for the case of thermodynamic equilibrium, they will do so for any other kind of equilibrium. As an extreme example consider the case when the 2-state is "metastable," i.e., $a_{12}=a_{21}=0$. We then obtain from (18) and (25) and (26)

$$n_2/n_1=\frac{p_2}{p_1}e^{-\frac{\chi_2-\chi_1}{kT}}\,\frac{1-(1-W)\,e^{-\frac{\chi_3-\chi_2}{kT}}}{1-(1-W)\,e^{-\frac{\chi_3-\chi_1}{kT}}} \tag{30}$$

This expression shows that the excitation to the metastable state may be approximately the same as in the case of thermodynamic equilibrium ($W=1$) at the temperature $T$, even if $W$ is very small. This result is of considerable interest for the theory of gaseous nebulae.[1]

The theory of radiative equilibrium developed in section 4 is valid even if ionization takes place. As a first approximation we shall consider the case of a single element, and take account of one quantum state only. Let the index 1 refer to the atom in an un-ionized state and 2 to the ionized state. The ionization formula takes the form

$$n_2/n_1=a_{12}/a_{21} \tag{31}$$

The transition coefficients $a_{12}$ and $a_{21}$ can be calculated as soon as the atomic absorption coefficient $x_\nu$ is known as well as the velocity distribution of the free electrons. To save repetition from earlier work[2] I give directly the expressions for the $a$'s

$$a_{12}=\int_0^\infty x_\nu c\rho(\nu)d\nu/h\nu \tag{32}$$

$$a_{21}=\frac{2\sigma_{12}n_e}{hm^2c^2}\int_0^\infty x_\nu\,\nu^2(1+\bar{\rho}_\nu)F(v)v^{-1}\frac{dv}{d\nu}\,d\nu \tag{33}$$

---

[1] *Nature*, 114, 859, 1924.

[2] Cf. especially E. A. Milne, *Philosophical Magazine*, 47, 209, 1924.

where $n_e F(v)dv$ is the number of free electrons per unit volume in the velocity interval $v$ to $v+dv$ and $\sigma_{12}$ the a priori probability of the atom with the electron bound relative to the a priori probability of the atom when the electron is missing.

As an illustration consider the explicit ionization formula for the case that the velocities of the electrons are distributed according to Maxwell's law. The energy density of radiation is given by (7), and, as an approximation, we assume that $x_\nu$ is zero in the interval $\nu=0$ to $\nu=\nu_m$ and proportional to $\nu^{-2}$ for higher frequencies. Reducing expressions (32) and (33) according to these assumptions, we find

$$\frac{n_2 n_e}{n_1}=\frac{WT}{T_0}\,\frac{(4\pi mkT_0)^{\frac{3}{2}}}{\sigma_{12}}\,\frac{\log\left(1-e^{-\frac{h\nu_m}{kT}}\right)}{\psi} \tag{34}$$

where

$$\psi=\int_{\nu_m}^{\infty}\left(1+\frac{W}{e^{\frac{h\nu}{kT}}-1}\right)e^{\frac{h\nu_m-h\nu}{kT_0}}\,\frac{h\,d\nu}{kT_0} \tag{35}$$

and where $T_0$ is the temperature of the electrons. Formula (34) should be of value in any discussion of the ionization of a gaseous nebula excited by radiation from a distant star. The special assumptions introduced concerning the velocity distribution of the electrons and the functional form of the absorption coefficient cannot have influenced the result very much.

7. *Bright lines in spectra of the late type.*—Turning to the stars of late type, we find that the problem of accounting for bright-line radiation assumes a much more complicated aspect. The surprising thing is not so much the appearance of bright lines as the fact that lines requiring such strong excitation in order to appear as the hydrogen lines should be so amply represented in the spectra of these low-temperature stars. The origin of this excitation appears to constitute the essential problem at issue, the solution of which must be known before any suggestion about the mechanism of the production of bright lines can be ventured.

The hydrogen lines appear as strong absorption lines in early-type stars, and decrease in intensity all the way through the spectral sequence from class A to classes F, G, and K. There is a remarkable difference between giants and dwarf stars in that giants are likely to exhibit hydrogen absorption lines much more strongly than dwarfs of the same spectral type. This peculiarity is particularly prominent for late-type stars, many giant K and M stars exhibiting prominent absorption lines while dwarf stars of the same types generally show very faint hydrogen absorption.

The general decrease in intensity of hydrogen absorption lines in passing from spectra of early to those of late type is satisfactorily explained by ordinary thermodynamic theory. The different behavior of giants and dwarfs may be due partly to different thickness of atmospheres, and partly to a real difference in absolute concentration of hydrogen atoms in the stars of the two branches. Such a difference is to be expected if, in the stars, heavy elements are built up from hydrogen, provided, of course, that the evolutionary course of a star is in the direction

$$M_{\text{giant}} \rightarrow A \rightarrow B \rightarrow A \rightarrow M_{\text{dwarf}}$$

as is usually assumed.

When it is a question of accounting for the presence of hydrogen lines in giant M stars, thermodynamic theory seems to break down. This theory would predict that at a temperature of 2000° K. only one atom out of every $10^{24}$ would be able to absorb or emit the Balmer lines. This proportion is so small that the thickness of atmosphere required to produce detectable lines, for the probable values of the mean density of such stars and of the absorption coefficient for the lines in question, appears to be much larger than the dimensions of the stars. This result seemingly points to the conclusion that the excitation of hydrogen atoms, especially in the atmospheres of long-period variable stars, is not connected in a simple manner with the mean temperature of the photospheric layers. From the appearance of lines of elements other than hydrogen, little can be concluded, either for or against this inference. The lines in question are mostly such as appear in consequence of so small an excitation that temperature alone might account for the main part of this excitation, and any differentiating agency would be sufficient to make them visible. They cannot, therefore, be invoked as evidence when it comes to a distinction between different modes of excitation.

Dropping the hypothesis that bright hydrogen lines in M stars are produced by pure fluorescence phenomena in a quiescent atmosphere, as assumed to be the case for early-type stars, we see that the discussion in section 2 leaves only two possibilities: (1) We are witnessing the effect of electric discharges, as would be the case if the atmospheres were the seat of emission of penetrating $\beta$ or $\alpha$ particles; or (2) the atmospheres are the seat of violent and local variations in temperature.

We cannot decide definitely which of these possibilities is the more important. The fact that the lines appear to be rather narrow and to possess a peculiar kind of structure[1] suggests that the part of the atmosphere from which they are emitted is in a relatively steady state and not subject to violent internal motion changing rapidly with the time, as would be expected if (2) were the important factor. A closer study of the problem in hand, from the observational as well as the theoretical side, might lead to interesting consequences regarding the state of the stellar atmospheres and to a better understanding of long-period variation in general.

Any complete theory of bright lines in late-type stars must account for the abnormal distribution of intensity among the lines of the Balmer series. This question appears to involve complications, and no suggestion as to the solution will be advanced here. It may be mentioned, however, that this distribution of intensity differs widely from that to be expected on any approximate application of formulae based on the equations corresponding to temperature equilibrium. The relative intensities seem, therefore, to afford an independent argument in support of the conclusions that any explanation of these phenomena based on the ordinary theory of radiative equilibrium is bound to be inadequate, and that consequently we are induced to consider alternative possibilities, as has tentatively been done above.

MOUNT WILSON OBSERVATORY
December 1925

---

[1] W. W. Campbell, *Astrophysical Journal*, **9**, 31, 1899.

Contributions from the Mount Wilson Observatory, No. 310
Reprinted from the *Astrophysical Journal*, Vol. LXIII pp. 236–274, 1926
Printed in the U.S.A.

# A SPIRAL NEBULA AS A STELLAR SYSTEM
## MESSIER 33

By EDWIN HUBBLE

## ABSTRACT

*The spiral nebula Messier 33.*—This object is the fainter of the two naked-eye spirals. Its great angular diameter and high degree of resolution, suggesting that it is one of the nearest objects of its kind, offer exceptional opportunities for detailed investigation.

*Resolution.*—Critical tests made with the 100-inch reflector, the highest resolving-power available, show no difference between the photographic images of the so-called condensations in Messier 33 and the images of ordinary galactic stars. Moreover, the application of ordinary methods of stellar research leads to consistent results, similar to those found in other systems of stars.

*Variable stars.*—Forty-two variable stars have been found in the spiral, in addition to the three previously known; thirty-five of these are typical Cepheids with periods ranging from thirteen to seventy days, and photographic magnitudes at maxima, from 18.0 to 19.1. Of the remaining ten variables, four are irregular, one is probably an eclipsing binary, while the types of five are as yet undetermined.

*Novae.*—Two novae have been observed, both apparently on the declining branch of their light curves. The maximum observed photographic magnitudes, 17.25 and 17.9, respectively, were brighter than that attained by any of the Cepheids.

*Nebulae.*—Several patches of diffuse emission nebulosity with blue stars involved are found in the arms of the spiral. The relation between the extent of the nebulosity and the magnitudes of the stars is similar to that in the galactic system. It is inferred that the spectral types of the involved stars are Oe5 and B0.

*Star colors.*—A comparison of photovisual with shorter direct exposures indicates that the brightest stars in the nebula are white or blue. No accurate calibration of the photovisual plates has been possible, but an approximate reduction curve was constructed from well-determined photographic magnitudes, corrected by color-indices corresponding to known or probable spectral types of a few exceptional stars.

*Star counts.*—The numbers of stars in successive intervals of photographic magnitude down to 19.2 have been counted over an area containing about one-fifth of all of the stars in the nebula. Stars begin to appear in the nebula at about 15.5. The form of the luminosity function is similar to the bright end of Kapteyn's function for stars in the vicinity of the sun.

*Distance.*—The period-luminosity relation is conspicuous among the thirty-five Cepheids and indicates a distance about 8.1 times that of the small Magellanic Cloud. Using Shapley's value for the latter, the distance of the spiral is about 263,000 parsecs. $m-M=22.1$. The order of this distance is supported by the independent evidence of the novae, the blue giants involved in diffuse emission nebulosity, and the form of the luminosity function for the brighter stars.

*Dimensions.*—The linear scale corresponding to this distance is $1''=1.27$ parsecs. The major diameter of the spiral is about 4600 parsecs, and the minor diameter probably a tenth of this amount. The total absolute magnitude is about $-15.1$. The dimensions and the luminosity are comparable with those for the Magellanic Clouds.

The nature of nebulae and their place in the scheme of the universe have been favorite subjects of controversy since the very dawn of telescopic observations. In these later days, when the non-galactic nebulae have been clearly differentiated from the diffuse and the planetary, the discussion has concentrated around the spectacular forms of the spirals. Some believe them to be subordinate members of the galactic system, and hence moderately small and relatively near; others consider them as comparable with the galactic system itself—island universes, scattered through the remote depths of space. The crucial point at issue is the order of their distance, and arguments concerning this quantity have been largely speculative.

The present contribution to the subject consists of observational data concerning the particular spiral, Messier 33. The data lead to a conception of the object as an isolated system of stars and nebulae, lying far outside the limits of the galactic system. To this extent the evidence favors the island-universe hypothesis, but, in respect to dimensions and luminosity, the spiral is more closely comparable with the Magellanic Clouds than with the galactic system itself.

The investigations described followed naturally upon the partial resolution of Messier 33 into swarms of actual stars, and ordinary methods of stellar research were employed throughout. The discovery of Cepheid variables[1] furnished a probably reliable criterion of absolute magnitude, and the order of the resulting distance was confirmed by other independent criteria. The same procedure, when applied to another spiral, Messier 31, led to similarly consistent results, strengthened in this case by the absolute-magnitude criterion for the numerous novae. The Andromeda spiral is the subject of a second paper, now in preparation, and the present discussion may be followed with this in mind.

## RESOLUTION OF MESSIER 33

The familiar condensations in the arms of spirals have been constantly interpreted, both casually and analytically, as stars in the process of formation. Messier 33 is especially rich in condensations, and its great angular dimensions, exceeded only by those of Messier 31, suggest that it is one of the nearest of all the spirals. For these reasons, Messier 33 affords the best opportunity for investigating the optical, or rather the photographic, nature of the condensations.

---

[1] A preliminary notice of the discovery of Cepheid variables will be found in *Publications of the American Astronomical Society* (33d meeting), Jan., 1925; reprinted in *Observatory*, 48, 139, 1925.

G. W. Ritchey, basing his judgment on the best material hitherto available, his own splendid photographs made with the 60-inch reflector, described them as soft, starlike condensations and designated them by the term "nebulous stars."[1]

The nebulous character, however, was inferred from the appearance of the images on long exposures made with fast reflectors centered on the nucleus of the spiral. The area of best definition was restricted to the central region where a considerable amount of unresolved nebulosity registered as a dense and fairly continuous background. In the outer regions of the nebula, where the background was relatively light, the various aberrations spread the images over considerable areas. Such conditions are not suitable for determining the character of the images. Considerations of this nature, supported by evidence from slitless spectrograms obtained with the 36-inch reflector at the Lick Observatory, led Knut Lundmark to the conclusion that the phenomena could be accounted for by assuming the spiral to consist of great numbers of ordinary stars with clusters of stars and some nebular material.[2]

---

[1] *Mt. Wilson Contr.*, No. 47; *Astrophysical Journal*, **32**, 26, 1910. Ritchey states: "All of these [spirals, including Messier 33] contain great numbers of soft starlike condensations which I shall call nebulous stars. They are probably stars in the process of formation." In Messier 33 he counted some 2400 "nebulous stars." This recalls the first description of the condensations in Messier 33 by Isaac Roberts based upon photographs made with his 20-inch reflector: "They are like nebulous stars in the midst of fainter nebulosity"; and again: "hundreds of stars having each a very small nucleus surrounded by fainter nebulosity" (*Photographs of Stars, Star Clusters and Nebulae*, **2**, 66, 1899).

[2] *Publications of the Astronomical Society of the Pacific*, **33**, 324, 1921. The statements are repeated in somewhat stronger terms in *Monthly Notices*, **85**, 890, 1925. It is, however, difficult to understand how the stellar nature of such faint light-sources can be "proved," as Lundmark claims, from spectrograms. To be assigned with certainty to the nebula, the objects must be of the order of the sixteenth photographic magnitude or fainter, and even prolonged exposures can do little more than distinguish between emission and continuous spectra. Lundmark found the latter and estimated them as approximately of solar type. This, of course, is just what is found for the small non-galactic nebulae scattered over the sky, and they, too, have often been called "nebulous stars." Moreover, there is considerable evidence, presented in the present paper, indicating that the brighter stars in Messier 33 are almost invariably white or blue. The discussion over the condensations in Messier 33, however, concerns the angular diameters of the small images, and, since they give continuous spectra, the spectrograms can have no advantage over direct photography, unless the ratio of camera to collimator is much larger than that ordinarily employed for faint objects.

The subject has been reinvestigated with the highest resolving-power available—the full aperture of the 100-inch reflector working under exceptionally fine conditions of mirror surface and seeing. The plates were centered on the outer regions of the arms as well as on the nucleus, and the exposures were short, not exceeding forty minutes, for the double purpose of avoiding the dense background of nebulosity and possible changes in observing conditions. On several plates, equal exposures were made to the nebula and to the neighboring Selected Area No. 45. This was primarily for the purpose of deriving magnitudes, but it also furnished an opportunity for comparing the images in the two regions.

A study of the plates clearly establishes the stellar appearance of the images of the condensations. They are as small and as sharp as those of ordinary stars of the same magnitude. The two most successful plates,[1] each of thirty minutes' exposure, centered on regions seven minutes of arc south and south-preceding the nucleus, show images with angular diameters smaller than any previously obtained on any astronomical photograph. The means of twenty of the smallest images are about 0″55 and 0″6, respectively. An enlargement from the central region of one of these photographs is shown in Plate VI. An equal area in Selected Area No. 45, photographed on the same plate with the same exposure time, shows about sixty stars; hence most of the images in the illustration can definitely be assigned to the nebula.

Occasional patches, which show appreciable dimensions on plates made with smaller instruments, the 100-inch resolved into groups of stars, a few of which are surrounded by what appears to be true unresolved nebulosity. The knots listed as N.G.C. 588, 592, and 604 are conspicuous examples of this structure, and the last has long been recognized as such. The nature of the surrounding nebulosities has been inferred from the emission character of their spectra.

These results, it may be emphasized, were obtained with the highest resolving-power at present available. There is no longer any reason for retaining the term "nebulous stars" in referring to the condensations in Messier 33. They may be considered as actual stars and fit subjects for the ordinary methods of stellar research until evidence to the contrary is forthcoming.[1] This alone is an indication of immense distance, for no isolated system is known in which the brightest stars are dwarfs.

---

[1] Seed 30 plates were used in order to shorten the exposures and hence avoid changing conditions. It is probable that somewhat smaller images may occasionally be obtained by using plates having a finer grain. With longer exposures, the images of the condensations build up as those of ordinary stars even where both are superposed on an unresolved background. The sharper images of the short exposures, however, offer the more critical test. There are no indications whatsoever of penumbra appearing on long exposures, such as were described by Roberts and suggested by Ritchey.

## VARIABLE STARS IN MESSIER 33

In 1922 J. C. Duncan[2] announced the discovery of three variable stars within the area covered by Messier 33. His data were insufficient for determining the nature of the light-curves, and he refrained from suggesting any connection between the variables and the nebula. Shortly afterward, M. Wolf,[3] at Heidelberg, independently discovered the variability of the brightest of these stars.

The Mount Wilson collection now contains about eighty photographs of Messier 33. A survey of these with the blink-comparator has led to the discovery of forty-two additional variables, making a total of forty-five, besides two novae, within the area covered by the nebula. The similar concentrations of variables in Messier 31, the Magellanic Clouds, N.G.C. 6822, and in the globular star clusters, together with the scarcity of such faint variables in other regions of the sky,[4] especially in the high galactic latitudes of the spirals, sufficiently establish the variables under discussion as connected with the nebula itself.

---

[1] It is still uncertain how far the resolution can be carried. The stars become more numerous with decreasing luminosity and, in the central region at least, appear to merge smoothly into the unresolved background. The luminosity function for the three brightest magnitudes agrees very closely with Kapteyn's luminosity function for stars in the vicinity of the sun, and the total luminosity of the nebulae is completely accounted for on the assumption that the similarity between the two functions extends throughout the entire range of magnitude. In Messier 31, however, the large central region gives no indication of resolution, although portions of the outer regions of the arms are as clearly resolved as those in Messier 33.

[2] *Publications of the Astronomical Society of the Pacific*, 34, 290, 1922.

[3] *Astronomische Nachrichten*, **217**, 476, 1923. Duncan's paper was published in October, 1922. Wolf's paper was dated December 20, 1922, and published January 15, 1923. He does not mention Duncan's earlier announcement and hence, while there is no question of priority, Wolf's discovery may be accepted as independent.

[4] For ten fields well distributed in galactic latitude, other than those of the systems mentioned, there are in the Mount Wilson collection six or more plates showing stars fainter than 19.0 photographic magnitude. An examination of these with the blink-comparator has resulted in the detection of two doubtful cases of faint variables.

The stars are so closely crowded on photographs of the nebula that identification of the variables by the usual method of measures referred to the nucleus is unsatisfactory. They have, instead, been marked on the various plates and identified by numbers corresponding to those used in the text and tables.[1] Variables Nos. 1, 2, and 3 are those discovered by Duncan and bear the numbers assigned by him.

Series of comparison stars have been selected for each of the variables, and their photographic magnitudes have been derived from comparisons with Selected Area No. 45, which is conveniently situated some 30′ preceding the nucleus of the nebula. Twelve comparisons made with the 100-inch reflector were used in determining the scale and the zero-point. The exposures ranged from 20 to 40 minutes on Seed 30 plates, and were centered on various regions of the nebula in order to reduce uncertainties in the distance corrections. Two additional comparisons with Selected Area No. 21 furnished a satisfactory check.[2] The adopted magnitudes are based on those of the Selected Area down to about 18.5, but beyond this point they are extrapolations. The measures are very consistent, the average deviation of individual plates from the mean being less than 0.05 mag., and the greatest range for an individual star (on five plates), less than 0.4 mag. For stars in the central region fainter than about 19.0 the magnitudes are not reliable because of the background of unresolved nebulosity. In the other regions the measures are consistent to about 19.2, but beyond this they are, in general, unreliable.[3]

[1] The variables appear on the following plates: Plate IV, all variables excepting Nos. 12, 13, 20, 21, 22, 37; Plate V, variables Nos. 5, 9, 10, 11, 12, 13, 18, 20, 21, 22, 23, 24, 25, 37, 40; Plate VI, variables Nos. 14, 29, 30, 31, 32, 33, 41, 42, 43, 44, 45; and Plate VII, variables Nos. 11, 12, 17, 18, 20, 21, 23, 27, 29, 37.

[2] In addition to these long exposures, ten comparisons with Selected Area No. 45 were made with the 60-inch, using exposures ranging from two to fifteen minutes, for the purpose of deriving magnitudes for the stars brighter than the seventeenth magnitude. Mr. Seares kindly furnished unpublished magnitudes on the international scale for the stars in the Selected Areas.

[3] For a discussion of the uncertainties in extrapolated magnitudes based on measures with scale-plates of long exposures with the 100-inch reflector, see *Mt. Wilson Contr.*, No. 304; *Astrophysical Journal*, **62**, 409, 1926.

PLATE IV

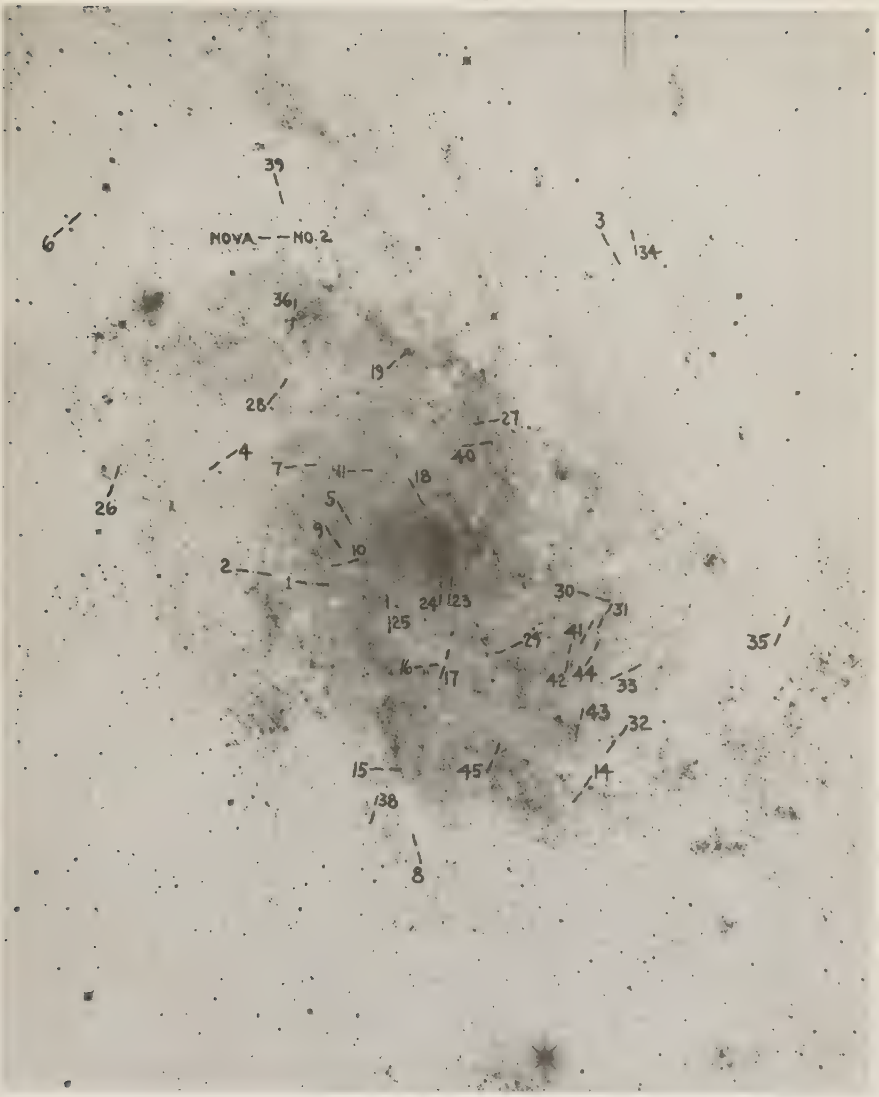

Negative Ri 115. Exposure 8.5 hours, Seed 23 plate, 60-inch reflector, August 5, 6, 7, 1910. Scale 1 mm = 14″.2. Nova No. 2 (1925) and all variables excepting Nos. 12, 13, 20, 21, 22, and 37 are marked.

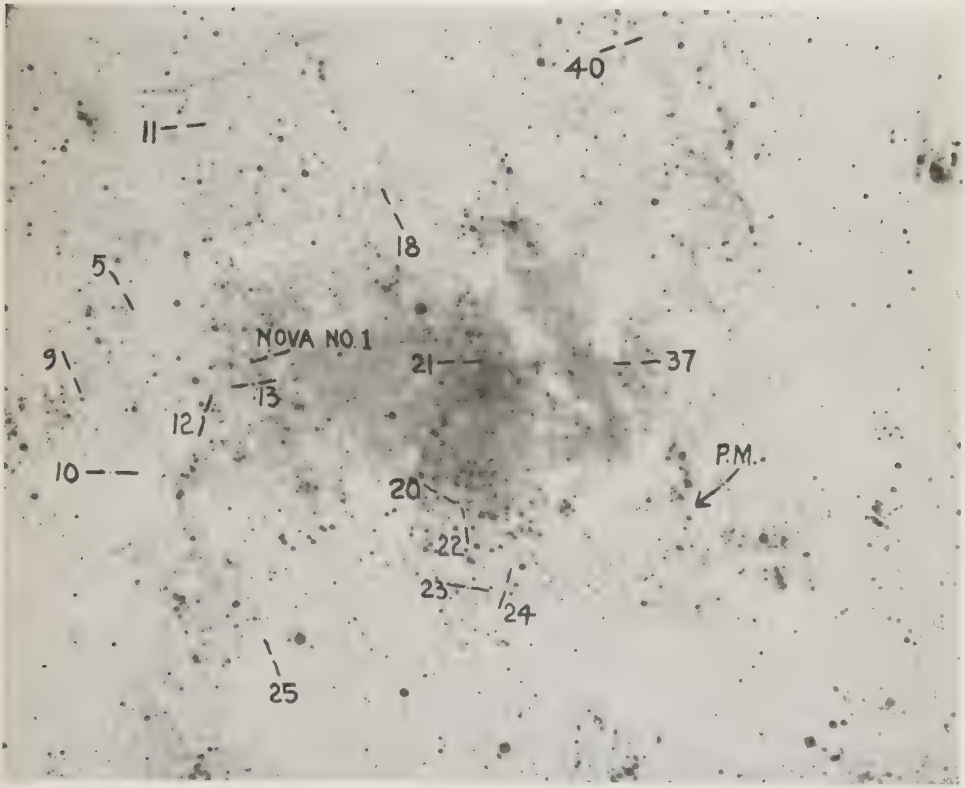

Negative H 584. Exposure 90 minutes, Seed 30 plate, 100-inch reflector, July 26, 1925. Scale 1 mm = 3″.8. Nova No. 1 (1919) and variables Nos. 5, 9, 10, 11, 12, 13, 18, 20, 21, 22, 23, 24, 25, 37, and 40 are marked. The star marked P.M., pg. mag. 18.25, is moving about 10″ per century in the direction of the arrow.

# PLATE VI

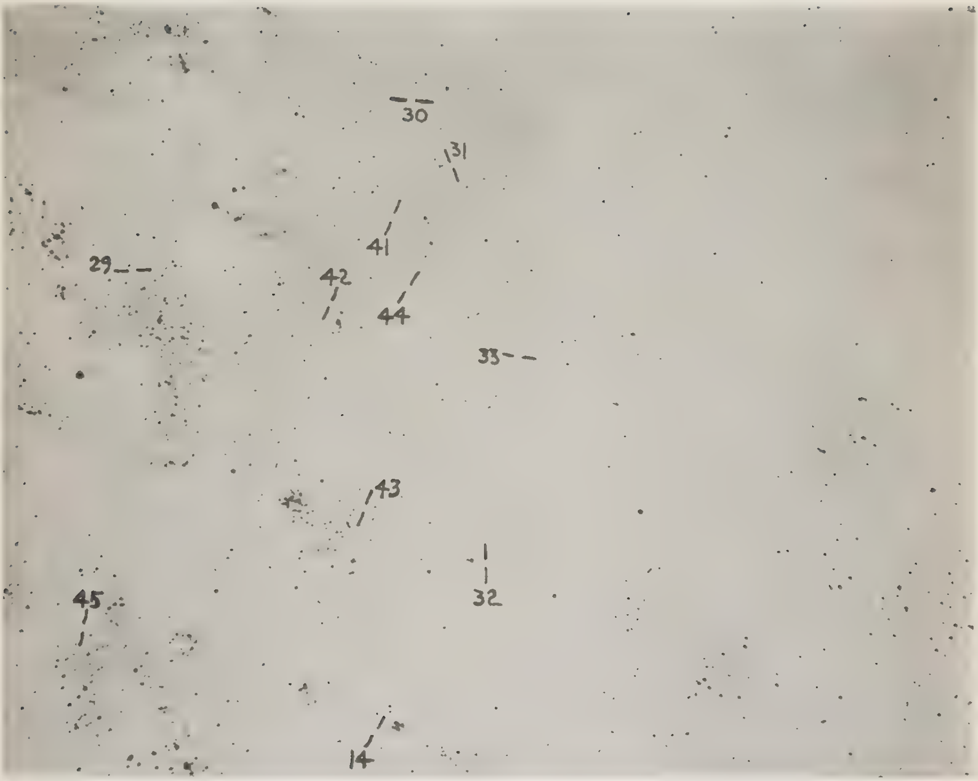

Negative H 485. Exposure 30 minutes, Seed 30 plate, 100-inch reflector, November 26, 1925; centered about 7′ south preceding the nucleus of Messier 33. Scale, 1 mm = 4″.3. Variables Nos. 14, 29, 30, 31, 32, 33, 41, 42, 43, 44, and 45 are marked. The mean diameter of the smallest star images is approximately 0″.5.

PLATE VII

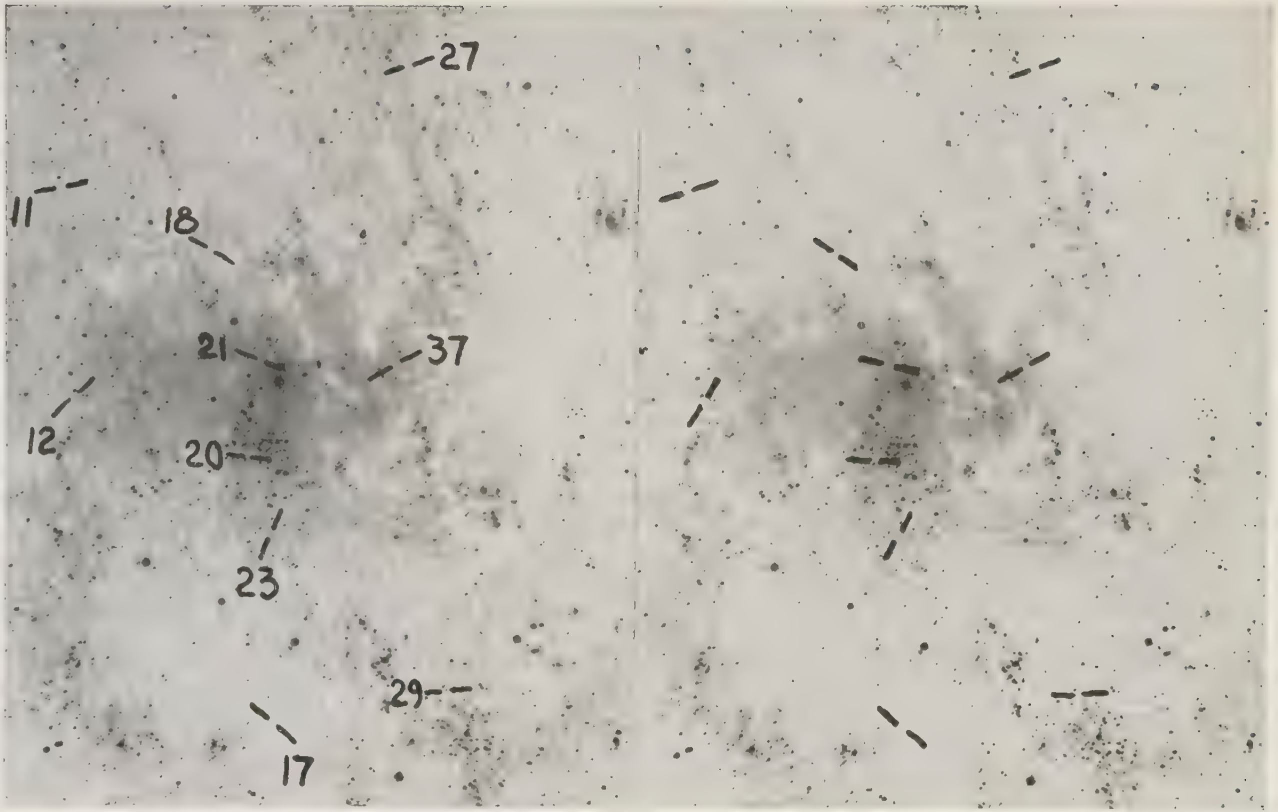

Light-Changes of Variables in Messier 33. Negatives H 440 (left) and H 475 (right), both made with the 100-inch reflector. Scale, 1 mm = 5″.2. All of the variables except No. 21 are Cepheids.

Magnitudes of variables on individual plates were estimated to the nearest tenth by reference to the sequences of comparison stars, the results being listed in Table I. A few of the stars, No. 21 in particular, are so involved with the unresolved nebulosity that the magnitudes have little or no meaning except at maximum. For most of the stars, however, it is believed that the data are sufficient to give fair values for the periods and the maximum magnitudes and some indications as to the general form of the light-curves. Magnitudes at minima, and hence the amplitudes of variation, are extremely uncertain. There are, in fact, several indications that the scale flattens out beyond about 19.0, and that the fainter magnitudes become increasingly too bright.

An examination of the data in Table I has established the nature of the variation of forty of the stars. Thirty-five are Cepheids, four are irregular, and one is very probably of an eclipsing type. Satisfactory solutions have not been found for the remaining five, but most of them are probably Cepheids.

## CEPHEID VARIABLES

The criteria used in determining Cepheid variation were: periods between two and one hundred days, amplitudes less than 2 mag., rapid brightening and slower fading, and no conspicuous secondary maxima. The limits for the first two of these are arbitrary, and, indeed, are more generous than necessary for the data under discussion. The maximum amplitude encountered is 1.2 mag., and the periods range from thirteen to seventy days.[1] The magnitudes at maximum range from 18.0 to 19.1. Minimum, and hence median, magnitudes are in general too uncertain for statistical discussion, but, although in several cases the minima are below the limits of the observations, there is no reason to suppose that any of the amplitudes approach the limiting value mentioned above.

In order to emphasize their Cepheid characteristics, several of the better-determined normal curves are illustrated in Figure 1.

---

[1] That some or all of the periods might be very close to one day, or some exact submultiple, was fully realized, and sufficient plates were obtained at different hour angles on the same night to eliminate this possibility. Each of the Cepheids was followed through several cycles after the period had been determined, and it is believed that the adopted elements are reliable.

## TABLE I

### PHOTOGRAPHIC MAGNITUDES OF VARIABLES IN MESSIER 33

| PLATE* | QUALITY | J.D.† | CEPHEIDS‡ | | | | | | |
|---|---|---|---|---|---|---|---|---|---|
| | | | 3 | 4 | 5 | 7 | 9 | 10 | 11 |
| R 15 | F | 18560.6 | 18.6 | 19.3 | 19.2 | 19.3 | 19.3 | 19.1 | 19.15 |
| 115 | E | 18890.6 | 18.3 | 19.3 | 19.4+ | 18.7 | 18.95 | 19.0 | 19.15 |
| D 34 | P | 22197.6 | 19.0 | 19.3 | 19.0 | 19.2 | 19.0 | 18.9 | 18.8 |
| P133 | F | 2307.4 | 18.45 | 19.3+ | 19.3+ | 19.2 | 18.8 | 19.15 | 19.2+ |
| 134 | P | 2311.4 | 18.45 | 19.0 | 19.3+ | 19.1 | 19.2 | 19.2 | 18.95 |
| 138 | G | 2314.4 | 18.7 | 18.1 | 18.8 | 18.75 | 19.3 | 19.2 | 18.75 |
| 139 | P | 2347.8 | 18.25 | 18.7 | 19.3 | 18.9 | 18.95 | 18.9 | 19.2 |
| D 48 | G | 2550.6 | 19.0 | 19.15 | 19.3+ | 19.3 | 18.7 | 18.8 | 18.85 |
| 83 | P | 2611.0 | 19.0 | 19.2+ | 19.2+ | 18.6 | ........ | ........ | ........ |
| 86 | F | 2612.5 | 18.95 | 19.3 | 19.3+ | 18.8 | 19.0 | 18.65 | 19.15 |
| 108 | P | 2669.4 | ........ | 18.1 | ........ | ........ | 19.0 | 19.15 | 18.9+ |
| 119 | F | 2694.3 | 18.95 | 19.3+ | 18.85 | ........ | 19.2+ | 18.5 | 18.9 |
| 130 | G | 2698.3 | 19.1 | 18.2 | 19.3 | 19.2 | 19.3 | 18.95 | ........ |
| 198 | G | 2903.2 | 18.9 | 19.3 | 19.3+ | 18.85 | 19.3 | 18.9 | 18.8 |
| 205 | G | 2907.2 | 18.9 | 19.15 | 19.4+ | 18.85 | 19.3 | 18.95 | 19.0 |
| A 4 | F | 2966.5 | 19.2 | ........ | ........ | 19.1+ | 18.75 | 18.65 | 18.95 |
| 8 | G | 3000.4 | 19.1 | 18.1 | 18.85 | 19.2 | 19.3 | 19.15 | 19.3 |
| 40 | G | 3319.6 | 19.0 | 19.15 | 19.3 | 19.3 | 19.3 | 18.7 | 18.8 |
| B 65 | G | 3322.1 | 19.0 | 19.4 | 18.85 | 19.1 | 19.3 | 18.95 | 18.9 |
| M335 | G | 3344.5 | 18.9 | 19.2+ | 19.3+ | 19.15 | 18.7 | 19.1 | 18.9 |
| H417 | E | 4004.7 | 19.3 | 19.4 | 19.3+ | 19.3 | 18.9 | 18.5 | 19.1 |
| D239 | G | 4024.6 | 18.8 | 19.3 | 19.1 | 19.15 | 18.65 | 19.0 | 18.9 |
| 245 | G | 4025.6 | 18.9 | 19.3 | 19.2 | 19.2 | 18.75 | 18.9 | 18.9 |
| S354 | F | 4026.6 | 18.85 | 19.3 | 19.1+ | 19.3 | 18.9 | 18.95 | 18.95 |
| 357 | F | 4027.6 | 18.9 | 19.3 | 19.1+ | 19.2+ | 19.0+ | 18.95 | 18.9+ |
| 363 | G | 4030.6 | 19.1 | 19.2+ | 19.1+ | 19.3 | 19.2 | 19.1 | 19.0 |
| H422 | G | 4031.6 | 19.1 | 19.4 | 19.3+ | 19.2 | 19.3 | 19.0 | 19.15 |
| 428 | F | 4033.6 | 19.0 | 19.4+ | 19.4+ | 19.2 | 19.3 | 19.0 | 19.15 |
| S367 | P | 4049.6 | 19.1 | 19.0 | ........ | 18.9 | ........ | ........ | 18.85 |
| 373 | P | 4050.6 | 19.2 | 19.2 | 19.1 | 19.1 | ........ | 19.15 | 18.9 |
| H433 | F | 4054.6 | 18.35 | 19.3+ | 18.9 | 19.1 | 19.1+ | 19.1 | 19.0 |
| S375 | F | 4055.6 | 18.45 | 19.25 | 19.05 | 19.3 | 19.3 | 19.15 | 19.1 |
| 383 | F | 4056.5 | 18.4 | 19.3 | 19.1+ | 19.2 | ........ | 19.1 | 19.0 |
| H441 | F | 4058.5 | 18.45 | 19.25 | 19.1+ | 18.9+ | ........ | ........ | ........ |
| 446 | E | 4059.5 | 18.45 | 19.15 | 19.25 | 19.2 | 19.0 | 19.15 | 19.15 |
| 452 | P | 4085.5 | 19.3 | 19.5 | 19.2+ | 19.2 | 18.95 | 18.7 | 19.2+ |
| S399 | P | 4089.5 | 19.2 | 19.3 | 19.1+ | 19.3+ | 19.0+ | 18.85 | 19.1+ |
| H458 | F | 4090.5 | 19.3 | 19.0 | 19.3+ | 19.3+ | 19.3 | 18.85 | 18.9 |
| 465 | F | 4092.5 | 19.2 | 18.4 | 19.1+ | 18.8+ | 19.3 | 18.95 | 18.85 |
| 467 | F | 4108.4 | 18.6 | 19.4 | 19.3 | 19.3 | 19.1 | 19.0 | 19.2 |
| 472 | F | 4109.4 | 18.65 | 19.5 | 19.2 | 19.2 | 19.4+ | 19.0 | 19.3+ |
| S407 | F | 4113.4 | 18.7 | 19.3 | 19.1+ | 19.3 | 19.0+ | 19.15 | 19.15 |
| H475 | E | 4115.4 | 18.75 | 19.35 | 19.3 | 19.2 | 19.3 | 19.15 | 19.0 |
| 486 | E | 4116.3 | 19.0 | 19.3 | 19.3 | 19.3 | 19.0 | ........ | 18.75 |
| 503 | F | 4147.3 | 18.8 | 18.45 | 19.3+ | 18.6 | 19.2 | 18.6 | 19.1 |
| 509 | G | 4149.3 | 18.8 | 18.6 | 19.2+ | 18.7 | 19.2 | 18.6 | 19.0+ |
| 517 | F | 4171.3 | 19.1 | 19.15 | 19.2 | 19.2 | 19.3 | 18.95 | 19.0 |
| 577 | G | 4348.6 | 18.3 | 19.4 | 19.2 | 19.2 | 18.9 | 18.95 | 19.1 |
| D253 | F | 4351.6 | 18.4 | 19.4 | 19.2 | 19.2 | 19.0 | 18.7 | 18.9 |
| H584 | E | 4357.6 | 18.6 | 19.5 | 19.1 | 19.2 | 19.3 | 18.55 | 19.0 |
| S497 | P | 4358.6 | 18.65 | ........ | 18.9 | ........ | ........ | ........ | ........ |
| H588 | G | 4377.6 | 19.3 | 19.1 | 19.1 | 19.15 | 19.3 | 18.95 | 18.8 |
| 593 | G | 4378.6 | 19.3 | 19.25 | 19.2 | 19.2 | 19.3 | 18.95 | 18.9 |
| 600 | G | 4379.6 | ........ | 19.3+ | ........ | ........ | ........ | ........ | 18.9 |
| D277 | E | 4384.6 | 19.2 | 19.4 | 19.4 | 18.9 | 18.7 | 19.0 | 19.25 |
| 288 | E | 4387.6 | 18.45 | 19.5 | 18.8 | 18.6 | 18.9 | 19.1 | 19.2 |
| H606 | P | 4405.5 | 18.85 | 19.1 | 19.3 | 19.2 | 18.75 | 19.05 | 19.0 |
| 611 | G | 4414.5 | 19.1 | 19.35 | 19.25 | 18.6 | 19.4 | 18.85 | 19.2+ |

---

* The prefixed letters refer to the observers: R = Ritchey, D = Duncan, P = Pease, A and B = Humason, M = van Maanen, S and H = Hubble.

† Add 2,400,000 to the first three dates, and 2,420,000 to the others. The decimal indicates Pacific Mean Time. In order to conform to the change to Civil Day Time, 0.5 must be added to each date.

‡ A plus sign following a magnitude indicates that the variable was invisible, but certainly fainter than the value indicated.

TABLE I—*Continued*

| Plate | Quality | J.D. | Cepheids | | | | | | |
|---|---|---|---|---|---|---|---|---|---|
| | | | 12 | 16 | 17 | 18 | 19 | 20 | 22 |
| R 15 | F | 18560.6 | 19.0+ | 19.0 | 18.95 | 18.8 | 18.1 | B | ........ |
| 115 | E | 18890.6 | 19.0 | 18.8 | 19.2 | 18.55 | 18.2 | 18.55 | 19.4 |
| D 34 | P | 22197.6 | ........ | 18.7 | 19.15 | 18.75 | 18.9 | ........ | ........ |
| P133 | F | 2307.4 | 19.2+ | 19.2 | 19.4+ | 19.05 | 18.7 | 18.65 | 19.1 |
| 134 | P | 2311.4 | 19.0 | 19.2 | 18.75 | 19.05 | 18.7 | 18.75 | 19.3 |
| 138 | G | 2314.4 | 18.6 | 19.3+ | 18.95 | 19.05 | 18.7 | 18.9 | 19.2+ |
| 139 | P | 2347.8 | 19.2+ | 19.2 | 19.4+ | 19.05 | 18.7 | 18.75 | ........ |
| D 48 | G | 2550.6 | ........ | 19.1 | 19.4 | 19.0 | 18.1 | B | 19.1+ |
| 83 | P | 2611.0 | ........ | ........ | ........ | ........ | 18.4 | ........ | ........ |
| 86 | F | 2612.5 | 19.2+ | 19.3 | 19.4 | 18.95 | 18.35 | ........ | ........ |
| 108 | P | 2669.4 | ........ | ........ | 19.2+ | 18.7 | 18.5 | ........ | ........ |
| 119 | F | 2694.3 | 19.2+ | 19.2+ | 19.2+ | 18.7 | 18.8 | ........ | 18.85 |
| 130 | G | 2698.3 | 19.2+ | 19.3 | 19.4+ | 18.55 | 18.6 | 18.4 | 19.0 |
| 198 | G | 2903.2 | 18.9 | 19.3 | 19.4+ | 18.65 | 18.8 | 18.9 | 19.1+ |
| 205 | G | 2907.2 | 19.3+ | 19.3 | 19.4 | 18.8 | 18.7 | 18.85 | 19.3+ |
| A 4 | F | 2966.5 | 18.8 | 18.75 | 19.1 | 18.7 | 18.85 | 18.9 | 19.2+ |
| 8 | G | 3000.4 | 19.4 | 18.8 | 19.4 | 18.7 | 18.5 | 19.0 | 19.0 |
| 40 | G | 3319.6 | 19.4 | 19.1 | 19.2 | 18.75 | 18.4 | 19.0 | 19.3+ |
| B 65 | G | 3322.1 | 19.3 | 19.3 | 19.4 | 18.8 | 18.4 | 18.9 | 19.4 |
| M335 | G | 3344.5 | 19.4 | 19.4 | 19.4 | 18.5 | 18.8 | 18.3 | 19.4 |
| H417 | E | 4004.7 | 18.6 | 19.3 | 19.4+ | 18.9 | 18.7 | 19.0 | 18.9 |
| D239 | G | 4024.6 | 18.6 | 19.2 | 19.4 | 18.5 | 18.0 | 18.2 | 18.95 |
| 245 | G | 4025.6 | 18.6 | 19.2 | 19.4+ | 18.55 | 18.2 | 18.3 | 18.9 |
| S354 | F | 4026.6 | ........ | 19.2+ | 19.4+ | 18.6 | 18.1 | ........ | ........ |
| 357 | F | 4027.6 | 18.75 | 19.0+ | 19.2+ | 18.7 | 18.3 | ........ | ........ |
| 363 | G | 4030.6 | 18.9 | 19.1+ | 19.4+ | 18.75 | 18.35 | 18.6 | ........ |
| H422 | G | 4031.6 | 19.1 | 19.2 | 19.4+ | 18.75 | 18.35 | 18.6 | 19.2 |
| 428 | F | 4033.6 | 19.1 | 18.6 | 19.4+ | 18.8 | 18.4 | 18.65 | 19.3 |
| S367 | P | 4049.6 | ........ | ........ | 19.3+ | ........ | 18.85 | ........ | ........ |
| 373 | P | 4050.6 | ........ | 18.7 | 19.4+ | ........ | 18.8 | ........ | ........ |
| H433 | F | 4054.6 | 19.3+ | 19.05 | 19.4+ | 18.9 | 18.7 | 18.9+ | 19.3 |
| S375 | F | 4055.6 | ........ | 19.1 | 19.4+ | 18.75 | 18.8 | 18.9+ | 19.3 |
| 383 | F | 4056.5 | ........ | 19.1 | 19.4+ | 18.5 | 18.7 | ........ | 19.3 |
| H441 | F | 4058.5 | 19.3+ | ........ | 18.75 | 18.45 | 18.7 | ........ | ........ |
| 446 | E | 4059.5 | 19.4 | 19.2 | 18.75 | 18.55 | 18.75 | 18.6 | 19.35 |
| 452 | P | 4085.5 | 19.1+ | 18.8 | 19.15 | 19.0 | 18.25 | 19.0 | 19.3+ |
| S399 | P | 4089.5 | 18.9 | 19.0+ | 19.1+ | ........ | 18.35 | ........ | ........ |
| H458 | F | 4090.5 | 18.6 | 19.1 | 19.3 | 19.55 | 18.3 | 19.1 | 18.9 |
| 465 | F | 4092.5 | ........ | 19.2+ | 19.3+ | 18.5 | 18.45 | 19.1 | 19.05 |
| 467 | F | 4108.4 | 19.3+ | 19.05 | 19.0 | 19.0 | 18.7 | 18.65 | 19.2+ |
| 472 | F | 4109.4 | 19.3 | 19.2 | 19.15 | 18.9 | 18.7 | 18.85 | 19.4 |
| S407 | F | 4113.4 | ........ | 19.2+ | 19.4+ | ........ | 18.8 | ........ | ........ |
| H475 | E | 4115.4 | 18.95 | 19.5 | 19.4+ | 19.0 | 18.7 | 19.0 | 19.05 |
| 486 | E | 4116.3 | 19.1 | 19.4 | 19.4 | 19.05 | 18.7 | 19.0 | 19.1 |
| 503 | F | 4147.3 | 19.1+ | 19.2 | ........ | 19.1 | 18.45 | ........ | ........ |
| 509 | G | 4149.3 | 19.4 | 19.2 | 19.4+ | 19.1 | 18.55 | 18.9 | 19.4 |
| 517 | F | 4171.3 | 19.4 | 19.2 | ........ | 18.8 | 18.65 | 18.2 | 19.4 |
| 577 | G | 4348.6 | 19.3+ | 18.7 | 19.3+ | 19.1 | 18.0 | 18.1 | 19.4 |
| D253 | F | 4351.6 | 18.8 | 18.85 | 19.4+ | 19.1 | 18.1 | 18.45 | 19.1 |
| H584 | E | 4357.6 | 19.1 | 19.4 | 19.45 | 19.0 | 18.3 | 18.6 | 19.2 |
| S497 | P | 4358.6 | ........ | ........ | ........ | ........ | 18.15 | ........ | ........ |
| H588 | G | 4377.6 | 19.1 | 19.4 | 19.4+ | 18.85 | 18.7 | 19.0 | 19.2 |
| 593 | G | 4378.6 | 19.1 | 19.4 | 19.4+ | 18.9 | 18.8 | 19.0 | 19.2 |
| 600 | G | 4379.6 | 19.1+ | 19.4 | ........ | ........ | 18.8 | 19.0 | ........ |
| D277 | E | 4384.6 | 19.1+ | 18.75 | 18.8 | 18.9 | 18.7 | 18.3 | 19.5 |
| 288 | E | 4387.6 | 19.4 | 19.2 | 19.0 | 18.9 | 18.7 | 18.4 | 19.4 |
| H606 | P | 4405.5 | 19.1+ | 19.1 | 19.4+ | 18.75 | 18.0 | ........ | ........ |
| 611 | G | 4414.5 | 18.8 | 19.4+ | 19.1 | 18.9 | 18.2 | 19.0 | 19.35 |

TABLE I—*Continued*

| Plate | Quality | J.D. | Cepheids | | | | | | |
|---|---|---|---|---|---|---|---|---|---|
| | | | 23 | 24 | 25 | 26 | 27 | 28 | 29 |
| R 15 | F | 18560.6 | ........ | ........ | ........ | 19.2 | 19.05 | 19.6 | 18.8 |
| 115 | E | 18890.6 | 18.95 | 19.3 | 19.3 | 19.6 | 19.3 | 19.7 | 19.2 |
| D 34 | P | 22197.6 | ........ | ........ | ........ | 19.4+ | 19.2 | 19.5+ | 19.0 |
| P133 | F | 2307.4 | 19.15 | 19.3 | ........ | 19.4+ | 19.0 | 19.6+ | 19.25 |
| 134 | P | 2311.4 | ........ | ........ | 19.6+ | 19.5+ | 19.1 | 19.6+ | 19.2+ |
| 138 | G | 2314.4 | 19.3 | 18.8 | 19.6+ | 19.4+ | 19.2 | 18.85 | 19.3 |
| 139 | P | 2347.8 | 19.2+ | 19.4+ | 19.4 | 19.1 | 19.2 | 19.6+ | 19.3 |
| D 48 | G | 2550.6 | 19.2+ | 19.4 | 19.3 | 19.4+ | 18.75 | 19.5+ | 18.5 |
| 83 | P | 2611.0 | ........ | ........ | ........ | ........ | ........ | 18.8 | 19.2+ |
| 86 | F | 2612.5 | 19.2+ | 19.1 | 19.4 | 19.5+ | 19.3 | 19.1 | 19.3 |
| 108 | P | 2669.4 | ........ | ........ | ........ | ........ | ........ | ........ | ........ |
| 119 | F | 2694.3 | ........ | ........ | 18.85 | ........ | ........ | ........ | 19.2 |
| 130 | G | 2698.3 | 19.2+ | 19.4+ | 19.3 | 19.4 | 19.2 | 19.5+ | 19.1 |
| 198 | G | 2903.2 | 19.3 | ........ | 19.5+ | 19.4 | 19.2 | 19.7 | 18.6 |
| 205 | G | 2907.2 | 19.0 | 19.2 | 19.5+ | 19.2 | 19.3 | 19.6+ | 19.3 |
| A 4 | F | 2966.5 | 19.2+ | ........ | 19.2 | ........ | 19.2 | ........ | 19.3 |
| 8 | G | 3000.4 | 18.85 | 19.3 | 19.7 | 19.35 | 18.7 | 19.6 | 19.1 |
| 40 | G | 3319.6 | 19.4+ | 19.1 | ........ | 19.2+ | 19.2 | 19.1 | 19.1 |
| B 65 | G | 3322.1 | 19.4 | 18.9 | 19.6+ | 19.2 | 19.3 | 19.6 | 19.1 |
| M335 | G | 3344.5 | 19.3+ | 19.3+ | 19.5+ | ........ | 19.1 | ........ | 19.3 |
| H417 | E | 4004.7 | 19.0 | 19.05 | 19.5+ | 19.5 | 19.4 | 19.5 | 18.7 |
| D239 | G | 4024.6 | 19.3 | 19.4+ | 19.1 | 19.4 | 19.3 | 18.75 | 19.3 |
| 245 | G | 4025.6 | 19.4 | 19.4+ | 19.15 | 19.3 | 19.3 | 19.0 | 19.3 |
| S354 | F | 4026.6 | ........ | ........ | ........ | 19.5+ | 19.3 | 19.3 | 19.2+ |
| 357 | F | 4027.6 | ........ | ........ | ........ | ........ | ........ | 19.5 | ........ |
| 363 | G | 4030.6 | ........ | ........ | ........ | 19.4+ | 19.2 | 19.5+ | 19.2+ |
| H422 | G | 4031.6 | 18.8 | 19.1 | 19.5+ | ........ | 19.2 | ........ | 19.3 |
| 428 | F | 4033.6 | 19.1 | 19.2 | 19.5+ | 19.4+ | 18.7 | 19.5+ | 19.3 |
| S367 | P | 4049.6 | ........ | ........ | 19.3 | 19.4+ | ........ | 19.5+ | ........ |
| 373 | P | 4050.6 | ........ | ........ | 19.1 | 19.4+ | ........ | 19.6+ | ........ |
| H433 | F | 4054.6 | ........ | ........ | ........ | ........ | 18.75 | ........ | 19.2 |
| S375 | F | 4055.6 | ........ | ........ | 19.45 | 19.6+ | 18.7 | 19.7 | 19.2 |
| 383 | F | 4056.5 | ........ | ........ | ........ | 19.4+ | 18.75 | 19.6+ | 19.3 |
| H441 | F | 4058.5 | ........ | ........ | ........ | ........ | ........ | ........ | ........ |
| 446 | E | 4059.5 | 19.0 | 19.35 | 19.6 | 19.4+ | 19.1 | 19.5+ | 19.3 |
| 452 | P | 4085.5 | 18.85 | 19.4 | 19.6 | 19.4+ | 19.3+ | 19.5+ | 19.1 |
| S399 | P | 4089.5 | ........ | ........ | ........ | 19.1 | 19.2+ | 19.6+ | 19.2 |
| H458 | F | 4090.5 | 19.3 | 19.4+ | 19.4 | 19.0 | 19.2 | 19.6+ | 19.2+ |
| 465 | F | 4092.5 | 19.2+ | 19.2 | 18.9 | 19.1 | 19.3 | ........ | 19.2+ |
| 467 | F | 4108.4 | 19.4 | 19.2 | 19.4+ | 19.4+ | 19.0 | 19.5+ | 19.3 |
| 472 | F | 4109.4 | 19.4 | ........ | ........ | 19.4+ | 19.25 | 19.5+ | 19.2 |
| S407 | F | 4113.4 | 18.7 | ........ | ........ | 19.2 | ........ | 19.5+ | 18.5 |
| H475 | E | 4115.4 | 19.2 | 19.5 | 19.7 | 19.2 | 19.3 | 19.6 | 18.7 |
| 486 | E | 4116.3 | 19.25 | 19.4+ | 19.4 | 19.1 | 19.2+ | 18.9 | 18.75 |
| 503 | F | 4147.3 | 19.4 | 19.2 | 19.4 | 19.4+ | 18.9 | 19.5+ | 18.65 |
| 509 | G | 4149.3 | 19.4 | 19.2 | 19.4 | ........ | 19.0 | ........ | 18.6 |
| 517 | F | 4171.3 | 19.4+ | 18.85 | 18.85 | 19.4+ | 18.95 | 19.5+ | 19.3 |
| 577 | G | 4348.6 | 19.4+ | 19.4+ | 19.35 | 19.2 | 18.9 | 19.5+ | 19.2 |
| D253 | F | 4351.6 | 19.2+ | 18.8 | 19.4+ | 19.4+ | 19.1 | 19.5+ | 19.3 |
| H584 | E | 4357.6 | 18.8 | 19.4 | 19.7 | 19.6 | 19.25 | 19.1 | 19.3 |
| S497 | P | 4358.6 | ........ | ........ | ........ | 19.4+ | ........ | 18.9 | ........ |
| H588 | G | 4377.6 | 19.4 | 18.95 | 19.5+ | 19.4+ | 19.2 | 19.0 | 19.0 |
| 593 | G | 4378.6 | 19.4 | 18.95 | 19.5+ | 19.4+ | ........ | 19.0 | 19.0 |
| 600 | G | 4379.6 | 19.3+ | ........ | ........ | 19.4+ | 19.0+ | 19.3 | 19.1 |
| D277 | E | 4384.6 | 18.95 | 19.5+ | 19.6 | 19.6+ | 19.3 | 19.7+ | 19.2 |
| 288 | E | 4387.6 | 19.25 | 19.5+ | 18.9 | 19.6+ | 19.2 | 19.7 | 19.35 |
| H606 | P | 4405.5 | 19.0+ | 18.9 | ........ | 19.4+ | ........ | 19.5+ | 18.65 |
| 611 | G | 4414.5 | 19.0+ | 19.2+ | 18.9 | 19.1 | 18.7 | 18.85 | 19.2 |

TABLE I—*Continued*

| Plate | Quality | J.D. | Cepheids | | | | | | |
|---|---|---|---|---|---|---|---|---|---|
| | | | 30 | 31 | 33 | 34 | 35 | 36 | 37 |
| R 15 | F | 18560.6 | 18.9 | 18.3 | ........ | 19.4 | 19.4 | 18.85 | ........ |
| 115 | E | 18890.6 | 19.1 | 19.3 | 19.7+ | 19.1 | 19.2 | 19.1 | 19.4+ |
| D 34 | P | 22197.6 | 18.7 | 19.3 | ........ | 19.2 | ........ | 19.0 | ........ |
| P133 | F | 2307.4 | 19.15 | 19.0 | 19.3 | 19.2 | 19.2 | 18.8 | ........ |
| 134 | P | 2311.4 | ........ | 19.1 | 19.7 | 19.3 | 19.3 | 18.45 | 19.4+ |
| 138 | G | 2314.4 | 19.2 | 19.15 | 19.5+ | 19.4 | 19.3 | 18.65 | 19.5+ |
| 139 | P | 2347.8 | 19.15 | 19.15 | 19.3+ | 19.1 | 19.4 | 18.65 | ........ |
| D 48 | G | 2550.6 | 19.1 | 19.15 | 18.8 | 19.0 | 19.3 | 19.1 | ........ |
| 83 | P | 2611.0 | 18.6 | ........ | ........ | 18.9 | 19.4 | 19.0 | ........ |
| 86 | F | 2612.5 | 18.9 | 19.15 | ........ | 18.95 | 19.45 | 19.0 | ........ |
| 108 | P | 2669.4 | ........ | ........ | ........ | ........ | ........ | ........ | ........ |
| 119 | F | 2694.3 | 18.3 | 19.15 | ........ | 18.75 | 18.7 | 19.0 | 19.2+ |
| 130 | G | 2698.3 | 18.45 | ........ | 19.5 | 18.85 | 18.9 | 19.0 | ........ |
| 198 | G | 2903.2 | 19.15 | 19.0 | 19.3+ | 19.3 | 18.65 | 19.0 | 19.3+ |
| 205 | G | 2907.2 | 19.15 | 19.0 | 19.7 | 19.3 | 18.7 | 19.0 | 19.5+ |
| A 4 | F | 2966.5 | 18.65 | 18.2 | 19.4 | ........ | 18.7 | 19.0 | 19.05 |
| 8 | G | 3000.4 | 19.15 | 18.35 | 18.75 | 19.4 | 18.9 | 18.75 | 19.4+ |
| 40 | G | 3319.6 | 19.15 | 19.0 | 19.7+ | 18.85 | 19.2+ | 18.7 | 18.75 |
| B 65 | G | 3322.1 | 19.15 | 19.3 | 19.7+ | 19.2 | 19.4 | 18.8 | 19.0 |
| M335 | G | 3344.5 | 18.5 | 18.5 | 19.7+ | 19.1 | 19.2+ | 19.1 | 19.4 |
| H417 | E | 4004.7 | 19.1 | 19.2 | 18.75 | 18.75 | 18.8 | 18.8 | 19.1 |
| D239 | G | 4024.6 | 18.8 | 19.0 | 19.5 | 18.55 | 19.4+ | 18.9 | 19.0 |
| 245 | G | 4025.6 | 18.45 | 19.15 | 18.75 | 18.6 | 19.4+ | 18.8 | 19.0 |
| S354 | F | 4026.6 | 18.3 | 19.15 | ........ | 18.6 | 19.4 | 18.8 | ........ |
| 357 | F | 4027.6 | 18.3 | 19.15 | ........ | ........ | ........ | 18.7 | ........ |
| 363 | G | 4030.6 | 18.5 | 19.2 | 19.1+ | 19.2 | 18.8 | 18.55 | 19.3 |
| H422 | G | 4031.6 | 18.4 | 19.2 | 19.2 | 19.1+ | 18.65 | 18.5 | 19.5 |
| 428 | F | 4033.6 | 18.45 | 19.1 | 19.5+ | 19.0 | 18.65 | 18.5 | 19.4 |
| S367 | P | 4049.6 | 19.1 | 18.3 | ........ | 18.6 | ........ | 19.0 | 19.1+ |
| 373 | P | 4050.6 | ........ | 18.4 | ........ | 18.6 | 19.2+ | 19.0 | ........ |
| H433 | F | 4054.6 | 19.1 | 18.4 | ........ | ........ | ........ | 19.0 | 19.3+ |
| S375 | F | 4055.6 | 19.1 | 18.45 | 19.7+ | 19.1 | 19.5 | 19.1 | 19.1+ |
| 383 | F | 4056.5 | 19.2 | 18.55 | 19.3+ | 19.2 | 19.2+ | 19.0 | 19.3+ |
| H441 | F | 4058.5 | ........ | ........ | ........ | ........ | ........ | ........ | 18.95 |
| 446 | E | 4059.5 | 19.15 | 18.95 | 19.7+ | 19.5 | 19.2 | 19.1 | 18.85 |
| 452 | P | 4085.5 | 18.9 | 18.2 | 19.6+ | 19.4 | 19.4+ | 19.0 | 19.3+ |
| S399 | P | 4089.5 | 19.0 | 18.4 | ........ | 19.1 | 19.2 | 19.0 | 19.2+ |
| H458 | F | 4090.5 | 19.1 | 18.45 | 18.9 | 18.75 | 19.1 | 19.0 | 19.3+ |
| 465 | F | 4092.5 | 19.1 | 18.8 | 19.4 | 18.6 | 18.6 | ........ | 19.35 |
| 467 | F | 4108.4 | 19.2 | 19.1 | 18.75 | 19.3 | 19.3 | 18.65 | 19.3 |
| 472 | F | 4109.4 | 19.25 | 19.2 | 18.9 | 19.4 | 19.4+ | 18.7 | 19.4+ |
| S407 | F | 4113.4 | 19.15 | 19.2 | 19.1+ | 18.55 | 19.45 | 19.0 | ........ |
| H475 | E | 4115.4 | 18.95 | 19.2 | 19.7 | 18.6 | 19.45 | 19.0 | 19.0 |
| 486 | E | 4116.3 | 18.8 | 19.3 | 19.5 | 18.75 | 19.45 | 19.0 | 19.0 |
| 503 | F | 4147.3 | 19.2 | 19.3 | 19.5 | 19.2 | ........ | 18.8 | 18.85 |
| 509 | G | 4149.3 | 19.2 | 19.15 | 19.0 | 19.2 | ........ | 18.8 | 19.0 |
| 517 | F | 4171.3 | 18.5 | 18.85 | 19.1 | 19.2 | 19.4 | 18.5 | 19.3+ |
| 577 | G | 4348.6 | 18.3 | 18.3 | 19.3+ | 19.3 | 19.2 | 18.7 | 19.2+ |
| D253 | F | 4351.6 | 18.45 | 18.5 | 19.3 | 19.3 | 19.2 | 18.7 | 19.3+ |
| H584 | E | 4357.6 | 18.5 | 18.85 | 19.1 | 18.45 | 19.2 | 18.6 | 18.9 |
| S497 | P | 4358.6 | ........ | ........ | ........ | 18.5 | ........ | 18.6 | ........ |
| H588 | G | 4377.6 | 19.2 | 19.2 | 19.0 | 19.2 | 19.0 | 19.0 | 18.9 |
| 593 | G | 4378.6 | 19.25 | 19.15 | 19.1 | 18.7 | ........ | 19.0 | 18.9 |
| 600 | G | 4379.6 | 19.2 | ........ | 19.2 | ........ | ........ | 19.1 | 19.2 |
| D277 | E | 4384.6 | 19.25 | 18.2 | 19.7 | 18.9 | 19.4 | 18.6 | 19.3 |
| 288 | E | 4387.6 | 19.25 | 18.5 | 19.8+ | 19.15 | 19.3 | 18.45 | 19.5 |
| H606 | P | 4405.5 | 18.9 | 19.1 | 19.3+ | 18.7 | 18.9 | 19.0 | ........ |
| 611 | G | 4414.5 | 19.0 | 19.3 | 19.0 | 19.2 | 19.4 | 19.1 | 19.05 |

TABLE I—*Continued*

| PLATE | QUALITY | J.D. | CEPHEIDS | | | | | | |
|---|---|---|---|---|---|---|---|---|---|
| | | | 38 | 39 | 40 | 41 | 42 | 43 | 44 |
| R 15 | F | 18560.6 | 18.7 | 19.2 | 19.1+ | 19.1 | 18.45 | 18.8 | ........ |
| 115 | E | 18890.6 | 19.1 | 19.5 | 19.2 | 19.25 | 19.0 | 19.3 | 19.2 |
| D 34 | P | 22197.6 | 18.8 | 19.1+ | 19.1 | ........ | ........ | ........ | ........ |
| P133 | F | 2307.4 | 19.1 | 19.1 | 19.4+ | 19.2 | 18.9 | 19.6 | 19.4 |
| 134 | P | 2311.4 | 18.2 | 19.3 | 19.0 | 18.7 | 19.0 | 18.7 | 19.2 |
| 138 | G | 2314.4 | 18.5 | 19.2+ | 19.3 | 19.1 | 19.0 | 18.95 | 18.6 |
| 139 | P | 2347.8 | 19.1 | 19.2+ | 19.4+ | 18.7 | 19.0 | 19.4+ | 19.1 |
| D 48 | G | 2550.6 | 19.1 | 19.1 | 19.3+ | 19.25 | 19.0 | 19.6 | 19.4 |
| 83 | P | 2611.0 | 18.6 | 18.9 | ........ | ........ | ........ | ........ | ........ |
| 86 | F | 2612.5 | 18.3 | 18.8 | 19.35 | 19.3 | 18.9 | 19.6 | ........ |
| 108 | P | 2669.4 | ........ | ........ | ........ | ........ | ........ | ........ | ........ |
| 119 | F | 2694.3 | 18.6 | ........ | 19.4+ | 19.2 | 18.8 | 19.15 | ........ |
| 130 | G | 2698.3 | 19.1 | 19.0+ | 19.3+ | 19.25 | 18.8 | 18.7 | 19.4 |
| 198 | G | 2903.2 | 18.95 | 18.8 | 19.4 | 19.1 | 18.6 | 19.4 | 19.3 |
| 205 | G | 2907.2 | 19.1 | 19.3 | 18.9 | 18.75 | 18.7 | 19.7 | 19.35 |
| A 4 | F | 2966.5 | 18.6 | ........ | 19.4+ | 19.25 | 18.8 | 19.4 | 19.2 |
| 8 | G | 3000.4 | 19.1 | 18.9 | 19.45 | 19.1 | 18.9 | 18.8 | 19.4 |
| 40 | G | 3319.6 | 18.6 | 19.2+ | 18.9 | 18.9 | 19.0 | 18.7 | 19.3 |
| B 65 | G | 3322.1 | 18.8 | 19.2 | 19.3 | 19.1 | 18.9 | 18.8 | 19.4 |
| M335 | G | 3344.5 | 18.6 | ........ | 19.4 | 19.25 | 19.0 | 19.1 | ........ |
| H417 | E | 4004.7 | 19.0 | 19.1 | 18.95 | 18.95 | 18.9 | 18.95 | 18.8 |
| D239 | G | 4024.6 | 19.0 | 19.2+ | 19.35 | 19.2 | 18.6 | 19.1 | 19.4 |
| 245 | G | 4025.6 | 18.9 | 19.2+ | 19.35 | 19.25 | 18.7 | 18.7 | 19.4 |
| S354 | F | 4026.6 | 19.0 | 19.2+ | ........ | ........ | 18.7 | 18.7 | 19.3 |
| 357 | F | 4027.6 | 19.0 | 19.0+ | ........ | 19.2 | 18.8 | 18.65 | 19.2 |
| 363 | G | 4030.6 | 19.0 | 19.2+ | 18.95 | 19.2 | 18.8 | 19.1 | 18.8 |
| H422 | G | 4031.6 | 19.1 | ........ | 19.15 | 19.25 | 18.9 | 19.3 | 18.6 |
| 428 | F | 4033.6 | 19.1 | 18.8 | 19.35 | 19.3 | 18.8 | 19.3 | 18.6 |
| S367 | P | 4049.6 | 19.0 | 18.9 | 19.1+ | 19.1+ | 18.8+ | 19.0 | 19.3+ |
| 373 | P | 4050.6 | 18.8 | 19.0 | 19.1+ | 19.1 | 18.6 | 19.1 | 19.3 |
| H433 | F | 4054.6 | 19.1 | ........ | 19.3 | 18.6 | 18.45 | 19.4 | 19.3 |
| S375 | F | 4055.6 | 19.1 | 19.2+ | 19.2 | 18.75 | 18.6 | 19.7 | 19.4 |
| 383 | F | 4056.6 | ........ | 19.1+ | 18.9 | 18.75 | 18.45 | 19.3 | 19.4 |
| H441 | F | 4058.5 | ........ | ........ | 19.1+ | 19.1 | 18.7 | 19.4 | 19.3 |
| 446 | E | 4059.5 | 19.1 | 19.0+ | 19.25 | 19.1 | 18.9 | 19.7 | 18.65 |
| 452 | P | 4085.5 | 19.15 | 19.1 | 19.3 | 19.25 | 18.6 | 19.3 | 19.3 |
| S399 | P | 4089.5 | 18.2 | 19.2+ | ........ | 19.2 | ........ | 19.1 | 19.3 |
| H458 | F | 4090.5 | 18.3 | 19.1+ | 19.35 | 18.6 | 18.8 | 18.8 | 18.8 |
| 465 | F | 4092.5 | 18.5 | ........ | 19.4 | 18.8 | 18.8 | 18.95 | 18.6 |
| 467 | F | 4108.4 | 19.1 | 19.1+ | 18.95 | 18.7 | 18.9 | 18.7 | 19.4 |
| 472 | F | 4109.4 | 19.1 | 19.2+ | 19.15 | 18.7 | 18.8 | 18.9 | 19.4 |
| S407 | F | 4113.4 | 18.4 | 19.1+ | 19.2+ | 18.95 | 18.45 | ........ | ........ |
| H475 | E | 4115.4 | 18.35 | 18.8 | 19.35 | 19.1 | 18.6 | 19.2 | 19.5 |
| 486 | E | 4116.3 | 18.45 | ........ | 19.3+ | 19.1 | 18.45 | 19.4 | 19.4 |
| 503 | F | 4147.3 | 18.8 | 18.75 | 19.0 | 18.9 | 18.6 | 18.6 | ........ |
| 509 | G | 4149.3 | 19.1 | ........ | 19.25 | 19.2 | 18.7 | 18.6 | 19.1 |
| 517 | F | 4171.3 | 18.7 | 19.1+ | 19.25 | 19.25 | 18.85 | 18.7 | 19.4 |
| 577 | G | 4348.6 | 18.8 | 19.3+ | 19.35 | 19.1 | 19.0 | 18.7 | 19.3 |
| D253 | F | 4351.6 | 19.1 | 19.2+ | 19.15 | 19.2 | 18.85 | 19.1 | 19.6 |
| H584 | E | 4357.6 | 19.1 | 18.8 | 19.35 | 19.2 | 18.55 | 19.35 | 19.6 |
| S497 | P | 4358.6 | ........ | 18.75 | ........ | ........ | ........ | ........ | ........ |
| H588 | G | 4377.6 | 19.1 | 19.1 | 19.25 | 18.65 | 19.0 | 19.4 | 19.4 |
| 593 | G | 4378.6 | 19.1 | 19.2+ | 18.95 | 18.65 | 19.0 | 19.7 | 19.4 |
| 600 | G | 4379.6 | 19.1 | 19.1+ | 19.0 | 18.7 | 19.0+ | 19.7 | 19.3 |
| D277 | E | 4384.6 | 19.3 | 19.3+ | 19.45 | 19.2 | 18.85 | 19.5 | 19.3 |
| 288 | E | 4387.6 | 18.8 | 19.2+ | 19.5 | 19.3 | 18.6 | 19.1 | 19.6 |
| H606 | P | 4405.5 | 19.1 | 18.8 | 19.1 | 19.1 | 19.0 | 19.7 | 19.2 |
| 611 | G | 4414.5 | 18.25 | 19.3 | 19.5+ | 18.7 | 18.85 | 19.2 | 19.6 |

TABLE I—*Continued*

| Plate | Quality | J.D. | Irregular | | | | Algol |
|---|---|---|---|---|---|---|---|
| | | | 1 | 2 | 6* | 13 | 8 |
| R 15 | F | 18560.6 | 17.7 | 17.3 | 18.4 | 18.4 | 18.6 |
| 115 | E | 18890.6 | 17.2 | 17.4 | 18.6 | 18.25 | 18.6 |
| D 34 | P | 22197.6 | 18.6 | 16.4 | 18.5 | 18.15 | 18.8 |
| P133 | F | 2307.4 | 18.6 | 16.4 | 18.6 | 18.15 | 18.6 |
| 134 | P | 2311.4 | 18.55 | 16.3 | 18.6 | 18.05 | 18.8 |
| 138 | G | 2314.4 | 18.6 | 16.4 | .......... | 17.95 | 18.7 |
| 139 | P | 2347.8 | 18.4 | 16.3 | 18.7 | 18.15 | 18.7 |
| D 48 | G | 2550.6 | 18.6 | 16.5 | 18.6 | 18.1 | 18.7 |
| 83 | P | 2611.0 | 18.5 | 16.5 | .......... | 18.2 | 18.7 |
| 86 | F | 2612.5 | 18.45 | 16.5 | 18.7 | .......... | 18.7 |
| 108 | P | 2669.4 | .......... | 16.6 | .......... | .......... | .......... |
| 119 | F | 2694.3 | .......... | 16.5 | .......... | 18.05 | 18.7 |
| 130 | G | 2698.3 | 18.4 | 16.3 | .......... | 18.1 | 18.8 |
| 198 | G | 2903.2 | 18.55 | 16.1 | 18.8 | 18.0 | 18.7 |
| 205 | G | 2907.2 | 18.45 | 16.0 | 18.7 | 18.1 | 18.7 |
| A 4 | F | 2966.5 | 18.7 | 16.1 | .......... | 18.05 | 18.7 |
| 8 | G | 3000.4 | 18.7 | 15.8 | 18.8 | 17.9 | 18.7 |
| 40 | G | 3319.6 | 18.5 | 16.3 | .......... | 17.8 | 18.7 |
| B 65 | G | 3322.1 | 18.5 | 16.1 | 18.8 | 17.9 | 18.8 |
| M335 | G | 3344.5 | 18.4 | 16.3 | .......... | 17.8 | 18.7 |
| H417 | E | 4004.7 | 18.55 | 15.5 | 18.8 | 17.75 | 18.6 |
| D239 | G | 4024.6 | 18.5 | 15.6 | .......... | 17.9 | 18.75 |
| 245 | G | 4025.6 | 18.4 | 15.6 | 18.8 | 18.0 | 18.8 |
| S354 | F | 4026.6 | 18.4 | 15.5 | 18.8 | 18.1 | 18.7 |
| 357 | F | 4027.6 | 18.5 | 15.5 | .......... | 18.05 | 18.7 |
| 363 | G | 4030.6 | 18.4 | 15.5 | 18.8 | 18.15 | 18.7 |
| H422 | G | 4031.6 | 18.6 | 15.5 | .......... | 17.75 | 18.8 |
| 428 | F | 4033.6 | 18.55 | 15.6 | 18.8 | 17.7 | 18.75 |
| S367 | P | 4049.6 | 18.4 | 15.5 | .......... | 18.1 | 18.75 |
| 373 | P | 4050.6 | 18.3 | 15.6 | 18.8 | 18.1 | 18.75 |
| H433 | F | 4054.6 | 18.4 | 15.6 | .......... | 18.0 | 18.7 |
| S375 | F | 4055.6 | 18.4 | 15.6 | 18.8 | 18.1 | 18.7 |
| 383 | F | 4056.5 | 18.4 | 15.5 | .......... | 17.9 | 19.15 |
| H441 | F | 4058.5 | 18.4 | 15.5 | .......... | 17.75 | 18.6 |
| 446 | E | 4059.5 | 18.45 | 15.5 | 18.8 | 17.75 | 18.75 |
| 452 | P | 4085.5 | 18.3 | 15.5 | 18.8 | 18.1 | 18.7 |
| S399 | P | 4089.5 | 18.3 | 15.6 | 18.8 | 18.15 | 18.75 |
| H458 | F | 4090.5 | 18.5 | 15.5 | .......... | 17.95 | 18.6 |
| 465 | F | 4092.5 | 18.3 | 15.6 | .......... | 17.9 | 18.6 |
| 467 | F | 4108.4 | 18.3 | 15.5 | 18.8 | 17.9 | 18.7 |
| 472 | F | 4109.4 | 18.4 | .......... | 18.8 | 17.95 | 18.7 |
| S407 | F | 4113.4 | 18.35 | 15.6 | 18.8 | 18.0 | 18.6 |
| H475 | E | 4115.4 | 18.5 | 15.5 | 18.8 | 17.8 | 18.75 |
| 486 | E | 4116.3 | 18.5 | 15.5 | .......... | 17.75 | 18.7 |
| 503 | F | 4147.3 | 18.6 | 15.6 | 18.8 | 17.8 | 18.5 |
| 509 | G | 4149.3 | 18.5 | 15.5 | 18.8 | 17.9 | 18.6 |
| 517 | F | 4171.3 | 18.4 | 15.5 | 18.8 | 17.75 | 18.75 |
| 577 | G | 4348.6 | 18.4 | 15.7 | 18.8 | 17.9 | 18.7 |
| D253 | F | 4351.6 | 18.45 | 15.7 | 18.8 | 17.85 | 18.7 |
| H584 | E | 4357.6 | 18.3 | 15.9 | 18.8 | 17.8 | 18.6 |
| S497 | P | 4358.6 | 18.5 | 15.6 | .......... | 17.8 | 18.7 |
| H588 | G | 4377.6 | 18.3 | 15.9 | 18.8 | 17.8 | 19.1 |
| 593 | G | 4378.6 | 18.4 | 15.9 | 18.8 | 17.75 | 18.6 |
| 600 | G | 4379.6 | 18.35 | 15.8 | 18.8 | 17.8 | 18.7 |
| D277 | E | 4384.6 | 18.3 | 15.9 | 18.8 | 17.8 | 18.7 |
| 288 | E | 4387.6 | 18.4 | 16.0 | 18.8 | 17.85 | 19.2 |
| H606 | P | 4405.5 | 18.3 | 15.9 | 18.8 | 17.8 | 18.7 |
| 611 | G | 4414.5 | 18.3 | 15.9 | 18.8 | 17.9 | 18.7 |

* Var. No. 6. Magnitudes are estimated.

TABLE I—*Continued*

| Plate | Quality | J.D. | Undetermined | | | | |
|---|---|---|---|---|---|---|---|
| | | | 14 | 15 | 21 | 32 | 45 |
| R 15 | F | 18560.6 | .......... | 19.3+ | .......... | .......... | 18.8 |
| 115 | E | 18890.6 | 19.2 | 19.2 | 18.75 | 18.8 | 18.55 |
| D 34 | P | 22197.6 | .......... | 19.25 | .......... | .......... | .......... |
| P133 | F | 2307.4 | 19.35 | 19.35 | 18.5 | 19.1 | 19.0 |
| 134 | P | 2311.4 | 18.8 | 19.45 | 18.5 | 18.6 | 18.9 |
| 138 | G | 2314.4 | 18.9 | 19.35 | 18.65 | 19.35 | 18.9 |
| 139 | P | 2347.8 | 19.3+ | 19.25 | 18.85 | 19.2+ | 18.45 |
| D 48 | G | 2550.6 | 19.2 | 19.35 | 18.85 | 18.85 | 19.0 |
| 83 | P | 2611.0 | .......... | .......... | .......... | .......... | .......... |
| 86 | F | 2612.5 | 19.35 | 19.5 | 18.9 | 19.1 | 18.8 |
| 108 | P | 2669.4 | .......... | .......... | .......... | .......... | .......... |
| 119 | F | 2694.3 | .......... | 19.25 | 18.85 | 19.2 | .......... |
| 130 | G | 2698.3 | 19.1 | 19.45 | 18.85 | 19.5+ | 19.0 |
| 198 | G | 2903.2 | 19.4 | 19.1 | 18.7 | 19.5+ | 19.0 |
| 205 | G | 2907.3 | 19.4 | 19.45 | 18.55 | 19.25 | 18.95 |
| A 4 | F | 2966.5 | 19.05 | .......... | 18.8 | 19.2+ | 18.7 |
| 8 | G | 3000.4 | 19.4 | 19.0 | 18.7 | 19.5 | 19.0 |
| 40 | G | 3319.6 | 19.2 | 19.3 | 18.45 | 19.5 | 18.4 |
| B 65 | G | 3322.1 | 19.4 | 19.45 | 18.65 | 19.5 | 18.5 |
| M335 | G | 3344.5 | 19.4 | 19.3+ | 18.9 | 19.4+ | 18.55 |
| H417 | E | 4004.7 | 19.6 | 19.45 | 18.75 | 19.5+ | 18.45 |
| D239 | G | 4024.6 | 19.05 | 19.4+ | 18.9 | 19.5+ | 18.95 |
| 245 | G | 4025.6 | 19.0 | 19.5 | 18.85 | 19.25 | 18.9 |
| S354 | F | 4026.6 | 19.0 | 19.4+ | .......... | .......... | .......... |
| 357 | F | 4027.6 | .......... | .......... | .......... | .......... | .......... |
| 363 | G | 4030.6 | 19.0 | .......... | .......... | .......... | 19.0 |
| H422 | G | 4031.6 | 19.2 | 19.25 | 18.85 | 19.4 | 18.9 |
| 428 | F | 4033.6 | 19.2 | 19.45 | 18.85 | 19.0 | 19.0 |
| S367 | P | 4049.6 | 19.2 | .......... | 18.5 | .......... | .......... |
| 373 | P | 4050.6 | .......... | .......... | 18.5 | .......... | 18.95 |
| H433 | F | 4054.6 | .......... | 19.4 | 18.55 | .......... | 18.75 |
| S375 | F | 4055.6 | 19.6+ | 19.1 | 18.55 | 19.2 | 18.9 |
| 383 | F | 4056.5 | 19.4+ | 19.1 | 18.55 | 19.2 | 18.9 |
| H441 | F | 4058.5 | .......... | .......... | 18.55 | .......... | 18.35 |
| 446 | E | 4059.5 | 19.2 | 19.4 | 18.55 | 19.5+ | 18.5 |
| 452 | P | 4085.5 | 19.2 | 19.45 | 18.75 | 19.4 | 18.55 |
| S390 | P | 4089.5 | .......... | 19.4+ | .......... | .......... | .......... |
| H458 | F | 4090.5 | 19.3 | 19.3+ | 18.75 | 18.9 | 18.7 |
| 465 | F | 4092.5 | 19.05 | 19.4+ | 18.75 | 19.2 | 18.6 |
| 467 | F | 4108.4 | 19.4 | 19.15 | 18.75 | 18.8 | 18.95 |
| 472 | F | 4109.4 | .......... | 19.3 | 18.75 | 18.75 | 18.95 |
| S407 | F | 4113.4 | .......... | 19.3+ | .......... | .......... | 19.0 |
| H475 | E | 4115.4 | 19.2 | 19.3 | 18.7 | 19.4 | 19.0 |
| 486 | E | 4116.3 | 19.2 | .......... | 18.5 | 19.5 | 19.0 |
| 503 | F | 4147.3 | 19.5 | 19.4 | 18.7 | 18.6 | 18.5 |
| 509 | G | 4149.3 | .......... | 19.3 | 18.75 | 18.8 | 18.3 |
| 517 | F | 4171.3 | 19.2 | 19.4 | 18.85 | 19.0 | 18.9 |
| 577 | G | 4348.6 | 18.8 | 19.4 | 18.8 | 18.6 | 18.8 |
| D253 | F | 4351.6 | 18.95 | 19.2 | 18.8 | 19.4 | 18.7 |
| H584 | E | 4357.6 | 19.05 | 19.1 | 18.75 | 19.4 | 18.25 |
| S497 | P | 4358.6 | 18.9 | .......... | .......... | .......... | 18.4 |
| H588 | G | 4377.6 | 19.6 | 19.45 | 18.8 | 19.5 | 18.4 |
| 593 | G | 4378.6 | 19.4 | 19.5 | 18.85 | 19.5 | 18.45 |
| 600 | G | 4379.6 | 19.4+ | 19.3 | 18.7 | 18.8 | 18.5 |
| D277 | E | 4384.6 | 19.3 | 19.5 | 18.65 | 19.45 | 18.5 |
| 288 | E | 4387.6 | 19.5 | 19.5 | 18.85 | 18.7 | 18.5 |
| H606 | P | 4405.5 | 18.9 | 19.2 | 18.9 | 19.2 | 19.0 |
| 611 | G | 4414.5 | 19.1 | 19.3 | 19.0 | 19.4 | 19.1 |

The necessary data for the construction of light-curves for all the Cepheids are given in Table II. The period-luminosity relation is conspicuous among these Cepheids, and is illustrated in Figure 2, where logarithms of the periods are plotted against magnitudes at maximum. Long exposures on Cramer Iso plates through a visual filter, while not accurately calibrated as yet, indicate moderately large color-indices, quite consistent with solar-type spectra, for those Cepheids which could be identified.[1]

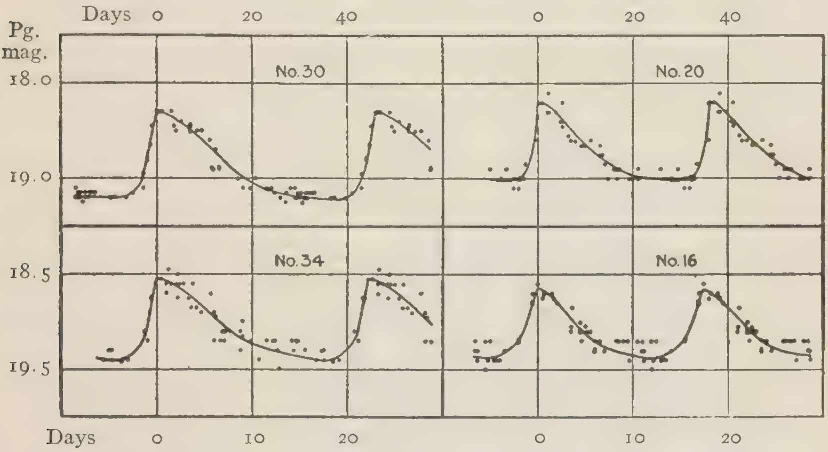

FIG. 1.—Mean light-curves for four Cepheids in Messier 33. The magnitudes are photographic.

These considerations all indicate that the variables are ordinary Cepheids, such as are known in the galactic system, the Magellanic Clouds, and the globular clusters, and hence that they can be employed for determining the distance of the spiral. An examination of Figure 2 suggests that the data are reasonably complete for maximum magnitudes down to about 18.8, but that for fainter maxima they are occasional and probably not representative.[2] This restriction, together with the limited range and considerable scattering, de-

---

[1] This conclusion is based on the fact that for stars having the same order of photographic magnitude the Cepheids fall about midway between the brightest and faintest photovisual images.

[2] Eighteen of the Cepheids are within 5′ of the nucleus, and seventeen are more distant. The two groups are thoroughly intermingled on the plot in Fig. 2, and show no appreciable difference that can be attributed to the influence of unresolved nebulosity.

## TABLE II

### CEPHEIDS IN MESSIER 33

| Var. No. | Period | | Pg. Mag. | | Epoch J.D. | Distance from Nucleus | Position Angle‡ | Identification Plates |
|---|---|---|---|---|---|---|---|---|
| | Days | Log $P$ | Maximum | Range* | | | | |
| 10† | 69.50 | 1.842 | 18.55 | (0.6) | 2424004.5 | 188″ | 105° | IV, V |
| 19 | 54.706 | 1.738 | 18.0 | .8 | 4018.0 | 346 | 15 | IV |
| 30 | 46.03 | 1.663 | 18.3 | .9 | 4026.0 | 301 | 250 | IV, VI |
| 3 | 41.68 | 1.620 | 18.35 | 0.9 | 4054.5 | 633 | 330 | IV |
| 31 | 37.33 | 1.572 | 18.25 | 1.0 | 4084.0 | 337 | 245 | IV, VI |
| 29 | 36.31 | 1.560 | 18.55 | (0.8) | 4111.5 | 237 | 210 | IV, VI, VII |
| 20 | 35.95 | 1.556 | 18.2 | ( .8) | 4024.0 | 53 | 160 | V, VII |
| 36 | 35.80 | 1.554 | 18.5 | ( .5) | 4028.0 | 506 | 35 | IV |
| 18 | 34.00 | 1.531 | 18.5 | ( .6) | 4057.0 | 104 | 30 | IV, VII |
| 35 | 30.514 | 1.484 | 18.65 | ( .8) | 4031.0 | 665 | 255 | IV |
| 42 | 30.34 | 1.482 | 18.45 | ( .5) | 4051.0 | 323 | 225 | IV, VI |
| 44 | 30.123 | 1.479 | 18.6 | 0.8 | 4029.5 | 353 | 230 | IV, VI |
| 4 | 27.366 | 1.437 | 18.25 | 1.2 | 4091.5 | 444 | 70 | IV |
| 7 | 26.556 | 1.424 | 18.6 | (0.7) | 4147.0 | 296 | 60 | IV |
| 38 | 25.04 | 1.398 | 18.2 | .9 | 4089.0 | 523 | 165 | IV |
| 11 | 23.43 | 1.370 | 18.8 | ( .5) | 4116.0 | 201 | 50 | IV, V, VII |
| 17 | 23.297 | 1.367 | 18.8 | ( .9) | 4058.5 | 229 | 180 | IV, VII |
| 26 | 23.258 | 1.366 | 19.1 | ( .7) | 4089.5 | 618 | 80 | IV |
| 27 | 22.448 | 1.351 | 18.7 | ( .6) | 4054.5 | 233 | 340 | IV, VII |
| 34 | 22.16 | 1.346 | 18.55 | ( .9) | 4024.5 | 668 | 325 | IV |
| 22 | 21.816 | 1.339 | 18.9 | ( .5) | 4002.5 | 64 | 175 | V |
| 12 | 21.681 | 1.336 | 18.6 | (0.9) | 4024.5 | 140 | 95 | V, VII |
| 33 | 20.50 | 1.312 | 18.75 | (1.1) | 4004.5 | 430 | 235 | IV, VI |
| 43 | 20.166 | 1.305 | 18.7 | 1.0 | 4025.5 | 424 | 215 | IV, VI |
| 9 | 18.90 | 1.277 | 18.7 | (0.6) | 4023.0 | 204 | 90 | IV, V |
| 28 | 18.58 | 1.269 | 18.85 | ( .8) | 4116.5 | 412 | 50 | IV |
| 41 | 17.98 | 1.255 | 18.65 | ( .6) | 4090.5 | 321 | 235 | IV, VI |
| 37 | 17.602 | 1.246 | 18.9 | ( .8) | 4058.0 | 77 | 280 | V, VII |
| 16 | 17.50 | 1.243 | 18.7 | ( .7) | 4033.0 | 239 | 170 | IV |
| 39 | 16.166 | 1.208 | 18.8 | ( .7) | 4114.0 | 722 | 25 | IV |
| 5 | 14.60 | 1.165 | 18.85 | ( .6) | 4051.5 | 186 | 75 | IV, V |
| 23 | 13.564 | 1.132 | 18.85 | ( .6) | 4112.5 | 96 | 180 | IV, V, VII |
| 25 | 13.438 | 1.129 | 18.95 | ( .8) | 4386.0 | 169 | 140 | IV, V |
| 40† | 12.922 | 1.111 | 18.95 | ( .5) | 4003.5 | 188 | 340 | IV, V |
| 24 | 12.894 | 1.110 | 18.85 | (0.7) | 3990.0 | 96 | 190 | IV, V |

* The amplitudes, in general, are very uncertain; the few which seem to be fairly reliable are printed without parentheses.

† In the preliminary notice (*Publications of the American Astronomical Society*, 4, 261, 1925) the periods of Nos. 10 and 40 were given as 19.6 and 26.0 days, respectively. New observational data have led to the revised values listed above. The period previously published for No. 15 was also found to be erroneous.

‡ Position angles are measured from the north through the east (following side). The accuracy of both position angles and distances is sufficient only to indicate the regions in which the variables are located. Identification may be made on the various plates.

tracts materially from the significance of correlation curves computed from the data, and recourse was had to a direct cut-and-try method for determining $m-M$, the modulus of the distance.

Shapley's period-luminosity curve,[1] expressing the relation between log $P$ and median photographic magnitude for more than a hundred Cepheids in a single system, the small Magellanic Cloud, is the latest and most reliable standard for comparison. The individual points were replotted, using magnitudes at maxima instead of median magnitudes,[2] and a corresponding diagram on transparent paper was constructed, to the same scale, for the Cepheids in Messier 33. The latter was laid upon the former so that the ordinates for log $P$ were superposed and then adjusted to the best fit by shifting along the magnitude axis. This method assumes that the amplitudes of the Cepheids in the two systems are similar; otherwise, an error amounting to half the systematic difference in the amplitudes is introduced. In general, the two diagrams are comparable, although the scattering among the Cepheids in the spiral appears to be slightly less than among those in the cloud, while the deficiencies in the spiral for the fainter magnitudes and shorter periods are strikingly evident.

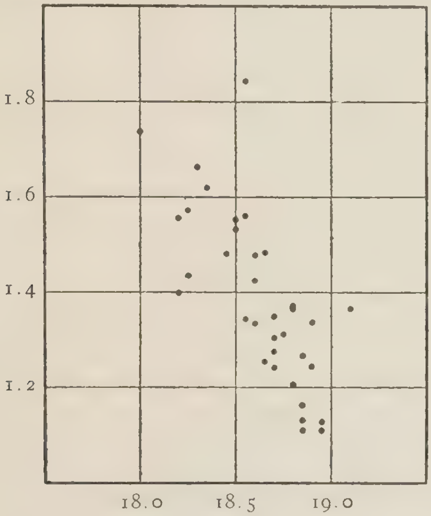

FIG. 2.—Period-luminosity relation among Cepheids in Messier 33. Photographic magnitudes at maximum (abscissae) are plotted against logarithms of period in days.

The best fit, illustrated in Figure 3, appears to be for a difference of 4.55 mag. in the moduli of the two systems, and the adjustment is sensibly unbalanced by a shift of 0.1 mag. in either direction. The latest value[1] for the modulus of the cloud is 17.55; hence for Messier 33

---

[1] *Harvard Circular*, No. 280, 1925.

[2] In two cases, where the amplitudes were not specifically stated, probable values were derived from a curve expressing the relation between amplitude and log $P$.

$$
\begin{aligned}
m-M &= 22.1 \\
\pi &= 0.''000{,}0038 \\
\text{Distance} &= 263{,}000 \text{ parsecs} \\
&= 850{,}000 \text{ light-years.}^{2}
\end{aligned}
$$

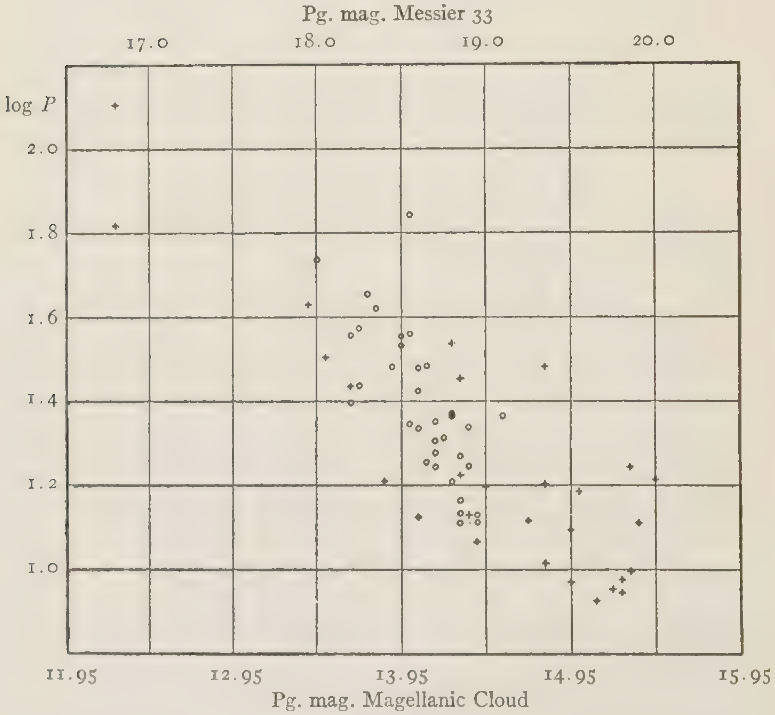

FIG. 3.—Comparison of period-luminosity relations for Cepheids in Messier 33 (circles) and in the Small Magellanic Cloud (crosses).

The accuracy of the results, the universal validity of the Cepheid criterion being assumed, depends largely upon the accuracy of the zero-point of Shapley's period-luminosity curve.[1] It is hoped that the probable error arising from the system of magnitudes and the comparison with the Cepheids in the Magellanic Cloud is not greater than 0.2 mag. in the modulus, or 10 per cent in the distance.

---

[1] *Harvard Circular*, No. 280, 1925.

[2] The values published in the preliminary notice, derived from twenty-two Cepheids and Shapley's unrevised period-luminosity relation, were: $m-M=22.3$; distance = 930,000 light-years. The difference is due almost entirely to the revised form of the period-luminosity curve in the portion covering the Cepheids in the spiral.

Hitherto, wherever Cepheids have been found in isolated systems, the criterion has led to distances entirely consistent with other characteristics that could be observed. The latest application has been to N.G.C. 6822, a system very similar to the Magellanic Clouds, but at a distance of about 214,000 parsecs, comparable with that of Messier 33 itself.[2] Here, also, the period-luminosity relation functioned normally, and the order of the resulting distance was confirmed by several independent criteria. A presumption is thus raised in favor of the general validity of the Cepheid criterion which only strong and cumulative evidence to the contrary will destroy.

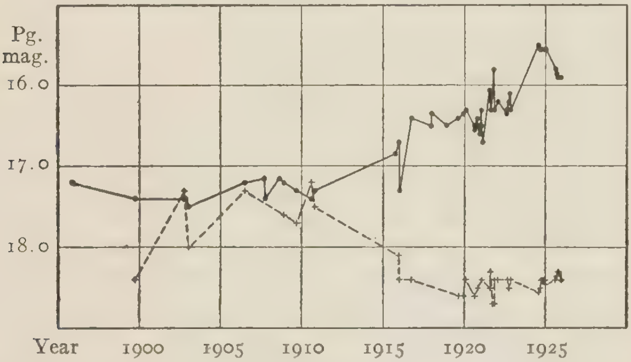

FIG. 4.—Two irregular variables in Messier 33; No. 1, crosses; No. 2, points

IRREGULAR VARIABLES

The four irregular variables are Nos. 1, 2, 6, and 13. A number of observations of Nos. 1 and 2 from early plates, not included in Table I, were published by Duncan[3] and by Wolf.[4] These, together with a few additional data, are listed in Table III. The magnitudes have been reduced to the photographic system derived from comparisons with Selected Areas Nos. 21 and 45, and differ appreciably from those published by the above-mentioned investigators.[1] Independent estimates of the magnitudes have been made on such of the original plates as were available.

---

[1] Recent results on radial velocities and proper motions of galactic Cepheids indicate the possibility of a moderate correction to the zero-point, but until the new data have been discussed in a definitive manner, it seems preferable to use the current value, with full realization, however, of the possibility of a subsequent revision.

[2] *Mt. Wilson Contr.*, No. 304; *Astrophysical Journal*, **62**, 409, 1926.

[3] *Publications of the Astronomical Society of the Pacific*, **34**, 290, 1922.

[4] *Astronomische Nachrichten*, **217**, 476, 1923.

TABLE III

ADDITIONAL MAGNITUDES FOR VARIABLES NO. 1 AND NO. 2

| Date | | Obs.† | Variable | |
|---|---|---|---|---|
| | | | No. 1 | No. 2 |
| 1895 | Nov. 14*.......... | R | 17.3‡ | 17.2 |
| 1899 | Sept. 12*.......... | K | 18.4 | 17.4 |
| 1902 | Sept. 5*.......... | Ri | 17.3 | 17.4 |
| | Sept. 26.......... | W | .......... | 17.4 |
| 1903 | Jan. 16*.......... | R | 18.0? | 17.5 |
| 1906 | *.......... | L | 17.3? | 17.2 |
| 1907 | Aug. 8.......... | W | .......... | 17.15 |
| | Aug. 12.......... | W | .......... | 17.4 |
| 1908 | July 25.......... | W | .......... | 17.15 |
| | Nov. 17.......... | P | 17.6 | 17.2 |
| 1910 | Oct. 24.......... | C | 17.5 | 17.3 |
| 1915 | Oct. 1*.......... | M | .......... | 16.85 |
| | Oct. 30*.......... | L | 18.1 | 16.7 |
| | Nov. 5.......... | C | 18.4 | 17.3 |
| 1916 | Sept. 28*.......... | L | 18.4 | 16.4 |
| 1917 | Dec. 10.......... | W | .......... | 16.5 |
| | Dec. 16.......... | W | .......... | 16.35 |
| 1918 | Nov. 11*.......... | M | .......... | 16.5 |
| 1920 | Aug. 15.......... | W | .......... | 16.55 |
| | Oct. 4*.......... | M | .......... | 16.4 |
| 1921 | Aug. 30.......... | Lu | 18.3 | 16.3 |
| | Nov. 28.......... | Lu | 18.4 | 16.3 |
| 1922 | Jan. 20.......... | Lu | 18.4 | 16.2 |
| | Aug. 14.......... | W | .......... | 16.35 |
| | Aug. 25.......... | W | .......... | 16.35 |
| | Aug. 25*.......... | D | 18.4 | 16.3 |
| | Oct. 14*.......... | M | .......... | 16.1 |
| | Oct. 15*.......... | M | .......... | 16.3 |

* Plates from which magnitudes have been independently determined. Otherwise the magnitudes are those published by Duncan and by Wolf, reduced to the system of the international photographic scale.

† The photographs were made by the observers indicated in the second column: R = Isaac Roberts, K = Keeler, Ri = Ritchey, W = Wolf, L = Lampland, P = Perrine, C = Curtis, M = van Maanen, Lu = Lundmark, D = Duncan.

‡ Limit of the plate. Variable No. 1 was not visible.

---

[1] Magnitudes of a sequence of comparison stars were derived from four short-exposure comparisons with Selected Area No. 45 in addition to those found from the available long exposures.

Light-curves of these two variables, based on Tables I and III, are shown in Figure 4. Number 2 appears to have remained quiescent at about 17.4 mag. from 1895 to somewhere between 1911 and 1915. By 1915, the variable had entered upon a period of activity which is still in progress. It brightened gradually, with minor fluctuations, until it reached a maximum of 15.55, which it maintained during the season 1924–1925. It was then the brightest star which could definitely be assigned to the nebula, the absolute photographic magnitude corresponding to the distance indicated by the Cepheids being $-6.55$. A faint slitless spectrogram was obtained during this period with two prisms and a 3-inch camera at the Newtonian focus of the 100-inch reflector. The continuous spectrum held up well into the violet, suggesting an early type, and a bright $H\beta$ could be seen. Several other bright lines, including $H\gamma$ and $H\delta$, were suspected. The spectrum can best be described as an early type with bright lines, and this is consistent with the photovisual plates which indicate a very small color-index. During the summer and autumn of 1925, the star faded about 0.5 mag. Variation of this type is not sufficiently known among galactic stars for analogies to be traced.

Variable No. 1 is similar in many respects to No. 2. Its normal magnitude appears to be near 18.4, but about 1900 it entered upon a seventeen-year period of activity, during which it attained a maximum magnitude of at least 17.2. By 1917 it was back to normal, and since then has shown only slight evidence of unrest. The mean magnitude during 1924–1925, however, was 18.3 as against 18.5 for the period 1920–1922. Photovisual observations indicate a moderate positive color-index of the order of 0.5 mag.

Variable No. 6 has remained steady at about 18.8 since 1921. Plates for 1910, 1911, and 1919 indicate, however, a luminosity some 0.3 or 0.4 mag. brighter. Variable No. 13 is fainter on the early plates than on the later. In 1910–1911 it was about 18.4; in 1919–1921, about 18.0; in 1924–1925, about 17.7. The color-index during the last epoch was of the order of +0.8 mag.

### OTHER VARIABLES

Variable No. 8 appears to be an eclipsing star. On three plates it was 19.1 or fainter; otherwise it has remained steady at about 18.6. The minima were

| | Photographic Magnitude |
|---|---|
| J.D. 2424056.49 | 19.15 |
| 4377.59 | 19.1 |
| 4387.60 | 19.25 |

The images on these plates have been critically examined, and there seems to be no reason for supposing them defective.

No periods have been found for variables Nos. 14, 15, 21, 32, and 45. The small amplitudes and recurring maxima suggest, however, the Cepheid type of variation, and it is probable that more and better observations will establish it for several of the stars.

### NOVAE

Two novae have been observed in the spiral, the first about 1.′8, and the second about 10.′8, from the nucleus, both in the north-following quadrant. Nova No. 1 was found on four plates obtained by Pease in the winter of 1919–1920. The position, indicated on Plate V, was about 1.″5 south of a star of 18.15 mag., and the photographic images of the two overlapped. This detracted from the reliability of the estimates of magnitude. Moreover, an interval of one hundred and ten days separated the plate on which the nova was first seen from the next preceding plate, and thus the date and the magnitude of maximum are unknown.

Nova No. 2, whose position is marked on Plate IV, appeared on the first photograph obtained in the season 1925–1926. It was obviously on the declining branch of its light-curve, although it was followed for some two months longer. The data of observation for both novae are given in Table IV, in which are included absolute magnitudes computed from the distance indicated by the Cepheids, and also the dates of the photographs next preceding and following those on which the novae were visible.

The observed portions of the two light-curves are shown in Figure 5. The data are insufficient to serve as a reliable criterion of distance, and would be so even were the frequency distribution of absolute magnitudes attained by galactic novae definitely known. Among those in Messier 31, however, of which some sixty have been observed,[1] there is a sharply defined maximum frequency about

TABLE IV

Apparent and Absolute Photographic Magnitudes of Novae in Messier 33

| Plate | Date | m | M† |
|---|---|---|---|
| Nova No. 1 | | | |
| D 34* | 1919 Aug. 26 | .......... | .......... |
| P 133 | Dec. 14 | 17.25 | −4.85 |
| 134 | Dec. 18 | 17.25 | 4.85 |
| 138 | Dec. 21 | 17.8 | 4.3 |
| 139 | 1920 Jan. 23 | 18.0 | −4.1 |
| D 48* | Aug. 13 | .......... | .......... |
| Nova No. 2 | | | |
| H 517* | 1925 Jan. 17 | .......... | .......... |
| 577 | July 17 | 17.9 | −4.2 |
| D 253 | July 20 | 18.0 | 4.1 |
| H 584 | July 26 | 18.4 | 3.7 |
| 588 | Aug. 15 | 19.2 | 2.9 |
| 600 | Aug. 17 | 19.25 | 2.85 |
| D 277 | Aug. 21 | 19.4 | 2.7 |
| 288 | Aug. 24 | 19.5 | 2.6 |
| H 606 | Sept. 12 | 19.5 | 2.6 |
| 611 | Sept. 21 | 19.7 | −2.4 |
| S 507* | Oct. 18 | .......... | .......... |

* The photographs next preceding that of the first appearance and next following the last appearance are also listed.

† Absolute magnitudes are derived from the distance indicated by the Cepheids in Messier 33.

apparent magnitude 17.0. The Cepheids in the two spirals have the same apparent magnitudes for corresponding periods, and it is to be expected that the novae, also, will show a similar behavior. The fragmentary observations of the two novae in Messier 33 are consistent with this supposition. They indicate, at least, that the novae are brighter than the Cepheids, a relation that holds in both Messier 31 and in the galactic system. The lack of data on the magnitudes at maxima is a serious handicap, but on the very reasonable assumption that the apparent magnitudes attained in Messier 33 are similar to those in Messier 31, the mean absolute magnitude of the novae, at the distance indicated by the Cepheids, would be −5.1, which is of the same order as that for novae in the galactic system.[1]

---

[1] This number includes those discovered up to December, 1925. Nos. 23–60 have been found by the writer; details will be published later.

## DIFFUSE NEBULAE IN MESSIER 33

Several patches of diffuse nebulosity with stars involved are found in the outer arms of Messier 33. The brightest of these, catalogued separately as N.G.C. 588, 595, and 604, show emission spectra. Slit spectrograms are available for N.G.C. 604, and show that $H\beta$ is brighter than $N_2$, a relation characteristic of diffuse emission nebulosity in the galactic system. Photovisual observations indicate that the brighter stars involved are blue.[2] Moreover, as will be shown later, the relation between the apparent magnitudes of the involved stars and the angular extent of the nebulosities is the same as that among diffuse galactic nebulae.[3]

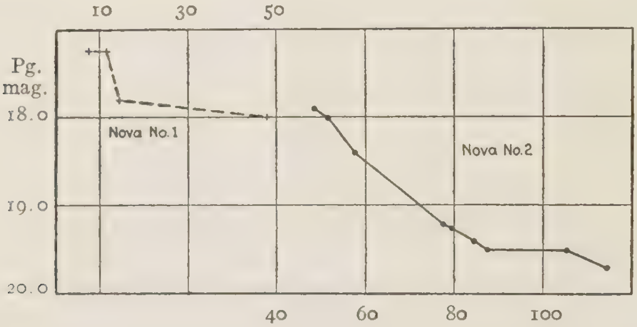

FIG. 5.—Light-curves of two novae in Messier 33. The Julian dates may be found by adding to the abscissae, 2422300 for Nova No. 1, and 2424300 for Nova No. 2.

These various features offer strong cumulative evidence that the patches in Messier 33 are indeed diffuse emission nebulae similar in every respect to those in the galactic and other systems. On this assumption, the brighter stars involved are blue giants[1] of spectral types Bo or Oe5, and can be used to test the order of the distance derived from the Cepheids. The photographic magnitudes of the brighter stars in the three groups[2] are given in Table V along with the absolute magnitudes computed from the modulus $m-M=22.1$.

---

[1] Lundmark (*Monthly Notices*, **85**, 885, 1925) has made use of the reverse procedure. Combining a mean apparent magnitude of 16.34 for twenty-two novae in Messier 31 with a mean absolute magnitude of −6.9 for galactic novae, he derived a distance of $1.4 \times 10^6$ light-years for the spiral.

[2] The photovisual images are as small as, or smaller than, those of any other stars in the nebula of the same order of photographic magnitude.

[3] *Mt. Wilson Contr.*, No. 250; *Astrophysical Journal*, **56**, 400, 1922.

TABLE V*

MAGNITUDES OF STARS INVOLVED IN EMISSION NEBULOSITY IN MESSIER 33

| N.G.C. 588 | | N.G.C. 595 | | N.G.C. 604 | |
|---|---|---|---|---|---|
| $m$ | $M$ | $m$ | $M$ | $m$ | $M$ |
| 16.55 | −5.55 | 16.6 | −5.5 | 15.75 | −6.35 |
| 16.85 | 5.25 | 16.7 | 5.4 | 15.8 | 6.3 |
| 17.5 | 4.6 | 16.8 | 5.3 | 15.9 | 6.2 |
| 17.7 | −4.4 | 16.9 | 5.2 | 15.95 | 6.15 |
| | | 17.0 | 5.1 | 16.0 | 6.1 |
| | | 17.2 | 4.9 | 16.15 | 5.95 |
| | | 17.5 | 4.6 | 16.15 | 5.95 |
| | | 17.6 | 4.5 | 16.3 | 5.8 |
| | | 17.6 | 4.5 | 16.45 | 5.65 |
| | | 17.7 | −4.4 | 16.55 | 5.55 |
| | | | | 16.55 | 5.55 |
| | | | | 16.75 | 5.35 |
| | | | | 16.8 | 5.3 |
| | | | | 16.85 | −5.25 |

* The table contains photographic magnitudes, both apparent and absolute, of the brighter stars involved in three patches of diffuse nebulosity having emission spectra, in the arms of Messier 33. The lists are complete to the faintest star measured in each group.

These absolute magnitudes must be compared with those of the brightest blue giants known in other systems. The most recent estimates of mean absolute photographic magnitude for the blue giants in the galactic system are

Bo (sharp lines) = −3.5 (Adams)[3]
O (absorption lines) = −4.4 (Plaskett)[4].

---

[1] *Mt. Wilson Contr.*, No. 241; *Astrophysical Journal*, 56, 162, 1922.

[2] N.G.C. 592, the only other knot in the arms of Messier 33 which is catalogued separately, is an open group of stars with no trace of diffuse nebulosity. One star, about 15.5 and thus considerably brighter than the others, is red and may be a field star. The three next brightest, ranging from about 16.5 to 16.8, are of early types, blue or white.

[3] *Mt. Wilson Contr.*, No. 262; *Astrophysical Journal*, 57, 294, 1923.

[4] *Publications of the Dominion Astrophysical Observatory*, 2, No. 16, 1924.

The original values, expressed in visual magnitudes, have been corrected for a mean color-index of −0.4 mag. in each case. Plaskett suggests a dispersion of the order of 3 mag. for the O stars, which would make the upper limit about −5.9, less than a half-magnitude fainter than the brightest star in Table V. When we consider the influence of selection on the stars in the spiral, the probability that some of the brightest images are clusters rather than single stars,[1] and the uncertainty in the dispersion among the galactic stars, the discrepancy becomes unimportant, so that the two sets of absolute magnitudes may be regarded as comparable. The blue giants in Messier 33 therefore confirm the order of the distance derived from the Cepheids.

Dimensions of the nebulosities themselves, measured on long exposures with the 100-inch reflector, together with the linear dimensions in parsecs are as follows:

| | Seconds of Arc | Parsecs |
|---|---|---|
| N.G.C. 588 | 30×25 | 40×30 |
| 595 | 55×32 | 70×40 |
| 604 | 65×55 | 80×70 |

The brighter portion of N.G.C. 604, in which the stars are closely crowded, is about 50″, or 65 parsecs, in diameter. These dimensions are comparable with those of the largest nebulae in other systems. N.G.C. 2070 in the large Magellanic Cloud is about 80 parsecs;[2] nebula No. III in N.G.C. 6822 is about 55 parsecs;[3] and in the galactic system the great exterior loop in the constellation of Orion is about 40 parsecs in diameter.[1]

---

[1] Groups of stars in Messier 33 one second (1.27 parsecs) or less in diameter would certainly appear as ordinary images of single stars on all but limiting exposures under excellent observing conditions, and hence would be counted as single stars. Groups of such dimensions are fairly numerous in the galactic system, especially among the blue giants involved in nebulosity. Within this limit, for instance, are included such aggregations as five of the six brightest stars in the Pleiades, all the brighter stars in the Orion nebula, the major portions of the clusters in Messier 8 and N.G.C. 2237, and such multiple stars as those in Messier 20 and N.G.C. 281. Phenomena of a similar nature would readily account for several of the excessively bright objects listed as single stars in Messier 33, especially among those in the crowded cluster involved in N.G.C. 604. The excess of very bright stars, all apparently blue, over those to be expected from an analogy with Kapteyn's luminosity function also can be explained, in part at least, along these lines.

[2] Shapley, *Harvard College Observatory Bulletin*, No. 816.

[3] *Mt. Wilson Contr.*, No. 304; *Astrophysical Journal*, **62**, 409, 1926.

Among the diffuse nebulae in the galactic system, the following relation has been established for measures on Seed 30 plates exposed sixty minutes with a reflector of focal ratio 1:5,

$$m+5\log a=11.1$$
$$\text{Mean deviation}=\ 0.8,$$

where $m$ is the apparent photographic magnitude of the associated star or group of stars and $a$ is the angular distance, in minutes of arc, to which the luminous nebulosity can be traced.[2] For the nebulae in Messier 33, using integrated magnitudes from Table V and measuring the extent of the nebulosity from the center of gravity of the stars, we find

| | $m$ | $a$ | $m+5\log a$ |
|---|---|---|---|
| N.G.C. 588 | 15.5 | 0'.15 | 11.4 |
| 595 | 14.6 | 0.33 | 12.2 |
| 604 | 13.2 | 0.5 | 11.7 |
| Mean | .......... | .......... | 11.8 |

These results are sufficiently consistent with the foregoing relation to support the assumption that the stars and nebulae in the spiral are similar to those in the galactic system.

### LUMINOSITY FUNCTION

In order to determine the upper limit of luminosity for the stars in Messier 33, counts were made over three areas, each about six minutes of arc square, centered on the nucleus and on points six minutes north and eight minutes south, respectively. The sum of the areas is 107 square minutes of arc, which was estimated to contain about one-fifth of the stars in the nebula. The same method was employed as in making counts[1] in N.G.C. 6822, the final results being expressed as numbers of stars in successive intervals of apparent photographic magnitude. Field stars were eliminated by means of the stellar distribution tables recently published by Seares and van Rhijn.[2]

---

[1] Measured on long exposures with small cameras. The original plates are in the Mount Wilson collection.

[2] *Mt. Wilson Contr.*, No. 250; *Astrophysical Journal*, 46, 400, 1922.

TABLE VI

LUMINOSITY FUNCTION FOR MESSIER 33

| Pg. Mag. | Stars Counted | Normal Number Gal. Lat. 30°5 | $\phi$ ($m$)* Messier 33 | $\phi$ ($M$)† Galaxy | $M$ |
|---|---|---|---|---|---|
| 19.2–19.0 | 990 | 16 | 974 | 972 | −3.0 |
| 18.9–18.7 | 540 | 14 | 526 | 580 | 3.3 |
| 18.6–18.4 | 340 | 12 | 328 | 341 | 3.6 |
| 18.3–18.1 | 265 | 10 | 255 | 197 | 3.9 |
| 18.0–17.8 | 233 | 9 | 224 | 114 | 4.2 |
| 17.7–17.5 | 110 | 8 | 102 | 64 | 4.5 |
| 17.4–17.2 | 45 | 7 | 38 | 35 | 4.8 |
| 17.1–16.9 | 29 | 6 | 23 | 19 | 5.1 |
| 16.8–16.6 | 25 | 5 | 20 | 10.4 | 5.4 |
| 16.5–16.3 | 17 | 4.3 | 12.7 | 5.5 | 5.7 |
| 16.2–16.0 | 10 | 3.5 | 6.5 | 2.9 | 6.0 |
| 15.9–15.7 | 4 | 2.9 | 1.1 | 1.5 | 6.3 |
| 15.6–15.4 | 6 | 2.4 | 3.6 | 0.8 | 6.6 |
| 15.3–15.1 | 2 | 2.0 | 0 | 0.4 | 6.9 |
| 15.0–14.8 | 3 | 1.7 | 1.3 | 0.2 | 7.2 |
| 14.7–14.5 | 1 | 1.4 | −0.4 | 0.1 | −7.5 |
| 14.4–14.2 | 1 | 1.1 | − .1 | .......... | .......... |
| 14.1–13.9 | 1 | .9 | 0.1 | .......... | .......... |
| 13.8–13.6 | 2 | .7 | 1.3 | .......... | .......... |
| 13.5–13.3 | 2 | .5 | 1.5 | .......... | .......... |
| 13.2–13.0 | 2 | .4 | 1.6 | .......... | .......... |
| 12.9–12.7 | 0 | .3 | −0.3 | .......... | .......... |
| 12.6–12.4 | 0 | .2 | − .2 | .......... | .......... |
| 12.3–12.1 | 0 | .2 | −0.2 | .......... | .......... |

* $\phi(m)$ represents the numbers of stars in successive intervals of apparent photographic magnitude in a portion of Messier 33. The intervals are 0.3 mag., and the area over which the counts were made is estimated to include about one-fifth of the stars in the nebula.

† $\phi(M)$ gives the numbers of stars in successive intervals of absolute visual magnitude in a volume of space $3.6\times10^8$ cubic parsecs in which stars are distributed according to Kapteyn's luminosity function for the vicinity of the sun. The intervals are the same as for $\phi(m)$, namely, 0.3 mag. The median absolute magnitudes of the intervals in both functions are given in the last column. These are visual for Kapteyn's function and photographic for that of the nebula. The latter absolute magnitudes are based on the distance indicated by the Cepheids.

The data are collected in Table VI and are represented diagrammatically in Figure 6. The results for the brighter stars have little weight because of the small numbers in so restricted an area, but it is evident[1] that the stars in the nebula begin about 15.5 mag. For the distance derived from the Cepheids, this corresponds to an absolute magnitude of −6.6.

---

[1] *Mt. Wilson Contr.*, No. 304; *Astrophysical Journal*, **62**, 409, 1926.

[2] *Proceedings of the National Academy of Sciences*, **11**, 358, 1925.

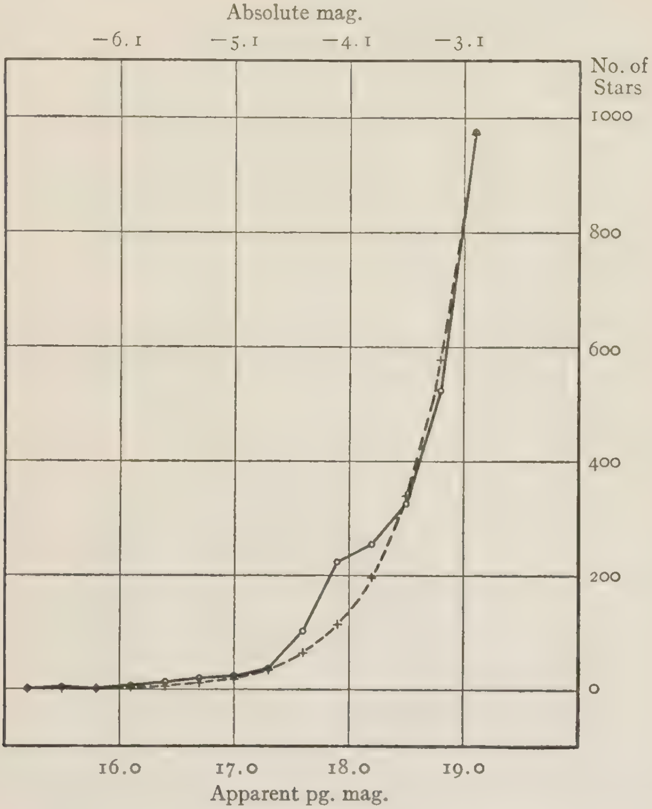

FIG. 6.—Luminosity function for the brighter stars in Messier 33, compared with Kapteyn's luminosity function.

Such a value for the upper limit of stellar luminosity is consistent with the conception of Messier 33 as a great isolated system, and is comparable with the corresponding limits for other systems.[1] The brightest Cepheid, at maximum, is about 2.5 mag. fainter than this limit and, indeed, has been outshone by several of the irregular variables. One of the latter, No. 2, practically reached the limit when, during the recent maximum, it attained an absolute magnitude of −6.55. Among the stars of constant luminosity, the five brightest of the blue giants in N.G.C. 604 are all within a half-magnitude of the limit.

---

[1] There are about six stars between 13.0 and 15.5 in excess of the number to be expected from the distribution tables. These are readily explained as accidental deviations incident upon the restricted areas counted, or resulting from the counting of close groups as single stars; but it is possible that they may indicate the presence of a few extremely luminous stars in the nebula. More extensive counts will be required in order to settle the question.

The nucleus, if it were truly stellar, would be an exception. The apparent magnitude is about 14.1, or −8.0 absolute. Since the spectral type is G5, the absolute visual magnitude, −9.0, would rival that of S Doradus in the large Magellanic Cloud. The image of the nucleus as shown on short exposures is not sharp, however, and suggests a small, highly concentrated globular nebula rather than a star. This is consistent with the behavior of nuclei in other spirals, among which the only ones that appear to be truly stellar have planetary spectra.[2]

The plot of the luminosity function, shown in Figure 6, exhibits a striking similarity to the corresponding section of Kapteyn's luminosity curve for stars in the vicinity of the sun, even though the latter is expressed in visual magnitudes, while the former is photographic. Kapteyn's function[3] is drawn as a dotted curve. The minor discrepancies between this and the full broken line, representing the data for Messier 33, can be explained partly as due to clusters in the nebula having been counted as single stars of higher luminosity and partly on the assumption, for which observational evidence will be adduced in the following section, that the brightest stars in the nebula are blue, and that the mean color-index increases as the magnitudes grow fainter.

---

[1] Upper limits of luminosity for other systems, in photographic magnitudes, are as follows: galactic system, −5.5 (brightest reliable measure, $\beta$ Orionis); large Magellanic Cloud, −8.0 (*Harvard Circular*, No. 271); small Magellanic Cloud, −4 to −7 (*ibid.*, No. 260); N.G.C. 6822, −5.9 (*Mt. Wilson Contr.*, No. 304); and globular clusters, −4.0 (*Proceedings of the National Academy of Sciences*, **6**, 293, 1920).

[2] N.G.C. 4051 and 4151 are examples. The emission spectra are confined to the nuclei and do not represent the light from the body of the nebulae.

[3] The data are found in *Mt. Wilson Contr.*, No. 229; *Astrophysical Journal*, **55**, 242, 1922.

Since the star counts are estimated to include about one-fifth of all the stars in the nebula down to the limit of the counts, the volume coefficient applied to Kapteyn's function as shown in Figure 6 must be increased fivefold in order to include all the stars in the nebula in the successive intervals of absolute magnitude. The resulting value is $1.8\times10^9$ cubic parsecs.

The integration of Kapteyn's function over the entire range of magnitudes gives a space density of 8.16 absolute visual magnitudes per cubic parsec.[1] For the volume coefficient corresponding to the counts in Messier 33, the total magnitude would be

$$\begin{aligned} 8.16-2.5\log(1.8\times10^9) &= -15.0 \text{ (absolute)} \\ 22.1-15.0 &= \phantom{-1}7.1 \text{ (apparent)} . \end{aligned}$$

The apparent visual magnitude of the spiral has been measured by Holetschek[2] and by Kritzinger,[3] and both find the same value, 7.0. This excellent agreement immediately suggests that the similarity between Kapteyn's luminosity function and that for the stars in Messier 33, although actually observed for only the three brightest magnitudes, extends throughout the range of magnitudes significant in determining integrated luminosities. The lower limit of this range is about the fourth absolute magnitude.[4] Fainter stars contribute less than 0.2 mag. to the total luminosity.

[1] Seares, *Mt. Wilson Contr.*, No. 191; *Astrophysical Journal*, **52**, 162, 1920.

[2] *Annalen der Wiener Sternwarte*, **20**, 1907.

[3] *Sirius*, **48**, 111, 1915.

[4] In a system of stars whose luminosities are distributed according to Kapteyn's function, the luminosity contributed by stars fainter than magnitude $M$, expressed as a correction which must be applied to the result of integration over the range $-\infty$ to $M$ in order to obtain the total magnitude of the entire system, is as follows:

| $M$ | Correction | $M$ | Correction |
|---|---|---|---|
| −3 | 3.52 mag. | +3 | 0.32 mag. |
| 2 | 2.65 | 4 | .17 |
| −1 | 1.93 | 5 | .08 |
| 0 | 1.35 | 6 | .036 |
| +1 | 0.90 | 7 | .013 |
| +2 | 0.56 | +8 | 0.004 |

For stars fainter than about $M=8$, Seares (*Mt. Wilson Contr.*, No. 273; *Astrophysical Journal*, **59**, 310, 1924) has shown that Kapteyn's function does not represent the observed distribution in the vicinity of the sun. Probable differences for this part of

The total luminosity of the spiral is thus fully accounted for on the assumption that it is a system of stars, the ten brightest magnitudes of which are distributed in a manner similar to that observed in the neighborhood of the sun. This assumption is supported by the directly observed similarity in the distribution of the three brightest magnitudes. It is tempting to extrapolate and argue that, since the ten brightest magnitudes appear to be similarly distributed in the two systems, the fainter magnitudes also should conform. There are, however, no observational controls for such a venture. Even the first assumption is by no means established. For instance, it might well be suggested that stars beyond the limits of observation are entirely lacking and that the luminosity which would otherwise be derived from them is supplied by true nebulosity which would ultimately produce the stars. This, of course, would be a forced interpretation, but would conform, in a measure, to current speculations on the evolution of spirals.

The volume of space filled by Messier 33 can be approximately derived by considering it as an ellipsoid of revolution with the minor axis one-tenth the major axis. The true form is probably a lens shape, but the order of the volume can be obtained on the simpler assumption. Since the maximum diameter is about sixty minutes of arc and the linear scale, at the distance indicated by the Cepheids, is $1'' = 1.27$ parsecs, the volume will be of the order of

$$\tfrac{4}{3}\pi(2.3)^3 \times 10^8 = 5 \times 10^9 \text{ cubic parsecs.}$$

This is about three times the volume coefficient derived by adjusting Kapteyn's luminosity function to fit the star counts in the nebula. It indicates that the average space density for the nebula as a whole is about one-third that in the vicinity of the sun, or about 9.26 absolute visual magnitudes per cubic parsec. The space density in the nuclear region and in the arms would, of course, be much greater.

An approximation for the mass of the spiral can be obtained from the difference in the radial velocities of the nucleus and the patch

---

the curve have, however, no appreciable effect on the integrated luminosity. When stars no fainter than $M = 15$ are considered, the radically different form of the function which Seares has suggested for the faint stars corresponds to a difference in the integrated luminosities of less than 0.002 mag.

of emission nebulosity, N.G.C. 604, some 700″ from the nucleus in the general direction of the major axis. The measures are

| | Km/sec. |
|---|---|
| Nucleus[1] | − 70 |
| N.G.C. 604[2] | −270 |
| Difference | 200 |

The ratio of minor to major axis appears to be about 2:3; the tilt is therefore about 42°, and the differential velocity of 200 km/sec. can be interpreted as the radial component of a linear velocity of rotation about the nucleus of

$$200 \sec 42^\circ = 270 \text{ km/sec.}$$

This corresponds to a period of rotation of the order of twenty million years at a distance of $1.83\times10^8$ astronomical units from the nucleus. The mass within this orbit, in terms of the sun's mass,[3] will be

$$M=\frac{a^3}{p^2}=1.5\times10^{10}\ .$$

The additional mass for the outer regions is probably less than the errors involved in the determination.

The mean density on these assumptions is approximately $3\odot$ per cubic parsec, or about twenty times that in the vicinity of the sun. This suggests the possibility of large quantities of non-luminous material in the central region of the nebula, but until more accurate data are available no emphasis can be placed on the numerical values. The method employed in calculating the mass is very sensitive to errors in the radial velocities—the mass varying directly with the square of the linear velocity of rotation. The radial velocity of N.G.C. 604 was derived from narrow emission lines and should be fairly reliable. That for the nucleus,[1] however, depends upon three absorption lines measured on a single plate of very small dispersion, −0.9 mm from $H\gamma$ to K. The result represents only the order of the velocity, and the probable error is a large fraction of the difference between the velocities of the nucleus and N.G.C. 604. Moreover, it is by no means certain that even an accurate differential velocity would represent merely the line-of-sight component of rotation about the nucleus.

---

[1] Pease, *Publications of the Astronomical Society of the Pacific*, **28**, 33, 1916.

[2] Mean of two determinations, by Pease and by Slipher. One, −278 km/sec., is given in the paper just cited; the other, −260 km/sec., is quoted by Strömberg, *Mt. Wilson Contr.*, No. 292; *Astrophysical Journal*, **61**, 353, 1925.

[3] When the distance from the nucleus, $a$, is expressed in parsecs, and the linear velocity of rotation, $v$, in km/sec., then $M\odot=235\,av^2$. The mass varies directly as the distance from the observer and as the square of the linear velocity. Due to the uncertainty in the latter quantity and the possibility that something more is observed than simple rotation around the nucleus, the computed mass may be in error by as much as a factor of 10.

## COLORS OF STARS IN MESSIER 33

Some information concerning the colors of the brighter stars in Messier 33 has been derived from isochromatic plates exposed through a visual color-filter. One of these, an exposure of three hours with the 100-inch reflector, shows stars which are estimated to be fainter than the eighteenth photovisual magnitude, including many of the Cepheids. Comparisons on the blink-comparator with appropriate direct exposures suggest that most of the brighter stars in the nebula are white or blue. The conclusion is based on the differences in the photovisual images of stars of approximately equal photographic magnitudes. For example, in the central region of the nebula, twenty-eight stars have photographic magnitudes between 16.5 and 17.5. On the plates examined, twenty-five of these show photovisual images that are comparable with the photographic images, while the remaining three stars have much larger photovisual images. From the well-determined photographic scale, which in this region appears to be not very different from the photovisual, the color-indices of the three outstanding stars were estimated to be about a magnitude greater than those of the other twenty-five. Moreover, two faint stars in the immediate neighborhood, having conspicuous proper motions,[1] are obviously much redder than the three just mentioned. The most reasonable interpretation of these observations is that the proper-motion stars are red dwarfs, that the three exceptional stars are yellow, and that the twenty-five other stars are white or blue. Moreover, since faint stars of early spectral types are extremely rare in this galactic latitude, it is probable that such stars belong to the nebula.

---

[1] Six stars within 11′ of the nucleus show conspicuous proper motions on the blink-comparator on plates of fifteen years' interval made with the 60-inch reflector. The photographic magnitudes of two have been measured as 17.3 and 18.25, the proper motions being of the order of 13″ and 10″ per century, both toward the south-following quadrant. The brighter of these is No. 367 in van Maanen's measures of Messier 33 for rotation (*Mt. Wilson Contr.*, No. 260; *Astrophysical Journal*, 57, 264, 1923). The magnitudes of the other four are estimated to be 14.2, 15.8, 16.4, and 17.8, with proper motions between 5″ and 10″ per century.

Although it has not yet been possible to calibrate the photovisual plates by direct comparisons with the polar sequence, an approximate reduction curve, connecting photovisual magnitudes with scale measures, has been constructed by correcting the photographic magnitudes for color-indices corresponding to known or probable spectral types. For the bright end of the curve, the nucleus itself and a star 1ʹ.8 north following were used. Photovisual magnitudes of 13.1 and 12.3, respectively, were derived from the observed spectral types G5 and F8. Seven Cepheids gave a point for the faint end at about 18.3. A mean spectral type of Go was assumed, in accordance with data from spectrograms of sixteen typical galactic Cepheids having periods ranging from ten to twenty-seven days with a mean of about seventeen days. The mean period of the seven Cepheids in Messier 33 is twenty-three days, but this larger value is balanced, to a certain extent, by the fact that most of the Cepheids were observed near maximum. The midpoint of the curve, the most important for the present purpose, depends upon a single star. This has a proper motion of the order of 10ʺ per century and a photographic magnitude of 18.25. It is obviously very red, and has been assumed to be a dwarf M with a color-index of +1.8. It is improbable that the color-index is greater than this amount, and hence the photovisual luminosities derived from this region of the reduction curve, together with the resulting color-indices, can be considered as upper limits.

By means of the reduction curve, color-indices have been determined for one hundred and ten stars, all but one[1] of which are within 2ʹ of the nucleus. The results are exhibited in Figure 7, where color-indices are plotted against photographic magnitudes. The data are practically complete to the eighteenth magnitude. The dotted

[1] The exception is the faint proper motion star used in determining the reduction curve. It is about 2ʹ.2 south preceding the nucleus, and is identified on Plate XV.

curve represents the minimum values of color-indices for stars of corresponding magnitudes in the polar sequence.[1] Since the galactic latitude of the pole is only 2° less than that of the spiral, it is reasonable to assume that field stars will be confined to the region above the dotted line in Figure 7. This region includes nine stars brighter than the eighteenth magnitude, one of which, the irregular variable No. 13, 17.85 mag., +0.8 color-index, certainly belongs to the nebula. The number of field stars to be expected on the basis of the mean distribution tables of Seares and van Rhijn[2] is seven.

The restricted area and the small number of stars do not permit definite conclusions to be drawn from this close agreement. The indications are, however, that all the stars brighter than the eighteenth magnitude, having color-indices less than, say 0.5 mag., belong to the nebula. Moreover, no star, excepting the variable, brighter than this limit, with a color-index greater than 0.5 mag., can with certainty be assigned to the central region of the nebula. The mean color-index of the stars assigned to the nebula is slightly negative, but since this probably represents an upper limit, the stars may actually be blue giants. It is possible that the brightest red stars in the spiral are all variables.

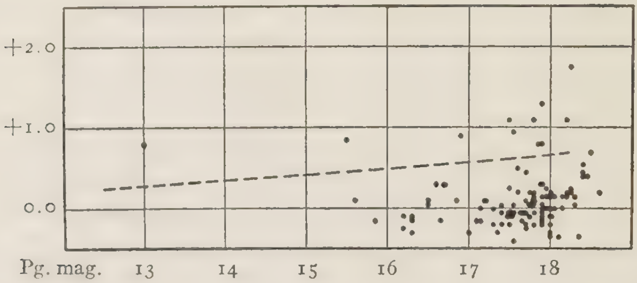

FIG. 7.—Color-indices (ordinates) of stars in the central region of Messier 33. The dotted line indicates the probable minimum color-index of stars outside the nebula.

These results, although approximate and possibly subject to serious errors and limitations, are sufficient to differentiate the brighter stars in the central region of Messier 33 from those in the globular clusters and in the irregular nebulae such as N.G.C. 6822, and probably from those in the Magellanic Clouds, all of which appear to be red. This contrast, which may be important, invites speculation on the larger problems of cosmic evolution.

---

[1] Seares, *Mt. Wilson Contr.*, No. 81; *Astrophysical Journal*, **39**, 361, 1914.

[2] *Mt. Wilson Contr.*, No. 301; *Astrophysical Journal*, **62**, 320, 1925.

In this connection, attention may be called to Seares's results[1] on the distribution of colors in Messier 51, 94, and 99. These are all well-developed spirals in which the arms are partially resolved into stars. The central regions of unresolved nebulosity (and also the amorphous mass at the end of an arm of Messier 51) were found to be much redder than the outer arms. Messier 33 exhibits the same phenomenon. The unresolved nebulosity around the nucleus is much stronger on photovisual than on unfiltered plates, as compared with star images both in the central region and in the outer arms. This agrees with the fact that the nucleus and the surrounding remnant of apparently unresolved nebulosity give a spectrum of the solar type, while the brighter stars have no appreciable color-index. The contrast in color between stars and nebulosity is in harmony with Seares's results for the other spirals, which in turn suggest that there is no conspicuous difference in color between the brighter stars in the central region and those in the outer arms of spirals. An inspection of the images in the arms of Messier 33 appears to support this latter suggestion, but, since the photovisual exposures were centered on the nucleus, the aberrations of the images in the outer regions prevented any reliable quantitative conclusions.

The observational data are insufficient to determine whether the unresolved central nebulosity with its solar type spectrum and considerable color-index is actually amorphous nebulosity or a cluster of faint stars. If the latter is the case, the color-indices must be assumed to increase as the luminosities of the stars decrease, after the manner of stars in the galactic system. It is well known, however, that spirals can be arranged in a series in which the arms build up at the expense of the unresolved nuclear region, unwinding and breaking up into condensations as they grow. The nuclear region of such late-type spirals as Messier 33 can be thus considered as the remnant of much larger central masses, such, for instance, as seen in Messier 31 or N.G.C. 4594. The nuclear regions of these in turn are almost indistinguishable from the elliptical nebulae (possibly prespiral forms) such as N.G.C. 3115 and Messier 32. In all these cases, the apparently unresolved nebulosity is associated with approximately solar-type spectra and appropriate color-indices. Even in Messier 31, however, which is highly resolved in the outer arms, the nuclear region shows not the slightest trace of resolution with the 100-inch reflector working under exceptionally fine observing conditions.

---

[1] *Proceedings of the National Academy of Sciences*, **2**, 553, 1916.

## CONCLUSION

The present investigations indicate that Messier 33 is an extremely distant system of stars and nebulae, similar in many respects to the Magellanic Clouds. It differs, however, in two important characteristics: The great majority at least of the brightest stars are of early spectral types, and there is a symmetrical arrangement of material with respect to a dominating nucleus. Detailed study of the stars within the limits of observation—the three or four brightest magnitudes—indicates that they are normal giants such as are known in other systems. The application of all available criteria leads to this one interpretation of the data.

The distance, derived from the period-luminosity relation applied to thirty-five apparently normal Cepheids, is about 8.1 times that of the small Magellanic Cloud, or, using Shapley's distance for the latter, about 263,000 parsecs. The order of this distance is confirmed by evidence from independent sources—novae, emission nebulosity with blue stars involved, and the luminosity function. The distance being known, the apparent dimensions of the spiral can be converted into absolute dimensions, assuming the form, from analogy with other spirals, to be lenticular, with a minor axis about one-tenth of the major axis. These dimensions are listed in Table VII with those of the two Magellanic Clouds for comparison.[1]

It is evident that Messier 33 must be considered as comparable in size with the Clouds rather than with the galactic system. It is not, however, of an entirely different order from the latter, and, in this connection, it may be mentioned that in size the other great spiral, Messier 31, occupies an intermediate position. Including the Magellanic Clouds, which are most readily interpreted as irregular non-galactic nebulae, five systems are now known which are believed to be distinct from the galactic system. The diameters range from 1250 parsecs for N.G.C. 6822 to about 14,000 parsecs for Messier 31. The ratio is about 1 to 11. The multiplication of the dimensions of Messier 31 in the same ratio would include the galactic system, even as outlined by the globular clusters.

---

[1] *Mt. Wilson Contr.*, No. 304; *Astrophysical Journal*, **62**, 409, 1926.

TABLE VII

Absolute Dimensions of Messier 33 and the Magellanic Clouds

| | Messier 33 | Magellanic Clouds | |
|---|---|---|---|
| | | Large | Small |
| Distance* | 263,000 | 34,500 | 31,600 |
| Total magnitude | −15.1 pv.† | −16.5 pg. | −15.5 pg. |
| Diameter | 4600 | 4300 | 2000 |
| Volume | $5\times10^{9}$ | $4.2\times10^{10}$ | $4.2\times10^{9}$ |
| Density | 9.3 | 10.0 | 8.5 |

* Distances and diameters are expressed in parsecs, volumes in cubic parsecs, and densities in absolute magnitudes per cubic parsec.

† The total magnitude of Messier 33 is expressed in visual absolute magnitudes, but, since the brighter stars in the spiral are white or blue, it is thought that the total photographic magnitude will not be very different.

Mount Wilson Observatory
February 1926

Contributions from the Mount Wilson Observatory, No. 311
Reprinted from the *Astrophysical Journal*, Vol. LXIII, pp. 281–341, 1926
Printed in the U.S.A.

# A SPECTROGRAPHIC STUDY OF MIRA CETI

By ALFRED H. JOY

## ABSTRACT

*Spectral variations.*—131 spectrograms taken with the 60-inch and 100-inch reflectors cover the whole range of the star's variation during the last ten years. Spectral changes are recurrent. The titanium bands vary with magnitude (Table III). Bright lines of ionized iron are seen near maximum. Although at minimum there are no emission lines, bright hydrogen lines appear soon after and have their greatest intensity near maximum. Low-temperature emission lines of iron, magnesium, and silicon appear after maximum is well past. The weaker absorption lines fade out at minimum. Spectral changes depend mostly on the magnitude of the star.

*Absorption spectrum.*—Measures of individual lines of band structure show that the bands give the same velocities as the absorption lines. Seven new titanium oxide bands to the violet of λ 4354 have been identified by laboratory comparisons. The absorption lines belong to temperature classes I and II. The most prominent elements are iron, vanadium, chromium, manganese, calcium, and magnesium. Titanium lines are weak. Radial velocity measures give a curve (Table VI) which is represented by elliptical elements.

*Emission lines.*—The bright lines measured are given in Table VIII; the probable identification of 32 of these lines is in Table X. Estimates of the intensities at different phases have been made for 36 of the stronger lines (Table IX). The emission lines give a velocity curve (Table XIV) which shows outward motion relative to the absorption-line curve except at minimum, when the difference is zero. The maximum difference is 19 km/sec. at phase 56 days. The velocities of both bright and dark lines are the same at recurring cycles (Table XVII). The intensities of the bright lines at maximum depend on the magnitude of the star (Table XIX). At the unusually faint maximum of 1924 several peculiar features were noted in the region λ 4584–λ 4905, which, in part, are tentatively attributed to magnesium hydride.

*Physical conditions.*—The spectroscopic absolute magnitude at the normal maximum of magnitude 3.5 is estimated to be −0.3, corresponding to a parallax of 0.″017. From the angular diameter of 0.″056 measured with the interferometer, the linear diameter is found to be 490,000,000 km, and the surface brightness 7.5 mags. fainter than the sun. For an assumed mass 5 times that of the sun the density is $1.1\times10^{-7}$, and the surface gravity $4\times10^{-5}$, that of the sun. The temperature is estimated to vary from 2300° to 1800° K. The observed bolometric variation in energy of about one magnitude agrees with the observed variation in visual magnitude, when account is taken of the shift in the energy-curve toward the red for these temperatures, and the excessive absorption of the titanium oxide bands at minimum.

*The visual companion.*—The spectrum of a companion was seen on plates taken near minimum. Its approximate position was determined from the spectrograms. Later its presence was confirmed visually by Aitken. In 1923 the magnitude was 9.8, but it seems to be a variable. It has an early type spectrum with bright lines of hydrogen, helium, and ionized iron and calcium. No absorption lines are present except those connected with emission bands of the hydrogen series. The violet component of the hydrogen lines is affected by the variation of both stars.

*Discussion.*—The application of recent results to the problem of the variation of Mira and similar stars is briefly discussed.

The purpose of this contribution is to give a summarized description of the extraordinary changes which take place in the spectrum of the long-period variable *o* Ceti, to extend the material published in several papers[1] by Adams and the writer, and to give the results of further study of the spectrograms of the star made with the 60-inch and 100-inch reflectors during the years 1916–1925.

Mira is the brightest and the best-known star of its class. In most respects its behavior is typical. The long-period variables are distinguished by periods averaging about 300 days. Most of them have M-type spectra with emission lines, particularly of hydrogen.

Since the discovery of its variation in 1596, the light changes in Mira have been followed with very few interruptions. The mean period is 330 days, but the interval from maximum to maximum may vary by as much as 30 days. The magnitude at maximum is normally about 3.5, with extremes of 1.5 and 5.6. The minimum is also uncertain, varying from 8.0 to 10.0, but most frequently is about 9.2. The red color of the variable has made the estimates of its brightness somewhat uncertain, especially at minimum phase.

A number of observers have studied the spectrum of the star at or near maximum. Stebbins[2] in his extended research in 1903 was able to follow it to lower magnitudes, but the faintness of the star at minimum phase made it impossible at that time to secure satisfactory spectrograms.

Observations were begun at Mount Wilson in 1916, primarily to note the effects of changing absolute magnitude on the spectrum. As observations continued, points of astrophysical interest developed which had not previously been considered in full, so that it was deemed advisable to try to cover the whole cycle of variation. Accordingly more time has been devoted to this star than to any other thus far observed spectroscopically at this Observatory.

The completion of the 100-inch reflector in 1919 made it possible to secure spectrograms at minimum with sufficient dispersion to study the velocity variation of bright and dark lines throughout the period, as well as to note numerous other data bearing on the physical conditions in and about the star. The intrusion of a secondary spectrum at minimum led, in 1920, to the consideration of the existence of a faint companion,[1] and to its visual detection[2] in 1923.

---

[1] *Publications of the Astronomical Society of the Pacific*, **29**, 112, 1917; **30**, 193, 1918; **32**, 163, 1920; **33**, 107, 1921; **35**, 168, 1923; **36**, 290, 1924. *Publications of the American Astronomical Society*, twenty-ninth meeting, p. 14, 1922; thirtieth meeting, p. 64, 1923.

[2] *Lick Observatory Bulletins*, **2**, 78, 1903; *Astrophysical Journal*, **18**, 341, 1903.

## I. THE GENERAL COURSE OF THE SPECTRAL VARIATIONS

The major physical processes taking place in the star seem to repeat themselves without essential change in succeeding cycles of its light variation. The outstanding features of the spectrum depend for the most part upon the magnitude of the star as well as upon the phase.

At maximum the star is of spectral type M5–M6, with strong bands of titanium oxide and sharp hydrogen emission lines. The bright lines of hydrogen have their maximum intensity at or soon after the maximum of light. They are accompanied by faint emission lines of ionized iron. The appearance of most of the other bright lines is delayed for three or four months until the star has reached fainter magnitudes.

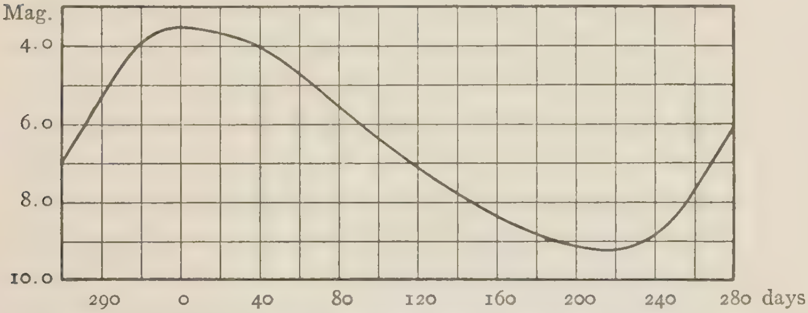

FIG. 1.—Light-curve of Mira from observations of the American Association of Variable Star Observers.

When the star is fainter than the eighth magnitude the bright lines of the companion are well seen and its continuous spectrum shows sufficient strength to give the combined spectrum a curious distorted effect which is especially noticeable in the region of the bands. As the brightness diminishes the bands increase in strength and the absorption lines fade until at minimum only a few lines can be seen. Certain lines of chromium, calcium, and vanadium seem to be the most persistent. The strong calcium line at λ 4226 undergoes a tremendous change, reaching a width of about 25 A at minimum.

---

[1] *Publications of the American Astronomical Society*, twenty-ninth meeting, p. 14, 1922.

[2] Aitken, *Publications of the Astronomical Society of the Pacific*, 35, 323, 1923.

The sharp emission lines of hydrogen disappear at about magnitude 8.5 and reappear at about the same brightness on the rising branch of the light-curve. There are numerous other emission lines, mostly sharp in character like the hydrogen lines, the time of whose appearance is apparently determined by their temperature class. The silicon lines λλ 3905 and 4103 are seen near maximum, but the extremely low-temperature magnesium line λ 4571 is not found until a magnitude of 5.5 is reached about 80 days after maximum. All bright lines disappear at minimum, or very soon after, so that during an interval of 20–40 days soon after minimum no emission lines whatsoever are given out by the variable itself.

## 2. THE OBSERVATIONS

The observations have extended over a sufficient length of time to be fairly representative of the spectrographic behavior of the star. All portions of the light-curve have been covered. The maxima observed have varied from 2.8 in 1923 to 4.7 in 1924; the extremes of minima were 9.4 in 1921 and 8.5 in 1922.

In general the spectrograms were taken with a single prism and an 18-inch (46 cm) camera at the Cassegrain focus of the 60-inch and 100-inch reflectors. The usual dispersion was about 35 A to the millimeter. In a few cases a 40-inch (102 cm) camera was used near maxima, and cameras of 7 and 10 inches at the fainter minima. When possible the exposures were timed to show the continuous and dark-line spectrum rather than bright lines only. The plates have been made by a number of observers to whom much credit is due for the results obtained. Some of the spectrograms taken at minimum of light during the poor observing conditions of winter were particularly difficult to obtain.

The magnitudes used in this discussion are based on curves generously furnished from the Harvard College Observatory by Professors Bailey and Shapley and on observations published by the American Association of Variable Star Observers. The brighter magnitudes agree closely with the estimates published in the *Astronomische Nachrichten* by Nijland, but those below 7.5 are systematically brighter, chiefly because of the different system of magnitudes for the comparison stars adopted by Nijland.

The dates of observed maxima and minima for the years in question are given in Table I.

TABLE I

MAXIMA AND MINIMA

| MAXIMA | | | | MINIMA | |
|---|---|---|---|---|---|
| Mag. | Observed Date | Calculated Date | O−C | Mag. | Observed Date |
| 3.7 | 1916, Nov. 14 | Nov. 16 | $-2^{\mathrm{d}}$ | .......... | .......... |
| 3.6 | 1917, Oct. 1 | Oct. 12 | $-11$ | .......... | .......... |
| 3.5 | 1918, Sept. 20 | Sept. 7 | $+13$ | .......... | .......... |
| 3.3 | 1919, Aug. 6 | Aug. 3 | $+3$ | 9.6 | 1920, Mch. 21 |
| 3.1 | 1920, June 30 | June 28 | $+2$ | 9.4 | 1921, Jan. 27 |
| .......... | .......... | May 24 | .......... | 9.5 | 1921, Dec. 28 |
| .......... | .......... | Apr. 19 | .......... | 8.5 | 1922, Nov. 6 |
| 2.8 | 1923, Mch. 6 | Mch. 15 | $-9$ | 9.2 | 1923, Oct. 6 |
| 4.7 | 1924, Feb. 1 | Feb. 8 | $-7$ | 9.3 | 1924, Sept. 1 |
| 3.8 | 1925, Jan. 4 | Jan. 3 | $+1$ | 9.0 | 1925, Aug. 1 |
| 3.3 | 1925, Dec. 4 | Nov. 29 | $+5$ | .......... | .......... |

The question of phase in a case of this kind is a difficult problem, and thus far no adequate method has been suggested by which observations made in different cycles can be satisfactorily combined. Some have taken as phases proportional parts of the time actually elapsing between maxima and minima or between one maximum and the next. In this discussion of *o* Ceti, where the irregularities are small as compared with the whole period and where phases are used chiefly in connection with radial velocities which, at best, have a large probable error, the use of a mean period has seemed admissible. All phases given in this paper are based upon maxima determined from the mean elements

$$\text{Max.} = 2421184 + 330 \text{ days.}$$

These elements give the calculated maxima of Table I. It will be observed that the deviations of the observed maxima from the calculated values do not exceed 13 days.

Table II is a list of the 131 spectrograms of *o* Ceti used in this

## TABLE II

### OBSERVATIONS OF *o* CETI

| Plate | Date | J.D. | Mag. | Phase | Spectrum | Dark Lines | | Bright Lines | |
|---|---|---|---|---|---|---|---|---|---|
| | | | | | | *V* | Wt. | *V* | Wt. |
| | 1916 | | | | | km/sec. | | km/sec. | |
| γ 5252..... | Nov. 11 | 1179 | 3.7 | 325 | M7 | +63.4 | 1 | +42.8 | 1 |
| 5258..... | 12 | 1180 | 3.7 | 326 | 7 | 62.4 | 3 | 46.4 | 2 |
| 5299..... | Dec. 5 | 1203 | 3.8 | 19 | 7 | 64.2 | 2 | 46.3 | 2 |
| | 1917 | | | | | | | | |
| 5413..... | Jan. 4 | 1233 | 4.4 | 49 | 7 | 70.3 | 3 | 40.3 | 2 |
| 5480..... | 31 | 1260 | 5.2 | 76 | 8 | 58.2 | 3 | 40.7 | 2 |
| 5492..... | Feb. 1 | 1261 | 5.3 | 77 | 8 | 58.5 | 3 | 40.3 | 2 |
| 5559..... | 9 | 1269 | 5.5 | 85 | 8 | 66.2 | 2 | 46.4 | 2 |
| 5615..... | Mch. 3 | 1291 | 6.2 | 107 | 8 | 54.5 | 2 | 39.5 | 2 |
| 6120..... | Aug. 27 | 1468 | 5.9 | 284 | 8 | 63.5 | 2 | 47.4 | 2 |
| 6235..... | Sept. 30 | 1502 | 3.6 | 318 | 6 | 65.4 | 2 | 49.7 | 2 |
| 6236..... | 30 | 1502 | 3.6 | 318 | 6 | 64.1 | 2 | 46.0 | 2 |
| 6243..... | Oct. 1 | 1503 | 3.6 | 319 | 6 | 62.7 | 3 | 51.5 | 1 |
| 6270..... | 5 | 1507 | 3.6 | 323 | 6 | 64.6 | 2 | 45.2 | 2 |
| 6306..... | 26 | 1528 | 3.7 | 14 | 7 | 63.8 | 3 | 49.2 | 2 |
| 6338..... | Nov. 1 | 1534 | 3.8 | 20 | 7 | 63.4 | 3 | 49.3 | 1 |
| 6369..... | 23 | 1556 | 4.1 | 42 | 7 | 69.7 | 2 | 48.3 | 2 |
| | 1918 | | | | | | | | |
| 6531..... | Jan. 2 | 1596 | 5.1 | 82 | 7 | 60.0 | 2 | 40.6 | 3 |
| 6594..... | 23 | 1617 | 5.7 | 103 | 8 | 64.1 | 3 | 40.2 | 3 |
| 6724..... | Mch. 2 | 1655 | 7.1 | 141 | 8+Bβ | 48.7 | 1 | 38.3 | 2 |
| 7413..... | Sept. 23 | 1860 | 3.5 | 16 | 6 | 59.1 | 2 | 48.0 | 2 |
| 7524..... | Oct. 26 | 1893 | 3.9 | 49 | 6 | ........ | .... | ...... | .... |
| 7551..... | Nov. 16 | 1914 | 5.2 | 70 | 7 | 68.5 | 2 | 49.1 | 2 |
| 7645..... | Dec. 15 | 1943 | 6.5 | 99 | 8 | ........ | .... | 45.2 | 3 |
| | 1919 | | | | | | | | |
| 7773..... | Jan. 16 | 1975 | 7.7 | 131 | e | ........ | .... | 48.4 | 1 |
| 7795..... | 18 | 1977 | 7.8 | 133 | 8+Bβ | 53.4 | 1 | 46.3 | 3 |
| 8597..... | Aug. 16 | 2187 | 3.4 | 13 | 5 | 65.8 | 3 | 44.3 | 2 |
| 8694..... | Sept. 10 | 2212 | 3.8 | 38 | 6 | 56.2 | 2 | 40.8 | 1 |
| 8789..... | Oct. 14 | 2246 | 5.3 | 72 | 7 | 60.1 | 2 | 41.6 | 3 |
| 8805..... | Nov. 3 | 2266 | 6.2 | 92 | 8 | 56.9 | 3 | 38.9 | 3 |
| C 185..... | 8 | 2271 | 6.4 | 97 | .......... | ........ | .... | ...... | .... |
| γ 8872..... | 13 | 2276 | 6.6 | 102 | 8 | ........ | .... | 45.8 | 3 |
| 8918..... | Dec. 12 | 2305 | 7.7 | 131 | e+Bβ | ........ | .... | 53.3 | 3 |
| | 1920 | | | | | | | | |
| C 230..... | Jan. 7 | 2331 | 8.4 | 157 | e+Bβ | ........ | .... | 51.8 | 2 |
| 246..... | 14 | 2338 | 8.5 | 164 | e+Bγ | ........ | .... | 55.3 | 2 |
| 250..... | 15 | 2339 | 8.6 | 165 | 9+Bδ | ........ | .... | 56.6 | 3 |
| 260..... | 29 | 2353 | 8.9 | 179 | 9+Bδ | ........ | .... | 55.4 | 2 |
| 278..... | Feb. 6 | 2361 | 9.1 | 187 | e+Bβ | ........ | .... | 57.2 | 1 |
| 287..... | 12 | 2367 | 9.2 | 193 | e+Bδ | ........ | .... | 54.0 | 1 |
| 500..... | June 29 | 2505 | 3.1 | 1 | 6 | 65.0 | 3 | 56.4 | 2 |
| γ 9395..... | July 27 | 2533 | 3.4 | 29 | 5 | 64.6 | 3 | 47.6 | 2 |
| 9436..... | Aug. 5 | 2542 | 3.6 | 38 | 5 | 60.1 | 3 | 42.4 | 2 |
| 9454..... | 23 | 2560 | 4.4 | 56 | 7 | 61.5 | 3 | 37.8 | 2 |
| 9567..... | Sept. 22 | 2590 | 6.0 | 86 | 8 | 59.5 | 1 | ...... | .... |
| C 760..... | Nov. 20 | 2649 | 8.1 | 145 | 9+Bγ | 67.5 | 0.5 | 50.2 | 3 |
| 766..... | 21 | 2650 | 8.2 | 146 | 9+Bδ | 46.3 | 1 | 49.2 | 3 |
| 801..... | 29 | 2658 | 8.4 | 154 | 9+Bγ | +46.1 | 0.5 | +48.5 | 2 |

TABLE II—*Continued*

| Plate | Date | J.D. | Mag. | Phase | Spectrum | Dark Lines | | Bright Lines | |
|---|---|---|---|---|---|---|---|---|---|
| | | | | | | *V* | Wt. | *V* | Wt. |
| | 1921 | | | | | km/sec. | | km/sec. | |
| C 847..... | Jan. 4 | 2694 | 9.2 | 190 | M9+Bδ | ........ | .... | +47.6 | 2 |
| 859..... | 21 | 2711 | 9.4 | 207 | −+Bγ | ........ | .... | ...... | .... |
| 861..... | 24 | 2714 | 9.4 | 210 | −+Bβ | ........ | .... | ...... | .... |
| 867..... | 29 | 2719 | 9.4 | 215 | 9+Bϵ | +47.5 | 0.5 | ...... | .... |
| 874..... | Feb. 15 | 2736 | 9.3 | 232 | 9+Bγ | ........ | .... | ...... | .... |
| 878..... | 17 | 2738 | 9.3 | 234 | 9+Bγ | 49.1 | 0.5 | ...... | .... |
| γ 10276..... | July 14 | 2885 | 4.9 | 51 | 7 | 57.1 | 3 | 40.5 | 2 |
| 10381..... | Aug. 18 | 2920 | 6.4 | 86 | 8 | 54.5 | 2 | 37.8 | 3 |
| 10435..... | Sept. 10 | 2943 | 7.2 | 109 | 8 | 59.8 | 2 | 51.8 | 3 |
| 10503..... | 21 | 2954 | 7.6 | 120 | 8+Bβ | 56.1 | 3 | 44.0 | 3 |
| C 1364..... | Oct. 6 | 2969 | 8.0 | 135 | 8 | ........ | .... | 49.6 | 3 |
| 1375..... | 8 | 2971 | 8.1 | 137 | 8+Bδ | 52.7 | 1 | 45.9 | 3 |
| 1401..... | 13 | 2976 | 8.3 | 142 | .......... | ........ | .... | ...... | .... |
| 1442..... | Nov. 7 | 3001 | 8.8 | 167 | 9+Bδ | 58.0 | 2 | 54.4 | 3 |
| 1474..... | 22 | 3016 | 9.0 | 182 | 9+Bγ | ........ | .... | 45.8 | 1 |
| 1478..... | Dec. 7 | 3031 | 9.2 | 197 | 9+Bδ | ........ | .... | 48.6 | 2 |
| 1482..... | 8 | 3032 | 9.3 | 198 | −+Bβ | ........ | .... | 49.4 | 1 |
| 1483..... | 9 | 3033 | 9.3 | 199 | −+Bβ | ........ | .... | 49.6 | 1 |
| 1488..... | 11 | 3035 | 9.3 | 201 | −+Bγ | ........ | .... | 59.6 | 1 |
| 1494..... | 14 | 3038 | 9.4 | 204 | 9+Bδ | ........ | .... | 50.6 | 1 |
| | 1922 | | | | | | | | |
| 1515..... | Jan. 9 | 3064 | 9.3 | 230 | e+Bγ | ........ | .... | ...... | .... |
| 1546..... | Feb. 4 | 3090 | 8.9 | 256 | 9+Bγ | ........ | .... | ...... | .... |
| 1547..... | 5 | 3091 | 8.9 | 257 | 9+Bδ | 49.4 | 1 | ...... | .... |
| 1597..... | Mch. 9 | 3123 | 7.1 | 289 | 8+Bγ | 60.2 | 1 | ...... | .... |
| γ 11148..... | July 6 | 3242 | 5.7 | 78 | 8 | 58.2 | 2 | 46.0 | 2 |
| 11254..... | Aug. 11 | 3278 | 6.8 | 114 | 8 | 59.5 | 3 | 40.0 | 3 |
| C 1845..... | 31 | 3298 | 7.5 | 134 | 9+Bβ | 57.2 | 2 | 49.8 | 3 |
| 1897..... | Sept. 28 | 3326 | 8.2 | 162 | 9+Bγ | 63.7 | 0.5 | 47.2 | 3 |
| 1950..... | Oct. 9 | 3337 | 8.3 | 173 | .......... | ........ | .... | ...... | .... |
| 1996..... | Nov. 5 | 3364 | 8.5 | 200 | 9+Bδ | 46.2 | 2 | ...... | .... |
| 2013..... | Dec. 5 | 3394 | 8.3 | 230 | 9+Bδ | 53.5 | 3 | ...... | .... |
| 2017..... | 26 | 3415 | 7.9 | 251 | 9+Bγ | 56.3 | 3 | ...... | .... |
| | 1923 | | | | | | | | |
| 2040..... | Jan. 2 | 3422 | 7.8 | 258 | 9+Bγ | 55.7 | 2 | ...... | .... |
| 2041..... | 2 | 3422 | 7.8 | 258 | 8+Bγ | 65.6 | 0.5 | ...... | .... |
| γ 11564..... | 25 | 3445 | 5.5 | 281 | 8 | 58.8 | 3 | 43.2 | 1 |
| C 2090..... | 27 | 3447 | 5.0 | 283 | 7 | 62.3 | 3 | 55.6 | 1 |
| 2091..... | 27 | 3447 | 5.0 | 283 | 7 | 60.9 | 3 | 52.0 | 1 |
| γ 11609..... | Feb. 7 | 3458 | 3.8 | 294 | 6 | 58.7 | 3 | 44.3 | 1 |
| 11622..... | 24 | 3475 | 2.9 | 311 | 5 | 64.3 | 3 | 41.1 | 1 |
| 11623..... | 24 | 3475 | 2.9 | 311 | 5 | 69.2 | 2 | 49.3 | 1 |
| C 2171..... | Mch. 28 | 3507 | 3.2 | 13 | 5 | 65.1 | 2 | 48.1 | 1 |
| 2353..... | July 24 | 3625 | 7.7 | 131 | 8+Bϵ | ........ | .... | 51.0 | 1 |
| 2383..... | Aug. 18 | 3650 | 8.4 | 156 | 8+Bϵ | 58.9 | 0.5 | 57.7 | 2 |
| 2482..... | Oct. 19 | 3712 | 9.2 | 218 | 9+Bδ | ........ | .... | +56.3 | 1 |
| 2487..... | Oct. 20 | 3713 | 9.2 | 219 | .......... | ........ | .... | ...... | .... |
| 2579..... | Dec. 17 | 3771 | 8.1 | 277 | 8+Bδ | +53.0 | 2 | ...... | .... |

TABLE II—*Continued*

| Plate | Date | J.D. | Mag. | Phase | Spectrum | Dark Lines | | Bright Lines | |
|---|---|---|---|---|---|---|---|---|---|
| | | | | | | *V* | Wt. | *V* | Wt. |
| | 1924 | | | | | km/sec. | | km/sec. | |
| γ 12363..... | Jan. 12 | 3797 | 5.6 | 303 | M7 | +61.7 | 2 | +51.0 | 0.5 |
| 12447..... | 26 | 3811 | 5.1 | 317 | 7 | 57.7 | 1 | 41.8 | 0.5 |
| C 2663..... | Feb. 11 | 3827 | 4.7 | 3 | 7 | 64.5 | 2 | 49.9 | 1 |
| γ 12461..... | 13 | 3829 | 4.8 | 5 | 7 | 63.9 | 3 | 43.2 | 1 |
| 12471..... | 14 | 3830 | 4.8 | 6 | 7 | ........ | .... | 45.6 | 1 |
| C 2710..... | Mch. 11 | 3856 | 5.4 | 32 | 7 | ........ | .... | 47.1 | 1 |
| 2930..... | Aug. 12 | 4010 | 9.0 | 186 | −+Bε | ........ | .... | 51.4 | 0.5 |
| 2934..... | 13 | 4011 | 9.0 | 187 | 9 | ........ | .... | 54.3 | 1 |
| 2989..... | Sept. 7 | 4036 | 9.1 | 212 | −+Bδ | ........ | .... | 47.6 | 1 |
| 3037..... | Oct. 8 | 4067 | 8.9 | 243 | 9+Bδ | 55.8 | 1 | 50.2 | 1 |
| 3068..... | Nov. 6 | 4096 | 8.4 | 272 | 9+Bδ | 61.3 | 3 | 44.8 | 0.5 |
| 3078..... | 14 | 4104 | 7.6 | 280 | 8+Bδ | 61.4 | 3 | ...... | .... |
| 3091..... | Dec. 3 | 4123 | 5.2 | 299 | 8 | 55.9 | 2 | 51.6 | 1 |
| | 1925 | | | | | | | | |
| G 47..... | Jan. 3 | 4154 | 3.8 | 0 | 7 | ........ | .... | ...... | .... |
| γ 13185..... | 8 | 4159 | 3.8 | 5 | 7 | 61.3 | 5 | ...... | .... |
| 13191..... | 10 | 4161 | 3.8 | 7 | 7 | ........ | .... | ...... | .... |
| 13192..... | 10 | 4161 | 3.8 | 7 | 7 | ........ | .... | ...... | .... |
| 13193..... | 10 | 4161 | 3.8 | 7 | 7 | ........ | .... | ...... | .... |
| 13200..... | 11 | 4162 | 3.8 | 8 | 7 | 67.5 | 2 | 48.2 | 1 |
| 13201..... | 11 | 4162 | 3.8 | 8 | 7 | 69.9 | 3 | 48.6 | 1 |
| 13202..... | 11 | 4162 | 3.8 | 8 | 7 | 61.7 | 3 | 47.8 | 1 |
| 13203..... | 11 | 4162 | 3.8 | 8 | 7 | ........ | .... | +41.9 | 0.5 |
| C 3406..... | July 29 | 4361 | 9.0 | 207 | 9+Bδ | ........ | .... | ...... | .... |
| 3410..... | 30 | 4362 | 9.0 | 208 | 9+Bδ | ........ | .... | ...... | .... |
| 3511..... | Sept. 8 | 4402 | 8.8 | 248 | 9+Bβ | 57.8 | 2 | ...... | .... |
| 3516..... | 23 | 4417 | 8.0 | 263 | 9 | ........ | .... | ...... | .... |
| γ 13819..... | Oct. 7 | 4431 | 6.4 | 277 | 8 | 61.4 | 3 | ...... | .... |
| 13828..... | 8 | 4432 | 6.3 | 278 | 8 | 61.5 | 2 | ...... | .... |
| 13849..... | 26 | 4450 | 4.5 | 296 | 7 | +61.9 | 3 | ...... | .... |
| 13891..... | Nov. 25 | 4480 | 3.4 | 326 | 6 | ........ | .... | ...... | .... |
| 13892..... | 25 | 4480 | 3.4 | 326 | 6 | ........ | .... | ...... | .... |
| C 3604..... | Dec. 7 | 4492 | 3.2 | 8 | 6 | ........ | .... | ...... | .... |
| 3605..... | 7 | 4492 | 3.2 | 8 | 6 | ........ | .... | ...... | .... |
| γ 13925..... | 22 | 4507 | 3.2 | 23 | 6 | ........ | .... | ...... | .... |
| 13926..... | 22 | 4507 | 3.2 | 23 | 6 | ........ | .... | ...... | .... |
| 13928..... | 23 | 4508 | 3.2 | 24 | 6 | ........ | .... | ...... | .... |
| 13931..... | 24 | 4511 | 3.2 | 25 | 6 | ........ | .... | ...... | .... |
| 13933..... | 25 | 4512 | 3.3 | 26 | 6 | ........ | .... | ...... | .... |
| | 1926 | | | | | | | | |
| 13990..... | Jan. 21 | 4539 | 4.0 | 53 | 7 | ........ | .... | ...... | .... |

## NOTES TO TABLE II

Plates γ 6243, 6338, and 9454 were taken with the 40-inch camera; γ 5252, 7524, C 867, 874, 878, 1546, 1547, 1597, 2041, 2353, and 2383 with the 7-inch camera; C 2487, 2930, 2934, 3037, 3068, 3078, 3410, 3511, and 3516 with the 10-inch camera. C 185, 1401, 1950, 2487, 3605, γ 13191, 13192, 13193, and G 47 show the red region of the spectrum. γ 13185 was taken by Mr. Sanford with 3 prisms and 18-inch camera; γ 13891, 13892, NOTES TO TABLE II—*Continued*

13925, 13926, 13928, 13931, and 13990 were taken with 3 prisms and 40-inch camera to study the structure of $H\gamma$ and $H\delta$. G 47 was taken by Mr. Merrill with a grating spectrograph attached to the 100-inch reflector. $\gamma$ 7645, 7773, 8872, 8918, C 230, 246, 801, 859, 861, 874, 1364, 1482, 1483, 1488, 1515 are too weak to show much of the continuous spectrum.

The slit was set at 45° position angle for C 1482, 1483, 1488, 1494, 2017, and at 135° for C 1474, 2013, 2040, 2041.

The exposure times vary from a few minutes up to four hours. The number of plates taken by various observers is: Hubble, 1; Duncan, 2; Humason, 2; Hoge, 5; Strömberg, 5; Sanford, 6; Merrill, 10; Adams, 31; Joy, 69.

study. The sixth column gives the estimated spectral type for each date. The classification used is based on the recommendation of the International Astronomical Union in 1922, which gives *o* Ceti at normal maximum as an example of type M6e, and R Leonis of type M8e. This system permits the inclusion of all the Me stars thus far observed, at minimum as well as maximum, within the subdivisions 0 to 10. Obviously it is a great advantage to be able to classify all the spectra showing well-developed titanium oxide bands in one spectral class. The typical stars used here in connection with this classification were chosen by Mr. Merrill and the writer and are given in *Contribution* No. 264, *Astrophysical Journal*, **58**, 241, 1923. The spectrum of the companion is B and the appended Greek letter shown in the sixth column of the table is that of the hydrogen bright line farthest to the violet seen in the spectrum of the companion.

The measured radial velocities of dark and bright lines with their corresponding weights are given in the last columns of the table.

### 3. SPECTRAL TYPE

A casual inspection of the plates taken at different phases shows, as has been noted by several observers, a considerable variation in type, which, in general, appears to follow the change in brightness. This relationship is indicated in Table III and Figure 2.

If the spectral type thus determined is a function of temperature, the relationship is important and indicates an actual physical change in temperature in the region where the bands and absorption lines originate.

While the general characteristics of the spectra certainly depend mostly on magnitude, there is no escape from the conclusion that many peculiarities of individual lines or regions vary in different cycles. Thus, the spectra at the bright minimum of 1922 and the faint maxima of February, 1924, without doubt, were somewhat different from the usual spectra at corresponding magnitudes.

TABLE III

Relationship of Type and Magnitude

| Mean Type | Mean Mag. | No. Plates |
|---|---|---|
| M5.2 | 3.1 | 6 |
| M6.3 | 3.7 | 13 |
| M6.9 | 4.6 | 8 |
| M7.6 | 5.5 | 11 |
| M8.0 | 6.4 | 8 |
| M8.4 | 7.7 | 15 |
| M9.0 | 8.9 | 26 |

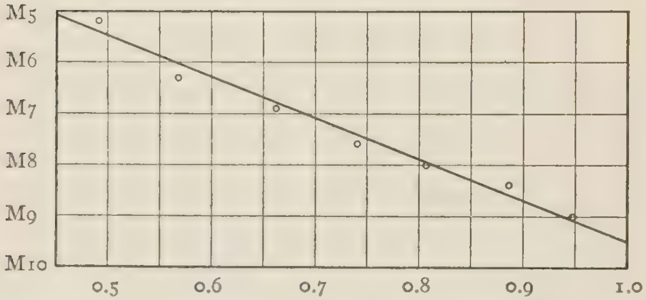

Fig. 2.—Variation of spectral type with logarithm of the magnitude (abscissae)

### 4. THE CONTINUOUS SPECTRUM AND BANDS

With slit spectrograms it is not possible to study satisfactorily the relative intensities of different portions of the continuous spectrum. Nevertheless, it is evident, as Stebbins[1] has shown, that the spectrum is relatively stronger in the region λ 4000–λ 4200 at minimum than at maximum. Mr. Merrill finds the same effect in other Me stars. Doubtless a similar result is indicated by studies of color indices of M-type stars, from which it appears that the color index increases very little, if any, after passing M0. It is also ap-

---

[1] *Lick Observatory Bulletins*, 2, 90, 1903.

## PLATE VIII

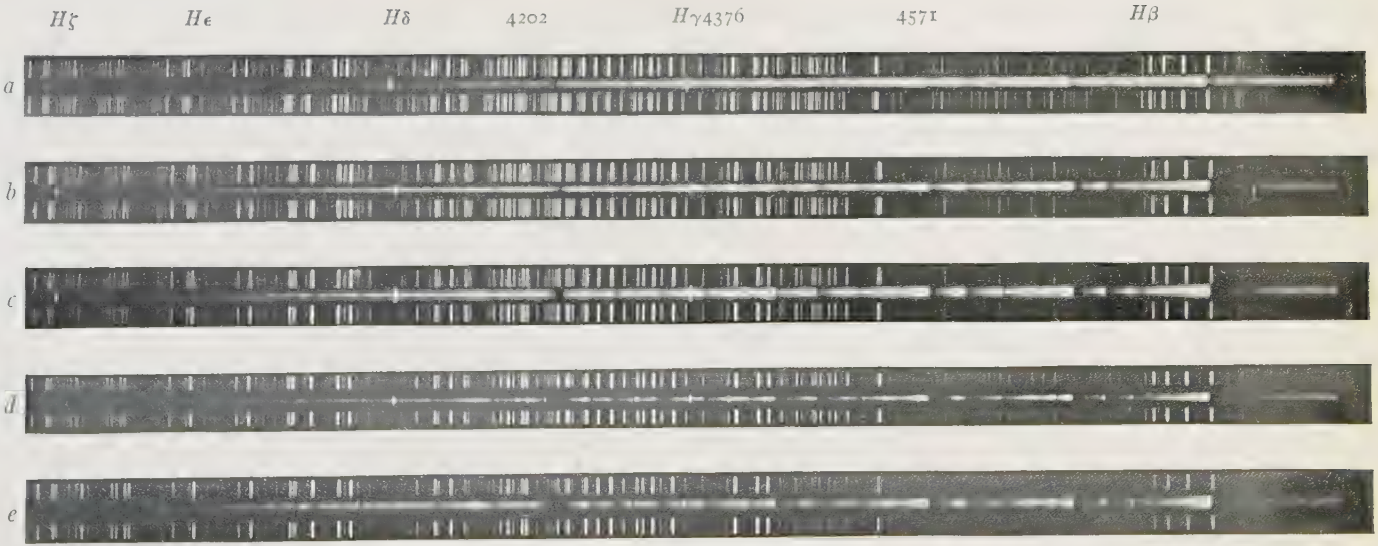

Spectrograms of Mira Illustrating Spectral Variation with Magnitude and Phase

(*a*) γ 8597, August 16, 1919; magnitude 3.4; type M5e; phase 13 days
(*b*) γ 5413, January 4, 1917; magnitude 4.4; type M7e; phase 49 days
(*c*) γ 6594, January 23, 1918; magnitude 5.1; type M8e; phase 82 days
(*d*) C 1845, August 31, 1922; magnitude 7.5; type M9e; phase 134 days
(*e*) C 2017, December 26, 1922; magnitude 7.9; type M9; phase 250 days

parent that the region to the red of λ 6200 is relatively strong as compared with the yellow and green regions. The relative intensities in the visual region at different phases are well shown in Shane's[1] curves.

The data are not sufficient for a quantitative interpretation of these changes in the continuous spectrum. It is only necessary to point out that two effects are certainly present. The spectrum falls off toward the violet as the energy shifts toward the red with decreasing temperature, and there is a large amount of absorption arising from the greatly increased strength and extent of the titanium oxide bands. These two causes appear to work together near minimum to produce the relatively weak continuous spectrum in the region λ 4200–λ 6200. Some general absorption may be present, but this cannot be proved without better photometric measures of the spectrum than are now available. The subject will be referred to again in Section 12 in connection with a discussion of the temperatures.

The predominating feature of the spectrum of *o* Ceti and the later-type long-period variable stars is the presence of the strong absorption bands identified by Fowler[2] with titanium oxide. The strengthening of these bands in the green and yellow regions of the spectrum plays a considerable part in the light-curve as determined from visual observations. Even if no other causes produced changes in magnitude, the light of the star would still be greatly cut down by the increasing absorption of the titanium oxide. Figure 3 illustrates the strength of the bands near $H\beta$. The figure is taken from Koch microphotometer curves of plate $\gamma$ 7795. The type is estimated as M8. The positions of these titanium bands in the photographic region have been determined by Stebbins, Plaskett, Sidgreaves, and others, and in the red region of the spectrum by Merrill[3] and Shane.[4] It has been usual to measure the position of the heads of these bands, and from such measures Frost and Lowater[5] have suspected that the bands give the same velocity as the emission lines; but the results have not been satisfactory, because photographic spreading makes it impossible with the dispersion usually employed in stellar observations to set accurately upon the head of the band. Measures by different observers show large discordances. Settings are not likely to be made in the same manner on plates of different density or upon different bands on the same plate. For these reasons it has not been thought worth while to attempt to measure the heads of the bands.

---

[1] *Ibid.*, **10**, 133, 1922.

[2] *Proceedings of the Royal Society*, A, **79**, 509, 1907.

[3] *Scientific Papers, Bureau of Standards*, No. 318, 1918.

[4] *Lick Observatory Bulletins*, **10**, 132, 1922.

[5] *Astrophysical Journal*, **58**, 272, 1923.

It was found possible, however, to measure a certain group of lines in the structure of one of the bands of *o* Ceti. The same structural details were identified on a plate of *α* Herculis. Plates *γ* 6243 and *γ* 6338, taken with the 40-inch camera, and *γ* 13185, with 3 prisms and 18-inch camera, show especially sharp detail in the region λ 4609–λ 4623, which is reproduced in Plate X *e*. The dispersion at this point is 20 A per millimeter for the first two plates, and 17 A per millimeter for the last plate. The lines used are blended pairs and triplets in the tail of a band whose head is at λ 4585. Although many such could have been measured, a series of twelve blends was thought sufficient for the investigation of the velocity given by the bands. The lines are beautifully defined on these plates and settings can be made with the utmost precision. The groups were identified and their wave-lengths determined from two different furnace plates kindly lent by Mr. King, using strontium and titanium lines as standards.

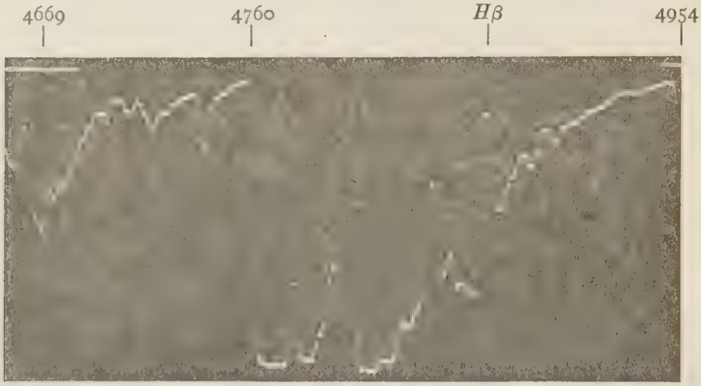

Fig. 3.—Koch microphotometer curve showing the absorption of titanium oxide bands from λλ 4650 to 4955. Spectral type M8.

The results of the measurements, on the Rowland system, are given in Table IV. The wave-lengths measured in *o* Ceti have been corrected by the amount of the velocity found from the absorption lines of the spectrum. The results show conclusively that the bands give the same displacements as the absorption lines of the star and indicate that the band absorption originates in the star's atmosphere under conditions similar to those producing the atomic absorption lines.

TABLE IV

COMPARISON OF $TiO_2$ IN *o* CETI AND IN THE LABORATORY

| Laboratory Mean λ (2 plates) | *o* Ceti Mean λ (3 plates) | Difference *o* Ceti − Laboratory |
|---|---|---|
| 4608.179 | 4608.090 | −0.089 |
| 4609.247 | 4609.152 | − .095 |
| 4610.199 | 4610.199 | .000 |
| 4611.337 | 4611.430 | + .093 |
| 4612.478 | 4612.490 | + .012 |
| 4613.624 | 4613.665 | + .041 |
| 4614.922 | 4614.955 | + .033 |
| 4616.090 | 4616.124 | + .034 |
| 4617.288 | 4617.344 | + .056 |
| 4618.593 | 4618.570 | − .023 |
| 4619.891 | 4619.839 | − .052 |
| 4621.102 | 4621.106 | + .004 |
| Mean difference | | +0.001 |

Several hitherto unrecorded bands appear near the usual minima, and also at the peculiar maximum of 1924. These are degraded toward the red, but the heads are not strongly marked. Their approximate positions are:

λλ 4130–50
4165–90
4212–38
λλ 4242–44*
4250–68
4270–78
λλ 4315–25
4328–34*
4338–48

All except the two which are starred have been identified as belonging to the titanium oxide band-spectrum. Plates for this purpose, taken with the furnace, into which had been introduced a considerable current of oxygen, were kindly supplied by Mr. King. Koch microphotometer curves assisted greatly in studying the structure of the bands. One of the most prominent of these new bands is that at λλ 4212–4238 which is of especial interest because it falls upon the great absorption region due to λ 4226 of calcium and is responsible for a part of the absorption heretofore attributed to neutral calcium.

### 5. ABSORPTION SPECTRUM

The dispersion used in the observations of *o* Ceti does not permit of a detailed study of a large number of lines at different phases of the star's light, but it does give a fair determination of the velocity and makes it possible to observe the behavior of the outstanding lines of the spectrum.

The spectrum at maximum, as has been pointed out by previous observers, contains a large number of absorption lines, especially in the region λ 3900–λ 4350, where the bands are less intense. The identification of these lines shows that those which are measurable with the dispersion used are, with very few exceptions, low-temperature lines of classes I and II belonging to the elements iron, vanadium, chromium, manganese, calcium, and magnesium. Mr. Merrill has called my attention to the presence of the pair λλ 4044 and 4047 of neutral potassium which is strengthened at fainter magnitudes.

The lines of vanadium are remarkable for their number and persistence. They are the only lines of moderate intensity which can be measured near the minimum. The weakness of titanium is striking. The explanation must be along the line of King's experiment.[1] He found that, when the bands of titanium oxide were strengthened by the introduction of oxygen into the furnace, the usual titanium lines practically disappeared. The supply of atomic titanium seems largely to be exhausted by the formation of the $TiO_2$ molecules which produce the bands. The presence of a considerable amount of oxygen is necessary to obtain this result.

The only lines of titanium actually measured on our plates with ordinary dispersion are λ 4314 and the stronger members of the low-temperature multiplets at λ 4300 and λ 4535, and these are notably weakened as the bands strengthen. Several other titanium lines appear faintly at maximum if higher dispersion is employed.

The absorption lines generally used in the velocity measures are given in Table V. The identifications and wave-lengths are given in the Rowland and International systems. The temperature class is that found by King in the electric furnace. Additional lines of less intensity are visible on the plates taken with greater dispersion, such

---

[1] *Mt. Wilson Contr.*, No. 114; *Astrophysical Journal*, **43**, 342, 1916.

TABLE V

ABSORPTION LINES

| ELEMENT | TEMP. CLASS | WAVE-LENGTH | | ESTIMATED INTENSITY | |
|---|---|---|---|---|---|
| | | Rowland | I.A. | Max. Mag. | Mag. 8.5 |
| *Fe* | I A | λ 4291.630 | .473 | 4 | e 2 |
| | I | 4144.038 | .873 | 2 | 1 |
| | | 4202.198 | .033 | 2 | e 14 |
| | | 4376.107 | .934 | 4 | e 14 |
| | | 4427.482 | .314 | 2 | e 2 |
| | II | 4005.408 | .247 | 4 | 1 |
| | | 4045.975 | .816 | 10 | 2 |
| | | 4063.759 | .598 | 5 | 3 |
| | | 4071.908 | .742 | 3 | 2 |
| | | 4250.626 | .471 | 4 | 1 |
| | | 4271.760 | .606 | 5 | 2 |
| | | 4294.301 | .130 | 3 | 1 |
| | | 4308.081 | .908 | 4 | e 15 |
| | | 4325.939 | .766 | 8 | 1 |
| | | 4383.720 | .550 | 6 | 1 |
| | | 4404.927 | .755 | 5 | 1 |
| | | 4415.293 | .128 | 2 | 1 |
| | III | 4260.640 | .482 | 1 | 1 |
| | | 4282.565 | .408 | 2 | 2 |
| | | 4408.582 | .420 | 4 | 3 |
| *V* | I | 4092.821 | .671 | 5 | 4 |
| | | 4109.905 | .753 | 3 | 3 |
| | | 4115.330 | .178 | 2 | 2 |
| | | 4116.634 | .482 | 4 | 4 |
| | | 4128.251 | .098 | 3 | 3 |
| | II | 4379.396 | .239 | 4 | 4 |
| | | 4390.149 | .992 | 4 | 3 |
| | | 4395.413 | .255 | 6 | 6 |
| *Cr* | I | 4497.023 | .859 | 6 | 6 |
| | | 4254.505 | .350 | 12 | 25 |
| | | 4274.958 | .804 | 10 | 20 |
| *Mn* | I | 4030.918 | .773 | 8 | 0 |
| | | 4033.224 | .079 | 5 | 4 |
| | | 4034.644 | .499 | 4 | 2 |
| *Ca* | I | 4226.904 | .748 | (3A) | (25A) |
| | | 4318.817 | .658 | 2 | 5 |
| *Ca*<br>*Cr* | I<br>II | 4289.725 | .569 | 12 | 25 |
| *Ti* | II | 4299.410 | .242 | 4 | 2 |
| | | 4314.964 | .805 | 8 | 6 |
| *Sr*+ | II | 4077.885 | .735 | 20 | 12 |
| | | 4215.703 | .546 | 15 | 4: |
| *Sr* | I | 4607.510 | .337 | 5 | 20 |
| *Mg* | I | 4571.275 | .105 | 4 | e 27 |
| *Ba*+ | II | 4554.211 | .044 | 4 | 1 |

as those of *Co*, *Cr*, *Fe*, *Ti*, and *V* belonging entirely to classes I and II. The intensity of the lines is estimated for maximum and for magnitude about 8.5. At minimum the continuous spectrum of the companion makes estimates too uncertain to be of value. As the star declines in brightness the fainter lines of the various elements tend to disappear. Several of the lines become emission lines and are marked with the letter *e*.

The multiplet group of titanium lines of class II at λ 4535 blends to form a strong line at maximum, which weakens and becomes emission in character as the star approaches minimum. λλ 4299.4 and 4314.9 of titanium behave in much the same way. These lines are probably affected by the shortage of titanium caused by the strengthening of the bands, as well as by the general weakening of absorption lines of the lowest temperature classes.

The ultimate lines of ionized calcium, barium, and strontium are very strong at maximum but are much weakened toward minimum. H and K of calcium are not easily photographed in *o* Ceti because of the weakness of the spectrum in the violet and because of the interference of the spectrum of the companion at minimum. On the few plates having sufficient exposure at this phase, the H and K lines appear to be present but decidedly weakened. The encroachment of the bright line λ 4216 may hasten the disappearance of the strontium line λ 4215 at about magnitude 7.5. When the star is fainter than the eighth magnitude, this region becomes engulfed in the tremendous absorption of the calcium line λ 4226 whose width at minimum light is fully 30 A.

Several enhanced lines of iron and titanium, such as λλ 4233, 4352, 4395, 4417, 4501, 4549, and 4584, are found in the spectrum of *α* Orionis, but the reduced temperature in *o* Ceti, even at maximum, and in stars of the later M-types, makes their appearance weak or doubtful. At minimum light they seem to be entirely lacking in the variable star.

The chromium lines λλ 4254 and 4274 and the calcium line λ 4226 strengthen with decreasing temperature and become enormously strong at minimum. An unknown strong line, or perhaps a bandhead, at λ 4738 acts similarly. The line is not sharp and is somewhat shaded toward the red. Its width is about 2 A at minimum, and its wave-length from 45 plates, corrected for the absorption-line velocity of the star, is λ 4738.297. A search among known lines and bands has failed to reveal the origin of this strong absorption line. It seems very probable that it may be the head of an absorption band which falls off toward the red.

## 6. THE RADIAL VELOCITIES DETERMINED FROM ABSORPTION LINES

The measurements for the determination of radial velocity have been shared in part by Mr. Adams and Misses Burwell and Stone, but all the plates have been measured once, and usually twice, by the writer.

TABLE VI

Absorption-Line Normal Points

| Weighted Mean Phase | Weighted Mean *V* | Weighted Mean Phase | Weighted Mean *V* |
|---|---|---|---|
| days | km/sec. | days | km/sec. |
| 0 | +64.0 | 113 | +57.5 |
| 7 | 64.3 | 147 | 54.9 |
| 16 | 63.7 | 238 | 53.8 |
| 41 | 63.0 | 278 | 59.8 |
| 70 | 60.9 | 288 | 61.2 |
| 89 | +60.0 | 312 | +63.0 |

Although the dispersion used is less than that desirable for radial velocity measurements involving a comparatively small range, it should be borne in mind that the absorption lines, especially near maximum, are numerous and of superior quality, and that the results are based upon a large number of measures. Furthermore, the absorption lines used throughout the whole period of the star's variation, which are listed in Table V, are unusually homogeneous in character, being without exception strong low-temperature or ultimate lines of a small number of elements. The average number measured on each plate is 12 for the whole series. At minimum fewer lines were available than at maximum. In forming the normal points, weights, based on the number of lines, the number of measures, the dispersion employed, and the quality, were assigned to each plate.

After arranging the dark-line velocities given in Table II in order of phase, eleven normal places, of comparable weight, were formed. These are given in Table VI and are represented by open circles on the curve of Figure 4.

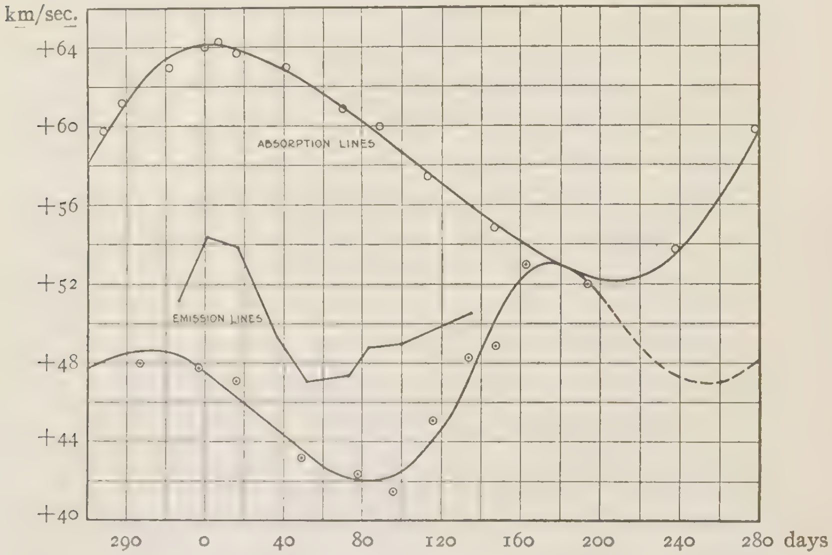

Fig. 4.—Velocity-curves for absorption lines (above) and emission lines (below). The broken middle line represents the velocities of the emission lines of ionized iron.

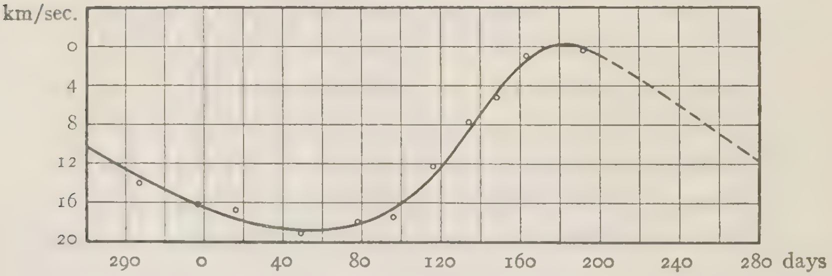

Fig. 5.—Curve showing differences between absorption and emission velocities

Although it is not thought that the variable star is a spectroscopic binary, the curve drawn through the normal points can be described best in terms of the usual elements of an elliptic orbit.

The following elements are satisfactory. A least-squares solution has not been attempted.

$$P = 330 \text{ days}$$
$$K = 5.9 \text{ km/sec.}$$
$$\gamma = +58.2 \text{ km/sec.}$$
$$\omega = 265^\circ\!.2$$
$$e = 0.20$$
$$a \sin i = 26{,}200{,}000 \text{ km}$$
$$\frac{m_1^3 \sin^3 i}{(m+m_1)^2} = 0.007 \odot$$

The striking feature of the velocity-curve is its resemblance in form to the light-curve. The maximum positive velocity occurs at maximum, and the greatest velocity of approach at minimum, light. The case is thus opposite in phase to that of the Cepheids, for which maximum velocity of approach occurs at maximum of light.

Previous observers[1] have not failed to consider the possibility of variable radial velocity but have made observations only at the star's brightest phases, which correspond to the broad maximum of the velocity curve. The evidence has accordingly pointed to the conclusion that the velocity was constant.

Thus Campbell's observations[2] in 1897 and 1898, including 7 plates with phases from −36 to +55 days from maximum, show a range of only 3 km/sec. His results, which were obtained with three prisms, are given in Table VII. In themselves, these observations show no indication of variation in velocity, but their deviations from the Mount Wilson curve are not larger than might be attributed to error in observation. On the other hand, the series of single-prism observations by Stebbins[3] in 1902, with phases up to +83 days, show a distinct tendency, when reduced to velocities, to follow the variable velocity-curve here given.

Merrill has made numerous observations of the velocities of other long-period variables, but as these photographs likewise show the absorption spectrum only near maximum, there is no evidence at hand from other stars of this class. He has reached the conclusion that in the case of X Ophiuchi,[1] where a companion star checks the velocity of the variable, and probably in other stars of this class, the absorption lines give the true velocity of the star. The present results for *o* Ceti, if typical, complicate the problem, inasmuch as it raises the question whether the velocity of translation of the star is the $\gamma$-velocity of the curve or the velocity at either maximum or minimum. Statistical methods may ultimately furnish the answer; but it is impossible at present, on account of the small range of variation and the lack of direct methods of attack, to come to any conclusion.

---

[1] Küstner, *Astrophysical Journal*, **27**, 301, 1908; Plaskett, *Journal of the Royal Astronomical Society of Canada*, **1**, 45, 1907; Merrill, *Publications of the Detroit Observatory*, **2**, 65, 1916; Lunt, *Astrophysical Journal*, **48**, 265, 1918; Harper, *Publications of the Dominion Observatory*, **4**, 334, 1920; Frost and Lowater, *Astrophysical Journal*, **58**, 265, 1923.

[2] *Astrophysical Journal*, **9**, 31, 1899.

[3] *Lick Observatory Bulletins*, **2**, 81, 1903.

TABLE VII

Observations by Campbell

| | Phase | *V* | C.—Mt. W. |
|---|---|---|---|
| Nov. 10—1897...... | −20 days | +63.4 km/sec. | +0.2 |
| Dec. 15............ | +15 | 62.0 | −1.8 |
| 15............ | +15 | 60.7 | −3.1 |
| Aug. 29—1898...... | −36 | 62.8 | +1.1 |
| Sept. 4............ | −30 | 63.7 | +1.3 |
| 19............ | −15 | 61.8 | −1.7 |
| Nov. 29............ | +55 | 62.3 | +0.4 |

The variable X Ophiuchi is visible for so short a period that it is not possible to determine whether the absorption-line velocity varies or not. The companion of Mira is so faint and so difficult to separate spectrographically that it cannot be satisfactorily used for determining the velocity of the system. The only evidence available is that from the bright lines of the companion, shown on a few plates mostly of small dispersion, which give the same velocity as the variable (both bright and dark lines) at minimum. It is possible that the bright lines are displaced to the violet, as in B.D. +11°4673. Merrill's[2] computations would seem to indicate that for the Me stars in general a small value of the K-term is given by use of the velocities of the absorption lines at maximum.

---

[1] *Mt. Wilson Contr.*, No. 261; *Astrophysical Journal*, **57**, 251, 1923.

[2] *Mt. Wilson Contr.*, No. 264; *Astrophysical Journal*, **58**, 255, 1923.

## 7. EMISSION LINES

The emission lines of hydrogen in *o* Ceti were first noticed[1] in 1886 by Pickering as one of the earliest results of the photographic observation of stellar spectra with the objective prism at the Harvard College Observatory. Later, other long-period variables were found to have the same bright lines. This characteristic then became the criterion by which numerous variables of this type were detected from inspection of their spectra, and thus far only a few M-type stars emitting bright hydrogen lines have failed to exhibit the Mira type of variation in light. The exceptional cases include six of the faintest dwarfs: W.B. $10^h234$, $16^h906$, Furujhelm 54 and 58, and the companions of Castor[2] and *o* Eridani;[3] and six giants:[4] W Cephei, Boss 1985, 5650, H.D. 42474, B.D. +61°8, and C.D.M. −33°16843. The dwarfs are not known to vary in brightness. Some of the giants have an irregular variation of small range. All but the last star have spectra which are essentially different from that of *o* Ceti and need not concern us in this discussion. C.D.M. −33°16843, to which our attention was directed by Miss Cannon, gives, however, a typical Me spectrum, yet among several hundred stars of this type it is the only one known to maintain constant brightness.

The hydrogen lines on our plates are usually considerably overexposed in order that the absorption lines of the spectrum may be measured. The Balmer series has been recorded from $H\alpha$ to $H\iota$ but the region for which this study is fairly complete extends only from λ 3950 to λ 5000. The behavior varies with the line and also depends to some extent upon the particular cycle considered, but, in general, the magnitude of the star seems to be the controlling factor. The cycles repeat themselves with only slight inconsistencies.

When the star reaches a minimum none of the hydrogen lines is bright. With increase in light there is a sudden appearance of hydrogen emission at about the seventh magnitude, which is first seen in $H\delta$ and, a short time later, in $H\gamma$. In the course of a week or two, these two lines attain great strength, $H\delta$ remaining the stronger until well past maximum. The greatest intensity is reached about a month after maximum light. The decline then sets in; $H\gamma$ becomes somewhat stronger than $H\delta$, and both disappear together near magnitude 8.0. Near minimum the emission lines go over into absorption lines. The relative changes in the hydrogen lines are illustrated in Plate IX.

---

[1] *First Annual Report of the Photographic Study of Stellar Spectra,* Cambridge, 1887; reprinted in *Nature,* **36,** 32, 1887.

[2] Adams and Joy, *Publications of the Astronomical Society of the Pacific,* **32,** 158, 1920; **34,** 174, 1922.

[3] Leonard, *ibid.,* **33,** 272, 1921.

[4] Adams and Joy, *ibid.,* **33,** 263, 1921; Adams, Joy, and Humason, *ibid.,* **34,** 175, 1922; **37,** 161, 1925.

$H\alpha$ is present as a bright line on the few plates sensitized for the red portion of the spectrum. Relative to the continuous spectrum, it appears to be weaker than $H\beta$. Shane[1] found $H\alpha$ nearly equal to $H\beta$ in intensity. He also noted that $H\alpha$ was displaced about 1 A toward the violet, relative to the other bright lines, on all his plates. This displacement appears to be confirmed, in part at least, by rough measures of the Mount Wilson plates.

$H\beta$ and $H\zeta$ have been seen and measured each cycle. They make their appearance near the time of maximum, and, on account of their weakness, vanish after three or four months, at about magnitude 6.5. $H\zeta$ seems to reach its maximum somewhat later than $H\beta$. $H\epsilon$ and $H\eta$ are similar in strength on our plates. They appear about a month after maximum and fade out at about the same time as $H\beta$ and $H\zeta$. $H\theta$ and $H\iota$ were found on two plates only, at phases of 49 and 77 days.

In a general way the hydrogen series has its greatest strength at $H\delta$ and declines toward red and violet. The weakness of $H\epsilon$, $H\kappa$, $H\lambda$, $H\mu$, and $H\xi$ are explained by local absorption, as suggested by Miss Clerke for $H\epsilon$, and by Shane for the other lines.

The hydrogen lines are fairly sharp on one-prism spectrograms and there is little indication of any lack of symmetry. Higher dispersion reveals $H\gamma$ and $H\delta$ to be composite, each consisting of three components. The separation of these components seems to be constant, but the relative intensity has changed since they were first observed. Campbell[2] found at the maxima of 1898 that $H\gamma$ was made up of a strong central component with a lesser one to the violet

---

[1] *Lick Observatory Bulletins*, **10**, 131, 1922; *Publications of the Astronomical Society of the Pacific*, **32**, 234, 1920.

[2] *Astrophysical Journal*, **9**, 31, 1899.

# PLATE IX

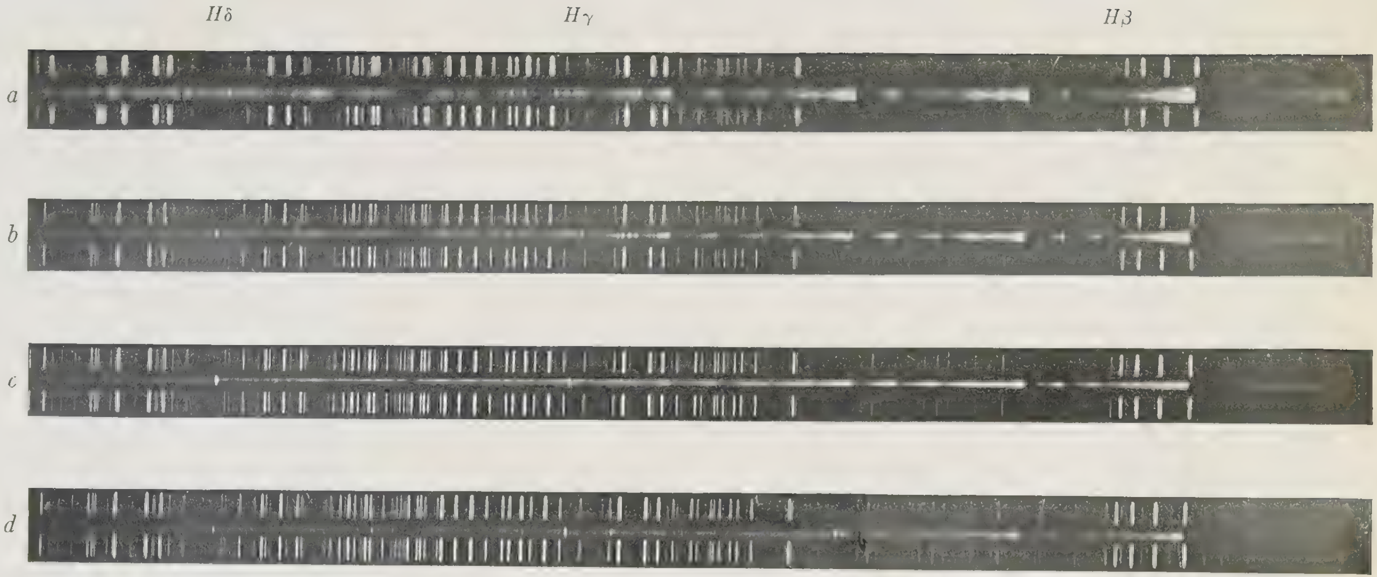

Spectrograms of Mira Illustrating the Behavior of the Hydrogen Emission Lines during a Cycle

(*a*) C 3511, September 8, 1925; magnitude 8.8, phase 248 days. No hydrogen emission lines are present except $H\beta$, which emanates from the companion.

(*b*) $\gamma$ 6120, August 27, 1917; magnitude 5.9, phase 284 days. $H\delta$ stronger than $H\gamma$.

(*c*) $\gamma$ 6306, October 26, 1917; magnitude 3.7, phase 14 days.

(*d*) $\gamma$ 6724, March 2, 1918; magnitude 7.1, phase 141 days. $H\gamma$ stronger than $H\delta$.

and a weak one on the red side. $H\delta$ was symmetrical with a strong central line and two equal side components. Wright[1] was able to see but two components of $H\gamma$ in 1899, but when he examined it in 1909 for indications of the Zeeman effect it was triple, with much the same intensity relations as found by Campbell in 1898. On plates taken with three prisms by Mr. Merrill and the writer at the last maximum in December, 1925, the three components of $H\gamma$ are not well resolved, but seem to decrease slightly in intensity toward the red, the violet component being the strongest. $H\delta$, however, shows a strong central line with a very weak companion to the violet and a line of intermediate intensity well separated on the red side. Plate X*f* shows its appearance on November 25, 1925. In the succeeding three months the central component of $H\delta$ strengthened relatively, so that the close violet component was almost lost. There was no certain change in $H\gamma$. The separations are practically the same as those found by Campbell, but the intensities are quite different. The whole line or band shifts its position in accordance with the velocity-curve given in Section 8. As far as observed, the other bright lines have been found single.

No explanation can be suggested which satisfactorily accounts for the peculiar structure of these hydrogen lines. The components are unsymmetrical in position and intensity. The separations of the components are 0.29 A to the violet side and 0.46 A to the red. The Zeeman and Stark effects seem to be ruled out. Since they shift as a unit, the components must originate in the same portion of the star's atmosphere. Unsymmetrical double reversal is a possible cause.

In addition to the emission lines of hydrogen, numerous other bright lines have been observed. Campbell[2] in 1897 and 1898 first measured λλ 4308 and 4376 and identified them, from 3-prism plates, with the corresponding iron lines. He concluded that they have the same displacements as the bright hydrogen lines. He also called attention to the bright line λ 4103 which Plaskett[3] later identified with Rowland's line λ 4103.1, *Si Mn*. Plaskett refers to seven other bright lines in addition to the hydrogen lines. Numerous emission lines are recorded by Stebbins, Küstner, Adams and Joy, and Frost and Lowater. Merrill finds that most of these lines occur in other long-period variable stars.

---

[1] *Lick Observatory Bulletins*, **6**, 60, 1910.

[2] *Astrophysical Journal*, **9**, 31, 1899.

[3] *Journal of the Royal Astronomical Society of Canada*, **1**, 56, 1907.

All the bright lines and bright places resembling lines, which have been measured, are listed in Table VIII. The wave-lengths from the Mount Wilson measures, given in the first two columns, have been corrected by the mean displacement of any or all of the following bright lines measured on the plate: $H\delta$, $H\gamma$, λλ 4202, 4216, 4291, 4308, 4376, 4571. These are among the strongest and most frequently recurring bright lines, and there can be no question of the correctness of their identification[1] with hydrogen and the low-temperature radiation of iron and magnesium.

The validity of the assumption that all the bright lines are subject to the same displacement is still open to question, but the agreement found here for the hydrogen lines and the low-temperature lines makes it reasonably certain that this is the case for these groups at least. The case is not so clear for some of the remaining lines, such as λ 4233 of ionized iron and λλ 3905 and 4103 of silicon, which belong to higher temperature classes and probably originate at different levels. For the many lines with no plausible identifications the corrections are presumably in the right direction.

The third column of Table VIII gives the probable error of the mean wave-lengths computed from the internal agreement of the measures, the fourth column the probable identification, and the fifth, the number of Mount Wilson plates upon which the wave-length is based. The line may have been present on other plates as well, but omitted in measurement on account of its weakness or poor definition. No lines are included which have not been found on at least three plates, unless measured by other observers.

The remaining columns contain the wave-lengths published by other observers. In the last column are the wave-lengths of the bright lines found by Merrill[2] in long-period variables other than *o* Ceti. The values which are starred have been supplied by Mr.

---

[1] Adams and Joy, *Publications of the Astronomical Society of the Pacific*, **35**, 168, 1923.

[2] *Mt. Wilson Contr.*, No. 265; *Astrophysical Journal*, **58**, 197, 1923.

## TABLE VIII

### EMISSION LINES IN *o* CETI

| Wave-Length | | Probable Error | Identification | No. Plates | Stebbins | Plaskett | Frost and Lowater | Me Stars Merrill |
|---|---|---|---|---|---|---|---|---|
| Rowland | I.A. | | | | | | | |
| ........ | ...... | ....... | $H\kappa$ | ...... | 3750.5 | .......... | .......... | ......... |
| 3770.83 | .70 | ±0.04 | $H\iota$ | 2 | 3770.85 | .......... | .......... | ......... |
| 3797.96 | .83 | .00 | $H\theta$ | 2 | 3798.09 | .......... | .......... | ......... |
| 3835.65 | .52 | .03 | $H\eta$ | 16 | 3835.53 | .......... | .......... | Standard |
| 3852.90 | .77 | .07 | ...... | 2 | 3852.84 | .......... | .......... | 3852.76 |
| 3889.33 | .20 | .01 | $H\zeta$ | 31 | 3889.24 | .......... | Standard | Standard |
| 3905.82 | .69 | .02 | *Si* | 13 | 3905.69 | .......... | 3905.78 | Standard |
| 3907.83 | .70 | .02 | ...... | 2 | 3907.51 | .......... | .......... | 3907.60* |
| ........ | ...... | ...... | ...... | ...... | 3932.78 | .......... | .......... | ......... |
| 3938.57 | .44 | .04 | ...... | 4 | 3938.43 | .......... | .......... | 3938.47* |
| ........ | ...... | ...... | ...... | ...... | 3967.82 | .......... | .......... | 3967.66* |
| 3970.30 | .16 | .03 | $H\epsilon$ | 11 | .......... | .......... | Standard | Standard |
| ........ | ...... | ...... | ...... | ...... | 3978.0 | .......... | .......... | 3977.92 |
| ........ | ...... | ...... | ...... | ...... | 3997.8 | .......... | .......... | 3997.87* |
| ........ | ...... | ...... | ...... | ...... | 4002.0 | .......... | .......... | 4001.90* |
| 4006.94 | .80 | .03 | ...... | 9 | 4007.07 | .......... | .......... | ......... |
| 4030.75 | .61 | .07 | *Mn* | 2 | 4030.8 | .......... | .......... | 4030.66 |
| 4101.89 | .74 | .00 | $H\delta$ | 51 | 4101.99 | Standard | Standard | Standard |
| 4103.15 | .00 | .01 | *Si* | 39 | .......... | 4103.20 | 4103.15 | 4103.18 |
| 4119.75 | .60 | .02 | ...... | 10 | .......... | 4119.81 | .......... | 4119.65* |
| 4122.92 | .77 | .03 | ...... | 6 | .......... | .......... | .......... | 4122.98* |
| 4138.75 | .60 | .02 | *Fe*+ | 23 | .......... | 4138.78 | 4138.80 | 4138.80 |
| 4166.00 | .84 | .01 | ...... | 16 | .......... | 4166.09 | 4166.03 | 4166.09* |
| 4170.81 | .65 | .05 | ...... | 5 | .......... | .......... | .......... | 4171.04* |
| 4173.63 | .47 | .04 | *Fe*+ | 3 | .......... | 4173.83 | .......... | 4173.60* |
| 4178.98 | .82 | .05 | *Fe*+ | 35 | 4178.9 | 4179.09 | .......... | 4178.98 |
| 4202.18 | .02 | .01 | *Fe* | 32 | 4202.24 | .......... | 4202.01 | Standard |
| 4206.86 | .70 | .03 | *Fe* | 10 | .......... | .......... | 4206.68 | ......... |
| 4216.35 | .19 | .01 | *Fe* | 18 | 4216.04 | .......... | .......... | 4215.90 |
| 4229.47 | .31 | .02 | ...... | 4 | .......... | 4229.76 | .......... | ......... |
| 4233.49 | .33 | .01 | *Fe*+ | 40 | 4233.45 | 4233.61 | 4233.42 | 4233.51 |
| 4249.49 | .34 | .06 | ...... | ...... | .......... | .......... | .......... | ......... |
| 4258.45 | .30 | .04 | *Fe* | 7 | .......... | .......... | .......... | ......... |
| 4291.64 | .49 | .01 | *Fe* | 10 | .......... | .......... | .......... | ......... |
| 4308.10 | .94 | .01 | *Fe* | 30 | 4308.03 | .......... | .......... | Standard |
| 4340.64 | .48 | .00 | $H\gamma$ | 58 | 4340.66 | Standard | Standard | Standard |
| 4352.52 | .36 | .04 | ...... | 9 | .......... | .......... | .......... | 4352.61* |
| 4372.74 | .58 | .03 | ...... | 12 | 4372.94 | .......... | .......... | 4372.74 |
| 4376.09 | .93 | .01 | *Fe* | 31 | 4376.11 | 4375.98 | .......... | 4376.00 |
| 4427.49 | .33 | .02 | *Fe* | 11 | 4427.2 | .......... | .......... | ......... |
| 4434.16 | .00 | .03 | ...... | 3 | 4433.8 | .......... | .......... | ......... |
| ........ | ...... | ...... | ...... | ...... | .......... | .......... | 4454.41 | ......... |
| ........ | ...... | ...... | ...... | ...... | .......... | .......... | 4457.06 | ......... |
| 4458.95 | .79 | .03 | ...... | 20 | .......... | .......... | 4458.79 | 4458.99 |
| 4461.47 | .31 | .03 | ...... | 12 | .......... | .......... | 4461.44 | 4461.52* |
| 4461.75 | .59 | .02 | *Fe* | 9 | .......... | .......... | .......... | ......... |
| 4482.27 | .11 | .10 | *Fe* | 5 | .......... | .......... | .......... | ......... |
| 4489.73 | .57 | .06 | *Fe* | 4 | .......... | .......... | .......... | ......... |
| 4511.66 | .50 | .02 | *In* | 13 | 4511.9 | .......... | 4511.73 | 4511.62 |
| 4521.56 | .40 | .02 | ...... | 4 | .......... | .......... | 4521.54 | 4521.70 |
| 4533.95 | .78 | ±0.09 | ...... | 4 | .......... | .......... | .......... | ......... |

TABLE VIII—*Continued*

| ROWLAND | | PROBABLE ERROR | IDENTIFICATION | NO. PLATES | STEBBINS | PLASKETT | FROST AND LOWATER | ME STARS MERRILL |
|---|---|---|---|---|---|---|---|---|
| Rowland | I.A. | | | | | | | |
| ........ | ...... | ....... | ...... | ...... | ......... | .......... | 4559.88 | ......... |
| ........ | ...... | ....... | ...... | ...... | ......... | .......... | 4562.15 | ......... |
| 4571.31 | .14 | ±0.01 | *Mg* | 27 | 4571.15 | .......... | .......... | Standard |
| 4578.96 | .79 | .05 | ...... | 3 | ......... | .......... | .......... | 4579.01 |
| 4584.05 | .88 | .20 | *Fe*+ | 2 | ......... | .......... | 4584.08 | ......... |
| ........ | ...... | ....... | ...... | ...... | ......... | .......... | 4633.72 | ......... |
| ........ | ...... | ....... | ...... | ...... | ......... | .......... | 4634.94 | ......... |
| ........ | ...... | ....... | ...... | ...... | ......... | .......... | 4639.26 | ......... |
| ........ | ...... | ....... | ...... | ...... | ......... | .......... | 4756.72 | ......... |
| ........ | ...... | ....... | ...... | ...... | ......... | .......... | 4801.33 | ......... |
| ........ | ...... | ....... | ...... | ...... | ......... | .......... | 4803.18 | ......... |
| ........ | ...... | ....... | ...... | ...... | ......... | .......... | 4838.68 | ......... |
| 4861.49 | .31 | .02 | *Hβ* | 26 | 4861.67 | Standard | Standard | Standard |
| 4923.95 | .78 | .07 | *Fe*+ | 6 | ......... | .......... | .......... | ......... |
| 5018.62 | .45 | ±0.23 | *Fe*+ | 4 | ......... | .......... | .......... | ......... |

Merrill from manuscript. In many cases the lines were measured on three or four plates only, but it is of great interest to note that they are found in other stars.

Wave-lengths are given on the Rowland system, except in the second column where the International values are given for comparison. Stebbins' wave-lengths are corrected by −0.67 A to allow for the displacement of the bright lines, while a correction of +0.25 A suggested by Plaskett has been applied to his wave-lengths to reduce them to the bright hydrogen lines as standards. Merrill omits the wave-lengths of six hydrogen lines and of λλ 3905, 4202, 4308, and 4571, used as standards by which the displacements of the other lines are corrected.

In some cases it is not easy to determine whether a measured point is actually an emission line or a narrow region of continuous spectrum between two absorption lines; but if the line has been seen by different observers under different instrumental conditions and with different dispersions there can be little doubt that the emission is real.

Of the 66 lines given in Table VIII, 49 have been measured on our plates and, after careful examination, have been considered to be real emission lines. The 17 remaining lines recorded by other observers, excluding *Hκ*, which is too far in the violet, have been looked for on our plates, but either they are not present or else appear to be continuous background rather than real lines. Nine lines are included which are not recorded by other observers; of these 7 have been identified with reasonable certainty.

It is of interest to consider the strength of the bright lines and the time of their appearance with respect to changes in brightness of the star. Table IX gives the relative intensities estimated on an arbitrary scale, as found on well-exposed plates chosen as representative of the line-intensities at different magnitudes and phases. The estimates must be regarded as rough comparisons only, since the atmospheric transmission, as well as photographic and instrumental effects, has not been taken into account. On the whole, it has seemed better to arrange the plates in the order of magnitude rather than phase, since temperature in the star is probably the controlling influence in the variation of the emission. The intensities observed follow the magnitudes more consistently than any other single factor.

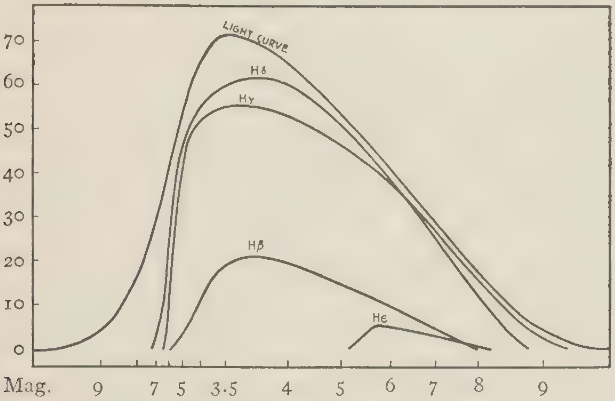

FIG. 6.—Intensities of hydrogen lines for different magnitudes. The ordinates are relative intensities on an arbitrary scale. The scale of the abscissae is given in magnitudes projected from the light-curve.

The strength of the continuous spectrum on a scale of 5 is given in the second column. The following columns give data for the 36 strongest and most important lines. Some of these appear as absorption lines for a portion of the cycle. The intensities of absorption are then preceded by the letter *a*. Asterisks in the table indicate that the line is not to be expected on account of over- or underexposure at that point in the spectrum.

Figures 6 and 7 represent graphically the changes in intensity of several of the lines. In order that the intensities may be compared with the normal light variation of the star, the mean light-curve has been included in Figure 6, and the scale of the abscissae is given in magnitudes projected down from the light-curve. Thus, intensities are plotted according to magnitude, but the horizontal spacing is the time scale of the light variation.

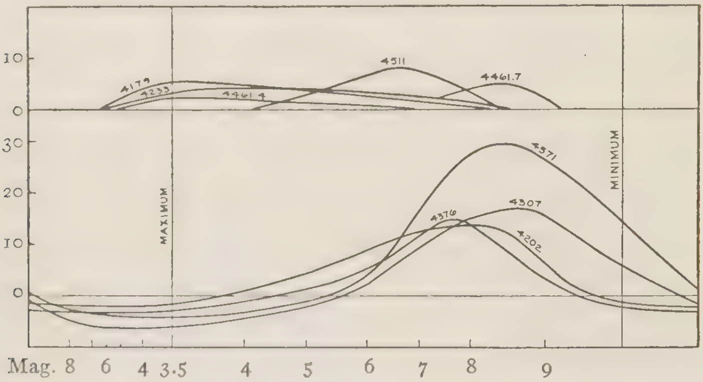

Fig. 7.—Intensities of emission lines for different magnitudes. The scale and coordinates are the same as in Fig. 6. In the lower part of the figure the curves below the zero-line represent the intensity of absorption on an independent scale.

Inspection of Table IX shows two principal groups of bright lines. The first, whose lines are strongest near the maximum of the star, includes the hydrogen series and the enhanced iron lines; the second comprises the low-temperature lines which have been attributed to iron, magnesium, manganese, and indium, and have their maximum intensity four to six months after maximum light.

$H\epsilon$ is apparently an exceptional case in the hydrogen series for it reaches its greatest intensity very much later than the other hydrogen lines. This peculiarity may be accounted for on the basis of Miss Clerke's[1] explanation of its weakness. The H line of calcium is so strong at the maximum of the star that it absorbs the radiation

---

[1] *Problems in Astrophysics*, p. 226, 1903.

## TABLE IX

### INTENSITIES OF EMISSION LINES

| Plate | Int. | Mag. | Phase | $H\eta$ | $H\zeta$ | 3905 | $H\epsilon$ | 4006 | 4030 | $H\delta$ | 4103 | 4119 | 4122 | 4138 | 4166 |
|---|---|---|---|---|---|---|---|---|---|---|---|---|---|---|---|
| C 3068 | 3 | 8.4 | 272 | * | * | * | .... | .... | a5 | .... | .... | .... | .... | .... | .... |
| C 2013 | 4 | 8.3 | 230 | * | * | * | .... | .... | a8 | .... | .... | .... | .... | .... | .... |
| C 2040 | 3 | 7.8 | 258 | * | * | * | .... | .... | a8 | 1 | .... | .... | .... | .... | .... |
| C 1597 | 2 | 7.1 | 289 | * | * | * | * | * | a8 | 2 | .... | .... | .... | .... | .... |
| 12363 | 4 | 5.9 | 303 | * | * | * | .... | .... | a8 | 8 | 2 | .... | .... | 1 | 1 |
| 11564 | 4 | 5.5 | 281 | * | 1 | * | .... | 1 | a8 | 35 | 2 | .... | 1 | 2 | 1 |
| C 2090 | 5 | 5.0 | 283 | * | 1 | * | .... | 2 | a8 | 70 | 2 | .... | 2 | 5 | 2 |
| 12447 | 4 | 4.9 | 317 | * | * | * | * | 1 | a7 | 25 | 2 | 2 | 2 | 5 | 4 |
| 11609 | 5 | 3.8 | 294 | * | * | * | .... | .... | a8 | 60 | 2 | 1 | 2 | 3 | 3 |
| 5258 | 3 | 3.7 | 326 | * | 2 | * | .... | .... | a8 | 50 | 3 | 2 | 1 | 4 | 1 |
| 6235 | 4 | 3.6 | 318 | * | 1 | * | .... | .... | a8 | 40 | 2 | 1 | 2 | 5 | 2 |
| 11622 | 4 | 2.9 | 311 | * | * | * | * | * | a4 | 55 | 2 | 2 | 3 | 10 | 4 |
| C 500 | 2 | 3.1 | 1 | * | * | * | * | * | * | 60 | 1 | .... | .... | 2 | 3 |
| 9395 | 5 | 3.4 | 29 | 1 | 15 | 1 | .... | 5 | a8 | 90 | 1 | 1 | 2 | 6 | 3 |
| 7413 | 3 | 3.5 | 16 | * | 4 | * | .... | 1 | a6 | 35 | 2 | 2 | 2 | 5 | 3 |
| 6306 | 3 | 3.7 | 14 | 1 | 4 | 1 | .... | 3 | a7 | 35 | 2 | 1 | 1 | 5 | 3 |
| 5299 | 3 | 3.8 | 19 | 2 | 10 | 1 | .... | 5 | a6 | 55 | 2 | 1 | 1 | 6 | 3 |
| 13201 | 4 | 3.8 | 8 | * | 2 | * | * | * | * | 80 | 3 | 1 | 1 | 3 | 2 |
| 6369 | 4 | 4.1 | 42 | 1 | 15 | * | .... | 4 | a7 | 70 | 3 | 1 | 2 | 5 | 2 |
| C 2663 | 2 | 4.7 | 3 | * | 1 | * | * | * | a7 | 45 | 3 | 1 | 1 | 2 | 2 |
| 10276 | 2 | 4.9 | 51 | * | 3 | * | * | * | * | 30 | 1 | 1 | 1 | 2 | 1 |
| 6531 | 4 | 5.1 | 82 | 1 | 6 | * | .... | * | a2 | 40 | 4 | .... | 1 | 1 | .... |
| 7551 | 3 | 5.2 | 70 | 1 | 10 | 1 | .... | 1 | a3 | 70 | 3 | .... | 1 | .... | .... |
| 8789 | 3 | 5.3 | 72 | 2 | 10 | 1 | 1 | 1 | a2 | 35 | 3 | .... | .... | 1 | .... |
| 5559 | 2 | 5.5 | 85 | * | * | * | * | * | * | 25 | 2 | .... | .... | .... | .... |
| 6504 | 4 | 5.7 | 103 | 3 | 18 | 2 | 5 | .... | a2 | 35 | 2 | .... | .... | 1 | .... |
| 9567 | 3 | 6.0 | 86 | 1 | 12 | 1 | 1 | .... | a2 | 40 | 3 | .... | .... | 1 | .... |
| 8805 | 4 | 6.2 | 92 | 1 | 10 | 2 | 3 | .... | 1 | 30 | 3 | .... | .... | 1 | .... |
| 10381 | 3 | 6.4 | 86 | 1 | 10 | 1 | 2 | .... | .... | 35 | 3 | .... | .... | 1 | .... |
| 8872 | 1 | 6.6 | 102 | * | * | * | * | * | * | 12 | 1 | * | * | * | * |
| 11254 | 3 | 6.8 | 114 | 1 | 10 | 1 | 1 | .... | 1 | 30 | 3 | .... | .... | .... | .... |
| 6724 | 1 | 7.1 | 141 | * | * | * | * | * | * | 12 | * | * | * | * | * |
| 10435 | 1 | 7.2 | 109 | 1 | 4 | 1 | 1 | * | * | 30 | 3 | .... | .... | .... | .... |
| C 1845 | 3 | 7.5 | 134 | * | 1 | * | 2 | * | * | 35 | 3 | .... | .... | .... | .... |
| 10503 | 3 | 7.6 | 120 | 2 | 6 | 5 | 4 | .... | 1 | 30 | 5 | .... | .... | .... | .... |
| 7795 | 2 | 7.8 | 133 | * | * | * | 2 | * | * | 15 | 3 | .... | .... | .... | .... |
| C 760 | 1 | 8.1 | 145 | * | * | * | * | * | * | 2 | 1 | * | * | * | * |
| C 1897 | 1 | 8.2 | 162 | * | * | * | * | * | * | 2 | .... | .... | .... | .... | .... |
| C 801 | 1 | 8.4 | 154 | * | * | * | * | * | * | * | * | * | * | * | * |
| C 246 | 1 | 8.5 | 164 | * | * | * | * | * | * | * | * | * | * | * | * |
| C 250 | 1 | 8.6 | 165 | * | * | * | * | * | * | * | * | * | * | * | * |
| C 1442 | 2 | 8.8 | 167 | * | * | * | * | * | * | 1 | .... | .... | .... | .... | .... |
| C 1474 | 1 | 9.0 | 182 | * | * | * | * | * | * | * | * | * | * | * | * |
| C 1478 | 1 | 9.2 | 197 | * | * | * | * | * | * | * | * | * | * | * | * |
| C 1488 | 1 | 9.3 | 201 | * | * | * | * | * | * | * | * | * | * | * | * |
| C 867 | 2 | 9.4 | 215 | * | * | * | * | * | * | .... | .... | .... | .... | .... | .... |
| C 878 | 1 | 9.3 | 234 | * | * | * | * | * | * | .... | .... | .... | .... | .... | .... |
| C 3037 | 1 | 8.9 | 243 | * | * | * | * | * | * | .... | .... | .... | .... | .... | .... |

TABLE IX—*Continued*

| Plate | Int. | Mag. | Phase | 4170 | 4173 | 4179 | 4202 | 4206 | 4216 | 4233 | 4258 | 4291 | 4308 | $H\gamma$ | 4352 |
|---|---|---|---|---|---|---|---|---|---|---|---|---|---|---|---|
| C 3068 | 3 | 8.4 | 272 | .... | .... | .... | .... | .... | .... | .... | .... | a1 | a2 | .... | .... |
| C 2013 | 4 | 8.3 | 230 | .... | .... | .... | a1 | .... | .... | .... | a1 | a2 | a3 | .... | .... |
| C 2040 | 3 | 7.8 | 258 | .... | .... | .... | a2 | .... | .... | .... | a1 | a3 | a2 | .... | .... |
| C 1507 | 2 | 7.1 | 289 | .... | .... | .... | a2 | .... | .... | .... | a2 | a2 | a2 | .... | .... |
| 12363 | 4 | 5.9 | 303 | 1 | .... | 1 | a2 | a2 | .... | 2 | a3 | a3 | a5 | 12 | .... |
| 11564 | 4 | 5.5 | 281 | 1 | 1 | 2 | a2 | a2 | .... | .... | a2 | a4 | a6 | 40 | .... |
| C 2090 | 5 | 5.0 | 283 | 2 | .... | 2 | a3 | a2 | .... | .... | a2 | a3 | a4 | 60 | .... |
| 12447 | 4 | 4.9 | 317 | .... | .... | 1 | a2 | a3 | .... | 1 | a2 | a4 | a2 | 35 | .... |
| 11609 | 5 | 3.8 | 294 | 3 | .... | 2 | a2 | a2 | .... | 1 | a2 | a4 | a4 | 75 | .... |
| 5258 | 3 | 3.7 | 326 | 1 | 1 | 2 | a2 | a1 | .... | 1 | a2 | a4 | a4 | 45 | .... |
| 6235 | 4 | 3.6 | 318 | 1 | 1 | 3 | a1 | a2 | .... | 2 | a2 | a4 | a2 | 35 | 1 |
| 11622 | 4 | 2.9 | 311 | 3 | 1 | 8 | a2 | a2 | .... | 1 | a2 | a4 | a2 | 80 | .... |
| C 500 | 2 | 3.1 | 1 | 1 | .... | 1 | a2 | a2 | .... | 1 | a2 | a5 | a2 | 55 | .... |
| 9395 | 5 | 3.4 | 29 | 2 | 1 | 5 | .... | a2 | .... | 3 | a2 | a4 | a1 | 80 | .... |
| 7413 | 3 | 3.5 | 16 | 1 | 1 | 4 | .... | a1 | .... | 1 | a1 | a3 | a3 | 30 | .... |
| 6306 | 3 | 3.7 | 14 | 1 | 1 | 5 | .... | a1 | .... | 2 | a1 | a3 | a2 | 25 | 1 |
| 5299 | 3 | 3.8 | 19 | 2 | 1 | 5 | .... | a1 | .... | 2 | a1 | a3 | a2 | 35 | .... |
| 13201 | 4 | 3.8 | 8 | 2 | 1 | 2 | .... | .... | .... | 1 | a3 | a3 | a2 | 60 | .... |
| 6369 | 4 | 4.1 | 42 | 1 | 2 | 5 | 1 | .... | .... | 2 | a1 | a3 | a2 | 35 | 1 |
| C 2663 | 2 | 4.7 | 3 | .... | .... | 1 | 1 | .... | .... | .... | a1 | a3 | a3 | 30 | .... |
| 10276 | 2 | 4.9 | 51 | 1 | 1 | 2 | 1 | .... | .... | 1 | a1 | a2 | a1 | 30 | .... |
| 6531 | 4 | 5.1 | 82 | .... | 1 | 2 | 4 | 1 | 2 | 3 | a1 | a1 | a1 | 50 | .... |
| 7551 | 3 | 5.2 | 70 | 1 | 1 | 3 | 3 | 1 | 1 | 3 | a1 | a2 | .... | 40 | 1 |
| 8789 | 3 | 5.3 | 72 | .... | 1 | 2 | 4 | 1 | 2 | 3 | a1 | a1 | 1 | 40 | .... |
| 5559 | 2 | 5.5 | 85 | .... | .... | 1 | 2 | 1 | 2 | 1 | .... | a2 | .... | 18 | .... |
| 6594 | 4 | 5.7 | 103 | .... | 1 | 2 | 6 | 1 | 2 | 3 | .... | a1 | 2 | 40 | .... |
| 9567 | 3 | 6.0 | 86 | .... | 1 | 2 | 5 | 1 | .... | 3 | .... | a2 | .... | 35 | 1 |
| 8805 | 4 | 6.2 | 92 | .... | 1 | 2 | 15 | 1 | 5 | 4 | 1 | .... | 15 | 40 | .... |
| 10381 | 3 | 6.4 | 86 | .... | 1 | 2 | 5 | .... | 1 | 2 | .... | .... | 1 | 40 | .... |
| 8872 | 1 | 6.6 | 102 | * | * | * | 3 | .... | 1 | 1 | .... | .... | 4 | 20 | .... |
| 11254 | 3 | 6.8 | 114 | .... | 1 | 2 | 5 | 1 | 3 | 1 | .... | 1 | 1 | 30 | .... |
| 6724 | 1 | 7.1 | 141 | * | * | * | 4 | 1 | 2 | 1 | .... | 1 | 6 | 25 | 1 |
| 10435 | 1 | 7.2 | 109 | .... | 1 | 2 | 5 | 1 | 2 | 1 | 1 | 1 | 3 | 20 | .... |
| C 1845 | 3 | 7.5 | 134 | .... | .... | 5 | 18 | 1 | 12 | 2 | 1 | 15 | 10 | 45 | .... |
| 10503 | 3 | 7.6 | 120 | .... | .... | 3 | 12 | 1 | 3 | 3 | 2 | 2 | 12 | 35 | .... |
| 7795 | 2 | 7.8 | 133 | .... | 1 | 2 | 12 | 2 | 5 | 2 | .... | 2 | 5 | 25 | .... |
| C 760 | 1 | 8.1 | 145 | * | * | * | 5 | * | * | * | 1 | .... | 10 | 5 | .... |
| C 1897 | 1 | 8.2 | 162 | .... | .... | .... | 5 | 3 | 4 | .... | .... | 3 | 8 | 3 | .... |
| C 801 | 1 | 8.4 | 154 | * | * | * | 3 | .... | 1 | .... | .... | 1 | 10 | 1 | .... |
| C 246 | 1 | 8.5 | 164 | * | * | * | 1 | * | * | * | * | * | 3 | .... | .... |
| C 250 | 1 | 8.6 | 165 | * | * | * | 2 | .... | 1 | * | * | 1 | 15 | 2 | .... |
| C 1442 | 2 | 8.8 | 167 | .... | .... | .... | 4 | 1 | 2 | 1 | 1 | 3 | 10 | 4 | .... |
| C 1474 | 1 | 9.0 | 182 | * | * | * | 1 | * | * | * | * | * | 5 | .... | .... |
| C 1478 | 1 | 9.2 | 197 | * | * | * | 1 | * | * | * | * | * | 5 | .... | .... |
| C 1488 | 1 | 9.3 | 201 | * | * | * | * | * | * | * | * | * | 5 | .... | .... |
| C 867 | 2 | 9.4 | 215 | .... | .... | .... | .... | .... | .... | .... | .... | .... | 4 | .... | .... |
| C 878 | 1 | 9.3 | 234 | .... | .... | .... | .... | .... | .... | .... | .... | .... | .... | .... | .... |
| C 3037 | 1 | 8.9 | 243 | .... | .... | .... | .... | .... | .... | .... | .... | .... | 2 | .... | .... |

TABLE IX—*Continued*

| Plate | Int. | Mag. | Phase | 4372 | 4376 | 4427 | 4434 | 4458 | 4461 | 4482 | 4489 | 4511 | 4521 | 4571 | *Hβ* |
|---|---|---|---|---|---|---|---|---|---|---|---|---|---|---|---|
| C 3068 | 3 | 8.4 | 272 | .... | a1 | .... | .... | .... | .... | .... | .... | .... | .... | .... | .... |
| C 2013 | 4 | 8.3 | 230 | .... | a2 | a1 | .... | 2 | 2 | a1 | a2 | .... | .... | .... | .... |
| C 2040 | 3 | 7.8 | 258 | .... | a2 | a1 | .... | 2 | 1 | a2 | a2 | .... | .... | .... | .... |
| C 1597 | 2 | 7.1 | 289 | .... | a2 | .... | .... | 2 | 1 | a2 | a1 | .... | .... | .... | .... |
| 12363 | 4 | 5.9 | 303 | .... | a3 | a1 | .... | .... | .... | a1 | a1 | .... | .... | a2 | 2 |
| 11564 | 4 | 5.5 | 281 | .... | a2 | a2 | 2 | 3 | 2 | a2 | a2 | .... | .... | a4 | 1 |
| C 2090 | 5 | 5.0 | 283 | .... | a2 | a2 | 4 | 2 | 2 | a2 | a2 | .... | .... | a4 | 2 |
| 12447 | 4 | 4.9 | 317 | .... | a2 | a2 | .... | 1 | .... | a1 | a1 | .... | .... | a1 | 1 |
| 11609 | 5 | 3.8 | 294 | .... | a1 | a1 | 4 | 2 | 2 | a2 | a1 | .... | .... | a2 | 20 |
| 5258 | 3 | 3.7 | 326 | .... | a2 | a2 | .... | 1 | 1 | a2 | a2 | .... | .... | a2 | 8 |
| 6235 | 4 | 3.6 | 318 | .... | a2 | a2 | 3 | .... | .... | a2 | a2 | .... | 2 | a4 | 5 |
| 11622 | 4 | 2.9 | 311 | .... | a2 | a2 | 4 | 1 | 1 | a2 | a2 | .... | 4 | a2 | 40 |
| C 500 | 2 | 3.1 | 1 | .... | a2 | a2 | 3 | .... | .... | a3 | a3 | .... | 3 | a4 | 30 |
| 9395 | 5 | 3.4 | 29 | .... | a1 | a2 | 10 | 2 | 2 | a2 | a2 | .... | 10 | a2 | 40 |
| 7413 | 3 | 3.5 | 16 | .... | a2 | a2 | 2 | 1 | 0 | a1 | a2 | .... | .... | a2 | 4 |
| 6306 | 3 | 3.7 | 14 | .... | a2 | a2 | 2 | 4 | 1 | a2 | a3 | 1 | 5 | a2 | 5 |
| 5299 | 3 | 3.8 | 19 | .... | a2 | a2 | 2 | 2 | 3 | a2 | a3 | .... | 15 | a2 | 12 |
| 13201 | 4 | 3.8 | 8 | .... | a1 | a2 | 10 | 2 | 2 | a2 | a2 | .... | 2 | a2 | 10 |
| 6369 | 4 | 4.1 | 42 | .... | a1 | a2 | 10 | 2 | 2 | a1 | a2 | 1 | 3 | a2 | 2 |
| C 2663 | 2 | 4.7 | 3 | .... | a1 | a2 | 1 | 1 | .... | a1 | a2 | 1 | 1 | a1 | 2 |
| 10276 | 2 | 4.9 | 51 | .... | .... | a1 | 1 | .... | .... | a1 | a2 | 1 | .... | .... | 3 |
| 6531 | 4 | 5.1 | 82 | .... | 1 | .... | 1 | 1 | 1 | a1 | a2 | 1 | 2 | .... | 2 |
| 7551 | 3 | 5.2 | 70 | .... | .... | a1 | .... | 2 | 1 | a1 | a1 | 1 | 2 | .... | 2 |
| 8789 | 3 | 5.3 | 72 | .... | 2 | .... | .... | 1 | 2 | a1 | .... | 4 | 1 | 1 | 12 |
| 5559 | 2 | 5.5 | 85 | .... | 1 | .... | .... | 1 | 2 | a1 | a1 | 1 | 1 | 1 | 2 |
| 6594 | 4 | 5.7 | 103 | .... | 4 | 1 | .... | 2 | 2 | a1 | a1 | 2 | .... | 2 | 12 |
| 9567 | 3 | 6.0 | 86 | .... | 2 | 1 | .... | 1 | 1 | .... | .... | 3 | 1 | 1 | 10 |
| 8805 | 4 | 6.2 | 92 | 1 | 10 | 2 | .... | 1 | 2 | .... | 1 | 12 | 1 | 16 | 18 |
| 10381 | 3 | 6.4 | 86 | .... | 2 | 1 | .... | .... | .... | .... | .... | 2 | 1 | .... | 10 |
| 8872 | 1 | 6.6 | 102 | .... | 2 | .... | .... | .... | 1 | .... | .... | 1 | .... | 4 | 3 |
| 11254 | 3 | 6.8 | 114 | .... | 5 | .... | 1 | 2 | 1 | .... | .... | 4 | .... | 2 | 1 |
| 6724 | 1 | 7.1 | 141 | 2 | 10 | 1 | 1 | 1 | 2 | 1 | .... | 1 | .... | 20 | 5 |
| 10435 | 1 | 7.2 | 109 | 1 | 3 | .... | .... | 1 | 1 | .... | .... | 3 | .... | 4 | .... |
| C 1845 | 3 | 7.5 | 134 | 2 | 25 | 2 | 1 | 1 | 2 | .... | .... | 10 | .... | 30 | 1 |
| 10503 | 3 | 7.6 | 120 | 2 | 8 | 1 | 2 | 1 | 1 | 1 | 1 | 4 | .... | 15 | 3 |
| 7795 | 2 | 7.8 | 133 | 4 | 10 | 2 | 1 | 1 | 4 | .... | .... | 4 | .... | 18 | .... |
| C 760 | 1 | 8.1 | 145 | 3 | 4 | 1 | .... | 1 | 2 | .... | .... | 1 | .... | 16 | .... |
| C 1897 | 1 | 8.2 | 162 | 1 | 18 | 2 | .... | 1 | 4 | 1 | 2 | .... | .... | 25 | .... |
| C 801 | 1 | 8.4 | 154 | 1 | 2 | 1 | .... | 1 | 2 | 1 | 2 | .... | .... | 18 | .... |
| C 246 | 1 | 8.5 | 164 | * | 1 | * | * | * | * | * | * | * | * | 15 | .... |
| C 250 | 1 | 8.6 | 165 | .... | 5 | 1 | .... | .... | 2 | 1 | 2 | .... | .... | 30 | .... |
| C 1442 | 2 | 8.8 | 167 | 2 | 5 | 3 | .... | 1 | 4 | 1 | 1 | .... | .... | 25 | .... |
| C 1474 | 1 | 9.0 | 182 | .... | 2 | .... | .... | .... | 1 | .... | .... | .... | .... | 20 | .... |
| C 1478 | 1 | 9.2 | 197 | .... | .... | * | * | * | * | * | * | .... | .... | 20 | .... |
| C 1488 | 1 | 9.3 | 201 | * | * | * | * | * | * | * | * | * | * | 15 | .... |
| C 867 | 2 | 9.4 | 215 | .... | 1 | .... | .... | .... | .... | .... | .... | .... | .... | 18 | .... |
| C 878 | 1 | 9.3 | 234 | .... | .... | .... | .... | .... | .... | .... | .... | .... | .... | 5 | .... |
| C 3037 | 1 | 8.9 | 243 | .... | .... | .... | .... | .... | .... | .... | .... | .... | .... | 10 | .... |

proceeding from $H\epsilon$. As the star decreases in brightness and becomes cooler H diminishes in width and allows the bright $H\epsilon$ to appear. This explanation requires the presence of at least a portion of the calcium gas at levels above the origin of the $H\epsilon$ emission. The change in the strength of H is well illustrated in the reproduction of Stebbins' spectrograms[1] and is likewise shown on several of the plates used in this investigation. Shane[1] has accounted for the weakness of $H\kappa$, $H\lambda$, $H\mu$, and $H\xi$ by the corresponding absorption of the low-temperature lines of iron and vanadium.

---

[1] *Lick Observatory Bulletins*, **2**, 81, 1903.

The lines of silicon seem to be less sensitive to temperature changes and do not show a distinct maximum. In the electric furnace King[2] has found that these lines occur at intermediate temperatures corresponding to the iron lines of class III. The lines of the low-temperature group, with the exception of λ 4308 and probably λ 4202, which are in class II, belong to temperature class I.

The bright lines whose identification seems to be reasonably certain are listed in Table X.

*Hydrogen lines.*—The identification of the hydrogen lines has been accepted since they were first observed by Pickering in 1886. The question of their relative intensities is as yet not completely solved. The Balmer series behaves in stars as a high-temperature series, and it is to be expected that these lines, if they occur at all, will be strengthened by the maximum temperature. As will be seen in Figure 6, the maximum intensity of the hydrogen lines occurs very near maximum light.

*Enhanced lines.*—As has previously been pointed out,[3] enhanced lines are found in giant M-type stars owing chiefly to their low density. They may well occur in the extreme tenuity of the atmosphere of *o* Ceti. Although the agreement of the wave-lengths is not fully convincing, especially in the case of λ 4233, the identification with ionized iron may be considered as entirely probable. Several of the enhanced lines found in *o* Ceti are bright in certain S-type stars and in M-type stars such as W Cephei, which are of the same order of temperature as Mira. They also appear together in emission in the bright-line B-type stars. The consideration of the atomic origin of the lines thus identified, as worked out by Russell,[4] has hastened the conclusion. They are without exception the strongest members of the multiplets arising from the lowest levels of the ionized atom and would presumably be the first to be affected by any cause tending to produce emission lines.

---

[1] *Lick Observatory Bulletins*, **10**, 133, 1922.

[2] *Publications of the Astronomical Society of the Pacific*, **33**, 106, 1921.

[3] Adams and Joy, *Publications of the Astronomical Society of the Pacific*, **35**, 328, 1923.

[4] Unpublished series relationships in $Fe+$.

TABLE X

IDENTIFICATION OF EMISSION LINES

| MEASURED WAVE-LENGTH ROWLAND | LABORATORY WAVE-LENGTH | | ELEMENT | TEMP. CLASS | ATOMIC ORIGIN | TIME OF MAX. INTENSITY | |
|---|---|---|---|---|---|---|---|
| | Rowland | I.A. | | | | Mag. | Phase |
| 3770.83 | 3770.75 | .58 | $H\iota$ | ........ | $2P-11D$ | 4.4 | $50^{d}$ |
| 3797.96 | 3798.02 | .85 | $H\theta$ | ........ | $2P-10D$ | 4.4 | 50 |
| 3835.65 | 3835.51 | .36 | $H\eta$ | ........ | $2P-9D$ | 5.0 | 65 |
| 3889.33 | 3889.18 | .05 | $H\zeta$ | ........ | $2P-8D$ | 5.0 | 65 |
| 3905.82 | 3905.66[*] | .53 | *Si* | III | ........... | 5.2 | 70 |
| 3970.30 | 3970.21 | .08 | $H\epsilon$ | ........ | $2P-7D$ | 5.7 | 85 |
| 4030.75 | 4030.90 | .77 | *Mn* | I | $1s^6-1p^6$ | 7.2 | 125 |
| 4101.89 | 4101.89 | .74 | $H\delta$ | ........ | $2P-6D$ | 3.8 | 20 |
| 4103.15 | 4103.10[†] | .95 | *Si* | III | ........... | 5.2 | 70 |
| 4138.75 | 4138.58[§] | .43 | *Fe+* | ........ | $2f^4-1p^4$ | 3.5 | 0 |
| 4173.63 | 4173.63 | .47 | *Fe+* | ........ | $2p^4-1d'^4$ | 3.5 | 0 |
| 4178.98 | 4179.02 | .86 | *Fe+* | ........ | $2p^4-1f'^4$ | 3.6 | 10 |
| 4202.18 | 4202.19 | .03 | *Fe* | I | $1f^3-1g'^3$ | 8.0 | 145 |
| 4206.86 | 4206.86 | .70 | *Fe* | I A | $1d^5-1p'^7$ | 8.0 | 145 |
| 4216.35 | 4216.35 | .18 | *Fe* | I | $1d^5-1p'^7$ | 7.8 | 140 |
| 4233.49 | 4233.32 | .16 | *Fe+* | ........ | $2p^4-1d'^4$ | 3.8 | 20 |
| 4258.45 | 4258.48 | .33 | *Fe* | I A | $1d^5-1p'^7$ | 7.8 | 140 |
| 4291.64 | 4291.62 | .47 | *Fe* | I A | $1d^5-1p'^7$ | 8.0 | 145 |
| 4308.10 | 4308.08 | .91 | *Fe* | II | $1f^3-1g'^3$ | 8.6 | 165 |
| 4340.64 | 4340.63 | .47 | $H\gamma$ | ........ | $2P-5D$ | 3.7 | 15 |
| 4376.09 | 4376.09 | .93 | *Fe* | I | $1d^5-1f'^7$ | 7.8 | 140 |
| 4427.49 | 4427.47 | .31 | *Fe* | I | $1d^5-1f'^7$ | 8.0 | 145 |
| 4461.75 | 4461.82 | .66 | *Fe* | I | $1d^5-1f'^7$ | 8.3 | 160 |
| 4482.27 | 4482.34 | .18 | *Fe* | I | $1d^5-1f'^7$ | 8.0 | 145 |
| 4489.73 | 4489.91 | .75 | *Fe* | I A | $1d^5-1f'^7$ | 8.0 | 145 |
| 4511.66 | 4511.47[‡] | .31 | *In* | I | $1p^2-1s^2$ | 6.5 | 110 |
| 4571.31 | 4571.28 | .11 | *Mg* | I | $1S-1p^3$ | 8.4 | 165 |
| 4584.05 | 4584.01 | .84 | *Fe+* | ........ | $2f^4-1d'^4$ | 3.5 | 0 |
| 4861.49 | 4861.51 | .33 | $H\beta$ | ........ | $2P-4D$ | 3.7 | 15 |
| 4923.95 | 4924.09 | .92 | *Fe+* | ........ | $1s^6-1p'^6$ | 3.5 | 0 |
| 5018.62 | 5018.61 | .44 | *Fe+* | ........ | $1s^6-1p'^6$ | 3.5 | 0 |
| ........... | 6563.04 | .82 | $H\alpha$ | ........ | $2P-3D$ | ........ | ........ |

[*] King, unpublished

[†] King, *Publications of the Astronomical Society of the Pacific*, 35, 330, 1923.

[§] Calculated from known terms.

[‡] *Ibid.*, 37, 27, 1925.

The strongest and most persistent of the enhanced bright lines are λλ 4233 and 4179. λ 4233 is sharper and better for measurement. As it occurs with great frequency, the measures should be of high accuracy. λ 4179 is stronger than λ 4233 at maximum light but often is not sharp. It seems to be involved in a strong portion of the continuous spectrum, which may affect its observed wave-length.

As shown in Table XI, the enhanced lines of iron, in the mean, are displaced somewhat toward the red as compared with the hydrogen and low-temperature lines used for determining the wave-length correction. In other words, if we assume that the identification of these lines is correct, they have on the average a positive velocity relative to the eight lines used in forming the bright-line curve. As shown in Figure 4, these lines give points falling between the bright- and dark-line curves. Their origin must then be at a level of the star's atmosphere between the low level producing the absorption lines and the higher levels emitting the bright lines of hydrogen and the low-temperature lines.

TABLE XI

WAVE-LENGTHS OF ENHANCED IRON LINES

| Measured Wave-Length | Laboratory Wave-Length | Diff. | Wt. |
|---|---|---|---|
| 4138.75 | 4138.58 | +0.17 | 1 |
| 4173.63 | 4173.63 | 0.00 | 1 |
| 4178.98 | 4179.02 | −0.04 | 2 |
| 4233.49 | 4233.32 | +0.17 | 4 |
| 4584.08 | 4584.01 | +0.07 | 1 |
| 4923.97 | 4924.09 | ............ | ............ |
| 5018.62 | 5018.61 | ............ | ............ |
| Weighted mean diff. | ............ | +0.09 | ............ |

A similar effect has been pointed out by Merrill[1] for the enhanced iron lines of B.D. +11°4673.

The middle broken line in Figure 4 shows the mean course of the velocities for the enhanced lines λλ 4138, 4173, 4178, and 4233. The lines λλ 4924 and 5018 have a few measurements only and are located in a region of the spectrum where the focus is not good on our plates. They are not satisfactorily determined, as will be seen from their probable errors, and have not been used in forming the mean curve. The individual lines do not agree closely with one another. Hence this curve should not be taken as comparable in accuracy with the other curves, but the evidence points to a solution along these lines.

*Bright lines of silicon and indium.*—Table IX shows that the silicon lines λλ 3905 and 4103, and λ 4511, which may belong to indium, have intensity-curves quite different from those belonging to the low-temperature group. A comparison of these lines, similar to that for the enhanced lines, is given in Table XII. Apparently these lines arise from levels not far from those producing the enhanced iron lines and have corresponding velocities.

---

[1] *Publications of the Astronomical Observatory, University of Michigan,* **2,** 74, 1916.

The identification of the indium line is still uncertain. This line, together with λ 4101.9, which is coincident with $H\delta$, is one of the ultimate lines of indium. A plate taken by King[1] with the electric furnace shows that these two lines are strong even at a temperature of 1600°. If present in the sun, λ 4511 is very weak; and it has not been found in absorption in Mira at maximum. The atomic weight of indium is high, but like most of the elements which show bright low-temperature lines, it has a low ionization potential. It is unfortunate that the presence of $H\delta$ makes it impossible to observe the other member of this pair.

TABLE XII

WAVE-LENGTHS OF SILICON AND INDIUM LINES

| Measured Wave-Length | Laboratory Wave-Length | Diff. |
|---|---|---|
| 3905.82 ....... | 3905.66 | +0.16 |
| 4103.15 ....... | 4103.11 | +0.04 |
| 4511.66 ....... | 4511.47 | +0.19 |
| Mean diff...... | .............. | +0.13 |

*The low-temperature lines.*—Among the lines which reach their greatest intensity when the star has cooled after its outburst at maximum brightness are several iron lines, λ 4571 of magnesium, and perhaps λ 4030 of manganese. These lines originate at the lowest levels of the atom and maintain a considerable intensity in the electric furnace at very low temperatures.

In view of the interest attaching to the series relationships of the iron multiplets and of the criticism[2] of the identification of these lines, it seems worth while to give the multiplets of iron involved here as worked out by Walters[3] and Delaporte.[4]

---

[1] *Publications of the Astronomical Society of the Pacific*, **37**, 27, 1925.

[2] Baxandall, *The Observatory*, **46**, 82, 1923.

[3] *Journal of the Optical Society of America*, **8**, 248, 1924.

[4] *Zeitschrift für Physik*, **23**, 135, 1924, and **26**, 1, 1924.

The lines which have been measured as bright in Mira are marked with an asterisk. The arc intensities in the laboratory and King's temperature classification are added. The wave-lengths are I.A.

IRON MULTIPLETS

| | | | | | |
|---|---|---|---|---|---|
| I. | | 4232.724 (8) I A | 4199.990 (9) I A | 4149.77 (calculated) | |
| | | | *4258.322 (10) I A | *4206.703 (12) I A | 4134.433 (1) |
| | | | | *4291.465 (10) I A | *4216.185 (10) I |
| II. | | 4466.557 (12) I | | | |
| | *4489.744 (12) I A | 4471.66 (calc.) | 4435.154 (10) I A | | |
| | | *4482.176 (4) I A | 4445.480 (1) I A | 4389.251 (10) I A | |
| | | | *4461.658 (12) I | 4405.01 (calc.) | 4325.73 (calc.) |
| | | | | *4427.313 (12) I | 4347.239 (1) I A |
| | | | | | *4375.934 (15) I |
| III. | | 4325.770 (35) II | 4250.791 (25) II | 4147.675 (10) III | |
| | | | *4307.910 (35) II | *4202.032 (30) I | |
| | | | | 4271.764 (35) II | |

The four strongest members of multiplet I are bright in Mira. The absence of the diagonal member λ 4232 is puzzling. It may be too faint in the star.

In multiplet II all lines of the diagonal, and no others, appear in emission. λ 4375 is by far the strongest member. λλ 4482 and 4489 are extremely weak. The strong satellites λλ 4435 and 4389 reach the condition where emission and absorption neutralize each other.

Multiplets I and II are inter-system combinations of quintets and septets. Both arise in the d′ level, which is the lowest level known in the neutral iron atom. The inter-system combination seems especially favorable to the production of the bright lines. All these lines belong to King's class I or I A, but they are not among the "raies ultimes" of De Gramont, which are farther in the violet.

Multiplet III is an f–g′ triplet combination arising from the lowest triplet level. Two members only are bright. The absorption of the other members is much diminished at the time when the bright lines have their greatest intensity. λλ 4250.8 and 4271.8 are blended with the neighboring high-temperature iron lines, λλ 4250.1 and 4271.2, respectively, but the latter are relatively weak at the temperature of Mira and should not affect the multiplet lines to any great extent. Merrill[1] has found that at the positive pole of the arc λλ 4202 and 4307 are unchanged in intensity, but that λλ 4250.8,

---

[1] *Mt. Wilson Contr.*, No. 253; *Astrophysical Journal*, **56**, 479, 1922.

4271.8, and 4325[1] are slightly strengthened. This difference is in the direction found in *o* Ceti. The star appears to furnish an exceedingly sensitive test of the response of these lines to different degrees of excitation, and, in turn, their behavior should reveal very accurately the conditions prevailing in the star. Doubtless the most important factor is that of temperature.

With this problem in mind, Mr. King has been kind enough to examine some spectrograms of iron taken with the furnace and carbon plug. He finds that as the temperature of the plug is increased the low-temperature lines are the first to appear in absorption. The line λ 4307 shows easily and λ 4202 very faintly, together with λ 4375 and several of the low-temperature iron lines which are bright in *o* Ceti, with a plug temperature of 2000° and a vapor temperature of about 1600°; but λ 4325 does not appear at all. For some unknown reason λλ 4202 and 4307 are more sensitive to changes in excitation than the other members of the multiplet.[2]

At maximum the lines of this multiplet, as well as the strong low-temperature lines of class I, are the usual type of absorption lines. Lower temperatures following maximum have the effect of increasing the emission, so that the core is filled up until the absorption is entirely neutralized, and later some of the lines appear entirely in emission. These emission lines increase in strength to a maximum at magnitude about 8.0 and then decrease again toward minimum.

The intensities of the strong lines of multiplet III are given in Table XIII and illustrate the behavior of these lines in absorption and emission at different phases of the star's variation. The cases for λλ 4202 and 4307 are somewhat puzzling, but when the behavior of all the other members of the multiplet is considered, the probability for the suggested identification is strengthened.

Several of the lines do not appear actually to become emission lines, but they can no longer be recognized as absorption lines on these plates; of the two emission lines, λ 4202 is the weaker and the first to appear as a bright line; λ 4307 appears later and remains bright until well past minimum.

---

[1] Unpublished.

[2] Note added to proof: Miss Moore finds that λλ 4202 and 4307 are less winged in the sun than λλ 4325 and 4271. *Astrophysical Journal*, **63**, 6, 1926.

The low-temperature line of magnesium at λ 4571, which is an inter-system combination between a single and threefold level, is strongest at minimum light and remains bright even longer than λ 4307.

*Unidentified lines.*—If we accept the identification of all the 32 lines given in Table X, there remain 18 lines whose origin cannot be traced. Some of these may in reality be only portions of the continuous spectrum giving the appearance of bright lines. Other lines appear to be real, but a search among the laboratory spectra of the elements fails to suggest any likely identification.

TABLE XIII

INTENSITIES IN f–g′ IRON MULTIPLET

| Plate | Phase | Mag. | 4147 | 4202 | 4250 | 4271 | 4307 | 4325 |
|---|---|---|---|---|---|---|---|---|
| $\gamma$ 8597 | 13 | 3.4 | a1 | a1 | a4 | a3 | a1 | a5 |
| $\gamma$ 5492 | 77 | 5.3 | a1 | e4 | a2 | a3 | 0 | a5 |
| $\gamma$10503 | 120 | 7.6 | a1 | e12 | a1 | a2 | e12 | a2 |
| C 2383 | 156 | 8.4 | 0 | e10 | 0 | 0 | e20 | 0 |
| C 867 | 215 | 9.4 | 0 | 0 | a1 | a1 | e4 | 0 |
| C 1597 | 289 | 7.1 | 0 | a2 | a1 | a2 | a2 | a2 |

From the times of their occurrence with respect to the star's changes, it is possible to predict the nature of the sources in which identifications may be expected. Thus λλ 4166, 4461.5, and 4521 occur at or near maximum and should be expected in comparatively high-temperature sources, while λλ 3852, 3907, 3938, 4372, and 4579 are evidently of low-temperature origin.

## 8. RADIAL VELOCITIES GIVEN BY THE EMISSION LINES

The hydrogen lines $H\delta$ and $H\gamma$, the iron lines λλ 4202, 4216, 4291, 4308, and 4376, and the magnesium line λ 4571 have been employed for determining the radial-velocity curve of the bright lines. These are the lines used as standards for correcting the wave-lengths of the bright lines. Since they are the strongest and most persistent of the bright lines, they are well suited for measurement over a considerable portion of the star's period. $H\delta$ and $H\gamma$ are the only lines of the group which appear during increasing light and near maximum. During decreasing light, the hydrogen lines are concurrent with several of the other lines for a large part of the time. There is no evidence that any of the lines give different velocities; in fact, curves for the individual lines show satisfactory agreement with the mean curve based on all eight lines.

These lines are sharp and of superior quality for measurement on our plates. Campbell[1] and Plaskett[2] found that the hydrogen lines at least are not symmetrical and that measurements were affected by the strength of the line on the plate. In practice the micrometer wire has been set upon the tips of the strongly exposed bright lines. This precaution, which is always possible with plates on which the spectrum of the star is narrow, seems to have avoided any systematic error that might have entered because of asymmetry.

TABLE XIV

NORMAL POINTS FOR EMISSION LINES

| Mean Phase | Mean *V* | Mean Phase | Mean *V* |
|---|---|---|---|
| days | km/sec. | days | km/sec. |
| 16 | +47.1 | 148 | +48.9 |
| 49 | 43.2 | 163 | 53.0 |
| 78 | 42.4 | 194 | 52.0 |
| 96 | 41.5 | 297 | 48.0 |
| 116 | 45.1 | 327 | +47.8 |
| 134 | +48.3 | | |

The measures of the whole series of plates have been examined with this in mind, and a special series of plates was taken on January 11, 1925, with exposures ranging from 1 to 35 min.; but no error of this kind seems to be present. Settings can be made on the bright lines with great accuracy. On the whole, it appears that, although the number of lines used is much smaller, the velocity-curve determined from the bright lines is not greatly inferior in accuracy to that determined from the absorption lines.

The velocities found from the eight standard bright lines, with their weights, are given in the last two columns of Table II. They have been combined into the eleven normals given in Table XIV. These are represented by circles with central points in the lower portion of Figure 4. The plates showing bright lines have been weighted arbitrarily, as in the case of the absorption lines. The normals are means with nearly equal total weight.

---

[1] *Astrophysical Journal*, **9**, 31, 1899.

[2] *Journal of the Royal Astronomical Society of Canada*, **1**, 52, 1907.

The plot of the normal points shows conclusively that the velocity given by the emission lines is not constant and does not follow the course of the velocities obtained from the absorption lines. Perhaps the most striking, and doubtless an important, feature of the curve is that at the time of minimum light the bright lines give a velocity which agrees closely with that found from the absorption lines. The portion of the bright-line curve showing the rise from least to greatest velocity is well determined on account of the number of lines available during this interval.

TABLE XV

ABSORPTION *minus* EMISSION VELOCITIES

| Phase | a−e | Phase | a−e |
|---|---|---|---|
| days | km/sec. | days | km/sec. |
| 16 | +16.7 | 148 | + 6.1 |
| 49 | 19.1 | 163 | 0.9 |
| 78 | 17.9 | 194 | 0.3 |
| 96 | 17.4 | 297 | 14.0 |
| 116 | 12.2 | 327 | +16.1 |
| 134 | +7.7 | | |

It is unfortunate that other observers have not followed the star to later phases, for it is often possible to photograph the bright lines when it is not practicable to make exposures of sufficient length to secure the continuous spectrum. The principal features of the bright-line curve are, however, supported by the observations of Stebbins[1] on Mira and by those of Merrill[2] for four other long-period variables. In both cases a range of about 8 km/sec. is shown with a minimum velocity at a phase of about 50 days, followed by a sharp rise. Stebbins failed to recognize this variation because of the small amount of material (9 plates) available and the inclusion of a number of lines which are not subject to this variation in velocity.

Standing by itself, the velocity-curve of the bright lines seems to suggest no explanation of its behavior. If, however, the velocity changes are compared with the dark-line curve a clue is unfolded which needs consideration and may be of considerable value in interpreting the phenomena of the emission lines.

---

[1] *Lick Observatory Bulletins*, **2**, 91, 1903.

[2] *Mt. Wilson Contr.*, No. 264; *Astrophysical Journal*, **58**, 237, 1923.

In Table XV the differences between the bright-line normal points and the corresponding points on the dark-line curve are given. Figure 5 is a plot of these points.

It will be noted that there are no points between phases 194 and 297 days on account of the weakness and absence of emission lines at that time. Nevertheless, the points seem to represent a curve whose maximum, minimum, and form can be expressed by the elliptic elements

$K = 9.5$ km/sec.
$\gamma = +10.8$ km/sec.
$e = 0.24$
$\omega = 311^\circ$
$T = 155$ days
$a \sin i = 42{,}000{,}000$ km

The maximum difference of velocity is found at phase 56 days, the periastron or most rapid velocity change is at 155 days, and at phase 180 days there is practically no difference in velocity between bright and dark lines. The curve through the bright-line normal points in Figure 4 has been derived by correcting the dark-line curve by the differences shown in the curve of Figure 5. The dotted portion of the curve is not covered by observations and it would, perhaps, be well to omit that portion entirely.

## 9. RELATIONSHIP BETWEEN SPECTRAL CHANGES AND LUMINOSITY VARIATION

With Figures 1–7 before us it is possible to obtain a comprehensive idea of the relations between the physical processes taking place in the star, even though we cannot clearly outline the forces which are at work.

The following points appear to be well taken:

1. All physical changes repeat themselves with only slight deviations in succeeding cycles.

2. The spectral type of the star, and presumably the temperature of the absorbing strata, vary with the total luminosity, the earliest type and highest temperature occurring at maximum light. This ap-

plies generally, to different cycles as well as to changes during a single cycle.

3. The appearance and intensity of the emission lines depend essentially on magnitude rather than on phase. It is necessary, however, to distinguish between the ascending and descending branches of the light-curve, which have quite different spectroscopic behavior. For example, in 1917 and 1918, when the light-curves were decidedly different in form, the appearance and intensity of the bright lines seemed to conform more closely to the magnitude changes than to the time elapsed since the preceding maximum. A number of illustrations of this effect may be seen in Table IX where both magnitude and phase are given. The relationship was discovered in an attempt to arrange all the spectrograms in an unbroken sequence.

4. The hydrogen and enhanced iron lines have their maximum intensity of emission when the star is brightest, or shortly after. Certain low-temperature lines appear as bright lines after maximum light and reach their greatest intensity at about magnitude 8.5.

5. The velocity-curve of the absorption lines is similar in shape and phase to the light-curve. It is opposite in phase to the usual Cepheid curve but has a similar eccentricity. This curve is doubtless the fundamental velocity-curve of the lower layers of the star's atmosphere. It is subject to correction owing to the fact that the velocities are integrated over the whole disk. Such a correction would increase the range of variation if the changes are due to pulsation or convection currents.

6. The emission lines of hydrogen and the bright low-temperature iron lines have the same displacement.

7. The velocity-curve of the hydrogen and low-temperature emission lines is more intelligible if referred to the absorption-line curve. At minimum the two curves give equal velocities. The greatest difference in velocity is 56 days after maximum. The bright lines always show an outward velocity with respect to the absorbing strata.

8. The low-temperature bright lines appear when the difference in velocity is greatest and disappear near minimum when the difference is zero.

9. The bright enhanced lines and the lines of silicon (and

indium) have smaller displacements than the hydrogen and low-temperature lines and probably lie at low levels in the atmosphere. They show in less degree the velocity changes indicated by the emission lines of higher level.

### 10. COMPARISON OF OBSERVATIONS AT DIFFERENT CYCLES

The radial velocity from the absorption lines has been measured near maximum by a number of observers during the last twenty-eight years. A comparison of the mean results obtained within thirty days of maximum is given in Table XVI.

TABLE XVI

VELOCITY AT MAXIMUM

| Maximum | Mag. | *V* | No. Plates | Prisms | Observer |
|---|---|---|---|---|---|
| | | km/sec. | | | |
| Nov. 1897........ | 3.7 | +62.0 | 3 | 3 | Lick, Campbell |
| Oct. 1898........ | 2.9 | 62.8 | 2 | 3 | Lick, Campbell |
| June 1902........ | 3.5 | 66. | 1 | 1 | Lick, Stebbins |
| Dec. 1906........ | 3.9 | 65.4 | 2 | 3 | Ottawa, Plaskett |
| Dec. 1906........ | 3.9 | 66.1 | 3 | 3 | Bonn, Küstner |
| Dec. 1906........ | 3.9 | 64.2 | 4 | 3 | Yerkes, Frost |
| Dec. 1906........ | 3.9 | 71. | 2 | 1 | Yerkes, Frost |
| Jan. 1915........ | 3.9 | 70. | 3 | 1 | Yerkes, Frost |
| Jan. 1915........ | 3.9 | 54. | 2 | 1 | Ottawa, Harper |
| Jan. 1915........ | 3.9 | 63.7 | 1 | 1 | Detroit, Merrill |
| Dec. 1915........ | 3.5 | 63.4 | 5 | 4 | Cape, Lunt |
| Dec. 1915........ | 3.5 | 66. | 1 | 1 | Yerkes, Frost |
| Nov. 1916........ | 3.8 | 63.3 | 3 | 1 | Mt. Wilson |
| Sept. 1917........ | 3.6 | 64.1 | 5 | 1 | Mt. Wilson |
| Sept. 1917........ | 3.6 | 66. | 2 | 1 | Yerkes, Frost |
| Sept. 1918........ | 3.6 | 68. | 2 | 1 | Yerkes, Frost |
| Sept. 1918........ | 3.6 | 70. | 1 | 1 | Ottawa, Harper |
| Sept. 1918........ | 3.6 | 59.1 | 1 | 1 | Mt. Wilson |
| Aug. 1919........ | 3.3 | 65.8 | 1 | 1 | Mt. Wilson |
| Aug. 1919........ | 3.3 | 69. | 1 | 1 | Yerkes, Frost |
| June 1920........ | 3.1 | 64.8 | 2 | 1 | Mt. Wilson |
| Mch. 1923........ | 2.8 | 66.2 | 3 | 1 | Mt. Wilson |
| Feb. 1924........ | 4.7 | 62.0 | 4 | 1 | Mt. Wilson |
| Jan. 1925........ | 3.8 | 66.4 | 3 | 1 | Mt. Wilson |
| Jan. 1925........ | 3.8 | +61.3 | 1 | 3 | Mt. Wilson |

These observations may be grouped according to magnitude as in Table XVII.

It is clear that the velocities from the absorption lines do not vary with the maximum magnitude of different cycles to any appreciable extent, and, in fact, are constant within the errors of measurement, as earlier observers have concluded. The velocity-curves for each season separately show that the whole velocity-curve, as well as the maximum, is very probably constant; but the conclusion does not carry much weight because of the lack of data.

On account of the different methods of measuring the bright lines used by various observers, it has not seemed worth while to include these lines in Table XVI. The Mount Wilson results for the maxima of eight different cycles give the values of the mean velocities of bright $H\delta$ and $H\gamma$ within 30 days of maximum as shown in Table XVIII.

TABLE XVII

VELOCITY AND MAGNITUDE AT MAXIMUM

| Mag. at Max. | V | Wt. |
|---|---|---|
| 2.8–2.9 | +64.3 | 2 |
| 3.1–3.6 | 64.7 | 7 |
| 3.7–3.9 | 64.6 | 10 |
| 4.7 | +62.0 | 1 |

TABLE XVIII

VELOCITIES FROM EMISSION LINES AT DIFFERENT MAXIMA

| Mag. at Max. | V | No. of Plates |
|---|---|---|
| | km/sec. | |
| 2.9–3.1....... | +48.5 | 5 |
| 3.4–3.6....... | 47.9 | 8 |
| 3.7–3.8....... | 47.4 | 7 |
| 4.7........... | +46.3 | 5 |

The tendency for larger values of the velocity to occur at brighter maxima is suggested, but the result may be accidental, since at maximum light only two lines are available for measurement.

From estimates of intensity, we have the approximate relationship of intensity of bright lines to maximum brightness at different epochs as grouped in Table XIX. The values are rounded off from those given in Table IX, and supplemented by a few estimates not included there. It is assumed that the effective exposure for the continuous spectrum is the same for all the plates considered. The results are very rough, but they give an idea of the strengthening of the emission lines with increased brightness at maximum.

The hydrogen lines are thus affected, not only at the time of maximum, but throughout a considerable portion of the particular cycle involved, as is apparent in the two cycles reaching maximum in June, 1920, and March, 1923, when the magnitudes were 3.1 and 2.8, respectively. The strength of $H\beta$ at bright maxima is remarkable. There seems to be some evidence that at times of unusual activity $H\gamma$ is strengthened with respect to $H\delta$. This was certainly true in 1923 (mag. 2.8). One is led to conjecture whether the normal order of intensities of the hydrogen lines might not prevail at a very bright maximum, such as that recorded by Herschel (mag. 1.5). The spectral type would then be expected to be M1 or M2, and the conditions would perhaps be the same as in those stars of class M1e, such as T Centauri, whose hydrogen lines decrease in strength toward the violet.

TABLE XIX

EMISSION-LINE INTENSITIES AT DIFFERENT MAXIMA

| MAG. AT MAX. | INTENSITY | | |
|---|---|---|---|
| | $H\delta$ | $H\gamma$ | $H\beta$ |
| 2.9–3.1 | 65 | 75 | 40 |
| 3.4–3.6 | 50 | 40 | 15 |
| 3.7–3.8 | 45 | 35 | 6 |
| 4.7 | 35 | 30 | 2 |

Lockyer[1] has collected the published data on this point. Of the 6 maxima fainter than the normal magnitude, 3.5, all have $H\delta$ stronger than $H\gamma$; but for the 6 maxima brighter than 3.5, $H\gamma$ is stronger than $H\delta$ on one occasion and equal to it at two other maxima. One of the latter two is the maximum of 1923 when the Mount Wilson observations indicate that $H\gamma$ was the brighter. Estimates show that for maxima of magnitude 3.5 or brighter, $H\delta$ averages 10 per cent stronger on the scale of Table XIX than $H\gamma$, while for maxima fainter than magnitude 3.5, $H\delta$ is 54 per cent brighter.

The spectral type at maximum varies in a marked degree with the magnitude, as is shown in Table XX.

During the last ten cycles of Mira's variation two extraordinary departures from the usual procedure have occurred. First, at the minimum of November, 1922, the star did not fall below magnitude 8.5, which is twice the normal brightness. Second, the maximum of February, 1924, was so feeble that the greatest brightness (mag. 4.7) did not exceed one-third its normal maximum. These remarkable occurrences seem to be due to causes extraneous to the forces which produce normal variations and the minor irregularities accompanying them.

---

[1] *Monthly Notices of the Royal Astronomical Society*, **84**, 563, 1924.

The spectrograms taken at these times are marked by several peculiar features. At the minimum of 1922 the usual conditions seemed to prevail, except that λ 4308 was abnormally weak until September 28, phase 162 days, magnitude 8.2. By November 5, phase 200 days, magnitude 8.5, a great change in the appearance of the spectrum had taken place. The whole series of bright hydrogen and low-temperature lines had disappeared, although only normal changes had taken place in the bands and in the few absorption lines which could be seen. Thirty days later, December 5, phase 229 days, magnitude 8.3, the star had begun to increase in brightness. The spectrum was strong in the region λ 4000–λ 4200 and great numbers of absorption lines were present which would not normally be seen in such strength until two months after minimum. Slow and gradual changes ensued while the star was reaching the maximum of February, 1923, which was the brightest (mag. 2.8) of the last 20 years. No unexpected features were noted after December 5. From a spectroscopic viewpoint the minimum of 1922 seems to have hurried through its changes with extraordinary rapidity. If the time allotted for the changes had been twice as great, the minimum would have passed as a normal one. The light-curve shows

TABLE XX

SPECTRAL TYPE AT DIFFERENT MAXIMA

| Mag. at Max. | Type | Mag. at Max. | Type |
|---|---|---|---|
| 2.9 | M5 | 3.6 | M6 |
| 3.1 | 6 | 3.7 | 7 |
| 3.4 | 5 | 3.8 | 7 |
| 3.5 | 6 | 4.7 | 7 |

the effect to a lesser degree; the minimum occurred 15 days, and the following maximum, 9 days in advance of the time predicted by mean elements; the preceding decline in brightness was nearly normal to the seventh magnitude; the minimum was flat, and the rise to maximum very steep.

The exceptionally low maximum of February, 1924, is especially interesting because of the appearance at that time of a new and unknown series of bright lines or bands and the presence of broad absorption bands in the region λ 4600–λ 4900, which have not hitherto been noted in any stellar spectrum. These peculiarities may be seen in Plate X where spectrogram C 2663 is reproduced alongside C 2171, taken March 28, 1923 (mag. 3.2), for comparison.

The most prominent bright band, after correction for the usual velocity of bright lines, has its center at λ 4844.7. Its width is about 7 A. Other strong bright regions less than 1 A in width are found at λλ 4535.5, 4649.15, 4672.76, 4695.40, and 4867.53. These have the appearance of rather wide bright lines, but must be related to the accompanying bands, for there seems to be an absorption band from 5 to 15 A in width to the violet of each of the bright regions. The absorption is not more than one-fourth the intensity of the titanium oxide band at λ 4803, and seems to fade toward the violet, opposite to the titanium bands.

In order to separate the peculiarities of the maximum of 1924 from a normal maximum, Koch microphotometer curves of plates C 2663 and C 2171 were compared. By subtracting the normal curve from the abnormal one, dark bands were disclosed in the regions

λλ 4584–4647 (6)
4658–4666 (1)
4686–4713 (1)
λλ 4722–4758 (2)
4760–4803 (6)
4815–4842 (2)

The relative intensity of absorption is given in parentheses. The two strongest bands are affected by titanium absorption, which, at the maximum of 1924, was somewhat greater than normal.

Regions of strengthened emission are indicated at:

λλ 4649–4661 (2)
4669–4695 (4)
4804–4816 (3)
4843–4905 (7)

The band structure may be tentatively identified with that of magnesium hydride, which has been positively recognized in the spectrum of sun-spots, but does not appear in the solar spectrum itself. A comparison of these wave-lengths with Fowler's laboratory spectrum[1] of magnesium hydride shows so many features in common that if there were any positive evidence of the presence of the strong absorption band in the green with its head at λ 5210, the identification would be quite certain. Spectrogram γ 12447 shows a portion of the green region faintly, but beyond λ 5167 the titanium band cuts down the continuous spectrum to a mere shadow. What little evidence this plate affords may be said to be favorable to the identification, but it is hardly conclusive.

These unusual features are found on all six plates from January 12 to March 11, 1924, and doubtless are intimately connected with the cause of the low maximum. It is unfortunate that no spectrograms were taken in the visual region at this maximum in order to show whether there were other absorption bands farther to the red. The weakness of the bright hydrogen lines at the 1922 maximum may be due, in part, to loss of hydrogen taken up by the molecules of the hydride.

The new titanium bands described in Section 4 are especially strong at this maximum.

## 11. ABSOLUTE MAGNITUDE, SURFACE BRIGHTNESS, MASS, AND DENSITY

Unfortunately, the distances of the Me stars are not well enough known to permit the calibration of the absolute-magnitude curves of spectral lines. Several of the lines which give acceptable values for the spectroscopic absolute magnitude of giant M stars may, however, be used to estimate the luminosity of *o* Ceti. Those found practicable are λλ 4077, 4215, 4258, and 4490. By using the curves for the ordinary M stars, the absolute magnitude of *o* Ceti at normal maximum is found to be −0.8. The computations of Merrill and Strömberg,[2] and also those of Wilson referred to in the same paper, indicate that the spectroscopic values thus found for Me variables

---

[1] *Philosophical Transactions of the Royal Society of London*, A, **209**, 478, 1909.

[2] *Mt. Wilson Contr.*, No. 267; *Astrophysical Journal*, **59**, 104, 1924.

# PLATE X

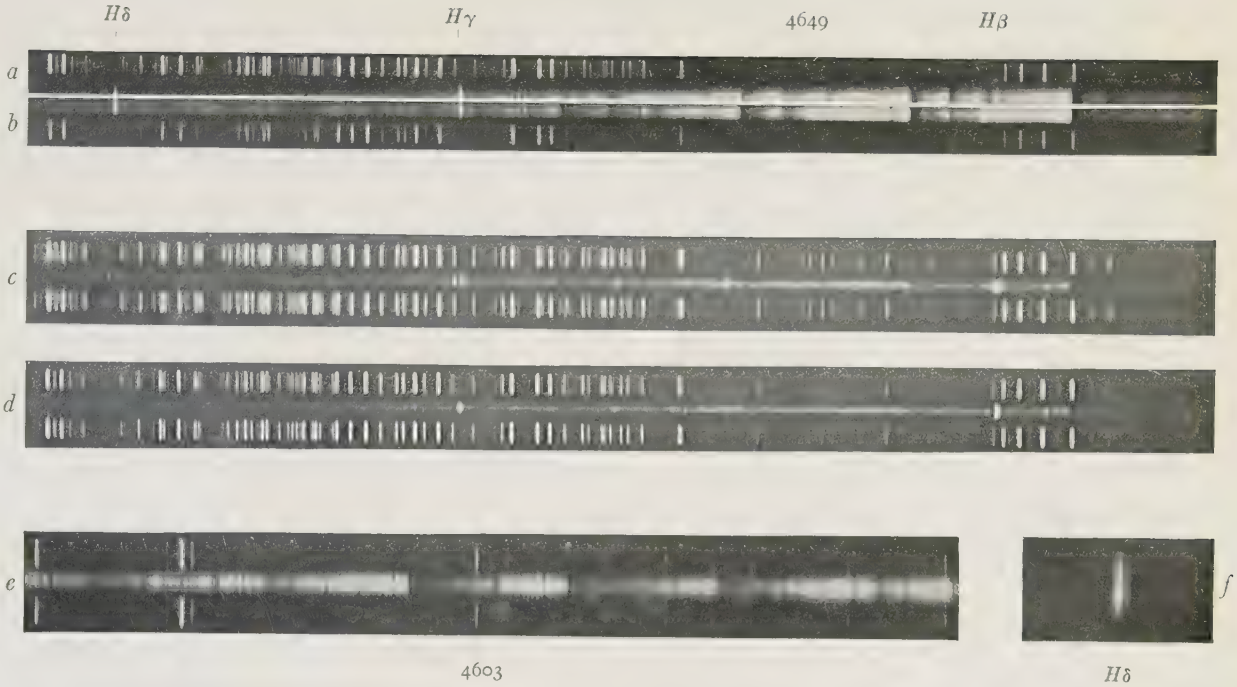

Spectrograms of Mira and Its Companion

(*a*) C 2171, March 28, 1923; magnitude 3.2. Normal maximum.
(*b*) C 2663, February 11, 1924; magnitude 4.7. Peculiar faint maximum.
(*c*) C 2482, October 19, 1923. Spectrum of the companion, with bands of Me star, showing hydrogen lines double.
(*d*) C 2989, September 7, 1924. Spectrum of the companion, with bands of Me star, showing violet component of hydrogen lines absent.
(*e*) γ 13185, January 8, 1925. Detailed structure of titanium bands near λ 4600, taken by Sanford with 3 prisms and 18-inch camera
(*f*) γ 13892, November 25, 1925. Triple structure of *H*δ near maximum, taken with 3 prisms and 40-inch camera.

are too bright by about one-half a magnitude. The corrected absolute magnitude of Mira at normal maximum would be $-0.3$. The corresponding parallax is $0\overset{''}{.}017$, which is in reasonable agreement with the best statistical determinations. With this we must be content for the present for, unfortunately, trigonometrical parallaxes of *o* Ceti cannot be used until they have been properly corrected for the effect of the companion in displacing the photographic images. It is probable, however, that in a few years the relative motion of the companion will be sufficient to permit the determination of a dynamical parallax.

The luminosity lines show sufficient change in intensity to indicate clearly that the spectroscopic absolute magnitude becomes considerably fainter as the visual brightness decreases. The lack of suitable reduction curves makes it impossible, however, to evaluate the corresponding absolute magnitude differences.

Using the parallax of $0\overset{''}{.}017$ found above and the angular diameter of $0\overset{''}{.}056$ measured by Pease[1] with the interferometer, we find the linear diameter to be 354 times that of the sun, or 490,000,000 km (310,000,000 mi.). At normal maximum (mag. 3.5) the average surface brightness per unit area is 7.5 magnitudes fainter than that of the sun.

The giant character of Mira leads us to believe that its mass is rather great, but there seems to be no direct method of determining it at present. The combined and individual masses may ultimately be found from its orbit and its orbital movement with respect to other stars.

The researches of Seares[2] indicate that the mass should be between 1 and 10 times that of the sun. If we take an intermediate value of $5\odot$, the corresponding density for the star is $1.1\times 10^{-7}$ as compared with the sun, or about one ten-thousandth that of our atmosphere. The surface gravity is very low, being $4\times 10^{-5}$ times that of the sun.

### 12. TEMPERATURE

An estimate of the effective temperature at normal maximum (mag. 3.5, type M6) may be obtained by extrapolation from Abbot's table.[1] He finds from radiometric measures of stellar spectra and comparison with black-body energy curves the values given in Table XXI. The normal maximum temperature of *o* Ceti must therefore be very nearly 2400° K. For the Me stars, many of which are of later type than Mira, Merrill,[2] from a comparative study of the behavior of stellar lines in the electric furnace, has estimated the temperature to be 2200° K.

---

[1] *Publications of the Astronomical Society of the Pacific*, **37**, 90, 1925.

[2] *Mt. Wilson Contr.*, No. 226; *Astrophysical Journal*, **55**, 202, 1922.

TABLE XXI

Abbot's Stellar Temperatures

| Star | Type | Temperature |
|---|---|---|
| α Tauri | K5 | 3000° K |
| β Pegasi | M2 | 2850 |
| α Orionis | M2 | 2600 |
| α Herculis | M5 | 2500 |

King[3] has shown that when sufficient oxygen is present the titanium oxide bands appear strongly in the electric furnace from 1900° to 2600°.

Nicholson and Pettit,[4] from thermocouple measures of total radiation, with and without a water cell, find temperatures of 2300° and 1800° K for average maximum and minimum, respectively, during the last four cycles. For the same period they observed an average total energy change from maximum to minimum of 1.1 magnitudes.

If we assume that the change in visual brightness varies as the radiation at λ 5750, which is the maximum of the visibility curve for these stars, we have from Planck's law of energy distribution,

$$\frac{B_1}{B_2}=\frac{e^{\frac{C_2}{\lambda T_2}}-1}{e^{\frac{C_2}{\lambda T_1}}-1}$$

---

[1] *Mt. Wilson Contr.*, No 280; *Astrophysical Journal*, **60**, 105, 1924.

[2] *Mt. Wilson Contr.*, No. 265; *Astrophysical Journal*, **58**, 200, 1923.

[3] *Mt. Wilson Contr.*, No. 114; *Astrophysical Journal*, **43**, 341, 1916; *Publications of the Astronomical Society of the Pacific*, **36**, 140, 1924.

[4] Unpublished.

where $B_1$ and $B_2$ are the visual luminosities at maximum and minimum, respectively, and $T_1$ and $T_2$ the corresponding temperatures. Taking $C_2 = 14300$, $T_1 = 2300°$ K, and $T_2 = 1800°$ K,

$$\frac{B_1}{B_2} = 3.3 \text{ mag.}$$

By the fourth-power law these temperatures indicate a difference in energy of 1.1 magnitudes.

Thus, according to black-body laws, a change in total energy of 1.1 magnitudes at these temperatures corresponds to a visual range of 3.3 magnitudes. The average visual variation of Mira for the same period is 5.3 magnitudes. The difference between the observed visual range and the amount calculated from the radiometric measures is 2.0 magnitudes. This difference can be attributed to the excessive absorption of the titanium oxide bands at minimum.

Suitable plates for photometric testing of the energy in different spectral regions at maximum and minimum are not available, but an idea of the absorption produced by the titanium bands may be gained from a comparison of Mira at maximum, when the type is M6, with a K5 giant star, in which the bands are not noticeably present.

For this test, spectrograms of Mira and Boss 646 were made with the 100-inch telescope on December 6, 1925, when the stars were at the same zenith distance. The regular Cassegrain spectrograph was employed, but to avoid troubles from atmospheric dispersion the slit was opened to one-half a millimeter. Ilford Panchromatic plates were used and developed together with dilute Rodinal. A strip at the edge of each plate was exposed to a Mazda lamp through a graduated photographic wedge whose energy transmission was calibrated by Mr. Pettit. Koch microphotometer curves of the spectra and the graduated strip were made. Areas under the curve were measured and reduced to relative energy by the wedge constants. In this way it is possible to compare the relative energy in the two stars for any part of the spectrum between λλ 4100 and 6800.

A rough estimate of the absorption of the titanium bands can now be made by comparing the energy distribution in *o* Ceti at maximum with that of Boss 646. If we equalize the energy of the two stars for the limited region λλ 4100–4300, where the bands do not show, by applying the proper factor to the measured energy of one of the stars, then the remaining portions of the two spectra, comprising practically the whole visual region, will show unequal energies arising from the difference in temperature and from titanium absorption. A comparison of black-body energy-curves for temperatures of 3000° and 2500° K shows that the visual region of the cooler star ought to give 2.0 times as much energy as that of the hotter star when the regions from λλ 4100–4300 are brought to equality. Measures of the microphotometer curves show, on the contrary, that, when the violet regions are equalized, *o* Ceti shows less energy in the visual region (λλ 4300–6700) than Boss 646 by a factor of 3.0. It is evident that the titanium oxide absorption is represented by a factor of 6.0, or 1.9 magnitudes. Inspection of plates taken at minimum indicates that the increase in strength of the bands at minimum is of the same order, and that the discrepancy of 2.0 magnitudes between visual and radiometric measures may be fully accounted for in this way. The greatest outstanding uncertainty is due to our lack of knowledge of the extension of the titanium bands into

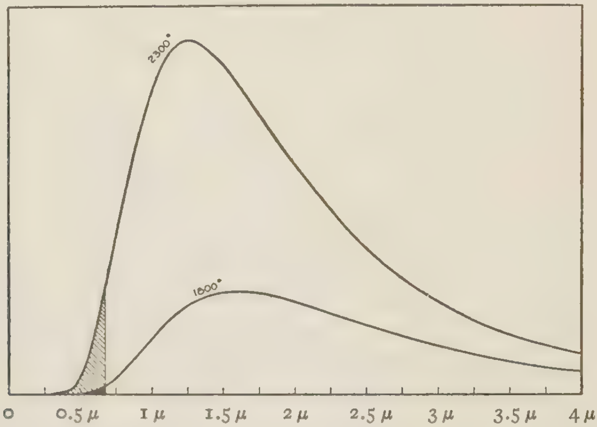

FIG. 8.—Black-body curves for 1800° and 2300° K, showing a difference in total radiation of 1.1 magnitudes. The shaded portions represent the region λλ 3000–6700 and indicate the much larger difference in the visible radiation, which at these temperatures is only a small fraction of the total radiation.

the infra-red. A study of the actual amount of titanium absorption at different phases would be a valuable contribution to the problem of the star's variation.

The overlapping of bands is so general at low temperatures that nearly all of the continuous spectrum in these regions is reduced more or less in intensity. The more refrangible rays on the violet side of λ 4200 are not absorbed and, as Stebbins[1] has pointed out, are thus relatively stronger at minimum.

Figure 8 shows the calculated energy-curves at maximum and minimum, for temperatures 2300° and 1800° K, and a difference in total radiation of 1.1 magnitudes. It is instructive to note the small percentage of energy falling within the visual region and the large effect of temperature change upon the amount of visible light.

The question of the applicability of black-body laws to a star of this character is still open. There may be complications connected with the nature of its variability and its bright lines, but it seems very probable that when the effects of bands and atmospheric absorption are taken into account, the radiation given out will closely follow the normal energy-curve.

## 13. THE DISCOVERY OF THE VISUAL COMPANION

Although the emission line of $H\beta$ belonging to the companion appears on spectrograms of *o* Ceti taken in 1918, it was not until the minimum of January, 1920, that it was possible to obtain spectra at minimum and to appreciate the extraordinary character of the hydrogen lines and the peculiar effect of the superposition of the continuous spectrum of the companion on the banded spectrum of the variable star. During the next two years minima occurred during the winter months and little progress was made in solving the problem. Although Professor Barnard failed to resolve the star under bad conditions of seeing, the impression of duplicity gained in strength. The position angle and distance of the source of the peculiar spectrum were roughly estimated from spectrograms taken with the slit in different position angles to be 135° and $0''.3$ respectively.[2]

---

[1] *Lick Observatory Bulletins*, **2**, 90, 1903.

[2] *Publications of the American Astronomical Society*, twenty-ninth meeting, p. 15, 1922; *Popular Astronomy*, **31**, 237, 1923.

In 1923 the star seemed to be elongated on the slit of the spectrograph. At our suggestion, Dr. Robert G. Aitken examined the star with the 36-inch refractor of the Lick Observatory on October 19 and found it to be an easy double; position angle, 130°3; distance, 0″90; magnitude of the companion, about 9.8.[1] At the minimum of 1924 there was "little or no evidence of change."[2]

The companion was noticeably fainter in 1925. On the spectrograms taken in July the continuous spectrum of the companion was relatively weak as compared with the two preceding years. On August 25, during a visit to Mount Hamilton, Drs. Aitken and Moore showed the writer the star with the 36-inch refractor. The companion was at least 1½ magnitudes fainter than the primary and was not easily seen under the rather poor conditions of seeing then prevailing. They pointed out that, under similar conditions, it would have been easy to observe at the two preceding minima. The September spectrograms show no trace of the continuous spectrum of the companion and only faint indications of the bright hydrogen lines. Unquestionably, the companion is also a variable star of long or irregular period. It was, doubtless, too faint to have been seen by Aitken in 1903 and Doolittle in 1905.

The maximum brightness seems to have been reached in 1922 or 1923 and to have fallen off rapidly in 1925. A number of the stars of its spectral type with bright lines have been found to be irregular variables.

### 14. THE SPECTRUM OF THE COMPANION

During minima of *o* Ceti it has been possible to secure spectrograms of the companion with very little interference from the brighter star. The outstanding features of the spectrum are: the hydrogen lines, made up of very strong emission components with absorption centers; the strong continuous spectrum whose intensity distribution resembles that of the late B-type stars; the bright bands of helium and ionized calcium; and the fairly sharp but weak bright lines of ionized iron.

No absorption lines are seen except those accompanying the hydrogen series. The spectral type is probably about B8. This determination is based on the continuous spectrum, on the fact that bright helium is present, and on analogy with similar stars in which helium absorption lines make their classification possible.

---

[1] *Publications of the Astronomical Society of the Pacific*, **35**, 323, 1923.

[2] *Ibid.*, **36**, 296, 1924.

H.D. 50138 has similar hydrogen lines, while H.D. 161114[1] has bright lines of ionized iron. The bright bands of helium and of H and K of calcium seem to be unique. They are 4 or 5 A in width and usually are not suitable for accurate measurement. They have approximately the same displacement as the sharp bright lines of iron. The helium lines, λλ 4026, 4388, 4471, 4713, $D_3$, and probably 4922 and 5016, are present.

The hydrogen series has been observed from $H\alpha$ to $H\epsilon$. The lines fall off in intensity toward the violet, as is usually the case with bright-line stars other than the Me variables. $H\alpha$ has been seen on three photographs, but its exact character and strength cannot be determined on account of overexposure in that region. $H\epsilon$ is faintly seen on a few plates. The other lines, $H\beta$, $H\gamma$, and $H\delta$, are much alike in structure and, on account of their great intensity, are easily observed with moderate exposures. $H\gamma$ is much stronger with respect to its continuous spectrum than $H\gamma$ of the Me star at its maximum intensity. $H\beta$ is about three times the intensity of $H\gamma$, and $H\delta$ is correspondingly weaker.

The hydrogen lines are made up of three parts: a strong emission component about 4 A in width, displaced about 2 A to the red from its normal position after allowing for the velocity of the star; a strong absorption line 2 A in width, displaced to the violet about 1 A; and a violet emission component of variable strength lying 3 A to the violet of the normal position of the hydrogen lines.

The hydrogen lines, at times, resemble those of P Cygni. The violet components of $H\beta$, $H\gamma$, and $H\delta$ are nearly equal in intensity, showing only a slight strengthening from violet toward the red. As a result the violet component is stronger with respect to the red in $H\delta$ than at $H\beta$. At some minima the violet component is very faint, while in 1923 it was comparable with the red component. The relative maximum strength of the violet component of $H\beta$ at the successive minima from February, 1920, to August, 1925, was 1, 5, 5, 5, 10, 2, 2. Further, the violet component is proportionately brighter near the minimum phase of the Me star. Its maximum strength is found in every case on plates taken between the phases 205 and 230 days. The intensity increases up to the time of minimum and decreases

---

[1] Merrill, *ibid.*, p. 225, 1924.

TABLE XXII

INTENSITIES OF THE VIOLET COMPONENT OF $H\beta$

| Phase | Intensity | Phase | Intensity |
|---|---|---|---|
| days | | days | |
| 167 | 1 | 201 | 4 |
| 182 | 2 | 204 | 5 |
| 197 | 2 | 230 | 2 |
| 198 | 2 | 256 | 0 |

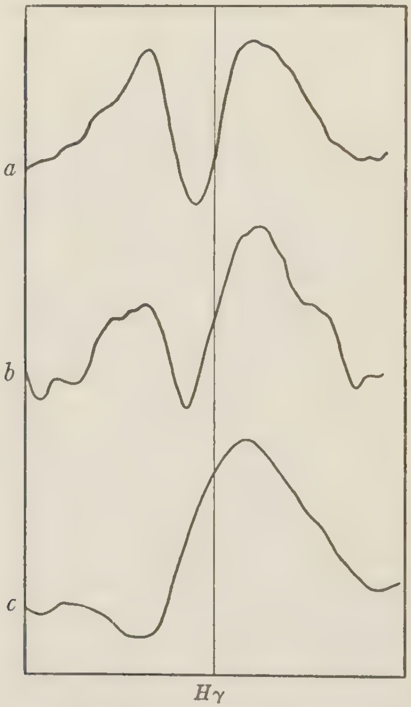

FIG. 9.—Curves drawn from thermocouple deflections showing photographic intensities of $H\gamma$ in the spectrum of the companion of Mira. (*a*) C 2482, October 19, 1923; phase 218 days. (*b*) C 1494, December 14, 1921; phase 204 days. (*c*) C 1547, February 5, 1922; phase 257 days. The vertical line represents the normal position of $H\gamma$. Scale, 3 mm = 1 A.

thereafter. For example, in 1921 the estimated intensities were as given in Table XXII.

The intensity thus appears to vary with the brightness of the companion and inversely with that of Mira.

There is no certain indication of variation in the position or intensity of the red emission component. Figure 9 illustrates the $H\gamma$ line at three different phases. The curves are formed from thermocouple deflections taken with a narrow slit at intervals in the region of $H\gamma$ and give accurate relative intensities of the photographic blackening in that region of the spectrum. The vertical line indicates the position of $H\gamma$ displaced toward the red to allow for the velocity of the star as determined from the bright lines.

TABLE XXIII

EMISSION LINES OF COMPANION

| λ (Rowland) | λ (I.A.) | λ (Rowland) | λ (I.A.) |
|---|---|---|---|
| 4233.33...... | .16 | 4520.40.... | .24 |
| 4302.35...... | .18 | 4522.80.... | .64 |
| 4303.34...... | .18 | 4534.34.... | .17 |
| 4351.93...... | .77 | 4549.64.... | .48 |
| 4416.98...... | .81 | 4556.06.... | .90 |
| 4489.35...... | .21 | 4584.02.... | .84 |
| 4491.57...... | .41 | 4924.11.... | .92 |
| 4508.45...... | .29 | 5018.63.... | .44 |

It will be noted that the absorption line is so strong that, in each case, the curve falls well below the level of the neighboring continuous spectrum. The absorption seems to fall farther to the violet as the violet component becomes weaker, but this effect may be apparent rather than real.

The whole band extends about equal distances on either side of the normal position of $H\gamma$, but the absorption line is situated well to the violet of the center.

Emission lines of ionized iron, as given in Table XXIII, have been identified. Many of these lines are very faint on our spectrograms. As they are also of poor quality for measurement, the results show a wide range and should be given small weight. Table XXIV shows the velocities resulting from the identification given above.

The mean velocity of +51.0 km/sec. is nearly that of both dark and emission lines of the Me star at minimum. During the three years covered by these observations there was probably no change in velocity.

The bright lines comprise most of the stronger lines of ionized iron in the blue region of the spectrum. Lines belonging to other elements, if present, are too faint to be seen.

If the maximum apparent magnitude of the companion star is 9.8 and the absolute magnitude of the principal star is −0.3 at normal maximum (mag. 3.5), the absolute magnitude of the companion is +6.0. It must be considered as an early-type dwarf star, and is the only one thus far found to have a bright-line spectrum.

TABLE XXIV

Velocity of Companion from Bright Lines

| Plate | No. Lines | $V$ |
|---|---|---|
| | | km/sec. |
| C 2482........ | 3 | +53.3 |
| 2930........ | 8 | 52.3 |
| 2989........ | 13 | 52.0 |
| 3037........ | 5 | 47.8 |
| 3406........ | 8 | 53.9 |
| 3410........ | 3 | 45.6 |
| Weighted mean...... | | +51.0 |

## 15. DISCUSSION

It is not the purpose of this paper to attempt a theory of the variation of the stars of the Mira type. The problem of the underlying cause of the periodic physical convulsion which produces the variation of these stars is one which will ultimately yield to theoretical attack when sufficient observational material is at hand. It may be well to consider briefly the bearing of recent study on the question.

If the velocity-curve shown by the absorption lines can be interpreted as a spherical pulsation of the star, it would mean a considerable change in the size of the disk and a corresponding variation in the total luminosity. The largest size would be during the star's increasing light and the smallest on the decreasing branch. At maximum and minimum it would have intermediate dimensions. The semi-variation of radius given by the elements of the orbit of the dark lines is 26,200,000 km, which is a pulsation of about 11 per cent about a mean position. Since the velocities are integrated over the whole disk of the star, the actual changes would be about one-third greater.[1] This amount is comparable with the relative change found for Cepheids and is a much smaller percentage variation than that found in $\alpha$ Orionis by interferometer measures of diameter. It appears doubtful, indeed, whether the full change, which would produce a variation in brightness of one-half a magnitude or more due to variation in the size of the disk, actually occurs. Such a distortion of the light-curve should be detected in the visual curve and will certainly be noticed, if present, in the bolometric curve. In case the spherical pulsation is disproved, alternative explanations may be sought in non-spherical pulsations or atmospheric currents such as have recently been considered in the case of the sun.

It is not possible to admit of a two-body system in explanation of the radial velocity changes, since, even with the most favorable inclination and masses, the orbit of the secondary star would be well within the limit of the known dimensions of the primary.

The emission lines themselves play little or no part in the light variation, for the total light given out by bright lines is less than 1 per cent of the total visual light. They are, however, of the greatest interest from a physical standpoint. A thorough knowledge of their origin and behavior might open up the whole problem and would shed much light on the question of stellar atmospheres under conditions of extremely low density and gravity.

The emission lines of hydrogen and the low-temperature lines of iron and magnesium give the same velocities, irrespective of the time of their first appearance. Thus, they seem to originate in a moving stratum or shell, rather than in explosions or prominences shot out at intervals from the atmosphere. Even the emission lines of silicon and ionized iron, which are produced under conditions of greater excitation, seem to share the same velocity changes in a less degree.

Except at the time of minimum light, the movements of this shell, as recorded by the emission lines, are always outward with respect to the reversing layer where the absorption lines are produced. The hydrogen lines appear with the rise in temperature and show increasing intensity until well after maximum. The low-temperature lines appear after maximum when the temperature has fallen sufficiently, but do not find favorable conditions for excitation during the time of rising temperature. When the temperature has dropped to minimum all bright lines disappear for a time.

---

[1] Shapley and Nicholson, *Proceedings of the National Academy of Sciences*, **5**, 422, 1919.

The location of the emitting layer relative to the absorbing layer cannot be determined conclusively. Emission is usually to be expected at the higher levels, but the behavior of $H\epsilon$ and several of the ultra-violet hydrogen lines suggests an overlying layer or diffuse cloud of absorbing calcium and iron. Possibly the peculiar distribution of intensities found among the hydrogen lines having wave-lengths longer than $H\epsilon$ may also be accounted for by absorbing hydrogen.

It should be kept in mind that we see the integrated light from the whole disk of the star and that lines which are bright at the center may or may not be bright at the limb; and, further, that variation of the darkening at the limb would tend to mask luminosity changes.

Recognition of the temperatures involved at maximum and minimum connects the problem of the star's variation more closely with that of other types of physical variation of stars. For, taking into account the fact that a large loss of light in the visual region results from a small change in bolometric magnitude at these temperatures and allowing for the increasing absorption of the titanium oxide bands, we find that variation in energy arising from internal causes is of the order of one magnitude. This leads to the conclusion that the physical changes may be traced to sources similar to those prevailing in the hotter variable stars and that the whole group of physical variables may be found to form a sequence from the shortest to the longest periods.

Temperature estimates have been derived from studies of the spectra and, more recently, have been amply confirmed by radiometric observations. The agreement of these results indicates that the temperatures are known within about 5 per cent.

The important part played by the titanium bands is evident upon inspection of spectrograms taken at different phases of the star's variation. General absorption may also be present, but it seems clear that its effect must be small as compared with the titanium absorption.

The companion is a most unusual star. It will be interesting to observe its future variation in brightness, as well as its motion, and to confirm the influence of the principal star on its emission lines.

It is a pleasure to acknowledge the assistance rendered by many members of the Observatory staff during the progress of this study. All the members of the spectroscopic department have taken part in the observations, measurements, or computations. Mr. Ellerman has reproduced photographs for study and prepared the illustrations. Miss Ware has made the microphotometer curves. Messrs. Nicholson and Pettit have assisted very greatly in the sections concerning temperature and energy distribution. Mr. King has supplied laboratory plates which have helped in the solution of several puzzling questions. Mr. Merrill has given advice on many occasions. Mr. Adams has shared in much of the work, especially in the earlier part of the investigation covered by our joint papers, and has continued his interest throughout.

Mount Wilson Observatory
March 1926

Contributions from the Mount Wilson Observatory, No. 312
Reprinted from the *Astrophysical Journal*, Vol. LXIV, pp. 93–121, 1926
Printed in the U S.A.

# SOLAR HYDRODYNAMICS

By V. BJERKNES[1]

## ABSTRACT

*Hydrodynamical discussion of internal solar motions, especially vortex motions for explaining sun-spots.*—It is shown that the *low temperatures* of sun-spots may be explained if the vortices connected with them decrease in intensity from the surface downward. The excess of centrifugal force in the upper part of the vortex then gives rise to a centrifugal pumping effect, by means of which the gases in the central region are lifted from below and adiabatically cooled.

A simple view of the numerous collective *properties of sun-spots* is obtained if we make the following suppositions: Sun-spot phenomena originate in two sub-photospheric zonal vortices, one for each cycle, which have opposite rotations. These vortices occasionally rise to the surface and penetrate the sun's atmosphere, and then return again below the photosphere. Wherever a sinuous vortex rises and cuts the photosphere a sun-spot of the corresponding cycle makes its appearance or may be discovered. The direction of rotation is supposed to determine the sign of the magnetic field. In virtue of the internal circulation of the sun, which may also explain the phenomenon of the equatorial acceleration, the two vortices revolve round each other, the period of revolution being the complete sun-spot period of 22 years.

Hale's discovery of magnetic fields in the sun-spots, of the regular succession of the polarities in binary groups, and of the reversal of these polarities from cycle to cycle has created an entirely new situation as regards the theory of sun-spots and of solar phenomena in general.

No attempt has yet been made, as far as I know, to give a connected interpretation of these phenomena. Any interpretation, however improbable, may therefore have a certain relative value. But in taking up the subject I must emphasize the fact that I enter a field entirely new to me. All my knowledge of solar phenomena has resulted from the recent opportunity for discussion with the astronomers of the Mount Wilson Observatory, to whom I here express my appreciative thanks for their interest and assistance.

## I. RESULTS AND PRINCIPLES OF PHYSICAL HYDRODYNAMICS

We shall begin by summarizing certain general principles and results which will be used later, and then add a number of supplementary developments.[2]

---

[1] Research Associate of the Carnegie Institution of Washington.

[2] Cf. the lectures given at the California Institute of Technology, Pasadena, September to December, 1924, which will be published later. The concluding lecture gave the sun-spot theory which is the subject of this paper.

1. *Dynamics of circulation.*—The internal dynamics of a perfect fluid depends upon two fields, that of *pressure* and that of *mass.* In the field of pressure the *pressure gradient* points in the direction of decreasing pressure and represents the force per unit volume originating from pressure. In the field of mass the *inertia gradient* points in the direction of decreasing inertia, i.e., of decreasing density or increasing specific volume. If the two vectors do not coincide, the inertia will be asymmetrically distributed relative to the force due to pressure. This will give rise to rotation about an axis normal to the two vectors, tending to bring the densest masses in the rear. The rotation will thus be directed from the inertia gradient toward the pressure gradient.

To give the law quantitative form we may represent the field of pressure by isobaric surfaces drawn for unit differences of pressure, and the field of mass by surfaces of equal specific volume (isosteric surfaces) drawn for unit differences of this quantity. These surfaces divide space into a set of unit tubes, characterizing the asymmetry which the field of mass presents relative to the field of pressure. The positive direction of rotation around these tubes is by definition that mentioned, i.e., from the inertia gradient to the pressure gradient. Defining with Lord Kelvin the circulation along a closed curve as the line integral of the tangential component of velocity,

$$C=\int v_t ds \ , \tag{1}$$

and calling $N$ the number of unit tubes comprised by the curve, we have

$$\frac{dC}{dt}=N \ , \tag{2}$$

i.e., *any closed fluid curve has at any time a rate of increase of circulation in the positive direction round the unit tubes which is numerically equal to the number of these tubes included within the curve.*[1]

Classical hydrodynamics restricts its considerations to "barotropic" conditions, according to which the field of pressure entirely governs the field of mass. The inertia gradient then coincides with the pressure gradient, no unit tubes exist, $N=0$, and (2) reduces to

---

[1] Cf. V. Bjerknes, "Ueber die Bildung von Cirkulationsbewegungen und Wirbeln in reibungslosen Flüssigkeiten," *Videnskabsselskabets Skrifter*, Christiania, 1898.

$$C=\text{const.} \tag{3}$$

Thus, the circulation of any closed fluid is invariable. This is the Helmholtz-Kelvin principle of the conservation of circulations and vortices. All circulations in fluid or gaseous masses, such as those surrounding or constituting the celestial bodies, must be according to law (2), and may be calculated from it if we can determine the isosteric surfaces, or the equivalent isothermal surfaces, *as something different from the isobaric surfaces.* When, vice versa, variations of circulation are known, we may derive the corresponding numbers of unit tubes, and thus derive relative distributions of mass and pressure. Only one example, which is instinctively understood, will be given here:

Let a horizontal curved current be given, which for simplicity is assumed to be steady or approximately steady. If the current has an upward-increasing intensity, the upper masses will have an excess of centrifugal force. This produces a centrifugal pumping effect, which lifts heavy masses (adiabatically cooled gas) on the inner concave side of the current. If, vice versa, the current has an upward-decreasing intensity, the lower masses will have an excess of centrifugal force. This causes a centrifugal sucking effect, which brings light masses (adiabatically heated gas) down on the inner concave side of the current. A vortex with an upward-increasing velocity will, therefore, have a core of heavy masses or cold gas; a vortex with upward-decreasing velocity, a core of light masses or of hot gas.[1]

The theorem of circulation (2) gives completely the dynamics of these pumping and sucking effects, and leads to a convenient formula characterizing the equilibrium conditions ultimately reached. In deriving such a formula, we may use the gas equation, and thus introduce the absolute temperature $\vartheta$ instead of the specific volume. Let $dv$ be the increase in velocity for an increase in height $dz$, $g$ the acceleration of gravity, $d\vartheta$ the increase in temperature for an increase in length *ds* measured along a curve *s* which is contained in the isobaric surface, runs normal to the lines of flow, and is counted positive outward, i.e., from the concave to the convex side of the current. Finally, on account of the curvature of the current, the moving particles have a certain angular velocity Ω around an axis which forms the angle $\phi$ with the isobaric surface. Then Ω represents the component of angular velocity round the normal to the isobaric surface. We then have the formula

---

[1] Cf. V. Bjerknes, "On the Dynamics of the Circular Vortex with Applications to Atmospheric Vortex and Wave Motion," *Geofysiske Publikationer*, Christiania, 1921.

$$\frac{1}{\vartheta}\frac{d\vartheta}{ds}=\frac{2\Omega\sin\phi}{g}\frac{dv}{dz} \tag{4}$$

which may be used as long as the vertical accelerations are zero or moderate and the state of motion steady or nearly steady.

The principle of pumping or sucking effects of curved currents takes a slightly different form when, from absolute motion, we pass to the motion relative to a rotating body like the earth or the sun. A current which is straight, relative to the rotating rigid body, will be curved from the viewpoint of absolute motion. Instead of referring to the concave and convex side of the curved current, we refer to the left and right side of the apparently straight current, and find the following rule:

*In the northern hemisphere of the earth or the sun a current will carry cold masses on its left side, if it has an upward-increasing intensity, and on its right side, if it has upward-decreasing intensity.*[1]

As an example, we may mention that the general atmospheric motion of the northern hemisphere of the earth is an eastward drift with upward-increasing intensity, which carries the cold polar air masses on its left side. Formula (4) applies directly to these relative motions when $\phi$ is the latitude and Ω the angular velocity of the earth or the sun.

A more complex formula can be derived to cover the case of a current which appears curved in its relative motion. But the simple formula (4) will be sufficient, if in each case we interpret Ω as the greater of the two angular velocities: that of the vortex, and that of the solid rotating body, the sun or earth.

---

[1] Cf. T. W. Sandström, "Ueber die Beziehung zwischen Temperatur und Luftbewegung in der Atmosphäre unter stationären Verhältnissen," *Öfversigt af K. Vetenskaps-akademiens Förhandlinger*, Stockholm, 1901; *Meteorologische Zeitschrift*, **19**, 161, 1902.

2. *Thermodynamics of circulation.*—To illustrate, from a thermodynamical viewpoint, the conditions for producing circulation, consider a closed tube, for simplicity, of uniform section, filled with fluid or gas in adiabatic, i.e., indifferent, equilibrium. The slightest heating of a single element $E$ will disturb barotropic conditions, and the whole fluid mass will come into a circulating motion which will not stop until this element has reached the highest point of the tube.

To maintain circulation systematically against a resisting force such as friction, we can, in one branch of the tube, at a certain height, place a source of heat (Fig. 1, $A$) which the fluid cannot pass without assuming a definite increase of temperature and, at a certain other height in the other branch, a source of cold which the heated fluid cannot pass without a corresponding drop in temperature. The entire fluid mass will then be kept in circulation by a force which is equal to the difference in weight between two fluid columns of different temperatures but of the same height, the height being equal to the difference in elevation of the two sources. The circulation considered is upward through the branch containing the source of the heat, and down the branch containing the source of the cold. The tube becomes filled with heated fluid above the two sources, and with cooled fluid below.

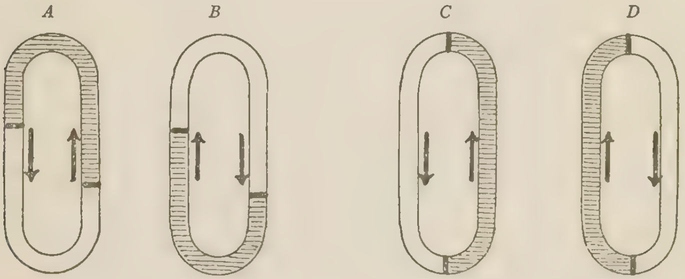

FIG. 1

It is an important peculiarity of the engine that it may run in the opposite direction. For this it suffices that, by an impulse, we produce a certain initial retrograde circulation (Fig. 1, $B$). The fluid passing down through the source of heat will then be heated, while that moving up through the source of cold will be cooled. The two columns of different temperatures have thus interchanged places, and during the motion the part of the tube below the two sources will contain warm fluid, and that above them, cold fluid. The efficiency of the engine is exactly the same for direct and for inverse motion. The engine is self-starting for direct motion, while an initial impulse is required to start the retrograde circulation.

The efficiency is greatest when the source of heat is at the lowest point and the source of cold at the highest point of the tube (Fig. 1, *C* and *D*). In this case the difference between direct and retrograde motion disappears. The engine then ceases to be self-starting, but an infinitely small impulse will start it in either direction; and, when started, it then works with higher efficiency than for any other arrangement of the sources.

When the source of cold is at a lower level than the source of heat, the efficiency is negative, i.e., the engine will transfer more heat to the source of cold than it receives from the source of heat. Instead of transforming heat into kinetic energy, it will transform kinetic energy into heat as long as there exists a circulating motion from which kinetic energy can be derived.

3. *Stratified circulation.*—In the preceding example the fluid is supposed, initially, to be in barotropic equilibrium. Whatever the form of the vessel, the slightest heating of a single element then brings the whole mass of fluid into circulation, which continues until the heated element has reached the highest position possible. Similarly, a cooled element cannot stop before it reaches the bottom.

It is quite different if the fluid is intrinsically heterogeneous, with heavier masses below and lighter masses above, corresponding to stable internal equilibrium. A heated element will then ascend only to the level of fluid having its own density. In common experiments with small fluid masses a heated element, as a rule, soon reaches the surface and the heterogeneities are rapidly smoothed out. But when the volume is large in comparison with the differences of temperature, we meet with the very characteristic phenomenon of *stratified circulation*. Very instructive is the following experiment due to Alf Sinding-Larsen.[1]

---

[1] *Annalen der Physik*, **9**, 1190, 1902.

A test tube containing a heterogeneous salt solution is put in a glass of hot water. The salt solution then divides into a series of superimposed strata, each having its independent circulation (Fig. 2, *A*). If after heating, the tube is put in cold water, the opposite circulation occurs within the strata (Fig. 2, *B*). Circulations produced in this way are symmetrical with respect to the axis of the tube. Circulations across the tube may be obtained by heating it on one side and cooling it on the other. In these experiments the circulation evidently tends to produce homogeneity within each stratum, with the result that the heterogeneities are concentrated in narrow transitional layers separating the homogeneous strata. If the physical and chemical conditions of the fluid permit the formation of a single homogeneous stratum, such a stratum will be the ultimate result, the existence of several strata being merely a transitional state; but if the strata pre-exist through physical or chemical reasons as with oil and water for instance, they will resist this tendency to form a single homogeneous mass.[1]

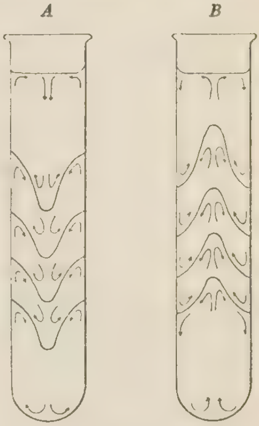

FIG. 2

In the preceding experiment heating produced and friction counteracted the circulation. But under favorable circumstances friction may also produce stratified circulation. Experiments and observations on the phenomenon have been made especially by J. W. Sandström.[1]

---

[1] It does not seem necessary to assume with Sinding-Larsen that in his experiments the strata are pre-existent because of difference in molecular structure, and merely become visible in consequence of circulation. The limited ascending power of the heated masses in the heterogeneous fluid system seems sufficient to explain the formation of the strata and to be in full accordance with his results: namely, that the strata are the more striking the greater the difference between the specific weights of the solvent and the concentrated solution; that the number of strata seems to depend partly upon the differences of concentration in the solution; that the depth of the strata increases in general with decreasing concentration; that the bounding surfaces of the strata move upward, in general, as a consequence of the steadily increasing depth of the individual strata, from which it follows that the number of strata decreases.

My attention has only recently been directed to a paper by Mendenhall and Mason, "The Stratified Subsidence of Fine Particles," *Proceedings of the National Academy of Sciences*, **9**, 199, 1923, in which stratified circulations of thermal origin are examined.

Consider a series of superimposed strata, each stratum for simplicity being a homogeneous salt solution, with a sudden increase in salinity as we pass from one stratum to that next underlying (Fig. 3). A wind on the free surface of the top stratum will set this stratum in circulation. By friction the next underlying stratum then comes into opposite circulation. This in turn acts upon the next lower stratum, and so on, with the result that all strata circulate like toothed wheels, but with decreasing intensity as we proceed from stratum to stratum downward. Sandström also describes phenomena of this type produced by the wind on stratified sea water along a beach.

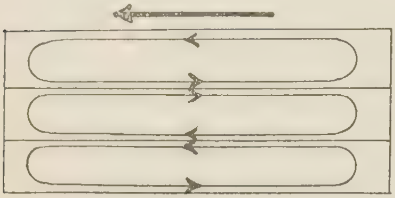

FIG. 3

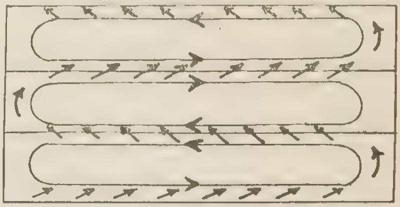

FIG. 4

We have supposed the homogeneous superimposed strata to be pre-existent. But if the solution has initially a continuously varying concentration, the wind will evidently tend to produce an upper homogeneous circulating layer, which will then tend to produce a second homogeneous layer immediately below, and so on. It would be interesting to examine experimentally how far this process can proceed.

In the experiments of Sinding-Larsen, friction counteracts the circulation produced by heating. But evidently conditions may arise such that heat and friction co-operate in producing and maintaining stratified circulation. Figure 4 illustrates a possible motion where this is the case. The fluid mass is supposed to be heated from below and cooled at its free surface. Initially conditions are unstable, as in the tubes of Figure 1, *C* or *D*. But an initial impulse may be used to determine the direction of circulation in the lowest layer. Friction will then give an opposite circulation to the next higher layer, and so on. But friction will not be the only cause maintaining the circulation of the higher layers. Each of them will be heated from below, and take part in the convection transport of heat. The small arrows in Figure 4 indicate the flow of heat.

---

[1] "Windströme im Gullmarfjord," *Svenske Hydrografiske-biologiske Kommissionens Skrifter*, II, Göteborg, 1905.

It would also be interesting to test experimentally the conditions for realization and stability of this kind of stratified circulation, both when the strata pre-exist and when formed as a result of the circulation. The initial impulse determining the direction of the circulation could be avoided by slightly inclining the heated bottom, and an inclined rigid surface which is cooled could be substituted for the upper horizontal free surface.

## II. EMPIRICAL DATA CONCERNING THE SUN

4. The sun rotates on its axis in about twenty-five days. The rotation is not that of a rigid body, the angular velocity being considerably greater at the equator than in higher latitudes. The highest layers in the sun's atmosphere seem to follow closely the motion at the equator. Thus, in passing from the photosphere upward in the atmosphere of the sun, we approach, in all extra-tropical latitudes, layers of increasing velocity.

5. Sun-spots seem to be depressions in the photosphere. They occur in lower latitudes, and seldom appear as much as 45° from the equator.

6. The sun-spots of each cycle always appear within two relatively narrow zones 10° or 15°, or at most, 20° wide, symmetrically situated in the two hemispheres. These zones are most distant from the equator at the beginning of a cycle, and during the eleven years of the cycle gradually approach, so that toward the end they may almost reach the equator; but they never cross it. Before the spots of one cycle have disappeared, those of the next have made their appearance in the higher latitudes and begun their motion toward the equator.

7. In the majority of cases sun-spots appear in pairs forming binary systems. The axis of a binary system is, on the average, near-

ly parallel to the equator. In general, the closer the parallelism, the nearer the system is to the equator.

8. Sun-spots always show magnetic polarity, the members of a binary system having opposite polarities. A single spot may consist of two halves of opposite polarity, and thus, from the magnetic point of view, be a binary system. At the time of their appearance spot groups very frequently are bipolar. They usually end as single spots.

9. The preceding spots of binaries, almost without exception, have during the whole cycle a definite polarity, characteristic of that cycle. The polarities of preceding spots are opposite in the two hemispheres, and the whole system of polarities reverses with the beginning of a new cycle.

10. Within a binary system a certain asymmetry generally prevails. The preceding spot, as a rule, is the larger and has the longer life; the companion is smaller, often consists of a number of smaller spots, and may disappear long before the preceding spot.

11. Hydrogen spectroheliograms in the region of sun-spots often show spiral structure. The curvature is usually opposite in the two hemispheres, but does not change from cycle to cycle. If the spiral structure represents lines of flow, the motion must be both radial and circular. Since it has been obtained only by the use of hydrogen lines, it is believed to belong to the high levels of the solar atmosphere and to be merely a secondary effect of what is going on deeper down, in or below the photosphere. Occasionally hydrogen clouds have been drawn into a spot, with velocities up to 170 km/sec. Motion outward from the spot in the lower layers of the sun's atmosphere has also been observed.

The line structures surrounding bipolar systems seem sometimes to suggest an outflow from one spot and a corresponding inflow into the other; but the structures are generally complicated and not easy to interpret.

## III. GENERAL SUPPOSITIONS CONCERNING THE SUN

As a basis for an attempt to interpret the observed phenomena, the following suppositions will be made:

12. As the sun consists of gases of different specific weights, it will be near a state of *stable* internal equilibrium; i.e., the equilibri-

um is not of the adiabatic or indifferent type which would exist if density (and temperature) varied downward as a function merely of pressure. The difference may be illustrated thus: In the case of adiabatic equilibrium a mass which has been cooled at the sun's surface would sink to the sun's center, but in the case of stable internal equilibrium it would sink only to a certain equilibrium level from which it would ascend again when heated to the temperature of this layer.

Conditions in the sun will, therefore, be favorable for the formation of stratified circulation, and the conditions for this kind of circulation will be still more favorable if relatively homogeneous strata pre-exist, such that each stratum consists mainly of one chemical constituent or of constituents having approximately the same specific weight, but separated from the higher and lower strata by transitional layers in which chemical constitution and corresponding physical properties are subject to rapid variations.

13. The origin of all that happens on the sun is in the solar radiation. This may be taken to include the expulsion of electrically charged particles, which may be of importance for the electric conditions of the sun. The luminous and thermal radiation, on the other hand, will be considered responsible for the internal dynamics of the sun. It cools the upper layers of the photosphere and thereby disturbs the equilibrium conditions.

14. The heat thus lost by the photosphere is restored from the deeper layers by internal radiation, convection, and conduction. Internal radiation is believed to be the dominant factor, especially in the deep layers of very high temperature. But a sufficient percentage is left for setting up powerful convectional currents. The importance of convection increases near the surface, where, on account of the lower temperature, the internal radiation becomes less dominant.

15. The rotation of the sun acts as an organizing factor, tending to produce a general zonal symmetry around the axis of rotation.

16. The sun-spots are a kind of vortex. No hypothesis is made concerning the origin of their magnetic fields, but it is supposed that the fields are connected with the vortical motion in such a way that the magnetic polarity is reversed by a reversal of the vortex motion.

## IV. SUGGESTED INTERPRETATION OF THE SOLAR PHENOMENA

17. *Vortex theory of sun-spots.*—The well-known comparison of sun-spots with tropical cyclones involves the assumption that dynamically a sun-spot is a vortex. If this is correct, the comparison of sun-spots with the greatest vortices known on the earth, the tropical cyclones, will be useful in many respects, and, first, may give us a mental picture of the dimensions. The diameter of a small tropical cyclone is 120–130 kilometers. Let us now enlarge both the earth and the cyclone a hundred times. The earth will then have approximately the dimensions of the sun, the cyclone will be of the dimensions of the equatorial plane of the earth, and thus represent the area of a good-sized sun-spot. We know nothing of the height or depth of the sun-spot vortex; but taking again a hundred times the height of a tropical cyclone, which is between 5 and 10 km, we arrive at 500 to 1000 km. The body of a fair-sized sun-spot vortex would then be represented by the section contained between the equatorial plane of the earth and a parallel plane between 4° and 9° latitude.

A first fundamental question to be examined is whether a vortex theory can account for the visibility of sun-spots, i.e., of their relative darkness or low temperature. Formula (4) may be used for discussing this question. It gives the temperatures in what we may call a balanced vortex, in which the cooled heavy masses are just carried by the centrifugal pumping effect, and no ascending motion is present. Sun-spot vortices will, as a matter of course, not have this balanced character. The lifted cooled masses are subject to continuous radiation from below, and the pumping must go on continuously to lift the cooled masses at a sufficient rate to keep them sufficiently cool in spite of the radiation. Nevertheless, the formula for the balanced vortex will give a useful first approximation. To bring it into a convenient form for our special purpose, we remark that $ds \sin \phi$ is the element $dr$ of a radius vector from the axis of the vortex. We may thus write:

$$\frac{d\vartheta}{\vartheta}=\frac{2\Omega}{g}\frac{dv}{dz}dr$$

Then, for the sake of argument, we shall make a simple assumption concerning the rate at which the velocity $v$ increases with the height

$z$ in the vortex. For simplicity let the velocity be zero at a certain depth $H$ below the surface of the photosphere and increase upward according to a linear law until it reaches the value $v$ or $\Omega r$ at the surface of the photosphere. We may then substitute

$$\frac{dv}{dz}=\frac{v}{H}=\frac{\Omega r}{H}$$

and thus obtain

$$\frac{d\vartheta}{\vartheta}=\frac{2\Omega^2 r}{Hg}\,dr\ .$$

But the ratio of the centrifugal force $\Omega^2 r$ to the acceleration of gravity $g$ is the tangent of the angle of inclination of an element $ds$ of the photosphere, and this multiplied by the horizontal line element $dr$ gives the vertical projection $dz$ of a line element $ds$ contained in the inclined surface of the photosphere. Integrating this equation along the surface of the photosphere from a great distance to the center of the vortex, we obtain a relation between the drop in temperature $\Delta\vartheta$ and the corresponding dip $D$ below the normal level of the photospheric surface (Fig. 5). For simplicity we may assume the thickness $H$ of the vortex to be constant. Considering at the same time the drop in temperature $\Delta\vartheta$ to be small as compared with the temperature itself, we find by the integration the simple formula

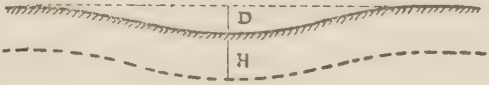

FIG. 5

$$\Delta\vartheta=2\vartheta\,\frac{D}{H}\ . \tag{5}$$

For large values of the drop in temperature we must use the result of the exact integration, viz.,

$$\log_e\frac{\vartheta_0}{\vartheta}=\frac{2D}{H}\ . \tag{6}$$

The approximate formula (5) represents the following exceedingly simple law: The drop in temperature is proportional to the dip in the surface of the photosphere. The dynamics of the phenomenon is obvious: The dip is due to the excess weight of the relatively cool gases forming the core of the vortex; these are prevented from leaving the surface by the centrifugal pumping effect arising from the excess of circulatory motion in the higher strata. On the other hand, for the same value of the dip, the drop in temperature is inversely proportional to the thickness $H$ of the vortex; the thinner the cooled stratum, the more must it be cooled to give the required excess of weight.

Introducing $\vartheta = 6000°$ as the surface temperature of the sun, we find

$$\Delta\vartheta = 12{,}000\,\frac{D}{H}$$

or, in the exact logarithmic form,

$$\log_e \vartheta_0 - \log_e \vartheta = 0.8686\,\frac{D}{H}\,.$$

These formulae give numerically

| $D/H$ | 0.001 | 0.01 | 0.1 | 0.2 | 0.3 | 0.4 | 0.5 |
|---|---|---|---|---|---|---|---|
| $\Delta\vartheta$ | 12° | 120° | 1100° | 2000° | 2700° | 3300° | 3800° |

Thus a dip in the photosphere amounting to only one-tenth of the thickness of the stratum taking part in the vortex motion will be sufficient to produce a drop in temperature of 1100°, while a greater dip will produce an even greater decrease in temperature. Now let the diameter of the vortex be ten times its thickness. The average inclination required to produce the dip of 1/10 would then be 1/100. The velocities required to produce this inclination at different distances $r$ from the axis of rotation are

| $r=$ | 10 | 100 | 1000 | 10,000 | 100,000 km |
|---|---|---|---|---|---|
| $v=$ | 0.2 | 0.6 | 1.7 | 5.5 | 17.5 km/sec. |

For the conditions on the sun these velocities seem very moderate. For a fourfold inclination, which gives a temperature drop of

3300°, the velocities would have only to be doubled. They thus remain small compared, for instance, with the velocity of 170 km/sec. found for a hydrogen cloud in the sun's atmosphere, not to speak of the amazing velocities observed in the prominences. There will be no difficulty therefore in accounting for the somewhat greater velocities which would be required to give the same temperature depressions in the unbalanced vortices. The simple case of the balanced vortex will, however, give the easiest available first approximation. Detailed examples of such sun-spot vortices, with full representation of the fields of velocity, pressure, mass, and temperature, may easily be worked out by use of the formulae given in my paper on the circular vortex, quoted above.

An important question is also the depth from which the vapors must be pumped up in order to give the required drop in temperature, for instance, 1100°. The adiabatic decrease of temperature in the earth's atmosphere is 1° C. per hundred meters of height. On the sun, with gravity 27 times stronger, the decrease would be 27° per hundred meters for an atmosphere like that of the earth, and we may assume for the solar gases a value differing not greatly from this. When these gases are lifted 10,000 meters or 10 km, they should cool down 2700°. How much this would reduce their temperature below that at the new level depends upon the solar temperature gradient. If, as in the earth's atmosphere, this is half the adiabatic gradient, the result would be 1300°. For smaller differences between the actual and the adiabatic rate, the required vertical displacement might be some multiple of 10 km. But great vertical displacements will not come into the question.

The vortex theory thus gives a straightforward explanation of the darkness of sun-spots; no great effort of any kind is required to explain their low temperatures. As a matter of fact, the trouble is, not to explain why sun-spots are seen, but rather why many more of them do not become visible and then disappear on a body where conditions for the formation and annihilation of vortices are as favorable as on the sun. This raises the question of the long life of a sun-spot, which may extend to months or to even more than a year. Under the intensive radiation from below, the cooled masses forming at any moment the core of the vortex cannot long retain their low temperature. But as they become heated they will be replaced by new masses pumped from below and float out radially over the surface of the photosphere. This process will continue as long as sufficient energy is at hand for the pumping operation. During the outward motion the circulation around the center of the spot will rapidly decrease, and the radial component will prevail. We have emphasized this radial outflow along the surface of the photosphere as a typical characteristic of sun-spots.

The radial motion outward at the bottom of the sun's atmosphere, as remarked by Hale, must give rise to a sink and a corresponding radial inflow in the upper strata. Because of the rotation of the sun the inflow will assume a spiral character, which may explain the spiral structure sometimes appearing in the high layers. Since this is determined by the direction of the sun's rotation and not by that of the photospheric vortex below, these spiral structures would have no reason to change when the magnetic polarities change at the beginning of a new sun-spot cycle.

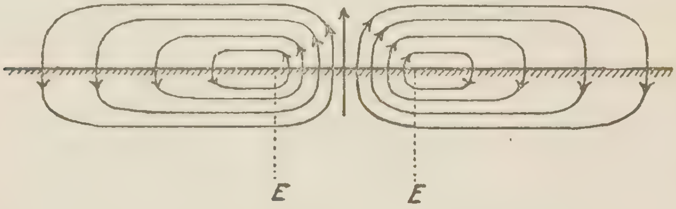

Fig. 6

For further discussion of the structure of sun-spot vortices, we shall make use of the vortex lines. Each element of a vortex line is an axis of local rotation, the direction of which is given by the positive screw rule. The vortex line, by geometric necessity, can never stop; it must run back into itself. This is also the fundamental property of the lines of magnetic induction. This common property facilitates the parallel discussion of the vortical and magnetic properties of sun-spots. In the first rough approximation, the vortex lines and the lines of magnetic induction may be identified. Where these lines are strongly concentrated we thus have intensive vorticity and strong magnetic field; where they are dispersed, we have weak vorticity and weak magnetic field.

The simplest hypothesis which can be made is that each sun-spot is an independent vortex. Figure 6 gives the vortex-line representation of such a vortex. The lines come up in great numbers through the photosphere in the central part of the vortex, spread out in the solar atmosphere, and return through the photosphere to the central vortex region. We have no idea as to the heights to which the vortex lines ascend in the solar atmosphere. Most likely they are concentrated near the surface of the photosphere, thus representing here an intensive sliding motion. As the visibility of the sun-spot demands a rapid decrease of velocity downward, the vortex lines will not reach great depths below the photosphere. At the surface itself, between the points $E$ and $E'$, we have a limited area of intensive positive vorticity and strong magnetic field; outside we have weak negative vorticity and a weak magnetic field, opposite to that in the internal area. We do not know the correspondence between the direction of rotation and the sign of the magnetic field, and a reliable determination thereof would be of fundamental importance for the theory of sun-spots, and perhaps also for that of magnetism.

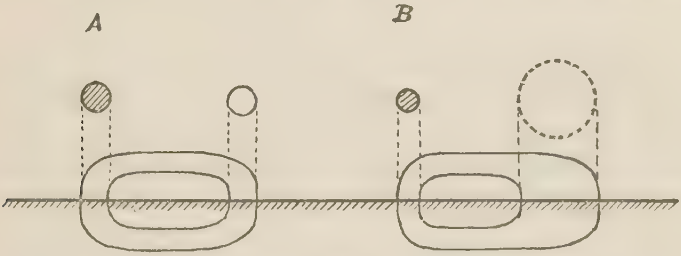

FIG. 7

If each sun-spot were an independent vortex, a binary system would appear only by accident, two vortices of opposite rotation happening to be near each other. To explain the binaries Hale has therefore suggested a coupled system forming a vortex ring, the two spots of the binary being the intersection of this ring with the photosphere. One half of the ring then belongs to the atmosphere, while the other half, dynamically the more important, forms a sub-photospheric connection between the spots (Fig. 7, $A$). Nothing prevents us from assuming that all sun-spots belong to binary systems of this type, for a spot which appears single may have an invisible companion, the vortex ring cutting the surface so diffusely that nothing is observed (Fig. 7, *B*).

The vortex-ring theory gives a simple explanation of the tendency of sun-spots to appear as binaries; but it fails to give any natural explanation of the characteristic collective properties of spots, which seem to point strongly toward a more complete coupling, not only between the spots of the same binary but also between the different binaries of the same cycle. As a matter of fact, a complete vortical connection between all spots of the same cycle can also be imagined. Thus all the spots may belong to a single zonal vortex, which surrounds the sun approximately as a parallel and gives rise to a spot, wherever it passes from the photosphere to the atmosphere or vice versa. The assumption may be made in two different forms: The zonal vortex may belong mainly to the atmosphere and occasionally dip below the photosphere from spot to spot of a binary (Fig. 8, *A*); or, vice versa, it may be mainly subphotospheric, and occasionally ascend into the atmosphere from member to member of a binary system (Fig. 8, *B*). Leaving until later the choice between these alternatives, we shall first derive the consequences which are common to both forms of the zonal vortex theory.

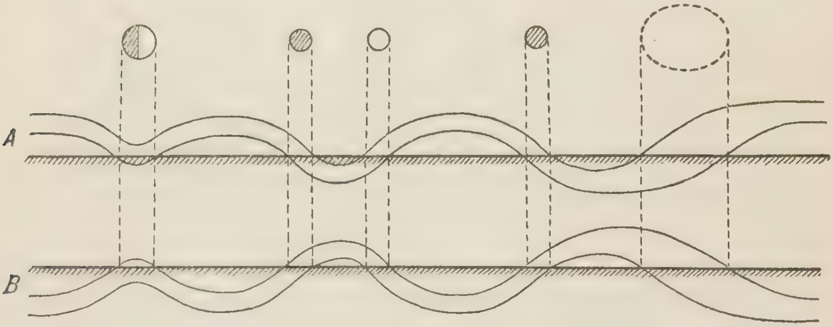

FIG. 8

While conserving the advantages of the vortex-ring theory, the zonal vortex gives a simple picture of the most striking collective properties of sun-spots, namely, that spots of the same cycle appear within a relatively narrow zone of latitude; that spots appear generally in binary systems; that the axis of a binary tends to be parallel to the equator; that binaries of the same cycle, almost without exception, show the same succession of polarities; that groups at their first appearance are very frequently bipolar; that a single spot is generally the last phase, one member of the binary system becoming diffuse and invisible before the other; that a companion to a single spot appears in the rear, if the original spot has the leading polarity for the cycle, and ahead if the opposite state of affairs prevails.

In addition, the theory reduces the progression of sun-spot phenomena from higher to lower latitudes to a motion of the single zonal vortex, while the reversed succession of polarities from cycle to cycle is explained as a reversal of the rotation of the zonal vortex.

The various advantages which the zonal-vortex theory of sun-spots thus seems to possess makes it desirable to find ways of testing its possibility. The simplest preliminary test would be to plot from day to day the probable course of the zonal vortex, in order to see if this gives an adequate representation of the distribution and propagation of sun-spots. In doing this it is recommended that areas of different polarity be marked with different colors, say red and blue. The simplest curve is then drawn which connects these areas in the regular succession red, blue, red, blue, etc. When necessary, a hypothetical invisible spot is to be inserted where the regular succession of polarities requires it. Remarking that this is permissible, and, further, that a vortex tube is infinitely flexible and may branch out and join again, we see that it will always be possible to draw the required curve. The difficulty is that its course is not uniquely determined. The aim should, therefore, be to draw it with the smallest possible number of assumed invisible spots and with as few branches and sinuosities as possible. Figure 9 indicates a possible course for such a curve, illustrating both a division into two branches and an S-shaped return of the curve used to explain the case of reversed polarity.

If it should prove possible to draw these curves so that they do present the distribution and progression of sun-spots, and if the survey of the sun's surface, magnetically and optically, along the course of the curves facilitates the discovery of invisible sun-spots, etc., the zonal vortex theory would at least be useful as a working hypothesis.

All the collective properties of sun-spots enumerated follow from the zonal-vortex theory in both its forms; but there is a decided reason in favor of the assumption that the zonal vortex is mainly sub-photospheric. Just below the radiating stratum of the photosphere we shall find the strongest tendency to form convective circulations of thermal origin. A sub-photospheric vortex, along its whole length, will bring hot gases to the surface and carry cooled gases down again. Throughout its entire extent it is a thermodynamically driven engine of the type Figure 1, *C* or *D*, and has the important property of running in both directions equally well, which provides for the two directions of rotation required for reversing the succession of polarities from cycle to cycle. That such a vortex does not take an irregular form, but tends to lie parallel to the equator, follows from the rotation of the sun, which favors symmetrical arrangements relative to the axis of rotation.

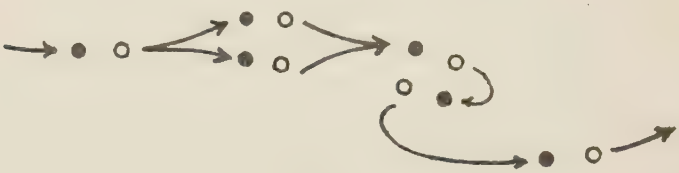

FIG. 9

Finally, it may be asked why such a sub-photospheric vortex should occasionally ascend to the surface. To answer this question we must recall the attraction or repulsion existing between parallel vortices and the attraction of a vortex toward a rigid plane. The surface of the photosphere, on account of its stability, will act as a practically rigid plane, which in general will attract the vortex. The force will disappear in one case only, namely, when the vortex yields completely to the current which tends to carry it along parallel to the surface. But such a complete yielding is excluded in the case of a vortex maintained convectively and receiving its energy from hot strata which never have the exact motion of the upper current. The attracting force will, therefore, always exist; and, if the vortex has an upward sinuosity, this sinuosity will come under increased attraction, as the force varies inversely as the distance from the plane. Ultimately the sinuosity may thus reach and cut the surface and form the two separate horizontal vortices of a binary, and even after this the continued attraction will tend to bring more of the vortex up and thus separate the two spots from each other.

There is another reason also, and perhaps more important, for the tendency of the sub-photospheric vortex to rise and cut the photosphere. The regular state below the surface of the sun is one of stable stratification. Circulation can take only the stratified form, with limited vertical excursions, whereas no special forces limit the horizontal excursions. The sub-photospheric vortex must, therefore, be very flat, the circulating curves having very flat elliptic forms, with horizontal major axis and vertical minor axis. This is a strained type of circulation, guided by a certain balance of forces. It may, therefore, have a strong tendency, when an opportunity offers, to turn over in the horizontal plane. Here a circulation, once started, goes on undisturbed, as a perfectly stable motion. This tendency to realize the most stable motion may, therefore, be the main reason why the vortex rises and cuts the photosphere, and why afterward new lengths of the photospheric vortex are drawn up to the already-formed horizontal sun-spot vortex, thus giving it a continuous supply of sub-photospheric energy.

When the vortex tube is thus bent up, the strained elliptic circulation in the vertical plane changes automatically into a circular circulation in the horizontal plane (Fig. 10). For the same area of cross-section this gives much shorter circulating curves, and therefore an intensified circulation. This intensified circulation again gives the pumping effect which lifts up gases from below and makes the spot visible by its lowered temperature. The kinetic energy of this localized vorticity is by and by absorbed in the work of pumping. But new energy becomes available according as new lengths of the sub-photospheric vortex are raised to the surface. In this way the sub-photospheric vortex may be drawn upon for energy for any length of time, and secure to the sun-spot any length of life.

18. *General solar circulation.*—Our view of sun-spots as a link in the internal circulation of the sun brings up the question of the general character of this circulation.

As in all likelihood strata of different density pre-exist in the interior of the sun, it seems very probable, if not necessary, that the circulation should be of the stratified type. In addition, the circulation itself will tend to develop the stratification further. The main question will be the vertical and horizontal extent, and the mutual arrangement of the individual circulating strata. Here the rotation of the sun enters as a determining factor. Without this rotation there would be no organizing principle. The stratification would have an irregular and turbulent character; but with rotation there must enter a tendency toward symmetry relative to the axis of the sun. How far the organizing power of the solar rotation may extend can be only vaguely estimated.

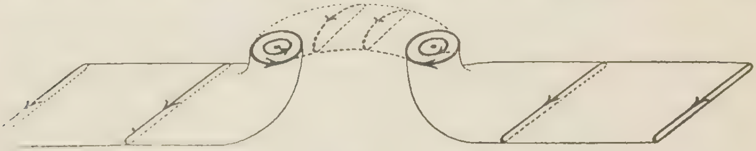

FIG. 10

An example of the simplest possible scheme of stratified circulation is given in Figure 11. Here the highest stratum is supposed to have a circulation from the poles to the equator at the surface, and from the equator back to the poles below. The next lower stratum should then circulate from equator to pole in its upper part, and from the pole to the equator below, and so on. One may ask why the highest layer should not rather circulate as in the case of the earth's atmosphere, namely, from equator to poles in the higher levels and from poles to equator below. The answer is that the circulation of the earth's atmosphere is self-starting in the direction observed because the main source of heat is at the ground level at the equator. On the sun, to the contrary, it is difficult to see why the circulation should start in either direction in preference to the other, since we have initially a symmetry corresponding to that of Figure 1, *C* and *D*. But *if* the circulation is started in a given direction, it should then persist in that direction.

The motive power of the circulation in the upper stratum is the cooling of the photosphere by radiation, and the corresponding heating lower down by radiation from within and by contact with the next lower stratum. Since the power of radiation decreases outward as the temperature decreases, the lowest part of the stratum has better access to the radiated heat than the upper part. This will favor heat transport by convection. The next lower stratum then comes into circulation by frictional effect, assisted by the cooling of its upper part by contact with the upper stratum and the heating of its lower part by the hot gases below.

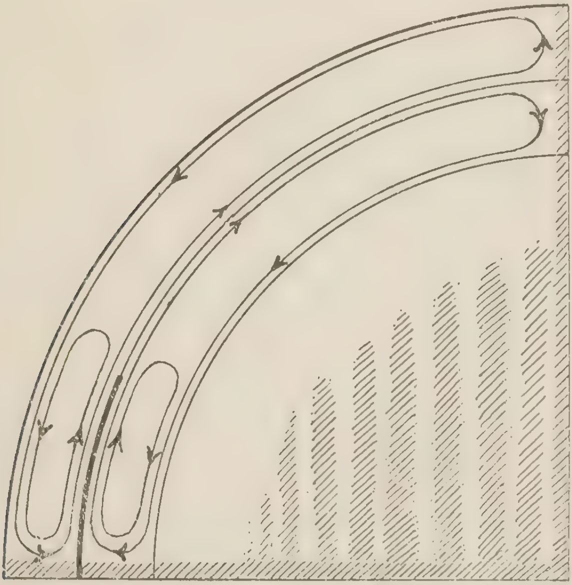

FIG. 11

If such a circulation exists, the surface of the sun as seen from the earth will not rotate as a rigid body. We cannot define any definite angular velocity of the entire solar surface, but only a certain zonal distribution of angular velocity, the character of which we shall now examine.

Evidently those parts of the sun which participate least in the circulation will move most nearly as a rigid body. These will be the great internal masses on both sides of the equatorial plane and surrounding the axis of rotation. The corresponding areas are shaded in Figure 11. Then for the masses participating in the circulation we must use the general law, so well known from the earth's atmosphere, that masses moving from pole to equator lag behind, while masses moving from the equator to the poles advance relative to the rigid, or apparently rigid, core. This always occurs to such an extent that the main motion becomes pratically a pure EW motion, accompanied only by a slow displacement of the masses in the NS direction. The upper layer of the highest circulating stratum should, therefore, in all latitudes appear retarded relative to the equatorial masses. Thus the internal circulations of the sun seem to open the possibility of explaining the so-called *equatorial acceleration*, which, from this viewpoint, should rather be called a *retardation in the higher latitudes*. A difficulty for this theory may be met in the fact that, as far as we can see, a retardation relative to the pole is to be expected; in other words, a polar acceleration should appear near the pole, where it will be difficult, however, to obtain good determinations of the angular velocity.

The amount of retardation of the upper masses will be limited mainly by friction against and mixing with the lower masses of the layer, which have a corresponding acceleration because of their motion from the equator to the poles. On the other hand, the fact that the observed retardation in the higher latitudes is so moderate shows that the motion from the poles to the equator must be very gradual, thus leaving time for an effective smoothing out of the difference in velocity between the retarded upper part and the accelerated lower part of the stratum. Observations indicate that the retarded masses in moderately high latitudes have had their angular velocities around the sun's axis reduced by about 1/20. This would represent an east wind relative to the quasi-rigid body of the sun which would traverse the solar circumference in about 20 solar days or in something more than a terrestrial year. The corresponding velocity would be about 130 meters per second. The motion from the poles to the equator should, therefore, require several years, and the corresponding north wind would be very weak.

The sub-photospheric zonal vortex from which sun-spots develop must belong to the lower, slow-moving layers of this east-current stratum. Then, when the vortex tube rises, cuts the photosphere, and forms a binary spot, the two separated parts of the tube must be affected differently by the stronger east wind near the surface. Attention is directed to this as a possible origin for the asymmetrical properties of binaries, although no attempt to consider details is made at present.

During their slow motion from the poles to the equator, the masses forming the surface of the photosphere must be gradually cooled. In consequence the sun should have its highest temperature at the poles and its lowest at the equator. We may adapt formula (4) to the discussion of this temperature, interpreting now $\phi$ as the latitude and $\Omega$ as the angular velocity of the sun. We may then introduce

$$ds = +R d\phi \ ,$$

$R$ being the radius of the sun, and write

$$\frac{dv}{dz} = \frac{v}{h} \ ,$$

$h$ being the thickness of the overlying current of the upper circulating stratum. Writing further

$$v_E = \Omega R$$

for the circumferential velocity at the sun's equator, we find from formula (4)

$$\frac{d\vartheta}{\vartheta} = \frac{2v_E \ v}{gh} \cos\phi d\phi \ .$$

This must now be integrated from the equator to the pole, i.e., from $\phi = 0$ to $\phi = \pi/2$. Writing the first member in the approximate form $\Delta\vartheta/\vartheta$, we obtain

$$\frac{\Delta\vartheta}{\vartheta} = \frac{2v_E v}{gh} \ .$$

For comparison we may first apply the formula to the earth's atmosphere. Here the height of the circulating stratum is roughly

10,000 meters, and for the circumferential velocity of the equator we may write $v_E = 500$ m/sec. Using the average temperature $\vartheta = 273°$, we obtain

$$\Delta\vartheta = 2.73\, v\ ,$$

$v$ representing the eastward velocity of the highest strata of the troposphere, that at the ground for simplicity being taken as zero. The formula gives

for $v = 10$ m/sec. $\Delta\vartheta = 27°$ ;
for $v = 20$ m/sec. $\Delta\vartheta = 54°$ .

Thus a velocity of 10 m/sec. in the upper part of the troposphere is sufficient to maintain a temperature-difference of 27° between pole and equator, while the double velocity of 20 m/sec. corresponds to the double temperature difference of 54°. The actual difference, when we disregard the thin locally cooled stratum at the surface in the polar regions, is somewhere between 30° and 40°, corresponding to a velocity in the upper troposphere between 11 and 15 m/sec.

Applying the same formula to the sun, we have the circumferential velocity at the equator $v = 2000$ m/sec., the acceleration of gravity $g = 275$, and for the eastward velocity of the highest circulating stratum the value just found, $v = 130$ m/sec., while the thickness $h$ of this stratum remains unknown. Setting $\vartheta = 6000°$ for the surface temperature of the sun, we find for the temperature difference between pole and equator

$$\Delta\vartheta = \frac{12,000,000}{h}\ .$$

This gives

for $h = 10$ km, $\Delta\vartheta = 1200°$ ;
for $h = 100$ km, $\Delta\vartheta = 120°$ ;
for $h = 1000$ km, $\Delta\vartheta = 12°$ .

If we venture a guess harmonizing with the conjectured thickness of about 100 km for sun-spot vortices, something between 100 km and 1000 km would be the most probable depth for the solar eastward current. The temperature difference of 12° to 120° between pole and equator would then be of the same order as that on the earth, and probably difficult to detect, and still more so when we remember that these temperatures correspond to the balanced motion, in which we neglect the disturbance by the radiation. But for a greater internal stability of the sun, the depth of sun-spot vortices and of the individual layers participating in the stratified circulation would decrease. Thus, greater temperature differences are quite possible, and actual measurement of such a difference between pole and equator would be of great interest.

Finally, it may be remarked that the circulation assumed for the photosphere should, by frictional coupling, give the solar atmosphere a circulation like that of the earth's atmosphere, i.e., from the poles to the equator in the lower strata, and from equator to poles in the high layers. Under these conditions the high masses should show acceleration relative to those below, limited by friction against and mixing with these lower masses. As a consequence of balance between accelerating and retarding effects, a rotation practically equal to that of the equator might occur for the high strata, in accordance with the result found for the highest parts of the sun's atmosphere.

To the attempts here made to explain the equatorial acceleration of the sun as a result of internal circulations, an important remark must be added: The planet Jupiter shows the same equatorial acceleration. The question must remain open whether the internal constitution of this planet is such as to allow the same explanation as suggested for the sun.

19. *The sun-spot cycle and the reversal of polarities.*—The preceding considerations have led to an interpretation of both sun-spots and equatorial acceleration as phenomena related to the internal circulation of the sun. Sun-spots depend upon intensive local circulations, and the equatorial acceleration upon the slow general circulation. The remaining question is whether these two suggested explanations fit into each other in such a way as to explain the fact that sun-spot phenomena are restricted to the lower latitudes of the sun and have their characteristic periodicity.

Figure 11 shows that we meet with the greatest contrast of temperature on both sides of the equator where the cooled masses of the photosphere, which have been radiating since they left the poles, descend and come in contact with the hot ascending masses of the next lower circulating layer. This provides conditions favorable, on the one hand, for a concentration of the general circulation in the lower latitudes, which is indicated by an inner circulating curve in each stratum of Figure 11 and, on the other, for the formation of the extra vortices of zonal character to which we have referred the sun-spots. If these zonal vortices have a certain persistency, they will be carried round by the general circulation into the lower latitudes.

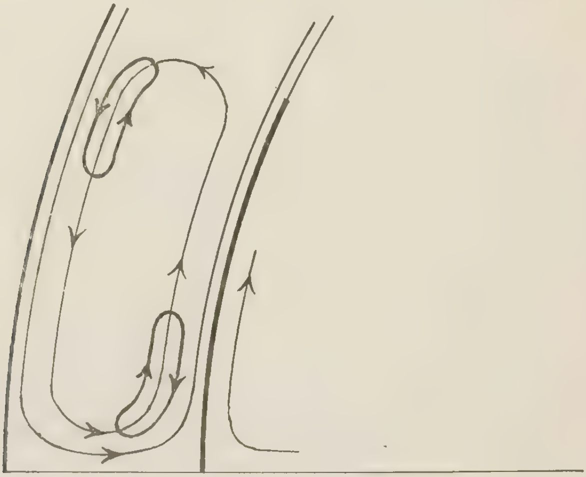

FIG. 12

It is only necessary to admit the existence of two zonal vortices having opposite directions of rotation which are carried round by the general circulation (Fig. 12). From a thermal point of view this supposition is possible, inasmuch as both directions of rotation are compatible with the thermal origin of the vortex zones. And, mechanically, vortices rotating like toothed wheels assist each other by their mutual frictional effect. Since we have estimated that the circulation between the poles and the equator requires many years, a period of twenty-two years for the revolution of the zonal vortices about each other does not seem unreasonable. The succession of the phenomena will be just as observed: The new cycle, with opposite rotation and opposite polarity, will begin in the higher latitudes while the old cycle is disappearing at the equator. When the zonal vortex at the equator dives below, we shall have only spots of the succeeding cycle which has then come to full development. Then, as this zonal vortex approaches the equator, the other vortex rises in higher latitudes and produces the spots of the next cycle with their reversed polarities, and so on.

From a kinematical point of view the process is exceedingly simple; but we have made only the very first steps in the discussion of its dynamics and thermodynamics.

The frictional coupling of the circulations of the two hemispheres may be responsible for the fact that sun-spots in the two hemispheres have the same periodicity and show opposite magnetic polarities in any given cycle.

The theory thus developed seems to favor the vortical nature of sun-spots. The vortex theory leads to a simple explanation of the low temperatures of sun-spots and gives, as a matter of course, the explanation of the fact that the low temperatures are found in depressions on the sun's surface. It provides conditions under which the low temperatures in these depressions may be maintained for any length of time, and suggests connections between sun-spots which would explain their striking collective properties, including their periodicity and the remarkable reversal of their magnetic polarities. It is not to be supposed that the complex of suggestions here tentatively developed will remain unchanged. Weak points are obvious and others may turn up; but many modifications of the suggested scheme are possible. That proposed will have done its service if it prepares the way for a better one.

BERGEN, NORWAY
November 1925

Contributions from the Mount Wilson Observatory, No. 313
Reprinted from the *Astrophysical Journal*, Vol. LXIII, pp. 342–367, 1926
Printed in the U.S.A.

# ON THE TRANSMISSION OF RADIATION THROUGH AN ABSORBING MEDIUM IN MOTION, WITH APPLICATIONS TO THE THEORY OF SUN-SPOTS AND SOLAR ROTATION

By SVEIN ROSSELAND[1]

## ABSTRACT

*Transmission of radiation through an absorbing and emitting medium.*—The theory is developed in a general way so as to include cases in which the medium is in motion and the state not stationary in time (§§ 1–5). In §§ 1–4 the properties of the radiation field alone are studied, and in § 5 the equation for the combined flow of material and ethereal energy are given. In § 6 the preceding theory is applied to sun-spots. It is assumed that the energy of solar radiation proceeds mostly from the sun's interior, and that in the spots this uniform stream of radiation is modified by convectional currents. This picture of the phenomenon leads to a simple formula connecting the mean density, mean vertical velocity, and mean vertical thickness of a spot. The theory leads to values of the thickness and velocities corresponding to the observed reduction of temperature in spots which are reasonable, but lack of observations prevents a more rigorous test.

In the last section the theory of solar rotation is discussed. It is emphasized that the equatorial acceleration of the sun may be intimately connected with the manner in which the energy of solar radiation is generated, and that pre-existing theories of the evolution of rotating stars need revision in order to take account of internal motions other than a rigid rotation. Friction being neglected, it is shown by a simple example how the source of energy determines the variation of angular velocity parallel to the axis of rotation, the variation perpendicular to this direction remaining undetermined to this degree of approximation.

1. In all theoretical work on the transfer of energy by radiation through an absorbing medium it is assumed that the medium is at rest. This assumption is sufficiently general to give valuable information about the large-scale structure of the stars. When it comes to the detailed explanation of the phenomena which occur in stellar atmospheres, however, it is obvious that the simple theory of radiative equilibrium is conceived on too narrow a scale, and the development of the theory in its most general aspect, allowing for the motion of the medium as well as for variations in the radiation field with time, becomes a necessity for astrophysical theory.

In the familiar case of the sun the phenomena most urgently calling for a discussion of this kind are the spots. How can a sunspot retain for months a temperature which is lower than that of the surrounding solar surface by a thousand degrees? The most probable answer to this question, on the basis of ordinary physical facts, seems to be that somewhere in the spot matter is in motion upward, and that the expansion of the gases consequent to this motion is sufficient to reduce systematically the flow of radiant energy which would characterize a state of hydrostatic equilibrium. Observations on the reduction of temperature in sun-spots below that of the undisturbed radiating surface contain, therefore, a store of implicit information on the general nature of the vertical motion in spots.

---

[1] Fellow of the International Education Board, 1924–1926.

When we study stellar atmospheres in general a number of problems turn up, such, for example, as the Cepheids and long-period variables, and all kinds of spectral variability not directly due to duplicity, the solution of which will probably require the consideration of transmission of radiation through moving media. In what follows, special stress will be placed upon the development of the general theory, while the application to stellar problems, which is by far the more difficult task, will be more in the nature of examples illustrative of this theory.

2. Consider any medium which is capable of emitting and absorbing radiation. Let $E_\nu d\nu$ denote the energy of radiation contained in the frequency interval $\nu$ to $\nu+d\nu$, which is emitted per unit time, volume, and solid angle from the matter at the point $x$, $y$, $z$ at the time $t$. Further, let $x_\nu$ denote the absorption coefficient of the matter at the same point and time, and in the same frequency interval, and let this be defined in such a way that $x_\nu ds$ is the fractional reduction of a linear beam of radiation in the given frequency interval in traversing the distance $ds$ through the medium in the immediate vicinity of the point in question.

The radiation field will be described statistically by a function $I_\nu$ which is defined by the requirement that

$$I_\nu \, d\nu \, dw \, d\sigma$$

is the energy of radiation in the frequency interval $d\nu$, directed within the elementary solid angle $dw$, which per unit time passes perpendicularly through the surface element $d\sigma$. Thus $I_\nu$ will be a function of $x$, $y$, $z$, $t$, $\nu$ and the direction cosines of the normal to $d\sigma$

counted in the direction of the flow of radiation. The function $I_\nu$ will occasionally be referred to as the *intensity* of the radiation field. Consider a small fixed cylinder with $d\sigma$ as a base, of height $ds$, and with its axis in the direction of $I_\nu$. The amount of radiation which in the time interval $t$ to $t+\tau$ enters the cylinder through $d\sigma$ is

$$d\nu\ d\sigma\ dw \int_t^{t+\tau} I_\nu\, dt\ .$$

If no absorption or emission of radiation took place within the cylinder, this same amount would escape through the top of the cylinder in the time interval $t+ds/c$ to $t+ds/c+\tau$. The radiation in question will, however, be weakened by absorption to an amount

$$d\nu\ d\sigma\ dw\ ds\ x_\nu\ I_\nu\ \tau$$

correct to the first order of the small quantity $ds$, and $\tau$, and reinforced through emission by the amount

$$d\nu\ d\sigma\ dw\ ds\ E_\nu\ \tau$$

which is correct to the same degree of approximation. The equation expressing the balance of energy in the field of radiation takes the form

$$\int_t^{t+\tau} I_\nu\, dt = \int_{t+ds/c}^{t+\tau+ds/c} \left(I_\nu + \frac{\partial I_\nu}{\partial s}\, ds\right) dt - (E_\nu - x_\nu\, I_\nu) ds\ \tau\ .$$

Developing the integrals to the first order in $\tau$ and $ds$, we obtain the final relation

$$\frac{\partial I_\nu}{\partial s} + \frac{1}{c}\frac{\partial I_\nu}{\partial t} + x_\nu\, I_\nu = E_\nu\ . \qquad (1)$$

In order to apply equation (1) to actual problems, $x_\nu$ and $E_\nu$ must be known. These functions regulate the interchange of energy between the radiation field on one hand and the field of matter on the other. The solution of equation (1) involves, therefore, the simultaneous solution of all equations which determine the state of the material field. Before entering upon this latter question we shall consider the problem of the integration of (1), assuming $x_\nu$ and $E_\nu$ to be known functions of the co-ordinates and the time.

Consider first the case in which the state of the system is steady, i.e., in which $I_\nu$, $x_\nu$, $E_\nu$ are independent of the time. Assume that we wish to calculate $I_\nu$ at the point $x$, $y$, $z$, and for direction cosines, $\alpha$, $\beta$, $\gamma$. We then draw a straight line in the direction $\alpha$, $\beta$, $\gamma$ and specify the position of the point $x$, $y$, $z$ on this line by a linear co-ordinate $s$. Equation (1) then becomes an ordinary linear differential equation of the first order in $s$. Putting

$$\tau_{AB}=\int_A^B x_\nu\, ds\,, \tag{2}$$

the integration being carried out on the straight line on which $s$ is the co-ordinate and from the point $A$ to the point $B$, we may write equation (1) in the form

$$e^{-\tau_{AB}}\frac{\partial}{\partial s}(I_\nu\, e^{\tau_{AB}})=E_\nu \tag{3}$$

where the point $B$ has been assumed to be variable while $A$ is a fixed point. Multiplying (3) by $e^{\tau_{AB}}$ and integrating from any point $C$ to a point $D$, we obtain as the integrated form of (1)

$$(I_\nu)_D=(I_\nu)_C e^{-\tau_{CD}}+\int_C^D (E_\nu)_B e^{-\tau_{BD}}\, ds_B \tag{4}$$

where we have made use of the identical relations

$$\tau_{AB}+\tau_{BC}=\tau_{AC}\text{ , etc.}$$

Equation (4) might have been written down directly, as it expresses only the fact that the intensity of radiation at $D$ is made up of the intensity at $C$ and the intensity of the radiation emitted from the layer between $D$ and $C$, allowance being made for the absorption, which in both cases takes place on the passage from the point of origin to $D$.

3. Let us now proceed to the solution of (1) for the case in which the term involving differentiation with respect to the time is retained. Put $s=x$, $ct=y$, and $I_\nu=z$, and assume that the final solution will be given in the form

$$V(x, y, z)=0\,.$$

Equation (1) then transforms into

$$\frac{\partial V}{\partial x}+\frac{\partial V}{\partial y}-(x_\nu z-E_\nu)\frac{\partial V}{\partial z}=0 \tag{5}$$

which expresses the fact that the vector whose components are 1, 1, and $-(x_\nu z-E_\nu)$ is contained in surfaces $V=$const. The stream lines of this vector are given by

$$\frac{dx}{1}=\frac{dy}{1}=-\frac{dz}{x_\nu z-E_\nu}\,. \tag{6}$$

Let

$$f_1=\text{const.}\ ; \qquad f_2=\text{const.}$$

be the integrals of (6). Then

$$V=\Phi(f_1\,,f_2)=0 \tag{7}$$

constitutes the general solution of (5), $\Phi$ being an arbitrary function[1] of $f_1$ and $f_2$. In the present case it is easy to find the integrals $f_1$ and $f_2$ of the ordinary differential equations (6). The first equation gives directly

$$f_1=x-y\,. \tag{8}$$

The second equation then reduces to

$$\frac{dz}{dx}=-x_\nu(x,\,x-f_1)z+E_\nu(x,\,x-f_1)\,. \tag{9}$$

This is an ordinary linear differential equation having the solution

$$f_2=ze^{\int^x x_\nu(p,\,p-f_1)dp}-\int^x E_\nu(q,\,q-f_1)e^{\int^q x_\nu(p,\,p-f_1)dp}dq\,. \tag{10}$$

Introducing these values of $f_1$ and $f_2$ in (7), solving for $z$, and introducing the original notation we obtain the generalized equivalent of (4)

$$I_\nu=\phi(s-ct)e^{-\int^s x_\nu(p,\,p-s+ct)dp} + \int^s E_\nu(q,\,q-s+ct)e^{-\int_q^s x_\nu(p,\,p-s+ct)dp}dq \tag{11}$$

---

[1] See, for instance, E. Goursat, *Cours d'Analyse Mathématique*, 2 (Paris 1915), 551.

where $\phi$ is an arbitrary function of one argument, and where the constant limits of integration are left arbitrary. We may revert to (4) by assuming the left-hand side of (11) to be independent of the time. The arbitrary function must then reduce to a constant, since it contains $s$ only in the combination $s-ct$, and by a proper adjustment of the limits of integration the two solutions become identical.

4. *Flux of radiation.*—In order to study the resultant streaming of radiant energy in the field it is convenient to introduce a certain vector $\boldsymbol{F}_\nu$ having the rectangular components $F_{\nu x}$, $F_{\nu y}$, $F_{\nu z}$, defined by the condition that $(\boldsymbol{F}d\sigma)$ is the net amount of the radiant energy in the frequency interval $d\nu$ which per unit time passes through the fixed surface element $d\sigma$.[1] The vectorial nature of $\boldsymbol{F}_\nu$ may be inferred from the fact that $(\boldsymbol{F}_\nu d\sigma)$ necessarily has the form[2]

$$(\boldsymbol{F}_\nu\, d\sigma)=A\;d\sigma_{yz}+B\;d\sigma_{zx}+C\;d\sigma_{xy} \tag{12}$$

---

[1] Vectors and tensors will be denoted by heavy type, and the following symbolism from the vector calculus will be used: Let $\boldsymbol{a}$, $\boldsymbol{b}$, denote any two vectors with rectangular components $a_x$, $a_y$, $a_z$, while $\varphi$ is an invariant. We then write

Inner product of $\boldsymbol{a}$ and $\boldsymbol{b}=(\boldsymbol{ab})=a_xb_x+a_yb_y+a_zb_z=$ invariant,

Vector product of $\boldsymbol{a}$ and $\boldsymbol{b}=[\boldsymbol{ab}]=$ vector with components $a_yb_z-a_zb_y$; $a_zb_x-a_xb_z$; $a_xb_y-a_yb_x$,

Differential vector operator $\nabla=$ vector with components $\dfrac{\partial}{\partial x}$; $\dfrac{\partial}{\partial y}$; $\dfrac{\partial}{\partial z}$; consequently

$$\nabla\varphi=\text{vector: } \frac{\partial\varphi}{\partial x};\ \frac{\partial\varphi}{\partial y};\ \frac{\partial\varphi}{\partial z},$$

$$\text{div } \boldsymbol{a}=(\nabla\boldsymbol{a})=\frac{\partial a_x}{\partial x}+\frac{\partial a_y}{\partial y}+\frac{\partial a_z}{\partial z}=\text{invariant},$$

$$\nabla^2\varphi=\frac{\partial^2\varphi}{\partial x^2}+\frac{\partial^2\varphi}{\partial y^2}+\frac{\partial^2\varphi}{\partial z^2}=\text{invariant}.$$

Invariant differential operator $(\boldsymbol{a}\nabla)=a_x\dfrac{\partial}{\partial x}+a_y\dfrac{\partial}{\partial y}+a_z\dfrac{\partial}{\partial z}$,

$$\text{curl } \boldsymbol{a}=[\nabla\boldsymbol{a}]=\text{vector: } \frac{\partial a_z}{\partial y}-\frac{\partial a_y}{\partial z};\ \frac{\partial a_x}{\partial z}-\frac{\partial a_z}{\partial x};\ \frac{\partial a_y}{\partial x}-\frac{\partial a_x}{\partial y}.$$

Let $\boldsymbol{A}$ stand for a tensor of second rank with components $A_{xx}$, $A_{xy}$, etc. . . . . $A_{zz}$, while $\boldsymbol{a}$ is a vector. Then we define as inner product of $\boldsymbol{A}$ and $\boldsymbol{a}$ a vector with rectangular components $A_{xx}a_x+A_{xy}a_y+A_{xz}a_z$; $A_{yx}a_x+A_{yy}a_y+A_{yz}a_z$; $A_{zx}a_x+A_{zy}a_y+A_{zz}a_z$, which we denote by $(\boldsymbol{aA})$. Taking for $\boldsymbol{a}$ the differential operator $\nabla$, we obtain a vector which we call div $\boldsymbol{A}$, the components of which are $\dfrac{\partial}{\partial x}A_{xx}+\dfrac{\partial}{\partial y}A_{xy}+\dfrac{\partial}{\partial z}A_{xz}$, etc.

[2] See, for example, Carslaw, *Mathematical Theory of the Conduction of Heat in Solids* (London, 1921).

where $A$, $B$, $C$ are certain coefficients and $d\sigma_{yz}$, $d\sigma_{zx}$, $d\sigma_{xy}$ are the projections of the surface element $d\sigma$ on the $yz$, $zx$, and $xy$ planes of coordinates, respectively. Integrating this expression over a closed surface and transforming the surface integral into a volume integral by Gauss's theorem, we find that

$$\frac{\partial A}{\partial x}+\frac{\partial B}{\partial y}+\frac{\partial C}{\partial z}$$

is an invariant. Consequently $A$, $B$, $C$ form the components of a vector, and the right-hand side of (12) is the scalar product of two vectors. Thus $\boldsymbol{F}_\nu$ is a vector with components $F_{\nu x}=A$, $F_{\nu y}=B$, $F_{\nu z}=C$, and this vector will be referred to as the *flux of radiation.*

From the definition of $\boldsymbol{F}_\nu$ we have

$$(\boldsymbol{F}_\nu d\sigma)=d\sigma\int I_\nu \cos\widehat{I_\nu d\sigma}\, dw\,,$$

the integration being extended to $4\pi$ of solid angle. Thus the $\boldsymbol{x}$-component of $\boldsymbol{F}_\nu$ is given by

$$F_{\nu x}=\int I_\nu \frac{dx}{ds}\, dw \tag{13}$$

where $ds$ is a line element in the direction of $I_\nu$ and $dx$ the $x$-component of $ds$. The expression of $F_{\nu y}$ and $F_{\nu z}$ may be obtained from (13) by substituting $dy$ or $dz$ for $dx$. By using equation (1) it is possible to transform (13) into a remarkable form which affords the most convenient starting-point for any application of the theory to actual problems. We assume the material medium to be isotropic, as will necessarily be the case if we are dealing with gases or liquids. The function $x_\nu$ must then be a pure function of position, and independent of the direction of emission or absorption.

Writing (1) in the form

$$I_\nu=E_\nu/x_\nu-\left(\frac{\partial I_\nu}{\partial s}+\frac{1}{c}\frac{\partial I_\nu}{\partial t}\right)x_\nu^{-1} \tag{14}$$

and introducing this value of $I_\nu$ in (13) and expanding the differentials with respect to $s$, we obtain, finally,

$$\frac{1}{c}\frac{\partial F_{\nu x}}{\partial t}+x_\nu F_{\nu x}=-\frac{\partial P_{xx}}{\partial x}-\frac{\partial P_{xy}}{\partial y}-\frac{\partial P_{xz}}{\partial z}+S_{\nu x} \tag{15}$$

where

$$\left.\begin{aligned} P_{xx}&=\int I_\nu\left(\frac{dx}{ds}\right)^2 dw\;; & P_{xy}&=\int I_\nu\frac{dx}{ds}\frac{dy}{ds}\,dw\;; \\ P_{xz}&=\int I_\nu\frac{dx}{ds}\frac{dz}{ds}\,dw\;; & S_{\nu x}&=\int E_\nu\frac{dx}{ds}\,dw\;. \end{aligned}\right\} \tag{16}$$

Thus the vector $\boldsymbol{F}_\nu$ satisfies the differential equation

$$\frac{1}{c}\frac{\partial \boldsymbol{F_\nu}}{\partial t}+x_\nu\boldsymbol{F_\nu}+\text{div.}\,\boldsymbol{P}=\boldsymbol{S_\nu} \tag{17}$$

where $\boldsymbol{P}$ stands for the symmetric tensor of the second rank, the components of which are $P_{xx}$, $P_{xy}$, $P_{xz}$, $P_{yy}$, $P_{yz}$, $P_{zz}$, and which henceforth will be referred to as the "flux tensor."

5. It is of great interest for stellar theory to derive the most general conditions which must be complied with in order that the tensor $\boldsymbol{P}$ shall reduce to an invariant. The principal diagonal components of the tensor are then equal, while the skew components are all zero. Introduce angular co-ordinates of direction $\theta$ and $\phi$ by the expressions

$$\frac{dx}{ds}=\sin\theta\cos\phi\;;\qquad \frac{dy}{ds}=\sin\theta\sin\phi\;;\qquad \frac{dz}{ds}=\cos\theta\;.$$

In these co-ordinates the element of solid angle has the form

$$dw=\sin\theta\,d\theta\,d\phi$$

and the equation for one of the skew tensor components, $P_{xy}$ say, thus becomes

$$P_{xy}=\int_{\theta=0}^{\pi}\int_{\phi=0}^{2\pi} I_\nu(\theta,\phi)\sin^3\theta\sin\phi\cos\phi\,d\phi\,d\theta\;.$$

This expression will be zero, provided $I_\nu\,(\theta,\phi)$ is an even function of $\phi$, and the same will be the case for the other skew components.

For practical applications the dependence of $P$ on $\theta$ is of most importance. Written out in full the expressions of $P_{xx}$, $P_{yy}$, $P_{zz}$ are

$$\left.\begin{aligned} P_{xx} &= \int_{\theta=0}^{\pi}\int_{\phi=0}^{2\pi} I_\nu(\theta,\phi)\sin^3\theta\cos^2\phi\,d\theta\,d\phi \quad (a) \\ P_{yy} &= \int_{\theta=0}^{\pi}\int_{\phi=0}^{2\pi} I_\nu(\theta,\phi)\sin^3\theta\sin^2\phi\,d\theta\,d\phi \quad (b) \\ P_{zz} &= \int_{\theta=0}^{\pi}\int_{\phi=0}^{2\pi} I_\nu(\theta,\phi)\cos^2\theta\sin\theta\,d\theta\,d\phi \quad (c) \end{aligned}\right\} \tag{18}$$

The equation $P_{xx}=P_{yy}$ is satisfied, provided $I_\nu(\theta, \phi)$ is an even function of $\phi$. The requirement $P_{xx}=P_{zz}$, on the other hand, restricts the dependence of $I_\nu$ on $\theta$. Assume $I_\nu$ to be developed in a power series of $\mu=\cos\theta$:

$$I_\nu=\sum_{n=0}^{\infty} A_n\mu^n\,. \tag{19}$$

The coefficients $A_n$ in this series will be functions of position and of the angle $\phi$. The condition $P_{xx}=P_{zz}$ now takes the form

$$\sum_{n=0}^{\infty}\int_0^{2\pi} A_n\,d\phi\int_{-1}^{1}\mu^{n+2}\,d\mu=\sum_{n=0}^{\infty}\int_0^{2\pi} A_n\cos^2\phi\,d\phi\int_{-1}^{1}(1-\mu^2)\mu^n\,d\mu\,. \tag{20}$$

As this condition imposes only a single restriction on an infinite number of coefficients $A_1, A_2 \,.\,.\,.\,.\, A_\infty$, it is clear that the desired result can be attained in an infinite number of ways. The case of special interest for practical applications occurs when only the few first terms in the series (19) are appreciable and the coefficients $A_n$ are independent of $\phi$. For the zero term alone, that is, when $I_\nu$ is independent of $\mu$, relation (20) is satisfied identically. This is also the case for the first-power term and all terms involving odd powers of $\mu$. The terms involving even powers of $\mu$ will, however, not drop out of formula (20). Thus the form

$$I_\nu(\mu)=A_0+A_1\mu+A_2\mu^2 \tag{21}$$

cannot be reconciled with the requirement $P_{xx}=P_{zz}$ unless $A_2=0$. As soon as terms beyond $A_3$ are included, the coefficients may be so adjusted as to comply with the requirement without putting any of them equal to zero. The foregoing result is of interest in so far as it shows that, in the limiting case when the deviations of $I_\nu$ from perfect spherical symmetry are very small, the tensor $\boldsymbol{P}$ deviates very little from an isotropic potential function, and that the tensorial nature becomes apparent as soon as the second-order term in (19) is of importance.

For the case that $A_2$ is zero in (21) we have

$$P_{xx}=P_{yy}=P_{zz}=2\pi\int_{-1}^{+1}(A_0+A_1\mu)\mu^2\,d\mu=\frac{4\pi}{3}A_0\,.$$

The energy density of the radiation field per unit frequency is, on the other hand,

$$A_\nu=\frac{2\pi}{c}\int_{-1}^{+1}(A_0+A_1\mu)d\mu=4\pi\,\frac{A_0}{c}$$

or

$$P_{xx}=\frac{c}{3}A_\nu\,. \tag{22}$$

Thus, for the limiting case in question, the only surviving components of the flux tensor $\boldsymbol{P}$ are equal to one-third of the energy density of radiation, multiplied by the velocity of light. From expressions (18) it will further be noticed that (22) gives a good approximation in all cases in which the term in $I_\nu$, which is independent of $\theta$ and $\phi$, is large compared to the sum of the terms containing $\theta$ and $\phi$. This circumstance justifies the application of (22) to most problems of transmission of radiation in the interior of a star.[1]

The foregoing considerations all refer to radiation in a specified spectral interval. Integrating $\boldsymbol{F}_\nu$ over all frequencies, we obtain a vector

$$\boldsymbol{F}_r=\int_0^\infty \boldsymbol{F}_\nu\,d\nu \tag{23}$$

which describes the combined flow of radiation for all frequencies.

6. Consider a closed surface $S$ fixed in space. The energy which at any time is contained within $S$ is the sum of three terms: the

---

[1] *Monthly Notices, R.A.S.*, **84**, 52, 1924.

electromagnetic energy of radiation, the thermal and subatomic energy, and the macroscopic kinetic energy of the substance. The corresponding energy densities we denote by $E_e$, $\rho E$, and $\frac{1}{2}\rho V^2$, $\rho$ and $V$ being mass-density and vectorial velocity of the substance at the point in question. The change in the total energy within $S$ which takes place in the time element $dt$ is thus

$$dt\int\left\{\frac{\partial E_e}{\partial t}+\frac{\partial}{\partial t}(\rho E)+\frac{\partial}{\partial t}(\tfrac{1}{2}\rho V^2)\right\}d\tau\,, \tag{24}$$

the integration being extended to the volume inclosed by the surface $S$. This energy must be equal to the sum of the net amount of energy which in the same time interval flows through the surface, and the work performed on the substance within the surface by external forces.

It is convenient to separate from the flux of internal and thermal energy a term $\rho E_s V$ which gives the flux of subatomic energy, the interatomic energy due to rotation of molecules, the excitation of atoms to higher quantum states, etc., $\rho E_s$ being the density of this part of internal energy. The total flux of translational energy of the atoms, on the other hand, is calculated as follows: Denote the velocity of *an individual atom* by $V_i$ and write

$$V_i=V+V_r \tag{25}$$

where $V_r$ is the random velocity of thermal agitation. If we could neglect the effect of collisions between the atoms, the total flux of translational kinetic energy would be given by the expression

$$F_t=\sum_i\left\{\frac{m_i}{2}V_i^2V_i\right\} \tag{26}$$

where $m_i$ is the mass of the $i$th atom and where the summation is to be extended to all atoms in unit volume. The collisions we take account of by introducing in (26) a zero-dimensional quantity $P_i$ which is a function of the mean free path of the atoms in question. Expanding (26) by using (25) we obtain

$$F_t=\sum_i\frac{m_i}{2}P_i\{V^2V+V_r^2V+V_r^2V_r+2(VV_r)V_r+2(VV_r)V+V^2V_r\}\,. \tag{27}$$

The first term in this expression gives the flux of macroscopic kinetic energy $\frac{1}{2}\rho V^2 \boldsymbol{V}$. The second and third terms give the flux of thermal energy, the second term corresponding to a flux

$$\rho E_t \boldsymbol{V}\ ; \qquad \rho E_t = \sum_i \frac{m_i}{2} P_i V_r^2$$

where $E_t$ is the thermal translational energy of the atoms per unit mass. The third term corresponds to what we are accustomed to call the "conductive flux of energy," which we shall denote by $\boldsymbol{F}_c$. The $x$-component of the fourth term we write in the form

$$V_x \sum_i m_i P_i V_{rx}^2 + V_y \sum_i m_i P_i V_{rx} V_{ry} + V_z \sum_i m_i P_i V_{rx} V_{rz} \tag{28}$$

which shows that this term is nothing but the inner product of the velocity $\boldsymbol{V}$ with the (symmetric) hydrodynamic stress tensor. It is customary to separate the hydrostatic pressure $p$ from the frictional terms in this tensor, and thus to write its components in the form $p+\pi_{xx}$; $p+\pi_{yy}$; $p+\pi_{zz}$; $\pi_{xy}$; $\pi_{xz}$; $\pi_{yz}$. The last two terms in (27) disappear identically. Thus, finally, the expression for $\boldsymbol{F}_t$ is

$$\boldsymbol{F}_t = \boldsymbol{F}_c + \tfrac{1}{2}\rho V^2 \boldsymbol{V} + \rho E_t \boldsymbol{V} + p\boldsymbol{V} + (\boldsymbol{V}\boldsymbol{\pi})\ . \tag{29}$$

If $f$ is the external force per unit mass, there will be an additional increase in energy per unit time and volume of amount $\rho(\boldsymbol{f}\boldsymbol{V})$. Adding up all these terms, we find that expression (24) must be equal to

$$\int \rho(\boldsymbol{f}\boldsymbol{V})d\tau - \int \{\boldsymbol{F}_r + \boldsymbol{F}_c + (p+\rho E)\boldsymbol{V} + (\boldsymbol{V}\boldsymbol{\pi})\}_n dS \tag{30}$$

where the first integral is to be extended to the volume within $S$, and the second to the surface $S$ itself, the index $n$ meaning that the components along the outward normal to $dS$ are to be taken for the vectors inclosed in brackets. Transforming the surface integral into a volume integral by Gauss's theorem, and remembering that the surface $S$ is arbitrary and thus may be infinitesimal, we find by combination of (24) and (30)

$$\frac{\partial E_c}{\partial t} + \frac{\partial}{\partial t}(\rho E) + \frac{\partial}{\partial t}\left(\tfrac{1}{2}\rho V^2\right) + \operatorname{div}\{\boldsymbol{F}_r + \boldsymbol{F}_c + (\rho E + p)\boldsymbol{V} + (\boldsymbol{V}\boldsymbol{\pi})\} = \rho(\boldsymbol{f}\boldsymbol{V})\ . \tag{31}$$

This expression may be further simplified by using the hydrodynamical equations

$$\frac{\partial}{\partial t}(\rho V)=\rho f-\nabla p-\operatorname{div}\pi-\operatorname{div}M\,;\qquad \frac{\partial \rho}{\partial t}+\operatorname{div}\rho V=0 \tag{32}$$

where the tensor $M$ represents the macroscopic flow of momentum:

$$(\operatorname{div}M)_x=\operatorname{div}(\rho V_x V)\,,\quad \text{etc.}$$

Hence

$$\frac{\partial}{\partial t}\left(\tfrac{1}{2}\rho V^2\right)=\rho(fV)-(V\nabla p)-(V\operatorname{div}\pi)-\operatorname{div}\left(\tfrac{1}{2}\rho V^2 V\right). \tag{33}$$

By using this expression, (31) transforms into

$$\frac{\partial E_e}{\partial t}+\frac{\partial(\rho E)}{\partial t}+\operatorname{div}(F_r+F_c+\rho EV)=(V\operatorname{div}\pi)-\operatorname{div}(V\pi)\,. \tag{34}$$

For viscous fluids $\pi$ has the form

$$\left.\begin{array}{l}\pi_{xx}=\mu\operatorname{div}V-\lambda\dfrac{\partial V_x}{\partial x}\,;\quad \pi_{yy}=\mu\operatorname{div}V-\lambda\dfrac{\partial V_y}{\partial y}\,;\quad \pi_{zz}=\mu\operatorname{div}V-\lambda\dfrac{\partial V_z}{\partial z}\\[2ex] \pi_{xy}=-\tfrac{1}{2}\lambda\left(\dfrac{\partial V_x}{\partial y}+\dfrac{\partial V_y}{\partial x}\right);\quad \pi_{xz}=-\tfrac{1}{2}\lambda\left(\dfrac{\partial V_x}{\partial z}+\dfrac{\partial V_z}{\partial x}\right);\quad \pi_{yz}=-\tfrac{1}{2}\lambda\left(\dfrac{\partial V_y}{\partial z}+\dfrac{\partial V_z}{\partial y}\right).\end{array}\right\} \tag{35}$$

In these formulae $\lambda$ and $\mu$ are two coefficients of viscosity which, for the case of a gaseous medium, are connected by the relation $\lambda=3\,\mu$. Carrying out the differentiation processes involved, we find further[1]

$$\begin{aligned}\Phi=\operatorname{div}(V\pi)-V\operatorname{div}\pi&=\pi_{xx}\frac{\partial V_x}{\partial x}+\pi_{yy}\frac{\partial V_y}{\partial y}+\pi_{zz}\frac{\partial V_z}{\partial z}\\ &\quad+\pi_{xy}\left(\frac{\partial V_x}{\partial y}+\frac{\partial V_y}{\partial x}\right)+\pi_{xz}\left(\frac{\partial V_x}{\partial z}+\frac{\partial V_z}{\partial x}\right)+\pi_{yz}\left(\frac{\partial V_y}{\partial z}+\frac{\partial V_z}{\partial y}\right).\end{aligned} \tag{36}$$

---

[1] Denoting the co-ordinates by $x_1$, $x_2$, $x_3$, formula (36) may be written in the form

$$\operatorname{div}(V\pi)-V\operatorname{div}\pi=\sum_{i=1}^{3}\sum_{k=1}^{3}\pi_{ik}\frac{\partial V_i}{\partial x_k}. \tag{36a}$$

The right-hand side of (36*a*) is thus seen to be equal to the *spur* of the tensor product of $\pi$ with the derivative of $V$. (See Eddington's *Mathematical Theory of Relativity*, 1st ed., p. 58.)

With the aid of (35) and (36), equation (34) takes the final form

$$\frac{\partial E_e}{\partial t}+\frac{\partial}{\partial t}(\rho E)+\text{div}\,\{\boldsymbol{F}_r+\boldsymbol{F}_c+\rho E\boldsymbol{V}\}+p\,\text{div}\,\boldsymbol{V}=\Phi \qquad (37)$$

where

$$\Phi=2\lambda\left\{\left(\frac{\partial V_x}{\partial x}\right)^2+\left(\frac{\partial V_y}{\partial y}\right)^2+\left(\frac{\partial V_z}{\partial z}\right)^2+\tfrac{1}{2}\left(\frac{\partial V_x}{\partial y}+\frac{\partial V_y}{\partial x}\right)^2\right.$$
$$\left.+\tfrac{1}{2}\left(\frac{\partial V_x}{\partial z}+\frac{\partial V_z}{\partial x}\right)^2+\tfrac{1}{2}\left(\frac{\partial V_y}{\partial z}+\frac{\partial V_z}{\partial y}\right)^2-\frac{\mu}{\lambda}(\text{div}\,\boldsymbol{V})^2\right\}. \qquad (38)$$

The quantity $\Phi$ represents the heat energy generated by friction per unit time and volume of the fluid.[1]

Equations (37) and (38) in conjunction with the hydrodynamical equations of motion (32) constitute the general system of differential equations by which the internal state of a star may be described as a function of the time.

If there is no friction in play ($\lambda=0$, $\mu=0$), and if there is no interchange of energy between radiation and matter ($\partial E_e/\partial t+\text{div}\,\boldsymbol{F}_r=0$) and no temperature conduction ($\boldsymbol{F}_c=0$), (37) reduces to the adiabatic relation

$$\frac{dE}{dt}+p\,\frac{d\,1/\rho}{dt}=0\,; \qquad \frac{d}{dt}=\frac{\partial}{\partial t}+(\boldsymbol{V}\nabla)\,. \qquad (39)$$

In the case of an ideal gas, $p$ is equal to $\frac{2}{3}\rho\,E$, and thus equation (39) may be written in the form

$$\frac{d}{dt}\left(E^{\frac{3}{2}}\rho^{-1}\right)=0\,, \qquad (40)$$

showing that $E^{\frac{3}{2}}\rho^{-1}$ remains constant for any individual mass element during its motion. If such a relation between $\rho$ and $E$ is fulfilled, not only for an individual mass element, but for all mass elements, the involved constant being the same, the star is said to be in *convective* equilibrium.

Consider, on the other hand, the case in which there is no motion. As the state of the system is thus stationary in time, no term involving the explicit time can appear in the equations. Thus the internal energy density of matter can at most involve a linear term in $t$, and equation (37) reduces to

---

[1] For an analogous, though less general, treatment of the problem considered in this section, see G. Kirchhoff, *Vorlesungen über Mathematische Physik*, 4 (Leipzig, 1894), 113.

$$\rho\frac{\partial E}{\partial t}+\text{div}\,\{F_r+F_c\}=0\;;\qquad \frac{\partial^2 E}{\partial t^2}=0 \tag{41}$$

which, in conjunction with the hydrostatic equations, is the general condition for the existence of radiative and conductive equilibrium.

Previous investigations concerning the internal constitution of the stars by other authors are, without exception, concerned with purely adiabatic or purely radiative equilibrium. In the sequel we shall consider cases which belong to neither of these classes, and, in particular, study the perturbing effect of local convective atmospheric currents on the flux of radiation from a star, the interior of which is in purely radiative equilibrium. This phase of the problem is likely to have an important bearing on sun-spot phenomena.

7. *Sun-spots.*—We are now prepared to discuss the following hypothesis concerning the origin of sun-spots, in so far as it relates to the reduction in temperature: *The sun as a whole is assumed to be in radiative equilibrium. The spots are regions in which this equilibrium is disturbed by vertical currents.* We shall approach the solution of this problem by successive approximations, beginning with the limiting case of radiative equilibrium.

For the case of radial symmetry the equations of radiative equilibrium may be written in the form

$$\left.\begin{array}{c} 4\pi\rho\varepsilon=\dfrac{1}{r^2}\dfrac{d}{dr}(r^2F_r)\;;\qquad 4\pi\rho G=-\dfrac{1}{r^2}\dfrac{d}{dr}(r^2f)\;;\qquad -4\pi\varepsilon=\dfrac{\partial E}{\partial t}\;; \\ \dfrac{dP}{dr}=-\rho f \end{array}\right\} \tag{42}$$

where $r$ is the distance from the stellar center to the point in question, $F_r$ the radial flux of radiation, $G$ the constant of gravitation, $f$ the gravitational acceleration, and $P$ the sum of gas pressure and radiation pressure. The weak point in all existing theories of stellar constitution lies in the fact that the quantity which we have denoted by $\varepsilon$ is entirely unknown; and we must proceed tentatively by testing different hypotheses concerning the nature of this quantity. The common practice is to assume $\varepsilon$ constant; in treating problems of stellar atmospheres it is frequently put equal to zero. Such a procedure has, of course, only a heuristic value, but we shall follow it here because the exact value of $\varepsilon$ does not greatly affect the results. For constant $\varepsilon$ it follows from (42) that

$$F_r = \lambda - \frac{\varepsilon}{G} f \qquad (43)$$

where $\lambda$ is a constant. As $f$ can vary but little in the stellar atmosphere, this means that $F$ is practically constant throughout the surface layer of the star. This result is not changed by assuming $\varepsilon$ to be zero, and indicates simply that we assume the bulk of the radiation to originate in the interior of the star and not in the surface region under consideration.

The flux vector $\boldsymbol{F}_r$ we assume to be of the form

$$\boldsymbol{F}_r = -\frac{A}{\rho x} \nabla U \qquad \text{or} \qquad F_r = -\frac{A}{\rho x} \frac{\partial U}{\partial r} \qquad (44)$$

throughout the whole atmosphere, where $U$ is the energy density of radiation, $A$ a constant, and $x$ the mass absorption coefficient, averaged in a certain way.[1] It follows directly from (22) that (44) is the limiting form for the case of the deep interior of the star, where the asymmetry in the radiant field is small. It is also the limiting form for the flux near the limit of the solar surface, where the radiation is approximately tubular, as considered in the Schuster-Schwarzschild approximation; but the constant $A$ will be several times larger in the latter case than in the former. Assuming $x$ to be a constant in (38), eliminating $dr$ from the hydrostatic equation in (42) by using (44), and integrating, we obtain

$$P = \frac{fA}{F_r x} (U - U_0) + \beta U_0 ; \qquad 1 > \beta > \tfrac{1}{3} \qquad (45)$$

where $U_0$ is the energy density of radiation corresponding to the temperature of matter at the top of the atmosphere. Hence, by Stefan's law, $P$ will be sensibly proportional to the fourth power of the temperature $T$ as soon as we are so far down in the atmosphere that $U_0$ is small compared to $U$. This result depends little upon the assumed constancy of $x$. Using, for instance, the formula

---

[1] *Monthly Notices, R.A.S.*, 84, 525, 1924.

$$x = \text{const. } \rho T^{-3}\ , \tag{46}$$

which may give a better approximation in consideration of the conditions in the star's interior,[1] we find, similarly, radiation pressure being neglected,

$$P = \text{const. } U \sqrt{1 - U_0^2/U^2} \tag{47}$$

which, for the case of the stellar photosphere, does not differ essentially from (45). Hence, for an atmosphere in radiative equilibrium, we assume that the gas pressure falls off as the fourth power of temperature. The mass density will consequently be proportional to the temperature in the third power. This result will be used in what follows.

As a next step we consider the case of an atmosphere in radiative equilibrium except for isolated places where local vortices and convection currents disturb the equilibrium conditions. We neglect the effect of friction and temperature conduction, put ε equal to zero, assume the state to be stationary in time, and write (37) in the consequent form

$$\operatorname{div} \boldsymbol{F}_r = \left\{ V\left( \nabla P - \rho \nabla E - \rho \nabla \frac{P}{\rho} \right) \right\}\ . \tag{48}$$

For an ideal gas mixture we have

$$P = \tfrac{2}{3} \rho E$$

and consequently

$$\nabla P - \rho \nabla E - \rho \nabla \frac{P}{\rho} = \tfrac{2}{3} E \nabla \rho - \rho \nabla E\ . \tag{49}$$

The vectors $\nabla \rho$ and $\nabla E$ may point in slightly different directions, but it lies in the nature of our assumptions that this difference will be small, and we assume that a good approximation will be obtained by taking $\rho$ a function of $E$. Thus for $\rho$ proportional to $E^n$, expression (49) assumes the form

$$\frac{n - \frac{3}{2}}{n + 1} \nabla P\ . \tag{50}$$

---

[1] *Mt. Wilson Contr.*, No. 296; *Astrophysical Journal*, **61**, 424, 1925.

If $n$ is equal to $\frac{3}{2}$, this expression is zero, and we have the case of convective equilibrium (cf. equation 40). The value of $n$ will, however, be considerably larger than $\frac{3}{2}$, since that corresponding to radiative equilibrium is of the order of 3. Thus

$$\alpha = \frac{n-\frac{3}{2}}{n+1} \tag{51}$$

is a positive quantity between zero and $\frac{3}{8}$. For small values of the vertical acceleration, the hydrostatic equation in (42) will give a good approximation to the pressure gradient, and thus (48) may be brought into the final form

$$\operatorname{div} \boldsymbol{F}_r = \alpha\rho(Vf) \; . \tag{52}$$

This equation expresses the fact that, apart from the multiplier $\alpha$, the increase in intensity of the flux of radiation is balanced by the work done by the gravitational forces on the streaming masses.

To obtain the total loss in intensity of radiation caused by local stationary convection current, we integrate (52) throughout a tube which runs parallel to the direction of $F$ from the base of the current to the top of the stellar atmosphere. Let $\sigma_1$, $\sigma_2$ be the lower and upper cross-sections of this tube, and $F_1$, $F_2$ the mean values of $F_r$ over $\sigma_1$ and $\sigma_2$, respectively. For the case under consideration the difference between $\sigma_1$ and $\sigma_2$ will be neglected, and the tube assumed to be straight, and of length $H$. The volume of the tube is thus $\sigma H$. Transforming the volume integral over the div-expression in (52) into a surface integral by Gauss's theorem, and denoting mean values over the volume $\sigma H$ by a horizontal bar, we find

$$F_2 - F_1 = \bar{\alpha} H \overline{V_z f} \bar{\rho} \tag{53}$$

where $V_z$ denotes the vertical component of the velocity. A rigorous test of this formula is not possible, because of our ignorance of most of the quantities which enter; but, on the assumption that (53) is true, it may be found useful in various ways. We know, for instance, with fair certainty that in the case of sun-spots the value of $\bar{\rho}$ cannot be much larger than $10^{-6}$ g/cm$^3$ and that $V_z$ cannot much exceed 10 km/sec. The temperature of the spots is frequently found to be about 1000° K below the average temperature of the solar surface, which is of the order 6000° K. Hence, by Stefan's law,

$$F_1-F_2=\tfrac{1}{2}F_1=4\,.\,10^{10}\ \text{c.g.s.}$$

Using these data and the limiting value $\frac{3}{8}$ for $\alpha$, we find from (47) that the thickness of a sun-spot cannot be less than fifty kilometers. This value is very small compared to the horizontal extension of spots, and it is, therefore, possible to assume very much smaller values of $\bar{\rho}$ and $V_2$ without arriving at improbably large values of the vertical thickness.

A more refined test of the theory is scarcely to be obtained, even with considerably improved observational material; and we must, provisionally, be content with the result that sun-spots may be the natural results of solar photospheric convection currents of moderate strength, even though observations do not provide a definite proof of this conclusion.[1]

7. *Solar rotation.*—It is a significant fact that the sun does not rotate like a rigid body for which the instantaneous angular velocity is the same for all mass elements. In the reversing layer of the sun the angular velocity $W$ follows the law[2]

$$W=W_0+W_1\cos^2\phi \tag{54}$$

where $\phi$ is the solar latitude; $W_0$ and $W_1$ are constants. It is naturally to be expected that the stars in general will exhibit similar deviations from a state of uniform rotation, which we shall call the *general circulation* of the star, in contradistinction to regions of local circulation such as sun-spots.

---

[1] Bjerknes (*Comptes Rendus*, **182**, 48, 1926) has suggested that the depression of the isothermal surfaces in a sun-spot may be connected with a special kind of horizontal circulation [cf. formula (66) of this paper]. Although the assumptions underlying the quantitative estimates in Bjerknes' paper may differ widely from actual conditions, it seems that a structure of the horizontal velocity field of a sunspot, essentially of the kind contemplated by Bjerknes, may just be necessary in order to produce the vertical motion contemplated in the foregoing theory, and the two theories may, therefore, be consistent in the end. For a further development of this theory, see also Bjerknes, *Mt. Wilson Contr.*, No. 312; *Astrophysical Journal*, **64**, 93, 1926.

[2] W. S. Adams, "An Investigation of the Rotation Period of the Sun," *Carnegie Institution Publications*, No. 138, p. 130.

The origin of the general circulation of the sun is probably similar in nature to that of the terrestrial atmosphere. The terrestrial circulation is maintained by the systematically higher temperature of the equatorial air masses relative to the polar masses, which disturbs the conditions of hydrostatic equilibrium and starts the complicated system of air currents between equatorial and polar regions. Although the general circulation of the terrestrial atmosphere arises from non-uniform heating *from without*, that of the sun may, on the other hand, be caused by non-uniform heating *from within*.

In order to see how a permanent circulation may thus be started, consider the case of a star having a steady motion such that the acceleration of an individual mass element arises from a potential $\Omega$. This implies the existence of a velocity potential $\omega$ which is connected with $\Omega$ by the relation[1]

$$\Omega=\frac{\partial\omega}{\partial t}+\tfrac{1}{2}(\nabla\omega)^2\ ; \qquad V=\nabla\omega\ ; \qquad \frac{dV}{\partial t}=\nabla\Omega\ .$$

Denoting gas *plus* radiation pressure by $P$, and the gravitational potential by $\phi$, we obtain the equations of motion in the form

$$\frac{1}{\rho}\nabla P=\nabla(\phi-\Omega)\ ; \qquad -\nabla^2\omega=\frac{d\rho}{\rho dt}\ , \tag{55}$$

frictional terms being neglected. Operating by curl on both sides of this equation, we find that the vector product of $\nabla\rho$ and $\nabla P$ is zero, and hence that these two vectors are parallel, and, by (55), parallel to $\nabla(\phi-\Omega)$. The surfaces of constant density and pressure will therefore coincide with the surfaces,

$$\phi-\Omega=\text{const.}\ ,$$

which we shall call "level surfaces." As the temperature is a function of density and pressure, it follows that temperature will also be constant over a level surface.

The thermal structure of the star is essentially determined by the distribution of energy-generating sources, as specified by the function $\varepsilon$ [cf. equation (41)]. Except for a transition layer somewhere in the stellar atmosphere, the flux vector will have the form (44). Since $U$ is a function of temperature only, the normal surfaces of $F_r$ are level surfaces. Denoting $\phi-\Omega$ by $\psi$, we may thus write

---

[1] See H. Lamb, *Hydrodynamics*, 5th ed. (Cambridge, 1924), art. 20.

$$F_r=-A\nabla\psi \tag{56}$$

where $A$ is some function of $\psi$, and by (37) and (41),

$$4\pi\varepsilon\rho=\text{div } F_r-P\text{ div } V=-A\nabla^2\psi-\frac{\partial A}{\partial\psi}(\nabla\psi)^2-P\nabla^2\omega \tag{57}$$

where, by Poisson's equation,

$$\nabla^2\psi=-4\pi G\rho-\nabla^2\Omega\,. \tag{58}$$

Although it is not known just what law $\varepsilon$ will follow, it is a fair guess that for regions in the same star having the same temperature and density $\varepsilon$ will also be the same. Thus $\varepsilon$ should be constant over a level surface: and hence, by (57),

$$A\nabla^2\psi+\frac{\partial A}{\partial\psi}(\nabla\psi)^2+P\nabla^2\omega=\text{function of }\psi\,. \tag{59}$$

In case of rigid rotation with constant angular velocity $W$

$$\nabla^2\Omega=-2W^2\,;\qquad \nabla^2\omega=0\,.$$

Since $(\nabla\psi)^2$ varies over a level surface, it is, by (59), necessary that $A$ be independent of $\psi$; and hence (57) assumes the form

$$\varepsilon=\text{const.}\left(1-\frac{W^2}{2\pi G\rho}\right)\,, \tag{60}$$

a relation first derived by von Zeipel.[1] If the internal heating system of the star does not conform to this particular law, rigid rotation becomes impossible, and a more general kind of motion will take its place. It seems physically impossible, however, as pointed out by Eddington,[2] that this law should be followed near the stellar surface, since $\varepsilon$ becomes negative in the region where $\rho<W^2/2\pi G$. Near the surface of a rotating star we must, therefore, always expect some kind of general circulation.

The result embodied in equation (60) is evidently of a more restrictive character than the analogous criterion of stability established by Poincaré,[1] which we shall recall briefly. If a star rotating with constant angular velocity $W$ is to remain in permanent equilibrium, it is necessary that the apparent force be directed inward all over the surface $S$ which forms the free surface of the star. Thus we have the condition that the integral of $\partial\psi/\partial n$ over the surface $S$ must be negative, $n$ denoting the outward normal to $S$. Using Gauss's theorem and equation (58), we thus have the relation

---

[1] *Monthly Notices, R.A.S.*, **84**, 665, 1924.

[2] *The Observatory*, 48, 73, 1925.

$$\int_S \frac{\partial\psi}{\partial n}\,dS = -\int_{\text{vol. } S} (4\pi G\rho + \nabla^2\Omega)\,d\tau\ . \tag{61}$$

Let $\bar{\rho}$ denote the mean density of the star, defined as total mass divided by total volume, which latter may be denoted by $T$. For rigid rotation $\nabla^2\Omega = -2W^2$, and the foregoing equation takes the form

$$\int_S \frac{\partial\psi}{\partial n}\,dS = -2T(2\pi G\bar{\rho} - W^2)\ . \tag{62}$$

For equilibrium to be possible the right-hand expression must be negative, and therefore

$$\frac{W^2}{2\pi G\bar{\rho}} < 1 \qquad \text{or} \qquad P > \frac{3\cdot 1}{\sqrt{\bar{\rho}}}\ \text{days} \tag{63}$$

where $P$ is the period of rotation, and $\rho$ is measured with the density of air as unity.

It seems to be implicitly assumed by all investigators of the theory of rotating stars that if a star, originally rotating with constant angular velocity, enters a state in which relation (63) is violated, cataclysmic motion must occur, resulting in fission or formation of a sharp edge from which matter is thrown off continuously. These conclusions, however, rest upon the hypothesis that the stars will always retain a state in which the angular velocity is the same for all mass elements. The impossibility of this hypothesis is clearly shown, however, by von Zeipel's relation (60); and in the sequel we shall examine some simple cases and show how a star may take up a state of motion with varying angular velocity, so as to conform to particular laws for the generation of stellar energy.

---

[1] *Figures d'Équilibre d'une Masse Fluide* (Paris, 1902), p. 11.

In examining the characteristics of the resulting motion, we shall first show that it is not sufficient to assume the angular velocity to be a function of only the distance $R$ from the axis of rotation. For in this case an acceleration potential exists:

$$\Omega = -\int W^2(R)R\,dR\ ; \qquad \nabla^2\Omega = -2W^2 - R\frac{\partial W^2}{\partial R}\ ; \qquad \nabla^2\omega = 0 \qquad (64)$$

and equation (59) must be satisfied. Even without detailed calculations, it is seen that the form (64) of $\Omega$ is, in general, incompatible with (59), since $\Omega$ will be constant over a certain class of cylindrical surfaces, while $(\nabla\psi)^2$ will be constant over certain oblate spheroidal surfaces, not very different from the surfaces of constant $\psi$.

In the next step we give up the assumption that an acceleration potential exists, but still assume that the motion takes place in circles around a fixed axis, such that the angular velocity $W$ is now also a function of the distance $z$ from the equatorial plane. Denoting by $r$ the radius vector from the center of the star to the point in question the hydrodynamic equation of motion takes the form

$$[WV] = \nabla\phi - \frac{1}{\rho}\nabla P\ ; \qquad V = [Wr]\ , \qquad (65)$$

viscosity being neglected. Operating by curl on both sides of (62), we find, after some calculations,[1]

$$2V\frac{\partial W}{\partial z} = [\nabla\alpha\nabla P]\ ; \qquad \alpha = \frac{1}{\rho}\ . \qquad (66)$$

This relation shows that when the angular velocity varies in a direction parallel to the axis of rotation, the isobaric and isosteric

---

[1] By ordinary vector formulae: curl $[WV] = V\,\mathrm{div}\,W + (W\nabla)V - (V\nabla)W - W\,\mathrm{div}\,V$. Since $\mathrm{div}\,V = 0$ and $W$ remain unaltered for an individual particle during the motion the last two terms disappear. Remembering that $W$ has only a $z$-component, the first two terms may be written in the form $\frac{\partial}{\partial z}(W_zV)$, and, by the fact that $V$ is proportional to $W_z$ and otherwise independent of $z$, it follows that

$$\frac{\partial}{\partial z}(W_zV) = 2\frac{\partial W_z}{\partial z}V\ .$$

Hence the left side of (66). The right side follows from the formula curl $\mu A = \mu$ curl $A + [\nabla\mu A]$ by putting $\mu = \alpha$ and $A = \nabla P$, and remembering that curl $\nabla P$ is identically zero.

surfaces will be inclined to each other by a finite angle. The flux of radiation, since temperature is a function of both density and pressure, will be parallel neither to the pressure nor to the density gradient. The variation of density along an isobaric surface is directly determined by (63). If $W$ is directed along the positive $z$-axis, as we have assumed, the vectors $\nabla P$ and $\nabla \alpha$ will lie in planes through this axis, and $V$ will be directed parallel to the positive $y$-axis.

Consider conditions in the upper right quadrant of the $xz$-plane. With the foregoing conventions the positive direction of the angle $\varphi$ between the vectors $\nabla \alpha$ and $\nabla P$ is to be counted in the direction from the positive $z$ to the positive $x$-axis. If $\partial W/\partial z$ is positive, the right-hand side of (63) must also be positive, meaning that $\varphi$ is less than $\pi$ which again means that at that point the isobaric surfaces ($P =$ const.) are *more* oblate than the isosteric surfaces ($\alpha =$ const.). If $\partial W/\partial z$ is positive all the way from pole to equator over a particular isobaric surface, this surface will consequently be coldest at the pole and hottest at the equator. If $\partial W/\partial z$ is negative, conditions are exactly reversed.[1]

We have thus seen that by suitably varying the angular velocity parallel to the axis of rotation, the isobaric surfaces can be tilted with respect to the isosteric and isothermic surfaces to any desired angle, so that any particular law of generation of energy can be complied with. A certain amount of convection is, however, necessary in all cases, because of internal friction. Let us assume for a moment that the angular velocity is adjusted to the correct tilt of the surfaces. The effect of viscosity will always be to reduce this tilt, and a reinforcement of the motion can be obtained only by introducing a current system from pole to equator, or vice versa, which by the principle of conservation of angular momentum, will increase or decrease the angular velocity by any required amount. From the previous calculations concerning the temperature of sun-spots it may be concluded, however, that any large-scale, vertical convection currents possibly existing in the sun must be of an exceedingly feeble intensity in order not to disturb the uniform illumination of the solar surface. It seems doubtful, therefore, that such currents can, for the case of the sun, materially affect the distribution of different elements in the sun's interior, as has been suggested.[1]

---

[1] These results were originally found by Bjerknes, "Dynamics of the Circular Vortex," *Geofysiske Publikationer*, **2**, No. 4, 1921, p. 44 ($A$), p. 45 ($B$).

In order to illustrate the conditions more clearly, consider a simple example. Assume the liberation of energy to be proportional to density, and the flux vector to have the form

$$F_r = -\nabla U$$

where $U$ is a function of the absolute temperature $T$ only. We have then the following system of equations:

$$\left.\begin{array}{lllll} -W^2R=\dfrac{\partial\phi}{\partial R}-\dfrac{1}{\rho}\dfrac{\partial P}{\partial R} & (a) & \nabla^2 U=-4\pi\varepsilon\rho & (c) & P=k\rho T \quad (e) \quad k=\text{const.} \\ 0=\dfrac{\partial\phi}{\partial R}-\dfrac{1}{\rho}\dfrac{\partial P}{\partial z} & (b) & \nabla^2\phi=-4\pi G\rho & (d) & \varepsilon=\text{const.}\,, \end{array}\right\} \quad (67)$$

frictional terms as well as radiation pressure being neglected. By using $(e)$, equations $(a)$ and $(b)$ may be written in the form

$$W^2=\frac{1}{R}\frac{\partial}{\partial R}(kT-\phi)+k\frac{T}{R}\frac{\partial \log\rho}{\partial R} \qquad (68)$$

$$\frac{\partial\log\rho}{\partial z}=-\frac{1}{kT}\frac{\partial}{\partial z}(kT-\phi)\;. \qquad (69)$$

These equations show that for the entire class of solutions of $(c)$ and $(d)$, in which the boundary conditions for $U$ and $\phi$ are the same, in consequence of which $T$ is a function of $\phi$, the density is given by an expression of the form

$$\log\rho=-\int\frac{d(kT-\phi)}{kT}+\text{function of } R\;. \qquad (70)$$

By introducing expression (70) in (68) it follows that the angular velocity is given by the expression

$$W^2=kTA(R) \qquad (71)$$

where $A$ is an arbitrary positive function of $R$ only.

Thus, passing along a line parallel to the axis of rotation, $W$ increases from the surface to the interior, being proportional to the square root of the temperature, and the star will, by (66), be hottest at the poles and coldest at the equator. For cases which are more general than those considered above, the function $A$ will probably be completely determined except for an arbitrary constant. If this should prove to be true, observations of the rotation of the sun might provide a direct source of information about the origin of the energy of solar radiation.

---

[1] A. S. Eddington, *The Observatory*, 48, 73, 1925.

Mount Wilson Observatory
March 1926

Contributions from the Mount Wilson Observatory, No. 314
Reprinted from the *Astrophysical Journal*, Vol. LXIV, pp. 136–141, 1926
Printed in the U.S.A.

# ON THE THEORY OF THE CONTINUOUS SPECTRUM OF THE CORONA

By EDISON PETTIT and SETH B. NICHOLSON

## ABSTRACT

*The distribution of energy in the coronal spectrum.*—Woltjer's calculations, based on scattering by free electrons, indicate that the ratio of far infra-red to visual radiation is greater for the corona than for the sun. A recalculation without his approximations gives an even richer infra-red radiation for the corona.

*Computation of the water-cell transmission of the coronal radiation.*—It is shown that, even with the revised calculations, the difference between the spectral distributions of energy in the coronal and solar radiations could not be detected by using the water cell to separate two spectral regions, as was done at the eclipse of January 24, 1925.

*Agreement of computed and observed water-cell transmissions.*—The theoretical water-cell transmission for the corona agrees as closely as can be expected with that observed by us at the eclipse of January 24, 1925.

In a recent paper, Woltjer[1] has calculated the distribution of energy in the continuous spectrum of the corona based on the scattering of radiation by free electrons. Two approximations are given, the first depending on the classical theory of scattering, and the second, which he accepted as more conclusive, depending on the introduction of the theory of quanta. The effect of positive ions is referred to, but their influence and that of neutral atoms is not discussed; hence the result tacitly assumes the corona to be an atmosphere of free electrons. The conclusion is that, while the continuous spectrum of the corona is practically identical in energy distribution with the solar spectrum in the photographic and visual region, it is much richer in energy in the far infra-red. It is our purpose to discuss the bearing of the radiometric observations on the author's theory.

In the approximations based on the classical theory of scattering Woltjer gives the following expression for the radiation scattered toward the earth from a point $P$ in the corona:

$$2\pi r_0^2\int_0^{\psi_0}\frac{I_\nu}{r^2}\cos\theta\sin\psi(1+\cos^2\chi\cos^2\alpha+\tfrac{1}{2}\sin^2\chi\sin^2\alpha)d\psi\ . \qquad (1)$$

---

[1] *Bulletin of the Astronomical Institutes of the Netherlands*, 3, 103, 1926.

To integrate this expression, he neglected the higher powers of $\chi$ and arrived at the approximate solution

$$F_\nu\left(1+\cos^2\alpha+\tfrac{1}{10}\,\frac{r_0^2}{\Delta^2}\,\sin^2\alpha\,\frac{15a_\nu+8b_\nu}{3a_\nu+2b_\nu}\right)\,, \tag{2}$$

where $F_\nu$ measures the energy of frequency $\nu$ in the mean solar spectrum, $a_\nu$ and $b_\nu$ are the coefficients of darkening for the solar atmosphere, and the relations

$$\frac{r_0}{\Delta}=1\,, \qquad \alpha=\frac{\pi}{2}$$

hold when the point $P$ is at the limb and on the sun.

If the higher powers of $\chi$ are not neglected, the solution for a point at the limb and on the sun is

$$F_\nu\left(1+\tfrac{1}{4}\,\frac{20a_\nu+7b_\nu}{3a_\nu+2b_\nu}\right)\,. \tag{3}$$

The coefficient of $F_\nu$ is the ratio of intensity of the coronal radiation to that of the integrated solar radiation for any frequency $\nu$. Table I gives the values of this ratio derived from Woltjer's expression (2) and from the rigorous expression (3) in units of their values for wave-length 0.3 $\mu$.

TABLE I

| Wave-Length | Approximate (2) | Rigorous (3) |
|---|---|---|
| $0\overset{\mu}{.}3$ | 1.00 | 1.00 |
| 0.6 | 1.03 | 1.15 |
| 1 | 1.04 | 1.23 |
| 2 | 1.05 | 1.27 |
| 3 | 1.05 | 1.27 |
| 4 | 1.05 | 1.28 |
| 5 | 1.05 | 1.28 |

It will be noted that the rigorous formula (3) indicates more infra-red radiation in the corona than formula (2).

Introducing the quantum relations, the author gives the coefficient of scattering, according to Pauli[1] and others, as proportional to

$$1+\frac{c^3}{8\pi h\nu^3}\,\rho_\nu\,, \tag{4}$$

---

[1] *Zeitschrift für Physik*, **18**, 283, 1923.

where the frequency of the incident and scattered radiation is taken to be the same, and the function is supposed to be roughly applicable to non-isotropic radiation.

In this expression, $\rho_\nu$ is the density of radiation at the point $P$, and is equal to

$$2\pi\frac{r_0^2}{c}\int_0^{\psi_0}\frac{I_\nu}{r^2}\cos\theta\sin\psi\, d\psi\ . \tag{5}$$

In the integration of (5) the higher powers of $\chi$ were again neglected with the following result:

$$\rho_\nu=\frac{F_\nu}{c}\left(1+\frac{1}{20}\frac{r_0^2}{\Delta^2}\frac{15a_\nu+8b_\nu}{3a_\nu+2b_\nu}\right)=\frac{F_\nu}{c}(1+\beta)\ . \tag{6}$$

Substituting in (4) the value of $\rho_\nu$ from (6) and taking

$$F_\nu=\frac{r_0^2}{\Delta^2}\frac{2\pi h\nu^3}{c}\frac{1}{e^{\left(\frac{h\nu}{kT_e}\right)}-1}\ ,$$

we find for the factor which expresses the dependence of the coefficient of scattering on $\nu$

$$1+\frac{1}{4}\frac{r_0^2}{\Delta^2}\frac{1+\beta}{e^{\left(\frac{h\nu}{kT_e}\right)}-1}\ . \tag{4a}$$

In evaluating this coefficient Woltjer neglected $\beta$. Integration of equation (5) without approximations gives for a point at the limb and on the sun

$$\rho_\nu=\frac{F_\nu}{c}\left(1+\frac{3a_\nu+b_\nu}{3a_\nu+2b_\nu}\right)=\frac{F_\nu}{c}(1+\beta_1)\ . \tag{6a}$$

Table II shows the factors of proportionality (4$a$) as derived by Woltjer, neglecting $\beta$, and as derived from equation (6$a$), including the value of $\beta_1$.

Here again the rigorous formula indicates more infra-red radiation than the approximate formula.

In discussing the observational data it will be recalled that the distribution of energy in the coronal spectrum was determined radiometrically at the eclipse of January 24, 1925, by measuring the water-cell transmission.[1] The transmission constants of this cell have already been given.[1] The distribution of coronal radiation under the conditions of observation may be computed by applying the theoretical factors given in Tables I and II to the intensities in the solar spectrum after transmission by the earth's atmosphere, and then applying the water-cell transmission constants to the resultant intensities. The data in Tables I and II refer to a point on the sun at the limb, and with less approximation to other points in the corona situated in the same line of sight. Since the intensity in the corona falls off rapidly with increasing distance from the limb, it is clear that points which approximate the conditions for which Tables I and II were computed will have the predominating effect; but these limitations should be kept in mind when comparing the theoretical and observational data.

---

[1] *Mt. Wilson Contr.*, No. 299; *Astrophysical Journal*, **62**, 202, 1925.

TABLE II

| Wave-Length | Approximate (2) | Rigorous (3) |
|---|---|---|
| 0$^{\mu}$3 | 1.00 | 1.00 |
| 0.6 | 1.00 | 1.01 |
| 1 | 1.02 | 1.04 |
| 2 | 1.10 | 1.19 |
| 3 | 1.20 | 1.38 |
| 4 | 1.30 | 1.58 |
| 5 | 1.40 | 1.78 |

If we could place equal confidence in the theories from which the values in Tables I and II are derived, the combined result, represented by the products of the two solutions, would be adopted as the more reliable; but since it is difficult to estimate the effect of several rather violent assumptions made in the applications of the theory of quanta, we give, in Table III, two solutions, one depending on the classical theory alone and one depending on the classical theory as modified by Woltjer's application of the quantum theory.

In Table III the numbers in the second column are proportional to the solar energy between the limits of wave-length indicated in the first column. These values, which were taken from Table 550 of the *Smithsonian Physical Tables* (7th rev. ed.), are for air-mass 3, which was traversed by the radiation. The third column gives the products of these values into the transmission coefficients of water-vapor inferred from Table 377 (*ibid.*) for 1 cm of precipitable water. No measures of precipitable water were made at this eclipse; but, considering the observing conditions, 1 cm is a reasonable estimate. A change of 50 per cent in this variable will scarcely affect the argument. The numbers in the third column therefore represent the energy distribution in the solar spectrum under the conditions of observation at the eclipse of January 24, 1925. It is not necessary to consider the reflection of silver, since it will have the same effect on the coronal and solar radiation, which are identical in the region of selective reflection.

---

[1] *Mt. Wilson Contr.*, No. 246; *Astrophysical Journal*, **56**, 295, 1922.

TABLE III

| Range of Wave-Length | Solar Energy | | Coefficient of Proportionality Corona/Sun | | Coronal Energy | |
|---|---|---|---|---|---|---|
| | Air-Mass 3 Dry | Air-Mass 3 $H_2O$, 1 cm | Table I | Tables II and I Combined | Classical | Modified |
| 0.3–0.4$\mu$ | 0.10 | 0.10 | 1.02 | 1.02 | 0.10 | 0.10 |
| 0.4–0.5 | 0.70 | 0.70 | 1.06 | 1.06 | 0.74 | 0.74 |
| 0.5–0.6 | 1.00 | 1.00 | 1.12 | 1.13 | 1.12 | 1.13 |
| 0.6–0.7 | 0.98 | 0.98 | 1.16 | 1.18 | 1.14 | 1.16 |
| 0.7–0.8 | 0.87 | 0.80 | 1.18 | 1.20 | 0.94 | 0.96 |
| 0.8–0.9 | 0.72 | 0.70 | 1.20 | 1.23 | 0.84 | 0.86 |
| 0.9–1.0 | 0.60 | 0.50 | 1.22 | 1.26 | 0.61 | 0.63 |
| 1.0–1.1 | 0.51 | 0.50 | 1.23 | 1.29 | 0.62 | 0.64 |
| Sum (0.3–1.1$\mu$) | ...... | 5.28 | ...... | ...... | 6.11 | 6.22 |
| 1.1–2.0 | 2.43 | 1.80 | 1.26 | 1.41 | 2.27 | 2.54 |
| 2.0–3.0 | 0.45 | 0.20 | 1.27 | 1.63 | 0.25 | 0.33 |
| 3.0–4.0 | 0.10 | 0.04 | 1.27 | 1.88 | 0.05 | 0.08 |
| 4.0–5.0 | 0.05 | 0.02 | 1.28 | 2.15 | 0.03 | 0.04 |
| Sum (0.3–5.5$\mu$) | ...... | 7.34 | ...... | ...... | 8.71 | 9.21 |
| $\frac{0.3\text{–}1.1\mu}{0.3\text{–}5.5\mu}=\left\{\text{Water-cell transmission}\right\}$ | ...... | 0.72 | ...... | ...... | 0.70 | 0.68 |

The fourth and fifth columns give the mean values of the coefficients of proportionality between the energies in the coronal and solar spectrum, computed according to the classical theory, and that modified by the quantum theory as outlined by Woltjer. Multiplying intensities of the solar radiation in the third column by these coefficients, we obtain the sixth and seventh columns, which represent the distribution of coronal energy according to these two theories, respectively.

While the water cell transmits some energy to 1.3 $\mu$, its practical limits are 0.3–1.1 $\mu$, the transmission between 1.1 and 1.3 $\mu$ being insignificant. The summations of the third, sixth, and seventh columns between the limits 0.3 and 1.1 $\mu$ then represent the energies isolated by the water cell, and those between the limits 0.3 and 5 $\mu$, the total energies in the solar spectrum and in the coronal spectrum as computed from theory. This shows that, according to the classical and the combined classical and quantum theories of scattering by free electrons, the water-cell transmissions of coronal radiation should be 70 and 68 per cent, respectively, as against 72 per cent for integrated solar radiation. These small differences are scarcely detectable by a single set of observations made at one eclipse even under the best observing conditions.

TABLE IV

| Source of Radiation | | Percentage of Energy 0.3–1.3$\mu$ | O−C | |
|---|---|---|---|---|
| | | | Classical | Modified |
| Calculated | Sun | 72. | .......... | .......... |
| | Corona, classical theory | 70. | .......... | .......... |
| | Corona, modified theory | 68. | .......... | .......... |
| Observed | Sun, Pettit and Nicholson | 71.4 | − 1. | − 1. |
| | Corona, Pettit and Nicholson | 77.6 | − 8. | −10. |
| | Corona, Stetson and Coblentz | 33. | +37. | +35. |

A comparison of the observed and calculated values is given in Table IV. The last column gives the differences between the observed and computed percentages of transmission, for both the classical theory and that modified by the theory of quanta as outlined by Woltjer. The first two pairs of values for O − C are probably not beyond the errors of observation, which may have either sign. It will be recalled that our observations with a thin glass screen showed no measurable radiation beyond 5.5 $\mu$ in the far infra-red, which is in agreement with the theory when we consider the negligible value of the energy in the solar spectrum in this region.

We wish to express our thanks to Mr. Rosseland for independent solutions and checks on points connected with the theory.

Mount Wilson Observatory
June 1926

Contributions from the Mount Wilson Observatory, No. 315
Reprinted from the *Astrophysical Journal*, Vol. LXIV, pp. 149–166, 1926
Printed in the U.S.A.

# REMARKS ON VARIOUS STATISTICAL PROPERTIES OF GALACTIC CEPHEIDS HAVING PERIODS LONGER THAN ONE DAY

By J. SCHILT[1]

## ABSTRACT

*Maximum frequency of Cepheids in different galactic longitudes.*—In the region of Sagittarius and Aquila the frequency-curve shows a maximum for log $P=0.84$. The maximum for other regions of the galaxy is for a decidedly shorter period. The period of maximum frequency for the Cepheids in the Small Magellanic Cloud is about the same as for the galactic Cepheids in the hemisphere opposite to the Sagittarius-Aquila region.

*Relation between magnitude, proper motion, and period.*—The present material shows that the median apparent magnitude, median proper motion, and median absolute magnitude are systematically small for log $P$ between 0.8 and 1.0. There is no decrease of apparent magnitude and proper motion for periods longer than ten days, as would be expected from a uniform distribution in density and velocity.

*Absolute magnitudes.*—The fact that the absolute magnitudes derived from the motions of the fainter Cepheids differ appreciably from the generally adopted values based on thirteen Boss stars indicates the importance of obtaining both accurate proper motions and additional radial velocities for these stars.

The present investigation is based upon the variable stars listed in the "Katalog und Ephemeriden veränderlicher Sterne für 1926,"[2] having periods between one and eighty days, which are not known to be eclipsing binaries. The number of these stars is one hundred sixty-three; twenty-one additional stars having Cepheid characteristics are of unknown period. Three groups have been formed according to period as follows:

| Group | Period in Days | Stars |
|---|---|---|
| I | 1–6 | 46 |
| II | 6–12 | 51 |
| III | 12–80 | 66 |

The definition of a Cepheid is rather vague, especially for stars of unknown spectrum. Constancy of period is not a reliable criterion, since variation in the period is not uncommon for true Cepheids and may amount, as in the case of ζ Geminorum,[3] to 10 per cent of the period. On the other hand, as observations accumulate, many stars will be found to have varying periods.

---

[1] Fellow of The International Education Board.

[2] *Vierteljahrsschrift der Astronomischen Gesellschaft*, **60**, 228, 1925.

[3] *See* W. Rabe, *Astronomische Nachrichten*, **219**, 129, 1923.

Although the spectral types have not always been given in the "Katalog," it is possible to make a rough division into spectral classes for the stars concerned:

| Group | A8 | G | K | M | Rp | Nb | Unknown |
|---|---|---|---|---|---|---|---|
| I. . . . . . . . . . . . . . . | 18 | 16 | 2 | 1 | 1 | . . . . . . | 10 |
| II. . . . . . . . . . . . . . | 15 | 17 | 3 | 1 | . . . . . . | . . . . . . | 13 |
| III. . . . . . . . . . . . . | 7 | 25 | 9 | 8 | 2 | 1 | 14 |

The rule that longer periods are correlated with more advanced spectral types seems to be confirmed by the frequencies of group III, as compared with those of groups I and II; but whereas the bulk of the stars in groups I and II are probably Cepheids, this is not certainly true for group III. The relative number of K and M stars in this group is larger than in the preceding groups, as is to be expected; but the group may include some Md variables, which are usually treated as a separate class, for it is difficult to decide where the longer-period Cepheids end and the class of long-period variables begins. For the present I have excluded all stars of known spectral type later than K and, moreover, the stars of group III of unknown spectral type. Two additional stars have also been excluded, viz., RU Doradus, which probably belongs to the Magellanic Cloud, and RX Camelopardalis, since the elements, $P = 7.908$, $M - m = 5.57$, give rise to doubt. The remaining stars for the three groups are forty-four, forty-eight, and forty-one in number, respectively.

The distribution in galactic longitude is given in Table I.

The mean of the galactic latitudes without regard to sign and the algebraical mean latitudes are also entered in the table. The difference in number for different galactic longitudes is for the most part spurious. The lack of Cepheids in longitudes 180° to 240°, or more accurately between the limits 173° and 230°, may, however, be real in part, since a considerable number of long-period and eclipsing variables are known in this region. The number of Cepheids found in different galactic longitudes is influenced by the study of special regions, but no such selective effect is to be expected in the distribution of periods among the different longitudes. Table I shows, however, that the number of stars of group I in the region 300° to 30° is very small as compared with those of groups II and III, the numbers being two, twenty, and twelve, respectively. It seems worth while, therefore, to investigate the distribution of periods more in detail.

The numbers of stars having different values of log $P$ ($P$ = period in days) have been entered in Table II for three intervals of galactic longitude, viz., 30°–150°, 150°–270°, and 270°–30°. Similar data for the Small Magellanic Cloud, taken from *Harvard Circular*, No. 280, have been added for comparison.

TABLE I

DISTRIBUTION OF CEPHEIDS IN GALACTIC CO-ORDINATES

| GAL. LONG. | GROUP I | | | GROUP II | | | GROUP III | | | TOTAL No. |
|---|---|---|---|---|---|---|---|---|---|---|
| | No. | Lat.* | Lat.† | No. | Lat.* | Lat.† | No. | Lat.* | Lat.† | |
| 0°– 30° .. | 0 | ...... | ...... | 5 | 9° | −4° | 5 | 10° | −7° | 10 |
| 30 – 60 .. | 2 | 6° | −4° | 3 | 6 | +1 | 5 | 6 | 0 | 10 |
| 60 – 90 .. | 8 | 4 | +4 | 3 | 1 | −1 | 1 | 2 | −2 | 12 |
| 90 –120 .. | 6 | 8 | +4 | 3 | 2 | −2 | 3 | 4 | 0 | 12 |
| 120 –150 .. | 2 | 11 | −11 | 3 | 1 | +1 | 3 | 10§ | −10§ | 8 |
| 150 –180 .. | 4 | 12 | −6 | 4 | 12 | +12 | 4 | 2 | 0 | 12 |
| 180 –210 .. | 0 | ...... | ...... | 0 | ...... | ...... | 1 | 0 | 0 | 1 |
| 210 –240 .. | 1 | 3 | −3 | 0 | ...... | ...... | 1 | 1 | +1 | 2 |
| 240 –270 .. | 15 | 2 | 0 | 7 | 4 | −1 | 10 | 4 | +1 | 32 |
| 270 –300 .. | 4 | 6 | −3 | 5 | 14 | −1 | 1 | 58 | +58 | 10 |
| 300 –330 .. | 0 | ...... | ...... | 4 | 10 | −8 | 1 | 4 | −4 | 5 |
| 330 –360 .. | 2 | 4 | −4 | 11 | 6‡ | −6‡ | 6 | 6 | +5 | 19 |

* Mean latitude without regard to sign.

† Algebraic mean latitude.

‡ Excluding RY Boötis, lat. +62°.

§ Excluding RS Ceti, lat. −52°.

The quantities $\Sigma\frac{1}{6}$ and $\Sigma\frac{1}{2}$, indicating the limits of log $P$ below which lie $\frac{1}{6}$ and $\frac{1}{2}$, respectively, of the stars, have been determined graphically from smoothed, integrated frequency-curves. The mean errors of the median values, $\Sigma\frac{1}{2}$, have been computed from the dispersion $\pm(\Sigma\frac{1}{2}-\Sigma\frac{1}{6})$. The results are in Table III.

The data of Table II are graphically represented in Figure 1, curves I–IV, the points representing means of three successive values. The maximum frequency from these plots is entered in the last column of Table III. As was to be expected from the data in

## TABLE II

FREQUENCIES OF LOG $P$ IN DIFFERENT LONGITUDES

| LOG $P$ | GALACTIC LONGITUDE | | | ALL | MAG. CLOUD |
|---|---|---|---|---|---|
| | 30°–150° | 150°–270° | 270°–30° | | |
| 0.00–0.20 | ... | ... | ... | ... | 4 |
| 0.20–0.25 | ... | 1 | ... | 1 | 2 |
| 0.25–0.30 | 1 | ... | ... | 1 | 6 |
| 0.30–0.35 | 1 | ... | ... | 1 | 5 |
| 0.35–0.40 | ... | ... | ... | ... | ... |
| 0.40–0.45 | ... | ... | 1 | 1 | 5 |
| 0.45–0.50 | 1 | 1 | ... | 2 | 5 |
| 0.50–0.55 | ... | 1 | 1 | 2 | 4 |
| 0.55–0.60 | 3 | 3 | ... | 6 | 7 |
| 0.60–0.65 | 4 | 3 | 1 | 8 | 9 |
| 0.65–0.70 | 3 | 5 | 1 | 9 | 12 |
| 0.70–0.75 | 5 | 5 | 1 | 11 | 6 |
| 0.75–0.80 | 5 | 2 | 3 | 10 | 4 |
| 0.80–0.85 | 1 | 4 | 6 | 11 | 5 |
| 0.85–0.90 | 1 | 2 | 4 | 7 | 1 |
| 0.90–0.95 | 1 | 1 | 3 | 5 | 2 |
| 0.95–1.00 | ... | 1 | 4 | 5 | 4 |
| 1.00–1.05 | 4 | 2 | 4 | 10 | 1 |
| 1.05–1.10 | 2 | 1 | ... | 3 | 2 |
| 1.10–1.15 | ... | 1 | 4 | 5 | 3 |
| 1.15–1.20 | 2 | 2 | ... | 4 | 3 |
| 1.20–1.25 | 4 | 1 | 3 | 8 | 4 |
| 1.25–1.30 | 1 | 2 | 1 | 4 | ... |
| 1.30–1.35 | ... | ... | 2 | 2 | ... |
| 1.35–1.40 | ... | 1 | ... | 1 | ... |
| 1.40–1.45 | ... | 3 | ... | 3 | 1 |
| 1.45–1.50 | ... | ... | ... | ... | 2 |
| 1.50–1.55 | ... | 1 | 1 | 2 | 2 |
| 1.55–1.60 | 2 | 1 | ... | 3 | ... |
| 1.60–1.65 | 1 | 1 | ... | 2 | 1 |
| 1.65–1.70 | 1 | 1 | ... | 2 | ... |
| 1.70–1.75 | ... | 1 | ... | 1 | ... |
| 1.75–1.80 | ... | ... | 1 | 1 | ... |
| 1.80–1.85 | ... | ... | 1 | 1 | 1 |
| 1.85–1.90 | ... | ... | 1 | 1 | ... |
| Totals | 43 | 47 | 43 | 133 | ... |

## TABLE III

MAXIMUM FREQUENCY AND MEAN ERROR

| Gal. Long. | $\Sigma \frac{1}{6}$ | $\Sigma \frac{1}{2}$ | $n$ | Mean Error | Max. Frequency |
|---|---|---|---|---|---|
| 30°–150° | 0.58 | 0.75 | 43 | ±0.03 | 0.70 |
| 150–270 | .55 | .78 | 47 | .03 | .70 |
| 270– 30 | .74 | .91 | 43 | .03 | .85 |
| Mag. Cloud | 0.38 | 0.62 | 103 | ±0.02 | 0.65 |

Table II, this is less than the median value, except in the case of the Small Magellanic Cloud. In the cloud a number of short-period stars produce a secondary maximum near $P=2$, but in the galaxy only a few Cepheids having these periods are known (such as SU and TU Cassiopeiae). In order to show still better the dependence of the frequency-curve on galactic longitude, the curves for somewhat narrower limits of longitude are given in Figure 1, curves V–VIII. The corresponding numerical data are in Table IV.

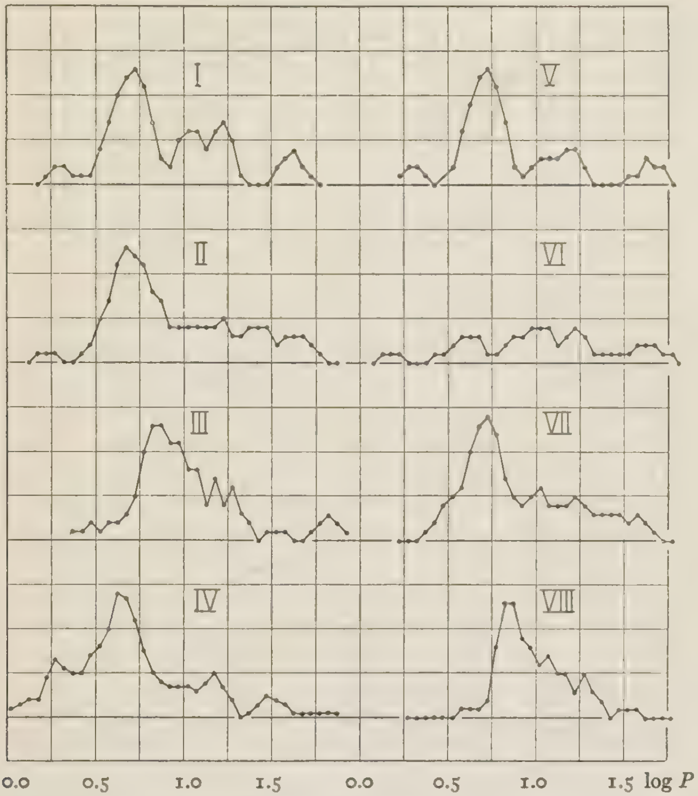

FIG. 1.—Frequency curves for galactic Cepheids

I. Gal. long. 30°–150°
II. Gal. long. 150 –270
III. Gal. long. 270 – 30
IV. Small Magellanic Cloud
V. Gal. long. 30°–110°
VI. Gal. long. 110 –180
VII. Gal. long. 180 –300
VIII. Gal. long. 300 – 30

For curve IV the scale of ordinates is one-half that of the other curves.

Sharp maxima are shown in Figure 1, V, VII, and VIII; for curve VI the number of stars is rather small as compared with the dispersion; but there is a suggestion of a maximum for a period shorter than for the other regions.

TABLE IV

| Curve | Gal. Long. | log *P* for Max. Freq. | Δ*m* | Median Mag. | Corr. for Distance | No. of Stars |
|---|---|---|---|---|---|---|
| V........... | 30°–110° | 0.70 | 0.0 | 8.8 | −0.6 | 33 |
| VI.......... | 110–180 | (.60) | +.35 | 8.3 | +.25 | 21 |
| VII......... | 180–300 | .70 | .0 | 8.2 | .0 | 45 |
| VIII........ | 300– 30 | 0.84 | −0.49 | 8.2 | −0.5 | 34 |

The period for maximum frequency is decidedly longer in the Sagittarius-Aquila region than in other parts of the galaxy, and shows a possible minimum near the opposite part of the sky (Fig. 1, curve VI).

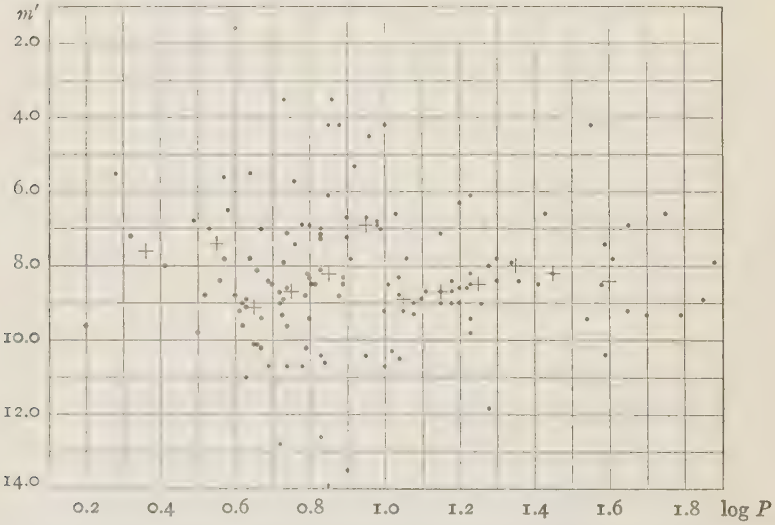

FIG. 2.—Apparent magnitudes of galactic Cepheids plotted against the logarithms of their periods. Crosses indicate median values of $m'$ for equal intervals in log $P$.

Let us compare the apparent magnitudes of Cepheids with the logarithms of their periods. The magnitudes used are the means of the maximum and minimum values given in the "Katalog."

A constant color correction of $-0.8$ has been applied to photographic magnitudes. Since the periods, and presumably the absolute magnitudes, differ in different galactic longitudes, it is desirable to correct the apparent magnitudes for systematic differences in log $P$. The corrections used, which are given in the fourth column of Table IV, are based on the assumption that 0.1 in log $P$ corresponds to $-0.35$ magnitude. The median apparent magnitudes given in the fifth column of the table are, moreover, to be reduced to a constant value, namely, 8.2. The total corrections finally applied to the apparent magnitudes are given in the sixth column.

TABLE V

MEDIAN MAGNITUDES AND PROPER MOTIONS

| log $P$ | Med. $m'$ | Mean Error | No. | Med. $p.m.$ | No. |
|---|---|---|---|---|---|
| $<0.36$ | 7.6 | ±0.6 | 6 | 0″.022 | 3 |
| 0.5–0.6 | 7.4 | .5 | 8 | .026 | 5 |
| 0.6–0.7 | 9.1 | .3 | 17 | .028 | 4 |
| 0.7–0.8 | 8.7 | .3 | 21 | .019 | 6 |
| 0.8–0.9 | 8.2 | .3 | 20 | .015 | 10 |
| 0.9–1.0 | 6.9 | .4 | 11 | .013 | 6 |
| 1.0–1.1 | 8.9 | .4 | 11 | .031 | 3 |
| 1.1–1.2 | 8.7 | .4 | 10 | .015 | 1 |
| 1.2–1.3 | 8.5 | 0.4 | 11 | .021 | 4 |
| 1.3–1.4 | 8.0 | 1.0 | 2 | .031 | 2 |
| $>1.6$ | 8.4 | ±0.3 | 16 | 0.025 | 9 |

The effect of these corrections, which is a reduction of the four galactic regions to the same median distance, is very small. They have been applied, however, in order to make it clear that systematic differences in the most frequent period and in the median apparent magnitude for the different galactic regions cannot be the origin of any possible correlation that may be found. The corrected magnitudes, $m'$, plotted against log $P$, give the scatter diagram reproduced in Figure 2. The median value of $m'$ for all periods together is 8.5 with a dispersion of ±1.4.

Two things are at once evident: (1) the dispersion in $m'$ is larger for stars having periods less than ten days ($\pm 1.8 \pm 0.2$, m.e.) than for those with periods greater than ten days ($\pm 0.95 \pm 0.14$, m.e.); (2) there is a lack of stars having log $P$ between 0.9 and 1.0 and magnitudes between the limits $8.5 \pm 1.4$. The significance of this is more clearly seen when we consider the median values of $m'$ for successive intervals of log $P$, which are indicated by crosses. The median values and their mean errors, computed from the dispersion in $m'$ for all stars together, are entered in Table V.

The difference in the median $m'$ for the stars with log $P$ equal to 0.95 and 1.05, respectively, is $2.0 \pm 0.6$ (m.e.). This difference in the median values for two groups of eleven stars each is remarkably large as compared with the dispersion of the individual magnitudes, viz., $\pm 1.4$. The discrepant value 6.9 is, however, supported more or less by a gradual decrease of the three preceding values. The reality of this gradual decrease and the sudden increase of two magnitudes near log $P = 1.0$ can hardly be determined from the present material. For a combination in larger intervals of log $P$, we find the following median values of $m'$:

| log $P$ | Median $m'$ | No. |
|---|---|---|
| 0.6–0.8 | 8.9 | 38 |
| 0.8–1.0 | 7.3 | 31 |
| 1.0–1.2 | 8.7 | 21 |

These show again that the median apparent magnitude for stars having log $P$ in the interval 0.8 to 1.0 is systematically bright.

If the irregularity is not simply a result of selection in the data, it might be attributed (1) to peculiarities in the correlation of luminosity with period; (2) to irregularities in the density distribution of the stars. The latter would reveal itself through systematic differences in the median distances. Since some correlation between absolute and apparent magnitude is to be expected, the existence of a period-luminosity relation would imply a correlation between apparent magnitude and period. If $\Delta(\rho)$ and $\Phi(M)$ represent the density and luminosity functions, respectively, the number of stars having apparent magnitudes between $m$ and $m+dm$, and absolute magnitudes between $M$ and $M+dM$, will be

$$N(m)dm = \frac{4\pi}{3} dM \Phi(M) \Delta(\rho) \rho^2 d\rho \,, \tag{1}$$

where

$$M = m - 5 \log \rho \ .$$

As an illustration, assume

$$\Delta(\rho) = e^{h + k(\log \rho) + l(\log \rho)^2} \ . \tag{2}$$

Since

$$\rho^2 d\rho = a e^{3a(m-M)} dm \ , \qquad a = 1/Mod.,$$

(1) has the form

$$N(m)dm = \frac{4\pi}{3} \Phi(M) dM e^{\alpha + \beta m + \gamma m^2} dm \ .$$

Since $\Phi(M)$ is independent of $m$, the apparent magnitude for stars in the interval $M$ to $M+dM$ has the mean value

$$\bar{m} = -\frac{\beta}{2\gamma} = -\frac{3a + 0.2k}{0.08l} + M \ , \tag{3}$$

which does not depend on the luminosity function, and, aside from $M$, involves only the constants $k$ and $l$ of the density function.

For a linear period-luminosity relation

$$M = A + B \log P \ , \tag{4}$$

we shall have a linear correlation between $\bar{m}$ and log $P$, provided the assumption (2) for the density law is justified. Something of the sort seems to apply in the case of stars having log $P < 1.0$. It is to be remarked, however, that $\bar{m}$ is extremely sensitive to small changes in the density law, for $l$ is a small quantity, while the numerator of the first term in (3) is not small. The discontinuity in $\bar{m}$ near log $P = 1.0$ might therefore be ascribed to a difference in the density distribution of the stars having long and short periods. On the other hand, any deviation from the period-luminosity relation (4) would disturb the correlation of $\bar{m}$ with log $P$.

The second alternative, which would require greater distances for stars having log $P > 1.0$, makes it desirable to examine the known proper motions. This has already been done by R. E. Wilson,[1] who found a continuous decrease in the parallactic motions of stars having periods up to forty days. He also found, however, that the $\tau$-components *increase* for stars having $P>9$ days, and that the total proper motions for the stars of longer period are also systematically large, which is just the opposite of what is to be expected on the basis of the second alternative above.

---

[1] *Astronomical Journal*, **35**, 36, 1923.

Values of the median $\mu$ for the intervals of log $P$ used here and the numbers of stars are given in the last two columns of Table V and illustrated in Figure 3. RY Boötis and W Virginis, having galactic latitudes $+62^\circ$ and $+57^\circ$, respectively, have been omitted, and also the stars in Wilson's list having the low weight 0.2. The omission of RY Boötis is justified on account of its spectrum, which does not show the Cepheid characteristics. The Cepheid character of W Virginis seems, however, to be well established, which disproves the rule that no Cepheids occur outside the galactic plane. The star has been omitted from the discussion because of its high velocity. On the other hand, stars having $P>40$ days are included in Table V. The median values for the fifty-three stars and the dispersion have been determined in the usual way: $\Sigma\frac{1}{2}$ = median value $= 0''.021$; $\pm\frac{1}{2}(\Sigma\frac{5}{6}-\Sigma\frac{1}{6})$ = dispersion $=\pm\frac{1}{2}(0''.033-0''.010)=\pm 0''.0115$. The median values show a decrease from log $P=0.6$ to 1.0, followed by a sudden increase near $P=10$ days, after which they are sensibly constant. In this respect their behavior is very similar to that of the apparent magnitudes $m'$. The mean differences between successive median values of $\mu$ are small with respect to their mean errors.

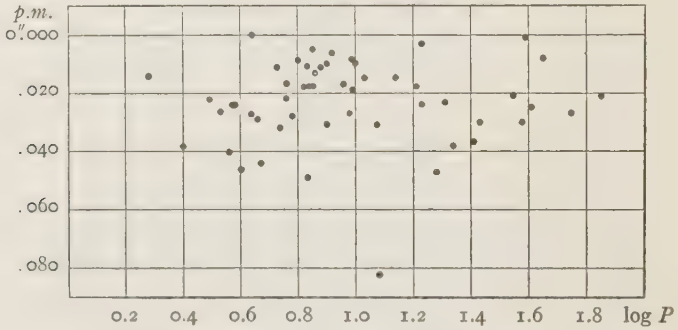

FIG. 3.—Proper motion plotted against log $P$ for galactic Cepheids

It is therefore advisable to combine the proper motions for larger intervals of log $P$ than those used in Table V. Thus, for three groups we have

| log $P$ | Median $\mu$ | Corrected $\mu$ | No. |
|---|---|---|---|
| <0.8 | 0″.025 | 0″.024 | 18 |
| 0.8–1.0 | .015 | .014 | 16 |
| >1.0 | 0.024 | 0.020 | 19 |

Since the motions of these stars as a class are small, their median values are appreciably affected by the systematic increase in the total proper motion arising from the effect of accidental error. Allowance, on the basis of the indicated probable errors, has been made for this in the "corrected" values.

The result is essentially the same as that found by Wilson. It should be remarked, however, that Wilson has shown the existence of a marked correlation between the size of the proper motion and its probable error. Since the indicated uncertainty for the third group is about twice that for the first two groups, this very suspicious circumstance may account for the unexpectedly large median for the long-period Cepheids.

The first attempt to determine the mean absolute magnitude for Cepheids was made by Hertzsprung[1] as early as 1906. He found from Auwers' proper motions for $\delta$ Cephei, $\zeta$ Geminorum, and $\eta$ Aquilae the mean absolute magnitude −2.4. After the appearance of Boss's *Catalogue* he extended his material to thirteen stars, for which practically the same value was found (−2.3; sun's velocity, 20 km/sec.). Wilson has extended this material to forty-one stars, for which he finds a mean parallactic motion of 0″.0142. Taking again the solar velocity of 20 km/sec., we find the mean absolute magnitude −1.0, which is surprisingly low. Meantime, the material for radial velocities has also increased. The thirteen Boss stars give a normal solar velocity of about 20 km/sec. in the direction of the general apex.[2] Recently Strömberg[3] derived a solar motion of 12.3 km/sec.

[1] *Zeitschrift für wissenschaftliche Photographie*, **5**, 94, 1907.

[2] The writer made a solution according to Bravais' method some years ago which has not been published.

[3] *Mt. Wilson Contr.*, No. 293; *Astrophysical Journal*, **61**, 363, 1925.

for Cepheids having periods longer than two days, which would raise the mean absolute magnitude from Wilson's parallactic motion to +0.1. The tendency of additional material, both for proper motion and radial velocity, to increase the absolute magnitude makes it worth while to treat the non-Boss stars separately. A graphical solution has been made for the parallactic motion of the non-Boss Cepheids having periods longer than one day, whereby $v/\sin\lambda$ was plotted against the weights, both quantities being taken from Wilson's paper. A solution for the sun's velocity in the galactic plane has also been made, based on the same material as used by Strömberg. The results for the assumed apex, galactic longitude 23°, latitude +22°, are as follows:

| Non-Boss Stars | Boss Stars |
|---|---|
| $\Sigma\frac{1}{2}=q=+0''.0095\pm 0''.0048$ (m.e.) | $\Sigma\frac{1}{2}=q=+0''.013\pm 0''.0052$ |
| $\Sigma\frac{1}{6}=-0''.015$ | $\Sigma\frac{1}{6}=-0''.003$ |
| $\Sigma\frac{5}{6}=+0''.029$ | $\Sigma\frac{5}{6}=+0''.025$ |
| Weight, 20.6 | Weight, 8.3 |
| $V$*$=+6\pm 2$ km/sec. | $V=+16\pm 2$ km/sec. |
| Weight, 13.4 (28 stars) | Weight, 6.4 (13 stars) |
| $M=+1.3\pm 1.6$ | $M=-2.5\pm 0.8$ |

* Solar velocity in galactic plane.

A factor 0.9 has been applied to the parallactic motions in order to reduce them to the galactic plane. Moreover, the present rather meager material for non-Boss stars shows a decrease of solar velocity with increasing period which counterbalances the decrease of parallactic motion as found by Wilson:

NON-BOSS STARS

| Period | $V$ | Weight | No. Stars | Paral. Motion | Weight | No. Stars |
|---|---|---|---|---|---|---|
| $1^d$–$4^d$ | +23 | 1.9 | 5 | $+0''.020\pm.005$ | 3.0 | 6 |
| 4–10 | 9 | 4.7 | 11 | $+\ .013\pm.005$ | 10.7 | 18 |
| >10 | + 1 | 6.7 | 12 | $-0.007\pm.007$ | 7.0 | 19 |

These results would indicate that the solar motion for the stars having periods longer than ten days is probably not in the direction assumed. From a plot of the radial velocities it seems hopeless, however, to find any other direction.

A rough solution from the proper motions has been made, in which, for convenience, the stars have been assumed to be exactly in the galactic plane. Since the galactic latitudes are small, this will not materially affect the results. Components of the proper motion in the galactic plane, $\mu \sin \chi$, and at right angles to it, $\mu \cos \chi$, directed to the north galactic pole, have been computed with the aid of tables which Mr. Strömberg kindly put at my disposal. In order to include a possible rotation effect, a term $W$ was introduced so that the equations of condition are of the form

$$x \cos \lambda + y \sin \lambda + W = \overline{\mu \sin x} \, .$$

The results indicate a rotation effect of $-0''.0075 \pm 0.0032$ (m.e.)[1] in the direction of Charlier's[2] rotation and about twice as large. A rotation of this order of magnitude is not a priori improbable, and might at least partly account for the existence of the proper motions. The parallactic motion in the galactic plane is $0''.0054 \pm .0038$ (m.e.), but does not justify any conclusion since the solar velocity in the same direction is inappreciable. From inspection, I found that the rotational effect is also indicated by stars having periods from about six to ten days, whereas for shorter periods there is no such indication. Repeating the foregoing calculation for all the non-Boss stars having periods longer than six days, which have been combined into seven groups, I find

$$\begin{aligned} x &= -0''.0068 \pm 0''.0026 \text{ (m.e.)} \\ y &= -0.0046 \pm 0''.0032 \\ W &= -0.0076 \pm 0''.0022 \end{aligned}$$

The equations for the components $\mu \cos \chi$ are

$$u \cos \lambda + v \sin \lambda + z = \overline{\mu \cos \chi} \, ,$$

---

[1] The mean error has been computed here on the assumption of a mean error of $0''.010$ in the p.m. having unit weight in Wilson's table.

[2] *Meddelanden från Lunds Astronomiska Observatorium*, Serie II, No. 9, 1913.

which give

$$\begin{aligned} u &= -0''.0034 \pm 0''.0026 \text{ (m.e.)} \\ v &= -0.0020 \pm 0.0032 \\ z &= -0.0088 \pm 0.0022 \end{aligned}$$

where $z$ is the component of parallactic motion toward the north galactic pole, and $u$ and $v$ the rotations about two axes in the galactic plane. The latter are insignificant, whereas $z$ is well above its mean error. When the apex is assumed to be in longitude 23°, the parallactic motion in the galactic plane and the rotational effect are

$$\begin{aligned} p &= \phantom{-}0''.0000;\ \text{weight, } 9.9 \\ W &= -0''.0086;\ \text{weight, } 22.2 \end{aligned}$$

Assuming that the peculiar motions can be represented by $\mu \sin \chi + W$ and $\mu \cos \chi + z$, we find symmetrical frequency-curves for both components. For the combined frequency the observed dispersion is $\pm 0''.015$ and the corrected dispersion $\pm 0''.011$. The observed dispersion of the radial velocities for stars having the same periods (viz., > 6 days) is ±16 km/sec. If we consider that part of the velocities rest on only a few observations, the mean error of a radial velocity will certainly not be overestimated by putting it ±8 km/sec. In this case the corrected dispersion is ±14 km/sec., from which the mean parallax is $4.74 \times 0''.011/14 = 0''.0037$, and the absolute magnitude 0.0.

Since, normally, the component of parallactic motion in the galactic plane is about three times that perpendicular to the plane, these results indicate either the existence of serious systematic errors in the proper motions or a systematic stream motion affecting the non-Boss stars having $P > 6$ days. The lack of uniformity in the distribution of the periods in longitude shown by the data in Tables II–IV and the curves in Figure 1 point toward a clustering of Cepheids, which would carry with it a tendency toward stream motion affecting individual groups. Until this question is settled, nothing positive can be affirmed as to the systematically low value found for the absolute magnitudes of these stars.

In connection with the first alternative on page 8, it is of interest to recall that the spectroscopic absolute magnitudes of Cepheids,[1] which were derived by the criteria for stars of constant light and a mean spectrum corresponding to that of the Cepheids, do not show the range in luminosity to be expected on the basis of period-luminosity relation. A plot of the published data, together with magnitudes for six additional stars, kindly placed at my disposal by Mr. Adams and Mr. Joy, is shown in Figure 4, where the points represent individual stars. The plot shows an increase in brightness with log $P$ from about 0.6 to 1.0. The median absolute magnitude of stars having periods longer than ten days is $-1.5$; for stars in the particular interval 0.8 to 1.0 it is $-2.4$;[2] in the interval 0.6 to 0.8, $-1.9$; and for log $P$ less than 0.6 it is $-1.4$. The circles in Figure 4 show the median values of $m'$ taken from Figure 2; $m'=8.0$ has arbitrarily been made to coincide with $-2.3$ on the scale of the spectroscopic absolute magnitudes.

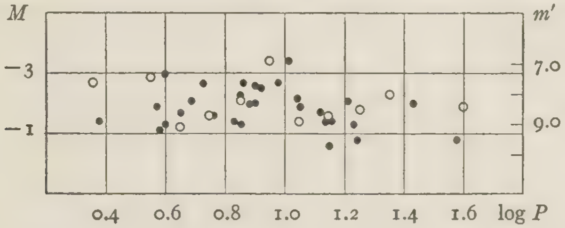

FIG. 4.—Spectroscopic absolute magnitudes of Cepheid variables. Open circles denote the median values of $m'$ from Fig. 2.

Although the material is scanty, it may be stated that a few special measurements on spectral lines with the microphotometer indicate a maximum in the intensity ratio of critical pairs of lines for a period of about ten days, followed by a drop in the ratio for stars having longer periods. The results are in Table VI. The tabulated quantity is the ratio of the intensity of an enhanced line to that of a neutral line. Settings were made at intervals of 0.01 mm on spectrograms having a dispersion of 36 A at $H\gamma$. The results have been plotted, and from these plots the intensities of the lines have been obtained.

---

[1] Adams, Joy, Strömberg, and Burwell, *Mt. Wilson Contr.*, No. 199; *Astrophysical Journal*, 53, 13, 1921.

[2] Including ζ Geminorum; period, 10.15±1.05 days.

Although these results suggest an irregularity in the absolute magnitudes at a point corresponding to $P = 10$ days, it must be noted that the spectroscopic criteria used for the limited material published do not allow for differences in spectral type, which, in the case of the Cepheids, increases with $P$. This matter, which seems important, is under investigation by Mr. Adams and Mr. Joy.

The decrease of absolute magnitude for stars having periods from a little less than four days to about ten days is, curiously enough, also shown by the early-type binaries. Adams and Joy have pointed out that the Harvard spectral classification affords a basis for the determination of absolute magnitudes for stars of early type.[1] The absolute magnitudes for sixteen binaries having spectral types B0 to B3 on the Harvard scale, and for which periods are known, have been taken from the paper cited. Mr. Adams kindly permitted me to use the unpublished results for thirteen more stars, spectrograms of which have been taken mainly by Mr. Milton Humason. The material used thus consists of twenty-nine stars, of which twenty-four have periods longer than one day. The five remaining stars have periods between 3.16 and 0.26 days, and their ranges are exceedingly small. The absolute magnitudes are plotted in Figure 5

TABLE VI

RATIO OF INTENSITY OF ENHANCED TO NEUTRAL LINES FOR STARS OF DIFFERENT PERIODS

| Star | Phase | Period | $\frac{4215}{4250}$ | $\frac{4233}{4236}$ | $\frac{4246}{4250}$ | Mean for Each Plate | Mean for Two Plates |
|---|---|---|---|---|---|---|---|
| SZ Tauri | Max. | $3\overset{\mathrm{d}}{.}15$ | 1.17 | 0.96 | 1.36 | 1.16 | 1.18 |
| | Min. | ........ | 1.28 | .80 | 1.56 | 1.21 | |
| RT Aurigae | Max. | 3.75 | 1.13 | .86 | 1.58 | 1.16 | 1.14 |
| | Min. | ........ | 1.05 | 0.92 | 1.37 | 1.11 | |
| S Sagittae | Max. | 8.38 | 1.24 | 1.02 | 1.43 | 1.23 | 1.20 |
| | Min. | ........ | 1.30 | 0.87 | 1.30 | 1.16 | |
| ζ Geminorum | Max. | 10.15 | 1.40 | 1.13 | 1.68 | 1.40 | 1.33 |
| | Min. | ........ | 1.17 | 1.08 | 1.53 | 1.26 | |
| X Cygni | Max. | 16.38 | 1.05 | 0.84 | 1.30 | 1.06 | 1.08 |
| | Min. | ........ | 1.08 | 0.92 | 1.28 | 1.09 | |
| T Monocerotis | Max. | 27.00 | 0.85 | 1.00 | 1.30 | 1.05 | 1.16 |
| | Min. | ........ | 1.38 | 1.46 | 1.00 | 1.28 | |

---

[1] *Mt. Wilson Contr.*, No. 262; *Astrophysical Journal*, **57**, 294, 1923.

against log $P$. This diagram shows a decrease in the mean $M$ with increasing period from log $P=0.6$ to somewhat more than 1.0. Still longer periods correspond to fainter magnitudes, and for periods greater than about twelve days the mean $M$ seems no longer to vary with the period. The mean values of $M$ are given in Table VII.

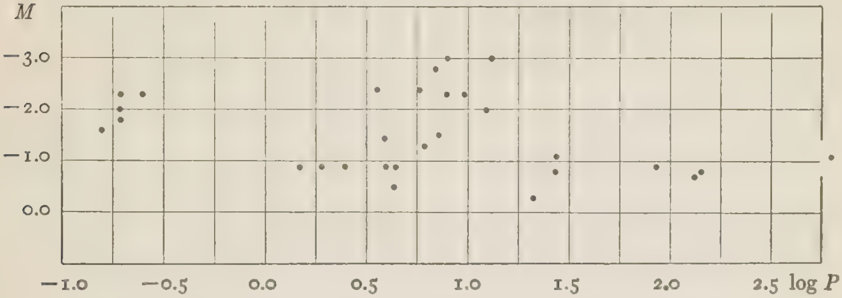

FIG. 5.—Spectroscopic absolute magnitude for spectroscopic binaries of types B0–B3 plotted against logarithm of period.

A few remarks may be added regarding the five stars having periods of about a fifth of a day. Several investigators have considered stars of this type to be pulsating stars rather than binaries, and, as Henroteau[1] has pointed out, there is an accumulation of evidence requiring the consideration of these stars as Cepheids. If so, they can scarcely fit the period-luminosity law, because of their high luminosity. The proper motions are rather small, even for B stars, and the mean reduced magnitude $H=M+5\log\mu$ is equal to $-6.74$. Putting $H=-6.74=-0.4+5\log T-8.38$, where $T$ is the

TABLE VII

PERIODS AND ABSOLUTE MAGNITUDES OF SPECTROSCOPIC BINARIES

| log $P$ | Mean $M$ | No Stars |
|---|---|---|
| −0.7 | −2.00 | 5 |
| +0.29 | 0.90 | 3 |
| .60 | 1.24 | 5 |
| .80 | 2.00 | 4 |
| 1.00 | 2.52 | 5 |
| 1.53 | 0.78 | 4 |
| 2.37 | −0.87 | 3 |

---

[1] *Publications of the Dominion Observatory*, **9**, 1, 1925.

linear tangential velocity and $-0.4$ the adopted absolute magnitude, we find $T = 2.5$ km/sec., which is an improbably low value, although the mean radial velocity, without regard to sign, is not very large, viz., 15 km/sec.

As they stand, the data from various sources—median apparent magnitudes, proper motions, radial velocities, and spectroscopic absolute magnitudes—appear to indicate a discontinuity or irregularity in the various characteristics corresponding to a period of about ten days. Were the data themselves above suspicion, we should be tempted to say that the galactic Cepheids are composed of two classes. But in no case is the evidence convincing. It is not certain that the apparent magnitudes form a representative collection; the proper motions may be affected by systematic error, and those of the questionable stars of long period are relatively uncertain, perhaps to a much greater degree than indicated by the calculated probable errors; the radial velocities are too few in number to give a trustworthy value of the all-important solar motion; and, finally, it is probable that the usual spectral criteria for luminosity do not apply to Cepheids unless differences in spectral type are taken into consideration.

Some of these difficulties may be associated with the more positive results of the discussion, namely, the lack of Cepheids having short periods in the Sagittarius-Aquila region and the evidence of peculiarities in the radial velocities, both of which indicate a lack of homogeneity that is perhaps to be explained by a clustering of stars into groups affected by stream motion. Until these questions have been cleared up it is evidently premature to assert dogmatically that the present assumptions concerning the absolute magnitudes of the Cepheids are either right or wrong. Perhaps the most important result, however, is the indication brought out by the discussion of the urgent necessity for additional data on both proper motions and radial velocities.

I wish to express my indebtedness to Mr. Seares for the development of the relation between mean apparent magnitude, density, and absolute magnitude given on page 9.

Mount Wilson Observatory
June 1926

Contributions from the Mount Wilson Observatory, No. 316
Reprinted from the *Astrophysical Journal*, Vol. LXIV, pp. 215–224, 1926
Printed in the U.S.A.

# TWO NEW VARIABLE STARS OF THE TYPE OF W URSAE MAJORIS

By J. SCHILT

## ABSTRACT

*Two new variables like W Ursae Majoris.*—The variability of 44*i* Boötis (fainter component) = Boss 3846 = Σ 1909 (ft.), and of B.D. +75°752 = Cin. 4000, has been investigated on account of *peculiarities in their spectra*. The variability of both stars is demonstrated. The periods of revolution (i.e., the double light-period) are of the order of 0ᵈ3, and the light-curves very much resemble that of W Ursae Majoris. The range of magnitude is about 0.7 for 44*i* Boötis and 0.35 for B.D. +75°752. 44*i* Boötis is of special interest because it is a *component* of a *visual binary* of well-marked orbital motion and of large parallax. Both stars have large proper motions.

## 44*i* BOÖTIS (FAINTER COMPONENT)

$15^h\ 0^m\ 29^s, +48°\ 2'\ 34''$ (1900), Harvard Visual Magnitude 6.1

This star is the fainter component of the well-known binary Σ 1909. The two components show a well-marked binary motion. The companion reached apastron about 1870 at a distance of 5″ from the brighter star. Since then the distance has decreased with an accelerating rate and amounts at present to about 3″, so that it is still just possible to get separate images with a long-focus instrument for the purpose of photographic photometry. Measurements by Hertzsprung[1] of four plates taken in the years 1915–1916 show differences which at the time were not regarded as real. The present observations were suggested by the resemblance of the spectrum to that of W Ursae Majoris.[2] The 60-inch telescope has been used with the Cassegrain (80 ft.) focus, for which the distance between the components on the plates is 0.36 mm. The plates used were Eastman 33.

About one hundred exposures of 5 and 10 seconds, alternately, were usually made on each plate. The total number of plates is thirty. The images have been measured with a thermopile photome-

---

[1] *Publikationen des Astrophysikalischen Observatoriums zu Potsdam*, **24**, Stück 2, 32, 1920.

[2] Adams, Joy, Strömberg, and Burwell, *Mt. Wilson Contr.*, No. 199; *Astrophysical Journal*, **53**, 94, 1921. Estimated spectrum G2p; measured, G4. Lines described as very poor, resembling those of W Ursae Majoris.

## TABLE I

### OBSERVATIONS OF 44*i* BOÖTIS

| Plate No. | Astronomical Date | No. Images Measured | J.D. Hel. G.M.T. | Epoch and Phase* | Δ*m* | Quality† |
|---|---|---|---|---|---|---|
| | 1926 | | 2424000+ | | | |
| SS 161...... | April 18 | 23 | 642.7996 | 0.013 | 0.61 | p |
| SS 162...... | April 18 | 16 | .8948 | .369 | 1.03 | f |
| | | 23 | .8981 | .381 | 1.00 | |
| SS 163...... | April 18 | 14 | .9310 | .437 | 0.80 | f |
| | | 13 | .9152 | .445 | .75 | |
| | | 22 | .9179 | .455 | .76 | |
| SS 164...... | April 18 | 21 | .9410 | .541 | .55 | p |
| | | 33 | .9452 | .557 | .60 | |
| SS 168...... | April 19 | 22 | 625.7158 | 3.435 | .95 | p |
| | | 13 | .7190 | .447 | .87 | |
| SS 169...... | April 19 | 20 | .8916 | 4.091 | .80 | p |
| | | 21 | .8946 | .102 | .80 | |
| | | 21 | .8977 | .114 | .75 | |
| | | 18 | .9009 | .126 | .70 | |
| SS 192...... | May 7 | 25 | 643.7495 | 70.784 | .95 | f |
| | | 22 | .7532 | .798 | 0.99 | |
| | | 24 | .7572 | .812 | 1.04 | |
| | | 22 | .7608 | .826 | 1.15 | |
| SS 193...... | May 10 | 24 | 646.6754 | 81.711 | 0.85 | f |
| | | 14 | .6796 | .726 | .84 | |
| | | 20 | .6827 | .738 | 0.97 | |
| SS 194...... | May 10 | 24 | .6988 | .798 | 1.18 | f |
| | | 26 | .7034 | .815 | 1.28 | |
| | | 28 | .7075 | .831 | 1.38 | |
| | | 18 | .7113 | .845 | 1.15 | |
| | | 25 | .7141 | .855 | 1.15 | |
| SS 195...... | May 10 | 22 | .7258 | .899 | 1.07 | f |
| | | 30 | .7293 | .912 | 0.98 | |
| | | 25 | .7376 | .943 | .87 | |
| | | 24 | .7411 | .956 | .86 | |
| SS 196...... | May 10 | 27 | .7584 | 82.021 | .75 | f |
| | | 34 | .7625 | .036 | .73 | |
| | | 29 | .7674 | .054 | .72 | |
| | | 26 | .7736 | .078 | .71 | |
| SS 197...... | May 10 | 27 | .7930 | .150 | .85 | p–f |
| | | 30 | .8006 | .178 | .90 | |
| | | 32 | .8068 | .202 | .96 | |
| | | 28 | .8131 | .225 | 0.98 | |
| SS 198...... | May 10 | 30 | .8311 | .292 | 1.19 | g |
| | | 26 | .8608 | .403 | 0.98 | |
| | | 27 | .8663 | .424 | .82 | |
| | | 27 | .8705 | .439 | .88 | |
| SS 199...... | May 10 | 25 | .8864 | .499 | .78 | g |
| | | 27 | .8906 | .514 | .72 | |
| | | 23 | .8955 | .533 | .69 | |
| SS 200....... | May 10 | 28 | .9101 | .587 | .75 | f |
| | | 30 | .9156 | .608 | .75 | |
| | | 24 | .9239 | .639 | .86 | |
| | | 24 | .9288 | .657 | 0.80 | |

* Phase is expressed as a fraction of the period.

† p = poor; f = fair; g = good.

TABLE I—*Continued*

| Plate No. | Astronomical Date | No. Images Measured | J.D. Hel. G.M.T. | Epoch and Phase* | $\Delta m$ | Quality† |
|---|---|---|---|---|---|---|
| | 1926 | | 2424000+ | | | |
| SS 201...... | May 10 | 32 | 646.9455 | 82.720 | 1.00 | f |
| | | 27 | .9517 | .743 | 0.99 | |
| | | 29 | .9579 | .766 | 1.07 | |
| | | 31 | .9627 | .784 | 1.34 | |
| SS 202...... | May 10 | 26 | .9800 | .848 | 1.19 | p |
| | | 21 | .9869 | .874 | 1.06 | |
| | | 26 | .9911 | .890 | 1.04 | |
| | | 22 | .9952 | .905 | 0.96 | |
| SS 240...... | June 11 | 28 | 678.6665 | 201.185 | .80 | f |
| | | 26 | .6702 | .199 | .81 | |
| | | 25 | .6737 | .212 | .87 | |
| SS 241...... | June 11 | 24 | .7662 | .558 | .77 | f |
| | | 20 | .7709 | .575 | .71 | |
| | | 18 | .7756 | .593 | .82 | |
| | | 27 | .7795 | .607 | .75 | |
| SS 242...... | June 11 | 25 | .7954 | .667 | .75 | f |
| | | 29 | .8032 | .696 | .87 | |
| | | 30 | .8078 | .713 | .87 | |
| | | 26 | .8120 | .729 | 0.87 | |
| SS 243...... | June 11 | 30 | .8271 | .785 | 1.10 | f–p |
| | | 24 | .8334 | .809 | 1.19 | |
| | | 24 | .8376 | .824 | 1.25 | |
| | | 24 | .8411 | .837 | 1.37 | |
| SS 244...... | June 11 | 21 | .8684 | .939 | 0.84 | f–p |
| | | 28 | .8752 | .965 | .89 | |
| | | 24 | .8829 | .994 | .85 | |
| | | 26 | .8862 | 202.006 | .83 | |
| SS 245...... | June 11 | 25 | .8993 | .055 | .80 | f |
| | | 25 | .9055 | .078 | .80 | |
| | | 25 | .9103 | .096 | .77 | |
| | | 22 | .9136 | .108 | .76 | |
| SS 246...... | June 11 | 29 | .9279 | .162 | .78 | p–f |
| | | 24 | .9318 | .176 | .80 | |
| | | 25 | .9374 | .197 | .84 | |
| | | 23 | .9428 | .217 | .87 | |
| SS 247...... | June 11 | 23 | .9555 | .265 | 0.98 | p–f |
| | | 24 | .9590 | .278 | 1.02 | |
| | | 21 | .9621 | .289 | 1.10 | |
| | | 10 | .9642 | .297 | 1.09 | |
| SS 293...... | July 9 | 23 | 706.6682 | 305.761 | 1.05 | f–p |
| | | 25 | .6725 | .777 | 1.04 | |
| | | 20 | .6756 | .788 | 1.19 | |
| | | 23 | .6786 | .800 | 1.17 | |
| SS 294...... | July 9 | 15 | .6843 | .821 | 1.40 | f |
| | | 21 | .6868 | .830 | 1.25 | |
| | | 15 | .6892 | .839 | 1.35 | |
| SS 295...... | July 9 | 21 | .7799 | 306.178 | 0.75 | g |
| | | 26 | .7836 | .192 | .80 | |
| | | 24 | .7884 | .210 | .85 | |
| | | 24 | .7932 | .228 | 0.85 | |

* Phase is expressed as a fraction of the period.

† p = poor; f = fair; g = good.

TABLE I—*Continued*

| Plate No. | Astronomical Date | No. Images Measured | J.D. Hel. G.M.T. | Epoch and Phase* | $\Delta m$ | Quality† |
|---|---|---|---|---|---|---|
| | 1926 | | 2424000+ | | | |
| SS 296...... | July 9 | 26 | 706.8121 | 306.298 | 1.08 | f |
| | | 22 | .8160 | .313 | 1.07 | |
| | | 24 | .8203 | .329 | 1.17 | |
| | | 23 | .8237 | .342 | 1.14 | |
| SS 297...... | July 9 | 24 | .8321 | .373 | 1.18 | g |
| | | 29 | .8380 | .395 | 1.13 | |
| | | 25 | .8426 | .412 | 1.10 | |
| | | 24 | .8467 | .428 | 1.05 | |
| SS 298...... | July 9 | 18 | .8547 | .457 | 0.92 | g |
| | | 18 | .8575 | .468 | .94 | |
| | | 22 | .8605 | .479 | .92 | |
| | | 23 | .8640 | .492 | 0.87 | |

* Phase is expressed as a fraction of the period.

† p = poor; f = fair; g = good.

ter, an occasional image being rejected because of poor quality. The readings for successive exposures of the same duration were combined into means of from two to five groups for each plate. The difference in brightness of the two components of the binary was then computed for each group from

$$\Delta m=\frac{(f_{10}+f_5)-(b_{10}+b_5)}{(f_{10}-f_5)+(b_{10}-b_5)}\times 0.75 \, ,$$

where $b_5$, $b_{10}$, $f_5$, and $f_{10}$ are the mean readings for the 5- and 10-second exposures on the bright and faint images, respectively, and where it is assumed that the difference between the images of a 5- and 10-second exposure is equivalent to 0.75 mag. The results are given in Table I. The corresponding epochs of observation are in J.D. Heliocentric G.M.T., and refer to the mean of the beginning of the first and the end of the last exposure of each group.

The period of revolution, derived by least squares, is 0.267765 ± 0.000012 day. The corresponding epoch numbers and phases given in Table I have been counted from an arbitrary zero. The phases are expressed in fractions of the period. The individual observations are plotted in Figure 1. Combining them into groups of five in order of phase, we obtain the normal points given in Table II. These are indicated by the crosses in Figure 1 which are connected by the broken line.

The figure shows a number of discordant observations. An attempt has been made to connect these with the quality of the plates, but with only partial success. It is to be expected that the measured difference $\Delta m$ between the rather close components will depend on the seeing. The seeing was often rather bad and, in consequence, the images are frequently large and even tend to overlap. In these cases the measured $\Delta m$ is probably too small, since a setting on the larger star does not include the whole image, while one on the smaller star may include a portion of the image of the larger star; further, the Eberhard effect may also enter as a possible source of disturbance. In fact, the three measures giving $\Delta m$ less than 0.68 are all from poor plates.

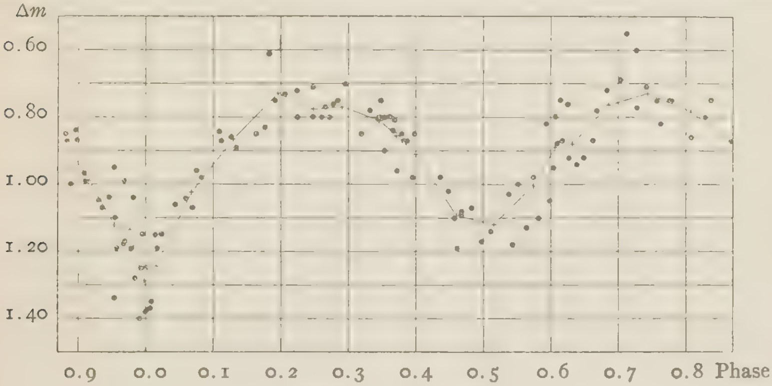

FIG. 1.—44*i* Boötis

Considering the difficulty of the object and the poor conditions under which part of the plates have been taken, the light-curve is satisfactory, and reveals at once a variation of the type of W Ursae Majoris. Without laying too much stress on the observed inequality in the depth of the minima, the one to the left in the figure may be considered as the primary. The primary minimum has been determined to be at phase $0.832P$, the secondary at $0.332P$. The resulting elements are

$$\text{Min. Hel. J.D. G.M.T.} = 2424646.976 + 0.267765\,E.$$
$$\pm 0.002 \pm 0.000012 \text{ (m.e.)}$$

$\Delta m$ at maximum is 0.76; at primary minimum, 1.29; at secondary minimum, 1.12.

*Remarks.*—1. A spectrogram obtained on May 28, 1926, with the 18-inch camera at the 60-inch telescope, during predicted time of maximum light, gives good indication of double lines, which, however, are wide and diffuse. The separation corresponds to about 350 km/sec. Spectrograms taken during minimum on July 17 and 18 by Mr. Joy with the 10-inch camera at the 100-inch reflector, and by the writer with the 7-inch camera at the 60-inch, show the lines to be distinctly narrower at the time of eclipse. Mr. Joy states: "The lines are quite measurable during minimum. They diminish in width during the half-hour preceding minimum."

TABLE II

NORMAL POINTS FOR 44*i* BOÖTIS

| Phase | $\Delta m$ | Phase | $\Delta m$ | Phase | $\Delta m$ |
|---|---|---|---|---|---|
| 0.015 | 1.24 | 0.399 | 0.91 | 0.806 | 0.78 |
| .066 | 1.02 | .461 | 1.10 | .883 | 0.89 |
| .129 | 0.86 | .515 | 1.12 | .917 | 0.99 |
| .196 | 0.73 | .573 | 1.01 | .954 | 1.12 |
| .248 | 0.78 | .607 | 0.89 | .976 | 1.14 |
| .290 | 0.77 | .631 | 0.88 | 0.996 | 1.29 |
| .346 | 0.81 | .686 | 0.76 | | |
| 0.370 | 0.85 | 0.744 | 0.73 | | |

2. The proper motion for the center of gravity of the visual pair, assuming equal masses, is 0".407. The trigonometric parallax is 0".076, the mean of the Allegheny and Yerkes determinations. The star is evidently a dwarf; the spectroscopic absolute magnitude is +5.2;[1] and its apparent magnitude, 6.1, is the brightest known for this class of variation.

3. As a consequence of the motion in the visual orbit, the apparent period of the variable in all probability cannot be constant. The projected distance between the visual components at present is about 40 astronomical units, and a rough calculation shows that the change in period should be perceptible as soon as uniform observations cover a period of about ten years.

4. The observed amplitude corresponds to a range of 0.1 mag. in the total light of the visual pair, which is perfectly within the reach of the photo-electric cell. This perhaps affords the only meth-

---

[1] *Mt. Wilson Contr.*, No. 199, p. 57; *Astrophysical Journal*, **53**, 69, 1921.

od by which the variation can be followed when the distance between the components becomes very small.

5. From the range in radial velocity, provisionally adopted as 350 km/sec., the distance of the components is 1.33 million km; and the masses, assumed equal, are $m_1 = m_2 = 0.64 \odot$. A rough calculation gives for the average radius of the ellipsoidal bodies 0.43 million km, and a density 2.2 times that of the sun. Since the absolute magnitude for each component is 6.25, the surface brightness is +0.38 mag. ($\odot = 0$). The value given by Seares for dwarfs of estimated spectrum G2 is +0.10 mag.[1] The effective temperature $T$ by Hertzsprung's[2] formula is 5500°. The star falls almost exactly on Eddington's curve, giving the relation between mass and absolute magnitude. The ratio of the distance between the eclipsing components to the projected distance on the sphere between the visual components is 1:4500.

TABLE III

COMPARISON STARS FOR B.D. +75°752

| STAR | B.D. No. | *Draper Catalogue* | | ADOPTED PG. MAG. |
|---|---|---|---|---|
| | | Pg. | Spectrum | |
| *a*............ | +75°765 | 7.93 | K2 | 8.00 |
| *b*............ | 74 890 | 7.47 | A3 | 7.36 |
| *c*............ | 74 889 | 8.7 | G5 | 8.52 |
| *d*............ | 76 809 | 7.41 | F2 | 7.48 |
| *e*............ | +74 877 | 8.6 | A2 | 8.83 |

### B.D. +75°752 = CIN. 4000

$20^h\ 38^m\ 42^s$, +75° 13′ 51″ (1900), Harvard Visual Magnitude 8.4, Sp. G5

The spectrum of this star has also been classified as resembling that of W Ursae Majoris by Mr. Adams, who kindly drew my attention to it.

One hundred and six plates have been obtained with the 10-inch Cooke refractor of 45-inch focal length. With the exception of the first two, which were test plates, they were all secured

---

[1] *Mt. Wilson Contr.*, No. 226, p. 34; *Astrophysical Journal*, **55**, 198, 1922.

[2] *Zeitschrift für Wissenschaftliche Photographie*, **4**, 43, 1906.

## TABLE IV

### OBSERVATIONS OF B.D.+75°752

| Plate No. | Astron. Date | J.D. G.M.T | Pg. Mag. | Plate No. | Astron. Date | J.D. G.M.T. | Pg. Mag. |
|---|---|---|---|---|---|---|---|
| | 1926 | 2424000+ | | | 1926 | 2424000+ | |
| 116 | May 8 | 644.9448 | 8.51 | 177 | May 12 | .9394 | 8.25 |
| 117 | | .9635 | 8.37 | 178 | | .9429 | 8.22 |
| 120 | May 9 | 645.7590 | 8.08 | 179 | | .9463 | 8.14 |
| 121 | | .7631 | 8.15 | 180 | | .9498 | 8.17 |
| 122 | | .7666 | 8.09 | 181 | | .9533 | 8.20 |
| 123 | | .7700 | 8.13 | 182 | | .9567 | 8.26 |
| 124 | | .7735 | 8.18 | 183 | | .9602 | 8.21 |
| 125 | | .7770 | 8.11 | 184 | | .9637 | 8.15 |
| 126 | | .7805 | 8.08 | 185 | | .9672 | 8.26 |
| 127 | | .7839 | 8.20 | 186 | | .9706 | 8.22 |
| 128 | | .7874 | 8.23 | 187 | | .9741 | 8.26 |
| 129 | | .7909 | 8.16 | 188 | | .9776 | 8.32 |
| 130 | | .7943 | 8.34 | 189 | | .9811 | 8.20 |
| 131 | | .7878 | 8.39 | 190 | | .9845 | 8.36 |
| 132 | | .8013 | 8.36 | 191 | | .9880 | 8.34 |
| 133 | | .8048 | 8.34 | 192 | | .9915 | 8.22 |
| 134 | | .8082 | 8.45 | 193 | | ............ | Rejected |
| 135 | | .8117 | 8.38 | 203 | June 13 | 680.6958 | 8.27 |
| 136 | | .8152 | 8.37 | 204 | | .7132 | 8.32 |
| 137 | | .8187 | 8.39 | 205 | | .7166 | 8.35 |
| 138 | | .8221 | 8.43 | 206 | | .7201 | 8.37 |
| 139 | | .8256 | 8.35 | 207 | | .7236 | 8.33 |
| 140 | | .8659 | 8.14 | 208 | | .7270 | 8.43 |
| 141 | | .8693 | 8.13 | 209 | | .7305 | 8.45 |
| 142 | | .8728 | 8.08 | 210 | | .7340 | 8.47 |
| 143 | | .8763 | 8.11 | 211 | | .7375 | 8.52 |
| 144 | | .8798 | 8.23 | 212 | | .7409 | 8.48 |
| 145 | | .8832 | 8.13 | 213 | | .7444 | 8.56 |
| 146 | | .8867 | 8.11 | 214 | | .7479 | 8.55 |
| 147 | | .8902 | 8.13 | 215 | | .7514 | 8.53 |
| 148 | | .8937 | 8.19 | 216 | | .7548 | 8.53 |
| 149 | | .8971 | 8.10 | 217 | | .7583 | 8.48 |
| 150 | | .9006 | 8.14 | 218 | | .7618 | 8.43 |
| 151 | | .9041 | 8.25 | 219 | | .7652 | 8.40 |
| 152 | | .9075 | 8.21 | 220 | | .7687 | 8.36 |
| 153 | | .9110 | 8.26 | 221 | | .7722 | 8.37 |
| 154 | | .9145 | 8.24 | 222 | | .7757 | 8.33 |
| 155 | | .9180 | 8.26 | 223 | | .7791 | 8.29 |
| 162 | May 12 | 648.8873 | 8.44 | 224 | | .7826 | 8.27 |
| 163 | | .8908 | 8.44 | 225 | | .7861 | 8.25 |
| 164 | | .8942 | 8.33 | 226 | | .7896 | 8.13 |
| 165 | | .8977 | 8.33 | 227 | | .7930 | 8.24 |
| 166 | | .9012 | 8.41 | 228 | | .7965 | 8.05 |
| 167 | | .9047 | 8.32 | 229 | | .8000 | 8.12 |
| 168 | | .9081 | 8.24 | 230 | | .8034 | 8.25 |
| 169 | | .9116 | 8.36 | 231 | | .8069 | 8.12 |
| 170 | | .9151 | 8.26 | 232 | | .8104 | 8.27 |
| 171 | | .9185 | 8.22 | 233 | | .8139 | 8.15 |
| 172 | | .9220 | 8.22 | 234 | | .8173 | 8.13 |
| 173 | | .9255 | 8.20 | 235 | | .8208 | 8.13 |
| 174 | | .9290 | 8.13 | 236 | | .8243 | 8.25 |
| 175 | | .9324 | 8.15 | 237 | | .8277 | 8.12 |
| 176 | | .9359 | 8.22 | 238 | | .8313 | 8.17 |

during three runs. Each plate has one exposure of 3 minutes,[1] and, as a rule, the beginning of successive exposures is every fifth minute. The plates used were Eastman 40 for the May runs and Eastman 33 for the series of June 13. The use of a separate plate for each exposure has the advantage that no systematic plate errors occur. The variable and five comparison stars have been measured with the thermopile photometer. One plate was rejected. Separate reduction curves have been drawn for all the plates. The comparison stars are given in Table III. The adopted magnitudes are smoothed values derived from measures on the plates.

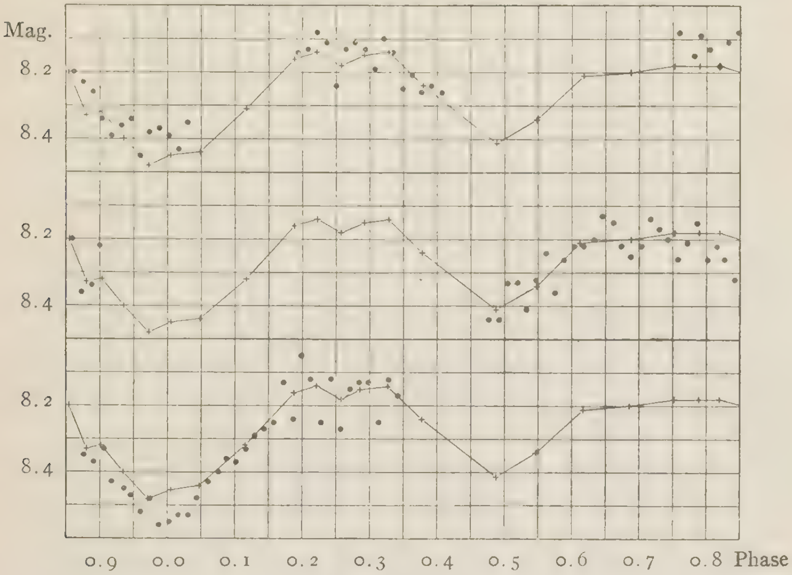

FIG 2.—B. D.+75° 752

The results of the measurements are given in Table IV. The times of mid-exposure are given in J.D. G.M.T., not reduced to the sun. The three main runs of observations are represented graphically in Figure 2, which shows that the variable is of the type of W Ursae Majoris.

The provisional interval of 0.123 day from minimum to minimum gives a revolution time of only $5^h 54^m$, which is three-fourths of the period of W Ursae Majoris. The maximum brightness is 8.13, and the depth of the minimum 0.35 mag. There is some uncertainty in the number of epochs[1] between the two minima of May 9 and June 13, and, on this account, the phases are not printed in Table IV. The number adopted is 284 (number of half-periods), which fits all of the observations. The revolution period thus derived is 0.2460±0.0002 day, the reciprocal of which has been used for the computation of the normal points. These are given in Table V, and are shown graphically in Figure 2 by the broken lines. The minima occur at phases $0.99P$ and $0.49P$, whence the elements are:

---

[1] Plates 116 and 117 had an exposure time of $5^m$.

TABLE V

NORMAL POINTS FOR B.D.+75°752

| Phase | Pg. Mag. | Phase | Pg. Mag. | Phase | Pg. Mag. |
|---|---|---|---|---|---|
| 0.005 ......... | 8.45 | 0.328 ........ | 8.14 | 0.790 ........ | 8.18 |
| .048 ......... | 8.44 | .378 ........ | 8.24 | .820 ........ | 8.18 |
| .116 ......... | 8.32 | .488 ........ | 8.41 | .854 ........ | 8.20 |
| .188 ......... | 8.16 | .548 ........ | 8.34 | .880 ........ | 8.33 |
| .222 ......... | 8.14 | .617 ........ | 8.21 | .903 ........ | 8.32 |
| .257 ......... | 8.18 | .688 ........ | 8.20 | .935 ........ | 8.40 |
| 0.292 ......... | 8.15 | 0.753 ........ | 8.18 | 0.972 ........ | 8.48 |

$$\begin{aligned}\text{Min. J.D. G.M.T. } 2424680.744 &+ 0.2460\,E.\\ \pm 0.0003 &\pm 0.0002 \text{ (m.e.)}\,.\end{aligned}$$

Attention may be called to the large proper motion, viz., $+0^{s}.0895$ and $+0''.531$. The trigonometric parallax, the mean of the determinations at Greenwich and Yale, is $0''.044$.

MOUNT WILSON OBSERVATORY
July 1926

---

[1] The uncertainty as to the period has been much decreased by a minimum observed by Mr. van Gent at Leiden, which Professor Hertzsprung kindly communicated. This minimum, June 28, 1926, G.M.T. $11^{h}49^{m}7$, occurs at phase $0.945P$.

Contributions from the Mount Wilson Observatory, No. 317
Reprinted from the *Astrophysical Journal*, Vol. LXIV, pp. 172–193, 1926
Printed in the U.S.A.

# ON THE ORBITS OF FOUR SPECTROSCOPIC BINARIES

By R. F. SANFORD

## ABSTRACT

*Orbits of spectroscopic binaries.—Four systems,* $\eta$ Orionis A, $\epsilon$ Hydrae C, Boss 4247, and B.D.$+57°2309$ are studied by means of slit spectrograms of one-prism dispersion made for the most part with the large reflectors at the Mount Wilson Observatory.

$\eta$ *Orionis A.*—The velocity of the center of mass varies in a *period* of *9.5 years* with a semi-amplitude of about 18 km/sec. Beal's earlier estimate of between 9 and 10 years for the period of variation in $\gamma$ is thus confirmed. If explainable as a triple system, the velocity of the system is about $+20$ km/sec. The three *masses* would be comparable and of the order of 10 ⊙ for each as a minimum. Radial velocities from the *D lines* of sodium are *constant*, thus agreeing with Slipher's observations for the H and K lines and exhibiting what has already been found for several other spectroscopic binaries of early B spectrum. Velocities for the triple system, for the D lines, and for the Orion nebula are in fairly good agreement, which may be significant since $\eta$ Orionis is near the inner edge of the large ring of nebulosity surrounding the Orion nebula.

$\epsilon$ *Hydrae C.*—The orbit found for this member of the well-known visual triple has an *eccentricity* among the *largest* associated with spectroscopic binaries and comparable with that of the orbit of AB of the same system. The period is 9.9 days; the velocity of the system is about 6 km/sec. less than that found for A and B, which may be a consequence of the motion of C about the pair AB.

*Boss 4247.*—Since the lines of both spectra appear, it has been possible to determine the orbital elements of *both components* of the spectroscopic binary. The period is 2.3 days; the orbits are *circular*, and the two semi-amplitudes of velocity variation are 97.4 and 108.7 km/sec. These data give 1.11 and 0.99 ⊙ as the values of $m \sin^3 i$ and $m_1 \sin^3 i$, respectively.

*B.D.$+57°2309$.*—This star is *imbedded in nebulosity*. Its spectral class is B3. The radial velocity varies in *two periods:* one 5.4 days, the other 225 days. Both orbits are elliptical, with small eccentricities; the semi-amplitudes of velocity variation are 40 and 22 km/sec., respectively. If interpreted as a *triple system*, the velocity of the center of mass would be $-17.2$ km/sec. The H and K lines are strong and sharp, and are provisionally accepted as showing a *constant* velocity of $-19.4$ km/sec., which, there is reason to believe, is the velocity of the surrounding nebulosity. Since the difference between this mean and the velocity for the assumed triple system can easily be accounted for by their respective probable errors, equality may be assumed to exist, whence it follows that the *triple system is at rest within the nebulosity.* Some evidence indicates that the D lines also do not oscillate with the lines which furnish the data for the two orbits found.

This paper derives orbits from the variable radial velocities of the four stellar systems listed in Table I. In three cases the data consist wholly of spectrograms made with the one-prism spectrographs attached to the 60- and 100-inch reflectors in Cassegrain form, while in the fourth they also include earlier measures, antedating the Mount Wilson series. The second, third, and fourth binaries were discovered at this Observatory.[1] The introduction to a previous paper[2] gives general details concerning instruments, observations, and methods of reduction.

### $\eta$ ORIONIS A AS A TRIPLE SYSTEM

$\eta$ Orionis ($\beta$G.C. 2712) is a stellar system whose complexities have been resolved one by one by various observational methods as astronomical equipment has improved. Sir William Herschel in the latter part of the eighteenth century noted a tenth-magnitude companion, to which Burnham ascribes a proper motion identical with that of $\eta$ Orionis. In the middle of the last century Dawes found the bright star to be a close double, the magnitudes of the components A and B being 3.7 and 4.9, respectively. Orbital motion has not been detected with certainty, the position angle and distance remaining about 80° and 1″, respectively.

TABLE I

| Star | H.D. No. | Mag. | $\alpha$ 1900 | $\delta$ 1900 | Spectrum |
|---|---|---|---|---|---|
| $\eta$ Orionis A............. | 35,411 | 3.7 | $5^h19^m.4$ | $-2°29'$ | B1 |
| $\epsilon$ Hydrae C............ | .......... | 7.5 | 8 41.5 | + 6 47 | F5 |
| Boss 4247.............. | 150,682 | 5.9 | 16 37.5 | +27 7 | F2,F2 |
| B.D.+57°2309.......... | 203,025 | 6.4 | 21 14.6 | +58 10 | B3 |

Frost and Adams[3] at the Yerkes Observatory found the radial velocity to be variable. About a year later, Adams[4] published an orbit for the spectroscopic binary which is so nearly circular that it may be described by the period 7.9896 days; the semi-amplitude of velocity variation, 144.75 km/sec.; and the epoch of maximum negative velocity, J.D. 2415723.849. These give a very good representation of the Yerkes observations.

The pair is so close that integrated light from both stars passes into the slit of the spectrograph, but the difference of magnitude is such that the resulting spectrum is essentially that of star A. Its spectral class is B1.

---

[1] *Publications of the Astronomical Society of the Pacific*, **36**, 137, 1924.

[2] *Mt. Wilson Contr.*, No. 201; *Astrophysical Journal*, **53**, 201, 1921.

[3] *Publications of the American Astronomical Society*, **1**, 179, 1902.

[4] *Astrophysical Journal*, **17**, 68, 1903.

In 1909 and again in 1915, a series of spectrograms of $\eta$ Orionis A was made at the Allegheny Observatory. A. F. Beal[1] measured these and found good agreement with Adams' elements, provided it was assumed that $\gamma$, the velocity of the center of mass, varied in a sine curve with a period between nine and ten years. Many of the Allegheny plates showed the spectra of two components, from which Baker[2] obtained 10.6 and 11.2 $\odot$ as the two mass functions pertaining to the short period.

A half-dozen spectrograms made by Slipher[3] at about the same epochs as the Allegheny series gave a constant velocity for the sharp H and K lines of calcium.

Next in order came observations by Stebbins[4] with a photoelectric cell, which showed $\eta$ Orionis to be an eclipsing binary with a principal minimum of at least 0.15 mag. below normal light and a secondary minimum of 0.02 or 0.03 mag. Stebbins states that "eclipses last probably less than half a day and seem to occur slightly before the predicted times." The period is so nearly an exact number of days that the complete photometric observation of the star becomes a slow process; but such results will be extremely valuable for the determination of the inclination of the orbit of the spectroscopic binary, and hence of the true semi-major axis and the masses.

A set of thirteen spectrograms was made at the Vienna Observatory in 1920, which Hnatek[5] combined with the early Yerkes plates for a redetermination of the elements. The results agreed well with those by Adams, the period, however, being increased 0.0034 day.

Still another series of radial velocity determinations has been made by the writer at Mount Wilson about the mean epoch 1925.0, the details for which are given in Table II. Phase is reckoned from J.D. 2415723.849, the epoch found by Adams for maximum negative velocity.

Since both the Allegheny and Vienna plates indicate changes in the elements, it seemed best to discuss all the radial velocities together. The values for the Yerkes, Vienna, and Mount Wilson Observatories were at hand. Dr. Curtis was kind enough to send the twenty-seven determinations comprising the Allegheny series of 1909 and the seventeen for 1915, with permission to make use of them. Dr. V. M. Slipher was so good as to send me his six plates for measurement. These have been used only as a confirmation of the much longer Allegheny series, made at the same epochs.

---

[1] *Publications of the American Astronomical Society*, **3**, 117, 1915.

[2] *Lick Observatory Bulletins*, **11**, 170, 1925.

[3] *Ibid.*

[4] *Publications of the American Astronomical Society*, **3**, 272, 1916.

[5] *Astronomische Nachrichten*, **217**, 53, 1922.

Each series of velocities was projected back upon Adams' velocity-curve with his period, from which it became apparent that only a slight shortening of his period would make all the series agree (except the Vienna observations), with $\gamma$ alone variable. An increase of 0.0034 day is the minimum change in Adams' period which will reconcile the Yerkes and Vienna observations; and since this change is inadmissible for all the other series, the Vienna observations have been ignored, except in determining the value of $\gamma$. The new period, 7.98922 days, which harmonizes the remaining series, is 0.00038 day shorter than Adams' original period. This is not to be interpreted as a real change in the period, but as the improvement contributed by the long interval now available. In qualitative

TABLE II

MOUNT WILSON OBSERVATIONS OF $\eta$ ORIONIS A

| Plate | Date | G.M.T. | Phase | Vel. | Corr. for Variable $\gamma$ | Corrected Velocity |
|---|---|---|---|---|---|---|
| | | | | km/sec. | km/sec. | km/sec. |
| $\gamma$ 12196....... | 1923 Oct. 21 | $0^{h}28^{m}$ | $0^{d}982$ | −89 | +22.5 | −66.5 |
| $\gamma$ 13034....... | 1924 Oct. 17 | 0 17 | 3.428 | +131 | +28.5 | +159.5 |
| $\gamma$ 13048....... | Oct. 18 | 23 28 | 5.397 | +75 | ......... | +103.5 |
| $\gamma$ 13060....... | Oct. 19 | 23 32 | 6.397 | −19 | ......... | +9.5 |
| $\gamma$ 13088....... | Nov. 7 | 23 47 | 1.439 | −60 | ......... | −31.5 |
| $\gamma$ 13118....... | Dec. 2 | 19 26 | 2.291 | +29 | ......... | +57.5 |
| $\gamma$ 13124....... | Dec. 3 | 21 45 | 3.388 | +119 | ......... | +147.5 |
| $\gamma$ 13128....... | Dec. 8 | 19 2 | 0.285 | −122 | ......... | −93.5 |
| $\gamma$ 13140....... | Dec. 15 | 17 42 | 7.130 | −93 | ......... | −64.5 |
| $\gamma$ 13171....... | 1925 Jan. 6 | 18 25 | 5.292 | +84 | ......... | +112.5 |
| $\gamma$ 13173....... | Jan. 6 | 19 8 | 5.332 | +82 | ......... | +110.5 |
| C 3121....... | Jan. 9 | 18 34 | 0.309 | −134 | ......... | −105.5 |
| $\gamma$ 13195....... | Jan. 10 | 18 48 | 1.318 | −77 | ......... | −48.5 |
| $\gamma$ 13769....... | Sept. 27 | 23 59 | 5.879 | +16 | +29.5 | +45.5 |
| C 3587....... | Dec. 2 | 20 7 | 7.802 | −137 | ......... | −107.5 |
| $\gamma$ 3591....... | Dec. 3 | 20 36 | 0.834 | −118 | ......... | −88.5 |
| $\gamma$ 14052....... | 1926 Feb. 24 | 18 21 | 3.804 | +133 | ......... | +162.5 |

agreement with this modification is the fact noted by Stebbins that eclipses occur before the epochs predicted with the old period.

With each series plotted against Adams' curve, the value of $\gamma$ for each set of plates was easily found by the mean departure from Adams' $\gamma$. Two series of plates, which have been made since Beal found nine to ten years as the probable period for the change in $\gamma$, confirm his estimate, for all the values fall on a smooth curve with $P=9.5$ years, as shown in the lower part of Figure 1. Table III lists the separate values of $\gamma$.

The values do not define a velocity-curve with sufficient precision to distinguish between a circular and an elliptic orbit, although, as plotted, some eccentricity is indicated. This uncertainty affects to some extent the mean $\gamma$, which was obtained in the usual way by finding the line which divides the $\gamma$-curve into equal areas. This line corresponds to +20 km/sec., which is probably a fair approximation to the velocity of the system, if triple. The semi-amplitude of velocity variation is about 17.5 km/sec.

TABLE III

VALUES OF $\gamma$ FOR $\eta$ ORIONIS A

| No. | Epoch | Vel. | Series |
|---|---|---|---|
| | | km/sec. | |
| 1 | 1902.4 | +35.5 | Yerkes |
| 2 | 1909.4 | +24.8 | Allegheny |
| 3 | 1915.0 | + 9.4 | Allegheny |
| 4 | 1920.2 | +37.0 | Vienna |
| 5 | 1925.0 | + 7.2 | Mt. Wilson |

The ordinates of the curve for $\gamma$ give the corrections required to reduce each series of observations to Adams' curve. The upper part of Figure 1 shows this curve, the two series of Allegheny observations thus corrected and combined into normal places, and, finally, my individual values similarly corrected for variation in $\gamma$. Phase is reckoned from greatest negative velocity. Although minor improvements might still be made, the agreement is satisfactory. The Vienna observations, if plotted, would be well represented by Adams' curve displaced 3.1 days to the right, no adequate explanation for which has been found.

To predict the radial velocity of $\eta$ Orionis A, it is therefore only necessary to use Adams' elements with the new period, 7.98922 days, and modify the velocity thus found by the difference between Adams' value of $\gamma$ and that found from the curve in the lower part of Figure 1. This seems the safest procedure, since to give elements for the variation in $\gamma$ would perhaps suggest a degree of accuracy certainly not at present attainable.

If we assume that the spectroscopic system involves three bodies and that the inclinations of both short- and long-period orbits are

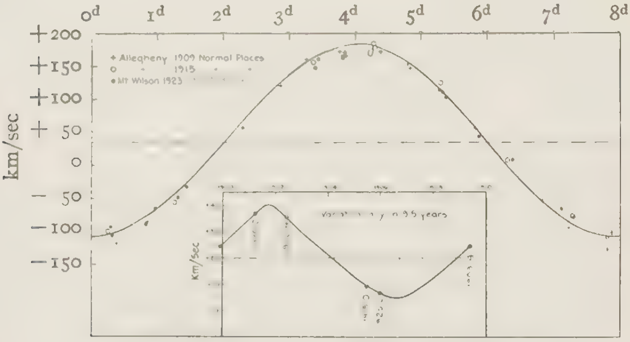

FIG. 1.—Radial velocity curves for $\eta$ Orionis A

nearly 90°, then it follows that the mass function for the long-period orbit is

$$\frac{M_1^3 \sin^3 i}{(M+M_1)^2} = 1.9 \odot ,$$

where $M$ is the combined mass of the two stars whose period is eight days, and $M_1$ the mass of the third star. But if $i = 90°$, $M = (10.6 + 11.2) \odot$, whence $M_1$ is of the order of $13 \odot$, so that we appear to be dealing with three comparable masses.

These three components comprise star A of the visual system, magnitude 3.7, which is 1 mag. brighter than the value usually assigned to star B. It is of interest that spectra of two of the stars in A are shown on many spectrograms without serious interference from the spectrum of B. Of course the latter may be fainter than estimated, at least photographically. At any rate, the differences in magnitude must be most favorably distributed to insure the selection actually found upon spectrograms resulting from the combined light of all four stars. It is hoped that with first-class seeing conditions the spectrum of B may be obtained free from that of A.

Spectroscopic binaries of type B3, or earlier, are quite numerous in which the H and K lines of calcium are sharp and give velocities which do not seem to vary. In several such cases, Miss Heger[1] has found a similar behavior for the D lines of sodium. Since Slipher finds that the H and K lines in $\eta$ Orionis A give a constant velocity, I have obtained two plates covering the region of the D lines. The dispersion of the plane-grating spectrograph used for this purpose is 65 A per millimeter. A neon comparison spectrum was used. From two measures of each plate, I have derived one velocity from $D_3$ of helium and another from the D lines of sodium, and have also computed the velocity from the elements already found. The results are in Table IV. The agreement between the computed velocities and those from $D_3$ is quite as good as one could expect from a single rather weak line and such dispersion. Although the phases are such as to give a large difference in the orbital velocities, the results for the D lines are not greatly different, and their mean, +17 km/sec., is not far from +20 km/sec., which has been found for the velocity of the triple system. It is of interest that $\eta$ Orionis is located on the inner edge of the great ring of nebulosity surrounding the Orion nebula, and that the velocities from the D lines as well as for the triple system are nearly the same as the mean of many determinations for the Orion nebula itself (+17 km/sec.) as published by Campbell and Moore.[2]

TABLE IV

$\eta$ ORIONIS A—D-LINE VELOCITIES

| Plate No. | Date | Computed Vel. | Meas. Vel. $D_3$ | Meas. Vel. $D_1$ and $D_2$ |
|---|---|---|---|---|
| | | km/sec. | km/sec. | km/sec. |
| G113....... | 1926 Jan. 27 | −137 | −134 | +26.8 |
| 127....... | Mar. 27 | + 82 | + 51 | + 6.6 |
| Mean... | .............. | .......... | .......... | +16.7 |

---

[1] *Lick Observatory Bulletins*, **10**, 59, 1919; *ibid.*, p. 141, 1921.

[2] *Lick Observatory Publications*, **11**, 107, 1918.

## THE ORBIT OF THE SPECTROSCOPIC BINARY $\epsilon$ HYDRAE C

The multiple system, $\epsilon$ Hydrae ($\beta$G.C. 4771), is of more than ordinary interest, for it includes a visual pair whose data were complete enough in 1912 to enable Aitken[1] to derive both its visual and spectrographic orbits, and thus obtain the linear dimensions of the orbit and the parallax. In addition, there is a third star, C, at a distance of $3''$, of about 7 mag., which has described an arc of some $40^\circ$ about AB during the one hundred years since its discovery. The spectrum obtained from the close visual pair (separation $0''.23$) is F8, and is that of the brighter component A. The spectral class of star C is F5.

To obtain the spectrum of C free from that of AB, it is necessary to keep the image very nearly at the same point on the slit, thereby producing a very narrow spectrum. Furthermore, the seeing must be good; otherwise the enlarged images merge and the spectrum becomes a composite of A, B, and C. Effort has always been made to meet these requirements, but some of the measures may be affected by blending with the brighter star, either because the rate of the driving clock made close guiding very difficult or because the seeing was variable throughout the exposure.

The first two spectrograms early in 1917 gave velocities which differed from each other and from the value of the velocity of the center of mass for AB so much and in such a direction that the binary character of C seemed certain. The seventh and eighth plates, taken in December, 1922, definitely settled the matter, after which the star was placed on a selected list of spectroscopic binaries for regular observation.

In all, forty-four spectrograms were obtained, covering satisfactorily the entire velocity-curve. Less than one-sixth of the period is required for the drop from maximum to minimum velocity; this and the other conditions already referred to delayed considerably the completion of the observations covering this branch of the velocity-curve.

The final adjustment of the observations gave $P = 9^d.9047$, which is judged to be correct within 0.001 day, since any greater change

---

[1] *Publications of the Astronomical Society of the Pacific*, **24**, 216, 1921.

## TABLE V

### OBSERVATIONS OF ε HYDRAE C

| Plate | Date | G.M.T. | Phase | Velocity | O−C | Wt. | Notes |
|---|---|---|---|---|---|---|---|
| | | | | km/sec. | km/sec. | | |
| γ 5361.... | 1916 Dec. 12 | 22$^{h}$31$^{m}$ | 5$^{d}$962 | +38.7 | − 4 | ½ | (1) |
| γ 5419.... | 1917 Jan. 4 | 21 54 | 9.128 | +56.7 | + 3 | 1 | |
| γ 5573.... | Feb. 9 | 20 35 | 5.454 | +43.7 | + 4 | 1 | |
| γ 7771.... | 1919 Jan. 15 | 20 08 | 7.201 | +44.8 | − 5 | 1 | |
| γ 7946.... | Mar. 11 | 20 11 | 2.774 | +20.7 | − 2 | 1 | |
| γ 8038.... | Apr. 11 | 17 15 | 3.938 | +30.2 | − 1 | 1 | |
| γ 11456.... | 1922 Dec. 5 | 00 25 | 0.103 | − 5.8 | − 1 | ½ | (2) |
| γ 11463.... | Dec. 5 | 22 51 | 1.038 | −10.0 | − 9 | 1 | |
| γ 11498.... | 1923 Jan. 2 | 22 01 | 9.193 | +43.9 | − 9 | ¼ | (2), (3) |
| γ 11543.... | Jan. 8 | 22 01 | 5.290 | +34.0 | − 6 | ½ | (3), (4) |
| γ 11576.... | Jan. 27 | 20 18 | 4.407 | +42.2 | + 8 | 1 | |
| C 2100.... | Jan. 31 | 23 07 | 8.520 | +51.8 | − 3 | ¼ | (3), (4) |
| γ 11616.... | Feb. 7 | 18 35 | 5.431 | +40.6 | 0 | ¼ | (3), (4) |
| γ 11625.... | Feb. 24 | 18 39 | 2.626 | +25.8 | + 5 | 1 | |
| γ 11645.... | Mar. 1 | 20 48 | 7.711 | +46.3 | − 6 | ½ | |
| γ 11655.... | Mar. 5 | 17 18 | 1.663 | + 7.4 | − 2 | 1 | |
| γ 11748.... | May 2 | 16 30 | 0.203 | −16.3 | − 6 | 1 | |
| C 2236.... | May 4 | 15 18 | 2.153 | +16.4 | + 1 | 1 | |
| γ 11759.... | May 5 | 15 45 | 3.172 | +25.4 | 0 | 1 | |
| γ 11766.... | May 6 | 15 20 | 4.154 | +26.6 | − 6 | 1 | |
| γ 11772.... | May 7 | 15 48 | 5.173 | +36.5 | − 2 | 1 | |
| C 2280.... | May 31 | 15 42 | 9.361 | +54.9 | + 6 | 1 | |
| C 2546.... | Nov. 22 | 0 55 | 5.459 | +43.1 | + 2 | 1 | |
| γ 12304.... | Nov. 25 | 21 35 | 9.416 | +52.6 | + 6 | 1 | |
| C 2599.... | Dec. 28 | 21 28 | 2.696 | +18.6 | − 3 | ½ | (1), (3) |
| γ 12367.... | 1924 Jan. 12 | 21 52 | 7.810 | +51.7 | − 1 | 1 | |
| C 2606.... | Jan. 12 | 23 54 | 7.884 | +49.0 | − 4 | ½ | (1) |
| γ 12407.... | Jan. 17 | 22 40 | 2.937 | +27.6 | + 4 | 1 | |
| C 2643.... | Jan. 20 | 19 46 | 5.817 | +50.4 | + 8 | 1 | |
| γ 12449.... | Jan. 26 | 18 57 | 1.878 | + 8.7 | − 3 | 1 | |
| γ 12565.... | Apr. 16 | 15 16 | 3.486 | +22.1 | − 6 | 1 | |
| γ 12578.... | Apr. 18 | 15 21 | 5.491 | +55.7 | +15 | ½ | (2), (3) |
| γ 13174.... | 1925 Jan. 6 | 19 40 | 1.243 | + 8.3 | + 5 | 1 | |
| γ 13382.... | Apr. 14 | 15 14 | 0.012 | − 6.8 | −10 | 1 | |
| γ 13417.... | May 6 | 15 43 | 2.222 | +16.8 | 0 | 1 | |
| γ 13430.... | May 14 | 15 53 | 0.324 | − 0.9 | +12 | 1 | |
| γ 13996.... | 1926 Jan. 25 | 21 54 | 8.959 | +52.1 | − 3 | 1 | |
| γ 14002.... | Jan. 26 | 17 20 | 9.768 | +20.9 | + 2 | 1 | |
| γ 14006.... | Jan. 26 | 21 21 | 0.031 | − 4.8 | − 6 | 1 | |
| γ 14014.... | Jan. 27 | 21 22 | 1.031 | − 2.9 | − 2 | 1 | |
| C 3677.... | Feb. 5 | 19 08 | 0.033 | + 8.2 | + 7 | 1 | |
| γ 14126.... | Mar. 27 | 17 26 | 0.438 | −14.3 | − 2 | 1 | |
| C 3765.... | Apr. 25 | 14 58 | 9.527 | +37.7 | + 4 | 1 | |
| C 3767.... | Apr. 25 | 16 03 | 9.572 | +29.4 | − 1 | 1 | |

(1) Short camera.
(2) Poor focus.
(3) Not used in forming the normal places.
(4) Poor plate.

would seriously upset the assemblage of velocities on the very steep and therefore critical branch of the curve. This element has been assumed to be known.

Because of the uncertainties already alluded to which may affect individual radial velocity determinations, it was deemed best to use normal places for the derivation of the preliminary elements and their subsequent correction by the method of least-squares. The data for the forty-four plates are in Table V; the normal places are given in Table VI. Notes to the tables indicate that a few of the spectrograms were not used for the normal places and give the reasons for rejection. Individual observations with phases such that they cover an essentially linear portion of the velocity-curve have been combined to form a normal place. Although there are objections to combining into one normal place observations separated by many periods, that liberty has been taken because the period was already rather well determined.

TABLE VI

NORMAL PLACES FOR $\epsilon$ HYDRAE C

| No. | Limits of Phase | Phase | Velocity | O−C | Wt. | Plates Included in Normal Place |
|---|---|---|---|---|---|---|
| | | | km/sec. | km/sec. | | |
| 1 ....... | ............. | $0^{\mathrm{d}}.103$ | − 5.8 | −0.5 | ½ | γ 11456 |
| 2 ....... | $0^{\mathrm{d}}.019$–$0^{\mathrm{d}}.331$ | .163 | − 3.8 | +5.1 | 2 | γ 13382, 13430 |
| 3 ....... | ............. | .203 | −16.3 | −6.0 | 1 | γ 11748 |
| 4 ....... | ............. | 0.438 | −14.3 | −1.5 | 1 | γ 14126 |
| 5 ....... | ............. | 1.038 | −10.0 | −8.7 | 1 | γ 11463 |
| 6 ....... | 1.031–1.243 | 1.137 | + 2.7 | +1.6 | 2 | γ 13174, 14014 |
| 7 ....... | 1.663–1.878 | 1.771 | + 8.0 | −3.0 | 2 | γ 11655, 12449 |
| 8 ....... | 2.153–3.172 | 2.647 | +22.1 | +1.0 | 6 | C2236, γ 7946, 11625, 11759, 12407, 13417 |
| 9 ....... | 3.486–4.154 | 3.859 | +26.3 | −4.3 | 3 | γ 8038, 11766, 12565 |
| 10 ....... | 4.407–5.459 | 5.123 | +41.4 | +3.1 | 4 | γ 5573, 11576, 11772, C 2546 |
| 11 ....... | 5.817–5.962 | 5.865 | +46.5 | +4.0 | 1½ | C2643, γ 5361 |
| 12 ....... | 7.201–7.884 | 7.603 | +48.0 | −3.7 | 3 | γ 7771, 11645, 12367, C2606 |
| 13 ....... | ............. | 8.959 | +52.1 | −3.1 | 1 | γ 13996 |
| 14 ....... | ............. | 9.128 | +56.7 | +2.9 | 1 | γ 5419 |
| 15 ....... | 9.361–9.416 | 9.388 | +54.8 | +7.2 | 2 | C2280, γ 12304 |
| 16 ....... | 9.527–9.572 | 9.550 | +33.6 | −5.7 | 2 | C3765, C3767 |
| 17 ....... | 9.768–0.033 | 9.881 | + 8.1 | +1.0 | 3 | γ 14002, 14006, C3677 |

The preliminary elements used are the mean of sets obtained by the methods of Russell and Lehmann-Filhés. These have been once corrected by least-squares, which yielded appreciable corrections only in the case of the velocity of the center of mass, $\gamma$, and the semi-amplitude of velocity variation, $K$. The preliminary elements, corrections, and final elements are in Table VII.

The eccentricity, 0.62, is among the very large values for spectroscopic binaries, and is much like the value 0.65 found for both the visual and spectroscopic orbits of components A and B.

If the plane of the orbit of C around AB were normal to the line of sight, we should expect the value of $\gamma$ for the spectroscopic binary C to be the same as that found by Aitken for AB, provided neither system contained a third body. The velocity of the center of mass for C is, however, about 6 km/sec. less than that derived for AB. Campbell's K-term cannot be responsible, since the two spectra are too nearly alike. There may be a third body in either system; to decide this would mean a great deal more observing. But the orbit of C around AB may not be normal to the line of sight, and the velocity difference of 6 km/sec. may be the component of the orbital velocity of C around AB. Assuming this to be the case, and that the observed difference is the component at the descending node, and further, that the angular separation of C from AB converted into linear measure by the parallax is the projected radius of a circular orbit, we find that the period of C about AB would be of the order of six hundred years. The angular rate of revolution of C about AB thus far observed gives six hundred and fifty years as the period, on the assumption of a circular orbit. Hence the difference in the veloci-

TABLE VII

ELEMENTS FOR $\epsilon$ HYDRAE C

| | Preliminary Elements | Corrections | Final Elements |
|---|---|---|---|
| $P$ ...... | ................ | ............ | $9\overset{d}{.}9047$ |
| $e$ ....... | 0.62 | 0.000 | 0.62 |
| $\omega$ ....... | $117\overset{\circ}{.}7$ | $-0\overset{\circ}{.}1$ | $117\overset{\circ}{.}6$ |
| $K$ ...... | 36.2 | −1.2 | 35.0 km/sec. |
| $T$ ...... | J.D. 2423800.000 | +0.007 | 3800.007 |
| $\gamma$ ....... | +30.0 | +1.2 | +31.2 km/sec. |
| $a \sin i$ ... | ................ | ............ | 3,700,000 km |
| $\frac{m_1^3 \sin^3 i}{(m+m_1)^2}$ | ................ | ............ | 0.0206 ☉ |

ties of the center of mass for C and AB is compatible with the known motion in position angle.

It may be well to point out that all but the first six observations of the radial velocity of C have been made at times when the position angles of B referred to A were in the same quadrant as those of C referred to AB. Further, since aphelion in the system AB occurs in that quadrant, the configuration mentioned persists longer than for B in any one of the other three quadrants. It would be of interest to redetermine the orbit for star C when star B is in the quadrant opposite to C.

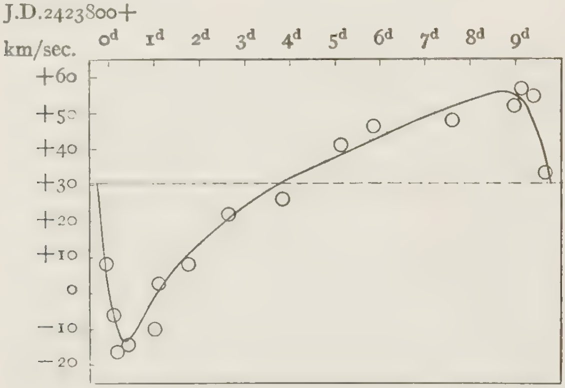

FIG. 2.—Radial velocity curve of $\epsilon$ Hydrae C

Table V gives the residuals for the individual observations as scaled from the velocity-curve based upon the final elements. Table VI shows the differences O − C between the velocities for the normal places and those computed by the final elements. When the practical difficulties are considered, the representation in both tables is quite as satisfactory as could be expected. In Figure 2 the normal places only have been plotted with the computed velocity-curve.

Besides stars A, B, and C, there is a fourth star, D, 19″ distant and of 12.5± mag., which has the same proper motion as the brighter stars and is therefore presumably a member of the system. Since its absolute magnitude is some 8 mag. fainter than that of star A, or about $M=9$, it would be of interest to know something of its spectrum. It is hoped that a spectrogram may be obtained in the near future with a spectrograph of low dispersion.

TABLE VIII

OBSERVATIONS OF BOSS 4247

| PLATE NO. | DATE | G.M.T. | PHASE | VELOCITY |  | O−C |  |
|---|---|---|---|---|---|---|---|
|  |  |  |  | Prim. | Second. | Prim. | Second. |
|  |  |  |  | km/sec. | km/sec. | km/sec. | km/sec. |
| γ 11848.... | 1923 June 6 | $19^h46^m$ | $0^d.108$ | + 84.0 | −105.5 | + 3.3 | +11.1 |
| γ 11859.... | June 21 | 21 11 | 1.323 | − 98.7 | + 95.9 | + 1.2 | +10.9 |
| γ 11899.... | June 28 | 18 04 | 1.270 | − 99.6 | + 87.5 | + 5.6 | − 3.2 |
| γ 11905.... | June 29 | 19 10 | 0.008 | + 88.0 | −122.2 | + 3.2 | − 0.8 |
| γ 12004.... | Aug. 5 | 15 20 | 2.234 | + 81.9 | −132.6 | − 1.0 | −13.5 |
| γ 12087.... | Sept. 1 | 14 52 | 1.524 | − 72.0 | + 50.2 | − 7.5 | + 4.8 |
| C 2425.... | Sept. 2 | 14 57 | 0.219 | + 67.2 | −116.2 | − 0.7 | −13.6 |
| C 2431.... | Sept. 4 | 14 51 | 2.215 | + 82.0 | −113.4 | + 0.3 | + 4.5 |
| C 2432.... | Sept. 4 | 15 05 | 2.224 | + 81.8 | −116.4 | − 0.5 | + 2.1 |
| γ 12534.... | 1924 Mar. 18 | 22 30 | 0.080 | + 81.3 | −117.9 | − 1.2 | + 0.9 |
| γ 12541.... | Mar. 19 | 22 20 | 1.073 | −108.4 | + 82.0 | − 0.8 | −11.4 |
| γ 12564.... | Apr. 15 | 21 49 | 0.360 | + 54.0 | − 71.8 | +12.4 | + 1.3 |
| γ 12569.... | Apr. 16 | 21 20 | 1.340 | − 93.1 | + 93.0 | + 4.7 | +10.0 |
| γ 12575.... | Apr. 17 | 21 58 | 0.058 | + 76.2 | −112.8 | − 6.3 | + 7.2 |
| C 2753.... | Apr. 18 | 22 08 | 1.065 | −101.7 | + 97.2 | + 5.5 | + 4.2 |
| γ 12640.... | May 15 | 18 39 | 0.229 | + 58.6 | − 98.6 | − 7.8 | + 2.3 |
| γ 12646.... | May 16 | 19 26 | 1.262 | −112.6 | + 90.7 | − 6.8 | − 0.7 |
| γ 12651.... | May 17 | 20 05 | 2.289 | + 80.6 | −118.9 | − 4.1 | + 2.3 |
| C 2785.... | May 18 | 22 46 | 1.093 | −109.7 | + 98.0 | − 1.1 | + 3.4 |
| γ 12664.... | May 19 | 22 24 | 2.077 | + 68.0 | −102.8 | + 1.8 | − 2.2 |
| γ 12738.... | June 17 | 19 50 | 0.973 | − 94.8 | + 85.2 | + 3.7 | + 1.9 |
| γ 12743.... | June 18 | 17 25 | 1.872 | + 16.8 | ........ | − 7.2 | ........ |
| γ 12782.... | July 13 | 15 42 | 1.416 | − 95.2 | + 56.4 | − 9.0 | −13.2 |
| γ 12789.... | July 14 | 15 52 | 0.116 | + 84.6 | −111.4 | + 4.7 | + 4.5 |
| γ 12795.... | July 15 | 16 35 | 1.145 | −112.9 | + 95.6 | − 2.9 | − 0.6 |
| C 3313.... | 1925 June 5 | 18 15 | 0.842 | − 71.8 | + 63.7 | + 5.2 | + 4.3 |
| γ 13438.... | June 7 | 17 32 | 0.505 | − 5.4 | ........ | −11.7 | ........ |
| γ 13444.... | June 7 | 23 26 | 0.750 | − 67.7 | + 41.3 | −10.9 | + 4.5 |
| γ 13445.... | June 8 | 15 30 | 1.420 | − 86.5 | + 61.5 | − 0.9 | − 7.4 |
| γ 13450.... | June 8 | 23 28 | 1.752 | − 13.8 | ........ | − 6.8 | ........ |

## ORBITS OF THE TWO COMPONENTS OF THE SPECTROSCOPIC BINARY BOSS 4247

The first spectrogram of this star showed the lines of two stars, both of spectral class about F2, and established its binary character.

Thirty spectrograms with one-prism dispersion were made with the 60- and 100-inch reflectors between June, 1923, and June, 1925. The data for these plates are in Table VIII. Both the phases and the residuals refer to the adopted elements. The period, which was soon found to be near 2 days, turned out to be 2.3076 days, and satisfactorily represents all observations in an interval which includes about three hundred and thirty revolutions in the orbit. The distribution of velocities would be very seriously affected were this period changed as much as 0.0005 day, which may be taken as an upper limit of the possible error in $P$. A freehand velocity-curve through the assembled observations was not distinguishable from a sine curve, and the orbit has been assumed to be circular. The elements are therefore period, velocity of the system, semi-amplitude of velocity variation for both components, and an arbitrarily chosen epoch, in this case the time when the primary attains its maximum positive velocity. These were determined by the graphical method of Lehmann-Filhés, and once corrected by the method of least-squares. Table IX gives these elements, the corrections, and the corrected elements which have been adopted. The representation is quite satisfactory as attested by the residuals in Table VIII and the fit of the observed velocities to the curve as shown in Figure 3.

TABLE IX

Elements for Boss 4247

| | Preliminary Elements | Corrections | Corrected Elements |
|---|---|---|---|
| $P$ | | | $2^{d}3076$ |
| $K$ | 97.5 | −0.11 | 97.4 km/sec. |
| $K_1$ | 107.5 | +1.22 | 108.7 km/sec. |
| $T$ | J.D. 2423923.862 | −0.006 | 3923.856 |
| $\gamma$ | −12.5 | −0.09 | −12.6 km/sec. |
| $(a+a_1)\sin i$ | | | 6,540,000 km |
| $m \sin^3 i$ | | | 1.1065 $\odot$ |
| $m_1 \sin^3 i$ | | | 0.9915 $\odot$ |
| $\frac{m}{m_1}=\frac{K^1}{K}$ | | | 1.11 |

The values of $a \sin i$ and $a_1 \sin i$ are 3,114,300 and 3,425,700 km, respectively. If the radii of the two stars are of the order of that of the sun, any inclination between 70° and 90° will result in a partial eclipse twice each revolution at phases corresponding to the intersections of the two curves in the radial velocity diagram. It might prove of interest to test this point by photometric observations.

Measures of the trigonometric parallax of this system are unknown to me, and the determination of the absolute magnitudes by spectral criteria is made difficult on account of the presence of the two sets of lines.

Boss's proper motion is small. The system appears, however, to consist of two stars not greatly different in absolute magnitude from that of the sun.

### B.D. +57°2309

Barnard found this star to be involved in nebulosity, as may be seen by reference to Plate 82, *Publications of the Lick Observatory*, **11**, 1913, where it appears as the first object listed in the appended table. This led Hubble, in 1920, to observe its spectrum with the one-prism spectrograph and 60-inch reflector. His five plates gave certain evidence of variability in the radial velocity of the star, and velocities from the H and K lines of calcium which did not agree with those from the other lines. He noted that $H\beta$ was an abnormally weak absorption line, and Humason found from objective-prism plates that $H\alpha$ appeared as an emission line.[1] The character of $H\alpha$ has been verified by slit spectrograms.

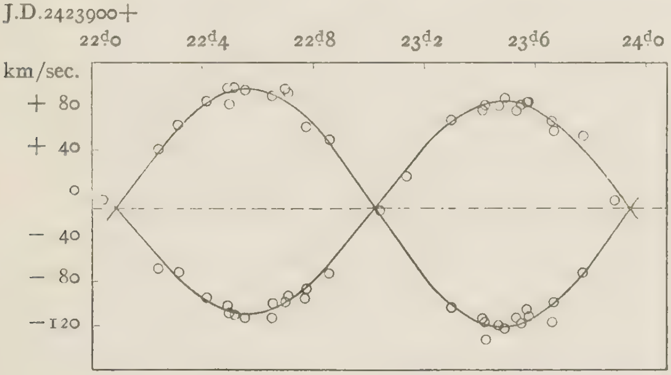

FIG. 3.—Radial velocity curves of Boss 4247

The star was placed on the program of spectroscopic binaries in 1921, and by the end of 1925 forty-two usable spectrograms had been obtained. These have furnished the data for the investigation of the orbit. Considerable difficulty was encountered in deriving a period until it was noted that observations which evidently established maxima and minima could not be harmonized with a single constant period. An attempt to establish a periodicity for these changes indicated a cycle of about 225 days. Further observation seemed to confirm this, so that a tentative curve having a period of 225 days was used as a starting-point for the correction of the observed velocities.

---

[1] Adams, Joy, and Sanford, *Publications of the Astronomical Society of the Pacific*, **36**, 137, 1924.

TABLE X

NORMAL PLACES; B.D.+57°2309; $P=225^d44$

| No. | Julian Day | Phase | Velocity Deviation from 5-Day Orbit | O−C | Wt. | Nos. from Column 1, Table XII |
|---|---|---|---|---|---|---|
| | | | km/sec. | km/sec. | | |
| 1 | 2424490.13 | $9^d73$ | +19 | + 4 | 2 | 40, 41 |
| 2 | 3599.42 | 20.88 | + 4 | − 3 | 4 | 10, 11, 12, 13 |
| 3 | 4514.61 | 34.31 | − 8 | − 4 | 1 | 42 |
| 4 | 4310.45 | 55.59 | −23 | − 7 | 2 | 30, 31 |
| 5 | 3636.63 | 58.10 | −11 | + 6 | 3 | 14, 15, 16 |
| 6 | 4339.67 | 84.81 | −19 | + 4 | 6 | 32, 33, 34, 35, 36, 37 |
| 7 | 3665.82 | 87.29 | −27 | − 4 | 5 | 17, 18, 19, 20, 21 |
| 8 | 3014.72 | 112.50 | −31 | − 9 | 1 | 6 |
| 9 | 3696.80 | 118.26 | −34 | −12 | 1 | 22 |
| 10 | 3923.97 | 119.99 | −22 | − 1 | 3 | 27, 28, 29 |
| 11 | 3720.73 | 142.19 | −10 | + 6 | 4 | 23, 24, 25, 26 |
| 12 | 2609.45 | 158.11 | −12 | − 2 | 4 | 1, 2, 3, 4 |
| 13 | 4420.18 | 165.32 | −11 | − 4 | 2 | 38, 39 |
| 14 | 3570.64 | 217.54 | +22 | + 1 | 3 | 7, 8, 9 |

TABLE XI

B.D.+57°2309—ELEMENTS OF LONG-PERIOD VARIATION

| | Preliminary Elements | Corrections | Adopted Elements |
|---|---|---|---|
| $P$ | | | $225^d44$ |
| $e$ | 0.095 | + 0.131 | 0.226 |
| $\omega$ | 0° | +16°6 | 16°6 |
| $K$ | 26.4 | − 4.5 | 21.9 km/sec. |
| $T$ | J.D. 2423797.50 | + 6.48 | 3803.98 |
| $\gamma$ | −4.5 | − 1.6 | −6.1 km/sec. |
| $a \sin i$ | | | 65,988,600 km |
| $\frac{M_1^3 \sin^3 i}{(M+M_1)^2}$ | | | 0.3956 ⊙ |

When the corrected velocities were studied, it was found that $P=5^{d}.41364$ provided an assembly which, in view of the nature of the spectrum from which the velocities were obtained, was fairly satisfactory. As the lines of only one star are visible, and their breadth and diffuseness make them somewhat difficult to measure, the velocities are subject to rather large probable errors. The calcium lines H and K are sharp and fairly strong, however, and special reference will be made to them later. The proximity to $H\epsilon$ makes the H line less satisfactory than the K line.

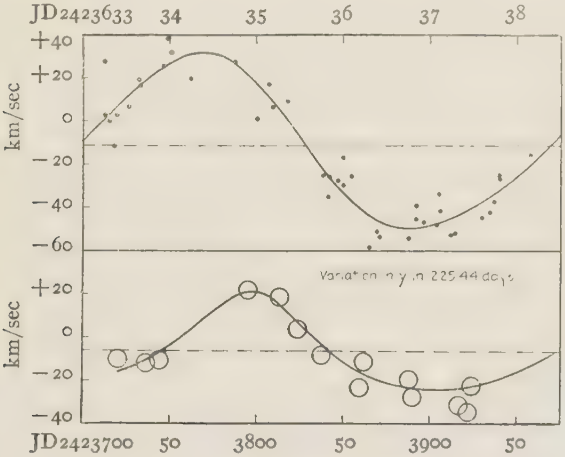

FIG. 4.—BD+57°2309

The adjustment between the two velocity-curves with periods of 225 days and 5 days, respectively, was one of successive approximations that led finally to $P=225^{d}.44$ for the long-period oscillation. Normal places for this variation were then formed, which are given in Table X. The weights are the numbers of plates used in forming the normal places. The spectrograms included in each normal place are indicated by the numbers in the last column, which refer to the successive plates in Table XII. The velocity deviations in Table X are residuals from the best approximation that could be gotten for the short-period velocity-curve. The velocity-curve which results from a plot of these data was used to derive preliminary elements by the method of Lehmann-Filhés. One least-squares solution for

## TABLE XII

### Observations of B.D.+57°2309

| No. | Plate No. | Date | G.M.T. | Phase | Obs. Vel. | Corr. from Long-Per. Var. | Corr. Vel. | O−C | H and K Vel. |
|---|---|---|---|---|---|---|---|---|---|
| | | 1920 | | | km/sec. | km/sec. | km/sec. | km/sec. | km/sec. |
| 1.... | γ 9609 | Oct. 2 | $18^h27^m$ | $5^d048$ | +13.4 | +14.5 | +27.9 | + 1 | ...... |
| 2.... | γ 9619 | Oct. 3 | 18 29 | 0.635 | −39.2 | +14.0 | −25.2 | − 3 | ...... |
| 3.... | γ 9626 | Oct. 20 | 14 58 | 1.248 | −57.6 | + 6.5 | −51.1 | − 5 | ...... |
| 4.... | γ 9627 | Oct. 20 | 15 45 | 1.280 | −60.3 | + 6.5 | −53.8 | − 7 | ...... |
| 5.... | γ 9717 | Nov. 19 | 17 46 | 4.296 | +42.3 | −10.5 | +31.8 | + 5 | ...... |
| | | 1921 | | | | | | | |
| 6.... | γ 10651 | Nov. 20 | 17 21 | 2.152 | −75.0 | +23.0 | −52.0 | − 8 | ...... |
| | | 1923 | | | | | | | |
| 7.... | γ 11814 | May 28 | 23 30 | 4.210 | +45.6 | −20.0 | +25.6 | 0 | ...... |
| 8.... | C 2279 | May 30 | 23 15 | 0.793 | − 7.4 | −20.0 | −27.4 | + 3 | ...... |
| 9.... | C 2283 | May 31 | 23 07 | 1.787 | −26.8 | −20.0 | −46.8 | + 2 | −15.7 |
| 10.... | C 2325 | June 26 | 22 18 | 0.685 | −26.6 | − 8.5 | −35.1 | −10 | −13.9 |
| 11.... | C 2330 | June 27 | 22 30 | 1.693 | −36.8 | − 8.5 | −45.3 | + 4 | ...... |
| 12.... | γ 11903 | June 28 | 21 51 | 2.665 | −18.8 | − 6.0 | −24.8 | + 6 | ...... |
| 13.... | γ 11908 | June 29 | 21 14 | 3.569 | + 6.0 | − 6.0 | 0.0 | − 3 | −11.8 |
| 14.... | γ 11996 | Aug. 3 | 20 16 | 0.704 | −41.8 | +16.0 | −25.8 | 0 | −11.2 |
| 15.... | γ 12002 | Aug. 4 | 20 05 | 1.707 | −54.9 | +16.0 | −38.9 | +10 | ...... |
| 16.... | γ 12007 | Aug. 5 | 19 29 | 2.672 | −43.7 | +17.0 | −26.7 | + 5 | ...... |
| 17.... | γ 12090 | Sept. 1 | 18 15 | 2.552 | −65.6 | +23.5 | −42.1 | − 7 | ...... |
| 18.... | γ 12091 | Sept. 1 | 19 13 | 2.593 | −60.6 | +23.5 | −37.1 | − 4 | ...... |
| 19.... | C 2428 | Sept. 2 | 19 56 | 3.622 | −35.5 | +23.5 | −12.0 | −16 | * |
| 20.... | C 2429 | Sept. 2 | 20 42 | 3.655 | −21.1 | +23.5 | + 2.4 | − 3 | −14.2 |
| 21.... | C 2435 | Sept. 4 | 20 27 | 0.230 | −14.2 | +23.5 | + 9.3 | + 8 | −16.1 |
| 22.... | C 2478 | Oct. 3 | 19 5 | 2.105 | −74.6 | +22.0 | −52.6 | − 7 | −15.5 |
| 23.... | C 2493 | Oct. 21 | 17 40 | 3.805 | −11.2 | +18.0 | + 6.8 | − 5 | −28.5 |
| 24.... | γ 12245 | Oct. 28 | 18 20 | 0.006 | + 1.3 | +16.0 | +17.3 | + 6 | + 4.2 |
| 25.... | γ 12249 | Oct. 29 | 16 44 | 0.939 | −41.5 | +16.0 | −25.5 | +11 | −18.0 |
| 26.... | γ 12257 | Oct. 30 | 16 59 | 1.950 | −49.3 | +15.5 | −33.8 | +12 | −38.6 |
| | | 1924 | | | | | | | |
| 27.... | γ 12649 | May 16 | 23 31 | 0.856 | −51.6 | +22.0 | −29.6 | + 3 | ...... |
| 28.... | γ 12653 | May 17 | 23 32 | 1.918 | −70.0 | +22.0 | −48.0 | − 1 | ...... |
| 29.... | C 2792 | May 19 | 23 56 | 3.934 | − 4.5 | +21.5 | +17.0 | 0 | −16.6 |
| | | 1925 | | | | | | | |
| 30.... | γ 13443 | June 7 | 22 52 | 3.522 | −13.0 | +15.5 | + 2.5 | + 2 | + 2.3 |
| 31.... | γ 13449 | June 8 | 22 50 | 4.520 | + 3.8 | +16.0 | +19.8 | −11 | ...... |
| 32... | γ 13518 | July 5 | 18 18 | 4.263 | +15.9 | +23.0 | +38.9 | +12 | ...... |
| 33.... | γ 13524 | July 6 | 18 28 | 5.270 | −22.2 | +23.0 | + 0.8 | −16 | ...... |
| 34.... | γ 13527 | July 6 | 22 50 | 0.038 | −16.5 | +23.0 | + 6.5 | − 3 | ...... |
| 35.... | γ 13531 | July 7 | 17 46 | 0.827 | −40.4 | +23.5 | −16.9 | +16 | ...... |
| 36.... | γ 13539 | July 8 | 21 18 | 1.974 | −65.1 | +23.5 | −41.6 | + 5 | ...... |
| 37.... | γ 13545 | July 9 | 22 14 | 3.013 | −38.6 | +23.5 | −15.1 | + 4 | ...... |
| 38.... | γ 13738 | Sept. 24 | 14 56 | 3.918 | +11.1 | + 8.0 | +19.1 | + 3 | ...... |
| 39.... | γ 13766 | Sept. 27 | 17 39 | 1.617 | −60.8 | + 6.5 | −54.3 | − 5 | ...... |
| 40.... | C 3588 | Dec. 3 | 14 42 | 3.532 | +43.8 | −16.0 | +27.8 | +27 | −34.4 |
| 41.... | γ 13912 | Dec. 6 | 15 20 | 1.144 | −44.6 | −14.5 | −59.1 | −15 | ...... |
| 42.... | γ 13942 | Dec. 29 | 14 34 | 2.458 | −46.8 | + 2.5 | −44.3 | − 7 | ...... |

* Red sensitive plate.

corrections to these elements was made, and Table XI gives preliminary elements, corrections, and corrected elements. The element called $\gamma$ in this case must be considered as a correction to the $\gamma$ corresponding to the short-period orbit, so that the velocity of the triple system is the sum of these two gammas.

The lower part of Figure 4 shows the curve defined by the corrected elements of Table XI and the normal points from which it was derived. It is doubtful whether these elements are quite right, but the limited data hardly warrant further refinement.

TABLE XIII

Normal Places; B.D.+57°2309; $P = 5^{\rm d}41364$

| No. | Phase | Velocity Freed from Long-Period Oscillation | O−C | Wt. | Plate Nos. from Table XII |
|---|---|---|---|---|---|
| | | km/sec. | km/sec. | | |
| 1........ | $0^{\rm d}118$ | +13.3 | + 7 | 2 | 21, 24 |
| 2........ | 0.795 | −28.7 | + 2 | 5 | 8, 10, 14, 25, 27 |
| 3........ | 0.986 | −38.0 | − 1 | 2 | 35, 41 |
| 4........ | 1.054 | −43.4 | − 3 | 3 | 2, 3, 4 |
| 5........ | 1.796 | −48.0 | 0 | 2 | 36, 39 |
| 6........ | 1.860 | −44.2 | + 4 | 6 | 9, 11, 15, 22, 26, 28 |
| 7........ | 2.152 | −52.0 | − 8 | 1 | 6 |
| 8........ | 2.620 | −32.7 | 0 | 4 | 12, 16, 17, 18 |
| 9........ | 2.740 | −29.7 | − 1 | 2 | 37, 42 |
| 10........ | 3.693 | − 0.7 | − 8 | 4 | 13, 19, 20, 23 |
| 11........ | 3.758 | + 9.8 | 0 | 2 | 29, 30 |
| 12........ | 4.088 | +26.4 | + 6 | 4 | 31, 32, 38, 40 |
| 13........ | 4.548 | +28.4 | − 2 | 3 | 1, 5, 7 |
| 14........ | 5.391 | + 3.6 | −10 | 2 | 33, 34 |

The lower curve in Figure 4 was then used to derive the corrections to the observed velocities to free them from the superposed long-period variation. Table XII gives the various data for the forty-two plates. The phases depend on the finally adopted elements of the short-period orbit; the corrections in the sixth column are those just referred to. The residuals are scaled from the upper part of Figure 4.

The assembly of the corrected velocities based on $P = 5^{\rm d}41364$ was so satisfactory that the period could be assumed to be known.

On account of the rather low weight for a single observation, it seemed best to form normal places, a procedure which also greatly diminished the labor of correcting the preliminary elements. These normal places are given in Table XIII. The weights are equal to the numbers of plates forming a normal. The phase and residuals refer to the final elements.

The freehand curve drawn through the plot of the normal places of Table XIII, assembled with the period 5.41364 days, gave by Russell's method a set of preliminary elements, which, as in the other case, were once corrected by least-squares. Table XIV gives the preliminary elements, corrections, and corrected elements. In this case, the corrections are satisfactorily small. By combining the $\gamma$ thus derived with that from Table XI, the velocity of the triple system is found to be $-17.2$ km/sec.

TABLE XIV

B.D.+57°2309—ELEMENTS OF SHORT-PERIOD VARIATION

| | Preliminary Elements | Corrections | Adopted Elements |
|---|---|---|---|
| $P$ .......... | .................. | .............. | $5^{\mathrm{d}}41364$ |
| $e$ .......... | 0.10 | +0.014 | 0.114 |
| $\omega$ .......... | $63^{\circ}5$ | $-5^{\circ}0$ | $58^{\circ}5$ |
| $K$ .......... | 41.3 | $-1.3$ | 40.0 km/sec. |
| $T$ .......... | J.D. 2423635.137 | +0.003 | 3635.140 |
| $\gamma$ .......... | $-11.3$ | +0.2 | $-11.1$ km/sec. |
| $a \sin i$ ....... | .................. | .............. | 2,959,900 km |
| $\frac{m_1^3 \sin^3 i}{(m+m_1)^2}$ .... | .................. | .............. | $0.0353\ \odot$ |

The values for $a \sin i$ and the mass function have both been added to Tables XI and XIV. In the former, $M_1$ is the mass of the third body, and $a$ and $K$ refer to the semi-major axis and projected semi-amplitude of the velocity variation of the pair of stars forming the short-period system about the center of gravity of the triple system; and $M$ is the combined mass of the two stars forming the short-period system and therefore the sum of $m$ and $m_1$ which appear in Table XIV. If we assume that the mass of the primary in the short-period system is twice that of the secondary and that $i$, the inclination of the orbit plane to the plane normal to the line of sight, is the same for both orbits, it is readily shown that we are dealing with moderate and entirely reasonable masses, whatever the value of $i$ between 30° and 90°. Further discussion of this point is hardly warranted, since the assumptions have no observational foundation.

The last column of Table XII gives the velocities derived from the H and K lines of calcium whenever these lines have been of satisfactory quality for measurement. There is considerable range in these velocities; but it has not been possible to find any smooth variation based on either the long or short period or a combination of the two. This does not preclude the possibility of periodicity, but the present data can be just as well represented by an invariable velocity whose apparent variability is only accidental. Hence the weighted mean is used as the best value of the velocity based upon the H and K lines, and this will probably not be far from the truth even if there is a periodic variation. This mean is $-19.4$ km/sec., which is not greatly different from the velocity of the triple system, $-17.2$ km/sec., or from the reflex of the solar motion in the direction of this system, namely, $-15$ km/sec. If it may be identified with the velocity of the triple system, which seems reasonable, and if the source of the H and K absorption is assumed to be in the immediate vicinity of the system, which is closely surrounded by nebulosity, it would be natural to infer that the velocity of the triple system is also that of the nebulosity, and that such nebulosity has ionized calcium as one of its constituents. So far as known, the spectrum of the nebulosity is continuous in character. The sodium lines $D_1$ and $D_2$ are present, a point of interest, because, except when these two lines manifest a behavior similar to the detached H and K lines, they do not ordinarily appear until later in the stellar spectral sequence.

Since, as already mentioned in connection with $\eta$ Orionis A, several spectroscopic binaries which have detached H and K lines also have detached sodium lines, a spectrogram covering the D region of B.D. $+57^\circ 2309$ was made on June 22, 1926. The photographic density is such that the spectrum can be measured from K of calcium to the D lines. The strength of the D lines is in itself sufficient to show that these lines are of the detached variety, since, otherwise, they would be almost vanishingly weak, inasmuch as the spectrum of the star is B3. The measured velocities also support this conclusion. The epoch was so chosen that the star's velocity was at the maximum for both the short and long periods, and hence deviated a maximum amount from the velocity of the triple system. The velocities for the K line and for the D lines and the mean velocity from the remaining lines are −2, −10, and +60 km/sec., respectively. The third velocity is to be compared with a computed velocity of +50 km/sec. The D-line velocity certainly differs markedly from this value, and is of the order of the previously determined mean for H and K and of the value for the single K line on the same plate. The evidence from this single plate is therefore for a similarity in behavior between the sodium lines and the H and K lines. In order to settle the question definitely, however, more plates are needed, especially such as have a greater precision for the D lines.

MOUNT WILSON OBSERVATORY
July 1926

Contributions from the Mount Wilson Observatory, No. 318
Reprinted from the *Astrophysical Journal*, Vol. LXIV, pp. 194–203, 1926
Printed in the U.S.A.

# MULTIPLETS IN THE SPARK SPECTRUM OF IRON

By HENRY NORRIS RUSSELL

## ABSTRACT

*Analysis of the spark spectrum of iron.*—All the lines of astrophysical importance have been classified with the aid of material prepared by Messrs. Merrill, Anderson, and Babcock. *Multiplets* belonging to *sextet and quartet systems* have been found. So far 214 lines have been grouped into 35 multiplets, involving combinations between 16 terms.

The *state of lowest energy* in the ionized atom corresponds to a $^6$D-term, the next to a $^4$F′-term. *The observed terms are in excellent agreement with the predictions of Hund's theory*, and are from the electronic configurations $s^2d^5$, $sd^6$, $d^7$, and $d^6p$. Only the lowest terms of the quartet system out of a large number predicted have yet been found, and an intricate system of doublets should exist. This agrees with the fact that many lines are still unclassified. Work on this spectrum will be continued.

An investigation of the enhanced lines of iron has been planned at this Observatory for some time. In connection with this, a list of all the iron lines which are known to belong to the spark spectrum was prepared by Mr. Merrill and Mr. Anderson, including the Zeeman effects as measured by Mr. Babcock, and used by the writer as a basis for an analysis of the structure of the spectrum.

The starting-point of this analysis was found in two multiplets in the ultra-violet discovered at the Bureau of Standards[1] which arose from combinations between a D- and D′-term of a sextet system ($^6$D and $^6$D′), and of a $^4$D- and $^4$P-term of a quartet system. With these as a beginning, a considerable number of other terms was found, and practically all the enhanced lines in the visible and near ultra-violet region were classified. A summary of the results appears in the writer's "List of Ultimate and Penultimate Lines,"[2] but the details have not yet been published.

Many lines remain unassigned, and it is hoped to continue the investigation in the near future; but as practically all the lines of astrophysical importance have already been classified, and there can be little doubt that the principal low energy-levels have been found, it seems desirable to publish the results thus far obtained, for the benefit of those who may be interested.

---

[1] Meggers, Kiess, and Walters, *Journal of the Optical Society of America*, **9**, 371, 1924.

[2] *Mt. Wilson Contr.*, No. 286; *Astrophysical Journal*, **61**, 274, 1925.

The lowest energy-level of the ionized atom of iron belongs to a $^6$D-term, which, with all the others so far found, is "inverted," the component with the greatest inner-quantum number having the lowest energy. Next above this and very near it comes a $^4$F′-term, and then a $^4$D- and a $^4$P′-term. These combine with terms of higher levels of types $^6$P $^6$D′ $^6$F, $^4$P $^4$D′ $^4$F, giving strong lines in the ultra-violet, which appear with considerable and often great intensity in the arc spectrum.

The spark lines in the visible region arise from the combination of higher-lying quartet and sextet terms with the same two "triads" of terms which have just been mentioned, as is shown in detail in the tables.

Table I gives the spectroscopic terms which have so far been identified. The notation is that now in general use, $^4P_3$ for example, denoting that component of a P-term of the quartet system which has the inner quantum number 3. Different terms of the same species are distinguished by letters a$^4$P, b$^4$P, etc., "a" denoting the lowest known term of the sort. The term values are counted upward from the lowest known energy-level, which appears to be much the best scheme when the ionization potential is unknown, and has much to recommend it as a permanent policy in the case of complex spectra.

A list of the lines which have been identified is given in Table II, which includes wave-lengths in I.A., intensities in the spark (from Merrill and Anderson's list), wave-numbers, and the designation by means of the terms whose combination produces the line.

The third column $(O-C)$ gives the difference between the observed wave-length and that computed from the term values given in Table I. The agreement is very close, except for the lines in the extreme ultra-violet, which are taken from Bloch's measures.[1] There is a systematic discordance of 0.10 A in this case, which, in view of the difficulties of exact standardization of measures of wave-length in this region, may be regarded as remarkably small.

When more such groups of lines of predictable wave-lengths have

---

[1] *Comptes Rendus*, 179, 1396, 1924.

### TABLE I

*$Fe^+$* TERMS

| Type | Term | Combinations |
|---|---|---|
| $a^4P_3'$ | 13474.36 | $a^4P$ $a^4D'$ $a^4F$ |
| | *198.68* | |
| $a^4P_2'$ | 13673.04 | |
| | *231.70* | |
| $a^4P_1'$ | 13904.74 | |
| $b^4P_3'$ | 20830.44 | $a^4P$ $a^4D'$ $a^4F$ |
| | *981.49* | |
| $b^4P_2'$ | 21811.93 | |
| | *597.78* | |
| $b^4P_1'$ | 22409.71 | |
| $a^4D_4$ | 7955.24 | $a^4P$ $a^4D'$ $a^4F$ |
| | *436.66* | |
| $a^4D_3$ | 8391.90 | $a^6P$ $a^6D'$ $a^6F$ |
| | *288.47* | |
| $a^4D_2$ | 8680.37 | |
| | *166.35* | |
| $a^4D_1$ | 8846.72 | |
| $b^4D_4$ | 31483.10 | $a^4P$ $a^4D'$ $a^4F$ |
| | *−95.28* | |
| $b^4D_3$ | 31387.82 | $b^4F$ |
| | *−23.51* | |
| $b^4D_2$ | 31364.31 | |
| | *3.99* | |
| $b^4D_1$ | 31368.30 | |
| $a^4F_5'$ | 1872.56 | $a^4D'$ $a^4F$ $b^4F$ |
| | *557.60* | |
| $a^4F_4'$ | 2430.16 | $a^6D'$ $a^6F$ |
| | *407.75* | |
| $a^4F_3'$ | 2837.91 | |
| | *279.58* | |
| $a^4F_2'$ | 3117.49 | |
| $b^4F_5'$ | 22637.15 | $a^4D'$ $a^4F$ $b^4F$ |
| | *173.13* | |
| $b^4F_4'$ | 22810.28 | |
| | *128.93* | |
| $b^4F_3'$ | 22939.21 | |
| | *92.04* | |
| $b^4F_2'$ | 23031.25 | |
| $a^4G_6$ | 25428.78 | $a^4D'$ $a^4F$ $b^4F$ |
| | *376.43* | |
| $a^4G_5$ | 25805.21 | |
| | *176.30* | |
| $a^4G_4$ | 25981.51 | |
| | *73.84* | |
| $a^4G_3$ | 26055.35 | |
| $a^6S$ | 23317.61 | $a^6P$ $a^6D'$ $a^6F$<br>$a^4D'$ $a^4F$ |
| $a^6D_5$ | 0.00 | $a^6P$ $a^6D'$ $a^6F$ |
| | *384.80* | |
| $a^6D_4$ | 384.80 | |
| | *282.85* | |
| $a^6D_3$ | 667.65 | |
| | *194.90* | |
| $a^6D_2$ | 862.55 | |
| | *114.41* | |
| $a^6D_1$ | 976.96 | |
| $a^4P_3$ | 46967.29 | $a^4P'$ $b^4P'$ $a^4D$ |
| | *422.34* | |
| $a^4P_2$ | 47389.63 | $b^4D$ |
| | *236.29* | |
| $a^4P_1$ | 47625.92 | |
| $a^4D_4'$ | 44446.81 | $a^4P'$ $b^4P'$ $a^4D$ |
| | *337.81* | |
| $a^4D_3'$ | 44784.62 | $b^4D$ $a^4F'$ $b^4F'$ |
| | *259.53* | |
| $a^4D_2'$ | 45044.15 | $a^4G$ $a^6S$ |
| | *162.23* | |
| $a^4D_1'$ | 45206.38 | |
| $a^4F_5$ | 44232.52 | $a^4P'$ $b^4P'$ $a^4D$ |
| | *521.20* | |
| $a^4F_4$ | 44753.72 | $b^4D$ $a^4F'$ $b^4F'$ |
| | *326.05* | |
| $a^4F_3$ | 45079.77 | $a^4G$ $a^6S$ |
| | *209.99* | |
| $a^4F_2$ | 45289.76 | |
| $b^4F_5$ | 65695.28 | $b^4D$ $a^4F'$ $b^4F'$ |
| | *681.63* | |
| $b^4F_4$ | 66376.91 | $a^4G$ |
| | *453.41* | |
| $b^4F_3$ | 66830.32 | |
| | *234.54* | |
| $b^4F_2$ | 67064.86 | |
| $a^6P_4$ | 42658.26 | $a^6S$ $a^6D$ $a^4D$ |
| | *580.26* | |
| $a^6P_3$ | 43238.52 | |
| | *382.46* | |
| $a^6P_2$ | 43620.98 | |

TABLE I—*Continued*

| Type | Term | Combinations | Type | Term | Combinations |
|---|---|---|---|---|---|
| $a^6D'_5$ | 38458.88 | $a^6S$ $a^6D$ $a^4D$ | $a^6F_6$ | 41968.05 | $a^6S$ $a^6D$ $a^4D$ |
| | *201.05* | | | *146.78* | |
| $a^6D'_4$ | 38659.93 | $a^4F'$ | $a^6F_5$ | 42114.83 | $a^4F'$ |
| | *198.91* | | | *122.17* | |
| $a^6D'_3$ | 38858.84 | | $a^6F_4$ | 42237.00 | |
| | *154.19* | | | *97.62* | |
| $a^6D'_2$ | 39013.03 | | $a^6F_3$ | 42334.62 | |
| | *96.10* | | | *66.58* | |
| $a^6D'_1$ | 39109.13 | | $a^6F_2$ | 42401.20 | |
| | | | | *38.51* | |
| | | | $a^6F_1$ | 42439.71 | |

been found, the problem of obtaining accurate standards in the Schumann region will be practically solved.

A number of lines in the red which fall exactly in the positions predicted by the combination principle, but have not been recorded in the laboratory, have been taken from the solar spectrum, in which they are readily distinguished by the fact that they are greatly weakened in sun-spots. These lines are indicated by an asterisk (*) in the intensity column. They are all faint. This behavior is characteristic of enhanced lines and suffices to show that they belong to a spark spectrum of some sort. The excellent agreement with the computed wave-lengths indicates that they are due to iron.

A few words may be added on the theoretical significance of these results.

According to Hund's theory,[1] which gives a remarkably complete account of the structure of all spectra to which it has been applied, the more complex spectra arise from the combined action of all the "outer" electrons on the atom (those which do not belong to complete groups or "shells"). Each of these electrons may be described in the usual way by the quantum number of its orbit, e.g., $4_1$, $4_2$, $3_3$, where the large figure denotes the total and the subscript the azimuthal quantum number, or by the equivalent notation 4s, 4p, 3d, which describes the type of spectroscopic term which would be produced by such an electron if acting alone (as in the cases of $K$, $Ca^+$, etc.).

To a given configuration of electronic orbits in the atom corre-

---

[1] *Zeitschrift für Physik*, 33, 345, 1925.

## TABLE II

### *Fe*+ IDENTIFIED LINES

(Unit for O−C, 0.01 A)

| λ | Int. | O−C<br>λ | ν Vac. | Multiplet |
|---|---|---|---|---|
| 1550.17 . . . . . . . . | 3 | −12 | 64509.07 | $a^4F_5-b^4F_4$ |
| 1552.7 . . . . . . . . . | 1 | −9 | 64403.95 | $a^4F_4-b^4F_3$ |
| 1562.60 . . . . . . . . | 00 | −9 | 63995.93 | $a^4F_3-b^4F_3$ |
| 1563.70† . . . . . . . | 3 | −10<br>−9 | 63950.87 | $a^4F_4-b^4F_4$<br>$a^4F'_2-b^4F_2$ |
| 1566.74 . . . . . . . . | 2 | −10 | 63826.81 | $a^4F'_5-b^4F_5$ |
| 1580.53 . . . . . . . . | 2 | −12 | 63269.93 | $a^4F_4-b^4F_5$ |
| 2270.29 . . . . . . . . | 1 | 0 | 44033.61 | $b^4F_2-b^4F_2$ |
| 2277.67 . . . . . . . . | 4 | +1 | 43890.91 | $b^4F'_3-b^4F_3$ |
| 2294.69 . . . . . . . . | 5 | +1 | 43565.42 | $b^4F'_4-b^4F_4$? |
| 2321.71 . . . . . . . . | 1 | −2 | 43058.46 | $b^4F_5-b^4F_5$ |
| 2327.39 . . . . . . . . | 5 | 0 | 42953.38 | $a^6D_3-a^6P_2$ |
| 2331.30 . . . . . . . . | 5 | −1 | 42881.35 | $a^4F_5-a^4F_4$ |
| 2332.80 . . . . . . . . | 6 | 0 | 42853.79 | $a^6D_4-a^6P_3$ |
| 2338.00 . . . . . . . . | 5 | 0 | 42758.48 | $a^6D_2-a^6P_2$ |
| 2343.49 . . . . . . . . | 7 | 0 | 42658.28 | $a^6D_5-a^6P_4$ |
| 2343.97 . . . . . . . . | 3 | +4 | 42648.87 | $a^4F'_4-a^4F_3$? |
| 2344.28 . . . . . . . . | 5 | 0 | 42643.95 | $a^6D_1-a^6P_2$ |
| 2348.12 . . . . . . . . | 6 | 0 | 42574.22 | $a^4F'_5-a^4D'_4$ |
| 2348.30 . . . . . . . . | 7 | −1 | 42570.96 | $a^6D_3-a^6P_3$ |
| 2354.88 . . . . . . . . | 3 | −1 | 42452.00 | $a^4F'_3-a^4F_2$ |
| 2359.11 . . . . . . . . | 6 | 0 | 42375.90 | $a^6D_2-a^6P_3$ |
| 2360.00 . . . . . . . . | 5 | 0 | 42359.91 | $a^4F'_5-a^4F_5$ |
| 2360.31 . . . . . . . . | 5 | +1 | 42354.36 | $a^4F_4-a^4D'_3$ |
| 2362.04 . . . . . . . . | 4 | +1 | 42323.33 | $a^4F'_4-a^4F_4$ |
| 2364.82 . . . . . . . . | 6 | −1 | 42273.59 | $a^6D_4-a^6P_4$ |
| 2366.59 . . . . . . . . | 4 | −1 | 42241.97 | $a^4F_3-a^4F_3$ |
| 2366.86 . . . . . . . . | 0 | +7 | 42235.75 | $a^6D_5-a^6F_4$? |
| 2368.60 . . . . . . . . | 6 | +1 | 42206.13 | $a^4F_3-a^4D'_2$ |
| 2370.50 . . . . . . . . | 3 | 0 | 42172.30 | $a^4F'_2-a^4F_2$ |
| 2373.733 . . . . . . . | 7 | 0 | 42114.87 | $a^6D_5-a^6F_5$ |
| 2375.103 . . . . . . . | 6 | −1 | 42088.98 | $a^4F'_2-a^4D'_1$ |
| 2379.276 . . . . . . . | 6 | −1 | 42016.75 | $a^4F'_4-a^4D'_4$ |
| 2380.763 . . . . . . . | 6 | +1 | 41990.52 | $a^6D_3-a^6P_4$ |
| 2382.030 . . . . . . . | 10 | 0 | 41968.05 | $a^6D_5-a^6F_6$ |
| 2383.02 . . . . . . . . | 3h | 0 | 41950.75 | $a^6D_4-a^6F_3$? |
| 2383.253 . . . . . . . | 4 | 0 | 41946.68 | $a^4F'_3-a^4D'_3$ |
| 2384.39 . . . . . . . . | 5 | 0 | 41926.65 | $a^4F'_2-a^4D'_2$ |
| 2385.00 . . . . . . . . | 2 | −1 | 41915.93 | $a^4F'_3-a^4F_4$ |
| 2388.631 . . . . . . . | 8 | 0 | 41852.22 | $a^6D_4-a^6F_4$ |
| 2391.485 . . . . . . . | 3 | 0 | 41802.36 | $a^4F'_4-a^4F_5$ |
| 2395.423 . . . . . . . | 5 | 0 | 41733.56 | $a^6D_3-a^6F_2$ |
| 2395.628 . . . . . . . | 8 | 0 | 41729.99 | $a^6D_4-a^6F_5$ |
| 2399.244† . . . . . . | 8 | −1<br>0 | 41667.09 | $a^6D_3-a^6F_3$<br>$a^4F'_2-a^4D'_3$ |
| 2402.60 . . . . . . . . | 3 | 0 | 41608.92 | $a^4F_3-a^4D'_4$ |
| 2404.435 . . . . . . . | 5 | 0 | 41577.16 | $a^6D_2-a^6F_1$ |
| 2404.888 . . . . . . . | 8 | 0 | 41569.33 | $a^6D_3-a^6F_4$ |
| 2406.663 . . . . . . . | 7 | 0 | 41538.67 | $a^6D_2-a^6F_2$ |
| 2410.526 . . . . . . . | 8 | +1 | 41471.98 | $a^6D_2-a^6F_3$ |
| 2411.071 . . . . . . . | 7 | 0 | 41462.74 | $a^6D_1-a^6F_1$ |

TABLE II—*Continued*

| λ | Int. | O−C λ | ν Vac. | Multiplet |
|---|---|---|---|---|
| 2413.313 | 6 | 0 | 41424.22 | $a^6D_1-a^6F_2$ |
| 2437.72 | 1 | 0 | 41009.51 | $a^4G_3-b^4F_2$ |
| 2447.32 | 3 | +1 | 40848.65 | $a^4G_4-b^4F_3$ |
| 2451.74 | 2 | 0 | 40775.01 | $a^4G_3-b^4F_3$ |
| 2464.03 | 4 | 0 | 40571.66 | $a^4G_5-b^4F_4$ |
| 2474.78 | 4 | 0 | 40395.44 | $a^4G_4-b^4F_4$ |
| 2476.67§ | 2 | −1 | 40364.61 | $a^4F'_5-a^6F_4$ |
| 2482.70 | 5 | 0 | 40266.58 | $a^4G_6-b^4F_5$ |
| 2484.188§ | 6 | −1 | 40242.45 | $a^4F'_5-a^6F_5$ |
| 2493.29 | 10 | 0 | 40095.56 | $a^4F'_5-a^6F_6$ |
| 2505.26 | 1 | +3 | 39904.00 | $a^4F'_4-a^6F_3$ |
| 2506.14 | 2 | +1 | 39889.99 | $a^4G_5-b^4F_5$ |
| 2511.36 | 2 | −2 | 39807.09 | $a^4F'_4-a^6F_4$ |
| 2519.09 | 6 | −2 | 39684.93 | $a^4F'_4-a^6F_5$ |
| 2540.12 | 4 | −2 | 39217.46 | $a^4F'_2-a^6F_3$ |
| 2562.543 | 9 | 0 | 39012.05 | $a^4D_4-a^4P_3$ |
| 2563.485 | 7 | 0 | 38997.72 | $a^4D_3-a^4P_2$ |
| 2566.921 | 5 | 0 | 38945.54 | $a^4D_2-a^4P_1$ |
| 2577.930 | 6 | 0 | 38779.20 | $a^4D_1-a^4P_1$ |
| 2582.590 | 8 | 0 | 38709.25 | $a^4D_2-a^4P_2$ |
| 2585.886 | 10 | 0 | 38659.91 | $a^6D_5-a^6D'_4$ |
| 2591.554 | 7 | 0 | 38575.38 | $a^4D_3-a^4P_3$ |
| 2593.70† | 4 | −4 | 38543.46 | $a^4D_1-a^4P_2$? |
| 2598.380 | 8 | 0 | 38474.04 | $a^6D_4-a^6D'_3$ |
| 2599.405 | 10 | 0 | 38458.88 | $a^6D_5-a^6D'_5$ |
| 2607.099 | 8 | 0 | 38345.39 | $a^6D_3-a^6D'_2$ |
| 2611.086 | 3 | 0 | 38286.82 | $a^4D_2-a^4P_3$ |
| 2611.885 | 9 | 0 | 38275.11 | $a^6D_4-a^6D'_4$ |
| 2613.835 | 8 | 0 | 38246.57 | $a^6D_2-a^6D'_1$ |
| 2617.627 | 8 | 0 | 38191.17 | $a^6D_3-a^6D'_3$ |
| 2620.419 | 3 | 0 | 38150.47 | $a^6D_2-a^6D'_2$ |
| 2621.677 | 7 | 0 | 38132.17 | $a^6D_1-a^6D'_1$ |
| 2625.676 | 9 | 0 | 38074.08 | $a^6D_4-a^6D'_5$ |
| 2628.303 | 8 | 0 | 38036.05 | $a^6D_1-a^6D'_2$ |
| 2631.053 | 7 | 0 | 37996.30 | $a^6D_2-a^6D'_3$ |
| 2631.332 | 7 | 0 | 37992.27 | $a^6D_3-a^6D'_4$ |
| 2692.842 | 3 | 0 | 37124.50 | $a^4D_4-a^4F_3$ |
| 2709.39 | 1 | +2 | 36897.62 | $a^4D_3-a^4F_2$ |
| 2714.419 | 8 | 0 | 36829.39 | $a^4D_4-a^4D'_3$ |
| 2724.892 | 5 | 0 | 36687.85 | $a^4D_3-a^4F_3$ |
| 2727.542 | 5 | 0 | 36652.21 | $a^4D_3-a^4D'_2$ |
| 2730.740 | 6 | +1 | 36609.30 | $a^4D_2-a^4F_2$ |
| 2732.46 | 5 | 0 | 36586.27 | $a^4F_5-a^6D'_5$ |
| 2736.970 | 7 | 0 | 36525.96 | $a^4D_2-a^4D'_1$ |
| 2739.551 | 10 | 0 | 36491.55 | $a^4D_4-a^4D'_4$ |
| 2743.199 | 8 | 0 | 36443.03 | $a^4D_1-a^4F_2$ |
| 2746.486 | 8 | 0 | 36399.41 | $a^4D_2-a^4F_3$ |
| 2746.988 | 7 | 0 | 36392.75 | $a^4D_3-a^4D'_3$ |
| 2749.182 | 4 | 0 | 36363.74 | $a^4D_2-a^4D'_2$ |
| 2749.327 | 10 | 0 | 36361.81 | $a^4D_3-a^4F_4$ |
| 2749.487 | 3 | 0 | 36359.69 | $a^4D_1-a^4D'_1$ |
| 2755.736 | 9 | 0 | 36277.24 | $a^4D_4-a^4F_5$ |
| 2761.809 | 4 | 0 | 36197.48 | $a^4D_1-a^4D'_2$ |
| 2768.938 | 3 | 0 | 36104.28 | $a^4D_2-a^4D'_3$ |

TABLE II—*Continued*

| λ | Int. | O−C λ | ν Vac. | Multiplet |
|---|---|---|---|---|
| 2861.20 | 2 | +4 | 34940.13 | $a^4D_2-a^6P_2$? |
| 2864.97 | 2 | −3 | 34894.16 | $b^4D_4-b^4F_4$? |
| 2868.88 | 2 | 0 | 34846.62 | $a^4D_3-a^6P_3$ |
| 2880.757 | 5 | +1 | 34702.94 | $a^4D_4-a^6P_4$ |
| 2892.85 | 1 | 0 | 34558.11 | $a^4D_2-a^6P_3$ |
| 2916.1 | 1u | −5 | 34282.36 | $a^4D_4-a^6F_4$ |
| 2922.02 | 2 | −6 | 34212.91 | $b^4D_4-b^4F_5$ |
| 2926.584 | 6 | 0 | 34159.55 | $a^4D_4-a^6F_5$ |
| 2944.400 | 6 | 0 | 33952.89 | $a^4P'_2-a^4P_1$ |
| 2947.661 | 6 | 0 | 33915.23 | $a^4P'_3-a^4P_2$ |
| 2953.778 | 5 | 0 | 33845.08 | $a^4D_3-a^6F_4$ |
| 2964.632† | 3 | 3<br>0 | 33721.17 | $a^4D_2-a^6F_2$<br>$a^4P'_1-a^4P_1$ |
| 2965.040 | 4 | +1 | 33716.53 | $a^4P'_2-a^4P_2$ |
| 2970.518 | 3 | −1 | 33654.37 | $a^4D_2-a^6F_3$ |
| 2975.94 | 1 | −1 | 33593.05 | $a^4D_1-a^6F_1$ |
| 2979.356 | 2 | 0 | 33554.52 | $a^4D_1-a^6F_2$ |
| 2984.834 | 8 | 0 | 33492.96 | $a^4P'_3-a^4P_3$ |
| 2985.552 | 6 | 0 | 33484.91 | $a^4P'_1-a^4P_2$ |
| 3002.651 | 7 | 0 | 33294.22 | $a^4P'_2-a^4P_3$ |
| 3170.346 | 2 | +1 | 31533.22 | $a^4P'_2-a^4D'_1$ |
| 3183.126 | 3 | +1 | 31406.60 | $a^4P'_2-a^4F_3$ |
| 3185.33 |  | +2 | 31384.87 | $a^4P'_1-a^4F_2$ |
| 3186.750 | 4 | +2 | 31370.88 | $a^4P'_2-a^4D'_2$ |
| 3192.806‖ | 3 | −12 | 31311.38 | $a^4P'_3-a^4D'_3$ |
| 3193.811 | 4 | +1 | 31301.53 | $a^4P'_1-a^4D'_1$ |
| 3196.086 | 3 | +1 | 31279.25 | $a^4P'_3-a^4F_4$ |
| 3210.458 | 4 | +2 | 31139.24 | $a^4P'_1-a^4D'_2$ |
| 3213.320 | 5 | +1 | 31111.50 | $a^4P'_2-a^4D'_3$ |
| 3227.756 | 7d | +1 | 30972.36 | $a^4P'_3-a^4D'_4$ |
| 3255.898 | 2 | 0 | 30704.67 | $a^4D_4-a^6D'_4$ |
| 3277.358 | 3 | 0 | 30503.62 | $a^4D_4-a^6D'_5$ |
| 3281.302 | 2 | 0 | 30466.95 | $a^4D_3-a^6D'_3$ |
| 3295.825 | 1 | −1 | 30332.72 | $a^4D_2-a^6D'_2$ |
| 3302.865 | 1 | 0 | 30268.06 | $a^4D_3-a^6D'_4$ |
| 3303.476 | 1 | 0 | 30262.44 | $a^4D_1-a^6D'_1$ |
| 3312.707 | 1 | +4 | 30178.12 | $a^4D_2-a^6D'_3$ |
| 3974.17 | * | 0 | 25155.38 | $b^4P'_2-a^4P_3$? |
| 4122.67 | * | +1 | 24249.26 | $b^4P'_3-a^4F_3$ |
| 4128.74 | * | +1 | 24213.67 | $b^4P'_3-a^4D'_2$ |
| 4173.475 | 5 | +1 | 23954.12 | $b^4P'_3-a^4D'_3$ |
| 4178.868 | 8 | +1 | 23923.22 | $b^4P'_3-a^4F_4$ |
| 4233.163 | 10 | 0 | 23616.36 | $b^4P'_3-a^4D'_4$ |
| 4258.16 | * | −1 | 23477.87 | $b^4P'_2-a^4F_2$ |
| 4273.31 | 1 | −1 | 23394.50 | $b^4P'_2-a^4D'_1$ |
| 4296.56 | 3 | −2 | 23267.93 | $b^4P'_2-a^4F_3$ |
| 4303.18 | 4 | +2 | 23232.10 | $b^4P'_2-a^4D'_2$ |
| 4351.77 | 10 | −1 | 22972.72 | $b^4P'_2-a^4D'_3$ |
| 4369.41 | * | +1 | 22880.01 | $b^4P'_1-a^4F_2$ |
| 4385.39 | 5 | +1 | 22796.60 | $b^4P'_1-a^4D'_1$ |
| 4416.81 | 8 | 0 | 22634.42 | $b^4P'_1-a^4D'_2$ |
| 4472.93 | * | 0 | 22350.56 | $b^4F'_3-a^4F_2$ |
| 4489.21 | 10 | +2 | 22269.38 | $b^4F'_4-a^4F_3$ |
| 4491.41 | 8 | +1 | 22258.48 | $b^4F'_2-a^4F_2$ |

TABLE II—*Continued*

| λ | Int. | O−C λ | ν Vac. | Multiplet |
|---|---|---|---|---|
| 4508.287 | 15 | − 1 | 22175.16 | $b^4F'_2-a^4D'_1$ |
| 4515.337 | 15 | 0 | 22140.55 | $b^4F'_3-a^4F_3$ |
| 4520.238 | 8 | 0 | 22116.55 | $b^4F'_5-a^4F_4$ |
| 4522.636 | 10 | + 2 | 22104.82 | $b^4F'_3-a^4D'_2$ |
| 4534.17 | * | − 3 | 22048.66 | $b^4F'_2-a^4F_3$ |
| 4541.52 | * | − 2 | 22013.01 | $b^4F'_2-a^4D'_2$ |
| 4549.477 | 20 | − 2 | 21974.45 | $b^4F'_4-a^4D'_3$ |
| 4555.904 | 15 | 0 | 21943.44 | $b^4F'_4-a^4F_4$ |
| 4576.31 | 10 | − 3 | 21845.56 | $b^4F'_3-a^4D'_3$ |
| 4582.84 | * | + 3 | 21814.39 | $b^4F'_3-a^4F_4$ |
| 4583.843 | 30 | 0 | 21809.68 | $b^4F'_5-a^4D'_4$ |
| 4595.72 | * | + 1 | 21753.30 | $b^4F'_2-a^4D'_3$ |
| 4601.38 | * | 0 | 21726.54 | $a^6S-a^4D'_2$ |
| 4620.52 | * | + 1 | 21636.50 | $b^4F'_4-a^4D'_4$ |
| 4629.327 | 20 | 0 | 21595.38 | $b^4F'_5-a^4F_5$ |
| 4648.32 | * | +10 | 21507.15 | $b^4F'_3-a^4D'_4$ |
| 4656.98 | * | − 3 | 21467.14 | $a^6S-a^4D'_3$ |
| 4663.71 | * | − 3 | 21436.23 | $a^6S-a^4F_4$ |
| 4666.75 | * | 0 | 21422.22 | $b^4F'_4-a^4F_5$ |
| 4731.488 | 1 | + 2 | 21129.11 | $a^6S-a^4D'_4$ |
| 4923.92 | 20 | 0 | 20303.37 | $a^6S-a^6P_2$ |
| 5018.437 | 20 | − 1 | 19920.95 | $a^6S-a^6P_3$ |
| 5169.029 | 20 | + 1 | 19340.60 | $a^6S-a^6P_4$ |
| 5197.56 | 4 | − 2 | 19234.47 | $a^4G_3-a^4F_2$ |
| 5234.62 | 4 | − 1 | 19098.29 | $a^4G_4-a^4F_3$ |
| 5256.94 | * | − 6 | 19017.22 | $a^6S-a^6F_3$ |
| 5264.81 | 1 | + 1 | 18988.77 | $a^4G_3-a^4D'_2$ |
| 5276.012 | 5 | + 2 | 18948.44 | $a^4G_5-a^4F_4$ |
| 5284.11 | * | − 1 | 18919.41 | $a^6S-a^6F_4$ |
| 5316.62 | 8 | 0 | 18803.74 | $a^4G_6-a^4F_5$ |
| 5316.78 | * | − 2 | 18803.17 | $a^4G_4-a^4D'_3$ |
| 5325.56 | 0 | + 2 | 18772.15 | $a^4G_4-a^4F_4$ |
| 5346.54 | * | 0 | 18698.37 | $a^4G_3-a^4F_4$ |
| 5362.87 | * | + 3 | 18641.49 | $a^4G_5-a^4D'_4$ |
| 5425.26 | * | − 2 | 18427.37 | $a^4G_5-a^4F_5$ |
| 6147.85 | 0 | +10 | 16261.35 | $b^4D_2-a^4P_1$ |
| 6149.25 | 00 | − 1 | 16257.65 | $b^4D_1-a^4P_1$ |
| 6238.39 | 0 | − 2 | 16025.36 | $b^4D_2-a^4P_2$ |
| 6239.95 | * | 0 | 16021.34 | $b^4D_1-a^4P_2$ |
| 6247.56 | 1 | − 1 | 16001.84 | $b^4D_3-a^4P_2$ |
| 6369.48 | * | + 8 | 15695.23 | $a^6S-a^6D'_2$ |
| 6407.30 | * | + 4 | 15602.89 | $b^4D_2-a^4P_3$ |
| 6416.92 | 0 | − 1 | 15579.50 | $b^4D_3-a^4P_3$ |
| 6432.69 | * | − 7 | 15541.40 | $a^6S-a^6D'_3$ |
| 6456.39 | 3 | − 3 | 15484.26 | $b^4D_4-a^4P_3$ |
| 6516.08 | 00 | − 4 | 15342.41 | $a^6S-a^6D'_4$ |
| 7222.415 | * | + 4 | 13842.00 | $b^4D_2-a^4D'_1$ |
| 7224.481 | * | + 3 | 13838.03 | $b^4D_1-a^4D'_1$ |
| 7301.587 | 000 | + 4 | 13691.88 | $b^4D_3-a^4F_3$ |
| 7308.09 | 000 | + 8 | 13679.69 | $b^4D_2-a^4D'_2$? |
| 7310.226 | 00(A) | +10 | 13675.66 | $b^4D_1-a^4D'_2$ |
| 7320.72§ | 0 | +12 | 13656.10 | $b^4D_3-a^4D'_2$ |
| 7449.36 | * | + 3 | 13420.26 | $b^4D_2-a^4D'_3$ |
| 7462.356‡ | 2 | − 9 | 13396.97 | $b^4D_3-a^4D'_3$ |

TABLE II—*Continued*

| λ | Int. | $\frac{O-C}{\lambda}$ | ν Vac. | Multiplet |
|---|---|---|---|---|
| 7515.89........ | * | + 1 | 13301.50 | $b^4D_4-a^4D'_3$ |
| 7533.418....... | * | + 5 | 13270.53 | $b^4D_4-a^4F_4$ |
| 7655.474....... | ooNA | + 3 | 13058.94 | $b^4D_3-a^4D'_4$ |
| 7711.759....... | * | + 3 | 12963.66 | $b^4D_4-a^4D'_4$ |

* (In intensity column) Not recorded in laboratory spectra, but present in the solar spectrum and weakened or absent in the sun-spot spectrum.

† Blend with $Fe^{+}$.

§ Blend with *Fe*.

|| Blend with arc line? Spark line should be at λ 3192.695 or mistake in identification. Z.E. is correct for spark line.

‡ May be masked by *Cr*.

spond not one, but many spectroscopic terms, which owe their differences presumably to different quantized orientations of the various orbits in space. What terms correspond to any given electronic configuration may be worked out on Hund's principles.

The singly ionized atom of iron contains seven electrons outside the complete "argon-shell." In the states of lowest energy these will be in 4s or 3d orbits—the state in which there are two of the former and five of the latter being represented for brevity by $s^2d^5$.

The spectroscopic terms resulting from these states, according to Hund's theory, are as follows:

|  | Sextets | Quartets | Doublets |
|---|---|---|---|
| $s^2d^5$.............. | S | P′DF′G | SDF′GI, P′DF′GH′, D |
| $sd^6$.............. | D | D, P′F′, P′DF′GH′ | SDF′GI, SDG |
| $d^7$............... | ........ | P′F′ | P′DF′GH′, D |

According to Hund, among the terms arising from a given configuration, those of the highest multiplicity will be the lowest. The $^6D$- and $^6S$-terms may therefore be assigned with certainty to the configurations $sd^6$ and $s^2d^5$. The lowest $^4F'$- and $^4P'$-terms may be assigned with practically equal certainty to $d^7$—the principal ground for this being comparison with terms arising from similar configurations in the spark spectra of *V*, *Cr*, and *Mn*, which show that the configurations $d^{n+1}$ and $sd^n$ always give terms at nearly the same energy-level. The higher quartet P′DF′G-terms probably arise from $sd^6$.

None of these terms should, theoretically, combine with one another to give spectral lines, but all of them should combine, when the inner-quantum rules allow, with the terms arising from the configurations $d^6p$, etc. The combinations $^6S-{}^6D'$, $^6S-{}^6F$ are instances of this. The number of such terms is very great. The configuration $d^6p$ alone accounts for the following:

| Type | S′ | P | D′ | F | G′ | H | I′ | J |
|---|---|---|---|---|---|---|---|---|
| Sextets | .... | 1 | 1 | 1 | .... | .... | .... | .... |
| Quartets | 2 | 4 | 6 | 5 | 4 | 2 | 1 | .... |
| Doublets | 2 | 7 | 8 | 9 | 7 | 5 | 2 | 1 |

The three observed sextet terms are of just the types predicted. Three of the quartet terms, which appear in most of the combinations, form a similar "triad" and are probably very closely related to the sextet terms, having as limits the same term, $^5D$, in the *Fe* III spectrum. From what arrangement of orbits the other $^4F$-term comes cannot yet be stated.

So many more terms are predicted, even by this one electronic configuration, that it is not surprising that there are many unclassified lines. The doublet system, which has not yet been unraveled, should be extremely intricate. It is practically certain that the levels predicted and not yet found lie higher up than those so far known, and give lines well out in the ultra-violet. A full analysis of this spectrum will probably demand complete lists of spark lines in the region from λ 2200 onward. The observed energy-levels are just those which might have been anticipated on the basis of Hund's theory as giving the most prominent lines. The only point of unusual interest is that three different electronic configurations, $s^2d^5$, $sd^6$, $d^7$, appear to contribute to the production of the low terms. In the spark spectra of the preceding elements of this period, so far as known to the writer, only the configurations $sd^n$ and $d^{n+1}$ produce such terms.

MOUNT WILSON OBSERVATORY
July 1926

Contributions from the Mount Wilson Observatory, No. 319
Reprinted from the *Astrophysical Journal*, Vol. LXIV, pp. 225–242, 1926
Printed in the U.S.A.

# THE ABSOLUTE MAGNITUDES AND PARALLAXES OF 410 STARS OF TYPE M

By WALTER S. ADAMS, ALFRED H. JOY, and M. L. HUMASON

## ABSTRACT

*Spectroscopic absolute magnitudes of M stars.—Magnitudes* and *spectral types* have been determined for 410 M-type stars (Table I). Nearly all Boss stars north of −30°, several stars from the Selected Areas, and about 100 dwarf stars of this type have been included. The stars were classified from M0 to M7 on the basis of the titanium bands.

The *absolute magnitudes* were determined according to methods previously employed with the aid of additional lines and *new reduction curves.* λλ 4077, 4207, 4215, 4258, $H\gamma$, 4389, 4489, and $H\beta$ were used for *giants* and λλ 4318, 4435, 4454, 4535, 4586, and 4607 for *dwarfs.* The reduction curves were calibrated with the aid of mean parallaxes derived from *peculiar motions* for the giants and *trigonometric parallaxes* for the dwarfs.

Twenty-eight stars are brighter than −1.0 mag. and are called "super-giants." The ordinary giants show very little dispersion in absolute magnitude. The dwarfs vary with advancing type from +7.0 to +12.5 mag. Figures 1 and 2 indicate the relationship between type and absolute magnitude.

The mean difference between the spectroscopic and the trigonometric parallaxes is less than 0.″001 for 71 giants. For dwarfs the mean difference is 0.″002. The absolute magnitudes of 165 giants average 0.4 mag. brighter than those previously published in a list of 1646 stars. A comparison with Young and Harper, and with Rimmer, shows the Mount Wilson values to be fainter by 0.8 and 0.7 mag., respectively.

During the past few years we have made a special study of the absolute magnitudes and spectral types of the stars of type M, including those with either giant or dwarf characteristics of spectrum. We have now completed observations of essentially all the stars of this type in Boss's *Catalogue* north of −30° of declination. In addition we have included in our investigation numerous stars listed as K5 in the *Henry Draper Catalogue*, but classified as of type M according to our system, several stars observed in the Selected Areas, and about one hundred dwarf stars of the eighth and ninth magnitudes, visually. The dwarf stars were, of course, selected on the basis of proper motion, but no selection was made in the case of the giant stars except that of apparent magnitude.

The system of classification employed is that adopted by the International Astronomical Union on the recommendation of the Committee on the Spectral Classification of Stars. It is based almost entirely on the intensities of the bands of titanium oxide, only minor consideration being given to other features of the spectrum. The stars are listed as M0, M1, M2, etc., according to increasing intensities of these bands. It is well known that many of the long-period variable stars of class M show a much more advanced type of spectrum than the normal stars of this class. Accordingly, since the system of classification is designed to include these variables, no stars of type more advanced than M6 or M7 are found in our list. The great majority of the stars are of types M0–M4. In the case of the dwarf stars it seems probable that those of type later than M5 would be so faint apparently that they could hardly be observed under present conditions.[1]

The method of deriving the absolute magnitudes of the giant M-type stars listed in the catalogue of 1646 stars[2] published several years ago was described as a provisional one based on the comparison of the intensities of two or three pairs of lines with those of certain standard stars. With the increase in the amount of observational material it has become possible to calibrate new reduction curves for the separate spectral subdivisions by the aid of mean parallaxes derived from peculiar and parallactic motions. An examination of the spectra of some of the stars of exceptional absolute magnitude, such as $\alpha$ Orionis for example, has increased the list of lines suitable for determinations of absolute magnitude and should add materially to the accuracy of the values. For giant M stars the low-temperature lines of iron at $\lambda\lambda$ 4207, 4258, 4389, and 4489, together with the hydrogen lines $H\gamma$ and $H\beta$, and the ionized strontium line at $\lambda$ 4077, have proved most useful. The ionized strontium line at $\lambda$ 4215 has been used occasionally but is complicated by the presence of a low-temperature iron line nearby. For dwarf stars calcium lines at $\lambda\lambda$ 4318, 4435, 4454, and 4586, the titanium blend at $\lambda$ 4535, and the low-temperature strontium line at $\lambda$ 4607 have been used successfully. The calibration of the reduction curves for the dwarf stars has been made by the aid of trigonometric parallaxes which give by far the most accurate values for such stars.

The determination of the preliminary reduction curves for the individual lines in the spectra of giant stars was made about a year ago and was based upon mean parallaxes derived from the parallactic and peculiar motions of the stars observed up to that time. Since the radial velocities of these stars are fairly large on the average, the values derived from the peculiar motions were assigned a much higher weight in the solution. Trigonometric parallaxes were not used in this calibration. Preliminary values of the absolute magnitudes of all the stars in the list were determined from the reduction curves obtained in this way, and then the entire material was rediscussed and the corrections to the preliminary system were calculated. The method is simply one of successive approximations. In nearly all cases the corrections were found to be a few tenths of a unit in absolute magnitude, the largest values applying to the brightest stars or "super-giants," for which the material available for calculating mean parallaxes is necessarily scanty. The corrections derived from the final computation were then applied to the preliminary values, and the resulting absolute magnitudes are those listed in our Table I. The extensive calculations involved in the determination of the mean parallaxes were carried out by Dr. Strömberg, to whom we are indebted most deeply.

---

[1] *Publications of the Astronomical Society of the Pacific*, **37**, 157, 1925.

[2] *Mt. Wilson Contr.*, No. 199; *Astrophysical Journal*, **53**, 13, 1921.

The method used by Strömberg in deriving the corrections to the provisional system of absolute magnitudes was to divide the stars into groups of different absolute magnitude (as based on the provisional values) and different spectral subdivisions, and to calculate the average peculiar radial velocity $\theta$ and the solar motion from the radial velocities of the stars in each group. The peculiar motions were found to give very consistent results for the mean parallaxes computed from the proper motions in right ascension and declination as well as from the $\tau$-component. The values of $\theta$ vary but little, in general less than 0.5 km/sec., so that the mean parallaxes derived from the peculiar motions appear to be very reliable. They have been corrected for a mean error of $\pm 0\overset{''}{.}004$ in the proper-motion components, but even were the error twice as great, the effect upon the absolute magnitudes would be small.

On the other hand, the mean parallaxes of these groups of stars derived from parallactic motions are very uncertain, the results from proper motion in right ascension and declination differing by as much as $0\overset{''}{.}004$ in some cases. The mean parallaxes from parallactic motions are systematically smaller than those derived from peculiar motions, the difference being 0″.0022 for the group of brightest stars, and 0″.0016 for the ordinary giants. These would correspond to differences of 1.0 and 0.5 in mean absolute magnitude. No explanation can as yet be given for this discrepancy, which has been found to exist in the case of some other stars, such, for example, as the long-period variables. Because of the uncertainty in the values derived from parallactic motions, the mean parallaxes and absolute magnitudes calculated from peculiar motions have been used exclusively in calibrating our final reduction curves, and this consideration should be borne in mind in making comparisons between our results and those of other observers who have used mean parallaxes based largely upon parallactic motions.

The successive columns of Table I give the data for the stars observed. Those listed in Boss's *Preliminary General Catalogue* are given by number with no further designation. Because of the convenience and accessibility of Porter's "Catalogue of Proper Motion Stars," *Publications of the Cincinnati Observatory*, No. 18, most of the dwarf stars have been listed according to their numbers in this catalogue. The visual apparent magnitudes are given under $m$, the values being taken, where possible, from the *Henry Draper Catalogue*. The spectral types are the means of our own determinations, and the total proper motions $\mu$ are mainly from the catalogues of Boss and Porter. The remaining columns give the absolute magnitudes $M$, the corresponding parallaxes, and the trigonometric parallaxes compiled by Schlesinger in his *Catalogue of Parallaxes*, 1924.

Although for the sake of uniformity all the spectroscopic parallaxes have been given to three places of decimals, attention should be called to the very marked difference in the influence of an uncertainty in the absolute magnitude on the parallaxes of giants as compared with dwarf stars. As an illustration, if we select two adjacent stars in the list, Boss 40 and Cin. 25, we find that an error of 0.3 in the absolute magnitude would affect the parallax of Boss 40 by 0″.0005 and that of Cin. 25 by 0″.043. The apparent magnitudes of the fainter dwarf stars, and especially of the components of visual binaries, are also subject to serious uncertainties which enter directly into the calculation of the spectroscopic parallaxes. Additional photometric observations of these stars would be of great value.

## TABLE I

| Name | α 1925 | δ 1925 | *m* | Sp. | μ | *M* | Spec. π | Trig. π |
|---|---|---|---|---|---|---|---|---|
| Comp. Lal. 47231. | $0^h$ $0^m.7$ | +45° 23′ | 10.2 | M2 | 0″.856 | +10.6 | 0″.120 | 0″.097 |
| Cin. 3161.... | 0 0.8 | −37 43 | 8.3 | M3 | 6.112 | +10.0 | .219 | .220 |
| Lal. 47231 Br. | 0 1.2 | +45 24 | 8.6 | M0 | 0.858 | + 8.7 | .105 | .097 |
| B.D. +61°8.... | 0 5.6 | +62 14 | 9.2 | M2ep | ...... | − 1.3 | .001 | ....... |
| B.D. +75°4.... | 0 9.8 | +75 37 | 7.6 | M4 | ...... | − 0.2 | .003 | ....... |
| 30.... | 0 10.6 | − 8 12 | 5.4 | M4 | .060 | − 0.2 | .008 | ....... |
| 31.... | 0 10.7 | +19 47 | 4.9 | M1 | .094 | + 0.7 | .014 | − .009 |
| 33.... | 0 10.8 | −19 21 | 4.7 | M1 | .068 | − 0.1 | .011 | ....... |
| 40.... | 0 12.8 | + 1 26 | 7.3 | M5 | 0.022 | − 0.2 | .003 | ....... |
| Cin. 25.... | 0 14.0 | +43 36 | 8.1 | M2 | 2.890 | +10.4 | .288 | .282 |
| Comp. Cin. 25.... | 0 14.0 | +43 36 | 10.5 | M5 | 2.890 | +12.4 | .240 | .282 |
| 64.... | 0 19.3 | −16 22 | 6.6 | M3 | 0.041 | − 0.1 | .005 | ....... |
| B.D. +30°59.... | 0 23.2 | +30 46 | 7.6 | M1 | ...... | 0.0 | .003 | ....... |
| 81.... | 0 24.1 | +17 29 | 5.3 | M3 | .117 | − 0.6 | .007 | ....... |
| 90.... | 0 26.2 | − 4 22 | 6.0 | M0 | 0.011 | + 0.2 | .007 | ....... |
| B.D. +66°34.... | 0 27.6 | +66 51 | 9.5 | M3 | 1.775 | + 8.7 | .069 | ....... |
| βG.C. 368 Ft.. | 0 37.0 | − 7 38 | 10.0 | M1 | 0.022 | + 7.6 | .033 | ....... |
| B.D.+45°181.... | 0 38.7 | +45 31 | 7.4 | M0 | ...... | + 0.2 | .004 | ....... |
| 161.... | 0 42.6 | +15 4 | 5.6 | M4 | 0.064 | + 0.1 | .008 | .013 |
| 168 Ft.. | 0 44.5 | +57 25 | 7.4 | M0 | 1.242 | + 8.2 | .145 | .182 |
| 191.... | 0 49.2 | − 1 33 | 4.9 | M0 | 0.017 | − 0.2 | .010 | ....... |
| 217.... | 0 55.9 | + 6 5 | 6.3 | M1 | 0.023 | − 0.9 | .004 | − .002 |
| B.D.+63°137.... | 1 1.9 | +63 32 | 8.7 | M1 | 1.55 | + 8.5 | .091 | .078 |
| 259.... | 1 5.5 | +35 13 | 2.4 | M0 | 0.216 | + 0.3 | .038 | .045 |
| 274.... | 1 8.2 | +44 56 | 6.6 | M1 | .042 | + 0.2 | .005 | ....... |
| B.D.+55°290.... | 1 14.7 | +55 56 | 8.9 | M6 | ...... | 0.0 | .002 | ....... |
| 306.... | 1 18.7 | + 1 20 | 6.5 | M0 | .069 | 0.0 | .005 | ....... |
| 342.... | 1 30.7 | +18 5 | 6.0 | M2 | .088 | + 0.3 | .007 | ....... |
| Cin. 238.... | 1 38.5 | +63 28 | 8.2 | M0 | .70 | + 8.2 | .100 | 0.082 |
| B.D.+55°394.... | 1 39.3 | +56 9 | 9.0 | M0 | ...... | − 0.5 | .001 | ....... |
| Cin. 251.... | 1 49.2 | −22 49 | 8.9 | M1 | .857 | + 9.0 | .105 | ....... |
| 451.... | 1 56.2 | −21 11 | 5.7 | M1 | .014 | + 0.1 | .008 | ....... |
| 453.... | 1 56.5 | −21 26 | 4.2 | M1 | .130 | + 0.2 | .016 | ....... |
| 455.... | 1 56.7 | − 8 53 | 5.7 | M5 | .086 | 0.0 | .007 | ....... |
| 491.... | 2 6.5 | +19 9 | 5.9 | M3 | .092 | − 0.1 | .006 | ....... |
| 502.... | 2 8.9 | +14 56 | 6.0 | M1 | .100 | + 0.1 | .007 | ....... |
| B.D.+56°547.... | 2 15.3 | +56 39 | 8.2 | M3 | ...... | − 1.4 | .001 | ....... |
| B.D.+56°551.... | 2 15.8 | +56 49 | 8.2 | M0 | ...... | − 1.4 | .001 | ....... |
| B.D.+57°550.... | 2 16.5 | +57 31 | 8.6 | M2 | ...... | − 1.4 | .001 | ....... |
| B.D.+55°597.... | 2 16.9 | +56 16 | 8.2 | M4 | ...... | − 1.3 | .001 | ....... |
| B.D.+56°583.... | 2 17.2 | +56 46 | 7.0 | M6 | ...... | − 0.7 | .003 | ....... |
| B.D.+56°595.... | 2 18.0 | +56 51 | 8.5 | M1 | ...... | − 1.8 | .001 | ....... |
| 539.... | 2 18.1 | + 0 3 | 5.9 | M1 | 0.006 | 0.0 | .007 | ....... |
| B.D.+56°597.... | 2 18.2 | +56 52 | 8.6 | M0 | ...... | − 1.7 | .001 | ....... |
| B.D.+56°609.... | 2 20.1 | +57 6 | 8.5 | M4 | ...... | − 1.1 | 0.001 | ....... |

TABLE I—*Continued*

| Name | α 1925 | δ 1925 | *m* | Sp. | μ | *M* | Spec. π | Trig. π |
|---|---|---|---|---|---|---|---|---|
| 570.... | $2^{h}27^{m}2$ | −22° 53′ | 6.4 | M2 | 0″.044 | + 0.1 | 0″.005 | ....... |
| 582.... | 2 31.2 | +34 22 | 5.6 | M3 | .061 | − 0.3 | .007 | 0″.012 |
| 617 Ft.. | 2 39.1 | +48 55 | 10.0 | M2 | .351 | + 8.2 | .044 | .080 |
| 646.... | 2 46.9 | +34 45 | 4.7 | Mo | .077 | + 0.3 | .013 | .009 |
| βG.C. 1490 Ft.. | 2 51.2 | +26 34 | 9.7 | M1 | .333 | + 8.7 | .063 | .060 |
| 660.... | 2 51.6 | +18 2 | 5.9 | M6 | .018 | 0.0 | .007 | .012 |
| 669.... | 2 56.0 | +79 7 | 5.7 | M2 | .039 | 0.0 | .007 | ....... |
| 691.... | 2 58.4 | + 3 48 | 2.8 | M2 | .078 | + 0.1 | .029 | .011 |
| 698.... | 3 0.4 | +38 33 | 3.7 | M4 | .173 | − 0.7 | .013 | .038 |
| B.D. +1°543.... | 3 2.7 | + 1 42 | 8.9 | Mo | .91 | + 8.4 | .079 | ....... |
| 707.... | 3 2.8 | − 6 23 | 5.6 | M3 | .002 | 0.0 | .008 | ....... |
| 712.... | 3 4.1 | +18 30 | 6.5 | Mo | .042 | + 0.5 | .006 | .028 |
| 759.... | 3 16.2 | −22 2 | 4.0 | M3 | .065 | − 0.3 | .014 | ....... |
| 765.... | 3 18.1 | +64 19 | 5.6 | Mo | .019 | − 1.8 | .003 | ....... |
| Cin. 456.... | 3 24.4 | −20 4 | 8.2 | Mo | .603 | + 8.7 | .126 | ....... |
| 826.... | 3 35.6 | +62 59 | 5.3 | M4 | .022 | − 0.6 | .007 | ....... |
| B.D.+68°278.... | 3 40.5 | +68 26 | 9.2 | M1 | .30 | + 7.8 | .052 | .073 |
| 868.... | 3 42.5 | −12 20 | 4.6 | M2 | .069 | 0.0 | .012 | ....... |
| 864.... | 3 42.6 | +65 18 | 4.7 | M1 | .004 | − 1.1 | .007 | ....... |
| 912.... | 3 52.9 | −13 49 | 6.7 | M2 | .010 | − 0.7 | .003 | ....... |
| 915.... | 3 54.5 | −13 43 | 3.2 | Mo | 0.130 | − 0.2 | .021 | .018 |
| *o* Eridani C...... | 4 11.8 | − 7 46 | 10.8 | M6e | 4.082 | +11.9 | .166 | .203 |
| 993... | 4 15.3 | +60 34 | 5.7 | Mo | 0.122 | − 0.3 | .006 | ....... |
| 1014... | 4 17.9 | +20 39 | 6.1 | Mo | .011 | 0.0 | .006 | − .003 |
| 1057... | 4 26.8 | +14 57 | 6.6 | M3 | .074 | − 0.1 | .005 | ....... |
| 1071... | 4 30.6 | − 8 23 | 5.4 | M3 | .035 | − 0.6 | .006 | ....... |
| Cin. 594... | 4 31.7 | +52 45 | 8.5 | M2 | .53 | + 9.0 | .126 | .091 |
| 1105... | 4 37.2 | −19 49 | 4.5 | M3 | .094 | + 0.1 | .013 | ....... |
| 1128... | 4 45.1 | +63 23 | 5.8 | M2 | .111 | 0.0 | .007 | .002 |
| 1149... | 4 48.3 | +14 8 | 5.2 | M4 | .059 | − 0.4 | .008 | ....... |
| 1154... | 4 49.5 | + 2 23 | 5.7 | M1 | .034 | 0.0 | .007 | .006 |
| B.D.+42°1180... | 5 3.5 | +42 28 | 8.8 | M6 | ...... | 0.0 | .002 | ....... |
| 1237... | 5 7.9 | −11 56 | 5.9 | M6 | .051 | − 0.8 | .005 | ....... |
| Comp. 1246... | 5 11.2 | +45 55 | 10.0 | M2 | .437 | + 9.6 | .083 | .069 |
| 1256... | 5 12.9 | +42 43 | 5.9 | M4 | .049 | − 0.4 | .005 | .004 |
| B.D.+29° 897... | 5 22.4 | +29 52 | 8.0 | M1 | ...... | − 2.4 | .001 | ....... |
| 1309... | 5 23.1 | +63 0 | 5.8 | M1 | .005 | − 0.3 | .006 | ....... |
| 1327... | 5 25.9 | − 1 9 | 5.0 | Mo | 0.028 | 0.0 | .010 | ....... |
| Cin. 705... | 5 27.6 | − 3 40 | 8.8 | M3 | 2.222 | +10.2 | .190 | 0.172 |
| 1335... | 5 27.8 | +18 32 | 4.7 | M2 | 0.013 | − 3.0 | .003 | ....... |
| 1334... | 5 29.7 | +75 0 | 6.4 | Mo | .019 | 0.0 | .005 | ....... |
| 1348... | 5 30.4 | +54 23 | 6.0 | Mo | .007 | − 0.2 | .006 | ....... |
| B.D.+43°1332... | 5 38.1 | +43 28 | 8.8 | M1 | .004 | − 0.4 | .001 | ....... |
| 1439... | 5 45.9 | +37 17 | 5.0 | M1 | 0.052 | + 0.3 | .011 | ....... |
| B.D.+27° 887... | 5 46.1 | +27 40 | 7.7 | M5 | ...... | + 0.1 | 0.003 | ....... |

TABLE I—*Continued*

| Name | $\alpha$ 1925 | $\delta$ 1925 | $m$ | Sp. | $\mu$ | $M$ | Spec. $\pi$ | Trig. $\pi$ |
|---|---|---|---|---|---|---|---|---|
| M 37, Br. star.... | $5^h47^m3$ | +32° 32′ | 9.7 | M1 | 0″007 | − 0.1 | 0″001 | ....... |
| 1468... | 5 51.1 | + 7 24 | 0.9 | M2 | .029 | − 4.3 | .009 | 0″017 |
| 1479... | 5 54.4 | +45 56 | 4.6 | M3 | .011 | − 1.0 | .008 | ....... |
| 1531... | 6 4.4 | −19 9 | 5.5 | M2 | .063 | − 0.6 | .006 | ....... |
| B.D.+23°1243... | 6 7.4 | +23 14 | 7.4 | M3ep | ...... | − 1.3 | .002 | ....... |
| 1549... | 6 7.8 | +22 56 | 6.3 | M2 | .027 | − 1.4 | .003 | .000 |
| 1561... | 6 10.4 | +22 32 | 3.8 | M3 | .065 | − 0.4 | .014 | .014 |
| 1560... | 6 11.0 | +61 33 | 5.3 | M3 | .005 | − 0.6 | .007 | ....... |
| 1596... | 6 15.8 | +14 41 | 6.0 | M0 | .019 | 0.0 | .006 | ....... |
| 1599... | 6 16.2 | − 2 55 | 5.2 | M1 | .009 | 0.0 | .009 | − .004 |
| $\beta$ G.C. 3319 Br. | 6 16.8 | + 5 47 | 8.1 | M4 | ...... | − 0.1 | .002 | .001 |
| 1604... | 6 18.4 | +22 33 | 3.2 | M3 | .128 | − 0.4 | .019 | .016 |
| 1606... | 6 19.1 | +49 20 | 5.1 | M0 | .014 | − 2.7 | .003 | .000 |
| B.D.+17°1320... | 6 32.9 | +17 37 | 9.5 | M1 | .88 | + 9.1 | .083 | .097 |
| B.D.+45°1330... | 6 33.2 | +45 8 | 8.8 | M2 | ...... | + 0.2 | .002 | ....... |
| 1715... | 6 38.4 | − 9 6 | 5.3 | M0 | .037 | + 0.3 | .010 | ....... |
| 1743... | 6 44.0 | − 8 55 | 5.3 | M1 | .036 | − 2.1 | .003 | ....... |
| Cin. 837... | 6 51.2 | +40 11 | 8.3 | M0 | .43 | + 7.5 | .069 | .030 |
| 1808... | 6 58.3 | − 5 37 | 5.4 | M2 | .009 | − 0.6 | .006 | ....... |
| 1810... | 6 58.7 | −27 50 | 3.7 | M0 | .011 | − 2.1 | .007 | ....... |
| 1801... | 7 5.9 | +87 10 | 5.3 | M2 | .051 | 0.0 | .009 | ....... |
| 1846... | 7 7.5 | +51 33 | 5.7 | M3 | .019 | + 0.2 | .008 | .003 |
| 1856... | 7 9.1 | +16 17 | 5.3 | M4 | .051 | − 0.4 | .007 | .004 |
| 1861... | 7 10.1 | +25 1 | 6.0 | M1 | .105 | + 0.3 | .007 | ....... |
| 1868... | 7 11.3 | +28 2 | 5.9 | M1 | .020 | + 0.1 | .007 | .004 |
| 1887... | 7 13.5 | −23 11 | 4.8 | M0 | .001 | − 2.2 | .004 | ....... |
| 1889... | 7 13.6 | −27 45 | 4.8 | M3 | .045 | − 0.2 | .010 | ....... |
| B.D.+33°1505... | 7 14.6 | +32 59 | 9.3 | M1 | .57 | + 8.9 | .079 | ....... |
| 1871... | 7 15.4 | +82 34 | 5.1 | M4 | .045 | − 0.1 | .009 | ....... |
| 1918... | 7 18.0 | −25 45 | 6.1 | M5 | .031 | 0.0 | .006 | ....... |
| Comp. 1979... | 7 29.8 | +32 3 | 9.6 | M1e | .203 | + 8.8 | .069 | .076 |
| 1985... | 7 30.4 | −14 22 | 5.1 | M3ep | .016 | − 1.5 | .005 | ....... |
| 1986... | 7 31.1 | +46 21 | 5.8 | M1 | .047 | + 0.2 | .008 | ....... |
| 1987... | 7 31.3 | +27 4 | 4.2 | M0 | .119 | + 0.1 | .015 | .011 |
| 2005... | 7 35.1 | +17 51 | 5.2 | M0 | .004 | − 0.3 | .008 | .000 |
| 2020... | 7 37.8 | +14 23 | 5.8 | M3 | .015 | − 0.8 | .005 | .002 |
| 2028... | 7 39.5 | +25 58 | 5.4 | M0 | .034 | 0.0 | .008 | ....... |
| 2037... | 7 41.7 | +37 42 | 5.4 | M3 | .030 | 0.0 | .008 | ....... |
| 2049... | 7 42.7 | +33 36 | 5.3 | M1 | .040 | − 0.1 | .008 | .010 |
| 2144... | 8 1.9 | +22 51 | 6.2 | M3 | .024 | − 0.5 | .005 | ....... |
| 2186... | 8 12.5 | +72 39 | 6.2 | M0 | .027 | 0.0 | .006 | ....... |
| 2223... | 8 19.8 | +10 53 | 6.3 | M2 | .021 | + 0.4 | .007 | ....... |
| 2245... | 8 22.6 | +12 54 | 5.8 | M3 | .116 | − 0.9 | .005 | .025 |
| 2265... | 8 27.3 | +18 21 | 5.6 | M1 | 0.087 | + 0.3 | .009 | ....... |
| B.D.+67° 552... | 8 29.8 | +67 33 | 9.3 | M0 | 1.101 | + 7.9 | 0.052 | 0.085 |

TABLE I—*Continued*

| Name | α 1925 | δ 1925 | *m* | Sp. | μ | *M* | Spec. π | Trig. π |
|---|---|---|---|---|---|---|---|---|
| 2378... | 8h48m.0 | +28° 33′ | 6.3 | M3 | 0″.022 | − 0.5 | 0″.004 | −0″.003 |
| β G.C. 4815 Br. | 8 48.5 | +71 5 | 8.6 | M1 | 1.390 | + 8.4 | .091 | .086 |
| β G.C. 4815 Ft. | 8 48.5 | +71 5 | 8.7 | M1 | 1.390 | + 8.4 | .087 | .086 |
| 2404BC. | 8 54.1 | +48 20 | 9.5 | M2 | 0.504 | + 7.8 | .046 | .070 |
| 2410... | 8 54.9 | +18 26 | 6.6 | M4 | .089 | 0.0 | .005 | ....... |
| 2411... | 8 55.8 | +67 55 | 5.0 | M3 | .021 | + 0.1 | .010 | ....... |
| B.D.−32°6877... | 9 1.4 | −32 8 | 7.7 | M5 | ...... | + 0.2 | .003 | ....... |
| 2434... | 9 1.8 | +67 11 | 5.3 | M0 | .050 | − 0.1 | .008 | ....... |
| 2450... | 9 4.7 | −25 33 | 4.8 | M1 | 0.040 | − 0.6 | .008 | ....... |
| 2469... | 9 9.3 | +53 1 | 8.1 | M0 | 1.677 | + 9.3 | .174 | .165 |
| 2470... | 9 9.3 | +53 1 | 8.1 | M0 | 1.686 | + 9.0 | .151 | .165 |
| 2474... | 9 10.3 | +57 3 | 5.5 | M0 | 0.036 | 0.0 | .008 | ....... |
| 2507... | 9 16.5 | +34 43 | 3.3 | M0 | .216 | − 0.3 | .019 | .002 |
| B.D.+81° 297... | 9 17.6 | +80 55 | 9.0 | M0 | .442 | + 7.1 | .042 | .058 |
| 2516... | 9 18.2 | −25 39 | 4.9 | M1 | .022 | + 0.4 | .013 | ....... |
| 2546... | 9 27.0 | +35 26 | 5.5 | M1 | .130 | + 0.2 | .009 | ....... |
| B.D.+36°1970... | 9 27.3 | +36 40 | 9.3 | M2 | .56 | + 9.0 | .087 | ....... |
| B.D. +8°2243... | 9 30.7 | + 8 33 | 8.1 | M3 | .019 | − 0.3 | .002 | ....... |
| 2578... | 9 32.3 | +31 30 | 5.7 | M2 | .044 | − 0.1 | .007 | ....... |
| 2612... | 9 39.7 | +14 22 | 5.6 | M2 | .014 | − 0.1 | .007 | ....... |
| 2614... | 9 41.2 | +57 28 | 5.4 | M3 | .025 | − 0.9 | .005 | ....... |
| 2621... | 9 42.2 | + 7 3 | 6.0 | M1 | .040 | 0.0 | .006 | ....... |
| 2633... | 9 45.6 | +39 59 | 6.8 | M2 | .016 | − 0.2 | .004 | ....... |
| 2639... | 9 47.0 | +13 25 | 6.7 | M0 | 0.037 | − 0.3 | .004 | ....... |
| Cin. 1167... | 9 47.4 | −11 55 | 9.4 | M2 | 1.848 | + 9.3 | .096 | .080 |
| B.D.+63° 869... | 9 50.6 | +63 9 | 8.5 | M1 | 0.600 | + 9.0 | .126 | ....... |
| 2658... | 9 51.3 | −18 39 | 5.2 | M1 | .050 | + 0.3 | .010 | ....... |
| 2680... | 9 56.3 | + 8 24 | 4.9 | M2 | 0.043 | 0.0 | .010 | ....... |
| Cin. 1218... | 10 6.8 | +49 51 | 6.8 | M0 | 1.451 | + 8.3 | .200 | .178 |
| Cin. 1225... | 10 9.1 | +52 55 | 9.0 | M0 | 0.74 | + 7.8 | .058 | .073 |
| 2731... | 10 12.7 | +14 6 | 5.7 | M2 | .035 | + 0.4 | .009 | ....... |
| Cin. 1244... | 10 15.6 | +20 15 | 9.0 | M4e | .490 | +11.2 | .275 | .207 |
| Cin. 1246... | 10 16.9 | − 1 5 | 8.9 | M0 | .679 | + 7.0 | .042 | ....... |
| 2766... | 10 21.3 | + 9 10 | 5.9 | M3 | .045 | + 0.1 | .007 | ....... |
| 2770... | 10 22.0 | − 6 41 | 5.8 | M2 | .189 | 0.0 | .007 | ....... |
| B.D.+46°1635... | 10 27.0 | +45 55 | 8.8 | M0 | .837 | + 8.2 | .076 | ....... |
| 2796... | 10 27.2 | − 7 15 | 6.4 | M0 | .045 | + 0.6 | .007 | ....... |
| 2800... | 10 28.2 | +14 31 | 5.7 | M2 | .041 | − 0.2 | .007 | − .004 |
| 2821... | 10 32.6 | −15 57 | 6.2 | M1 | .027 | − 0.5 | .007 | ....... |
| 2847... | 10 38.0 | +32 5 | 6.3 | M6 | .030 | + 0.1 | .006 | ....... |
| 2865... | 10 41.7 | +57 46 | 6.5 | M2 | .081 | + 0.5 | .006 | ....... |
| 2915... | 10 52.1 | + 6 35 | 6.0 | M5 | .023 | − 0.6 | .005 | − .009 |
| 2921... | 10 55.4 | +36 30 | 6.2 | M2 | .095 | + 0.1 | .006 | .019 |
| 2931... | 10 58.0 | − 2 5 | 5.0 | M1 | 0.041 | + 0.2 | .011 | ....... |
| 2935... | 10 59.3 | +36 28 | 7.6 | M2 | 4.778 | +10.4 | 0.363 | 0.392 |

TABLE I—*Continued*

| Name | α 1925 | δ 1925 | *m* | Sp. | μ | *M* | Spec. π | Trig. π |
|---|---|---|---|---|---|---|---|---|
| Lal. 21258... | $11^{\mathrm{h}}\ 1^{\mathrm{m}}.9$ | +43° 54′ | 8.9 | M2 | 4″.519 | +10.1 | 0″.174 | 0″.177 |
| Lal. 21368A.. | 11 6.9 | +30 52 | 8.8 | M1 | 0.623 | + 8.6 | .091 | .085 |
| Lal. 21368B.. | 11 6.9 | +30 52 | 9.8 | M2 | .623 | +10.3 | .126 | .085 |
| Cin. 1364... | 11 7.7 | −14 34 | 9.3 | M0 | .92 | + 8.0 | .055 | ....... |
| 2976... | 11 11.2 | +23 30 | 4.9 | M2 | .018 | − 0.8 | .007 | ....... |
| 2983... | 11 13.4 | + 2 25 | 5.4 | M0 | .159 | + 0.6 | .011 | ....... |
| Cin. 1375... | 11 13.5 | − 1 35 | 8.8 | M0 | 0.53 | + 7.7 | .060 | ....... |
| Cin. 1383... | 11 16.4 | +66 15 | 9.2 | M2 | 2.986 | + 9.0 | .091 | .126 |
| 3002... | 11 20.8 | −10 27 | 5.1 | M1 | 0.043 | − 0.1 | .009 | ....... |
| 3031... | 11 27.0 | +69 45 | 4.1 | M0 | .045 | − 0.2 | .014 | .022 |
| 3067... | 11 34.6 | + 8 33 | 5.5 | M6 | .013 | + 0.3 | .009 | ....... |
| B.D.+45°1955... | 11 37.7 | +44 37 | 7.8 | M3 | .021 | + 0.1 | .003 | ....... |
| 3089... | 11 42.0 | + 6 57 | 4.2 | M1 | .188 | − 0.2 | .013 | .007 |
| 3100... | 11 44.9 | −26 20 | 5.4 | M4 | .028 | − 0.3 | .007 | ....... |
| 3128... | 11 54.4 | + 3 54 | 7.0 | M4 | .009 | − 0.2 | .004 | ....... |
| 3136... | 11 56.4 | +81 16 | 6.4 | M4 | .068 | − 0.8 | .004 | ....... |
| B.D.+30°2217... | 11 59.7 | +30 6 | 7.7 | M5 | ...... | 0.0 | .003 | ....... |
| Cin. 1551... | 12 18.2 | +42 33 | 9.1 | M1 | .57 | + 8.9 | .091 | ....... |
| 3234... | 12 21.5 | +57 12 | 6.0 | M3 | .028 | + 0.4 | .008 | ....... |
| 3248... | 12 24.0 | +56 8 | 5.8 | M2 | .031 | + 0.6 | .009 | ....... |
| 3252... | 12 25.2 | − 2 1 | 7.6 | M4 | .049 | + 0.1 | .003 | ....... |
| 3259... | 12 26.4 | −23 17 | 5.9 | M0 | .030 | − 0.5 | .005 | ....... |
| 3265... | 12 26.8 | +69 37 | 5.2 | M4 | .084 | − 0.3 | .008 | ....... |
| B.D. +9°2636... | 12 27.5 | + 9 14 | 8.8 | M1 | .96 | + 8.6 | .091 | ....... |
| 3294... | 12 34.6 | + 2 16 | 6.0 | M3 | .090 | + 0.2 | .007 | ....... |
| 3295... | 12 34.9 | − 3 58 | 6.9 | M0 | .053 | + 0.1 | .004 | ....... |
| 3331... | 12 44.0 | + 3 59 | 6.7 | M4 | .013 | + 0.3 | .005 | ....... |
| Cin. 1633... | 12 46.9 | − 0 21 | 8.7 | M0 | .393 | + 8.7 | .100 | ....... |
| 3348... | 12 48.5 | +17 29 | 6.5 | M0 | .023 | − 0.3 | .004 | .022 |
| 3362... | 12 50.5 | − 9 8 | 4.9 | M3 | .032 | − 0.3 | .009 | ....... |
| 3367... | 12 51.8 | + 3 48 | 3.7 | M3 | .479 | 0.0 | .018 | .010 |
| 3374... | 12 55.2 | +17 49 | 5.0 | M0 | .036 | + 0.1 | .010 | ....... |
| Cin. 1661... | 12 56.5 | − 2 18 | 9.5 | M0 | .73 | + 8.3 | .058 | ....... |
| 3398... | 13 2.7 | +23 1 | 5.9 | M5 | .066 | − 0.2 | .006 | .032 |
| B.D.+18°2696... | 13 5.8 | +17 52 | 8.7 | M0 | .120 | + 0.0 | .002 | − .010 |
| 3434... | 13 10.8 | +11 44 | 5.8 | M0 | .090 | 0.0 | .007 | ....... |
| 3446... | 13 13.8 | + 5 52 | 5.0 | M2 | .016 | − 0.2 | .009 | ....... |
| Cin. 1719... | 13 16.1 | +35 31 | 9.0 | M2 | .884 | + 9.1 | .105 | .085 |
| 3460... | 13 18.2 | −12 11 | 7.1 | M2 | .027 | 0.0 | .004 | ....... |
| β G.C. 6476S.. | 13 20.1 | +29 36 | 9.4 | M0 | .535 | + 8.4 | .063 | ....... |
| 3488... | 13 24.2 | +72 47 | 6.1 | M1 | .030 | − 0.5 | .005 | ....... |
| 3499... | 13 28.1 | − 5 52 | 4.8 | M3 | .112 | + 0.2 | .012 | ....... |
| 3534... | 13 37.7 | − 8 20 | 5.2 | M2 | .108 | + 0.1 | .010 | ....... |
| 3536... | 13 37.9 | +55 4 | 4.8 | M2 | 0.028 | + 0.1 | .011 | ....... |
| Cin. 1784... | 13 41.4 | +18 13 | 9.6 | M1 | 1.86 | + 9.3 | 0.087 | 0.079 |

TABLE I—*Continued*

| Name | α 1925 | δ 1925 | m | Sp. | μ | M | Spec. π | Trig. π |
|---|---|---|---|---|---|---|---|---|
| Cin. 1786... | 13h41m9 | +15° 18′ | 8.5 | M2 | 2″.298 | +10.2 | 0″.219 | 0″.185 |
| 3553... | 13 43.3 | −17 29 | 5.8 | M2 | 0.065 | − 0.7 | .005 | ....... |
| 3572... | 13 45.9 | +16 10 | 4.3 | M0 | .106 | + 0.6 | .018 | ....... |
| 3581... | 13 47.8 | +35 2 | 6.0 | M1 | .072 | 0.0 | .006 | .001 |
| 3584... | 13 48.5 | +34 49 | 5.0 | M2 | .044 | − 0.3 | .009 | ....... |
| 3589... | 13 49.3 | +65 6 | 4.8 | M3 | .004 | − 0.4 | .009 | ....... |
| β G.C. 6710N.. | 13 59.5 | +46 42 | 9.5 | M4 | .609 | + 9.9 | .120 | ....... |
| B.D.+29°2486... | 14 1.1 | +29 30 | 8.2 | M3 | ...... | 0.0 | .002 | ....... |
| 3630... | 14 4.9 | +44 13 | 5.4 | M4 | .037 | − 0.7 | .006 | ....... |
| 3631... | 14 5.5 | +49 49 | 5.4 | M2 | .068 | 0.0 | .008 | ....... |
| 3632... | 14 6.7 | −15 57 | 5.1 | M3 | .027 | − 0.6 | .007 | ....... |
| 3656... | 14 10.7 | +69 47 | 5.4 | M2 | .068 | + 0.4 | .010 | ....... |
| B.D.+15°2690... | 14 13.9 | +15 36 | 6.0 | M3 | ...... | 0.0 | .006 | ....... |
| Cin. 1885... | 14 18.8 | +29 59 | 8.6 | M0 | 0.727 | + 8.1 | .079 | .067 |
| Cin. 1894... | 14 22.2 | +23 59 | 9.5 | M2 | 1.39 | + 8.7 | .069 | .053 |
| Cin. 1895... | 14 22.3 | +24 0 | 9.6 | M2 | 1.40 | + 9.1 | .079 | .053 |
| B.D. −7°3856... | 14 26.9 | − 8 18 | 9.3 | M0 | 1.26 | + 8.7 | .076 | ....... |
| Cin. 1920... | 14 31.9 | +34 4 | 9.0 | M0 | 0.76 | + 8.5 | .079 | ....... |
| 3733... | 14 32.0 | +49 42 | 5.9 | M1 | .067 | − 0.2 | .006 | ....... |
| 3761... | 14 40.1 | +26 51 | 4.9 | M3 | .024 | − 0.5 | .008 | ....... |
| B.D.+34°2559... | 14 42.1 | +34 41 | 7.8 | M2 | 0.044 | − 0.3 | .002 | ....... |
| 3812... | 14 53.1 | −21 4 | 8.9 | M2 | 1.916 | + 9.4 | .126 | .182 |
| 3827... | 14 56.4 | +66 14 | 4.9 | M5 | 0.082 | 0.0 | .010 | ....... |
| Cin. 1989... | 14 56.7 | −10 50 | 10.0 | M0 | .467 | + 9.0 | .063 | ....... |
| 3828... | 14 57.4 | − 2 28 | 5.7 | M1 | .048 | 0.0 | .007 | ....... |
| 3831... | 14 58.0 | + 0 9 | 5.9 | M2 | .030 | − 0.9 | .004 | ....... |
| 3837... | 14 59.7 | −24 59 | 3.4 | M4 | .094 | − 0.1 | .020 | ....... |
| B.D.+25°2874... | 15 4.2 | +25 13 | 9.2 | M0 | .961 | + 8.3 | .066 | .070 |
| 3867... | 15 8.7 | +19 15 | 6.0 | M4 | .004 | − 0.2 | .006 | − .007 |
| B.D. −3°3746... | 15 10.2 | − 3 32 | 9.2 | M0 | 0.69 | + 8.2 | .063 | ....... |
| B.D. −7°4003... | 15 15.6 | − 7 26 | 9.2 | M5 | 1.33 | +11.8 | .331 | ....... |
| 3931... | 15 22.3 | +15 41 | 5.5 | M1 | 0.033 | − 0.1 | .008 | ....... |
| 3938... | 15 24.4 | +25 22 | 6.3 | M1 | .039 | 0.0 | .005 | ....... |
| 3945... | 15 28.2 | +41 5 | 5.2 | M0 | .018 | − 0.1 | .009 | .023 |
| 3967... | 15 32.5 | +39 15 | 5.4 | M2 | .029 | 0.0 | .008 | ....... |
| 3969... | 15 33.0 | +15 21 | 6.8 | M6 | .011 | − 0.4 | .004 | ....... |
| 3990... | 15 37.6 | −19 26 | 5.0 | M0 | .127 | + 0.1 | .010 | ....... |
| 4015... | 15 45.4 | +18 22 | 4.3 | M1 | .110 | 0.0 | .014 | ....... |
| Cin. 2124... | 15 49.4 | +74 39 | 9.3 | M0 | .320 | + 8.4 | .066 | .034 |
| 4048... | 15 51.3 | +20 32 | 5.8 | M0 | .083 | − 0.7 | .005 | .029 |
| 4054... | 15 52.1 | +43 21 | 5.5 | M3 | .075 | − 0.1 | .008 | 0.022 |
| 4096... | 16 3.6 | −26 8 | 5.6 | M2 | .122 | − 0.5 | .006 | ....... |
| B.D.+35°2774... | 16 3.8 | +34 51 | 9.5 | M1 | .64 | + 8.8 | .072 | ....... |
| 4103... | 16 4.8 | + 8 44 | 5.9 | M3 | .024 | − 0.3 | .006 | ....... |
| 4125... | 16 8.5 | +23 41 | 6.0 | M4 | 0.028 | − 0.3 | 0.005 | ....... |

TABLE I—*Continued*

| Name | α 1925 | δ 1925 | *m* | Sp. | μ | *M* | Spec. π | Trig. π |
|---|---|---|---|---|---|---|---|---|
| 4134... | $16^{h}10^{m}.4$ | − 3° 30′ | 3.0 | M0 | 0″.161 | 0.0 | 0″.025 | 0″.040 |
| B.D. +75°585... | 16 13.1 | +74 51 | 8.4 | M5 | ...... | + 0.2 | .002 | ....... |
| 4159... | 16 16.0 | +59 56 | 5.6 | M4 | .022 | − 0.6 | .006 | ....... |
| Cin. 2184... | 16 16.6 | +67 25 | 8.9 | M0 | .505 | + 8.6 | .087 | .090 |
| 4173... | 16 19.5 | +33 58 | 5.4 | M2 | .049 | 0.0 | .008 | .017 |
| 4188... | 16 23.7 | − 7 26 | 5.4 | M2 | .176 | − 0.1 | .008 | .012 |
| 4193... | 16 24.8 | −26 16 | 1.2 | M1 | 0.034 | − 3.5 | .011 | .026 |
| B.D.−12°4523... | 16 26.2 | −12 28 | 9.5 | M5 | 1.24 | +11.8 | .288 | ....... |
| 4201... | 16 26.2 | +42 3 | 5.0 | M6 | 0.028 | 0.0 | .010 | ....... |
| 4211... | 16 28.7 | +33 40 | 6.7 | M0 | .039 | − 0.2 | .004 | ....... |
| 4212... | 16 29.1 | +11 39 | 4.9 | M0 | .204 | + 0.1 | .011 | − .011 |
| 4242... | 16 36.7 | +49 4 | 5.1 | M2 | .044 | 0.0 | .010 | ....... |
| 4262... | 16 42.0 | +15 53 | 5.8 | M3 | .054 | − 0.1 | .007 | .015 |
| 4264... | 16 42.2 | + 8 43 | 5.4 | M1 | .016 | 0.0 | .008 | ....... |
| Cin. 2238... | 16 42.3 | +33 38 | 8.6 | M0 | .37 | + 8.7 | .105 | .178 |
| 4286... | 16 47.7 | +27 56 | 5.9 | M1 | 0.011 | 0.0 | .007 | ....... |
| Cin. 2251... | 16 51.5 | − 8 12 | 9.2 | M4e | 1.234 | +10.5 | .182 | .148 |
| B.D.+25°3173... | 16 55.1 | +25 53 | 9.4 | M2 | 0.52 | + 9.1 | .087 | ....... |
| 4318... | 16 55.4 | −24 59 | 5.9 | M3 | .022 | + 0.1 | .007 | ....... |
| 4336... | 16 59.7 | +14 12 | 5.1 | M3 | .070 | + 0.2 | .010 | ....... |
| 4343... | 17 0.8 | +35 31 | 6.8 | M4 | 0.058 | − 0.8 | .003 | .000 |
| 4342... | 17 1.2 | − 4 57 | 7.9 | M0 | 1.464 | + 7.8 | .096 | .091 |
| Wolf 636... | 17 1.4 | − 4 57 | 9.3 | M3 | 1.465 | +10.1 | .145 | ....... |
| 4366... | 17 8.9 | +10 40 | 5.6 | M2 | 0.036 | − 0.4 | .006 | ....... |
| B.D.+45°2505... | 17 9.9 | +45 49 | 9.6 | M4 | 1.590 | + 9.9 | .115 | ....... |
| B.D.+42°2810... | 17 10.7 | +42 26 | 9.6 | M1 | 1.061 | + 8.7 | .066 | .030 |
| 4373... | 17 11.2 | +14 28 | 3.5 | M5 | 0.030 | − 1.6 | .010 | − .002 |
| B.D.−15°4502... | 17 12.0 | −15 8 | 6.8 | M1 | ...... | − 1.1 | .003 | ....... |
| 4400... | 17 17.0 | +18 8 | 5.2 | M2 | .051 | − 0.2 | .008 | ....... |
| 4408... | 17 18.2 | +46 19 | 5.8 | M0 | 0.050 | − 0.1 | .007 | ....... |
| Cin. 2347... | 17 34.5 | +18 36 | 9.1 | M1 | 1.39 | + 9.1 | .100 | .135 |
| Cin. 2354... | 17 36.9 | +68 25 | 9.1 | M4 | 1.334 | + 9.8 | .138 | .213 |
| B.D.+43°2796... | 17 41.7 | +43 26 | 9.5 | M3 | 0.616 | + 9.5 | .100 | ....... |
| Boss 4497B.. | 17 43.5 | +27 46 | 9.5 | M4 | .817 | +10.0 | .126 | .111 |
| 4526... | 17 52.6 | −23 56 | 6.9 | M1 | .003 | − 0.3 | .004 | ....... |
| B.D.+45°2627... | 17 54.7 | +45 22 | 6.2 | M6 | ...... | − 0.2 | .005 | ....... |
| 4555... | 17 57.8 | +45 30 | 5.9 | M0 | .044 | + 0.2 | .007 | 0.018 |
| 4578... | 18 2.9 | +22 13 | 5.3 | M2 | .023 | − 0.2 | .008 | ....... |
| 4606... | 18 9.1 | +31 23 | 5.0 | M3 | .018 | 0.0 | .010 | ....... |
| 4617... | 18 12.6 | −36 47 | 3.2 | M4 | .216 | + 0.2 | .025 | ....... |
| 4630... | 18 16.9 | −24 57 | 6.4 | M5 | .011 | − 0.6 | .004 | ....... |
| 4636... | 18 17.1 | +21 56 | 5.0 | M0 | .062 | 0.0 | .010 | ....... |
| 4649... | 18 19.0 | +23 15 | 5.7 | M0 | .076 | + 0.2 | .008 | ....... |
| 4653... | 18 19.6 | +49 5 | 5.1 | M3 | 0.058 | 0.0 | .010 | ....... |
| B.D.+43°2970... | 18 21.8 | +43 52 | 7.0 | M2 | ...... | − 0.5 | 0.003 | ....... |

TABLE I—*Continued*

| Name | α 1925 | δ 1925 | m | Sp. | μ | M | Spec. π | Trig. π |
|---|---|---|---|---|---|---|---|---|
| Cin. 2456 Br. | $18^{h}42^{m}0$ | +59° 30′ | 8.8 | M4 | 2″307 | +10.9 | 0″263 | 0″287 |
| Cin. 2456 Ft. | 18 42.0 | +59 30 | 9.3 | M5 | 2.307 | +11.9 | .331 | .287 |
| Cin. 2463... | 18 45.6 | +17 22 | 9.0 | M0 | 0.579 | + 8.5 | .079 | ....... |
| 4800... | 18 51.9 | +36 48 | 4.5 | M4 | .010 | − 1.4 | .007 | ....... |
| 4971... | 18 52.9 | +89 2 | 6.6 | M4 | .029 | − 0.4 | .004 | ....... |
| 4814... | 18 53.1 | +43 51 | 4.4 | M5 | 0.077 | − 0.6 | .010 | .006 |
| Cin. 2475... | 18 54.3 | + 5 50 | 9.7 | M2 | 1.247 | + 8.9 | .069 | .074 |
| B.D.+30°3409... | 19 2.1 | +30 37 | 6.4 | M2 | ...... | 0.0 | .005 | ....... |
| B.D.+29°3472... | 19 2.9 | +29 48 | 6.6 | M1 | ...... | 0.0 | .005 | ....... |
| 4877... | 19 5.7 | +39 2 | 7.6 | M6 | 0.007 | − 0.6 | .002 | ....... |
| 4966... | 19 22.6 | +50 6 | 7.1 | M7 | .016 | − 0.3 | .003 | ....... |
| 4976... | 19 25.6 | +24 31 | 4.6 | M1 | .170 | + 0.3 | .014 | .013 |
| 4983... | 19 26.7 | − 2 57 | 5.2 | M1 | .016 | − 0.2 | .008 | ....... |
| 4993... | 19 30.0 | −24 1 | 6.7 | M0 | .004 | 0.0 | .005 | ....... |
| Cin. 2556... | 19 30.9 | + 4 25 | 10.5 | M1 | .58 | + 8.6 | .042 | ....... |
| 5043... | 19 41.3 | +41 36 | 6.0 | M0 | .017 | 0.0 | .006 | .000 |
| 5052... | 19 44.0 | +18 21 | 3.8 | M2 | .009 | − 1.0 | .011 | .003 |
| B.D.+44°3242... | 19 44.1 | +44 53 | 9.2 | M2 | ...... | + 0.1 | .002 | ....... |
| 5069... | 19 47.9 | +38 32 | 5.4 | M2 | .098 | − 0.4 | .007 | ....... |
| 5106... | 19 53.5 | +60 37 | 7.3 | M1 | .012 | + 0.3 | .004 | ....... |
| 5118... | 19 55.4 | +19 17 | 3.7 | M0 | .062 | − 0.2 | .017 | .010 |
| 5125... | 19 56.7 | +17 19 | 5.6 | M4 | .015 | − 0.4 | .006 | ....... |
| 5129... | 19 58.0 | −27 55 | 4.6 | M4 | .037 | 0.0 | .012 | ....... |
| 5149... | 20 0.7 | +64 37 | 5.4 | M1 | .015 | 0.0 | .008 | ....... |
| 5154... | 20 1.8 | +76 16 | 6.4 | M3 | .059 | + 0.2 | .006 | ....... |
| B.D.+36°3883... | 20 4.7 | +36 21 | 7.4 | M2 | ...... | − 0.5 | .003 | − .003 |
| B.D.+76° 785... | 20 13.1 | +77 0 | 9.3 | M0 | .495 | + 8.6 | .072 | .059 |
| 5234... | 20 19.8 | +68 38 | 6.0 | M5 | .042 | 0.0 | .006 | ....... |
| 5231... | 20 20.1 | +40 47 | 6.1 | M0 | .054 | − 0.5 | .005 | ....... |
| 5248... | 20 25.1 | −22 39 | 6.2 | M1 | .029 | − 0.1 | .005 | ....... |
| 5271... | 20 29.0 | +48 58 | 5.6 | M2 | .037 | + 0.6 | .010 | ....... |
| Cin. 2676... | 20 35.8 | + 4 42 | 8.4 | M0 | .844 | + 7.9 | .079 | .063 |
| 5306... | 20 35.8 | −18 24 | 5.3 | M2 | .035 | − 0.3 | .008 | ....... |
| 5338... | 20 43.8 | − 5 18 | 4.6 | M3 | .039 | 0.0 | .012 | ....... |
| 5363... | 20 47.3 | −27 12 | 4.2 | M1 | .017 | − 0.3 | .013 | ....... |
| B.D.+61°2068... | 20 51.8 | +61 53 | 8.6 | M3 | .77 | + 9.2 | .132 | .141 |
| 5409... | 20 57.0 | +19 2 | 6.0 | M3 | .075 | + 0.3 | .007 | .006 |
| Furuhjelm 54... | 20 57.1 | +39 47 | 9.7 | M3e | .671 | +10.1 | .120 | .081 |
| 5430... | 21 2.7 | −25 18 | 4.6 | M0 | 0.059 | 0.0 | .012 | ....... |
| 5434... | 21 3.6 | +38 22 | 6.3 | M0 | 5.157 | + 8.4 | .263 | .300 |
| 5458... | 21 10.9 | +59 47 | 7.1 | M2 | 0.012 | − 1.6 | .002 | ....... |
| 5457... | 21 11.6 | −15 29 | 5.5 | M3 | .019 | 0.0 | .008 | ....... |
| 5462... | 21 12.3 | − 9 32 | 6.8 | M4 | 0.012 | 0.0 | .004 | ....... |
| Cin. 2757... | 21 13.0 | −39 9 | 6.6 | M1 | 3.532 | + 8.4 | .229 | 0.253 |
| 5479... | 21 17.4 | + 7 2 | 6.0 | M3 | 0.044 | 0.0 | 0.006 | ....... |

TABLE I—*Continued*

| Name | α 1925 | δ 1925 | m | Sp. | μ | M | Spec. π | Trig. π |
|---|---|---|---|---|---|---|---|---|
| 5487... | $21^{h}18^{m}7$ | −22° 59′ | 5.7 | M0 | 0″.041 | − 0.3 | 0″.006 | ....... |
| 5490... | 21 18.9 | − 9 38 | 6.2 | M0 | .050 | 0.0 | .006 | ....... |
| 5522... | 21 26.6 | +23 19 | 4.8 | M1 | .017 | 0.0 | .011 | 0″.010 |
| 5567... | 21 37.3 | +42 56 | 5.4 | M1 | .054 | + 0.4 | .010 | ....... |
| 5572... | 21 38.5 | + 5 20 | 5.6 | M2 | .022 | − 0.3 | .007 | ....... |
| 5583... | 21 40.1 | +40 49 | 5.5 | M2 | .026 | + 0.1 | .008 | ....... |
| 5593... | 21 41.2 | +58 26 | 4.4 | M2 | .002 | − 3.0 | .003 | .011 |
| 5595... | 21 42.3 | − 9 37 | 6.2 | M3 | .016 | − 0.2 | .005 | ....... |
| 5614... | 21 45.2 | +60 21 | 5.6 | M1 | .006 | + 0.5 | .010 | .020 |
| 5647... | 21 53.1 | +79 12 | 6.8 | M2 | .029 | − 0.3 | .004 | ....... |
| 5650... | 21 54.5 | +63 16 | 5.4 | M2e | .012 | − 2.0 | .003 | ....... |
| 5645... | 21 54.6 | −21 33 | 6.2 | M4 | .015 | − 0.2 | .005 | ....... |
| 5678... | 22 1.6 | +62 45 | 5.5 | M5 | .052 | + 0.1 | .008 | ....... |
| 5686... | 22 3.0 | +44 39 | 5.3 | M0 | .017 | + 0.1 | .009 | .004 |
| B.D.+14°4772... | 22 15.7 | +15 10 | 7.2 | M1 | ...... | 0.0 | .004 | ....... |
| Cin. 2922... | 22 25.4 | +57 19 | 9.2 | M3 | .870 | +10.4 | .174 | .257 |
| 5797... | 22 25.4 | + 8 45 | 5.8 | M0 | .062 | − 0.1 | .007 | ....... |
| 5804... | 22 26.4 | +47 19 | 4.6 | M0 | 0.021 | − 2.1 | .005 | .005 |
| B.D.+52°3240... | 22 29.6 | +53 21 | 9.5 | M5 | ...... | − 0.2 | .001 | ....... |
| B.D.+53°2911... | 22 29.7 | +53 25 | 9.5 | M1 | 1.482 | + 8.6 | .066 | .030 |
| 5820... | 22 30.8 | + 0 13 | 7.0 | M1 | 0.089 | − 0.1 | .004 | ....... |
| 5843... | 22 35.7 | +56 24 | 5.5 | M4 | .056 | − 0.3 | .007 | ....... |
| 5855... | 22 38.2 | −29 45 | 6.4 | M5 | .030 | − 0.1 | .005 | ....... |
| B.D.+43°4305... | 22 43.6 | +43 56 | 9.5 | M5e | .86 | +11.4 | .240 | ....... |
| 5884... | 22 45.6 | −13 59 | 4.2 | M0 | .039 | − 0.4 | .012 | ....... |
| 5897... | 22 48.6 | +42 55 | 5.2 | M0 | .106 | + 0.2 | .010 | ....... |
| 5895... | 22 48.7 | − 7 59 | 3.8 | M2 | .036 | − 0.1 | .017 | ....... |
| Cin. 3001... | 22 56.3 | −22 55 | 7.6 | M1 | .899 | + 8.8 | .174 | ....... |
| 5934... | 22 58.7 | − 6 59 | 6.5 | M2 | .039 | 0.0 | .005 | ....... |
| 5940... | 23 0.1 | +27 41 | 2.6 | M2 | 0.234 | − 0.4 | .025 | .016 |
| Cin. 3014... | 23 0.8 | −36 18 | 7.4 | M2 | 6.900 | + 9.4 | .251 | .292 |
| 5952... | 23 3.2 | + 9 0 | 4.7 | M2 | 0.016 | + 0.6 | .015 | − .003 |
| 5962... | 23 5.7 | + 8 16 | 5.4 | M4 | .004 | − 0.9 | .005 | ....... |
| 5978... | 23 10.4 | − 6 27 | 4.4 | M2 | .193 | + 0.6 | .017 | .005 |
| 5986... | 23 13.0 | − 8 8 | 5.1 | M5 | .022 | 0.0 | .010 | ....... |
| 5993... | 23 14.3 | +48 36 | 5.0 | M2 | .038 | 0.0 | .010 | ....... |
| 6003... | 23 16.3 | +41 40 | 6.0 | M0 | .044 | + 0.4 | .008 | ....... |
| 6006... | 23 17.2 | +30 0 | 5.8 | M0 | .102 | + 0.4 | .008 | ....... |
| 6025... | 23 21.5 | +61 52 | 5.2 | M2 | .014 | − 0.7 | .007 | ....... |
| 6058... | 23 29.7 | +22 5 | 5.5 | M5 | .036 | 0.0 | .008 | ....... |
| 6089... | 23 39.6 | + 9 55 | 5.4 | M2 | 0.007 | 0.0 | .008 | ....... |
| Lal. 46650... | 23 45.3 | + 2 0 | 8.7 | M2 | 1.393 | + 9.1 | .120 | .171 |
| 6121... | 23 47.5 | + 8 54 | 6.1 | M2 | 0.063 | − 0.1 | .006 | ....... |
| 6125... | 23 48.6 | +21 15 | 6.3 | M2 | .055 | + 0.5 | .007 | ....... |
| 6127... | 23 48.7 | +18 42 | 5.2 | M3 | .047 | 0.0 | .009 | 0.014 |
| 6137... | 23 50.9 | − 0 17 | 6.0 | M5 | .057 | − 0.5 | .005 | ....... |
| 6143... | 23 52.3 | −22 24 | 7.4 | M2 | .050 | 0.0 | .003 | ....... |
| 6150... | 23 53.9 | +24 43 | 4.8 | M3 | .056 | − 0.1 | .010 | ....... |
| B.D.+45°4378... | 23 54.8 | +46 19 | 9.2 | M0 | .64 | + 9.2 | .100 | ....... |
| 6171... | 23 58.1 | − 6 26 | 4.7 | M3 | 0.053 | − 0.5 | 0.009 | ....... |

An examination of the absolute magnitudes of the giant stars listed in Table I shows that the mean value is about −0.2, with some of the brightest stars ranging nearly to −4.5. The faintest of the giant M stars of early type is +0.7, and the brightest of the dwarf stars +7.0, thus leaving an interval of 6.3 mag. within which no stars are found. For stars of class M5 or later this interval increases to 11.0 mag. The mean absolute magnitude of the long-period variables as determined by Merrill and Strömberg is in good agreement with our values for the M stars of advanced type.

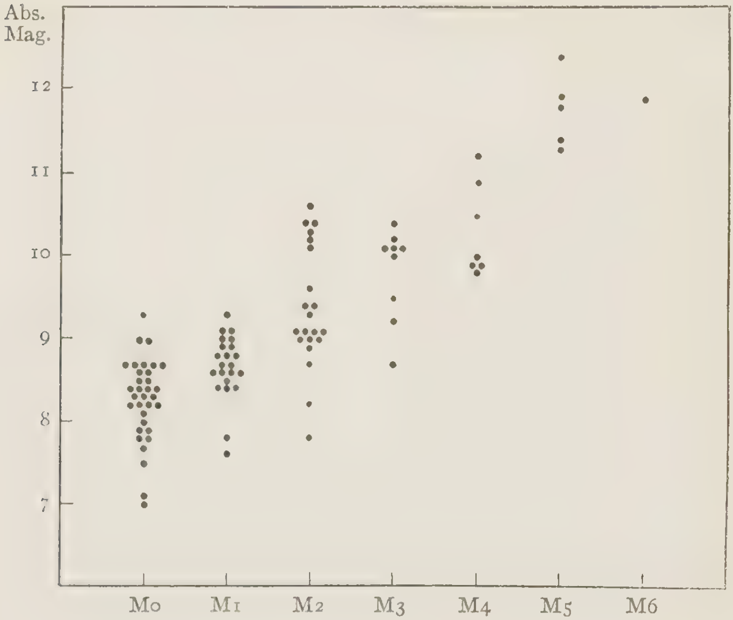

Fig. 1.—Absolute magnitudes and spectral types of dwarf M stars

The giant stars show little variation in mean absolute magnitude with spectral type, while the dwarfs decrease rapidly in luminosity as the type becomes more advanced. This characteristic of dwarf M stars has been noted by us previously, and reference has been made to the possibility it affords of deriving the parallaxes of faint stars of this type from spectrograms of very low dispersion. A diagram showing the absolute magnitudes of the dwarf stars of Table I plotted against spectral type is given in Figure 1. The corresponding mean curve is given in Figure 2. It seems clear that in the case of dwarf stars of the more advanced types, at least, a very fair approximation to the parallaxes may be derived from the estimation of spectral type and the assumption of a constant absolute magnitude for each type. Among the dwarf stars smaller dimensions appear to accompany lower temperatures and to lead to decreased luminosity, while among the giants the reduction in temperature is compensated by increase in size.

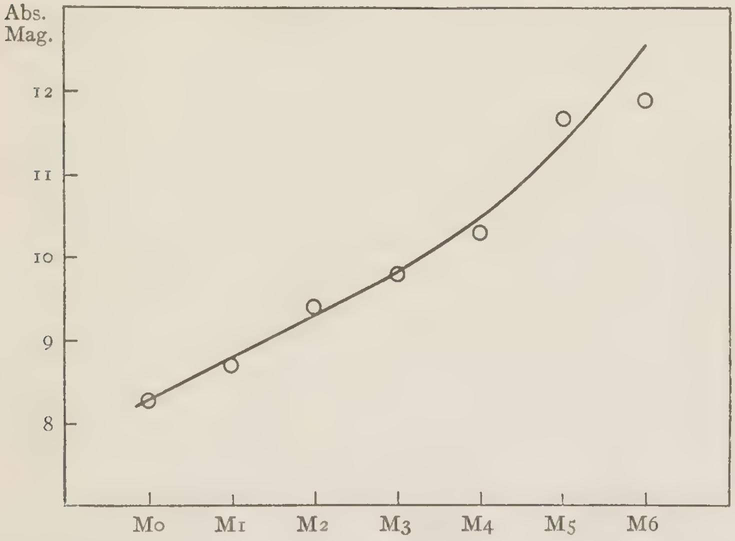

FIG. 2.—Normal points and plot of absolute magnitudes and spectral types of dwarf M stars.

Twenty-eight stars in the list have absolute magnitudes brighter than −1.0, and may for convenience be called "super-giants." Among them are α Orionis, α Scorpii, α Herculis, and several red variables in the *h* and χ cluster in Perseus. These intrinsically bright stars show a pronounced angular galactic concentration in conformity with the behavior of the brightest stars of other spectral types, although, as is well known, the M-type giants in general show no such effect. The average galactic latitude of these twenty-eight stars is 7°, only five stars having values above 10°.

Three of the super-giants belong to the W Cephei type of variable, and have spectra which show bright lines of hydrogen, as well as certain unidentified emission lines. Seven stars, of which four are irregular variables, are shown by their radial velocities to be members of the double cluster in Perseus. A parallax of between 0.″001 and 0.″002 is indicated by these stars. It is of interest to note that the mean proper motion of the seventeen super-giants for which values are known is only 0.″017, a value considerably smaller than that for the ordinary giants.

An outstanding feature of the absolute magnitudes of the giant stars other than the super-giants is their small dispersion. If this were due to any failure on the part of the spectral criteria to show differences of absolute magnitude among these stars, it would certainly be expected to show for the brightest stars as well. The spectral differences, however, between the ordinary giants and the super-giants are well marked. A comparison of the mean absolute magnitudes of groups of stars of different reduced proper motion $H = m + 5 \log \mu$ shows a fairly regular though small increase in luminosity with decrease in $H$. A similar comparison of $H$ with mean absolute magnitude derived from trigonometric parallaxes, of which about fifty are available, gives quite comparable results, and shows that trigonometric parallaxes also indicate small dispersion in absolute magnitude among the ordinary M-type giants. Since the reduced proper motion $H$ is a simple function of absolute magnitude and linear cross-motion, it is evident that the observed dispersion in $H$, which is not very large, may be accounted for by a considerable dispersion in linear cross-motion and little dispersion in absolute magnitude. The large dispersion in radial velocity observed among the normal M-type giants, larger than for any other class of giant stars, would indicate a similar dispersion in linear cross-motion and would be in excellent agreement with this view of a small range in absolute magnitude.

There are seventy-one giant stars in the list for which trigonometric parallaxes have been measured. Of these, sixty-seven are found in Schlesinger's *Catalogue of Parallaxes* and have been corrected for systematic errors on the basis of the system derived by him. The direct comparison of the spectroscopic and trigonometric parallaxes of these stars shows an excellent degree of agreement, the mean difference being less than 0ʺ.001, and the average deviation between 0ʺ.008 and 0ʺ.009. Since the reduction tables from which the spectroscopic absolute magnitudes and parallaxes are calculated were based on results derived from peculiar motions without any use of trigonometric parallaxes, this agreement affords important evidence for the accuracy of the system employed.

In the case of the dwarf stars the trigonometric parallaxes have been used exclusively in the derivation of the reduction curves, and close agreement of the mean results is to be expected. A comparison of sixty-four stars shows a systematic difference of about 0ʺ.002, the trigonometric parallaxes being the larger. This would correspond to considerably less than 0.1 in absolute magnitude.

Several stars among the dwarfs for which no trigonometric parallaxes have been measured are found to have values of 0ʺ.1 or larger. These are Cin. 251, Cin. 456, B.D. +63°869, Cin. 1633, $\beta$ G.C. 6710 N, B.D. −7°4003, B.D. −12°4523, Wolf 636, B.D. +45°2505, B.D. +43°4305, Cin. 3001, and B.D. +45°4378. If the spectroscopic parallaxes of B.D. −7°4003 and B.D. −12°4523 are confirmed by observers of trigonometric parallax they will be among the nearest known stars.

There are 155 giant stars in Table I which were included in the list of 1646 stars for which absolute magnitudes were published by us in 1921.[1] The present values are 0.4 mag. brighter on the average, a result which is quite satisfactory in view of the low weight of the earlier determinations. A similar comparison has been made for eighty-six giant stars common to our list and that of Young and Harper.[2] The Mount Wilson values are, on the average, nearly 0.8 mag. fainter than the Victoria results. The agreement is much better for the early than for the later subdivisions of type, the differences becoming progressively greater and amounting to as much as 1.5 mag. for the relatively few stars of classes M5 and M6. The explanation is probably to be found in the variation with spectral type of the intensities of the lines used for determinations of absolute magnitude.

---

[1] *Mt. Wilson Contr.*, No. 199; *Astrophysical Journal*, **53**, 13, 1921.

[2] *Publications of the Dominion Astrophysical Observatory*, **3**, No. 1, 1924.

A result similar to that obtained from a comparison with the Victoria values is found for the absolute magnitudes published by Rimmer.[1] The Mount Wilson values are slightly less than 0.7 mag. fainter for forty-seven stars observed in common. For stars of classes M0 and M1 the difference is 0.2 mag., but for the more advanced types the average difference is nearly a magnitude.

The present investigation has given no evidence of the existence of stars intermediate in absolute magnitude between the giants and the dwarfs, or of spectral types intermediate between these radically different spectra. In the case of dwarf stars which are observed because of their large proper motions, the effect of selection must necessarily be present, and if dwarf stars somewhat brighter than 7.0 in absolute magnitude exist, they may not have been detected because they are not included on our observing lists. For the giant stars, however, no effect of selection according to proper motion is present. If we may assume that the M stars given in Boss's *Catalogue* are complete to apparent magnitude 6.5, we find accordingly that no star of absolute magnitude 3.0 can be present within a distance from the sun defined by a parallax of $0\overset{''}{.}020$, and no star of absolute magnitude 2.0 within a distance defined by a parallax of $0\overset{''}{.}013$. The results for a considerable number of stars of fainter apparent magnitude, observed mainly in the Selected Areas, add strength to this conclusion, and make the existence in appreciable numbers of stars of intermediate absolute magnitude or spectral type exceedingly improbable.

MOUNT WILSON OBSERVATORY
August 1926

---

[1] *Memoirs of the Royal Astronomical Society*, **64**, Part 1, 1925.

Contributions from the Mount Wilson Observatory, No. 320
Reprinted from the *Astrophysical Journal*, Vol. LXIV, pp. 250-257, 1926
Printed in the U.S.A.

# THE DWARF COMPANION TO CASTOR AS A SPECTROSCOPIC BINARY AND ECLIPSING VARIABLE

By ALFRED H. JOY and R. F. SANFORD

## ABSTRACT

*Spectrographic observations.*—The spectral type of Castor C is dM1e. $H\alpha$, $H\beta$, $H\gamma$, $H\delta$, and H and K of calcium are present as emission lines. In 1916, the star was found to be a spectroscopic binary, both bright and dark lines being double, and both spectra being nearly alike, except that one was somewhat stronger than the other. The period was found to be 0.814266 day, with no indication of eccentricity. Thirty-five spectrograms have been obtained as listed in Table I. Spectrographic elements were determined and corrected by a least-squares solution: $e=0.0$ (assumed); $\gamma=+4.3$ km/sec.; $K_1=114.0$ km/sec.; $K_2=126.7$ km/sec. A comparison of the orbits of the system of Castor is given in Table III.

The *intensities of the two absorption spectra* are in the ratio of 5:4. The *emission lines* seem to be *stronger when on the side of greater wave-length.* They give the same velocities as the absorption lines. The *spectroscopic absolute magnitude* of the brighter component is estimated from plates showing single lines to be 9.2, which corresponds to a *parallax* of $0\overset{''}{.}083$.

*Absolute dimensions.*—With the aid of van Gent's light-curve, *photometric elements* and *absolute dimensions* have been computed: $a_0=0.88$; $k=0.89$; $i=86\overset{\circ}{.}4$; $a_1+a_2=2{,}700{,}000$ km; $r_1=0.76\odot$; $r_2=0.68\odot$; $m_1=0.63\odot$; $m_2=0.57\odot$; $\rho_1=1.4\odot$; $\rho_2=1.8\odot$. The surface brightness of both stars is 3.6 mag. fainter than that of the sun.

Star C of the system of Castor is distant $73''$ in position angle $165^\circ$, and is known to have the same proper motion ($0\overset{''}{.}207$ in $248^\circ$) and parallax as Castor. The apparent magnitude being 9.0, it must have an exceedingly low intrinsic luminosity.

The first slit spectrogram was made on March 15, 1916, and revealed the presence of two closely similar spectra showing absorption and emission lines whose characteristics are discussed in detail in another section of this paper. This first plate showed a large difference in wave-length between the two sets of lines, which, interpreted as a Doppler shift, indicated large orbital velocity. Subsequent observations gave spectra which confirmed this interpretation. The stellar magnitude of C is such that most of the spectrograms were necessarily made with a one-prism spectrograph equipped with a short camera giving a dispersion of 75 A per millimeter at $H\gamma$. The difficulties caused by the superposition of two spectra are therefore enhanced by the small dispersion, which makes for relatively low accuracy in the determination of the radial velocity. As far as can be judged from our measures, there seem to be no grounds for treating the velocities from the emission lines differently from those depending upon the absorption lines.

Observation of the separations of the lines of the two spectra upon successive nights for a considerable time gave the impression that the changes took place in a period slightly over four days, with, however, some disquieting inconsistencies. Pairs of plates from the same night were then made to test for a shorter period, with the result that, on the second attempt, the two plates, C 3718 and C 3721, whose mid-exposure times differ only 0.211 day, showed a totally different arrangement of the lines of the two component spectra. In the first case, the lines were single; and in the second, double, the indicated difference of velocity being about 230 km/sec. Evidently a period much shorter than four days had to be looked for, unless the velocity changes departed greatly from a sine curve.

Thirty-five spectrograms of a varied but still usable quality have been made as listed in Table I. Plates on which the lines of the two components are blended give, of course, but one velocity. Such velocities are entered in the column for the primary, but should be understood to be measures of plates whose lines could not be resolved. Except the first three plates, which were obtained with the 60-inch reflector, all exposures have been made with the 100-inch reflector.

The assumption that the velocity variation takes place in somewhat less than a day resulted in a satisfactory grouping of the observations about a single epoch with a period equal to 0.814266 day. More than forty-five hundred revolutions of the stars in their orbits are covered by the observations. Those velocities which are critical for a test of the correctness of the period can hardly admit of a shift of 0.05 day, which sets the upper limit of inaccuracy in the period at about 0.00001 day.

The freehand curve drawn through the observations plotted to one epoch indicated that the orbits might be assumed to be circular. Elements have been derived by a graphical method. The epoch from which the phases have been reckoned is the time of zero velocity of the components when the more massive star is passing from recession to approach.

TABLE I

Observations of the Companion to Castor

| Plate No. | Date | G.M.T. | Phase | Velocity | | O−C | |
|---|---|---|---|---|---|---|---|
| | | | | Prim. | Sec. | Prim. | Sec. |
| | | | | km/sec. | km/sec. | km/sec. | km/sec. |
| γ 4678.... | 1916 Mar. 15 | $16^h55^m$ | $0^d583$ | +100 | −130 | −18 | −10 |
| 4683.... | Mar. 16 | 17 59 | .812 | + 29 | ........ | ........ | ........ |
| 4745.... | Apr. 16 | 16 07 | .794 | + 16 | ........ | ........ | ........ |
| C 249.... | 1920 Jan. 14 | 23 04 | .304 | − 70 | + 82 | + 8 | −13 |
| 262.... | Jan. 29 | 22 03 | .602 | +120 | −111 | + 2 | +12 |
| 270.... | Feb. 4 | 18 57 | .773 | + 3 | ........ | ........ | ........ |
| 309.... | Mar. 6 | 16 30 | .730 | + 58 | − 68 | −14 | + 4 |
| 326.... | Mar. 11 | 19 50 | .169 | −118 | +124 | −12 | − 2 |
| 330.... | Mar. 12 | 18 36 | .303 | − 69 | + 85 | +10 | −11 |
| 377.... | Apr. 11 | 17 32 | .130 | − 91 | +123 | + 1 | +12 |
| 1634.... | 1922 Mar. 21 | 20 00 | .008 | + 7 | ........ | ........ | ........ |
| 1638.... | Mar. 22 | 18 12 | .119 | −103 | + 86 | −18 | −18 |
| 2490.... | 1923 Oct. 21 | 0 48 | .079 | − 57 | + 98 | + 5 | +21 |
| 2543.... | Nov. 21 | 19 38 | .108 | − 59 | +116 | +21 | +18 |
| 2552.... | Nov. 23 | 0 25 | .493 | − 6 | ........ | ........ | ........ |
| 2556.... | Nov. 24 | 0 20 | .678 | +124 | −103 | +21 | + 2 |
| 2560.... | Nov. 26 | 1 03 | .263 | −109 | +130 | − 2 | +12 |
| 2578.... | Dec. 17 | 0 23 | .064 | + 16 | ........ | ........ | ........ |
| 2683.... | 1924 Feb. 16 | 20 07 | .002 | − 2 | ........ | ........ | ........ |
| 3122.... | 1925 Jan. 9 | 20 25 | .680 | +110 | −113 | + 8 | − 8 |
| 3126.... | Jan. 10 | 20 30 | .054 | + 6 | ........ | ........ | ........ |
| 3129.... | Jan. 11 | 20 14 | .231 | −112 | +137 | − 5 | + 9 |
| 3142.... | Jan. 13 | 20 14 | .601 | +124 | −118 | + 6 | + 5 |
| 3145.... | Jan. 31 | 19 05 | .639 | +123 | −115 | + 9 | + 5 |
| 3153.... | Feb. 2 | 21 25 | .293 | − 83 | + 97 | + 1 | − 5 |
| 3202.... | Mar. 12 | 17 43 | .683 | + 95 | −108 | − 6 | − 7 |
| 3289.... | May 7 | 16 05 | .437 | + 17 | ........ | ........ | ........ |
| 3666.... | 1926 Jan. 24 | 17 00 | .275 | −107 | +112 | −13 | 0 |
| 3669.... | Jan. 24 | 23 05 | .532 | + 82 | − 84 | −14 | +16 |
| 3718.... | Feb. 27 | 15 25 | .010 | + 6 | ........ | ........ | ........ |
| 3721.... | Feb. 27 | 20 28 | .221 | −104 | +129 | + 5 | − 1 |
| 3725.... | Feb. 28 | 16 20 | .235 | −113 | +115 | − 7 | −13 |
| 3733.... | Mar. 24 | 18 53 | .716 | + 78 | −99 | − 3 | −17 |
| 3738.... | Mar. 29 | 17 53 | .799 | + 1 | ........ | ........ | ........ |
| 3772.... | Apr. 26 | 16 18 | 0.232 | − 91 | +132 | +16 | + 4 |

Only results from plates giving the velocities of both components have been used to correct these preliminary elements. Twelve normal places were determined for each component, and with these a set of normal equations was formed in the manner described by Harper.[1] In spite of very considerable disparity in quality, all individual velocities have been treated as of equal weight.

---

[1] *Publications of the Dominion Observatory*, 1, 327, 1914.

The preliminary elements, the corrections, and the adopted elements are given in Table II. The value of [*pvv*] for the normal places is 12 per cent less for the adopted elements than for the preliminary elements.

According to H. D. Curtis,[1] the velocities of the systems $\alpha^1$ and $\alpha^2$ Geminorum are −0.98 and +6.20 km/sec., respectively. The same element for star C is +4.3 km/sec. We thus have similar proper motions, parallaxes, and radial velocities, indicative of the close relationship between stars A, B, and C. The function $(a_1+a_2) \sin i$, the projected distance of the centers of the two components, is so small that even for rather dense stars the conditions are favorable for eclipses, whose epochs should correspond to the times when the spectral lines are superposed.

TABLE II

ELEMENTS OF THE COMPANION OF CASTOR

| | Preliminary Elements | Corrections | Adopted Elements |
|---|---|---|---|
| $P$ | | | 0.814266 day |
| $K_1$ | 117 | −3.0 | 114.0 km/sec. |
| $K_2$ | 130 | −3.3 | 126.7 km/sec. |
| $T$ | 2423746.520 | +0.004 | 3746.524 |
| $\gamma$ | +6 | −1.7 | +4.3 km/sec. |
| $(a_1+a_2) \sin i$ | | | 2,695,200 km |
| $m_1 \sin^3 i$ | | | 0.63 ⊙ |
| $m_2 \sin^3 i$ | | | 0.57 ⊙ |

Figure 1, where abscissae are phases and ordinates, velocities, shows the computed velocity curves. The velocities as measured upon the individual plates are plotted as circles. The column headed O−C in Table I gives the differences between the observed velocities and this curve. The representation, although ragged, is about what may be expected from such spectra obtained with comparatively low dispersion.

It may be of interest to recall the various orbits involved in this system. The visual orbit of $\alpha^1$ about $\alpha^2$, according to Burnham, is as yet quite indeterminate. It is certain, however, that its period is a matter of centuries, various computers deriving from 232 to

---

[1] *Lick Observatory Bulletins*, **4**, 55, 1906.

1000 years for this element. Each of the three stars is a spectrographic binary, but C is the only one that reveals the spectra of both components. A comparison of some of the characteristics of the stars and their orbits is given in Table III. The projected distance from AB to C is $1.43 \times 10^{10}$ km ($\pi = 0''.076$), or 960 astronomical units. It is interesting to find that $a \sin i$ for the primary members of the spectrographic binaries $\alpha^1$ and $\alpha^2$ is so closely the same as for the two components of star C.

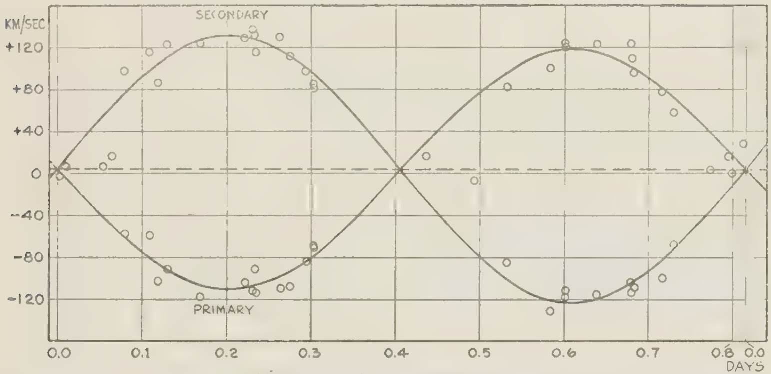

VELOCITY-CURVES. COMPANION TO CASTOR

FIG. 1

### THE SPECTRUM

The spectra of the components of the companion C are unusual and interesting. Both spectra show on all plates taken when the separation between the components is sufficient. The spectral type is dM1e with no certain difference in type between the components. The absorption spectrum pertaining to the more massive component is somewhat stronger than that of the less massive component, approximately, in the ratio of 5:4. The stars belong to the small group of M-type dwarfs which show H and K and the Balmer series of hydrogen as emission lines. Bright $H\alpha$ is present on one plate which shows the red portion of the spectrum. The hydrogen lines fall off in intensity from red to violet. No member of the series of wave-length shorter than $H\delta$ has been seen. H and K of ionized calcium are strong and sharp. All the bright lines give the same velocities as the absorption lines of the corresponding spectrum.

They double and become single with the absorption lines as illustrated in Plate XI.

The relative intensity of the emission lines of the two components varies in a marked degree. When they are on the red side, the lines of the more massive component are about twice as strong as those of the lesser component. When their positions are reversed, at the opposite phase, and the lines of the massive component are on the violet side, they no longer maintain their ascendency. They are, in fact, some 20 per cent weaker in the mean than the lines of the other component. In other words, when the velocities are such as to separate the lines, the red member of the pair is, with one or two exceptions, the stronger. A bright line originating from a given component is relatively enhanced when it is on the red side, that is, when the star is receding from us. The cause of this peculiar phenomenon is not clear. There seems to be nothing in the structure of the lines themselves as observed with low dispersion to suggest an explanation. The effect is the same for all the bright lines observed. The absorption lines behave normally. It is possible that the effect of the rapid orbital motion in a resisting medium might be such as to cause the higher atmosphere which produces the emission to be dragged behind. Thus, the receding star would show strengthened bright lines.

TABLE III

COMPARISON OF ORBITS OF CASTOR

| | AB (visual) | A($\alpha^2$) | B($\alpha^1$) | C |
|---|---|---|---|---|
| Spectrum | | A3s | A8s | dM1e |
| $m$ | | 2.0 | 2.8 | 9.6, 9.8 |
| $M$ ($\pi=0''.076$) | | 1.4 | 2.2 | 9.2, 9.4 |
| $P$ | 232–1000 years | 9.2 days | 2.9 days | 0.8 day |
| $e$ | 0.4 | 0.5 | 0.0 | 0.0 |
| $K$ | | 13.6km/sec. | 31.8km/sec. | 114.0km/sec.<br>126.7km/sec. |
| $\gamma$ | | +6.2km/sec. | −1.0km/sec. | +4.3km/sec. |
| $a \sin i$ | $a=$ 1,141,000,000km<br>76.4 ast. u. | 1,485,000 km | 1,279,000 km | 1,276,000 km<br>1,419,000 km |

ABSOLUTE MAGNITUDE

The spectrographic absolute magnitude has been determined by the use of the dwarf curves for six lines. Eleven plates showing single

# PLATE XI

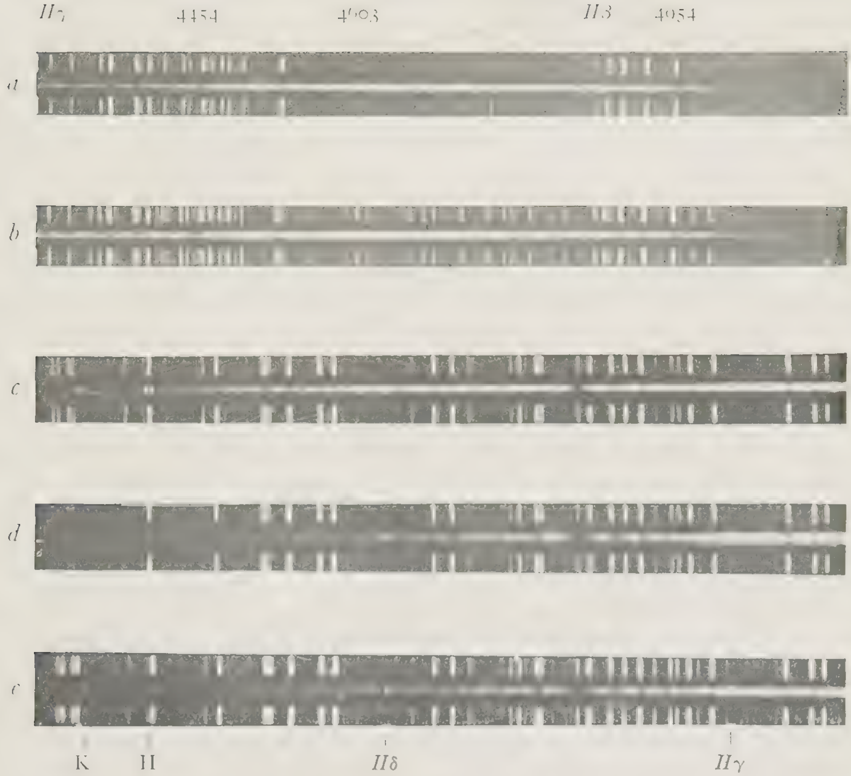

Spectrograms of the Companion to Castor

*a*) C262, double lines
*b*) C270, single lines
*c*) C3142, double lines, more massive component displaced to the violet
*d*) C3145, double lines, more massive component displaced to the red
*e*) C3718, single lines

lines are available for this purpose. The resulting absolute magnitude, which probably should be ascribed to the brighter star, is +9.2. The combined apparent magnitude is 9.0, which gives 9.6 and 9.8 for the separate components provided that one is 25 per cent brighter than the other. The parallax is, accordingly, 0".083. The value, 0".076, given in Schlesinger's catalogue as a mean of the trigonometric determinations for the different members of the system, would correspond to an absolute magnitude of 9.0 for the brighter component.

## THE PHOTOMETRIC ORBIT AND ABSOLUTE DIMENSIONS

After the preceding portions of this paper had been written and arranged for publication, the *Bulletin of the Astronomical Institutes of the Netherlands*, No. 97, came to hand. It contains an important communication by H. van Gent entitled "The Distant Companion C of Castor as an Eclipsing Variable Dwarf Star of Determinable Surface Brightness." Van Gent finds from photographic observations that the companion to Castor is an eclipsing variable[1] with equal minima. The period of the spectrographic orbit is confirmed. He makes use of a preliminary announcement[2] of early spectrographic observations to determine the absolute dimensions and other interesting physical conditions of the system. These results may be somewhat revised by applying the more complete data of the present paper.

The light-curve is not sufficiently well determined to admit of definitive elements from the photometric observations. It seems clear, however, that the minima are approximately equal and that the maxima show no effect of ellipticity, such as appears when the stars are elongated in the direction of the line joining their centers.

For uniformly illuminated disks with equal minima, the surface brightness must be the same for the two stars. The spectrographic observations confirm this conclusion.

According to van Gent, the loss of light at the minima is 0.538 mag., or 0.391 in intensity. From the strength of their spectral lines, we estimate the light of the two stars to be in the ratio of 4:5. Then, for the same surface brightness, the radius of the smaller in terms of the larger, or $k$ in Russell's notation, is 0.89.

---

[1] YY Geminorum, see *Astronomische Nachrichten*, **228**, 353, 1926.

[2] Adams and Joy, *Publications of the Astronomical Society of the Pacific*, **32**, 158, 1920.

From

$$a_0 = 1 - \lambda_1 + \frac{1 - \lambda_2}{k^2} ,$$

the fraction of obscuration is found to be 0.88. The light-curve indicates the duration of eclipse to be 0.12 of the period.

With the aid of Russell's Table I, $r_1$ and $i$ may now be found from the equations,

$$\cos^2 i \cos^2 \theta' + \sin \theta' = r_1^2 (1+k)^2$$
$$\cos^2 i = r_1^2 (1+kp)^2 .$$

Thus,

$$i = 86\overset{\circ}{.}4 , \qquad r_1 = 0.197 , \qquad r_2 = 0.175$$

A solution involving darkening at the limb gives values which are not essentially different from these results. In view of the large uncertainties of the light-curve, it seems hardly necessary to include them here.

Combining the photometric and spectrographic elements, we have the absolute dimensions:

| | |
|---|---|
| $a_1 + a_2 =$ | 2,700,000 km = 0.018 ast. u. |
| $r_1$ | 530,000 km = 0.76 ⊙ |
| $r_2$ | 472,000 km = 0.68 ⊙ |
| $m_1$ | 0.63 ⊙ |
| $m_2$ | 0.57 ⊙ |
| $\rho_1$ | 1.4 ⊙ |
| $\rho_2$ | 1.8 ⊙ |

The surface brightness is 3.6 mag. fainter than that of the sun.

The interest attaching to a more exact knowledge of the dimensions and physical conditions of these dwarf stars would make a more complete photometric study well worth while.

MOUNT WILSON OBSERVATORY
August 1926

Contributions from the Mount Wilson Observatory, No. 321
Printed in the U.S.A.

# THE PHOTOGRAPHIC DETERMINATION OF STELLAR PARALLAXES WITH THE 60- AND 100-INCH REFLECTORS

## NINTH SERIES

By ADRIAAN VAN MAANEN

## ABSTRACT

*Photographic parallaxes determined with the 60- and 100-inch reflectors.*—The detailed measurements are given for twenty-five fields, including twenty-nine stars and nebulae. The list contains six faint Wolf stars having large proper motions, Nos. 1056, 110, 437, 611, 612, 1106; the photographic absolute magnitudes range from +11.3 to +13.5. For B.D.−12°4523, which according to the *B.D. Catalogue* has a magnitude of 9.5, a parallax of +0″.350 was derived, giving it an absolute visual magnitude of +12.2. The mean parallax for the four Cepheids, T Monocerotis, RS Boötis, Y Ophiuchi, and Y Sagittarii, comes out slightly negative. For Nova Sagittae, No. 2, which is now of about fifteenth magnitude photographically, a parallax of +0″.013 was found; the star has a considerable proper motion for a nova, viz., +0″.078 and −0″.016 in $\alpha$ and $\delta$, respectively.

The present paper contains the results for twenty-five fields, which have recently been measured for parallax. The work has been carried out in the same way as for the previously published series.[1]

All plates were measured with the new stereocomparator. Table I contains the results of these measures; the last column indicates whether the plates were obtained with the 60-inch reflector at the Cassegrain focus (80 ft.) or with the 100-inch at the Newtonian focus (42 ft.).

The necessary data for each field are collected in tables, which are arranged as in the Sixth, Seventh, and Eighth Series. For the thirteen fields taken with the 60-inch the mean probable error of the parallaxes of the central stars is ±0″.0065; for the twelve fields taken with the 100-inch, ±0″.0127. This large error is partly due to the inclusion of N.G.C. 6891, for which the probable error is ±0″.037. The result for this object deserves little weight, as the nebulosity immediately around the central star is quite bright and visible on all of the photographs.

---

[1] *Mt. Wilson Contr.*, Nos. 111, 1916; 136, 1917; 158, 1918; 182, 1920; 204, 1921; 237, 1922; 270, 1923; 290, 1925.

Altogether twenty-eight fields have now been finished at the Newtonian focus of the 100-inch reflector. While this number is not large enough for a discussion of systematic errors, a few remarks may be made about the accuracy that can be attained. The mean probable error for all twenty-eight fields is ±0″.0100. If we exclude N.G.C. 6891 for the reasons given above, and *o* Ceti for the reason that the results may have been vitiated by the close companion discovered by Aitken and Joy, the mean probable error of the twenty-six fields is ±0″.0080. For seven of these fields which have a considerable southern declination, the plates were taken through a color screen in order to avoid distortion of the images by atmospheric refraction. This has the disadvantage that, for the same exposure time, considerably fewer stars per given area are available for com-

TABLE I

| Object | α 1900 | δ 1900 | Vis. Mag. Harvard | Mount Wilson Spectrum | Relative Parallax | $\mu_\alpha$ | P.E. | No. of Exp. | Instrument |
|---|---|---|---|---|---|---|---|---|---|
| Wolf 1056 | 0h33m29s | +30° 4′ | 12.9* | A 5‡ | +0″.077 | +1″.548 | 8 6 | 20 | 100 |
| Wolf 110 | 1 57 21 | + 5 14 | 13.2* | ......... | + .041 | +2.326 | 5 3 | 18 | 100 |
| B.D. +57°566 | 2 18 18 | +57 44 | 7.76 | A 5s | + .001 | +0.030 | 5 3 | 16 | 60 |
| Boss 936 | 3 58 47 | +21 49 | 4.50 | K0 | + .043 | + .070 | 12 11 | 14 | 60 |
| A.G. Berl. B 1366 | 4 8 37 | +22 6 | 8.9† | F0 | − .001 | + .433 | 4 2 | 16 | 60 |
| T Tauri | 4 16 10 | +19 18 | Var. | Ke | − .007 | + .018 | 6 6 | 18 | 100 |
| Boss 1217 | 5 2 10 | + 9 21 | 6.26 | G0 | + .040 | − .004 | 2 1 | 16 | 60 |
| T Monocerotis | 6 19 49 | + 7 8 | Var. | G3p | + .020 | − .008 | 5 2 | 16 | 60 |
| Lal. 15565 | 7 54 21 | +29 31 | 6.94 | G7 | + .061 | − .149 | 4 2 | 18 | 60 |
| N.G.C. 3242 | 10 19 58 | −18 8 | 12.2* | Pe § | + .031 | + .022 | 13 7 | 16 | 100 |
| Boss 3014 | 11 21 42 | + 3 33 | 6.19 | K0 | + .028 | − .720 | 12 5 | 16 | 60 |
| Boss 3015 | 11 21 43 | + 3 33 | 7.9 | K5 | + .070 | − .728 | 13 6 | 12 | 60 |
| Wolf 437 | 12 43 1 | +10 18 | 12.7* | ......... | + .106 | − .986 | 7 5 | 18 | 100 |
| Groom. 1969 | 13 9 18 | +57 12 | 8.6 | G5§ | + .048 | + .041 | 18 12 | 18 | 60 |
| Groom. 1970 | 13 9 31 | +57 14 | 6.74 | G0§ | + .046 | + .128 | 9 6 | 18 | 60 |
| RS Boötis | 14 29 17 | +32 12 | Var. | F3 | − .004 | + .025 | 2 0 | 16 | 60 |
| RU Coronae | 15 31 21 | +26 5 | Var. | ......... | + .001 | − .004 | 12 4 | 18 | 60 |
| Wolf 611 | 15 52 15 | + 5 25 | 16.0* | ......... | + .030 | + .042 | 8 3 | 14 | 100 |
| Wolf 612 | 15 52 17 | + 5 26 | 14.7* | ......... | + .033 | + .053 | 10 4 | 16 | 100 |
| B.D. −12°4523 | 16 24 45 | −12 24 | 9.5† | M5 | + .349 | − .064 | 17 16 | 16 | 100 |
| Lal. 31055 | 16 59 51 | − 4 54 | 7.90 | K5 | + .185 | − .922 | 26 15 | 18 | 100 |
| Strb. 5819 | 17 0 2 | − 4 55 | 9.3† | M3 | + .112 | − .870 | 27 15 | 18 | 100 |
| Y Ophiuchi | 17 47 17 | − 6 7 | Var. | cF9 | − .038 | + .016 | 9 6 | 16 | 100 |
| Boss 4595 | 18 4 54 | + 3 6 | 5.73 | F4 | + .019 | .000 | 2 1 | 14 | 60 |
| Y Sagittarii | 18 15 30 | −18 54 | Var. | G2p | + .012 | − .021 | 10 5 | 16 | 100 |
| Nova Sagittae, No. 2 | 20 3 4 | +17 24 | 15.2* | ......... | + .012 | + .078 | 5 4 | 16 | 100 |
| N.G.C. 6891 | 20 10 24 | +12 24 | 12.1* | Pd§ | + .017 | +0.008 | 37 25 | 16 | 100 |
| Wolf 1106 | 21 5 36 | +59 22 | 13.4* | ......... | + .039 | −1.040 | 3 3 | 16 | 60 |
| β Pegasi | 22 58 56 | +27 32 | Var. | M2 | +0.007 | +0.171 | 13 6 | 16 | 60 |

* These magnitudes are photographic, derived from counts of the number of stars of equal and brighter magnitude, and are based on Table IV of *Gronigen Publications*, No. 27.

† Magnitude from *B.D. Catalogue*.

‡ Spectrum from effective wave-length by Max Wolf.

§ Spectrum from the *Henry Draper Catalogue*.

parison purposes; accordingly, stars at greater distances from the center must be utilized. For these seven fields, N.G.C. 7293, ε Scorpii, Wolf 629, Wolf 922, N.G.C. 3242, B.D.−12°4523, and Y Sagittarii, the mean probable error is ±0″.0096, while for the other fields it is ±0″.0074. That the increase in the probable error is probably due to the fact that stars at greater distances from the center had to be used may be seen from Table II, which gives the mean distance of the comparison stars, the probable error of the parallaxes derived, and the numbers of fields used.

TABLE II

| $r$ | Mean $r$ | P.E. | No. |
|---|---|---|---|
| 2′.3–3′.9 | 3′.1 | ±0″.0070 | 7 |
| 4.0–4.9 | 4.7 | .0060 | 5 |
| 5.0–5.9 | 5.5 | .0080 | 10 |
| 6.0–7.5 | 6.7 | ±0.0122 | 4 |

The following fields require special comment:

*a*) *Wolf 1056, 110, 437, 611, 612, and 1106.*—All these stars have absolute magnitudes fainter than +10. In Table III are given the apparent photographic magnitudes as derived from counts of the numbers of stars of equal and brighter magnitude, together with the absolute magnitudes and proper motions.

TABLE III

| Name | Pg. Mag. | $\pi$ Abs. | $M$ | $\mu$ |
|---|---|---|---|---|
| Wolf 1056.... | 12.9 | +0″.078 | +12.4 | 1″.69 |
| 110.... | 13.2 | .042 | 11.3 | 2.43 |
| 437.... | 12.7 | .107 | 12.8 | 1.03 |
| 611.... | 16.0 | .032 | 13.5 | 1.54 |
| 612.... | 14.7 | .032 | 12.2 | 1.43 |
| 1106.... | 13.4 | +0.040 | +11.4 | 2.14 |

*b*) *B.D.−12°4523.*—This star, for which the *B.D. Catalogue* gives a magnitude of 9.5, was put on the program at the request of Mr. Adams as its spectrum seemed to indicate an extremely faint absolute magnitude. The parallax, +0″.350, gives the absolute magnitude +12.2; the spectroscopic absolute magnitude derived by Adams and Joy is +11.8.

*c) B.D.+57°566.*—The relative parallax is $+0''.001 \pm 0''.005$. This is a close double near the double cluster in Perseus. It is β.G.C. 1241; Burnham gives the magnitudes 8.1 and 10.4, $\Delta = 1''.79$, $p = 186^\circ.5$, with no observed change. I have measured the object for proper motion with the result $\mu_\alpha = +0''.030 \pm 0''.003$; $\mu_\delta = -0''.012 \pm 0''.006$. As its radial velocity is small, the system probably does not belong to the Perseus cluster.

*d) A.G. Berlin B 1366.*—This star has a large proper motion of $0''.54$ annually. Its parallax from several sources is, however, quite small, viz., Dearborn $\pi_{\mathrm{rel.}} = +0''.017$; McCormick, $-0''.016$; vM, $-0''.001$; while the spectroscopic parallax is $+0''.006$. The star accordingly must have a very large velocity at right angles to the line of sight. Its radial velocity, according to Adams and Joy, is 338 km/sec.

TABLE IV

| Name | α 1900 | δ 1900 | Median Mag. | Period | $\pi_{\mathrm{rel.}}$ | $\pi_{\mathrm{Sh.}}$ |
|---|---|---|---|---|---|---|
| SU Cas..... | $2^h43^m.0$ | +68°28′ | 5.9 | $1^d.950$ | $+0''.008$ | 0.0038 |
| RX Aur..... | 4 54.5 | +39 49 | 7.6 | 11.626 | − .001 | .00063 |
| T Mon.... | 6 19.8 | + 7 8 | 6.2 | 27.012 | + .020 | .00066 |
| RT Aur..... | 6 22.1 | +30 34 | 5.3 | 3.728 | + .006 | .0038 |
| RS Boö..... | 14 29.2 | +32 11 | 10.3 | 0.377 | − .004 | .00076 |
| RY Boö..... | 14 45.2 | +23 27 | 7.2 | 9.0 | + .023 | .00091 |
| UU Her..... | 16 32.5 | +38 10 | 9.1 | 45.39 | − .001 | .00010 |
| Y Oph.... | 17 47.3 | − 6 7 | 6.3 | 17.121 | − .038 | .00087 |
| Y Sag..... | 18 15.5 | −18 54 | 5.8 | 5.773 | + .012 | .0024 |
| RR Lyr..... | 19 22.3 | +42 36 | 7.25 | 0.567 | + .006 | .0030 |
| δ Cep..... | 22 25.4 | +57 54 | 4.14 | 5.366 | −0.002 | 0.0054 |

*e) T Tauri.*—The relative parallax is $-0''.007 \pm 0''.006$. This is the variable star connected with Hind's variable nebula. The magnitude changes irregularly from 9.3 to 13.5.

*f) T Monocerotis, RS Boötis, Y Ophiuchi, and Y Sagittarii.*—The mean parallax of these four Cepheids is practically zero. Altogether I have now derived parallaxes for eleven Cepheids. The results are collected in Table IV.

The mean relative parallax is $+0''.0026$, while Shapley's mean parallax is $+0''.0020$. Accepting Shapley's parallaxes as the true values, and $0''.0015$ as the corrections needed to convert my relative parallaxes into absolute values, this would indicate a correction to the Mount Wilson parallaxes of $-0''.0021$, in good agreement with the results derived in *Contribution* No. 237.

*g) Nova Sagittae*, No. 2.—The relative parallax is $+0''.0012 \pm 0''.005$. This nova reached its maximum magnitude, 7.2, on November 22, 1913. A remarkable feature is its proper motion, which is considerable for this class of objects, viz.,

$$\mu_\alpha = +0''.078 \pm 0''.004 ; \qquad \mu_\delta = -0''.016 \pm 0''.004 ; \qquad \mu = 0''.080 \ .$$

Accepting $+0''.013$ as the parallax, we find the absolute magnitude to have been $+2.8$ at maximum, while it is now $+10.8$; the tangential velocity would be 29 km/sec.

I wish to express my acknowledgment to Messrs. T. A. Nelson, A. N. Beebe, and Kenneth Pitt for their valuable aid in securing the plates, and to Mrs. Marsh, of the Computing Division, who has performed a large share of the necessary computations.

**Wolf 1056** $\alpha = 0^h 33^m 29^s$ $\delta = +30°4'$

| Mor. | Ev. | $t_1$ | $t_2$ | $\Delta_p$ | $M$ | $v$ |
|---|---|---|---|---|---|---|
| 10.654 | 8.854 | −12°.7 | −14°.2 | +1.07 | +572 | −14 |
| 10.654 | 8.849 | −11.5 | −12.2 | 1.04 | +597 | +12 |
| 7.635 | 8.854 | − 9.2 | −11.0 | 1.16 | −364 | + 4 |
| 7.635 | 8.849 | − 8.0 | −10.0 | 1.13 | −361 | + 3 |
| 10.652 | 9.901 | − 0.7 | − 4.5 | 1.28 | +258 | + 1 |
| 10.652 | 9.901 | + 0.5 | − 2.5 | 1.28 | +259 | + 2 |
| 7.638 | 6.920 | + 2.2 | + 5.0 | 1.40 | +262 | +12 |
| 7.638 | 9.972 | + 3.7 | + 7.2 | 1.51 | −716 | − 4 |
| 9.666 | 6.920 | + 9.7 | + 7.5 | 1.27 | +884 | − 5 |
| 9.667 | 9.972 | +12.7 | + 8.7 | +1.38 | − 85 | −12 |

$$+24.15\,\mu_\alpha + 3.50\,\pi = +7688$$
$$+3.50\,\mu_\alpha + 15.88\,\pi = +1357$$
$$\pi = +15.8 = 0''.077 \pm 0''.008$$
$$\mu_\alpha = +316.0 = 1''.548 \pm 0''.006$$

| No. | Br. | $x$ | $y$ | $\pi$ |
|---|---|---|---|---|
| 1..... | f | −3′.2 | +4′.3 | −0″.011 |
| 2..... | bf | −2.4 | +0.8 | + .014 |
| 3..... | ff | −1.7 | −5.2 | − .012 |
| 4..... | f | +0.2 | −1.8 | + .009 |
| 5..... | ff | +1.6 | −2.4 | + .010 |
| 6..... | f | +3.1 | +0.4 | − .009 |
| 7..... | bf | +0.6 | +2.3 | .000 |
| 8..... | f | +0.4 | +1.2 | +0.004 |

**Wolf 110** $\alpha=1^h57^m21^s$ $\delta=+5°14'$

| Mor. | Ev. | $t_1$ | $t_2$ | $\Delta_p$ | $M$ | $v$ |
|---|---|---|---|---|---|---|
| 7.636 | 9.972 | −15°.7 | − 7°.5 | +1.64 | −1088 | + 9 |
| 7.636 | 9.972 | −13.7 | − 6.0 | 1.64 | −1091 | + 6 |
| 7.638 | 9.018 | −10.7 | − 4.5 | 1.74 | − 645 | − 5 |
| 7.709 | 9.015 | − 5.0 | − 4.0 | 1.48 | − 610 | 0 |
| 7.709 | 9.018 | − 2.7 | − 3.0 | 1.48 | − 621 | −11 |
| 10.655 | 9.015 | + 2.5 | − 1.5 | 1.69 | + 787 | − 5 |
| 10.655 | 9.901 | + 3.7 | + 7.2 | 1.28 | + 368 | + 1 |
| 10.652 | 6.914 | + 4.2 | +14.0 | 1.36 | +1790 | + 4 |
| 10.652 | 6.914 | + 6.2 | +15.7 | +1.36 | +1790 | + 4 |

$+47.53\,\mu_a-\phantom{0}0.09\,\pi=+22559$

$-\phantom{0}0.09\,\mu_a+20.97\,\pi=+\phantom{22}134$

$\pi=+\phantom{47}8.4=+0''.041\pm0''.005$

$\mu_a=+474.6=+2''.326\pm0''.003$

| No. | Br. | $x$ | $y$ | $\pi$ |
|---|---|---|---|---|
| 1..... | f | −2′.0 | +5′.2 | +0″.003 |
| 2..... | bf | −3.4 | +3.0 | − .003 |
| 3..... | f | −7.8 | −0.8 | + .004 |
| 4..... | f | −1.4 | −5.7 | + .003 |
| 5..... | bf | +2.2 | −3.2 | − .011 |
| 6..... | bf | +6.4 | 0.0 | + .011 |
| 7..... | f | +5.3 | +2.9 | −0.005 |

**B.D.+57°566=β.G.C. 1241** $\alpha=2^h18^m18^s$ $\delta=+57°44'$

| Mor. | Ev. | $t_1$ | $t_2$ | $\Delta_p$ | $M$ | $v$ |
|---|---|---|---|---|---|---|
| 10.649 | 8.931 | −11°.0 | −11°.0 | +1.42 | +13 | − 7 |
| 10.649 | 8.928 | − 4.2 | + 0.7 | 1.40 | +17 | − 3 |
| 6.663 | 8.032 | − 4.5 | + 4.0 | 1.72 | −36 | −21 |
| 10.704 | 8.934 | − 3.2 | + 5.0 | 1.24 | +40 | +19 |
| 6.660 | 8.928 | + 1.2 | + 6.5 | 1.37 | −21 | + 6 |
| 10.704 | 8.032 | + 1.5 | + 8.0 | 1.58 | +36 | + 4 |
| 6.660 | 8.934 | + 5.5 | +12.0 | 1.40 | −30 | − 3 |
| 6.666 | 11.032 | + 7.5 | +11.5 | +1.72 | −39 | +11 |

$+47.46\,\mu_a-\phantom{0}4.91\,\pi=+553$

$-\phantom{0}4.91\,\mu_a+17.78\,\pi=-\phantom{0}51$

$\pi=+\phantom{0}0.3=+0''.001\pm0''.005$

$\mu_a=+11.7=+0''.030\pm0''.003$

| No. | Br. | $x$ | $y$ | $\pi$ |
|---|---|---|---|---|
| 1..... | f | +0′.3 | +1′.8 | +0″.014 |
| 2..... | bf | +0.5 | +3.2 | − .008 |
| 3..... | f | +4.4 | +2.6 | + .001 |
| 4..... | ff | +3.6 | +1.8 | − .007 |
| 5..... | f | +0.4 | −3.4 | + .001 |
| 6..... | bf | −2.7 | −4.7 | .000 |
| 7..... | bf | −4.1 | −3.0 | − .005 |
| 8..... | f | −1.9 | +0.7 | +0.004 |

**Boss 936** $\alpha=3^h58^m47^s$ $\delta=+21°49'$

| Mor. | Ev. | $t_1$ | $t_2$ | $\Delta_p$ | $M$ | $v$ |
|---|---|---|---|---|---|---|
| 7.791 | 10.057 | −16°.5 | − 3°.0 | +1.45 | − 7 | +31 |
| 7.786 | 9.086 | − 8.0 | + 0.7 | 1.55 | −42 | −33 |
| 10.794 | 10.059 | − 3.2 | + 1.5 | 1.44 | +31 | −14 |
| 7.786 | 10.057 | − 3.0 | + 4.0 | 1.47 | −41 | − 3 |
| 10.794 | 9.086 | + 1.0 | + 5.0 | 1.51 | +79 | + 6 |
| 10.792 | 10.059 | + 2.5 | + 8.2 | 1.46 | +34 | −11 |
| 10.792 | 9.986 | + 9.5 | +12.5 | +1.14 | +75 | +33 |

| No. | Br. | $x$ | $y$ | $\pi$ |
|---|---|---|---|---|
| 1..... | f | +1′.9 | +2′.9 | −0″.013 |
| 2..... | f | +4.3 | +2.5 | − .009 |
| 3..... | bf | +3.8 | −7.8 | + .007 |
| 4..... | f | −0.4 | −5.5 | + .004 |
| 5..... | bf | −2.1 | −3.3 | + .004 |
| 6..... | f | −6.6 | +2.9 | − .012 |
| 7..... | b | −1.5 | +8.2 | +0.021 |

$$+16.65\,\mu_a-\ 3.01\,\pi=+408$$
$$-\ 3.01\,\mu_a+14.44\,\pi=+165$$
$$\pi=+17.2=+0''.043\pm0''.012$$
$$\mu_a=+27.6=+0''.070\pm0''.011$$

**A.G. Berlin B 1366** $\alpha=4^h8^m37^s$ $\delta=+22°6'$

| Mor. | Ev. | $t_1$ | $t_2$ | $\Delta_p$ | $M$ | $v$ |
|---|---|---|---|---|---|---|
| 9.811 | 11.032 | − 9°.7 | −6°.7 | +1.26 | −210 | 0 |
| 6.737 | 11.032 | − 6.2 | −1.7 | 1.57 | −727 | +11 |
| 7.789 | 11.111 | − 5.7 | −1.0 | 1.61 | −569 | + 1 |
| 10.707 | 5.122 | − 5.7 | +2.5 | 1.90 | +946 | − 9 |
| 6.737 | 5.125 | − 2.0 | +3.7 | 1.82 | +265 | −10 |
| 10.707 | 11.111 | − 1.7 | +6.0 | 1.88 | − 77 | − 7 |
| 10.794 | 5.122 | + 6.2 | +6.7 | 1.60 | +984 | +13 |
| 10.794 | 5.125 | +11.7 | +8.5 | +1.60 | +979 | + 8 |

| No. | Br. | $x$ | $y$ | $\pi$ |
|---|---|---|---|---|
| 1..... | f | +3′.8 | +5′.4 | −0″.012 |
| 2..... | f | +9.2 | +1.6 | + .006 |
| 3..... | f | +0.3 | −9.6 | − .011 |
| 4..... | ff | −1.2 | −1.1 | + .023 |
| 5..... | f | −6.7 | −0.4 | + .006 |
| 6..... | bf | −5.2 | +3.0 | − .009 |
| 7..... | f | −1.6 | +1.6 | −0.003 |

$$+129.19\,\mu_a+17.28\,\pi=+22138$$
$$+\ 17.28\,\mu_a+22.21\,\pi=+\ 2952$$
$$\pi=-\ \ 0.4=-0''.001\pm0''.004$$
$$\mu_a=+171.4=+0''.433\pm0''.002$$

**T Tauri** $\alpha=4^h16^m10^s$ $\delta=+19°18'$

| Mor. | Ev. | $t_1$ | $t_2$ | $\Delta_p$ | $M$ | $v$ |
|---|---|---|---|---|---|---|
| 7.715 | 9.097 | − 3°.0 | + 2°.2 | +1.84 | −11 | − 3 |
| 6.833 | 9.092 | − 1.7 | + 4.5 | 1.36 | + 1 | +11 |
| 7.715 | 9.018 | + 1.5 | + 3.7 | 1.55 | −18 | −11 |
| 7.800 | 8.043 | + 4.0 | + 5.0 | 1.37 | − 8 | − 5 |
| 8.772 | 7.065 | + 3.5 | + 7.5 | 1.58 | +13 | + 9 |
| 9.741 | 9.018 | +11.5 | +10.7 | 1.49 | − 2 | − 3 |
| 9.743 | 8.043 | +10.5 | +11.0 | 1.59 | − 1 | − 5 |
| 7.797 | 7.065 | +10.7 | +11.2 | 1.47 | + 5 | + 4 |
| 7.797 | 9.092 | +15.0 | +11.5 | +1.55 | − 4 | + 3 |

$$+17.31\,\mu_a - 2.43\,\pi = +66$$
$$-2.43\,\mu_a + 21.33\,\pi = -41$$
$$\pi = -1.5 = -0''.007 \pm 0''.006$$
$$\mu_a = +3.6 = +0''.018 \pm 0''.006$$

| No. | Br. | $x$ | $y$ | $\pi$ |
|---|---|---|---|---|
| 1..... | bf | +2′.2 | +2′.4 | −0″.003 |
| 2..... | bf | +3.2 | +5.4 | .000 |
| 3..... | bf | +5.2 | −7.2 | + .010 |
| 4..... | f | +2.6 | −3.1 | − .002 |
| 5..... | bf | −3.2 | −3.2 | − .015 |
| 6..... | bf | −7.7 | +1.4 | + .012 |
| 7..... | bf | −2.5 | +4.3 | 0.000 |

**Boss 1217** $\alpha=5^h2^m10^s$ $\delta=+9°21'$

| Mor. | Ev. | $t_1$ | $t_2$ | $\Delta_p$ | $M$ | $v$ |
|---|---|---|---|---|---|---|
| 7.789 | 9.084 | −13°.0 | −12°.0 | +1.60 | +17 | −10 |
| 5.844 | 9.084 | −10.2 | − 7.7 | 1.35 | 26 | 0 |
| 7.789 | 9.087 | − 8.7 | − 5.2 | 1.62 | 35 | + 7 |
| 5.844 | 9.087 | − 5.2 | − 1.0 | 1.36 | 29 | + 2 |
| 7.792 | 5.119 | − 4.0 | + 3.2 | 1.71 | 19 | − 4 |
| 7.792 | 5.119 | + 0.2 | + 7.2 | 1.71 | 23 | 0 |
| 5.770 | 5.043 | + 1.5 | +10.0 | 1.48 | 25 | + 2 |
| 9.806 | 5.043 | + 4.2 | +15.5 | +1.35 | +19 | + 5 |

$$+61.83\,\mu_a + 3.68\,\pi = -26$$
$$+3.68\,\mu_a + 18.70\,\pi = +292$$
$$\pi = +15.9 = +0''.040 \pm 0''.002$$
$$\mu_a = -1.4 = -0''.004 \pm 0''.001$$

| No. | Br. | $x$ | $y$ | $\pi$ |
|---|---|---|---|---|
| 1..... | f | +0′.4 | +5′.9 | +0″.010 |
| 2..... | bf | +1.4 | +5.2 | − .005 |
| 3..... | f | +6.3 | −3.2 | − .007 |
| 4..... | bf | +1.9 | −7.1 | + .010 |
| 5..... | f | +0.8 | −4.9 | − .001 |
| 6..... | f | −2.2 | +0.4 | − .011 |
| 7..... | f | −4.3 | +1.2 | − .003 |
| 8..... | bf | −3.0 | +5.4 | +0.006 |

**T Monocerotis** $\alpha=6^h19^m49^s$ $\delta=+7°8'$

| Mor. | Ev. | $t_1$ | $t_2$ | $\Delta_p$ | $M$ | $v$ |
|---|---|---|---|---|---|---|
| 4.882 | 5.125 | −9°.0 | −7°.7 | +1.39 | +18 | + 6 |
| 4.805 | 9.087 | −8.5 | −3.5 | 1.51 | +38 | +12 |
| 9.806 | 5.125 | −7.7 | −3.2 | 1.68 | + 6 | + 8 |
| 4.882 | 9.087 | −4.7 | +0.7 | 1.22 | +10 | −14 |
| 4.805 | 5.117 | −4.5 | +2.7 | 1.65 | + 9 | − 5 |
| 9.806 | 5.114 | −2.2 | +3.0 | 1.63 | −18 | −16 |
| 9.811 | 5.117 | +2.5 | +7.0 | 1.63 | − 2 | 0 |
| 9.812 | 5.114 | +6.5 | +8.5 | +1.62 | + 2 | + 5 |

$$+124.11\,\mu_a+18.33\,\pi=-268$$
$$+\;18.33\,\mu_a+19.15\,\pi=+\;90$$
$$\pi=+7.9=+0''.020\pm0''.005$$
$$\mu_a=-3.3=-0''.008\pm0''.002$$

| No. | Br. | $x$ | $y$ | $\pi$ |
|---|---|---|---|---|
| 1..... | f | +0'.4 | +1'.1 | +0''.002 |
| 2..... | f | +1.2 | +1.2 | + .005 |
| 3..... | f | +3.3 | +1.1 | + .003 |
| 4..... | f | +3.6 | −2.2 | − .009 |
| 5..... | f | −1.9 | −1.2 | + .005 |
| 6..... | f | −3.2 | −2.1 | + .004 |
| 7..... | f | −3.3 | +0.4 | − .002 |
| 8..... | f | −2.7 | +2.1 | −0.009 |

**Lalande 15565** $\alpha=7^h54^m21^s$ $\delta=+29°31'$

| Mor. | Ev. | $t_1$ | $t_2$ | $\Delta_p$ | $M$ | $v$ |
|---|---|---|---|---|---|---|
| 4.964 | 9.163 | −14°.0 | −14°.2 | +1.16 | +273 | − 3 |
| 4.964 | 9.163 | −10.0 | − 7.2 | 1.16 | +264 | −12 |
| 9.904 | 7.232 | − 5.0 | − 5.0 | 1.68 | −107 | +10 |
| 4.959 | 7.229 | + 0.5 | − 3.0 | 1.43 | +175 | + 6 |
| 9.904 | 8.232 | + 0.7 | − 0.5 | 1.67 | − 45 | +14 |
| 10.879 | 8.229 | + 2.5 | + 0.7 | 1.76 | −116 | − 3 |
| 9.907 | 7.232 | + 7.0 | + 1.0 | 1.66 | −135 | −17 |
| 5.926 | 8.229 | + 7.7 | + 5.0 | 1.58 | +182 | + 8 |
| 10.880 | 6.276 | + 9.0 | +12.5 | +1.84 | −232 | − 6 |

$$+91.00\,\mu_a+\;8.23\,\pi=-5169$$
$$+\;8.23\,\mu_a+22.10\,\pi=+\;\;51$$
$$\pi=+24.2=+0''.061\pm0''.004$$
$$\mu_a=-59.0=-0''.149\pm0''.002$$

| No. | Br. | $x$ | $y$ | $\pi$ |
|---|---|---|---|---|
| 1..... | bb | +0'.4 | +4'.7 | 0''.000 |
| 2..... | f | +2.2 | +2.5 | + .002 |
| 3..... | bf | +1.9 | +1.0 | + .001 |
| 4..... | f | +5.6 | −4.7 | − .002 |
| 5..... | bf | 0.0 | −5.1 | − .002 |
| 6..... | f | −3.8 | −1.9 | + .006 |
| 7..... | f | −7.0 | −0.8 | − .005 |
| 8..... | f | −1.2 | +4.3 | −0.003 |

**N.G.C. 3242** $\alpha=10^h19^m58^s$ $\delta=-18°8'$

| Mor. | Ev. | $t_1$ | $t_2$ | $\Delta_p$ | $M$ | $v$ |
|---|---|---|---|---|---|---|
| 7.063 | 7.311 | −9°2 | −8°5 | +1.28 | +30 | +23 |
| 11.033 | 7.311 | −8.5 | −3.7 | 1.40 | +44 | +19 |
| 7.066 | 9.327 | −6.7 | −0.2 | 1.31 | −12 | −10 |
| 7.068 | 9.330 | −6.7 | −0.5 | 1.30 | −5 | −3 |
| 7.063 | 9.335 | −5.5 | +1.7 | 1.34 | −3 | −2 |
| 11.033 | 7.309 | −2.7 | +4.5 | 1.39 | +9 | −16 |
| 11.030 | 9.332 | +4.2 | +4.7 | 1.49 | +18 | +2 |
| 11.030 | 7.309 | +11.2 | +9.0 | +1.43 | +15 | −10 |

$$+59.84\,\mu_a+\ 8.97\,\pi=+321$$
$$+\ 8.97\,\mu_a+15.00\,\pi=+135$$
$$\pi=+6.4=+0''.031\pm0''.013$$
$$\mu_a=+4.4=+0''.022\pm0''.007$$

| No. | Br. | $x$ | $y$ | $\pi$ |
|---|---|---|---|---|
| 1..... | bf | −2′.1 | +6′.2 | +0″.001 |
| 2..... | b | −4.2 | +4.3 | − .004 |
| 3..... | b | −4.7 | +3.8 | − .005 |
| 4..... | f | −3.4 | −8.0 | + .018 |
| 5..... | bf | −0.2 | −8.2 | + .028 |
| 6..... | f | +0.3 | −2.6 | − .011 |
| 7..... | b | +4.6 | −2.0 | − .061 |
| 8..... | bf | +8.3 | +6.4 | +0.041 |

**Boss 3014** $\alpha=11^h21^m42^s$ $\delta=+3°33'$
3015 11 21 43 +3 33

| Mor. | Ev. | $t_1$ | $t_2$ | $\Delta_p$ | $M$(3014) | $M$(3015) | $v$ (3014) | $v$ (3015) |
|---|---|---|---|---|---|---|---|---|
| 3.992 | 7.317 | −8°5 | −9°0 | +1.52 | +1013 | +985 | +49 | −15 |
| 3.992 | 7.312 | −4.0 | −2.5 | 1.50 | +958 | +1029 | −5 | +29 |
| 4.066 | 7.317 | 0.0 | −3.0 | 1.31 | +906 | ........ | −35 | ........ |
| 9.087 | 8.355 | +2.5 | −1.0 | 1.36 | −199 | −187 | −6 | −14 |
| 4.066 | 8.353 | +4.2 | +0.5 | 1.44 | +1237 | ........ | −3 | ........ |
| 10.058 | 6.333 | +7.0 | +4.0 | 1.41 | −1022 | −1007 | +23 | +27 |
| 9.087 | 8.353 | +8.2 | +4.7 | 1.35 | −211 | −200 | −18 | −26 |
| 10.058 | 6.333 | +13.7 | +11.5 | +1.41 | −1059 | −1039 | −14 | −5 |

$$\left.\begin{aligned}+79.74\,\mu_a-\ 7.99\,\pi&=-22835\\-\ 7.99\,\mu_a+16.00\,\pi&=+\ 2455\end{aligned}\right\}3014$$

$$\left.\begin{aligned}+50.78\,\mu_a+\ 2.45\,\pi&=-14580\\+\ 2.45\,\mu_a+12.21\,\pi&=-\ 368\end{aligned}\right\}3015$$

$$\left.\begin{aligned}\pi&=+\ 11.0=+0''.028\pm0''.012\\\mu_a&=-285.3=-0''.720\pm0''.005\end{aligned}\right\}3014$$

$$\left.\begin{aligned}\pi&=+\ 27.7=+0''.070\pm0''.013\\\mu_a&=-288.5=-0''.728\pm0''.006\end{aligned}\right\}3015$$

| No. | Br. | $x$ | $y$ | $\pi$ |
|---|---|---|---|---|
| 1..... | f | +4′.1 | +0′.5 | −0″.013 |
| 2..... | ff | +2.9 | −0.4 | + .016 |
| 3..... | b | −1.8 | −3.0 | − .004 |
| 4..... | f | −5.9 | +2.1 | 0.000 |

On 4.066–7.317 and 4.066–8.353
Boss 3015 was not measured.

### Wolf 437 $\alpha = 12^h43^m1^s$ $\delta = +10°18'$

| Mor. | Ev. | $t_1$ | $t_2$ | $\Delta_p$ | $M$ | $v$ |
|---|---|---|---|---|---|---|
| 9.095 | 8.391 | −12°.5 | − 8°.2 | +1.47 | −104 | + 5 |
| 10.066 | 8.391 | − 0.5 | − 6.2 | 1.55 | −303 | + 1 |
| 10.066 | 11.361 | + 1.0 | − 2.2 | 1.43 | +293 | 0 |
| 9.098 | 11.361 | + 1.2 | − 0.2 | 1.34 | +498 | +14 |
| 9.098 | 11.358 | + 4.2 | + 1.0 | 1.32 | +472 | − 9 |
| 7.063 | 7.396 | + 5.2 | + 7.0 | 1.58 | + 98 | − 2 |
| 7.063 | 7.396 | + 6.7 | + 8.5 | 1.58 | + 95 | − 5 |
| 10.153 | 7.394 | +13.0 | +14.0 | 1.25 | −538 | − 9 |
| 10.153 | 7.394 | +15.2 | +15.2 | +1.25 | −520 | + 9 |

$$+30.68\,\mu_a + 1.62\,\pi = -6138$$
$$+1.62\,\mu_a + 18.26\,\pi = +69$$
$$\pi = +21.6 = +0''.106 \pm 0''.007$$
$$\mu_a = -201.2 = -0''.986 \pm 0''.005$$

| No. | Br. | $x$ | $y$ | $\pi$ |
|---|---|---|---|---|
| 1..... | f | −3′.8 | +8′.1 | +0″.009 |
| 2..... | f | −2.5 | +1.3 | − .006 |
| 3..... | bf | +2.8 | −7.4 | + .001 |
| 4..... | bf | +1.2 | −4.7 | + .001 |
| 5..... | bf | +2.6 | −3.5 | + .007 |
| 6..... | bf | +0.3 | +2.4 | − .020 |
| 7..... | bf | +2.2 | +5.6 | +0.004 |

### Groombridge 1970 = β.G.C. 6432 $\alpha = 13^h9^m31^s$ $\delta = +57°14'$

| Mor. | Ev. | $t_1$ | $t_2$ | $\Delta_p$ | $M$ | $v$ |
|---|---|---|---|---|---|---|
| 9.087 | 11.364 | −11°.0 | −5°.2 | +1.35 | − 81 | + 9 |
| 9.161 | 10.399 | − 8.2 | −1.2 | 1.26 | − 44 | − 4 |
| 11.191 | 8.355 | − 7.5 | −0.7 | 0.91 | +164 | + 3 |
| 9.087 | 11.364 | − 5.7 | −1.0 | 1.35 | − 93 | − 3 |
| 10.058 | 11.366 | − 4.0 | +1.2 | 1.41 | − 55 | −15 |
| 9.161 | 8.435 | − 3.7 | +2.5 | 1.39 | + 45 | −17 |
| 11.186 | 8.440 | 0 | +4.0 | 1.28 | +192 | +30 |
| 10.058 | 10.399 | + 3.0 | +4.2 | 1.56 | + 33 | +22 |
| 11.186 | 8.435 | + 6.5 | +6.7 | +1.26 | +133 | −29 |

$$+37.50\,\mu_a + 0.47\,\pi = +1905$$
$$+0.47\,\mu_a + 15.64\,\pi = +309$$
$$\pi = +18.2 = +0''.046 \pm 0''.009$$
$$\mu_a = +50.6 = +0''.128 \pm 0''.006$$

For Groombridge 1969 the following values were derived:

$$\pi = +19.1 = +0''.048 \pm 0''.018$$
$$\mu_a = +16.2 = +0''.041 \pm 0''.012$$

| No. | Br. | $x$ | $y$ | $\pi$ |
|---|---|---|---|---|
| 1..... | bf | + 4′.9 | + 8′.2 | 0″.000 |
| 2..... | f | + 5.6 | + 3.4 | − .020 |
| 3..... | b | +12.7 | − 2.1 | + .018 |
| 4..... | bf | + 3.8 | −10.0 | − .007 |
| 5..... | bf | − 2.1 | − 2.1 | + .018 |
| 6..... | f | −10.4 | − 3.2 | + .006 |
| 7..... | bf | −12.6 | + 1.8 | − .007 |
| 8..... | f | − 3.8 | + 5.2 | +0.021 |

### RS Boötis $\alpha = 14^h 29^m 17^s$ $\delta = +32°12'$

| Mor. | Ev. | $t_1$ | $t_2$ | $\Delta_p$ | $M$ | $v$ |
|---|---|---|---|---|---|---|
| 4.233 | 3.421 | −15°0 | −13°5 | +1.06 | + 8 | +2 |
| 11.191 | 3.424 | − 6.5 | −12.7 | 1.24 | +73 | −3 |
| 4.230 | 3.421 | − 4.7 | − 9.2 | 1.07 | +12 | +6 |
| 4.230 | 3.424 | 0.0 | − 8.5 | 1.08 | +11 | +5 |
| 5.199 | 9.505 | 0.0 | + 8.2 | 1.54 | −44 | +2 |
| 5.199 | 9.502 | + 4.5 | + 9.0 | 1.53 | −49 | −3 |
| 9.248 | 9.507 | + 9.2 | +10.0 | 1.32 | − 6 | −1 |
| 9.249 | 9.505 | +16.2 | +13.5 | +1.32 | − 9 | −4 |

$$+99.56\,\mu_\alpha - 1.67\,\pi = +997$$
$$-1.67\,\mu_\alpha + 13.16\,\pi = -39$$
$$\pi = -1.7 = -0''.004 \pm 0''.002$$
$$\mu_\alpha = +10.0 = +0''.025 \pm 0''.000$$

| No. | Br. | $x$ | $y$ | $\pi$ |
|---|---|---|---|---|
| 1..... | f | +0'.3 | +5'.1 | +0''.017 |
| 2..... | f | +6.9 | −0.8 | + .002 |
| 3..... | f | +9.9 | −0.5 | − .010 |
| 4..... | ff | +0.3 | −6.7 | + .002 |
| 5..... | bf | −1.5 | −8.0 | + .004 |
| 6..... | f | −4.9 | −3.2 | − .005 |
| 7..... | bf | −6.3 | +4.1 | − .002 |
| 8..... | f | −4.7 | +4.7 | − .010 |
| 9..... | f | −0.4 | +5.1 | +0.002 |

### RU Coronae $\alpha = 15^h 31^m 21^s$ $\delta = +26°5'$

| Mor. | Ev. | $t_1$ | $t_2$ | $\Delta_p$ | $M$ | $v$ |
|---|---|---|---|---|---|---|
| 6.276 | 7.465 | −14°5 | − 6°0 | +1.07 | − 8 | −10 |
| 5.284 | 7.465 | −14.0 | − 0.5 | 1.04 | + 9 | + 6 |
| 5.284 | 6.498 | −10.0 | + 2.5 | 1.20 | −24 | −26 |
| 6.276 | 7.462 | − 9.2 | + 4.5 | 1.06 | + 6 | + 4 |
| 11.192 | 6.498 | + 0.7 | + 7.0 | 1.55 | −11 | − 3 |
| 11.192 | 4.468 | + 6.0 | + 7.2 | 1.40 | − 1 | +10 |
| 11.293 | 7.462 | + 8.2 | + 8.7 | 0.98 | +15 | +21 |
| 9.249 | 7.471 | + 8.5 | +10.2 | 1.23 | +26 | +29 |
| 11.293 | 4.468 | +13.5 | +11.7 | +1.00 | −40 | −29 |

$$+140.56\,\mu_\alpha + 23.19\,\pi = -217$$
$$+23.19\,\mu_\alpha + 12.61\,\pi = -34$$
$$\pi = +0.2 = +0''.001 \pm 0''.012$$
$$\mu_\alpha = -1.6 = -0''.004 \pm 0''.004$$

| No. | Br. | $x$ | $y$ | $\pi$ |
|---|---|---|---|---|
| 1..... | bf | +4'.1 | +2'.7 | −0''.001 |
| 2..... | f | +7.4 | −1.4 | − .020 |
| 3..... | f | +5.2 | −2.5 | + .011 |
| 4..... | f | +3.0 | −1.1 | + .019 |
| 5..... | f | −1.9 | −1.9 | .000 |
| 6..... | bf | −6.0 | −3.0 | − .006 |
| 7..... | f | −3.2 | −1.0 | + .001 |
| 8..... | ff | −5.2 | +1.9 | − .001 |
| 9..... | bf | −4.3 | +5.4 | −0.001 |

**Wolf 611** $\alpha=15^h52^m15^s$ $\delta=+5°25'$
**612** 15 52 17 +5 26

| Mor. | Ev. | $t_1$ | $t_2$ | $\Delta_p$ | $M$(611) | $M$(612) | $v$ (611) | $v$ (612) |
|---|---|---|---|---|---|---|---|---|
| 10.154 | 11.522 | −11°7 | − 4°0 | +1.67 | − 7 | − 6 | − 5 | − 2 |
| 8.287 | 11.525 | − 5.0 | − 2.5 | 1.31 | −11 | −19 | + 9 | + 7 |
| 9.257 | 11.528 | − 3.5 | + 1.5 | 1.46 | −17 | −16 | − 7 | − 1 |
| 11.290 | 7.473 | + 4.2 | + 1.7 | 1.05 | +43 | +36 | + 4 | −12 |
| 9.257 | 11.522 | + 4.0 | + 6.0 | 1.44 | −14 | −21 | − 4 | − 7 |
| 11.288 | 7.473 | + 6.0 | + 6.2 | 1.06 | +26 | +56 | −13 | + 8 |
| 11.290 | 6.501 | + 8.2 | +13.7 | 1.19 | +54 | +48 | + 6 | −12 |
| 11.288 | 6.583 | +10.0 | +17.0 | +1.49 | ........ | +78 | ........ | +17 |

$$\left.\begin{aligned}+74.76\,\mu_a+\ 0.67\,\pi&=+639\\+\ 0.67\,\mu_a+12.35\,\pi&=+\ 82\end{aligned}\right\}611$$

$$\left.\begin{aligned}+96.85\,\mu_a+\ 7.67\,\pi&=+1102\\+\ 7.67\,\mu_a+14.57\,\pi&=+\ 182\end{aligned}\right\}612$$

$$\left.\begin{aligned}\pi&=+6.2=+0''\!.030\pm0''\!.008\\\mu_a&=+8.5=+0''\!.042\pm0''\!.003\end{aligned}\right\}611$$

$$\left.\begin{aligned}\pi&=+\ 6.8=+0''\!.033\pm0''\!.010\\\mu_a&=+10.8=+0''\!.053\pm0''\!.004\end{aligned}\right\}612$$

| No. | Br. | $x$ | $y$ | $\pi$ |
|---|---|---|---|---|
| 1..... | f | −3'.0 | +3'.2 | 0".000 |
| 2..... | f | −2.7 | −1.0 | − .011 |
| 3..... | f | −4.2 | −1.9 | + .010 |
| 4..... | f | +1.7 | −1.5 | − .011 |
| 5..... | bf | +4.9 | −2.3 | + .007 |
| 6..... | bf | +1.9 | +0.3 | + .002 |
| 7..... | f | +1.2 | +2.6 | +0.002 |

**B.D.−12°4523** $\alpha=16^h24^m45^s$ $\delta=-12°24'$

| Mor. | Ev. | $t_1$ | $t_2$ | $\Delta_p$ | $M$ | $v$ |
|---|---|---|---|---|---|---|
| 10.315 | 8.533 | − 8°7 | −6°2 | +1.23 | + 78 | +13 |
| 7.309 | 8.533 | − 7.7 | −2.7 | 1.26 | 137 | +31 |
| 10.315 | 8.528 | − 5.5 | −2.5 | 1.20 | 49 | −13 |
| 7.309 | 8.528 | − 4.0 | +1.0 | 1.23 | 92 | −12 |
| 10.320 | 9.513 | 0.0 | +1.5 | 1.11 | 55 | −13 |
| 10.320 | 11.528 | + 3.5 | +1.7 | 1.18 | 84 | −16 |
| 11.290 | 11.528 | +10.5 | +4.7 | 1.33 | 96 | − 2 |
| 11.290 | 9.513 | +13.7 | +4.7 | +1.26 | + 74 | + 7 |

$$+14.70\,\mu_a+\ 2.69\,\pi=\ 0$$
$$+\ 2.69\,\mu_a+12.03\,\pi=822$$
$$\pi=+71.2=+0''\!.349\pm0''\!.017$$
$$\mu_a=-13.0=-0''\!.064\pm0''\!.016$$

| No. | Br. | $x$ | $y$ | $\pi$ |
|---|---|---|---|---|
| 1..... | f | −2'.1 | +2'.7 | −0".024 |
| 2..... | f | −4.3 | +3.7 | + .010 |
| 3..... | f | −6.3 | −4.5 | − .004 |
| 4..... | f | −4.2 | −6.1 | + .008 |
| 5..... | bf | +3.9 | −3.6 | + .012 |
| 6..... | bf | +5.6 | −3.2 | − .008 |
| 7..... | bf | +5.9 | +5.3 | .000 |
| 8..... | f | +0.4 | +5.5 | +0.009 |

### Lalande 31055 $\alpha = 16^h 59^m 51^s$ $\delta = -4^\circ 54'$

| Mor. | Ev. | $t_1$ | $t_2$ | $\Delta_p$ | $M$ | $v$ |
|---|---|---|---|---|---|---|
| 10.315 | 11.525 | −8°2 | − 6°7 | +1.20 | +301 | +29 |
| 10.320 | 11.525 | +0.5 | − 3.7 | 1.17 | +281 | +11 |
| 10.315 | 7.558 | −4.5 | + 2.5 | 1.36 | −486 | −18 |
| 9.328 | 11.528 | +0.7 | + 2.5 | 1.16 | +411 | −47 |
| 11.288 | 7.561 | +2.5 | + 3.2 | 1.49 | −626 | +20 |
| 10.320 | 7.558 | +3.7 | + 4.7 | 1.33 | −466 | + 3 |
| 9.328 | 7.561 | +4.5 | + 6.2 | 1.31 | −319 | −35 |
| 9.333 | 11.523 | +4.2 | + 7.7 | 1.10 | +461 | + 8 |
| 11.288 | 11.523 | +6.2 | +11.2 | +1.30 | +122 | +28 |

$+44.88\,\mu_\alpha + 7.18\,\pi = -8171$

$+7.18\,\mu_\alpha + 14.62\,\pi = -799$

$\pi = +37.7 = +0''.185 \pm 0''.026$

$\mu_\alpha = -188.1 = -0''.922 \pm 0''.015$

For Strb. 5819, which is $11^s$ east and 1′5 south, but was not covered by the sector, the following values were derived:

$\pi = +22.9 = +0''.112 \pm 0''.027$

$\mu_\alpha = -177.6 = -0''.870 \pm 0''.015$

| No. | Br. | $x$ | $y$ | $\pi$ |
|---|---|---|---|---|
| 1..... | f | −4′8 | +6′7 | −0″021 |
| 2..... | f | −6.0 | +2.3 | + .021 |
| 3..... | f | −3.4 | −2.8 | − .035 |
| 4..... | f | −2.0 | −5.8 | + .010 |
| 5..... | bf | −0.4 | −5.4 | + .026 |
| 6..... | f | +5.8 | −1.5 | − .031 |
| 7..... | b | +4.9 | +0.3 | − .020 |
| 8..... | f | +7.2 | +2.5 | + .031 |
| 9..... | f | +0.1 | +3.5 | +0.015 |

### Y Ophiuchi $\alpha = 17^h 47^m 17^s$ $\delta = -6^\circ 7'$

| Mor. | Ev. | $t_1$ | $t_2$ | $\Delta_p$ | $M$ | $v$ |
|---|---|---|---|---|---|---|
| 7.312 | 6.583 | − 6°5 | − 2°0 | +1.48 | −14 | − 5 |
| 7.312 | 9.592 | − 4.5 | + 0.5 | 1.52 | −11 | + 9 |
| 9.328 | 6.583 | − 3.0 | 0.0 | 1.42 | − 1 | + 1 |
| 9.328 | 9.592 | − 1.2 | + 2.0 | 1.46 | −16 | − 4 |
| 9.333 | 6.586 | + 3.0 | + 3.0 | 1.41 | −12 | −10 |
| 9.333 | 9.666 | + 5.2 | + 3.2 | 1.68 | −26 | −12 |
| 10.321 | 6.586 | +10.2 | + 5.2 | 1.46 | +10 | + 9 |
| 10.321 | 9.589 | +12.5 | +10.7 | +1.47 | + 5 | +14 |

$+35.50\,\mu_\alpha + 10.98\,\pi = +33$

$+10.98\,\mu_\alpha + 17.75\,\pi = -101$

$\pi = -7.7 = -0''.038 \pm 0''.009$

$\mu_\alpha = +3.3 = +0''.016 \pm 0''.006$

| No. | Br. | $x$ | $y$ | $\pi$ |
|---|---|---|---|---|
| 1..... | f | −4′9 | +7′3 | −0″019 |
| 2..... | bf | −4.4 | +1.5 | + .025 |
| 3..... | bf | −8.0 | −4.6 | − .006 |
| 4..... | bf | +1.1 | −9.1 | + .001 |
| 5..... | f | +4.0 | −3.6 | .000 |
| 6..... | bf | +2.0 | −2.0 | ........ |
| 7..... | f | +7.2 | 0.0 | − .005 |
| 8..... | f | +2.2 | +5.3 | + .005 |
| 9..... | bf | +0.5 | +3.2 | +0.014 |

**Boss 4595 = β.G.C. 8388** $\alpha = 18^{h}4^{m}54^{s}$ $\delta = +3^{\circ}6'$

| Mor. | Ev. | $t_1$ | $t_2$ | $\Delta_p$ | $M$ | $v$ |
|---|---|---|---|---|---|---|
| 7.389 | 9.600 | −14°.7 | −5°.0 | +1.21 | + 8 | −1 |
| 7.389 | 9.600 | −10.5 | −0.5 | 1.21 | 10 | +1 |
| 11.364 | 7.621 | − 3.5 | 0.0 | 1.42 | 18 | +7 |
| 11.367 | 7.626 | − 3.5 | +1.5 | 1.43 | 4 | −7 |
| 7.392 | 7.621 | − 1.5 | +4.2 | 1.28 | 12 | +2 |
| 11.367 | 9.598 | + 2.0 | +4.5 | 1.31 | 8 | −2 |
| 7.392 | 9.598 | + 4.7 | +8.7 | +1.18 | + 9 | 0 |

$+45.80\,\mu_\alpha + 4.74\,\pi = +33$

$+4.74\,\mu_\alpha + 11.73\,\pi = +90$

$\pi = +7.7 = +0''.019 \pm 0''.002$

$\mu_\alpha = -0.1 = \phantom{+}0''.000 \pm 0''.001$

The 12.5 mag. companion, being covered by the sector, is not visible on the plates.

| No. | Br. | $x$ | $y$ | $\pi$ |
|---|---|---|---|---|
| 1..... | bf | +1′.9 | +0′.5 | −0″.002 |
| 2..... | bf | +1.4 | +1.0 | − .006 |
| 3..... | bf | +0.7 | +3.8 | + .008 |
| 4..... | bf | +4.1 | −1.9 | − .003 |
| 5..... | bf | +4.5 | −5.4 | + .009 |
| 6..... | b | −1.5 | −1.0 | − .016 |
| 7..... | bf | −5.5 | −0.4 | + .008 |
| 8..... | bf | −5.6 | +3.6 | +0.002 |

**Y Sagittarii** $\alpha = 18^{h}15^{m}30^{s}$ $\delta = -18^{\circ}54'$

| Mor. | Ev. | $t_1$ | $t_2$ | $\Delta_p$ | $M$ | $v$ |
|---|---|---|---|---|---|---|
| 8.392 | 9.587 | −8°.7 | −6°.0 | +1.14 | +18 | +10 |
| 8.392 | 9.587 | 6.7 | −3.5 | 1.14 | +13 | + 5 |
| 7.397 | 9.592 | 6.2 | −1.0 | 1.13 | − 9 | −21 |
| 11.362 | 6.667 | 4.5 | −0.2 | 1.59 | −17 | − 1 |
| 7.397 | 9.592 | 4.2 | +1.0 | 1.13 | +13 | + 1 |
| 7.394 | 6.668 | 2.7 | +1.7 | 1.44 | + 8 | + 7 |
| 11.362 | 6.586 | 2.0 | +3.5 | 1.28 | −23 | − 6 |
| 7.394 | 6.586 | −0.7 | +5.2 | +1.12 | + 1 | + 1 |

$+58.69\,\mu_\alpha + 7.83\,\pi = -230$

$+7.83\,\mu_\alpha + 12.65\,\pi = -2$

$\pi = +2.5 = +0''.012 \pm 0''.010$

$\mu_\alpha = -4.3 = -0''.021 \pm 0''.005$

| No. | Br. | $x$ | $y$ | $\pi$ |
|---|---|---|---|---|
| 1..... | bf | −0′.4 | +2′.4 | −0″.019 |
| 2..... | bf | −4.9 | +8.9 | + .003 |
| 3..... | bf | −4.2 | −6.7 | − .004 |
| 4..... | f | −1.5 | −7.7 | + .005 |
| 5..... | f | −2.4 | −5.2 | + .006 |
| 6..... | bf | +9.2 | +1.0 | − .004 |
| 7..... | f | +4.9 | +7.9 | +0.011 |

**Nova Sagittae, No. 2** $\alpha=20^h3^m4^s$ $\delta=+17°24'$

| Mor. | Ev. | $t_1$ | $t_2$ | $\Delta_p$ | $M$ | $v$ |
|---|---|---|---|---|---|---|
| 7.476 | 9.742 | −10°0 | −6°5 | +1.36 | −41 | − 8 |
| 11.460 | 9.745 | − 9.7 | −6.2 | 1.45 | +31 | + 1 |
| 7.476 | 9.666 | − 5.7 | −3.2 | 1.08 | −27 | + 5 |
| 7.474 | 9.745 | − 5.0 | −2.2 | 1.38 | −33 | 0 |
| 11.460 | 9.742 | − 2.5 | −1.7 | 1.44 | +33 | + 3 |
| 7.474 | 9.740 | − 1.0 | +0.2 | 1.37 | −29 | − 3 |
| 11.463 | 9.666 | − 0.5 | +0.7 | 1.15 | +28 | −11 |
| 11.463 | 9.740 | + 5.0 | +4.5 | +1.42 | +32 | + 2 |

$$+32.37\,\mu_a-\;2.22\,\pi=+508$$
$$-\;2.22\,\mu_a+14.31\,\pi=-\;1$$
$$\pi=+\;2.4=+0''.012\pm0''.005$$
$$\mu_a=+15.9=+0''.078\pm0''.004$$

| No. | Br. | $x$ | $y$ | $\pi$ |
|---|---|---|---|---|
| 1. . . . . | f | −0′.1 | 0′.0 | +0″.003 |
| 2. . . . . | f | −0.2 | +1.6 | + .001 |
| 3. . . . . | f | −1.6 | +1.4 | .000 |
| 4. . . . . | f | −3.1 | −1.1 | − .004 |
| 5. . . . . | f | −2.1 | −1.7 | − .008 |
| 6. . . . . | f | +1.0 | −2.2 | + .003 |
| 7. . . . . | f | +1.6 | −0.4 | .000 |
| 8. . . . . | f | +3.5 | +2.7 | −0.003 |

**N.G.C. 6891** $\alpha=20^h10^m24^s$ $\delta=+12°24'$

| Mor. | Ev. | $t_1$ | $t_2$ | $\Delta_p$ | $M$ | $v$ |
|---|---|---|---|---|---|---|
| 8.452 | 7.714 | − 3°5 | + 5°0 | +1.41 | +15 | + 9 |
| 7.476 | 7.794 | − 0.2 | 6.2 | 1.45 | −13 | −17 |
| 8.452 | 9.666 | 0.0 | 6.5 | 1.21 | + 8 | + 6 |
| 7.476 | 7.712 | + 2.2 | 6.2 | 1.27 | −12 | −16 |
| 8.444 | 7.714 | + 7.2 | 8.0 | 1.44 | +18 | +12 |
| 8.444 | 9.666 | +10.7 | 10.0 | 1.24 | +12 | +10 |
| 11.463 | 7.712 | +12.7 | 9.2 | 1.34 | +13 | + 2 |
| 11.463 | 7.794 | +16.2 | + 9.5 | +1.52 | + 7 | − 4 |

$$+31.72\,\mu_a+\;8.96\,\pi=+81$$
$$+\;8.96\,\mu_a+14.88\,\pi=+66$$
$$\pi=+3.5=+0''.017\pm0''.037$$
$$\mu_a=+1.6=+0''.008\pm0''.025$$

| No. | Br. | $x$ | $y$ | $\pi$ |
|---|---|---|---|---|
| 1. . . . . | f | −1′.0 | +2′.0 | +0″.001 |
| 2. . . . . | f | −5.2 | +2.8 | + .003 |
| 3. . . . . | bf | −3.2 | +0.8 | − .003 |
| 4. . . . . | bf | −0.3 | −4.4 | + .004 |
| 5. . . . . | bf | +1.4 | −4.6 | − .004 |
| 6. . . . . | f | +3.2 | −1.1 | + .007 |
| 7. . . . . | bf | +3.6 | 0.0 | − .001 |
| 8. . . . . | bf | +1.4 | +3.0 | −0.001 |

**Wolf 1106** $\alpha=21^h5^m36^s$ $\delta=+59^\circ22'$

| Mor. | Ev. | $t_1$ | $t_2$ | $\Delta_p$ | $M$ | $v$ |
|---|---|---|---|---|---|---|
| 8.517 | 6.739 | −11°.7 | −10°.0 | +1.20 | −709 | + 7 |
| 8.520 | 6.742 | − 8.7 | − 6.0 | 1.20 | −718 | − 2 |
| 8.518 | 9.748 | − 6.5 | − 4.5 | 1.23 | +590 | +52 |
| 8.520 | 6.739 | − 3.0 | − 3.0 | 1.19 | −715 | + 2 |
| 8.515 | 9.748 | − 2.5 | − 0.2 | 1.24 | +496 | −42 |
| 8.515 | 6.821 | + 2.7 | + 8.0 | 1.42 | −678 | − 3 |
| 9.505 | 9.751 | +11.7 | + 9.5 | 1.30 | +122 | − 9 |
| 9.505 | 9.751 | +17.0 | +16.0 | +1.30 | +123 | − 8 |

$+15.51\,\mu_\alpha+\phantom{0}5.11\,\pi=-6356$

$+\phantom{0}5.11\,\mu_\alpha+12.75\,\pi=-1867$

$\pi=+\phantom{0}20.5=+0''.052\pm0''.014$

$\mu_\alpha=-416.5=-1''.050\pm0''.013$

Omitting the two very discordant pairs of plates, 8.518–9.748 and 8.515–9.748, we get:

$\pi=+\phantom{0}15.5=+0''.039\pm0''.003$

$\mu_\alpha=-412.0=-1''.040\pm0''.003$

| No. | Br. | $x$ | $y$ | $\pi$ |
|---|---|---|---|---|
| 1..... | f | +0′.5 | +3′.4 | −0″.002 |
| 2..... | f | +3.3 | +3.6 | + .007 |
| 3..... | f | +3.2 | +3.0 | .000 |
| 4..... | f | +4.0 | −1.8 | − .007 |
| 5..... | ff | −0.5 | −3.2 | + .008 |
| 6..... | bf | −4.4 | −2.6 | + .004 |
| 7..... | bf | −3.3 | −1.4 | − .005 |
| 8..... | ff | −2.1 | −1.1 | −0.002 |

**β Pegasi** $\alpha=22^h58^m56^s$ $\delta=+27^\circ32'$

| Mor. | Ev. | $t_1$ | $t_2$ | $\Delta_p$ | $M$ | $v$ |
|---|---|---|---|---|---|---|
| 9.595 | 9.805 | −11°.5 | −11°.0 | +1.12 | − 6 | + 3 |
| 6.578 | 9.805 | −11.0 | − 5.2 | 1.20 | −209 | + 7 |
| 9.595 | 4.876 | − 7.2 | − 4.2 | 1.34 | +365 | +41 |
| 6.578 | 4.805 | − 6.2 | − 2.5 | 1.20 | + 87 | −36 |
| 7.553 | 4.876 | − 0.7 | 0.0 | 1.53 | +185 | − 1 |
| 7.553 | 4.805 | + 3.0 | + 1.5 | 1.30 | +162 | −29 |
| 7.551 | 9.811 | + 2.7 | + 2.0 | 1.34 | −157 | − 8 |
| 7.553 | 9.811 | + 7.5 | + 6.7 | +1.33 | −133 | +16 |

$+60.84\,\mu_\alpha+\phantom{0}5.96\,\pi=+4151$

$+\phantom{0}5.96\,\mu_\alpha+13.53\,\pi=+\phantom{0}442$

$\pi=+\phantom{0}2.9=+0''.007\pm0''.013$

$\mu_\alpha=+67.9=+0''.171\pm0''.006$

| No. | Br. | $x$ | $y$ | $\pi$ |
|---|---|---|---|---|
| 1..... | f | +0′.5 | +3′.2 | −0″.008 |
| 2..... | f | +5.2 | +0.4 | − .001 |
| 3..... | ff | +2.3 | −4.1 | + .007 |
| 4..... | f | +1.4 | −5.1 | + .004 |
| 5..... | bf | −2.6 | −2.7 | − .007 |
| 6..... | bf | −4.4 | +5.2 | + .016 |
| 7..... | f | −3.0 | +2.9 | −0.012 |

MOUNT WILSON OBSERVATORY
August 1926

Contributions from the Mount Wilson Observatory, No. 322
Reprinted from the *Astrophysical Journal*, Vol. LXIV, pp. 287–294, 1926
Printed in the U.S.A.

# PROVISIONAL ELEMENTS AND DIMENSIONS OF S ANTLIAE CONSIDERED AS AN ECLIPSING BINARY

By ALFRED H. JOY

## ABSTRACT

*Spectrographic observations.*—The spectrum is similar to that of W Ursae Majoris in that it shows wide double lines, but the type for both components is estimated to be A8. Luizet's double period, 0.64833872 day, fits the observations. *Nineteen spectrograms* (Table I), obtained with a single prism, serve to determine the *elements* of the orbit: $e=0.0$ (assumed); $\gamma=-5.0$ km/sec.; $K_1=81$ km/sec.; $K_2=148$ km/sec.

*Photometric orbit.*—The Harvard photometric observations have been used to determine a light-curve and an orbit, the star being considered as an eclipsing variable. The results indicate that the *components* are *very close* together and greatly *elongated*. The *eclipse* is *partial*. $a_0=0.36$; $k=0.77$; $i=62° 10'$. Judged from their spectra, the light of the brighter star is twice that of the fainter.

*Absolute dimensions.*—The spectrographic and photometric observations are combined to give the dimensions of the stars and the system: radius of relative orbit = 2,300,000 km; semi-major axis of large star = 1,160,000 km; semi-major axis of small star = 896,000 km; distance of surfaces = 251,000 km; $m_1=0.75\odot$; $m_2=0.42\odot$:, $\rho_1=0.31\odot$; $\rho_2=0.38\odot$.

The light-changes of the southern variable, S Antliae ($9^h\ 29^m.7$, $-28°\ 11'$, 1900), were first detected by H. M. Paul[1] at Washington in 1888. Its period was then the shortest known. The early observers, Sawyer, Yendell, and Chandler, placed the variable in the Algol class on account of the sharp minimum and flat maximum; but, in 1896, E. C. Pickering[2] made a series of observations with the meridian photometer and concluded that the star was not an eclipsing variable, because the minimum occupied such a large portion of the period and because the light-change at maximum was continuous. O. C. Wendell[3] observed portions of four minima in 1898 with the polarizing photometer, finding odd and even minima of nearly equal depth. Luizet,[4] in 1904, compared his observations with earlier measures and gave corrected elements of such accuracy as to hold very closely up to the time of the present observations. Since the light-curve does not differ widely from that which would be given by a single rotating ellipsoid, Shapley[1] included the star in his list of such objects. Plummer[2] has noted certain irregularities in the light-curve which led him to associate it with the short-period cluster-type of variables.

---

[1] *Astronomical Journal*, **9**, 180, 1890.

[2] *Astronomische Nachrichten*, **142**, 12, 1896.

[3] *Annals of the Harvard College Observatory*, **69**, 44, 1909.

[4] *Astronomische Nachrichten*, **165**, 291, 1904.

TABLE I

SPECTROGRAPHIC OBSERVATIONS

| PLATE | DATE | G.M.T. | PHASE | VELOCITY | | O−C | | WT. | |
|---|---|---|---|---|---|---|---|---|---|
| | | | | Prim. | Sec. | Prim. | Sec. | Prim. | Sec. |
| | | | | km/sec. | km/sec. | km/sec. | km/sec. | | |
| γ 6397 | 1917 Nov. 27 | $0^h$ $47^m$ | 0.3279 | +19 | . . . . . | +21 | . . . . . | 1.0 | . . . . . |
| 6435 | Dec. 4 | 0 52 | .1996 | −67 | +137 | +14 | + 4 | 0.5 | 1.0 |
| 6505 | 9 | 22 30 | .1717 | −80 | +140 | + 1 | + 1 | 1.0 | 0.5 |
| 6727 | 1918 Mar. 2 | 19 12 | .1411 | −87 | +149 | − 3 | + 9 | 0.5 | 0.5 |
| 6810 | 30 | 17 20 | .1848 | −82 | +122 | + 2 | −17 | 0.5 | 0.5 |
| 7708 | 1919 Jan. 18 | 21 25 | .0091 | −26 | . . . . . | −14 | . . . . . | 1.0 | . . . . . |
| 7970 | Mar. 17 | 18 12 | .1729 | −84 | +146 | + 2 | + 4 | 1.0 | 1.0 |
| 8023 | Apr. 10 | 15 35 | .0761 | −68 | + 55 | − 9 | −39 | 1.0 | 1.0 |
| 8024 | 10 | 16 35 | .1171 | −76 | +135 | + 2 | − 7 | 1.0 | 1.0 |
| 8037 | 11 | 16 14 | .4542 | +55 | −137 | −17 | + 9 | 1.0 | 0.5 |
| C 798 | 1920 Nov. 29 | 1 10 | .0581 | −56 | + 69 | − 6 | − 4 | 1.0 | 1.0 |
| C 930 | 1921 Mar. 16 | 17 37 | .0776 | −51 | + 91 | + 9 | − 5 | 1.0 | 1.0 |
| γ 10082 | Apr. 16 | 15 50 | .5731 | +54 | −146 | + 5 | −42 | 1.0 | 0.5 |
| 10084 | 16 | 17 05 | .6252 | +14 | . . . . . | + 3 | . . . . . | 1.0 | . . . . . |
| 10089 | 17 | 15 21 | .2564 | −77 | + 57 | −23 | −27 | 0.5 | 0.5 |
| 10092 | 17 | 17 07 | .3300 | − 4 | . . . . . | − 3 | . . . . . | 1.0 | . . . . . |
| 10109 | 21 | 15 40 | .3795 | +35 | −102 | − 2 | −21 | 1.0 | 0.5 |
| 10123 | 25 | 16 39 | .5304 | +83 | −172 | +15 | −33 | 0.5 | 0.5 |
| C 1012 | May 13 | 16 02 | 0.3512 | +22 | . . . . . | + 6 | . . . . . | 0.5 | . . . . . |

## SPECTROGRAPHIC OBSERVATIONS

The Harvard estimate of the spectral type is Fo. The first photographs of the spectrum obtained at this observatory were taken for the purpose of determining the absolute magnitude and parallax. It was immediately seen[3] that the spectrum is very different from that of Cepheid or cluster-type variables, the lines being wide and hazy, because of a large rotational effect like that found in W Ursae Majoris. In some cases the lines appeared to be double. On account of the character of the spectrum, the plates are extremely difficult to measure and the results are accordingly uncertain, especially in the case of the secondary spectrum. As more observations were obtained, it became evident that the period of light-variation could be used to plot the velocity changes only if the double period of sixteen hours were adopted. The predicted maximum of light occurs at the time of maximum separation of the two components of the spectrum, and minimum of light when the spectrum is single. It is therefore concluded that the star must be an eclipsing binary having ellipsoidal components of nearly the same surface brightness which partially eclipse each other. The spectral type is estimated as A8 for each star, but there is much uncertainty in the case of the fainter spectrum. On many of the plates, the weaker lines of both compo-

---

[1] *Astronomische Nachrichten*, 194, 353, 1913.

[2] *Monthly Notices of the Royal Astronomical Society*, 73, 659, 1913.

[3] Adams and Joy, *Publications of the Astronomical Society of the Pacific*, 31, 41, 1919.

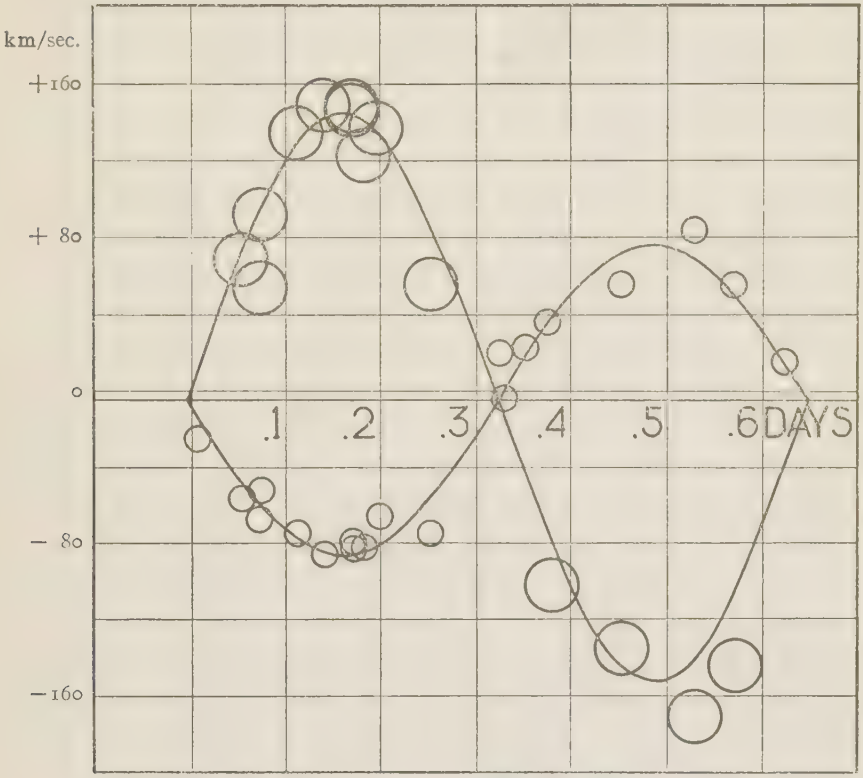

FIG. 1.—Velocity-curves of the components of S Antliae

nents are lacking, and the stronger lines very poorly defined. The lines of the secondary are always measured with difficulty. The low altitude of the star caused some of the spectrograms to be weak in the violet region.

Nineteen plates were obtained as given in Table I. All were measured at least once by the writer, and the weight for most of them is increased by the measures of Mr. Adams and Miss Burwell.

Since neither the photometric observations nor the velocity-curve show any indication of eccentricity, the orbit is assumed to be circular. Separate solutions were made to determine the correction to the remaining elements of the primary and secondary. The velocity of the system, $\gamma$, was not included in the secondary solution, since it was considered to be more accurately defined by the solution for the primary. When the period is doubled, the photometric elements of Luizet,

$$\text{Min.} = \text{J.D. } 2410741.5248 + 0.64833872 \text{ day (G.M.T.)}$$

satisfy the observations very exactly. Since more than eighteen thousand complete revolutions have taken place since the initial epoch, it is evident that the period cannot have changed by as much as one-tenth of a second in thirty years.

The corrected elements of the spectrographic orbit as determined by the observations are:

$e = 0.0$ (assumed) $\quad a_1 \sin i = 722{,}000$ km
$\gamma = -5.0 \pm 1.8$ km/sec. $\quad a_2 \sin i = 1{,}320{,}000$ km
$K_1 = 81 \pm 2.5$ km/sec. $\quad m_1 \sin^3 i = 0.52$
$K_2 = 148 \pm 11.6$ km/sec. $\quad m_2 \sin^3 i = 0.29$

The residuals in the seventh and eighth columns of Table I are computed from these elements.

## PHOTOMETRIC ORBIT

The outcome of the spectroscopic observations makes it worth while to re-examine the available photometric data, with a view to the determination of other facts concerning this well-known variable. It is of especial interest to see whether it is possible to account for the observed light-changes by assuming that the two bodies are ellipsoidal stars partially eclipsing each other.

The observations with the meridian photometer by Pickering[1] in 1896 and those of Wendell[2] in 1898 with the sliding-prism polarizing photometer have been used, the latter being adjusted to the meridian observations by applying a correction of +0.16 mag. The measures were grouped according to time in twenty-three normal places as given in Table II. The phases were determined from Luizet's elements.

TABLE II

Harvard Photometric Observations

| Mean Mag. | Mean Phase | No. | Mean Mag. | Mean Phase | No. | Mean Mag. | Mean Phase | No. |
|---|---|---|---|---|---|---|---|---|
| 6.84...... | 0.006 | 6 | 6.45...... | 0.227 | 12 | 6.38...... | 0.435 | 4 |
| 6.75...... | .016 | 7 | 6.53...... | .251 | 7 | 6.46...... | .460 | 18 |
| 6.67...... | .028 | 7 | 6.61...... | .272 | 7 | 6.38...... | .502 | 17 |
| 6.56...... | .051 | 9 | 6.76...... | .318 | 4 | 6.41...... | .545 | 3 |
| 6.52...... | .065 | 5 | 6.79...... | .325 | 5 | 6.55...... | .576 | 19 |
| 6.38...... | .098 | 6 | 6.71...... | .349 | 17 | 6.67...... | .610 | 15 |
| 6.31...... | .146 | 7 | 6.65...... | .371 | 23 | 6.79...... | 0.636 | 16 |
| 6.39...... | 0.204 | 28 | 6.53...... | 0.398 | 8 | | | |

The observations show large errors, probably because of the southern declination of the star. Too much confidence should not be placed upon the arbitrary light-curve, which has been drawn as shown in Figure 2. It is evident, however, that the minima are not exactly equal in depth, and that after allowing for a considerable ellipticity, there remains a small percentage loss of light which may be caused by eclipse.

Using Russell's[3] method and notation, we find by plotting $\cos^2\theta$ against $1-L^2$, the magnitudes being reduced to intensities, that $z=0.340$. The rectified curve then shows that the loss of light because of eclipse is 0.145 at primary and 0.120 at secondary minimum. The loss because of the ellipticity of the stars is 0.188.

By setting different values for $a_0$ and $k$ in the equation

$$a_0=1-\lambda_1+\frac{1-\lambda_2}{k^2}\ ,$$

---

[1] *Harvard Annals*, **46**, 124, 1903.

[2] *Ibid.*, **69**, 44, 1909.

[3] *Astrophysical Journal*, **35**, 315; **36**, 54, 1912.

it is seen that the orbit would be largely indeterminate were it not for the assistance of the spectroscopic data at this point. The spectrograms indicate that one star is brighter than the other in the ratio of approximately 2:1. After calculating the ratio of surface brightnesses by comparing the minima and the total light of the two stars, the ratio of the radii, $k$, is found to be 0.775. Had the ratio 3:2 been used instead of 2:1, the resulting dimensions of the stars would have been changed by less than 10 per cent. A light-curve was computed with $k=0.775$ and $a_0=0.36$ which fits the rectified light-curve at minimum within the uncertainties of the observations.

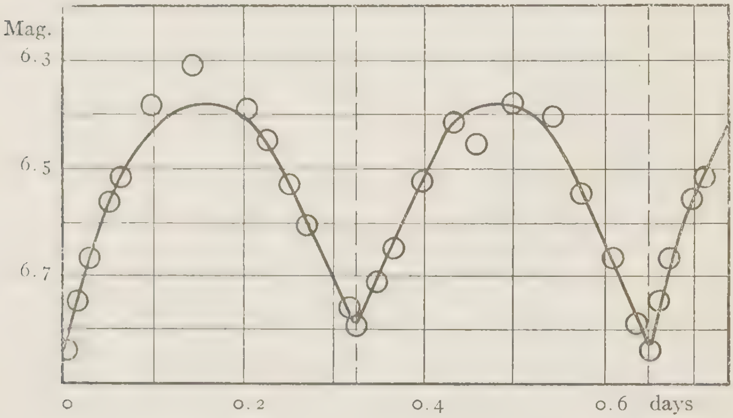

FIG. 2.—Light-curve of S Antliae

If we take 0.09 day before minimum as the beginning of eclipse, the corresponding value of the longitude, $\theta'$, may be computed, and the inclination, $i=62° 10'$, may be found from the equations

$$a_1^2(1-z)[1+kp(k, a_0)]^2=\cos^2 i$$

$$a_1^2(1-z\cos^2\theta')(1+k)^2=\cos^2 i\cos^2\theta'+\sin^2\theta' .$$

The dimensions of the stars in terms of the radius of the relative orbit are:

| | | |
|---|---|---|
| Semi-major axis of larger star | $a_1$ | 0.502 |
| Semi-minor axis of larger star | $b_1$ | .377 |
| Semi-major axis of smaller star | $a_2$ | .389 |
| Semi-minor axis of smaller star | $b_2$ | 0.292 |

The value of the inclination of the orbit having been determined from the photometric observations, it is possible to give absolute values for the dimensions of the system by combining the photometric and spectroscopic elements. We thus find:

| | | |
|---|---|---|
| Period | $P$ | 0.64833872 day |
| Orbital eccentricity | $e$ | 0.00 (assumed) |
| Light of bright star | $L_1$ | 0.67 |
| Ratio of surface brightness | $J_b/J_f$ | 1.2 |
| Spectral type, both stars | | A8 |
| Ratio of radii of stars | $k$ | 0.775 |
| Percentage of eclipse | $a_0$ | 0.36 |
| Duration of eclipse | | 0.180 day |
| Magnitude at maximum | | 6.39 |
| Magnitude at primary minimum | | 6.83 |
| Magnitude at secondary minimum | | 6.79 |
| Inclination of orbit | $i$ | 62° 10′ |
| Radius of relative orbit | $a_1+a_2$ | 2,300,000 km |
| Radius of primary orbit | $a_1$ | 817,000 |
| Radius of secondary orbit | $a_2$ | 1,490,000 |
| Semi-major axis, large star | | 1,160,000 |
| Semi-minor axis, large star | | 870,000 |
| Semi-major axis, small star | | 896,000 |
| Semi-minor axis, small star | | 674,000 |
| Distance of surfaces | | 251,000 |
| Mass, primary large star | $m_1$ | 0.75 $\odot$ |
| Mass, secondary small star | $m_2$ | 0.42 |
| Density, large star | $\rho_1$ | 0.31 |
| Density, small star | $\rho_2$ | 0.38 |
| Absolute magnitude, bright star | $M$ | 2.9 |
| Parallax | | 0.″017 |

The difference in velocity at the two limbs of the larger star due to rotation is 225 km/sec., which easily accounts for the character of the spectral lines. For determining the absolute magnitude the brighter star was assumed to have a surface brightness 1.1 mag. brighter than that of the sun. No darkened solution was attempted on account of the inaccuracy of the light-curve, but it seems probable from inspection that the observations would have been somewhat better represented by the assumption of darkening at the limb.

It therefore appears that the variable S Antliae should be classed among the eclipsing binaries. The light-changes can be accounted for by ellipticity of the stars and by the partial eclipse of the larger, brighter, and more massive star at primary minimum. The star will repay further accurate photometric observation, for the present results must be affected by a considerable degree of uncertainty.

Of those variable stars which have been suggested as single rotating ellipsoids, not one has been found to meet the necessary spectrographic requirements.

Mount Wilson Observatory
August 1926

Contributions from the Mount Wilson Observatory, No. 323
Reprinted from the *Astrophysical Journal*, Vol. LXIV, pp. 295-314, 1926
Printed in the U.S.A.

# GENERAL CHARACTERISTICS OF ELECTRICALLY EXPLODED WIRES

By J. A. ANDERSON and SINCLAIR SMITH

## ABSTRACT

A general discussion of the condenser circuit shows that *efficiency in producing high temperatures* with the method of electrically exploded wires requires primarily *high voltage;* secondarily, *large capacity* and *low inductance.* The best value for the resistance of the wire is $\sqrt{L/C}$, and the resistance of the rest of the circuit should be negligible.

Several methods of studying the explosions are outlined: (1) From *direct photographs* the temperature of the vapor may be measured when its pressure is equal to that of the surrounding atmosphere. (2) A convenient form of *rotating-mirror camera* is described, which is well adapted for studying sparks or explosions in circuits whose frequency is not much greater than $10^6$ cycles. (3) *Rotating-mirror spectrograph.* (4) *Velocity-of-sound method.* The sound pulse produced by the explosion is reflected back and caused to pass through the hot metallic vapor. Its path is photographed with the rotating-mirror camera. From this the *velocity of sound in the vapor* can be determined at various instants of time after the beginning of the explosion. A simple calculation then gives the *true temperature of the vapor* at these instants. The method does not apply to the early stages when the temperature exceeds 10,000° on account of the opacity of the vapor. (5) *Optical focal-plane shutter.* In the mechanical focal-plane shutter the image is stationary while the shutter moves. This is reversed in the present apparatus. The *image moves at high speed* produced by reflection from one face of a rotating mirror. After passing the opening in the shutter it is *reflected from a second face of the mirror* which exactly stops the motion, allowing the photograph to be made. Exposures of about $10^{-6}$ second are easily obtained. A motion-picture camera taking several such exposures in quick succession is suggested. Photographs made with this apparatus showing various phases of explosions are reproduced. (6) *Magneto-optic shutter.* A cell containing water is placed between crossed nicols. A small coil of wire connected in series with the wire to be exploded is wound around the cell. The coil is so designed that with the maximum current a rotation of the plane of polarization of about 20° is produced. With a suitable resistance in the circuit it follows that the shutter is open only near the maximum of the first half-cycle. Photographs of an early stage of the explosions are reproduced and discussed briefly. (7) *Parallel spark-gap.* A spark-gap parallel to the wire to be exploded is so adjusted that the current is shunted into it immediately after the wire is vaporized. This is possible for all metals tried except tungsten. A photograph of the wire then shows practically nothing but the very beginning of the explosion.

The appearance of explosions at the very beginning indicates that *the particles evaporating from electrically heated wires at high temperatures are charged.*

Six years ago one of us published an account of the spectra of electrically exploded wires[1] in which was included a description of some of the phenomena of an explosion. Since then methods and apparatus have been devised which greatly facilitate the study of such transient phenomena, and these, together with some of the conclusions we have reached, form the subject of the present paper.

---

[1] Anderson, *Mt. Wilson Contr.*, No. 178; *Astrophysical Journal*, **51**, 37, 1920.

The chief aim of the investigation is to produce very high temperatures. The method is that used first by Singer and later by Nipher, namely, to pass the current from a large condenser through a fine wire. Since by this means currents having an instantaneous value of several thousand amperes are readily obtained, it follows that a small wire will be heated and turned into vapor very suddenly. The word "explosion" was used by Nipher to describe the phenomenon, and we have followed him in this, although we do not agree with the reasoning which appears to have led him to choose this term.

In order to specify more or less precisely the conditions which favor the development of high temperatures it will be desirable to recall the well-known formulae which have been developed for condenser circuits. Such a circuit is defined by four constants, namely, the capacity $(C)$ of the condenser, the inductance $(L)$, the resistance $(R)$ of the circuit, and the voltage $(V)$ of the charged condenser. The current $(i)$ is then given by

$$i=\frac{Ve^{-\frac{RT}{2L}}}{L\sqrt{\frac{1}{LC}-\frac{R^2}{4L^2}}}\sin t\sqrt{\frac{1}{LC}-\frac{R^2}{4L^2}}\,, \tag{1}$$

provided $R$ is less than $2\sqrt{L/C}$, and by

$$i=\frac{Ve^{-\frac{RT}{2L}}}{L\sqrt{\frac{R^2}{4L^2}-\frac{1}{LC}}}\sinh t\sqrt{\frac{R^2}{4L^2}-\frac{1}{LC}} \tag{2}$$

in the general case.

It will be convenient to regard the resistance $R$ as made up of two parts, the resistance of the wire $(r)$ and that of the rest of the circuit $(R_0)$. Heat energy is developed in the wire at a rate given by $i^2r$, and in the rest of the circuit at the rate $i^2R_0$. Consequently, it is necessary that $r$ be large as compared to $R_0$, if the greater part of the energy is to appear in the wire. Practically, this means that $R_0$ must be made very small, for it will be shown later that the total resistance $r+R_0$ may not be large. The current $i$ which appears in the expression for the rate of energy input is of first importance, because it enters with the exponent 2. The product $i^2r$ must be made as large as possible. From equation (1) it follows that $i^2R$ will be a maximum when $R=\sqrt{L/C}$ nearly, and since $r$ will not differ very materially from $R$, this is very nearly the best value for the resistance of the wire.

There remains now to find what the relative values of the other constants $C$, $L$, and $V$ should be. Inserting in (1) the value of $R$ just found, we find that the maximum value of $i^2$ is

$$\tfrac{4}{3}V^2 \frac{C}{L} e^{-\frac{C}{L}t}\,.$$

Hence, $i^2$ varies as $V^2C/L$, from which it follows that a large value of $V$ is of first importance; that $C$ should be large also, and $L$ as small as possible.

Four condensers have been used in this work, and the constants of their circuits are given in Table I.

TABLE I

| Condenser No. | Capacity Microfarads | Inductance Millihenrys | Voltage Kilovolts | $i$ Max. Amperes | Frequency | Energy Joules |
|---|---|---|---|---|---|---|
| 1. . . . . . . . . . . | 0.4 | 0.0033 | 18–20 | 7,000 | 140,000 | 80 |
| 2. . . . . . . . . . . | 1.0 | .0034 | 18–20 | 10,800 | 87,000 | 200 |
| 3. . . . . . . . . . . | 0.6 | .0011 | 55–60 | 45,000 | 200,000 | 1080 |
| 4. . . . . . . . . . . | 2.0 | 0.0036 | 35–40 | 30,000 | 60,000 | 1600 |

Condensers 1 and 2 were built of sheets of window glass coated with tinfoil. Condenser 3 is of special plate glass, 11 mm thick. The electrodes are sheets of wire gauze imbedded in the center of each plate. These plates were made to order by the Mississippi Wire Glass Company, of New York, to whom, and especially to the superintendent of their factory, Mr. H. L. Carspecken, we are deeply grateful. Condenser 4 is made of window glass, but is coated with thin sheet copper, allowing the leads to be soldered on, thus insuring good electric contact throughout. It is made in eight units, each having a capacity of 1.0 microfarad. These units may be connected in various ways giving a number of different capacities and voltages. The arrangement for which constants are given in Table I is four pairs in series-parallel.

All of the condensers have been used in air, that is, not immersed in oil or any other special insulator, for the reason that in this kind of work glass plates occasionally fail, and if the condenser were immersed in oil, its repair would in general be a rather tedious matter, requiring much unpleasant work and a considerable loss of time.

### METHODS OF STUDY

1. *Direct photographs.*—Photographs[1] taken with a stop small enough to avoid over-exposure show the explosion to consist of two distinct parts: an inner very bright cylinder, usually from 2 to 3 cm in diameter and a little longer than the wire, and a much fainter flame, very irregular, both in shape and brightness, surrounding this cylinder. In the first paper, these parts were supposed to correspond to the limiting volume of vapor during the first and second half-oscillations of the current in the condenser circuit, but later methods of observation have shown that the flame develops chiefly after the current has ceased to flow. During the main explosion the vapor, which at first occupies a volume not much larger than the wire, expands with diminishing speed until, after two or three oscillations of the circuit, its volume becomes constant, or nearly so. It is this constant volume which is outlined by the bright inner cylinder shown by the direct photographs. In cooling, the vapor combines with the oxygen of the surrounding air, and this reaction produces the flame seen around the bright cylinder. Since the flame is caused by oxidation, it is in reality not a part of the explosion proper. A few wires have been exploded in atmospheres of hydrogen and of carbon dioxide; in these cases the bright cylinder appeared without the surrounding flame.

The fact that the bright cylinder soon attains a constant size is easy to explain and leads to a simple method of estimating the temperature. When first formed the metallic vapor must have a high pressure. As a result, it expands rapidly and the pressure falls. Equilibrium obtains only when the pressure becomes equal to that of the surrounding air, and observations described below show that this state is reached after a very few oscillations of the circuit, in something like 1/25,000 sec.

[1] *Mt. Wilson Contr.*, No. 178; *Astrophysical Journal*, **51**, 40, Plate VII*d*, *e*, 1920.

The volume occupied by the metallic vapor at atmospheric pressure may be determined from a direct photograph made to a known scale. The mass of the vapor is known, for it is equal to the mass of the wire used in the explosion. From the gas equation we then have

$$T=\frac{mvp}{MR}\,, \tag{3}$$

where $T$ is the absolute temperature, $m$ the molecular weight, $v$ the volume, $p$ the pressure, $M$ the mass, and $R$ the gas constant. There are two unknown quantities $T$ and $m$, and hence another equation is required. The equation first given by Saha, viz.,

$$\log_{10}\frac{x^2}{1-x^2}P=-\frac{5036\,I}{T}+2.5\log_{10}T-6.49\,, \tag{4}$$

will do since it involves only $I$, the ionization potential, and $x$, the percentage ionization. The ionization potential is known for most metallic elements, and $x$ is just what is required to compute the molecular weight of the vapor. At high temperatures metallic vapors are monatomic, and, consequently, if $A$ is the atomic weight, the mean molecular weight $m$ is given by

$$m=\frac{A}{1+x}\,. \tag{5}$$

With $p=1$, and $I$ equal to the ionization potential of the metal studied, a curve is drawn giving $x$ as a function of $T$ on the basis of equation (4). A value of $T$ is found from equation (3) by inserting the observed value of $v$, and taking $m=A$. In general, this value of $T$ will be much too high, but from the curve the corresponding value of $x$ is read off, which, inserted in $m$, gives a first approximation to the molecular weight. A new value of $T$ is then found from (3), which gives a second value of $x$, and hence by (5) a second approximation to $m$, and so on, until the correct value is found. The process converges quite rapidly, but in case the first value of $x$ is 0.5 or larger, the process can be much shortened by arbitrarily using one-half of this value in computing the first approximation to $m$.

The value of $T$ found by this process probably represents the average temperature of the vapor when the pressure has reached that of the surrounding atmosphere. This will be considerably lower than the highest temperature attained. There is every reason for believing that the maximum temperature is reached near the middle of the first half-oscillation of the circuit, because at this time the current has its greatest value, and the radiating surface of the mass of vapor is very much smaller than at later stages. Further, the photographs discussed in the following section show that the brightness is greatest during the first half-cycle. Still, for comparing explosions of different substances, or of the same substance produced under different conditions, this method of determining $T$ should prove of value.

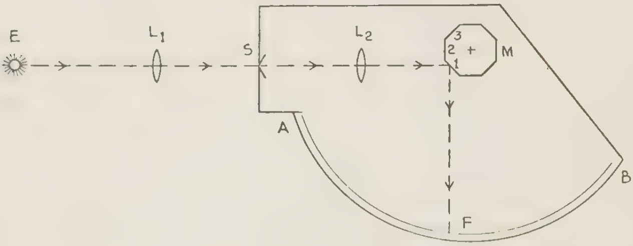

Fig. 1

2. *Rotating-mirror camera.*—The essential features of this apparatus may be seen in Figure 1. $E$ is the source (spark, explosion, etc.) to be studied. The lens $L_1$ forms an image of $E$ on the slit $S$, which is perpendicular to the plane of the paper. $L_2$ forms an image of $S$ on the photographic film $F$ after reflection from one of the faces of the mirror $M$. When $M$ is rotated, this image moves along the film from $A$ to $B$. The arc $AB$ is one-fourth of a circle, and, as the mirror has eight faces, it follows that when the slit image reflected from face 1 is just leaving the film at $B$, the image reflected from face 2 is just entering the film at $A$. Consequently, if the phenomenon at $E$ does not last longer than the time required for the slit image to move from $A$ to $B$, it must necessarily be recorded on the film, and by varying the speed of rotation of the mirror this condition can always be satisfied.

The distance from $M$ to $F$ is 25 cm. Hence, if $M$ makes 150 revolutions per second, the linear speed of the slit image along $F$ is $25\times 2\pi\times 300=47{,}250$ cm per second, which is sufficient for a study

# PLATE XII

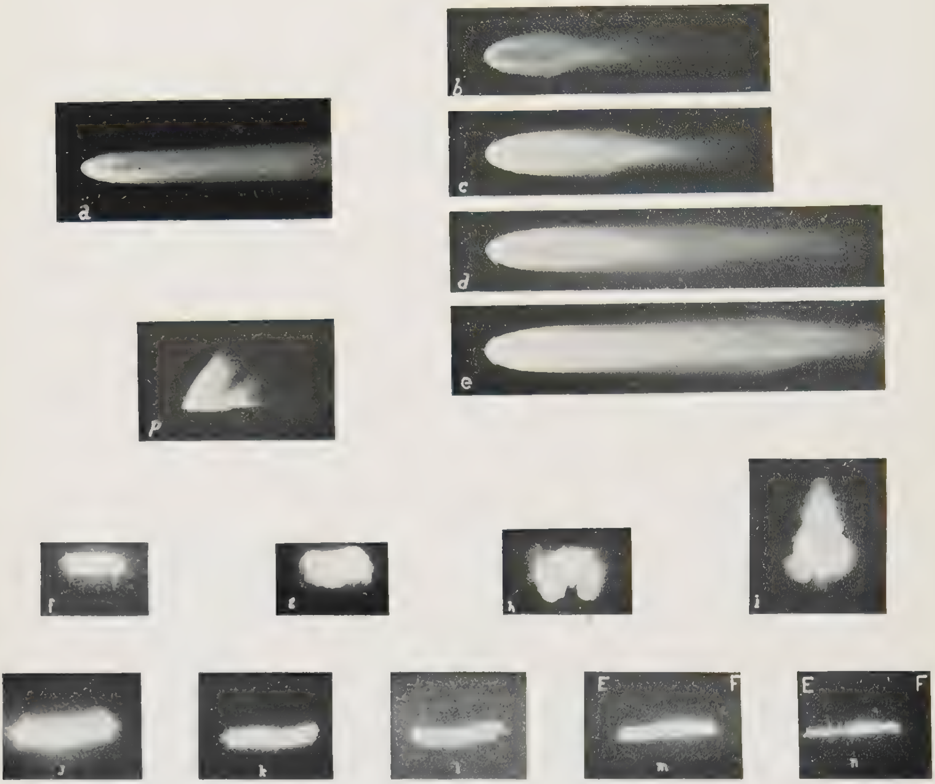

Photographs of Iron Wire Explosions

Rotating-mirror camera: *a*, open-air explosion, end on; *p*, confined explosion, end on; *b*, *c*, *d*, *e*, photographs showing passage of sound pulses through iron vapor.

Direct photographs of explosions: *f*, *g*, *h*, *i*, with optical focal-plane shutter; *j*, *k*, *l*, *m*, *n*, magneto-optic shutter.

of sparks in circuits whose frequency does not exceed one million cycles.

A photograph of the explosion of an iron wire taken with this camera is reproduced in Plate XII*a*. The frequency of the circuit was eighty-seven thousand cycles, so that the time interval between the bright bands which are faintly visible near the left end of the picture was $5.7 \times 10^{-6}$ sec. The slit was 1/50 mm in width, and its image moved from left to right. The beginning of the explosion is therefore at the left.

3. *Rotating-mirror spectrograph.*—The apparatus has been described by one of us.[1] The work done with the instrument shows that throughout at least the first half-cycle the spectrum of the explosion is continuous, and, consequently, that the vapor radiates essentially like a black body. Beginning with the second cycle, the continuous spectrum weakens rapidly and is replaced by a spectrum of bright lines similar to that of an arc.

4. *Velocity-of-sound method.*—This simple application of the rotating-mirror camera furnishes valuable information about the temperature, especially during the later stages when the vapor no longer radiates as a black body, and when, in consequence, it is impossible to make temperature determinations by radiation methods.

The explosion *E* (Fig. 1) is projected on the slit *S* end-on. A sound pulse is made to traverse the explosion in a direction parallel to that of the slit, that is, at right angles to the plane of the paper. If the sound pulse is a compression, the temperature within it will be somewhat higher than outside, and since it travels parallel to the slit, its trace on the photographic film will be a bright line inclined at some angle to the direction of travel of the slit image. The sound pulse utilized is that produced in the air by the rapid initial expansion of the explosion vapor. Two concave cylindrical mirrors are placed one on each side of the wire to reflect the sound pulse back to the explosion. In Figure 1, one of these mirrors would be directly above the plane of the paper at *E*, the other directly below. If their distances from the wire are exactly equal, the two reflected pulses will arrive simultaneously, and the two traces on the photographic film will cross at the center of the slit image. Several photographs of this sort are reproduced in Plate XII*b*, *c*, *d*, *e*.

---

[1] Sinclair Smith, *Mt. Wilson Contr.*, No. 285; *Astrophysical Journal*, **61**, 186, 1925.

The velocity of sound ($V$) in the vapor is readily determined by measuring the angle ($\theta$) between the two traces, the ratio ($M$) of the size of an object at $E$ to its image on the film $F$, and the linear speed ($V_0$) of the slit image on $F$. In the diagram (Fig. 2), let $AB$ and $CD$ be the two traces on the photograph. The sound wave travels the distance $M \times AP$ while the slit image moves from $P$ to $O$. Hence $M \times AP = Vt$; $PO = V_0 t$; therefore

$$\left.\begin{aligned} \frac{AP}{PO} &= \tan\frac{\theta}{2} = \frac{V}{MV_0}\ ; \\ \text{or}\qquad V &= MV_0 \tan\frac{\theta}{2}\ . \end{aligned}\right\} \tag{6}$$

The velocity of sound in a gas is given by

$$V = \sqrt{\frac{\gamma RT}{m}}\ , \tag{7}$$

where $\gamma$ is the ratio of the specific heats, and may be taken as 1.66 for all monatomic gases such as the metallic vapors at high temperatures. $R$ is the gas constant $8.316 \times 10^7$, $T$ is the absolute temperature, and $m$ the molecular weight. Hence, when $V$ has been determined by observation, equation (7) gives the ratio $T/m$, and consequently $T$, since $m$ may be found by the method discussed in connection with equations (4) and (5). This value of $T$ is the actual average temperature of the vapor at the moment when it is traversed by the sound pulse. By changing the distance between the wire and the cylindrical mirrors, the time interval between the beginning of the explosion and the moment at which the temperature is determined may be varied through a considerable range. It has been found that very good traces are obtained when the mirrors are from 3 to 7 cm from the wire. Since the radius of the cylinder of vapor is of the order of 1.5 cm, this gives from 3 to 11 cm for the length of path traveled by the sound pulse in air before it enters the hot vapor. The corresponding times measured from the beginning of the explosion are about 1/11,000 to 1/3000 sec. Fair traces are recorded when the mirrors are placed 2.5 cm from the wire, giving a path of 2 cm and an interval of about 1/17,000 sec. With the mirrors at 2 cm the traces are poorly defined and very difficult to measure. Probably this indicates that at such an early stage (less than 1/30,000 sec. from the beginning of the explosion) the vapor is not very transparent. Figure 3 will make this clear.

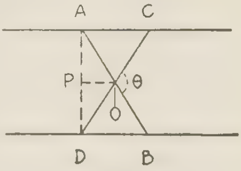

FIG. 2

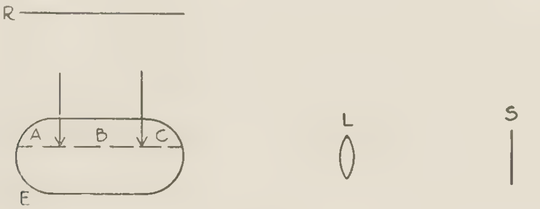

FIG. 3

Let *E* represent the vapor cylinder of the explosion, *R* one of the reflectors, and *ABC* the sound wave passing through *E* in the direction given by the arrows. The projecting lens and slit are at *L* and *S*. The surface *ABC* is at a slightly higher temperature than the surrounding vapors of *E*, and, if these are fairly transparent, light from all points of *ABC* will reach the slit *S*. If, however, the body of *E* is only partially transparent, the lens *L* will receive light from only a short distance within the vapor. Now in the neighborhood of *C* the temperature is not uniform, and, consequently, the sound pulse will travel with a lower velocity near the boundary than inside. The result will be a poorly defined image of the sound pulse, just as is observed when the mirrors are placed less than 2.5 cm from the wire.

Table II gives the results of one series of measures made on explosions of iron wires.

5. *Optical focal-plane shutter.*[1]—The rotating-mirror camera records only what happens in some one plane passed through the

---

[1] The absence of literature references does not mean that we regard any of the devices described in this paper as new. The principles are all well-known, and they have been frequently applied in the construction of apparatus by research workers everywhere.

source *E*, and it is often desirable to know just what the source as a whole looks like at any instant. It is certain that great changes take place in the explosion in $10^{-5}$ sec., and, at the beginning, in even much shorter time. Consequently, a camera is required which will take a picture of the source in something like $10^{-6}$ sec. Still better would be a motion-picture camera taking pictures with this exposure at the rate of say 500,000 per second. While neither of these requirements has been satisfied, a first step has been taken with the optical focal-plane shutter, and with the magneto-optic shutter described in the next section.

The optical focal-plane shutter, which is an adaptation of the rotating-mirror camera, is shown diagrammatically in Figure 4. A lens forms a small image of the source in the widely opened slit at *I*. The lens $L_2$ focuses this image after reflection from face 1 of the mirror *M* at some point on the circular arc *FF* ordinarily occupied by the photographic film. As *M* rotates, this image travels along *FF*. At *m* is placed a small plane mirror which reflects the light to face 2 of the rotating mirror. The length of *m* in the direction perpendicular to the plane of the paper is equal to the length of *M* in the same direction, while in the direction of travel of the image it is usually diaphragmed down to 1 mm or less as may be desired. The light, after reflection from $M_2$, passes through the lens $L_3$, which brings it to a focus on a photographic plate at *P*. Since the angular speed of $M_2$ is just one-half the angular speed of the light beam from *m*, it follows that the image at *P* is stationary. When *M* is rotating, the appearance on a ground-glass at *P* when the image of *m* sweeps by is precisely the same as that seen on the ground-glass of a camera fitted with a focal-plane shutter when the slot passes by. Hence, the name

TABLE II

| Distance from Wire to Mirrors in Centimeters | Inclination of Trace $=\theta/2$ | Percentage Ion. $x$ | Temp. (Ion. Pot. Assumed = 7 V.) |
|---|---|---|---|
| 3 | 66°0 | 40 | 8800° K |
| 4 | 62.8 | 20 | 7650 |
| 5 | 61.7 | 14 | 7260 |
| 6 | 60.4 | 9 | 6880 |
| 7 | 59.35 | 6 | 6410 |

"optical focal-plane shutter" is suggested for this device. It has, of course, all the faults of the ordinary shutter of this type. If, for example, the image *I* is wide compared to the width of *m*, and is changing very rapidly in position or shape, there is a certain amount of distortion of the picture produced at *P*. As far as speed is concerned, however, this device is much superior to the mechanical shutter. The linear speed of the latter does not often exceed 10 m per second, while in the present camera we have used 500 m per second regularly, and this can easily be increased.

In photographing the explosions, the image *I*, formed by a good lens, was about one-fifth of the natural size. Hence, the diameter of the bright cylinder at *I* measured about 5 mm. The image at *m* was of the same size as at *I*, while at *P* it was reduced in the ratio 7:5. The actual exposure time is that required for any point of the image to move across *m;* and, as this was 1 mm in width, it follows that a given point on the plate was illuminated for 1/500,000 sec. This always resulted in over-exposure for the bright cylinder, but was about right for the flame. The time required for the whole image to be impressed on the plate *P* is, of course, the time required for the image to move across *m*, and thus depends on the size of this image. In our case this time was about 1/100,000 sec.

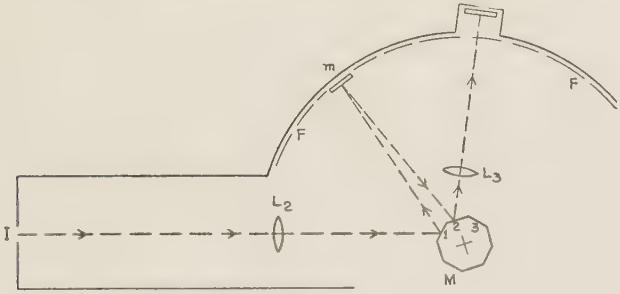

FIG. 4

Unfortunately, there is no way of synchronizing the explosion and the rotation of the mirror. Consequently, the beginning of the explosion may fall at any point along the arc *FF*, while only that stage is recorded which happens to fall on the small mirror *m*. Many photographs must therefore be taken in order to show all stages in the development of the phenomenon. In Plate XII*f*, *g*, *h*, *i*, are reproduced four photographs out of a series of seventy-five taken with this camera; *f* shows the explosion in a very early stage when the cylinder of vapor is expanding very rapidly. In Plate XII*g* it has reached its normal size, corresponding approximately to atmospheric pressure; *h* is somewhat later, while *i* shows the flame produced by the oxidation of the iron vapor.

If, in Figure 4, a second mirror like $m$ were placed quite near to $m$, but so adjusted as to reflect the light to face 3 instead of to face 2,

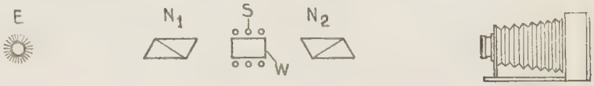

FIG. 5

and if the light so reflected were received by a second lens and plate like $L_3$ and $P$, properly placed, we should have an arrangement which would always take two photographs in quick succession. Indeed, the time interval separating them would be equal to the time required for the mirror $M$ to turn through one-half the angle subtended by the two mirrors $m$ as seen from $M$, and this could be made very short indeed. In general, it will be clear that if the mirror $M$ has $n$ faces, one could employ $(n/4)^2$ mirrors like $m$, and hence obtain $(n/4)^2$ photographs at perfectly arbitrary time intervals. With $n=16$, this would give a series of sixteen pictures showing sixteen successive stages of the explosion.

6. *Magneto-optic shutter.*—This device utilizes the magnetic rotation of the plane of polarization by a liquid such as water. A water-cell $W$ (Fig. 5) is placed between crossed nicols $N_1$ and $N_2$ directly in front of the camera $C$, suitable diaphragms being placed so that no light can enter the camera except that which has passed through the water cell. A few turns of wire, $S$, connected directly in the discharge circuit, are wound about $W$. The number of turns is so chosen that the plane of polarization for the average wave-length of photographic light is rotated some 10°–20° when the current has its first maximum value, and sufficient resistance is inserted in the circuit to make sure that the current in the second half-cycle will not "open" the shutter appreciably. Consequently, the photograph shows the explosion as

it appears during the middle of the first half-cycle. One might therefore conclude that the method has no flexibility but must always show only one phase of the explosion. This is not the case, for, by varying the current and, simultaneously, the number of turns in the coil *S*, the shutter-opening can be maintained sensibly constant while the phase of the explosion may be varied through a considerable range. For example, let the current be chosen so that the vaporization of the wire is completed just before the maximum value is reached; then if enough turns of wire have been placed around the water-cell to open the shutter the required amount, a photograph will be obtained showing a very early phase of the explosion. On the other hand, if the maximum possible current is used with say only one turn of wire in *S*, the vaporization of the wire will have been completed long before the shutter opens, and hence a relatively late phase will be recorded.

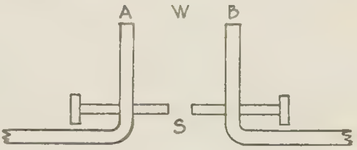

FIG. 6

Five photographs selected from a large number taken with this shutter are reproduced in Plate XII *j*, *k*, *l*, *m*, *n*. These were made with condenser 3 operated at a frequency of approximately one hundred thousand cycles. The coil *S* had ten turns of wire, and was not changed during the experiments. Some variation was produced by changing the current: the voltage of the condenser was varied from 40 to about 18 kv. In Plate XII, *j*, *k*, and *l* show explosions of nickel wires with voltages of 40, 30, and 22 kv, respectively. In Plate XII, *m* and *n* were taken with thin aluminum ribbons so placed that approximately half of the ribbon presented the flat face to the camera, the other half the edge. These are marked *F* and *E*. The peculiarities exhibited by these photographs will be considered in the discussion.

7. *Parallel spark-gap.*—This method enables us to photograph a very early stage of the explosion of all metals tried except tungsten. As seen in Figure 6, a spark-gap *S* is connected in parallel with the wire *W* and as close to the latter as possible. At the beginning of the discharge the current flows only through the conducting path *AWB*,

and it continues to do so until the voltage drop across $AB$ becomes greater than the potential difference required to break down the gap $S$, after which it flows through $S$. If $S$ is made very short, this will in general happen before the wire is vaporized; but by a proper adjustment of the spark-gap one can always insure that the wire is completely vaporized before the change of path takes place. A photograph of $AB$ shows in this case the early stage, plus the flame resulting from oxidation, if the experiment is performed in air. The flame can be largely suppressed, however, by the expedient of taking the picture with a heavily silvered quartz lens. This transmits only the 3150 A region of the spectrum, in which the flame is rather weak. Plate XIII*s*, *t*, shows two photographs made with this arrangement.

By projecting both the wire and the spark-gap simultaneously on the slit of the rotating-mirror camera, a photograph is obtained which shows clearly that the current jumps suddenly from the wire to the gap and stays there during the remainder of the discharge. Such a photograph, taken when $W$ was an aluminum wire and the spark-gap had a length of 12 mm, is reproduced in Plate XIII*o*. When a tungsten wire is used, the current does not pass wholly to the spark-gap, but divides, part going each way.

This method is interesting and very easy to apply. It has the disadvantage that it always shows the same very early phase of the explosion. Just why it works with most metals and cannot be made to work with tungsten is a problem which thus far has not been entirely solved.

8. *Miscellaneous studies.*—If the wire is placed in a slot 3 or 4 mm wide, 2 cm deep, and a little longer than the wire itself, the explosion differs very materially from one taken in the open air. Plate XII*p* shows a photograph of such an explosion made with the rotating-mirror camera (cf. this with the open-air explosion shown in Plate XII*a*). The luminosity of the vapor lasts only through the first three or three and one-half cycles, and the flame, as well as the long tail following the oscillations in the open-air explosion, is completely suppressed. The rotating-mirror spectrograph shows[1] that the spectrum remains continuous during the whole time. This will be called the

---

[1] *Mt. Wilson Contr.*, No. 285; *Astrophysical Journal*, **61**, 191–193, and Plate VIII*c*, 1925.

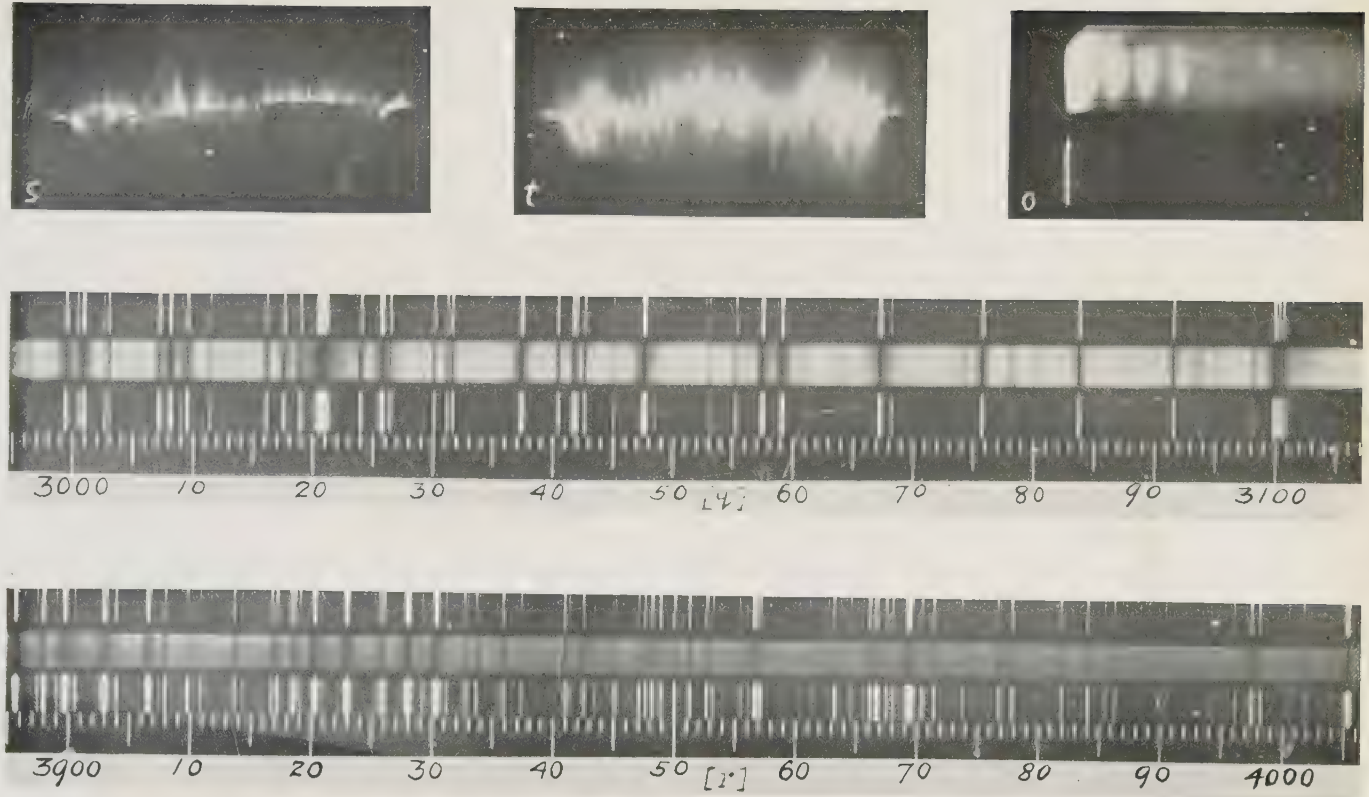

Photographs of Wire Explosions

*o*, Rotating-mirror camera, with parallel spark-gap, spark-gap above; *s*, *t*, direct photographs through silvered quartz lens, with parallel spark-gap; *q*, *r*, sections of iron spectrum, confined explosion in middle, iron-arc comparison outside.

"confined explosion" to distinguish it from the ordinary or "open-air" explosion. It has been used in most of the spectroscopic studies because all the arc lines and many spark lines appear in absorption. The spectrum of iron was photographed in the first and second orders of a 15-ft. concave grating, and a map extending from 2600 to 6600 A has been prepared from these plates. Plate XIII*q*, *r*, shows two sections of this map, which give a good idea of the richness of the spectrum and the character of the lines.

Energy curves of the confined explosion of iron have been determined by employing a vacuum thermocouple mounted so that it could be moved along the focal curve of a small quartz spectrograph. Ample deflections were obtained throughout the range 0.2–3$\mu$. Such a curve is not easy to interpret, since the radiation is integrated over the whole duration of the explosion, and in this time the temperature varies enormously. When reduced to a normal spectrum, so that the ordinates are proportional to $E_\lambda$, the maximum ordinate was found near 2650 A, with a second maximum of very nearly the same value at 2100 A. Throughout the ultra-violet region, low values of $E_\lambda$ were always found roughly to correspond to the larger groups of strong iron absorption lines.

Spectrograms of open-air explosions, which have been obtained for most of the metals, are difficult to interpret, because they are composite pictures of a number of different phenomena. During the first cycle the spectrum is mainly continuous with absorption lines. Beginning with the second cycle, the continuous spectrum decreases rapidly in intensity, and bright lines make their appearance, the spark lines showing first. Very soon the whole arc spectrum appears in emission, the low-temperature lines being strongly reversed. The flame which follows probably affects the integrated spectrum very little, owing to its inferior intensity. The spectrogram consequently shows a strong continuous background with the low-temperature arc lines appearing as rather narrow absorption lines; the spark lines and some high-temperature arc lines show bright, while lines of intermediate temperature classes may be practically absent. The appearance varies in different parts of the spectrum. In the ultra-violet, where reversals are relatively easy to obtain, many spark and most of the arc lines appear dark. In the visible portion most spark lines are bright and only the low-temperature arc lines appear in absorption. Near the red end of the spectrum dark lines are not frequently observed.

It is useless to attempt to draw conclusions from the study of an integrated spectrum such as this. Consider for a moment the photographs shown in Plate XII *b*, *c*, *d*, *e*. It will be observed that the passage of the sound wave through the vapor very soon quenches the luminosity of that stage which follows the oscillations and which has been referred to above as the "tail." Now this stage emits bright lines (the arc spectrum) with little or no continuous spectrum. Hence, by arranging two reflectors near the explosion, one can gradually remove from the integrated spectrum all the bright-line emission by merely moving the reflectors closer to the wire, without changing in any way the discharge conditions in the circuit. In fact, all stages between the open-air and the confined explosion can be produced in this way.

A somewhat more interesting series of changes can be produced by introducing self-induction into the circuit when studying open-air explosions. With a fair amount of inductance the continuous spectrum is suppressed entirely, and the spectrum approximates very closely a normal arc spectrum. Reducing the amount of inductance causes the spectrum to change gradually into that of the open-air explosion. In this case, the circuit conditions are changed. The current intensity, and hence the temperature, increases as the inductance is decreased.

Since the confined explosion has a continuous spectrum, it follows that the vapor should be opaque to radiation, unless the spectrum is due to minute solid or liquid particles, as is the case in the flame of a candle. It does not seem likely that the light of the confined explosion can come from solid or liquid particles, for its maximum brightness is equal to that of a black body at a temperature of about 20,000° C. The temperature of the supposed particles would have to be at least this high, and this is obviously impossible. The following experiment was tried, however, to test the point in question. An iron wire was used for the explosion. Close to the wire, but between it and the slit of the spectrograph, was placed a spark-gap with zinc terminals. This gap was connected in series with the wire so that the spark would be exactly simultaneous with the explosion. In a second experiment the arrangement was similar, except that the spark-gap was placed behind the explosion, so that the light from the spark passed through the iron vapor of the explosion on its way to the spectrograph. The exposures were made just sufficient to show the continuous spectrum of the explosion clearly. In the first experiment the bright zinc spark lines were very prominent on the weak continuous spectrum, while in the second no trace of any bright lines could be seen. It was estimated that if 5 per cent of the light from the spark had been transmitted, the strongest zinc lines should have been visible on the spectrogram. It follows that the layer of iron vapor 5 cm in thickness transmitted less than 5 per cent of the light. This gives an absorption coefficient per centimeter of at least 0.6, or a mass absorption coefficient of about 2000, if we take the average density of the iron vapor as $3 \times 10^{-4}$. At 20,000° C. this corresponds to a pressure of about 10 atmospheres. The average density is certainly no higher than this, for the zinc lines reach their greatest brightness in the second, third, and fourth half-cycles, and it is only during the first half-cycle that the pressure can exceed 10 atmospheres.

## DISCUSSION

The following is a general description of what probably takes place during an explosion:

1. The wire is heated, melted, and vaporized while the current through it increases from zero to a few thousand amperes. This part of the process may be followed quite easily by numerical calculation, for all the constants are fairly well known. Such a computation for condenser 2, with an iron wire weighing 1 mg, is plotted as a time-temperature curve in Figure 7. It shows that the wire was completely vaporized $6.4 \times 10^{-7}$ sec. after the beginning of the discharge. The current at this instant was 3,900 amp. Vaporization began at $4.5 \times 10^{-7}$ sec., when the current was 2,800 amp. The maximum possible diameter[1] of the cylinder of vapor at $6.4 \times 10^{-7}$ sec. may be found by assuming that the vapor moved outward during the vapor-

---

[1] It is here assumed that the evaporated particles are neutral atoms or molecules leaving the surface with the average velocity of molecular motion due to temperature. It appears from the photographs discussed in section 4 that in reality the phenome-

ization with the molecular velocity of iron at 2690° C., the boiling-point of iron. This diameter comes out 0.3 mm, and hence the pressure of the vapor would be high—in round numbers, 500 atmospheres. Beyond this point calculation fails, for the conductivity of iron vapor is not known.

2. Shortly after the wire has been completely vaporized the resistance is probably high, especially for metals which vaporize below 3000° C. This is indicated by the fact that the method of the parallel spark-gap works for just these metals. Tungsten, for which that method fails, is probably not completely vaporized until the temperature is well above 5000° C., and at such a high temperature it is probable that the ionization is appreciable, and, hence, that the conductivity is sufficient for the current to flow in spite of the parallel spark-gap.

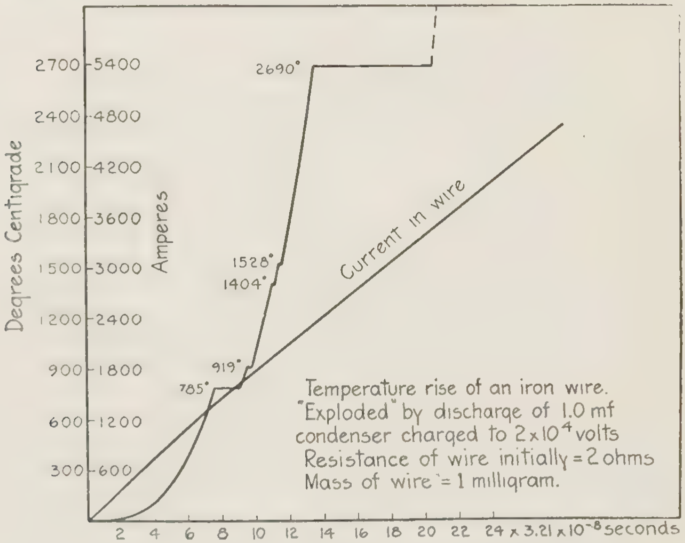

FIG. 7

For most metals, then, the voltage rises sharply immediately

---

non is not so simple as this. The particles forming the "jets" shown on the photographs escape from the wire with velocities up to 2 km per second. Consequently, the cylinder has at first no such regular boundary as assumed in the test, and the pressure is undoubtedly lower than the computed value.

after vaporization is complete. This means a very rapid rise in temperature, since the current is large, and, until the ionization becomes appreciable, the resistance is high. Ionization becomes important when the temperature reaches 10,000° C. From this point on, the resistance diminishes rapidly on account of increasing ionization due to both rising temperature and falling pressure caused by the rapid expansion.

The maximum temperature will be reached when the energy lost by radiation from the surface of the vapor is just equal to the input $i^2r$. Unfortunately, the resistance $r$ is unknown. It is quite certain, however, that a temperature of at least 20,000° C. is reached toward the end of the first quarter-cycle. The radiating area of the vapor may be measured from photographs taken with the rotating-mirror camera, the current is known, and consequently a value of the apparent resistance at this stage can be calculated. The result is in the neighborhood of 0.2 ohm. This includes, of course, the effect of the potential drop at the cold electrodes, which may be appreciable.

3. After the first quarter-cycle, the phenomena may be readily followed with the aid of the rotating-mirror camera. The temperature oscillates, but its trend is steadily downward. The pressure decreases and becomes sensibly equal to that of the surrounding air at the end of the second cycle. (A frequency of $10^5$ cycles is assumed.)

4. The photographs reproduced in Plate XII*j*, *k*, *l*, *m*, *n*, showing the earliest stages of explosions, are somewhat surprising, and suggest that the vaporization of the wire is not such a simple process as was assumed above. Instead of small smooth cylinders, these photographs show a complicated structure consisting chiefly of streamers issuing from the wire.

Two interpretations of the appearance suggest themselves at once: (*a*) that we have to do with a brush discharge from the wire to the air around it; (*b*) that the vapor escapes from the wire in the form of jets irregularly distributed over its surface. Photographs reproduced in Plate XII*m* and *n* show quite clearly that we are not dealing with a brush discharge, for the apparent jets all originate on the flat surface of the ribbons, the edge being quite free from any appearance of a discharge. If it were a brush discharge, practically all the brushes would spring from the edge, and few, if any, from the flat sides. Hence we must conclude that these are real jets of vapor issuing from the wire. A study of all the photographs taken with the magneto-optic shutter shows that the jets appear first at the places where the magnetic field produced by the current in the wire is weakest, for example, on the flat face of a ribbon, or around the outside angle of a wire bent sharply, etc. The intensity of the magnetic field at the surface of a wire when vaporization begins is generally from $10^5$ to $10^6$ gausses. It is easy to see that a charged particle would have some difficulty in escaping from the wire against such a field, but it could have no effect on a neutral atom. These photographs therefore indicate that the particles evaporating from an electrically heated wire at high temperatures are charged when they leave the wire.

Mount Wilson Observatory
September 1926

Contributions from the Mount Wilson Observatory, No. 324
Reprinted from the *Astrophysical Journal*, Vol. LXIV, pp. 321–369, 1926
Printed in the U.S.A.

# EXTRA-GALACTIC NEBULAE

By EDWIN HUBBLE

## ABSTRACT

This contribution gives the results of a statistical investigation of 400 extra-galactic nebulae for which Holetschek has determined total visual magnitudes. The list is complete for the brighter nebulae in the northern sky and is representative to 12.5 mag. or fainter.

*The classification* employed is based on the forms of the photographic images. About 3 per cent are irregular, but the remaining nebulae fall into a sequence of type forms characterized by rotational symmetry about dominating nuclei. The sequence is composed of two sections, the elliptical nebulae and the spirals, which merge into each other.

*Luminosity relations.*—The distribution of magnitudes appears to be uniform throughout the sequence. For each type or stage in the sequence, the total magnitudes are related to the logarithms of the maximum diameters by the formula,

$$m_T = C - 5 \log d ,$$

where $C$ varies progressively from type to type, indicating a variation in diameter for a given magnitude or vice versa. By applying corrections to $C$, the nebulae can be reduced to a standard type, and then a single formula expresses the relation for all nebulae from the Magellanic Clouds to the faintest that can be classified. When the minor diameter is used, the value of $C$ is approximately constant throughout the entire sequence. The coefficient of log $d$ corresponds with the inverse-square law, which suggests that the nebulae are all of the same order of absolute luminosity and that apparent magnitudes are measures of distance. This hypothesis is supported by similar results for the nuclear magnitudes and the magnitudes of the brightest stars involved, and by the small range in luminosities among nebulae whose distances are already known.

*Distances and absolute dimensions.*—The mean absolute visual magnitude, as derived from the nebulae whose distances are known, is $-15.2$. The statistical expression for the distance in parsecs is then

$$\log D = 4.04 + 0.2\, m_T ,$$

where $m_T$ is the total apparent magnitude. This leads to mean values for absolute dimensions at various stages in the sequence of types. Masses appear to be of the order of $2.6 \times 10^8 \odot$.

*Distribution and density of space.*—To apparent magnitude about 16.7, corresponding to an exposure of one hour on fast plates with the 60-inch reflector, the numbers of nebulae to various limits of total magnitude vary directly with the volumes of space represented by the limits. This indicates an approximately uniform density of space, of the order of one nebula per $10^{17}$ cubic parsecs or $1.5 \times 10^{-31}$ in C.G.S. units. The corresponding radius of curvature of the finite universe of general relativity is of the order of $2.7 \times 10^{10}$ parsecs, or about 600 times the distance at which normal nebulae can be detected with the 100-inch reflector.

Recent studies have emphasized the fundamental nature of the division between galactic and extra-galactic nebulae. The relationship is not generic; it is rather that of the part to the whole. Galactic nebulae are clouds of dust and gas mingled with the stars of a particular stellar system; extra-galactic nebulae, at least the most conspicuous of them, are now recognized as systems complete in themselves, and often incorporate clouds of galactic nebulosity as component parts of their organization. Definite evidence as to distances and dimensions is restricted to six systems, including the Magellanic Clouds. The similar nature of the countless fainter nebulae has been inferred from the general principle of the uniformity of nature.

The extra-galactic nebulae form a homogeneous group in which numbers increase rapidly with diminishing apparent size and luminosity. Four are visible to the naked eye;[1] 41 are found on the Harvard "Sky Map";[2] 700 are on the Franklin-Adams plates;[3] 300,000 are estimated to be within the limits of an hour's exposure with the 60-inch reflector.[4] These data indicate a wide range in distance or in absolute dimensions. The present paper, to which is prefaced a general classification of nebulae, discusses such observational material as we now possess in an attempt to determine the relative importance of these two factors, distance and absolute dimensions, in their bearing on the appearance of extra-galactic nebulae.

The classification of these nebulae is based on structure, the individual members of a class differing only in apparent size and luminosity. It is found that for the nebulae in each class these characteristics are related in a manner which closely approximates the operation of the inverse-square law on comparable objects. The presumption is that dispersion in absolute dimensions is relatively unimportant, and hence that in a statistical sense the apparent dimensions represent relative distances. The relative distances can be reduced to absolute values with the aid of the nebulae whose distances are already known.

## PART I. CLASSIFICATION OF NEBULAE

### GENERAL CLASSIFICATION

The classification used in the present investigation is essentially the detailed formulation of a preliminary classification published in a previous paper.[1] It was developed in 1923, from a study of photographs of several thousand nebulae, including practically all the brighter objects and a thoroughly representative collection of the fainter ones.[2] It is based primarily on the structural forms of photographic images, although the forms divide themselves naturally into two groups: those found in or near the Milky Way and those in moderate or high galactic latitudes. In so far as possible, the system is independent of the orientation of the objects in space. With minor changes in the original notation, the complete classification is as follows, although only the extra-galactic division is here discussed in detail:

---

[1] These are the two Magellanic Clouds, M 31, and M 33.

[2] Bailey, *Harvard Annals*, **60**, 1908.

[3] Hardcastle, *Monthly Notices*, **74**, 699, 1914.

[4] This estimate by Seares is based on a revision of Fath's counts of nebulae in Selected Areas (*Mt. Wilson Contr.*, No. 297; *Astrophysical Journal*, **62**, 168, 1925).

CLASSIFICATION OF NEBULAE

| I. Galactic nebulae: | Symbol | Example |
|---|---|---|
| A. Planetaries | P | N.G.C. 7662 |
| B. Diffuse | D | .............. |
| 1. Predominantly luminous | DL | N.G.C. 6618 |
| 2. Predominantly obscure | DO | Barnard 92 |
| 3. Conspicuously mixed | DLO | N.G.C. 7023 |
| II. Extra-galactic nebulae: | | |
| A. Regular: | | |
| 1. Elliptical ($n=1, 2, \ldots, 7$ indicates the ellipticity of the image without the decimal point) | E$n$ | N.G.C. 3379 E0<br>221 E2<br>4621 E5<br>3115 E7 |

---

[1] "A General Study of Diffuse Galactic Nebulae," *Mt. Wilson Contr.*, No. 241; *Astrophysical Journal*, **56**, 162, 1922.

[2] The classification was presented in the form of a memorandum to the Commission on Nebulae of the International Astronomical Union in 1923. Copies of the memorandum were distributed by the chairman to all members of the Commission. The classification was discussed at the Cambridge meeting in 1925, and has been published in an account of the meeting by Mrs. Roberts in *L'Astronomie*, **40**, 169, 1926. Further consideration of the matter was left to a subcommittee, with a resolution that the adopted system should be as purely descriptive as possible, and free from any terms suggesting order of physical development (*Transactions of the I.A.U.*, **2**, 1925). Mrs. Roberts' report also indicates the preference of the Commission for the term "extra-galactic" in place of the original, and then necessarily non-committal, "non-galactic."

Meanwhile K. Lundmark, who was present at the Cambridge meeting and has since been appointed a member of the Commission, has recently published (*Arkiv för Matematik, Astronomi och Fysik, Band 19B*, No. 8, 1926) a classification, which, except for nomenclature, is practically identical with that submitted by me. Dr. Lundmark makes no acknowledgments or references to the discussions of the Commission other than those for the use of the term "galactic."

CLASSIFICATION OF NEBULAE—*Continued*

| 2. Spirals: | Symbol | Example |
|---|---|---|
| *a*) Normal spirals | S | .............. |
| (1) Early | Sa | N.G.C. 4594 |
| (2) Intermediate | Sb | 2841 |
| (3) Late | Sc | 5457 |
| *b*) Barred spirals | SB | .............. |
| (1) Early | SBa | N.G.C. 2859 |
| (2) Intermediate | SBb | 3351 |
| (3) Late | SBc | 7479 |
| B. Irregular | Irr | N.G.C. 4449 |

Extra-galactic nebulae too faint to be classified are designated by the symbol "Q."

### REGULAR NEBULAE

The characteristic feature of extra-galactic nebulae is rotational symmetry about dominating non-stellar nuclei. About 97 per cent of these nebulae are regular in the sense that they show this feature conspicuously. The regular nebulae fall into a progressive sequence ranging from globular masses of unresolved nebulosity to widely open spirals whose arms are swarming with stars. The sequence comprises two sections, elliptical nebulae and spirals, which merge into each other.

Although deliberate effort was made to find a descriptive classification which should be entirely independent of theoretical considerations, the results are almost identical with the path of development derived by Jeans[1] from purely theoretical investigations. The agreement is very suggestive in view of the wide field covered by the data, and Jeans's theory might have been used both to interpret the observations and to guide research. It should be borne in mind, however, that the basis of the classification is descriptive and entirely independent of any theory.

*Elliptical nebulae.*—These give images ranging from circular through flattening ellipses to a limiting lenticular figure in which the ratio of the axes is about 1 to 3 or 4. They show no evidence of resolution,[2] and the only claim to structure is that the luminosity

---

[1] *Problems of Cosmogony and Stellar Dynamics*, 1919.

[2] N.G.C. 4486 (M 87) may be an exception. On the best photographs made with the 100-inch reflector, numerous exceedingly faint images, apparently of stars, are found around the periphery. It was among these that Belanowsky's nova of 1919 appeared. The observations are described in *Publications of the Astronomical Society of the Pacific*, **35**, 261, 1923.

PLATE XIV

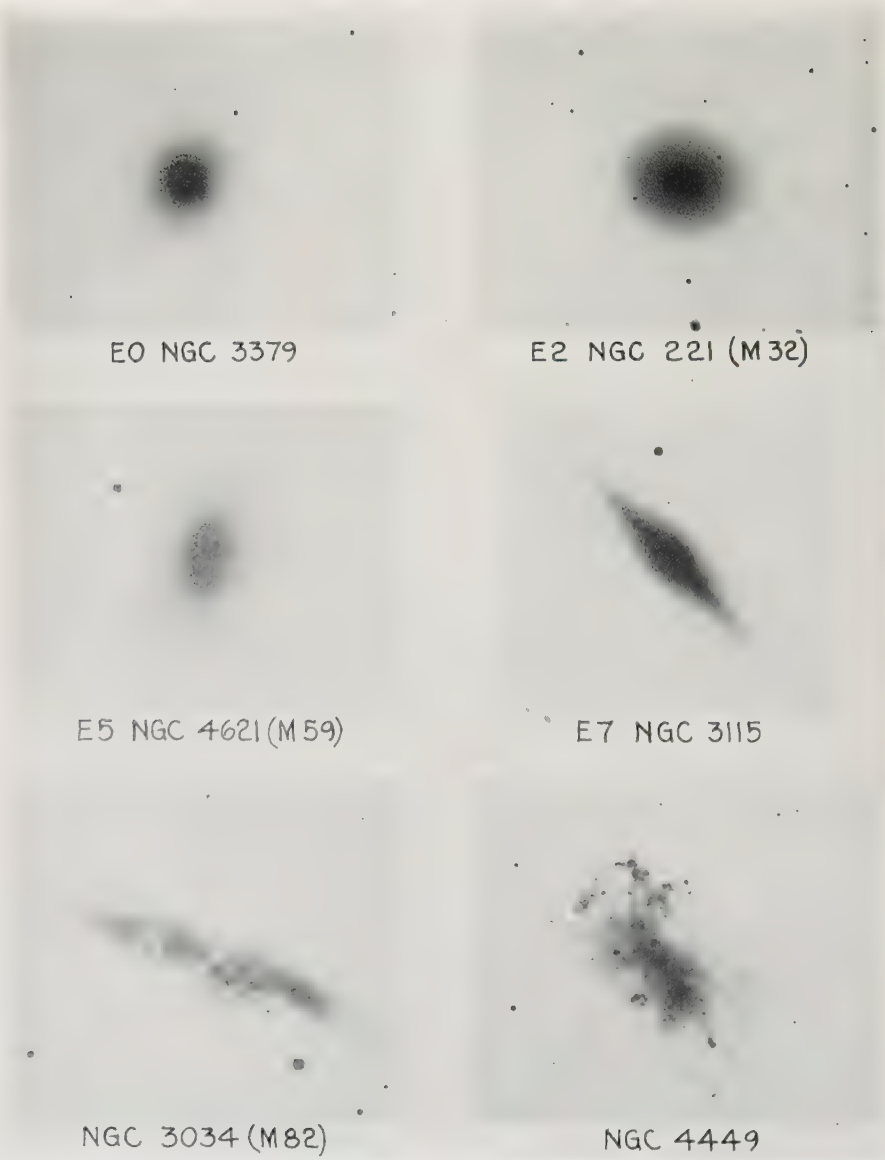
E0 NGC 3379

E2 NGC 221 (M 32)

E5 NGC 4621 (M 59)

E7 NGC 3115

NGC 3034 (M 82)

NGC 4449

Elliptical and Irregular Nebulae

fades smoothly from bright nuclei to indefinite edges. Diameters are functions of the nuclear brightness and the exposure times.

The only criterion available for further classification appears to be the degree of elongation. Elliptical nebulae have accordingly been designated by the symbol "E," followed by a single figure, numerically equal to the ellipticity $(a-b)/a$ with the decimal point omitted. The complete series is E0, E1, . . . . , E7, the last representing a definite limiting figure which marks the junction with the spirals.

The frequency distribution of ellipticities shows more round or nearly round images than can be accounted for by the random orientation of disk-shaped objects alone. It is presumed, therefore, that the images represent nebulae ranging from globular to lenticular, oriented at random. No simple method has yet been established for differentiating the actual from the projected figure of an individual object, although refined investigation furnishes a criterion in the relation between nuclear brightness and maximum diameters. For the present, however, it must be realized that any list of nebulae having a given apparent ellipticity will include a number of tilted objects having greater actual ellipticities. The statistical average will be too low, except for E7, and the error will increase with decreasing ellipticity.

*Normal spirals.*—All regular nebulae with ellipticities greater than about E7 are spirals, and no spirals are known with ellipticities less than this limit. At this point in the sequence, however, ellipticity becomes insensitive as a criterion and is replaced by conspicuous structural features which now become available for classification. Of these, practically speaking, there are three which fix the position of an object in the sequence of forms: (1) relative size of the unresolved nuclear region; (2) extent to which the arms are unwound; (3) degree of resolution in the arms. The form most nearly related to the elliptical nebulae has a large nuclear region similar to E7, around which are closely coiled arms of unresolved nebulosity. Then follow objects in which the arms appear to build up at the expense of the nuclear regions and unwind as they grow; in the end, the arms are wide open and the nuclei inconspicuous. Early in the series the arms begin to break up into condensations, the resolution commencing in the outer regions and working inward until in the final stages it reaches the nucleus itself. In the larger spirals where critical observations are possible, these condensations are found to be actual stars and groups of stars.

The structural transition is so smooth and continuous that the selection of division points for further classification is rather arbitrary. The ends of the series are unmistakable, however, and, in a general way, it is possible to differentiate a middle group. These three groups are designated by the non-committal letters "a," "b," and "c" attached to the spiral symbols "S," and, with reference to their position in the sequence, are called "early," "intermediate," and "late" types.[1] A more precise subdivision, on a decimal scale for example, is not justified in the present state of our knowledge.

In the early types, the group Sa, most of the nebulosity is in the nuclear region and the arms are closely coiled and unresolved. N.G.C. 3368 and 4274 are among the latest of this group.

The intermediate group, Sb, includes objects having relatively large nuclear regions and thin rather open arms, as in M 81, or a smaller nuclear region with closely coiled arms, as in M 94. These two nebulae represent the lateral extension of the sequence in the intermediate section. The extension along the sequence is approximately represented by N.G.C. 4826, among the earliest of the Sb, and N.G.C. 3556 and 7331, which are among the latest. The resolution in the arms is seldom conspicuous, although in M 31, a typical Sb, it is very pronounced in the outer portions.

---

[1] "Early" and "late," in spite of their temporal connotations, appear to be the most convenient adjectives available for describing relative positions in the sequence. This sequence of structural forms is an observed phenomenon. As will be shown later in the discussion, it exhibits a smooth progression in nuclear luminosity, surface brightness, degree of flattening, major diameters, resolution, and complexity. An antithetical pair of adjectives denoting relative positions in the sequence is desirable for many reasons, but none of the progressive characteristics are well adapted for the purpose. Terms which apply to series in general are available, however, and of these "early" and "late" are the most suitable. They can be assumed to express a progression from simple to complex forms.

An accepted precedent for this usage is found in the series of stellar spectral types. There also the progression is assumed to be from the simple to the complex, and in view of the great convenience of the terms "early" and "late," the temporal connotations, after a full consideration of their possible consequences, have been deliberately disregarded.

PLATE XV

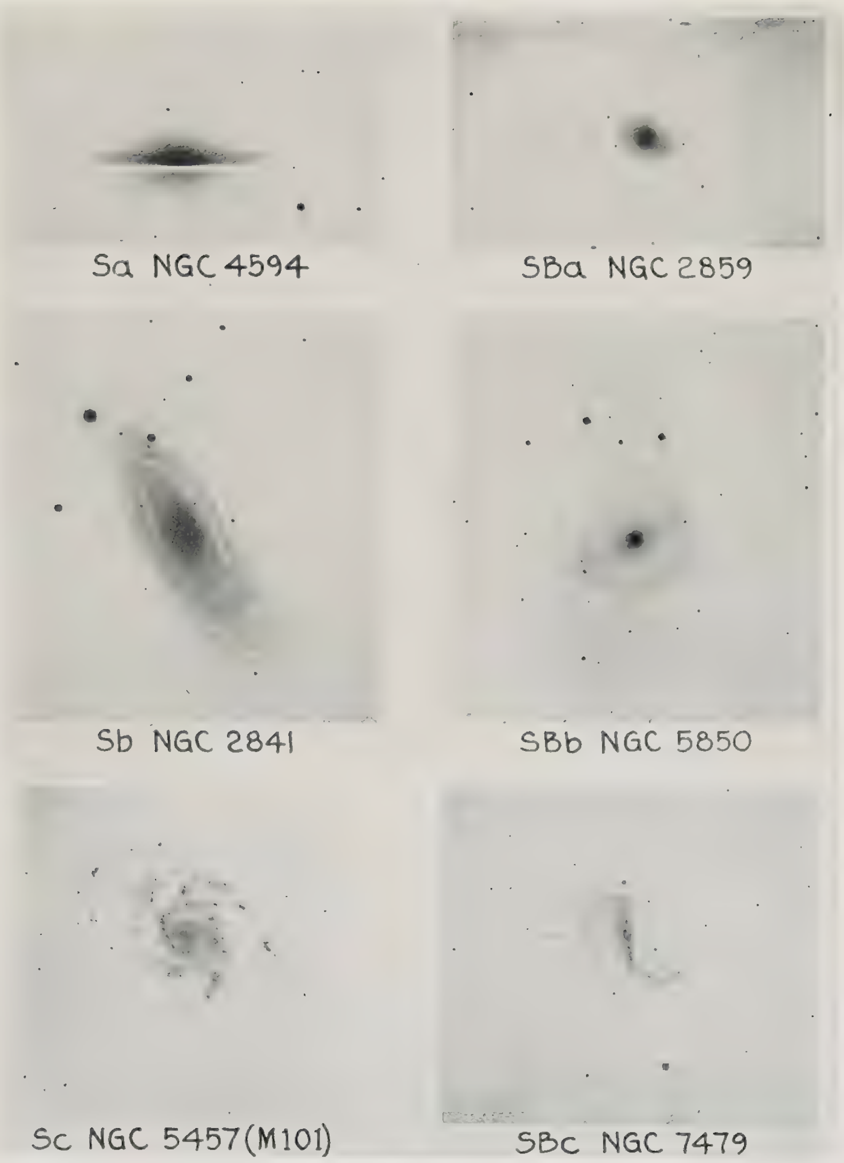

Sa NGC 4594

SBa NGC 2859

Sb NGC 2841

SBb NGC 5850

Sc NGC 5457 (M101)

SBc NGC 7479

NORMAL AND BARRED SPIRALS

The characteristics of the late types, the group Sc, are more definite—an inconspicuous nucleus and highly resolved arms. Individual stars cannot be seen in the smaller nebulae of this group, but knots are conspicuous, which, in larger objects, are known to be groups and clusters of stars. The extent to which the arms are opened varies from M 33 to M 101, both typical Sc nebulae.

*Barred spirals.*—In the normal spiral the arms emerge from two opposite points on the periphery of the nuclear region. There is, however, a smaller group, containing about 20 per cent of all spirals, in which a bar of nebulosity extends diametrically across the nucleus. In these spirals, the arms spring abruptly from the ends of this bar. These nebulae also form a sequence, which parallels that of the normal spirals, the arms apparently unwind, the nuclei dwindle, the condensations form and work inward.

H. D. Curtis[1] first called attention to these nebulae when he described several in the intermediate stages of the series and called them $\phi$-type spirals. The bar, however, never extends beyond the inner spiral arms, and the structure, especially in the early portion of the sequence, is more accurately represented by the Greek letter $\theta$. From a dynamical point of view, the distinction has considerable significance. Since Greek letters are inconvenient for cataloguing purposes, the English term, "barred spiral," is proposed, which can be contracted to the symbol "SB."

The SB series, like that of the normal spirals, is divided into three roughly equal sections, distinguished by the appended letters "a," "b," and "c." The criteria on which the division is based are similar in general to those used in the classification of the normal spirals. In the earliest forms, SBa, the arms are not differentiated, and the pattern is that of a circle crossed by a bar, or, as has been mentioned, that of the Greek letter $\theta$. When the bar is oriented nearly in the line of sight, it appears foreshortened as a bright and definite minor axis of the elongated nebular image. Such curious forms as the images of N.G.C. 1023 and 3384 are explained in this manner. The latest group, SBc, is represented by the S-shaped spirals such as N.G.C. 7479.

---

[1] *Publications of the Lick Observatory*, **13**, 12, 1918.

### IRREGULAR NEBULAE

About 3 per cent of the extra-galactic nebulae lack both dominating nuclei and rotational symmetry. These form a distinct class which can be termed "irregular." The Magellanic Clouds are the most conspicuous examples, and, indeed, are the nearest of all the extra-galactic nebulae. N.G.C. 6822, a curiously faithful miniature of the Clouds, serves to bridge the gap between them and the smaller objects, such as N.G.C. 4214 and 4449. In these latter, a few individual stars emerge from an unresolved background, and occasional isolated spots give the emission spectrum characteristic of diffuse nebulosity in the galactic system, in the Clouds, and in N.G.C. 6822.[1] These features are found in other irregular nebulae as well, notably in N.G.C. 1156 and 4656, and are just those to be expected in systems similar to the Clouds but situated at increasingly greater distances.

The system outlined above is primarily for the formal classification of photographic images obtained with large reflectors and portrait lenses. For each instrument, however, there is a limiting size and luminosity below which it is impossible to classify with any confidence. Except in rare instances, these small nebulae are extra-galactic, and their numbers, brightness, dimensions, and distribution are amenable to statistical investigation. For cataloguing purposes, they require a designating symbol, and the letter "Q" is suggested as convenient and not too widely used with other significations.

## PART II. STATISTICAL STUDY OF EXTRA-GALACTIC NEBULAE

### THE DATA

The most homogeneous list of nebulae for statistical study is that compiled by Hardcastle[2] containing all nebulae found on the Franklin-Adams charts. These are uniform exposures of two hours on fast plates made with a Cooke astrographic lens of 10-inch aperture and 45-inch focal length. The scale is 1 mm = 3′. The entire sky is cov-

---

[1] $H\beta$ is brighter than $N_2$. Patches with similar spectra are often found in the arms of late-type spirals—N.G.C. 253, M 33, M 101. The typical planetary spectrum, where $H\beta$ is fainter than $N_2$, is found in the rare cases of apparently stellar nuclei of spirals; for instance, in N.G.C. 1068, 4051, and 4151. Here also the emission spectra are localized and do not extend over the nebulae.

[2] *Monthly Notices*, 74, 699, 1914.

PLATE XVI

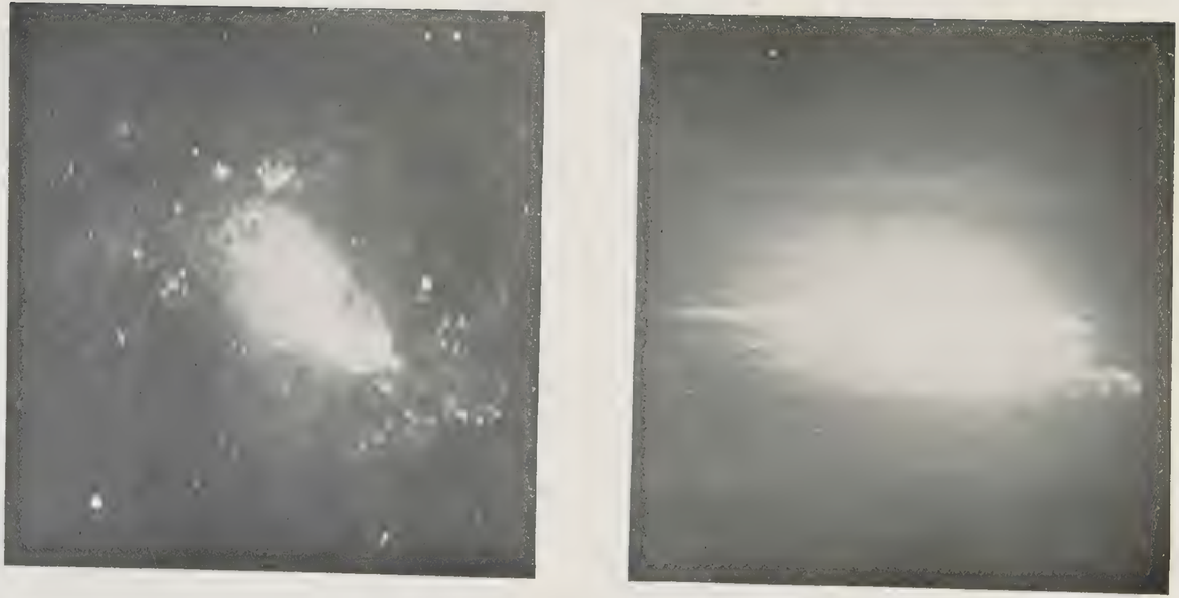

Irregular Nebula N.G.C. 4214

Direct photograph with 100-inch reflector March 18, 1925. Scale 1 mm = $3''.3$
Slitless spectrogram at primary focus of 100-inch reflector, March 19, 1925

ered, but since the plates are centered about 15° apart and the definition decreases very appreciably with distance from the optical axis, the material is not strictly homogeneous. Moreover, the published list suffers from the usual errors attendant on routine cataloguing; for instance, four conspicuous Messier nebulae, M 60, M 87, M 94, and M 101, are missing. In general, however, the list is thoroughly representative down to about the thirteenth photographic magnitude and very few conspicuous objects are overlooked. It plays the rôle of a standard with which other catalogues of the brighter nebulae may be compared for completeness, and numbers in limited areas may be extended to the entire sky.

When known galactic nebulae, clusters, and the objects in the Magellanic Clouds are weeded out, the remaining 700 nebulae may be treated as extra-galactic. Very few can be classified from the Franklin-Adams plates; for this purpose photographs on a much larger scale are required. Until further data on the individual objects are available, Hardcastle's list can be used only for the study of distribution over the sky. This shows the well-known features—the greater density in the northern galactic hemisphere, the concentration in Virgo, and the restriction of the very large nebulae to the southern galactic hemisphere.

Fortunately, numerical data do exist in the form of total visual magnitudes for many of the nebulae in the northern sky. These determinations were made by Holetschek,[1] who attempted to observe all nebulae within reach of his 6-inch refractor. He later restricted his program; but the final list is reasonably complete for the more conspicuous nebulae north of declination −10°, and is representative down to visual magnitude about 12.5. Out of 417 extra-galactic nebulae in Holetschek's list, 408 are north of −10°, as compared with 400 in Hardcastle's. The two lists agree very well for the brighter objects, but diverge more and more with decreasing luminosity. At the twelfth magnitude about half of Holetschek's nebulae are included by Hardcastle. Since the two lists compare favorably in completeness over so large a region of the sky, Holetschek's may be chosen as the basis for a statistical study and advantage taken of the valuable numerical data on total luminosities.

---

[1] *Annalen der Wiener Sternwarte*, **20**, 1907.

Hopmann[1] has revised the scale of magnitudes by photometric measures of the comparison stars used by Holetschek. New magnitudes were thus obtained for 85 individual nebulae and from these were derived mean correction tables applicable to the entire list. The revised magnitudes are used throughout the following discussion. Hopmann's corrections extend to about 12.0 mag., and have been extrapolated on the assumption that they are constant for the fainter magnitudes. The errors involved are unimportant in view of selective effects which must be present among the observed objects near the limit of visibility.

The nebulae were classified and their diameters measured from photographs of about 300 of them taken with the 60-inch and 100-inch reflectors at Mount Wilson. Most of the others are included in the great collection of nebular photographs at Mount Hamilton, which have been described by Curtis;[2] and, through the courtesy of the Director of the Lick Observatory, it has been possible to confirm the classification inferred from the published description by actual inspection of the original negatives.

Types, diameters, and total visual magnitudes are thus available for some 400 of the nebulae in Holetschek's list. The few unclassified objects are all fainter than 12.5 mag. The data are listed in Tables I–IV, in which the N.G.C. numbers, the total magnitudes, and the logarithms of the maximum diameters in minutes of arc are given for each type separately. A summary is given in Table V, in which the relative frequencies and the mean magnitudes of the various types will be found.

### RELATIVE LUMINOSITIES OF THE VARIOUS TYPES

The frequency distribution of magnitudes for all types together and for the elliptical nebulae and the spirals separately is shown in Table VI and Figure 1. With the exception of the two outstanding spirals, M 31 and M 33, the apparent luminosities are about uniformly distributed among the different types. The relative numbers of the elliptical nebulae as compared with the spirals decrease somewhat with decreasing luminosity, but this is very probably an effect

---

[1] *Astronomische Nachrichten*, **214**, 425, 1921.

[2] *Publications of the Lick Observatory*, **13**, 1918.

## TABLE I

### Elliptical Nebulae

| N.G.C. | $m_T$ | log *d* |
|---|---|---|
| E0 (17) | | |
| 404 | 11.1 | +0.11 |
| 474 | 12.6 | − .40 |
| 1407 | 10.9 | .15 |
| 3348 | 11.8 | − .15 |
| 3379* | 9.4 | + .30 |
| 4283 | 12.2 | − .52 |
| 4486* | 9.7 | + .30 |
| 4494* | 10.1 | − .15 |
| 4552* | 9.9 | + .23 |
| 4589 | 11.4 | − .30 |
| 4648 | 12.3 | .52 |
| 5044 | 11.8 | .30 |
| 5216 | 13.3 | .70 |
| 5273 | 12.1 | .52 |
| 5557 | 12.3 | .40 |
| 5812 | 12.0 | − .40 |
| 5846 | 10.9 | 0.0 |
| Mean | 11.40 | −0.204 |
| E1 (13) | | |
| 467 | 13.0 | −0.70 |
| 596 | 11.8 | .22 |
| 1400 | 11.1 | .22 |
| 2880 | 12.0 | .52 |
| 3226 | 12.0 | .10 |
| 3962 | 11.8 | − .30 |
| 4278* | 10.8 | .0 |
| 4374* | 9.9 | + .08 |
| 4472 | 8.8 | + .30 |
| 4478 | 11.5 | − .10 |
| 4636 | 10.9 | + .08 |
| 5813 | 12.6 | − .30 |
| 7626 | 12.3 | −0.30 |
| Mean | 11.43 | −0.177 |
| E2 (14) | | |
| 221* | 8.8 | +0.42 |
| 1453 | 11.9 | − .10 |
| 2672 | 12.8 | − .40 |
| 3193 | 12.1 | 0.0 |
| E2 —*Continued* | | |
| 3599 | 12.0 | −0.30 |
| 3608 | 11.6 | .22 |
| 3640 | 11.1 | − .05 |
| 4261 | 11.1 | + .20 |
| 4291 | 12.3 | − .52 |
| 4377 | 11.9 | − .05 |
| 4406* | 10.0 | + .30 |
| 4476 | 12.8 | − .30 |
| 4649* | 9.5 | + .30 |
| 5127 | 13.3 | −0.52 |
| Mean | 11.52 | −0.088 |
| E3 (10) | | |
| 1052 | 11.8 | −0.15 |
| 1600 | 12.7 | + .17 |
| 3222 | 13.3 | − .15 |
| 4319 | 12.8 | − .52 |
| 4365 | 11.4 | + .04 |
| 4386 | 12.3 | − .52 |
| 5322* | 9.6 | + .15 |
| 5982 | 11.4 | .0 |
| 7562 | 12.8 | − .22 |
| 7619 | 11.8 | −0.15 |
| Mean | 11.99 | −0.133 |
| E4 (13) | | |
| 584 | 10.9 | +0.30 |
| 1700 | 12.5 | − .10 |
| 2974 | 11.8 | .15 |
| 3605 | 12.5 | − .52 |
| 3610 | 11.8 | + .15 |
| 3894 | 12.8 | − .05 |
| 4125* | 10.3 | + .30 |
| 4378 | 12.1 | − .15 |
| 4382* | 10.0 | + .48 |
| 4551 | 12.8 | + .04 |
| 4742 | 12.3 | .0 |
| 5576 | 12.3 | − .15 |
| 7454 | 13.3 | 0.0 |
| Mean | 11.95 | −0.011 |

TABLE I—*Continued*

| N.G.C. | $m_T$ | log *d* |
|---|---|---|
| E5 (6) | | |
| 720 | 10.9 | +0.11 |
| 2693 | 12.3 | − .15 |
| 3377 | 10.9 | + .17 |
| 4473 | 10.3 | .11 |
| 4621* | 10.0 | + .30 |
| 4660 | 11.4 | 0.0 |
| Mean | 10.97 | +0.090 |
| E6 (7) | | |
| 821 | 11.8 | 0.0 |
| 2768 | 10.7 | + .18 |
| 3613 | 11.8 | .25 |
| 4179 | 11.8 | .34 |
| 4435* | 10.5 | .11 |
| 4546* | 10.3 | .18 |
| 4697* | 9.6 | +0.48 |
| Mean | 10.93 | +0.220 |
| E7 (5) | | |
| 3115* | 9.5 | +0.60 |
| 4111 | 10.1 | .54 |
| 4270 | 12.1 | .0 |
| 4570 | 11.1 | .38 |
| 5308 | 12.3 | +0.28 |
| Mean | 11.02 | +0.360 |
| Peculiar (8) | | |
| 185 | 12.3 | +0.48 |
| 205* | 9.3 | .90 |
| 524† | 11.9 | .41 |
| 3607‡ | 9.9 | .11 |
| 3998† | 12.1 | + .23 |
| 4459‡ | 11.3 | − .22 |
| 5485‡ | 12.3 | .05 |
| 5739 | 13.3 | −0.40 |

of selection. The elliptical nebulae are more compact than the spirals and become more stellar with decreasing luminosity. For this reason some of the fainter nebulae are missed when small-scale instruments are used, although the same luminosity spread over a larger area would still be easily detected. The effect is very pronounced on photographic plates. It accounts also for the slightly brighter mean magnitude of the elliptical nebulae as compared with the spirals in Table V.

The various types are homogeneously distributed over the sky, their spectra are similar, and the radial velocities are of the same general order. These facts, together with the equality of the mean magnitudes and the uniform frequency distribution of magnitudes, are consistent with the hypothesis that the distances and absolute luminosities as well are of the same order for the different types. This is an assumption of considerable importance, but unfortunately it cannot yet be subjected to positive and definite tests. None of the individual similarities necessarily implies the adopted interpretation, but the totality of them, together with the intimate series relations among the types, which will be discussed later, suggests it as the most reasonable working hypothesis, at least until inconsistencies should appear.

TABLE II

Barred Spirals

| N.G.C. | $m_T$ | log *d* |
|---|---|---|
| SBa (26) | | |
| 936 | 11.1 | +0.48 |
| 1023* | 10.2 | .78 |
| 2732 | 12.3 | .11 |
| 2781 | 12.3 | .11 |
| 2787 | 11.4 | .36 |
| 2859 | 11.1 | .28 |
| 2950 | 11.6 | .15 |
| 3384* | 10.7 | .48 |
| 3412* | 11.2 | + .40 |
| 3418 | 13.1 | .0 |
| 3458 | 12.8 | − .22 |
| 3945 | 11.5 | + .20 |
| 4026 | 11.1 | .48 |
| 4203 | 11.1 | .36 |
| 4346 | 12.0 | .20 |
| 4371 | 12.0 | .18 |
| 4421 | 12.8 | .17 |
| 4442 | 10.9 | .50 |
| 4477 | 10.9 | .40 |
| 4596 | 12.0 | .25 |
| 4643 | 11.1 | .26 |
| 4754 | 10.9 | .48 |
| 5473 | 12.0 | + .08 |
| 5574 | 13.0 | − .05 |
| 5689 | 12.0 | + .30 |
| 5701 | 12.3 | +0.17 |
| Mean | 11.66 | +0.267 |
| SBb (16) | | |
| 1022 | 11.8 | +0.04 |
| 2650 | 12.8 | .0 |
| 3351* | 11.4 | + .48 |
| 3400 | 12.5 | − .10 |
| 3414 | 11.5 | + .26 |
| 3504 | 11.4 | .30 |
| 3718 | 11.8 | +0.48 |
| SBb—*Continued* | | |
| 4102 | 12.0 | +0.36 |
| 4245 | 11.1 | .15 |
| 4394 | 11.5 | .60 |
| 4548 | 11.1 | .60 |
| 4699* | 10.0 | .57 |
| 4725* | 9.2 | .70 |
| 5218 | 12.8 | .25 |
| 5566 | 11.1 | .20 |
| 7723 | 11.8 | +0.18 |
| Mean | 11.48 | +0.317 |
| SBc (15) | | |
| 613 | 10.6 | +0.60 |
| 779 | 12.1 | .48 |
| 3206 | 13.3 | .45 |
| 3344 | 11.4 | .60 |
| 3346 | 12.3 | .40 |
| 3625 | 13.3 | .0 |
| 3686 | 12.0 | .30 |
| 3769 | 12.8 | .43 |
| 3953 | 11.1 | .74 |
| 3992 | 11.5 | .85 |
| 4303* | 10.6 | .78 |
| 4579* | 9.7 | .45 |
| 5383 | 12.6 | .40 |
| 5921 | 12.8 | .70 |
| 7479 | 12.1 | +0.48 |
| Mean | 11.87 | +0.509 |
| Peculiar (2) | | |
| 2782 | 12.3 | +0.26 |
| 4314 | 11.1 | +0.34 |

### RELATION BETWEEN LUMINOSITIES AND DIAMETERS

Among the nebulae of each separate type are found linear correlations between total magnitudes and logarithms of diameters. These

## TABLE III

### NORMAL SPIRALS

| N.G.C. | $m_T$ | log *d* | N.G.C. | $m_T$ | log *d* |
|---|---|---|---|---|---|
| Sa (49) | | | | | |
| 488 | 11.8 | +0.48 | 4281 | 11.5 | +0.18 |
| 676 | 13.3 | .30 | 4429 | 11.5 | .48 |
| 1332 | 10.9 | .43 | 4452 | 12.6 | .15 |
| 2655 | 11.1 | .60 | 4526 | 11.1 | .70 |
| 2681 | 10.7 | .48 | 4550 | 12.1 | .43 |
| 2775 | 10.9 | .32 | 4570 | 11.1 | .38 |
| 2811 | 12.3 | .28 | 4594 | 9.1 | .85 |
| 2855 | 12.8 | .11 | 4665 | 11.8 | + .08 |
| 3169§ | 12.3 | .60 | 4684 | 12.2 | − .22 |
| 3245 | 11.8 | .30 | 4698 | 11.9 | + .43 |
| 3301 | 12.4 | .15 | 4710 | 11.8 | .54 |
| 3368* | 10.0 | .85 | 4762 | 11.5 | .57 |
| 3516 | 12.1 | .20 | 4866 | 12.0 | .50 |
| 3619 | 12.3 | .0 | 4958 | 11.4 | .60 |
| 3626* | 11.3 | .28 | 5377 | 11.8 | .48 |
| 3665 | 12.0 | .0 | 5389 | 12.5 | .25 |
| 3682 | 12.1 | .08 | 5422 | 12.1 | + .40 |
| 3898 | 12.0 | .43 | 5631 | 12.0 | − .05 |
| 3941 | 10.3 | .30 | 5866* | 11.7 | + .48 |
| 4036 | 10.9 | .60 | 7013 | 12.8 | .08 |
| 4138 | 12.1 | .20 | 7457 | 12.8 | .30 |
| 4143 | 11.3 | .11 | 7727 | 11.3 | .43 |
| 4150 | 12.0 | .11 | 7814* | 11.4 | +0.48 |
| 4251 | 10.4 | .26 | | | |
| 4268 | 12.8 | .0 | Mean | 11.69 | +0.333 |
| 4274 | 11.1 | +0.54 | | | |
| Sb (70) | | | | | |
| 224 | 5.0 | +2.25 | 3556 | 11.1 | +0.90 |
| 672 | 12.8 | 0.54 | 3593 | 11.9 | .60 |
| 772 | 11.1 | .70 | 3623* | 9.9 | .90 |
| 949 | 13.3 | .0 | 3627* | 9.1 | 0.90 |
| 955 | 12.9 | .40 | 3628§ | 11.4 | +1.08 |
| 1068 | 9.1 | .40 | 3632 | 13.3 | −0.10 |
| 1309 | 12.0 | .15 | 3675 | 11.4 | + .48 |
| 2639 | 12.2 | .0 | 3681 | 13.0 | .0 |
| 2715 | 12.5 | .40 | 3684 | 13.0 | + .08 |
| 2748 | 12.0 | .32 | 3895 | 13.3 | − .05 |
| 2841* | 9.4 | .78 | 3900 | 12.1 | + .25 |
| 2985 | 11.4 | 0.48 | 3938 | 12.1 | .65 |
| 3031* | 8.3 | +1.20 | 4020 | 12.3 | .17 |
| 3182 | 12.9 | −0.22 | 4030 | 11.1 | .30 |
| 3190 | 11.9 | + .48 | 4051* | 11.9 | .60 |
| 3227 | 12.0 | .48 | 4085 | 12.5 | .36 |
| 3277 | 12.6 | .0 | 4151 | 12.0 | .40 |
| 3310 | 10.4 | + .18 | 4192 | 10.9 | .90 |
| 3380 | 12.1 | − .05 | 4216* | 10.8 | 0.85 |
| 3489* | 11.2 | +0.40 | 4244§ | 12.3 | +1.11 |

TABLE III—*Continued*

| N.G.C. | $m_T$ | log *d* | N.G.C. | $m_T$ | log *d* |
|---|---|---|---|---|---|
| | | Sb—*Continued* | | | |
| 4258* | 8.7 | +1.30 | 5394 | 13.3 | +0.17 |
| 4273 | 11.8 | 0.20 | 5633 | 13.0 | − .10 |
| 4438* | 10.3 | .54 | 5713 | 12.3 | + .32 |
| 4448 | 11.8 | .48 | 5740 | 12.3 | .48 |
| 4450 | 10.6 | + .57 | 5746 | 10.4 | .87 |
| 4451 | 12.8 | − .15 | 5750 | 12.8 | .15 |
| 4500 | 12.8 | +0.17 | 5772 | 12.0 | .25 |
| 4565*§ | 11.0 | 1.17 | 5806 | 12.3 | .30 |
| 4736* | 8.4 | 0.70 | 5985 | 12.0 | .60 |
| 4750 | 11.8 | .26 | 6207 | 11.8 | .30 |
| 4800 | 11.8 | .04 | 6643 | 11.9 | .48 |
| 4814 | 12.7 | .56 | 7331* | 10.4 | .95 |
| 4826 | 9.0 | .90 | 7541 | 12.7 | .41 |
| 5055* | 9.6 | .90 | 7606 | 12.0 | +0.78 |
| 5376 | 12.8 | + .17 | | | |
| 5379 | 12.9 | −0.05 | Mean | 11.55 | +0.471 |
| | | Sc (115) | | | |
| 157 | 11.4 | +0.40 | 3395 | 12.6 | +0.11 |
| 253 | 9.3 | 1.34 | 3396 | 13.3 | − .10 |
| 278 | 12.0 | 0.08 | 3430 | 12.6 | + .49 |
| 470 | 13.1 | 0.20 | 3432 | 12.0 | .79 |
| 598 | 7.0 | 1.78 | 3437 | 12.4 | .28 |
| 615 | 12.3 | 0.43 | 3445 | 13.1 | .08 |
| 628* | 10.6 | .90 | 3448 | 12.3 | .26 |
| 908 | 11.9 | .60 | 3486 | 11.8 | .58 |
| 1084 | 11.4 | .34 | 3488 | 12.8 | .25 |
| 1087 | 12.1 | .36 | 3512 | 12.3 | .0 |
| 1637 | 12.6 | .48 | 3521* | 10.1 | .65 |
| 2339 | 13.1 | 0.28 | 3549 | 13.3 | .43 |
| 2403* | 8.7 | 1.20 | 3596 | 13.3 | .60 |
| 2532 | 13.3 | 0.17 | 3631 | 11.8 | .66 |
| 2683 | 9.9 | 1.00 | 3642 | 12.0 | .73 |
| 2712 | 12.3 | 0.20 | 3655 | 11.9 | .04 |
| 2742 | 11.8 | .40 | 3666 | 11.8 | .54 |
| 2776 | 12.3 | 0.34 | 3672 | 13.0 | .54 |
| 2903* | 9.1 | 1.04 | 3683 | 12.0 | .15 |
| 2964 | 11.6 | 0.40 | 3780 | 13.0 | .40 |
| 2976 | 12.0 | .50 | 3810 | 11.3 | .62 |
| 3003§ | 13.3 | .78 | 3813 | 12.3 | .32 |
| 3021 | 12.3 | .11 | 3877 | 11.8 | .64 |
| 3079§ | 12.0 | .90 | 3887 | 12.3 | .40 |
| 3147 | 11.4 | .30 | 3893 | 11.8 | .61 |
| 3166 | 12.0 | .0 | 3949 | 11.8 | .34 |
| 3184 | 12.7 | .78 | 3982 | 12.1 | .36 |
| 3198 | 13.0 | .95 | 4013 | 13.3 | .60 |
| 3254 | 12.8 | .60 | 4041 | 11.4 | .30 |
| 3294 | 12.0 | .48 | 4062 | 12.6 | .48 |
| 3389 | 13.1 | +0.30 | 4088 | 11.5 | +0.72 |

TABLE III—*Continued*

| N.G.C. | $m_T$ | log *d* | N.G.C. | $m_T$ | log *d* |
|---|---|---|---|---|---|
| | | Sc—*Continued* | | | |
| 4096 | 12.3 | +0.78 | 4995 | 11.8 | +0.36 |
| 4100 | 12.3 | .60 | 5005* | 11.1 | .70 |
| 4145 | 12.3 | .70 | 5012 | 11.9 | .43 |
| 4157§ | 12.3 | .77 | 5033* | 11.8 | 0.78 |
| 4212 | 12.3 | .30 | 5194* | 7.4 | 1.08 |
| 4220 | 12.1 | 0.40 | 5204 | 12.8 | 0.59 |
| 4236 | 12.8 | 1.04 | 5236 | 10.4 | 1.00 |
| 4254 | 10.4 | 0.65 | 5247 | 13.3 | 0.70 |
| 4321* | 10.5 | .70 | 5248 | 11.5 | .50 |
| 4414 | 10.1 | .48 | 5290 | 12.5 | .48 |
| 4419 | 11.8 | .36 | 5297 | 12.6 | .60 |
| 4460 | 12.1 | .20 | 5364 | 13.3 | .60 |
| 4490* | 10.2 | .60 | 5395 | 12.8 | 0.30 |
| 4501* | 10.5 | .70 | 5457 | 9.9 | 1.34 |
| 4504 | 12.1 | 0.48 | 5474 | 12.0 | 0.60 |
| 4517§ | 12.5 | 1.00 | 5585 | 12.3 | .60 |
| 4536§ | 12.3 | 0.85 | 5676 | 11.8 | .48 |
| 4559 | 10.7 | .90 | 5678 | 11.8 | .41 |
| 4569* | 10.9 | .65 | 5832 | 13.1 | 0.56 |
| 4580 | 12.3 | .15 | 5907§ | 11.9 | 1.04 |
| 4605 | 9.9 | 0.48 | 6181 | 12.5 | 0.30 |
| 4631* | 9.5 | 1.08 | 6217 | 12.1 | .25 |
| 4632 | 13.1 | 0.50 | 6503 | 9.9 | .70 |
| 4666 | 12.0 | .60 | 7448 | 11.8 | + .30 |
| 4713 | 12.3 | .38 | 7671 | 13.3 | −0.15 |
| 4781 | 11.8 | .48 | | | |
| 4793 | 12.4 | .20 | Mean | 11.75 | +0.537 |
| 4808 | 12.6 | +0.34 | | | |
| | | Peculiar Spirals (Unclassified) | | | |
| 972 | 13.3 | +0.17 | | | |
| 2537 | 13.3 | .0 | | | |
| 4900 | 11.8 | +0.23 | | | |

are shown in Figures 2–5 for the beginning, middle, and end of the sequence of types and also for the irregular nebulae. In Figures 2 and 3 adjacent types have been grouped in order to increase the material, and in Figure 5 the Magellanic Clouds have been added to increase the range.

The correlations can be expressed in the form

$$m_T = C - K \log d \,, \tag{1}$$

where $K$ is constant from type to type, but $C$ varies progressively throughout the sequence. The value of $K$ cannot be accurately determined from the scattered data for any particular type, but, within the limits of uncertainty, it approximates the round number 5.0, the value which is represented by the lines in Figures 2–5.

When $K$ is known, the value of $C$ can be computed from the mean magnitude and the logarithm of the diameter for each type. This amounts to reading from the curves the magnitudes corresponding to a diameter of one minute of arc, but avoids the uncertainty of establishing the curves where the data are limited.

TABLE IV

IRREGULAR NEBULAE

| N.G.C. | $m_T$ | log $d$ | N.G.C. | $m_T$ | log $d$ |
|---|---|---|---|---|---|
| 2968 | 12.6 | +0.08 | 4656§ | 11.5 | +1.30 |
| 3034* | 9.0 | .85 | 4753 | 11.4 | +0.43 |
| 3077 | 11.4 | .48 | 5144 | 12.8 | − .30 |
| 3729 | 11.8 | .17 | 5363 | 11.1 | +0.20 |
| 4214* | 11.3 | .90 | | | |
| 4449* | 9.5 | .65 | Mean | 11.34 | +0.469 |
| 4618 | 12.3 | +0.40 | | | |

NOTES TO TABLES I–IV

* Magnitude from Hopmann.

† N.G.C. 524 and 3998 are late elliptical nebulae in which the equatorial planes are perpendicular to the line of sight. They might be included with the E6 or E7 nebulae.

§ Absorption very conspicuous.

‡ N.G.C. 3607, 4459, and 5485 appear to be elliptical nebulae with narrow bands of absorption between the nuclei and the peripheries.

The progressive change in the value of $C$ throughout the sequence may be expressed as a variation either in the magnitude for a given diameter or in the diameter for a given magnitude. Both effects are listed in Table VII and are illustrated in Figure 6, in which magnitudes and diameters thus found are plotted against types. With the exception of the later elliptical nebulae, for which the data are wholly inadequate for reliable determinations, the points fall on smooth curves. In the region of the earlier elliptical nebulae, the curves should be somewhat steeper in order to allow for objects of greater ellipticities which are probably included.

### REDUCTION OF NEBULAE TO A STANDARD TYPE

The slope, $K$, in the formula relating magnitudes with diameters, appears to be closely similar for the various types, but accurate determinations are restricted by the limited and scattered nature of the data for each type separately. With a knowledge of the parameter $C$, however, it is possible to reduce all the material to a standard

TABLE V

FREQUENCY DISTRIBUTION OF TYPES

| Type | Number | Percentage | Mean Mag. |
|---|---|---|---|
| Elliptical Nebulae | | | |
| Eo | 17 | 18 | 11.40 |
| 1 | 13 | 14 | 11.43 |
| 2 | 14 | 15 | 11.52 |
| 3 | 10 | 11 | 11.99 |
| 4 | 13 | 14 | 11.95 |
| 5 | 6 | 6 | 10.97 |
| 6 | 7 | 8 | 10.93 |
| 7 | 5 | 5 | 11.02 |
| Pec | 8 | 9 | 11.55 |
| Total | 93 | 23* | 11.53 |
| Normal Spirals | | | |
| Sa | 49 | 21 | 11.69 |
| b | 70 | 29 | 11.55 |
| c | 115 | 49 | 11.75 |
| Pec | 3 | 1 | 12.80 |
| Total | 237 | 59* | 11.68 |
| Barred Spirals | | | |
| SBa | 26 | 44 | 11.66 |
| b | 16 | 27 | 11.48 |
| c | 15 | 26 | 11.87 |
| Pec | 2 | 3 | 11.70 |
| Total | 59 | 15* | 11.66 |
| Irregular Nebulae | | | |
| | 11 | 3* | 11.34 |
| Totals | | | |
| All types | 400 | 100 | 11.63 |

* Percentages of 400, the total number of nebulae investigated. The percentages of the subtypes refer to the number of nebulae in the particular type.

type and hence to determine the value of $K$ from the totality of the data. The mean of E7, SBa, and Sa was chosen for the purpose, as representing a hypothetical transition-point between the elliptical nebulae and the spirals, and was designated by the symbol "So." The corresponding value of $C$, in round numbers, is 13.0. Corrections were applied to the logarithms of the diameters of the nebulae of each observed class, amounting to

$$\Delta \log d = 0.2\ (13.0 - C)$$

where $C$ is the observed value for a particular class.[1] When the values of $C$ are read from the smooth curve in Figure 6, these corrections are as shown in Table VIII.

TABLE VI

FREQUENCY DISTRIBUTION OF MAGNITUDES

| MAGNITUDE INTERVAL | NUMBERS OF NEBULAE | | |
|---|---|---|---|
| | E | S | All |
| 8.1– 8.5 | 0 | 2 | 2 |
| 8.6– 9.0 | 2 | 4 | 7 |
| 9.1– 9.5 | 4 | 6 | 11 |
| 9.6–10.0 | 7 | 7 | 19 |
| 10.1–10.5 | 7 | 13 | 20 |
| 10.6–11.0 | 8 | 14 | 32 |
| 11.1–11.5 | 9 | 24 | 49 |
| 11.6–12.0 | 21 | 57 | 88 |
| 12.1–12.5 | 20 | 52 | 86 |
| 12.6–13.0 | 10 | 33 | 51 |

The corrected values of $\log d$ were then plotted against the observed magnitudes. This amounts to shifting the approximately parallel correlation curves for the separate types along the axis of $\log d$ until they coincide. Since the mean magnitudes of the various types are nearly constant, the relative shifts will very nearly equal the differences in the mean observed $\log d$, and hence the effect of errors in the first approximation to the values of $K$ will be negligible.

The plot is shown in Figure 7, in which the two Magellanic

---

[1] Since $C$ is constant for all nebulae in a given class, the linear relation between $\Delta \log d$ and $C$ for the different classes is something more than a mere geometrical relation arising from the observed equality of the mean $m_T$ in the various classes.

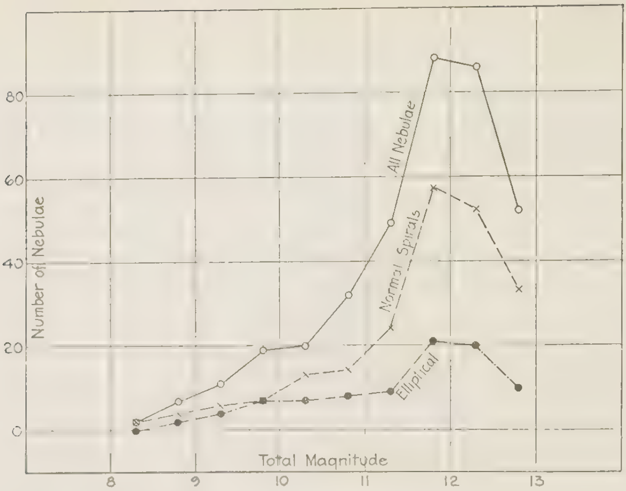

FIG. 1.—Frequency distribution of apparent magnitudes among nebulae in Holetschek's list.

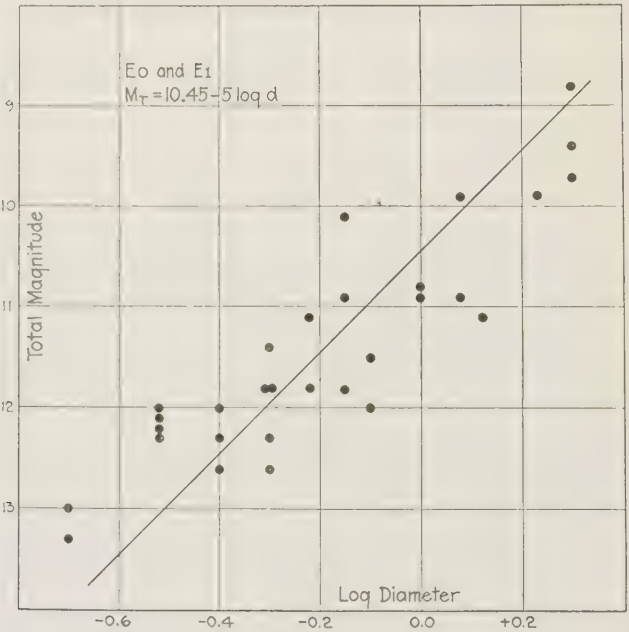

FIG. 2.—Relation between luminosity and diameter among nebulae at the beginning of the sequence of types—Eo and E1 nebulae.

Clouds have been included in order to strengthen the bright end of the curve which would otherwise be unduly influenced by the single

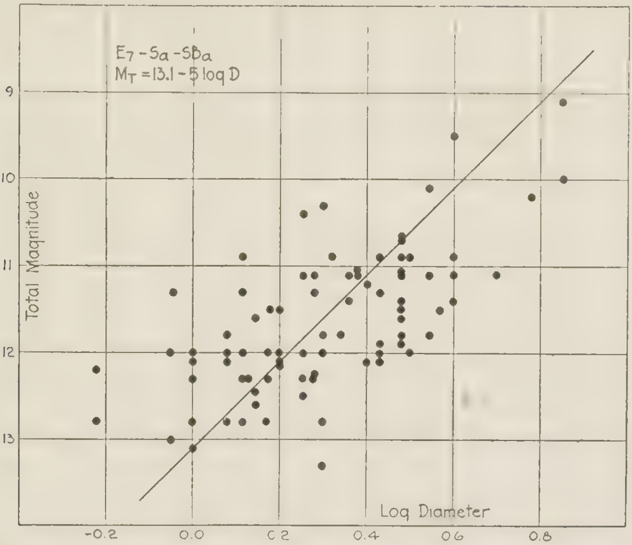

FIG. 3.—Relation between luminosity and diameter among nebulae at the middle of the sequence of types—E7, Sa, and SBa nebulae.

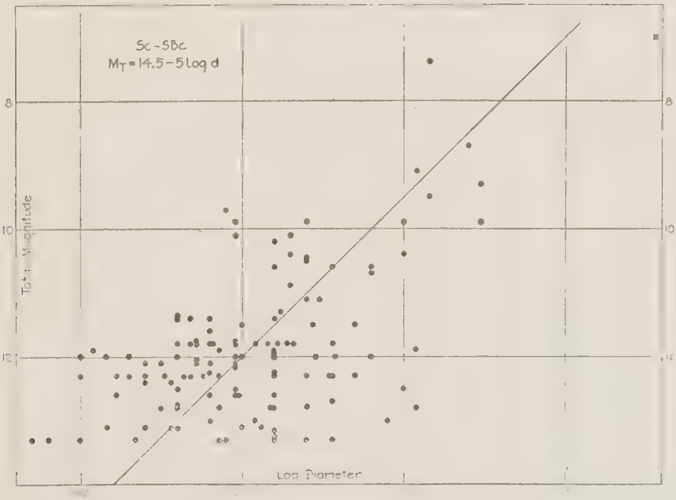

FIG. 4.—Relation between luminosity and diameter among nebulae at the end of the sequence of types—Sc and SBc nebulae.

object, M 31. The magnitudes +0.5 and +1.5, which were assigned to the Clouds, are estimates based upon published descriptions.

The correlation of the data is very closely represented by the formula

$$m_T = 13.0 - 5 \log d \, . \tag{2}$$

This falls between the two regression curves derived from least-square solutions and could be obtained exactly by assigning appropriate weights to the two methods of grouping. The nature of the data is such that a closer agreement can scarcely be expected. No correction to the assumed value of the slope appears to be required. The material extends over a range of 12 mag., and the few cases which have been investigated indicate that the correlation can be extended another 3 mag., to the limit at which nebulae can be classified with certainty on photographs made with the 100-inch reflector. The relation may therefore be considered to hold throughout the entire range of observations.

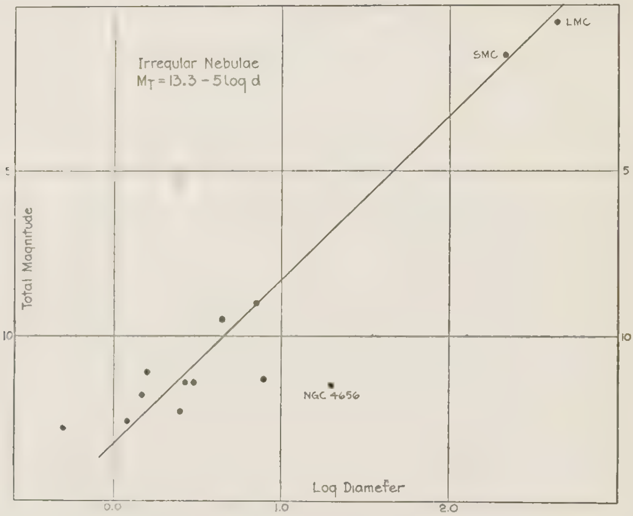

Fig. 5.—Relation between luminosity and diameter among the irregular nebulae. The Magellanic Clouds are included. N.G.C. 4656 is an exceptional case in that it shows a narrow, greatly elongated image in which absorption effects are very conspicuous; hence the maximum diameter is exceptionally large for its apparent luminosity.

The residuals without regard to sign average 0.87 mag., and there appears to be no systematic effect due either to type or luminosity. The scatter, however, is much greater for the spirals, especially in the later types, than for the elliptical nebulae. The limiting cases are explained by peculiar structural features. The nebulae which fall well above the line usually have bright stellar nuclei, and those which fall lowest are spirals seen edge-on in which belts of absorption are conspicuous.

TABLE VII

| Type | $\bar{m}_T$ | $\overline{\log d}$ | $C$* | $d$† |
|---|---|---|---|---|
| Eo | 11.40 | −0.204 | 10.38 | 1.2 |
| 1 | 11.43 | .177 | 10.54 | 1.3 |
| 2 | 11.52 | .088 | 11.08 | 1.6 |
| 3 | 11.99 | .133 | 11.33 | 1.8 |
| 4 | 11.95 | − .011 | 11.90 | 2.4 |
| 5 | 10.97 | + .090 | 11.42 | 1.9 |
| 6 | 10.93 | .220 | 12.03 | 2.5 |
| 7 | 11.02 | .360 | 12.82 | 3.7 |
| Sa | 11.69 | .333 | 13.35 | 4.7 |
| b | 11.55 | .471 | 13.90 | 6.0 |
| c | 11.74 | .540 | 14.44 | 7.7 |
| SBa | 11.66 | .267 | 13.00 | 4.0 |
| b | 11.48 | .317 | 13.16 | 4.3 |
| c | 11.87 | .509 | 14.41 | 7.6 |
| Irr | 11.34 | +0.469 | 13.68 | 5.4 |

* $C = m_T + 5 \log d$.

† $\log d = 0.2\,(C - m_T)$; $m_T = 10.0$.

### EFFECTS OF ORIENTATION

The effect of the orientation is appreciable among the spirals in general. In order to illustrate this feature, they have been divided into three groups consisting of those whose images are round or nearly round, elliptical, and edge-on, or nearly so. The mean values of $m_T + 5 \log d$ were then computed and compared with the theoretical value, 13.0. The residuals are negative when the nebulae are too bright for their diameters and positive when they are too faint. The results are given in Table IX, where mean residuals are followed by the numbers of nebulae, in parentheses, which are represented by the means.

The numbers of the barred spirals are too limited to inspire confidence in the results, but among the normal spirals there is conclusive evidence that the highly tilted and edge-on nebulae are fainter for a given diameter than those seen in the round. A study of the individual images indicates that the effect is due very largely to dark absorption clouds, which become more conspicuous when the nebulae are highly tilted. These clouds are generally, but not universally, peripheral features. An extensive investigation will be necessary before any residual effect due to absorption by luminous nebulosity can be established with certainty. Even should such exist, it clearly cannot be excessive.

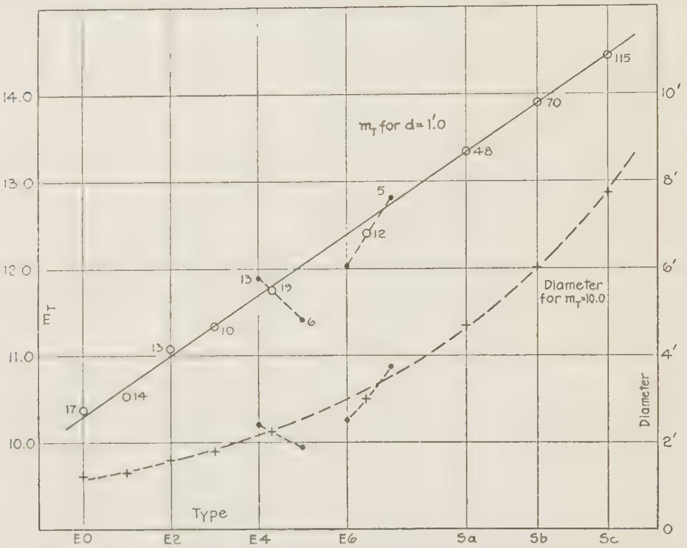

FIG. 6.—Progressive characteristics in the sequence of types. The upper curve represents the progression in total magnitude with type for nebulae having maximum diameters of one minute of arc. The elliptical nebulae and the normal spirals are included as representing the normal sequence, but the barred spirals and the irregular nebulae are omitted. The figures give the number of objects observed in each type. Among the later elliptical nebulae the numbers are so small that means of adjacent types have been plotted. The lower curve represents the progression in diameter along the normal sequence for nebulae of the tenth magnitude.

### SIGNIFICANCE OF THE LUMINOSITY RELATION

The correlations thus far derived are between total luminosities and maximum diameters. In the most general sense, therefore, they express laws of mean surface brightness. The value, $K = 5.0$, in formula (1) indicates that the surface brightness is constant for each separate type. The variations in $C$ indicate a progressive diminution in the surface brightness from class to class throughout the entire sequence. The consistency of the results amply justifies the sequence as a basis of classification, since a progression in physical dimensions

TABLE VIII

| Type | $C$ | $\Delta \log d$ | Type | $C$ | $\Delta \log d$ |
|---|---|---|---|---|---|
| E0 | 10.30 | +0.54 | Sa | 13.31 | −0.06 |
| 1 | 10.65 | .47 | Sb | 13.90 | .18 |
| 2 | 11.00 | .40 | Sc | 14.45 | .29 |
| 3 | 11.35 | .33 | SBa | 13.00 | .00 |
| 4 | 11.70 | .26 | SBb | 13.16 | .03 |
| 5 | 12.05 | .19 | SBc | 14.41 | .28 |
| 6 | 12.40 | .12 | Irr | 13.68 | −0.14 |
| 7 | 12.75 | +0.05 | | | |

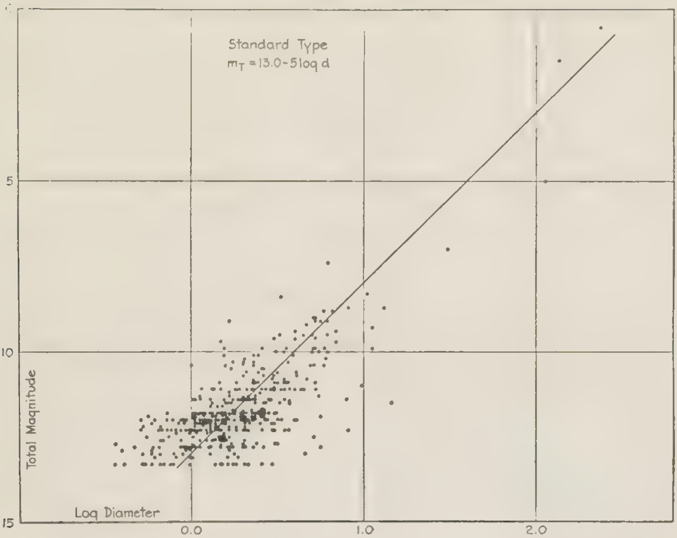

FIG. 7.—Relation between luminosity and diameter among extra-galactic nebulae. The nebulae have been reduced to a standard type, S0, which, being the mean of E7, Sa, and SBa, represents a hypothetical transition point between elliptical nebulae and spirals. The Magellanic Clouds have been included in order to strengthen the brighter end of the plot.

is indicated, which accompanies the progression in structural form. Although the correlations do not necessarily establish any generic relation among the observed classes, they support in a very evident manner the hypothesis that the various stages in the sequence represent different phases of a single fundamental type of astronomical body. Moreover, the quantitative variation in $C$ is consistent with this interpretation, as is apparent from the following considerations.

Among the elliptical nebulae it is observed that the nuclei are sharp and distinct and that the color distribution is uniform over the images. This indicates that there is no appreciable absorption, either general or selective, and hence that the luminosity of the projected image represents the total luminosity of the nebula, regardless of the orientation. If the observed classes were pure, that is, if the apparent ellipticities were the actual ellipticities, formula (1) could be written

TABLE IX

RESIDUALS IN $m_T+5 \log d$ AS A FUNCTION OF ORIENTATION

| Type | Round | Elliptical | Edge-On |
|---|---|---|---|
| Sa................ | −0.02 (13) | −0.27 (13) | +0.57 (23) |
| Sb................ | .77 (24) | .0 (35) | 1.71 (11) |
| Sc................ | −0.08 (35) | −0.13 (57) | +0.66 (22) |
| All S......... | −0.26 (72) | −0.11 (105) | +0.83 (56) |
| SBa.............. | 0.0 (10) | −0.30 (7) | +0.31 (8) |
| SBb.............. | − .16 (10) | + .07 (6) | ............ |
| SBc.............. | +0.19 (9) | −0.50 (4) | +0.32 (2) |
| All SB........ | +0.01 (29) | −0.21 (17) | +0.31 (10) |
| All spirals..... | −0.22 (101) | −0.13 (122) | +0.73 (66) |

$$C_e = m_T + 5 \log b - 5 \log (1-e) \ , \qquad (3)$$

where $b$ is the minor diameter in minutes of arc and $e$ is the ellipticity. The term $m_T+5 \log b$ is observed to be constant for a given type. If it were constant for all elliptical nebulae, then the term $C_e+5 \log (1-e)$ would be constant also. On this assumption,

$$C_e + 5 \log (1-e) = C_0 ,$$

where $C_0$ is the value of $C$ for the pure class E0. Hence

$$C_e - C_0 = -5 \log (1-e)\,, \tag{4}$$

a relation which can be tested by the observations. An analysis of the material indicates that this is actually the case, and hence that among the elliptical nebulae in general, the minor diameter determines the total luminosity, at least to a first approximation.[1]

The observed values of $C$ vary with the class, as is seen in Table VII and Figure 6, but, excepting that for E7, they are too large because of the mixture of later types of nebulae among those of a given observed class. It is possible, however, to calculate the values of $C_e - C_0$ for the pure classes and then to make approximate corrections for the observed mixtures on the assumption that the nebulae of any given actual ellipticity are oriented at random. In this manner, mean theoretical values can be compared with the observed values. The comparisons are shown in Table XII in the form $C_7 - C_e$, because E7 is the only observed class that can be considered as pure. The significance of the table will be discussed later.

The following method has been used to determine the relative frequencies with which nebulae of a given actual ellipticity, oriented at random, will be observed as having various apparent ellipticities.

In Figure 8, let the co-ordinate axes $OX$ and $OY$ coincide with the major and minor axes, $a$ and $b$, of a meridian section of an ellipsoid of revolution. Let $OO'$ be the line of sight to the observer, making an angle $i$ with $OX$, and let $OR$ be perpendicular to $OO'$. Let $PP'$ be a

---

[1] This is apparent even among the observed classes. Referring to formula (3), $m_T + 5 \log b$ will be constant in so far as $C_e + 5 \log (1-e)$ is constant. The following table indicates that the latter term is approximately constant throughout the sequence of elliptical nebulae. The values of $C_e$ were read from the smooth curve in Fig. 6.

| $e$ | $C_e$ | $5 \log (1-e)$ | $C_0$ | Res. |
|---|---|---|---|---|
| 0 | 10.30 | 0.0 | 10.30 | −0.14 |
| 1 | 10.65 | − .23 | 10.42 | − .02 |
| 2 | 11.00 | .48 | 10.52 | + .10 |
| 3 | 11.35 | 0.78 | 10.57 | + .13 |
| 4 | 11.70 | 1.11 | 10.59 | + .15 |
| 5 | 12.05 | 1.50 | 10.55 | + .11 |
| 6 | 12.40 | 1.99 | 10.41 | − .03 |
| 7 | 12.75 | −2.62 | 10.13 | −0.31 |
| Mean |  |  | 10.44 | 0.12 |

tangent to the ellipse, parallel to and at a distance $b_1$ from $OO'$. Let $x_0$ and $y_0$ be the intercepts of the tangent on the $X$- and $Y$-axis, respectively. The apparent ellipticity is determined by $b_1$, which, for various values of the angle $i$, ranges from $b$ to $a$. The problem is to determine the relative areas on the surface of a sphere whose center is $O$, within which the radius $OY$ must pass in order that the values of $b_1$, and hence of the apparent ellipticity, $e_1$, may fall within certain designated limits. This requires that the angle $i$ be expressed in terms of $b_1$.

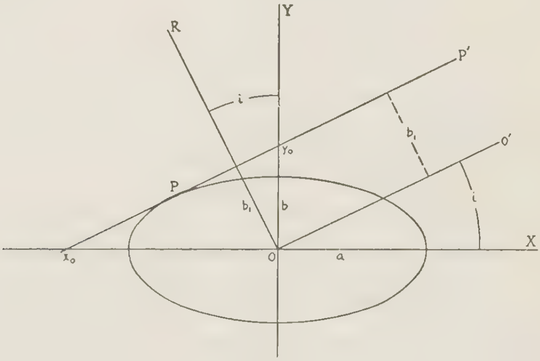

FIG. 8

From the equation of the tangent, $PP'$,

$$y=-x\tan i+\sqrt{a^2\tan^2 i+b^2}$$

$$y_0=\sqrt{a^2\tan^2 i+b^2}\,.$$

Since

$$b_1=y_0\cos i$$

$$b_1^2=a^2\sin^2 i+b^2\cos^2 i\,.$$

Let $a=1$, then

$$\cos^2 i=\frac{1-b_1^2}{1-b^2}\,,$$

where

$$b_1=1-e_1\,,\qquad b=1-e\,.$$

From these equations, the values of $i$ can be determined for all possible values of $e_1$. The limits for the observed classes E0 to E7 were chosen midway between the consecutive tenths, E0 ranging from $e=0$ to $e=0.05$; E1, from $e=0.05$ to $e=0.15$; E7, from $e=0.65$ to $e=0.75$. The relative frequencies of the various observed classes are then proportional to the differences in sin $i$ corresponding to the two limiting values of $e_1$. These frequencies must be calculated separately for nebulae of different actual ellipticities.

The results are given in Table X, where the actual ellipticities, listed in the first column, are followed across the table by the percentages which, on the assumption of random orientation, will be observed as having the various apparent ellipticities. The bottom row will be seen to show the percentages of apparent ellipticities observed in an assembly of nebulae in which the numbers for each actual ellipticity are equal and all are oriented at random.

TABLE X

| Actual | Apparent | | | | | | | | |
|---|---|---|---|---|---|---|---|---|---|
| | E0 | E1 | E2 | E3 | E4 | E5 | E6 | E7 | Total |
| E7 | 0.055 | 0.111 | 0.114 | 0.116 | 0.121 | 0.132 | 0.164 | 0.187 | 1.000 |
| 6 | .059 | .123 | .126 | .133 | .148 | .187 | 0.224 | ...... | ...... |
| 5 | .067 | .140 | .148 | .166 | .216 | 0.263 | ...... | ...... | ...... |
| 4 | .079 | .169 | .190 | .250 | 0.312 | ...... | ...... | ...... | ...... |
| 3 | .100 | .225 | .299 | 0.376 | ...... | ...... | ...... | ...... | ...... |
| 2 | .145 | .378 | 0.477 | ...... | ...... | ...... | ...... | ...... | ...... |
| 1 | 0.300 | 0.700 | ...... | ..... | ...... | ...... | ...... | ...... | ...... |
| 0 | 1.000 | ...... | ...... | ...... | ...... | ...... | ...... | ...... | ...... |
| Total | 1.805 | 1.846 | 1.354 | 1.041 | 0.797 | 0.582 | 0.388 | 0.187 | 8.000 |
| | 0.226 | 0.231 | 0.169 | 0.130 | 0.100 | 0.073 | 0.049 | 0.023 | 1.000 |

From this table and the actual numbers in the observed classes as read from a smoothed curve, the numbers of each actual ellipticity mingled in the observed classes can be determined. For instance, the four nebulae observed as E7 represent 0.187 of the total number of actual E7. The others are distributed among the observed classes E0 to E6 according to the percentages listed in Table X. Six nebulae are observed as E6, but 3.6 of these are actually E7. The remaining 2.4 actual E6 nebulae represent 0.224 of the total number of that actual ellipticity, the others, as before, being scattered among the observed classes E0 to E5. Table XI gives the complete analysis and is similar to Table X except that the percentages in the latter are replaced by the actual numbers indicated by the observations.

Finally, the mean values of $C_7 - C_e$ are calculated from the numbers of nebulae in the various columns of Table XI together with the values of $C_7 - C_e$ for the pure classes as derived from formula (4). The results are listed in the fourth column of Table XII following those for the pure and the observed classes. In determining the observed values, N.G.C. 524 and 3998 are included as E0 and E1, although in Table I they are listed as peculiar, because they are obviously much flattened nebulae whose minor axes are close to the line of sight.

The observed values in general fall between those for the pure classes and those corresponding to random orientation. They are of the same order as the latter, and the discrepancies are perhaps not unaccountably large in view of the nature and the limited extent of the material. There is a systematic difference, however, averaging about 0.2 mag., in the sense that the observed values are too large, and increasing with decreasing ellipticity. One explanation is that the observed classes are purer than is expected on the assumption of random orientation. This view is supported by the relatively small dispersion in $C$, as may be seen in Table I and Figure 2, among the nebulae of a given class, but it is difficult to account for any such selective effect in the observations. The discrepancies may be largely eliminated by an arbitrary adjustment of the numbers of nebulae with various degrees of actual ellipticity; for instance, the values in

TABLE XI

| Actual | Apparent | | | | | | | | |
|---|---|---|---|---|---|---|---|---|---|
| | E0 | E1 | E2 | E3 | E4 | E5 | E6 | E7 | Total |
| E7 | 1.2 | 2.4 | 2.5 | 2.5 | 2.6 | 2.9 | 3.6 | 4.0 | 21.7 |
| 6 | 0.6 | 1.3 | 1.4 | 1.5 | 1.6 | 2.0 | 2.4 | ...... | 10.8 |
| 5 | .8 | 1.7 | 1.8 | 2.0 | 2.7 | 3.1 | ...... | ...... | 12.1 |
| 4 | .8 | 1.7 | 1.9 | 2.5 | 3.1 | ...... | ...... | ...... | 10.0 |
| 3 | 0.9 | 2.1 | 2.8 | 3.5 | ...... | ...... | ...... | ...... | 9.3 |
| 2 | 1.1 | 2.9 | 3.6 | ...... | ...... | ...... | ...... | ...... | 7.6 |
| 1 | 1.7 | 3.9 | ...... | ...... | ...... | ...... | ...... | ...... | 5.6 |
| 0 | 9.9 | ...... | ...... | ...... | ...... | ...... | ...... | ...... | 9.9 |
| Total* | 17.0 | 16.0 | 14.0 | 12.0 | 10.0 | 8.0 | 6.0 | 4.0 | 87.0 |

* The totals represent the numbers in the observed classes as read from a smooth curve.

the last column of Table XII, calculated on the assumption of equal numbers, agree very well with the observed values, although the resulting numbers having the various apparent ellipticities differ slightly from those observed. The observed values, however, can again be accounted for by the inclusion of some flatter nebulae among the classes E6 and E7. Very early Sa or SBa nebulae might easily be mistaken for E nebulae when oriented edge-on, although they would be readily recognized when even slightly tilted. If the numerical results fully represented actual statistical laws, the explanation would be sought in the physical nature of the nebulae. The change from ellipsoidal to lenticular figures, noticeable in the later-type nebulae, would affect the results in the proper direction, as would also a progressive shortening of the polar axis. The discrepancies, however, are second-order effects, and since they may be due to accidental variations from random orientation, a further discussion must await the accumulation of more data.

TABLE XII

DIFFERENTIAL VALUES OF *C*

| Class | Pure Classes | Observed | Random Orientation | |
|---|---|---|---|---|
| | | | No. as Observed | Equal No. |
| *C*7–*C*7 | 0.00 | 0.00 | 0.00 | 0.00 |
| C6 | 0.63 | 0.35* | 0.25 | 0.35 |
| C5 | 1.10 | 0.70* | 0.58 | 0.70 |
| C4 | 1.51 | 0.85 | 0.87 | 1.01 |
| C3 | 1.84 | 1.42 | 1.11 | 1.28 |
| C2 | 2.13 | 1.67 | 1.33 | 1.55 |
| C1 | 2.39 | 2.01† | 1.54 | 1.83 |
| C0 | 2.62 | 2.17† | 2.15 | 2.25 |

* Read from smooth curve in Fig. 6. The small numbers of observed E5 and E6 nebulae justify this procedure. The other values are the means actually observed.

† N.G.C. 524 and 3998 are included as E0 and E1, respectively.

Meanwhile, it is evident that, to a first approximation at least, the polar diameters alone determine the total luminosities of all elliptical nebulae, and the entire series can be represented by the various configurations of an originally globular mass expanding equatorially. A single formula represents the relation, in which the value of *C* is that corresponding to the pure type E0. From Table

XII, this is found to be 2.62 mag. less than the value of $C_7$. The latter is observed to be 12.75, hence

$$m_T + 5 \log b = 10.13 \ . \tag{5}$$

If this relation held for the spirals as well, the polar diameters could be calculated from the measured magnitudes. Unfortunately, it has not been possible to measure accurately the polar diameters directly, and hence to test the question, but they have been computed for the mean magnitudes of the Sa, Sb, and Sc nebulae as given in Table III, and the ratios of the axes have been derived by a comparison of these hypothetical values with the means of the measured maximum diameters. The results, 1 to 4.4, 1 to 5.7, and 1 to 7.3, respectively, although of the right order, appear to be somewhat too high. An examination of the photographs indicates values of the order of 1 to 5.5, 1 to 8, and 1 to 10, but the material is meager and may not be representative. The comparison emphasizes, however, the homogeneity and the progressive nature of the entire sequence of nebulae and lends some additional color to the assumption that it represents various aspects of the same fundamental type of system.

From the dynamical point of view, the empirical results are consistent with the general order of events in Jeans's theory. Thus interpreted, the series is one of expansion, and the scale of types becomes the time scale in the evolutionary history of nebulae. In two respects this scale is not entirely arbitrary. Among the elliptical nebulae the successive types differ by equal increments in the ellipticity or the degree of flattening, and among the spirals the intermediate stage is midway between the two end-stages in the structural features as well as in the luminosity relations.

One other feature of the curves may be discussed from the point of view of Jeans's theory before returning to the strictly empirical attitude. The close agreement of the diameters for the stages E7 and Sa suggests that the transition from the lenticular nebula to the normal spiral form is not cataclysmic. If the transition were gradual, however, we should expect to observe occasional objects in the very process, but among the thousand or so nebulae whose images have been inspected, not one clear case of a transition form has been detected. The observations jump suddenly from lenticular nebulae with no trace of structure to spirals in which the arms are fully developed.

If the numerical data could be fully trusted, the SBa forms would fill the gap. Among these nebulae, the transition from the lenticular to the spiral with arms is gradual and complete. It is tempting to suppose that the barred spirals do not form an independent series parallel with that of the normal spirals, but that all or most spirals begin life with the bar, although only a few maintain it conspicuously throughout their history. This would also account for the fact that the relative numbers of the SBa nebulae are intermediate to those of the lenticular and of the Sa. The normal spirals become more numerous as the sequence progresses, while the numbers of barred spirals, on the contrary, actually decrease with advancing type.

### RELATION BETWEEN NUCLEAR LUMINOSITIES AND DIAMETERS

Visual magnitudes have been determined by Hopmann for the nuclei of 37 of the nebulae included in the present discussion. These data, together with types and diameters of the nebulae, are listed in Table XIII. When the magnitudes are plotted directly against the logarithms of the diameters, they show little or no correlation. When, however, the nebulae are reduced to the standard type (by applying corrections for differences in diameter along the sequence), a decided correlation is found whose coefficient is 0.76. This is shown in Figure 9. The simple mean of the two regression curves is

$$m_n = 14.45 - 4.94 \log d \,, \tag{6}$$

where the slope differs by about 1 per cent from that in formula (2). The list contains 16 elliptical nebulae, 15 normal, and 6 barred spirals. The nebulae are fairly representative, except that few late-type spirals are included. This is an effect of selection due to the fact that nuclei become less and less conspicuous as the sequence progresses.

The same result can be derived from a study of the differences, $m_n - m_T$, for the individual nebulae. The mean value is $1.55 \pm 0.08$, and the average residual is 0.60 mag. Means for the separate types are to be found in Table XIV.

The low value for Sa–SBa is due to N.G.C. 5866, for which the magnitude difference of 0.06 is certainly in error, and the high value for Sc and SBc, to M 51, for which the difference of 3.98 mag. is not representative. The latter is accounted for in part by the fact that the $m_T$ refers to the combined magnitude of the main spiral and the outlying mass, N.G.C. 5195. When these two cases are discarded, the final mean becomes 1.52±0.05, and the average residual, 0.52 mag., is consistent with the probable errors of the magnitude de-

TABLE XIII

Diameters and Nuclear Magnitudes

| N.G.C. | Type | log *d* | $m_n$ Hopmann | $m_n$ Reduced |
|---|---|---|---|---|
| 221 | E2 | +0.42 | 9.84 | 11.85 |
| 1023 | SBa | .78 | 11.86 | 11.86 |
| 2841 | Sb | 0.78 | 12.08 | 11.19 |
| 3031 | Sb | 1.20 | 10.94 | 10.05 |
| 3115 | E7 | 0.60 | 10.83 | 11.09 |
| 3351 | SBb | .48 | 12.31 | 12.15 |
| 3368 | Sa | .85 | 11.68 | 11.43 |
| 3379 | E0 | .30 | 11.55 | 14.27 |
| 3412 | SBa | .40 | 11.59 | 11.59 |
| 3489 | Sb | .40 | 11.54 | 10.65 |
| 3626 | Sa | .28 | 12.37 | 12.12 |
| 3627 | Sb | .90 | 12.03 | 11.14 |
| 4125 | E4 | .30 | 11.74 | 13.04 |
| 4216 | Sb | .85 | 11.65 | 10.76 |
| 4278 | E1 | .0 | 12.02 | 14.38 |
| 4374 | E1 | .08 | 11.43 | 13.79 |
| 4382 | E4 | .48 | 11.77 | 13.07 |
| 4435 | E6 | .11 | 11.65 | 12.26 |
| 4438 | Sb | .54 | 11.83 | 10.94 |
| 4486 | E0 | .30 | 11.23 | 13.95 |
| 4546 | E6 | .18 | 11.75 | 12.36 |
| 4552 | E0 | .23 | 11.59 | 14.31 |
| 4569 | Sc | .65 | 12.05 | 10.57 |
| 4579 | SBc | .45 | 11.48 | 10.07 |
| 4621 | E5 | .30 | 11.60 | 12.56 |
| 4636 | E1 | .08 | 11.97 | 14.33 |
| 4649 | E2 | .30 | 11.57 | 13.58 |
| 4697 | E6 | .48 | 10.90 | 11.51 |
| 4699 | SBb | .57 | 10.72 | 10.56 |
| 4725 | SBb | .70 | 11.97 | 11.81 |
| 4736 | Sb | .70 | 10.36 | 9.47 |
| 5005 | Sc | .70 | 12.04 | 10.56 |
| 5033 | Sc | 0.78 | 12.38 | 10.90 |
| 5194 | Sc | 1.08 | 11.38 | 9.90 |
| 5322 | E3 | 0.15 | 12.10 | 13.76 |
| 5866 | Sa | .48 | 11.76 | 11.51 |
| 7331 | Sb | +0.95 | 11.82 | 10.93 |
| Means |  | +0.509 | 11.60 | 11.90 |

terminations. The small numbers of objects within each class are insufficient for reliable conclusions concerning slight variations along the sequence. From the constancy of $m_n - m_T$, the relation expressed by formula (6) necessarily follows, the small difference in the constant being accounted for by the different methods of handling the data.

The parallelism of the two curves representing formulae (2) and (6) indicates that the regular extra-galactic nebulae, when reduced to the standard type, are similar objects. The mean surface brightness is constant, and the luminosity of the nucleus, as measured by Hopmann, is a constant fraction, about one-fourth, of the total luminosity of the nebulae. If there is a considerable range in absolute magnitude and hence in actual dimensions, the smaller nebulae must be faithful miniatures of the larger ones.

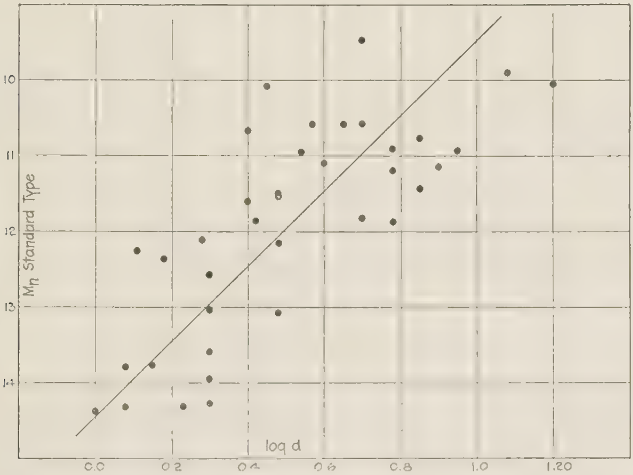

FIG. 9.—Relation between nuclear magnitudes and diameters. The nebulae have been reduced to the standard type by applying corrections to the magnitudes.

### ABSOLUTE MAGNITUDES OF EXTRA-GALACTIC NEBULAE

Reliable values of distances, and hence of absolute magnitudes, are restricted to a very few of the brightest nebulae. These are derived from a study of individual stars involved in the nebulae, among which certain types have been identified whose absolute magnitudes in the galactic system are well known. The method assumes that the stars involved in the nebulae are directly comparable with the stars in our own system, and this is supported by the consistency of the results derived from the several different types which have been identified.

TABLE XIV

| Types | $m_n - m_T$ | Number |
|---|---|---|
| E0–E3 | 1.64 | (9) |
| E4–E7 | 1.43 | (7) |
| Sa–SBa | 0.97 | (5) 1.27 when N.G.C. 5866 is omitted |
| Sb–SBb | 1.70 | (11) |
| Sc–SBc | 1.76 | (5) 1.19 when N.G.C. 5194 is omitted |
| Unweighted mean | 1.50 | (37) 1.45 (35) |
| Weighted mean | 1.55 | (37) 1.52 (35) |

TABLE XV

ABSOLUTE MAGNITUDES OF NEBULAE

| System | $M_T$ | $M_S$ |
|---|---|---|
| Galaxy | .......... | − 5.5 |
| M 31 | −17.1 | 6.5 |
| L M C | 17.0 | 8.0 |
| S M C | 16.0 | 5.5 |
| M 33 | 15.1 | 6.5 |
| N.G.C. 6822 | 13.7 | 5.8 |
| M 101 | 13.5 | − 6.3 |
| M 32 | −13.3 | ................ |
|  | .......... | − 6.3 |
|  | .......... | $-9.0 = M_S - M_T$ |
| Means | −15.1 | −15.3 |
| Adopted | −15.2 |  |

In Table XV are listed absolute magnitudes of the entire system and of the brightest stars involved, for the galaxy and the seven nebulae whose distances are known. The data for the Magellanic Clouds are taken from Shapley's investigations. The absolute magnitudes of the remaining nebulae were derived from Holetschek's apparent magnitudes and the distances as determined at Mount Wilson, where the stellar magnitudes were also determined. M 32 is generally assumed to be associated with the great spiral M 31, because the radial velocities are nearly equal and are unique in that they are the only large negative velocities that have been found among the extra-galactic nebulae. M 101 has been added to the list on rather weak evidence. The brightest stars involved are slightly brighter than apparent magnitude 17.0, and several variables have been found with magnitudes at maxima fainter than 19.0. Sufficient observations have not yet been accumulated to determine the light-curves of the variables, but from analogy with the other nebulae they are presumed to be Cepheids. On this assumption, both the star counts and the variables lead to a distance of the order of 1.7 times the distance of M 33. The inclusion of M 101 does not change the mean magnitude of the brightest stars involved, but reduces the mean magnitude of the nebulae by 0.2.

The range in the stars involved is about 2.5 mag., and in the total luminosities of the nebulae, about 3.8 mag. This latter is consistent with the scatter in the diagram exhibiting the relation between total luminosities and diameters. The associated objects, M 31 and 32, represent the extreme limits among the known systems, and the mean of these two is very close to the mean of them all.

## LUMINOSITY OF STARS INVOLVED IN NEBULAE

The number of nebulae of known distance is too small to serve as a basis for estimates of the range in absolute magnitude among nebulae in general. Further information, however, can be derived from a comparison of total apparent magnitudes with apparent magnitudes of the brightest stars involved, on the reasonable assumption, supported by such evidence as is available, that the brightest stars in isolated systems are of about the same intrinsic luminosity.

The most convenient procedure is to test the constancy of the differences in apparent magnitude between the brightest stars involved and the nebulae themselves, over as wide a range as possible in the latter quantities.

An examination of the photographs in the Mount Wilson collection has revealed no stars in the very faint objects or in the bright elliptical nebulae and early-type spirals. This was to be expected from the conclusions previously derived. Observations were therefore confined to intermediate- and late-type spirals and the irregular nebulae to the limiting visual magnitude 10.5. The Magellanic Clouds and N.G.C. 6822 were added to the nebulae in Holetschek's

## TABLE XVI

### Difference in Magnitude between Nebulae and Their Brightest Stars

| N.G.C. | $m_S$ | $m_T$ | $m_S-m_T$ |
|---|---|---|---|
| Sb | | | |
| 224 | 15.5 | 5.0 | 10.5 |
| 1068 | 17.5 | 9.1 | 8.4 |
| 2841 | >19.5 | 9.4 | >10.1 |
| 3031 | 18.5 | 8.3 | 10.2 |
| 3310 | >19.0 | 10.4 | > 8.6 |
| 3623 | >20.0 | 9.9 | >10.1 |
| 3627 | 18.5 | 9.1 | 9.4 |
| 4438 | >19.0 | 10.3 | > 8.7 |
| 4450 | 19.5 | 10.0 | 9.5 |
| 4736 | 17.3 | 8.4 | 8.9 |
| 4826 | >19.5 | 9.2 | >10.3 |
| 5055 | >19.0 | 9.6 | > 9.4 |
| 5746 | >19.5 | 10.4 | > 9.1 |
| 7331 | 19.0 | 10.4 | 8.6 |
| SBb | | | |
| 4699 | >19.5 | 10.0 | > 9.5 |
| Sc | | | |
| 253 | 18.3 | 9.3 | 9.0 |
| 598 | 15.6 | 7.0 | 8.6 |
| 2403 | 17.3 | 8.7 | 8.6 |
| 2683 | >20.0 | 9.9 | >10.1 |
| 2903 | 19.0 | 9.1 | 9.9 |
| 4254 | 18.5 | 10.4 | 8.1 |
| 4321 | 18.8 | 10.5 | 8.3 |
| 4414 | >19.5 | 10.1 | > 9.4 |
| 4490 | 18.8 | 10.2 | 8.6 |
| 5194 | 17.3 | 7.4 | 9.9 |
| 5236 | 18.6 | 10.4 | 8.2 |
| 5457 | 17.0 | 9.9 | 7.1 |
| Irr. | | | |
| L M C | 9.5 | 0.5 | 9.0 |
| S M C | 12.0 | 1.5 | 10.5 |
| 3034 | >19.5 | 9.0 | >10.5 |
| 4449 | 17.8 | 9.5 | 8.3 |
| 6822 | 15.8 | 8.5 | 7.3 |

list. Altogether, data were available for 32 objects, or about 60 per cent of the total number in the sky to the adopted limit. For this reason it is believed that the results are thoroughly representative.

The data are listed in Table XVI and are shown graphically in Figure 10. The luminosities of the brightest stars are given in photographic magnitudes. For the Magellanic Clouds, M 33, and N.G.C. 6822, these were obtained from published star counts. For M 31, 51, 63, 81, 94, and N.G.C. 2403, they depend upon unpublished counts, for which the magnitudes were determined by comparisons with Selected Areas. For the remaining nebulae, the magnitudes of stars were estimated with varying degrees of precision, but are probably less than 0.5 mag. in error.

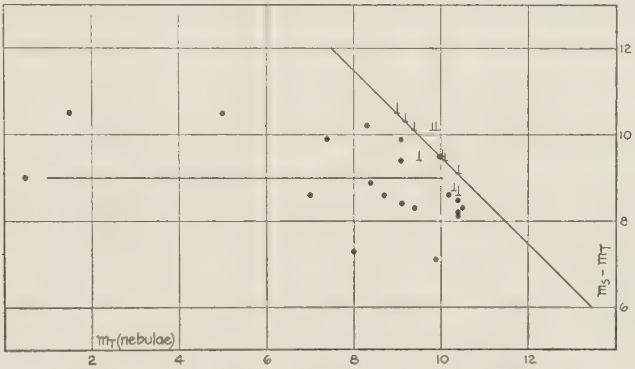

FIG. 10.—Relation between total magnitudes of extra-galactic nebulae and magnitudes of the brightest stars involved. Differences between total visual magnitudes of nebulae and the photographic magnitudes of the brightest stars are plotted against the total magnitudes. The dots represent cases in which the stars could actually be detected; the incomplete crosses represent cases in which stars could not be detected, and hence give lower limits for the magnitude differences. The diagonal line indicates the approximate limits of observation, fixed by the circumstance that, in general, stars fainter than 19.5 probably would not be detected on the nebulous background.

The sloping line to the right in Figure 10 represents the limits of the observations, for, from a study of the plates themselves, it appeared improbable that stars fainter than about 19.5 could be detected with certainty on a nebulous background. Points representing nebulae in which individual stars could not be found should lie in this excluded region above the line, and their scatter is presumably comparable with that of the points actually determined below the line. When allowance is made for this inaccessible region, the data can be interpreted as showing a moderate dispersion around the mean ordinate

$$m_s - m_T = 9.0 \, . \qquad (7)$$

The range in total magnitudes is sufficiently large in comparison with the dispersion to lend considerable confidence to the conclusion. The total range of four, and the average dispersion of less than 1 mag., are comparable with those in Table XV and in Figure 7, and agree with the former in indicating a constant order of absolute magnitude.

The mean absolute magnitude of the brightest stars in the nebulae listed in Table XV, combined with the mean difference between nebulae and their brightest stars, furnishes a mean absolute magnitude of $-15.3$ for the nebulae listed in Table XVI. This differs by only 0.2 mag. from the average of the nebulae in Table XV, and the mean of the two, $-15.2$, can be used as the absolute magnitude of intermediate- and late-type spirals and irregular nebulae whose apparent magnitudes are brighter than 10.5. The dispersion is small and can safely be neglected in statistical investigations.

This is as far as the positive evidence can be followed. For reasons already given, however, it is presumed that the earlier nebulae, the elliptical and the early-type spirals, are of the same order of absolute magnitude as the later. The one elliptical nebula whose distance is known, M 32, is consistent with this hypothesis.

Conclusions concerning the intrinsic luminosities of the apparently fainter nebulae are in the nature of extrapolations of the results found for the brighter objects. When the nebulae are reduced to a standard type, they are found to be constructed on a single model, with the total luminosities varying directly as the square of the diameters. The most general interpretation of this relation is that the mean surface brightness is constant, but the small range in absolute magnitudes among the brighter nebulae indicates that, among these objects at least, the relation merely expresses the operation of the inverse-square law on comparable objects distributed at different distances. The actual observed range covered by this restricted interpretation is from apparent magnitude 0.5 to 10.5. The homogeneity of the correlation diagrams and the complete absence of evidence to the contrary justify the extrapolation of the restricted interpretation to cover the 2 or 3 mag. beyond the limits of actual observation.

These considerations lead to the hypothesis that the nebulae treated in the present discussion are all of the same order of absolute magnitude; in fact, they lend considerable color to the assumption that extra-galactic nebulae in general are of the same order of absolute magnitude and, within each class, of the same order of actual dimensions. Some support to this assumption is found in the observed absence of individual stars in the apparently fainter late-type nebulae. If the luminosity of the brightest stars involved is independent of the total luminosity of a nebula, as is certainly the case among the brighter objects, then, when no stars brighter than 19.5 are found, the nebulae must in general be brighter than absolute magnitude $m_T - 25.8$ where $m_T$ is the total apparent magnitude. On this assumption, the faintest of the Holetschek nebulae are brighter than $-12.5$ and hence of the same general order as the brighter nebulae.

Once the assumption of a uniform order of luminosity is accepted as a working hypothesis, the apparent magnitudes become, for statistical purposes, a measure of the distances. For a mean absolute magnitude of $-15.2$, the distance in parsecs is

$$\log D = 0.2\, m_T + 4.04 . \tag{8}$$

### DIMENSIONS OF EXTRA-GALACTIC NEBULAE

When the distances are known, it is possible to derive actual dimensions and hence to calibrate the curve in Figure 6, which exhibits the apparent diameters as a function of type, or stage in the nebular sequence, for nebulae of a given apparent magnitude. The mean maximum diameters in parsecs corresponding to the different mean types are given in Table XVII. For the elliptical nebulae, values are given both for the statistical mean observed diameters and for the diameter as calculated for the pure types.

Spirals at the last stage in the observed sequence have diameters of the order of 3000 parsecs. Assuming 1:10 as the ratio of the two axes, the corresponding volume is of the order of $1.4 \times 10^9$ cubic parsecs, and the mean luminosity density is of the order of 7.7 absolute magnitudes per cubic parsec as compared with 8.15 for the galactic system in the vicinity of the sun. These results agree with those of Seares who, from a study of surface brightness, concluded that the galactic system must be placed at the end of, if not actually outside, the series of known spirals when arranged according to density.[1]

TABLE XVII

| Type | Diameter in Parsecs | | Type | Diameter in Parsecs |
|---|---|---|---|---|
| | Obs. | Cal. | | |
| E0 | 360 | 340 | Sa | 1450 |
| E1 | 430 | 380 | Sb | 1900 |
| E2 | 500 | 430 | Sc | 2500 |
| E3 | 590 | 490 | ........ | ........ |
| E4 | 700 | 570 | SBa | 1280 |
| E5 | 810 | 680 | SBb | 1320 |
| E6 | 960 | 850 | SBc | 2250 |
| E7 | 1130 | 1130 | Irr | 1500 |

### MASSES OF EXTRA-GALACTIC NEBULAE

Spectroscopic rotations are available for the spirals M 31[2] and N.G.C. 4594,[3] and from these it is possible to estimate the masses on the assumption of orbital rotation around the nucleus. The distances of the nebulae are involved, however, and this is known accurately only for M 31; for N.G.C. 4594 it must be estimated from the apparent luminosity.

Another method of estimating masses is that used by Öpik[4] in deriving his estimate of the distance of M 31. It is based on the assumption that luminous material in the spirals has about the same coefficient of emission as the material in the galactic system. Öpik computed the ratio of luminosity to mass for our own system in terms of the sun as unity, using Jeans's value[1] for the relative proportion of luminous to non-luminous material. The relation is

---

[1] *Mt. Wilson Contr.*, No. 191; *Astrophysical Journal*, 52, 162, 1920.

[2] Pease, *Mt. Wilson Comm.*, No. 51; *Proceedings of the National Academy of Sciences*, 4, 21, 1918.

[3] Pease, *Mt. Wilson Comm.*, No. 32: *ibid.*, 2, 517, 1916.

[4] *Astrophysical Journal*, 55, 406, 1922.

$$\text{Mass} = 2.6\,L\,. \qquad (9)$$

The application of this method of determining orders of masses seems to be justified, at least in the case of the later-type spirals and irregular nebulae, by the many analogies with the galactic system itself. Moreover, when applied to M 31, where the distance is fairly well known, it leads to a mass of the same order as that derived from the spectrographic rotation:

MASS OF M 31

| | |
|---|---|
| Spectrographic rotation | $3.5\times 10^{9}\,\odot$ |
| Öpik's method | $1.6\times 10^{9}$ |

The distance of N.G.C. 4594 is unknown, but the assumption that it is a normal nebula with an absolute magnitude of $-15.2$ places it at 700,000 parsecs. The orders of the mass by the two methods are then

MASS OF N.G.C. 4594

| | |
|---|---|
| Spectrographic rotation | $2.0\times 10^{9}\,\odot$ |
| Öpik's method | $2.6\times 10^{8}$ |

Here again the resulting masses are of the same order. They can be made to agree as well as those for M 31 by the not unreasonable assumption that the absolute luminosity of the nebula is 2 mag. or so brighter than normal.

Öpik's method leads to values that are reasonable and fairly consistent with those obtained by the independent spectrographic method. Therefore, in the absence of other resources, its use for deriving the mass of the normal nebula appears to be permissible. The result, $2.6\times 10^{8}\,\odot$, corresponding to an absolute magnitude of $-15.2$, is probably of the right order. The two test cases suggest that this value may be slightly low, but the data are not sufficient to warrant any empirical corrections.

### NUMBERS OF NEBULAE TO DIFFERENT LIMITING MAGNITUDES

The numbers of nebulae to different limiting magnitudes can be used to test the constancy of the density function, or, on the hypothesis of uniform luminosities, to determine the distribution in space. The nebulae brighter than about the tenth magnitude are known individually. Those not included in Holetschek's list are: the Magellanic Clouds, the two nebulae N.G.C. 55 and 1097, between 9.0 and 9.5 mag., and the seven nebulae N.G.C. 134, 289, 1365, 1533, 1559, 1792, and 3726, all between 9.5 and 10.0 mag.

---

[1] *Monthly Notices*, **82**, 133, 1922.

A fair estimate of the number between 10.0 and 11.0 mag. can be derived from a comparison of Holetschek's list with that of Hardcastle, an inspection of images on the Franklin-Adams charts and other photographs, and a correlation between known total magnitudes and the descriptions of size and brightness in Dreyer's catalogues. It appears that very few of these objects were missed by Holetschek in the northern sky—not more than six of Hardcastle's nebulae. For the southern sky, beyond the region observed by Holetschek, the results are very uncertain, but probable upper and lower limits were determined as 50 and 20, respectively. The brighter nebulae are known to be scarce in those regions. A mean value of 35 leads to a total 295 for the entire sky, and this is at least of the proper order.

The number of nebulae between 11.0 and 12.0 mag. can be estimated on the assumption that the two lists, Holetschek's and Hardcastle's, are about equally complete within this range. They are known to be comparable for the brighter nebulae, and, moreover, the total numbers included in the two lists for the same area of the sky, that north of declination $-10^\circ$, are very nearly equal—400 as compared with 408. The percentages of Holetschek's nebulae included by Hardcastle were first determined as a function of magnitude. Within the half-magnitude interval 11.0 to 11.5, for instance, 60 per cent are in Hardcastle's list. If the two lists are equally complete and, taken together, are exhaustive, the total number in the interval will be 1.4 times the number of Holetschek's nebulae. The latter is found to be 50 from smoothed frequency curves of the magnitudes listed in Tables I–IV. The total number north of $-10^\circ$ is therefore 70. This can be corrected to represent the entire sky by applying the factor 1.75, which is the ratio of the total number of Hardcastle's nebulae, 700, to the number north of $-10^\circ$, 400. In this manner a reasonable estimate of 123 is obtained for the number of nebulae in the entire sky between 11.0 and 11.5 mag. Similarly, between 11.5 and 12.0, where 50 per cent of Holetschek's nebulae are included in Hardcastle's list, the total number for the entire sky is found to be 236.

The greatest uncertainty in these figures arises from the assumption that the two lists together are complete to the twelfth magnitude. The figures are probably too small, but no standards are available by which they can be corrected. It is believed, however, that the errors are certainly less than 50 per cent and probably not more than 25 per cent. This will not be excessive in view of the possible deviations from uniform distribution where so limited a number of objects is considered.

Beyond 12.0 mag. the lists quickly lose their aspect of completeness and cannot be used for the present purpose. There are available, however, the counts by Fath[1] of nebulae found on plates of Selected Areas made with the 60-inch reflector at Mount Wilson. The exposures were uniformly 60 minutes on fast plates and cover the Areas in the northern sky down to and including the $-15°$ zone. The limiting photographic magnitudes for stars average about 18.5. The counts have been carefully revised by Seares[2] and are the basis for his estimate of 300,000 nebulae in the entire sky down to this limit.

Approximate limiting total magnitudes for the nebulae in two of the richest fields, S.A. 56 and 80, have been determined from extrafocal exposures with the 100-inch reflector. The results are 17.7 in each case, and this, corrected by the normal color-index of such objects, gives a limiting visual magnitude of about 16.7, which can be used for comparison with the counts of the brighter nebulae.

The various data are collected in Table XVIII, where the observed numbers of extra-galactic nebulae to different limits of visual magnitude are compared with those computed on the assumption of uniform distribution of objects having a constant absolute luminosity. The formula used for the computation is

$$\log N = 0.6\, m_T + \text{Constant}\,, \qquad (10)$$

[1] *Astronomical Journal*, **28**, 75, 1914.

[2] *Mt. Wilson Contr.*, No. 297; *Astrophysical Journal*, **62**, 168, 1925.

where the constant is the value of log $N$ for $m_T=0$. The value $-4.45$ is found to fit the observational data fairly well.

The agreement between the observed and computed log $N$ over a range of more than 8 mag. is consistent with the double assumption of uniform luminosity and uniform distribution or, more generally, indicates that the density function is independent of the distance.

The systematic decrease in the residuals O−C with decreasing luminosity is probably within the observational errors, but it may also be explained as due to a clustering of nebulae in the vicinity of the galactic system. The cluster in Virgo alone accounts for an appreciable part. This is a second-order effect in the distribution, however, and will be discussed at length in a later paper.

TABLE XVIII

NUMBERS OF NEBULAE TO VARIOUS LIMITS

| $m_T$ | LOG $N$* | | O−C | LOG $D$† |
|---|---|---|---|---|
| | O | C | | |
| 8.5........ | 0.85 | 0.65 | +0.20 | 5.74 |
| 9.0........ | 1.08 | 0.95 | .13 | 5.84 |
| 9.5........ | 1.45 | 1.25 | .20 | 5.94 |
| 10.0........ | 1.73 | 1.55 | .18 | 6.04 |
| 10.5........ | 1.95 | 1.85 | .10 | 6.14 |
| 11.0........ | 2.17 | 2.15 | + .02 | 6.24 |
| 11.5........ | 2.43 | 2.45 | − .02 | 6.34 |
| 12.0........ | 2.70 | 2.75 | .05 | 6.44 |
| 16.7........ | 5.48 | 5.57 | −0.09 | 7.38 |
| (18.0)........ | .......... | (6.35) | .......... | (7.64) |

* Log $N=0.6\,m_T-4.45$.

† Log $D=0.2\,m_T+4.04$.

Distances corresponding to the different limiting magnitudes, as derived from formula (8), are given in the last column of Table XVIII. The 300,000 nebulae estimated to the limits represented by an hour's exposure on fast plates with the 60-inch reflector appear to be the inhabitants of space out to a distance of the order of $2.4\times10^7$ parsecs. The 100-inch reflector, with long exposures under good conditions, will probably reach the total visual magnitude 18.0, and this, by a slight extrapolation, is estimated to represent a distance of the order of $4.4\times10^7$ parsecs or $1.4\times10^8$ light-years, within which it is expected that about two million nebulae should be found. This seems to represent the present boundaries of the observable region of space.

### DENSITY OF SPACE

The data are now available for deriving a value for the order of the density of space. This is accomplished by means of the formulae for the numbers of nebulae to a given limiting magnitude and for the distance in terms of the magnitude. In nebulae per cubic parsec, the density is

$$\left.\begin{aligned}\log \rho &= \log N - \log V\\ &= (0.6\, m_T - 4.45) - \log \frac{4\pi}{3} - 3(4.04 + 0.2\, m_T)\\ &= -17.19\end{aligned}\right\} \qquad (11)$$

This is a lower limit, for the absence of nebulae in the plane of the Milky Way has been ignored. The current explanation of this phenomenon in terms of obscuration by dark clouds which encircle the Milky Way is supported by the extra-galactic nature of the nebulae, their general similarity to the galactic system, and the frequency with which peripheral belts of obscuring material are encountered among the spirals. The known clouds of dark nebulosity are interior features of our system, and they do not form a continuous belt. In the regions where they are least conspicuous, however, the extra-galactic nebulae approach nearest to the plane of the Milky Way, many being found within 10°. This is consistent with the hypothesis of a peripheral belt of absorption.

The only positive objection which has been urged to this explanation has been to the effect that the nebular density is a direct function of galactic latitude. Accumulating evidence[1] has failed to confirm this view and indicates that it is largely due to the influence of the great cluster in Virgo, some 15° from the north galactic pole. There is no corresponding concentration in the neighborhood of the south pole.

[1] The latest and most reliable results bearing on the distribution of faint (hence apparently distant) nebulae are found in Seares's revision and discussion of the counts made by Fath on plates of the Selected Areas with the 60-inch reflector. When the influence of the cluster in Virgo is eliminated the density appears to be roughly uniform for all latitudes greater than about 25°.

If an outer belt of absorption is assumed, which, combined with the known inner clouds, obscures extra-galactic nebulae to a mean distance of 15° from the galactic plane, the value derived for the density of space must be increased by nearly 40 per cent. This will not change the order of the value previously determined and is within the uncertainty of the masses as derived by Öpik's method. The new value is then

$$\rho = 9 \times 10^{-18} \text{ nebulae per cubic parsec.} \qquad (12)$$

The corresponding mean distance between nebulae is of the order of 570,000 parsecs, although in several of the clusters the distances between members appear to be a tenth of this amount or less.

The density can be reduced to absolute units by substituting the value for the mean mass of a nebula, $2.6 \times 10^8 \odot$. Then, since the mass of the sun in grams is $2 \times 10^{33}$ and 1 parsec is $3.1 \times 10^{18}$ cm,

$$\rho = 1.5 \times 10^{-31} \text{ grams per cubic centimeter.} \qquad (13)$$

This must be considered as a lower limit, for loose material scattered between the systems is entirely ignored. There are no means of estimating the order of the necessary correction. No positive evidence of absorption by inter-nebular material, either selective or general, has been found, nor should we expect to find it unless the amount of this material is many times that which is concentrated in the systems.

### THE FINITE UNIVERSE OF GENERAL RELATIVITY

The mean density of space can be used to determine the dimensions of the finite but boundless universe of general relativity. De Sitter[1] made the calculations some years ago, but used values for the density, $10^{-26}$ and greater, which are of an entirely different order from that indicated by the present investigations. As a consequence, the various dimensions, both for spherical and for elliptical space, were small as compared with the range of existing instruments.

For the present purpose, the simplified equations which Einstein has derived for a spherically curved space can be used.[2] When

---

[1] *Monthly Notices*, 78, 3, 1917.

[2] Haas, *Introduction to Theoretical Physics*, **2**, 373, 1925.

$R$, $V$, $M$, and $\rho$ represent the radius of curvature, volume, mass, and density, and $k$ and $c$ are the gravitational constant and the velocity of light,

$$R=\frac{c}{\sqrt{4\pi k}}\cdot\frac{1}{\sqrt{\rho}}\,, \tag{14}$$

$$V=2\pi^2R^3\,, \tag{15}$$

$$M=\frac{\pi c^2}{2k}\cdot R\,. \tag{16}$$

Substituting the value found for $\rho$, $1.5\times10^{-31}$, the dimensions become

$$R=8.5\times10^{28}\text{ cm}=2.7\times10^{10}\text{ parsecs,} \tag{17}$$

$$V=1.1\times10^{88}\text{ cm}=3.5\times10^{32}\text{ cubic parsecs,} \tag{18}$$

$$M=1.8\times10^{57}\text{ grams}=9\times10^{22}\odot\,. \tag{19}$$

The mass corresponds to $3.5\times10^{15}$ normal nebulae.

The distance to which the 100-inch reflector should detect the normal nebula was found to be of the order of $4.4\times10^{7}$ parsecs, or about 1/600 the radius of curvature. Unusually bright nebulae, such as M 31, could be photographed at several times this distance, and with reasonable increases in the speed of plates and size of telescopes it may become possible to observe an appreciable fraction of the Einstein universe.

Mount Wilson Observatory
September 1926

Contributions from the Mount Wilson Observatory, No. 325
Reprinted from the *Astrophysical Journal*, Vol. LXV, pp. 23–49, 1927
Printed in the U.S.A.

# STELLAR SPECTRA OF CLASS S

## II. CHANGES IN SPECTRA OF LONG-PERIOD VARIABLE STARS

By PAUL W. MERRILL

### ABSTRACT

*Revised list of S-type stars.*—A revised list of 31 S-type stars, of which 20 are variable, is given in Table I. The presence of zirconium bands in the spectrum of $\chi$ Cygni is noted. The detailed classification of S-type spectra is a problem for the future.

*Spectroscopic data.*—Spectroscopic observations are listed in Table II, which includes the estimated intensities of the bright lines $H\beta$, $H\gamma$, and $H\delta$, and of the dark zirconium and titanium bands. Several variables, especially S Ursae Majoris and R Cygni, were extensively observed in order to determine the spectral variations during the light-cycle. Detailed descriptions of numerous lines follow Table II.

*Characteristic behavior of spectra of variables.*—The characteristic behavior of several features in the spectra of long-period variables is summarized. The zirconium bands are slightly weaker near maximum and the titanium bands much weaker. Bright hydrogen lines are absent at minimum and are strongest near maximum. The intensity decreases rapidly from $H\beta$ to $H\delta$ when titanium bands are absent, but $H\beta$ and $H\gamma$ are weaker when these bands are present. Bright enhanced lines of iron are visible at maximum and persist through a considerable portion of the light-cycle. The bright lines λλ 4202, 4308, 4511, 4521, 4571, and several others behave about as in Me variables, but certain differences are noted. The dark line λ 4554 $Ba^+$ is slightly stronger at maximum than at other phases while λ 4607 *Sr* is much weaker at maximum.

*Relationship between classes M and S.*—S-type spectra are closely related to those of giant stars of class M, and the temperature ranges of the two types of stars overlap. S-type stars probably have lower densities than M-type stars of the same effective temperatures. This is indicated by the spectra and by the relatively long periods of S-type variables.

*Special effects of titanium oxide.*—Certain peculiarities of advanced M-type spectra may be special effects of a relatively high stratum of absorbing titanium oxide. S-type stars will be useful in studying this and similar problems of red stars.

A general description of spectra of class S, together with an account of the observations leading to the inclusion of this class in the Draper system of stellar classification, may be found in *Mount Wilson Contribution*, No. 252; *Astrophysical Journal*, **56**, 457, 1922. This description contains references to prominent absorption bands apparently characteristic of class S, whose origin has since been identified with zirconium oxide.[1] It is planned later to publish a detailed discussion of the identification of lines and bands in spectra of this type.

The present contribution deals principally with certain long-period variable stars whose spectra are characterized by the chief features of class S. The spectral changes which accompany the periodic variations in brightness shed a strong light upon the relationship between classes M and S, and have a bearing on many other problems of long-period variables.

---

[1] *Publications of the Astronomical Society of the Pacific*, **35**, 217, 1923.

A revised list of thirty-one stars of class S is given in Table I. There is some doubt concerning the proper classification of W Cassiopeiae, R Orionis, and R Canis Minoris. These stars have the S-type characteristics, with the important exception of the zirconium oxide bands, which are very weak or absent. A fourth star, not included in Table I, which bears some resemblance to class S but does not exhibit definite zirconium bands, is VX Geminorum,[1] H.D. 55284.

Another question concerning classification is raised by spectra which contain both titanium and zirconium bands. In certain stars, for example $\pi^1$ Gruis, the S-type features are dominant and the spectra might be described as class S *plus* titanium bands. In other stars, for example H.D. 22649 (Boss 826), H.D. 35155,[2] and $\chi$ Cygni, the S-type features are less dominant, and the spectra appear to be intermediate between classes M and S. Intermediate spectra in which the zirconium and the titanium bands are both comparatively weak are apparently not very numerous, as H.D. 22649 is the only one found among the M-type stars on the absolute magnitude program of the Mount Wilson Observatory.[3]

Various combinations of zirconium and titanium bands have been observed in the spectra of variable stars. In a given spectrum both groups of bands may be strong, as in AA Cygni (see Plate XVII *b*); or the zirconium bands may be strong and the titanium weak, as in R Andromedae, or absent, as in S Ursae Majoris. In several variables the titanium bands undergo large variations in intensity during the light-cycle. In one well-known long-period variable, $\chi$ Cygni, zirconium bands of moderate intensity are associated with very strong titanium bands. In this case, the M-type spectrum appears dominant and the star is not included in Table I. It may,

---

[1] See remark in the *Henry Draper Catalogue;* also Sanford, *Mt. Wilson Contr.*, No. 276; *Astrophysical Journal*, **59**, 339, 1924.

[2] See Plate XII in *Mt. Wilson Contr.*, No. 252; *Astrophysical Journal*, **56**, 457, 1922.

[3] *Mt. Wilson Contr.*, No. 319; *Astrophysical Journal*, **64**, 225, 1926.

# PLATE XVII

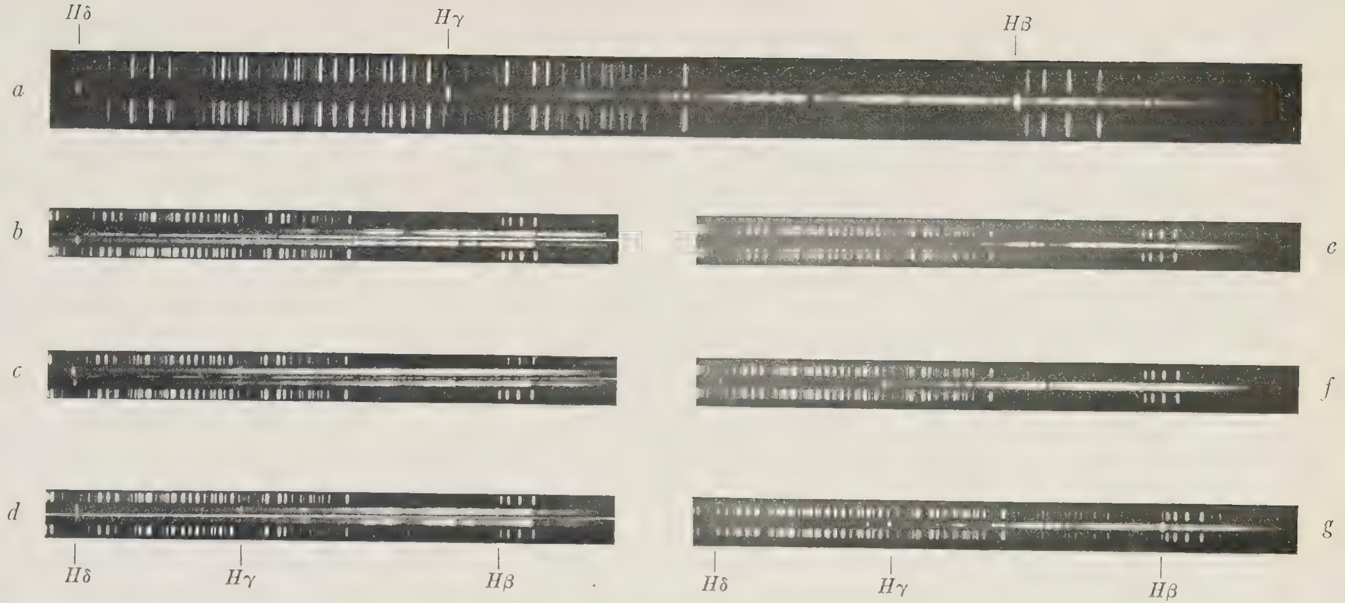

SPECTRA OF S-TYPE VARIABLE STARS

*a)* R Cygni, $\gamma$ 11117; mag. 8.0; phase +32 days.
*b)* Upper, AA Cygni, C3377; lower, RS Ursae Majoris, C3241, April 9, 1925; spectral class M5e.
*c)* U Cassiopeiae: upper, C3074; mag. 7.4; phase −11 days: lower, C3538; mag. 9.0; phase +22 days.
*d)* T Geminorum: upper, C3240; mag. 8.9; phase −10 days: lower, C 3186; mag. 9.4; phase −47 days.
*e)* R Cygni, C3492; mag. 9.6; phase −61 days.
*f)* R Cygni, C3572; mag. 6.8; phase − 3 days.
*g)* R Cygni, C1055; mag. 9.7; phase +115 days.

however, eventually prove expedient to classify such spectra with those of class S.

It will doubtless become desirable to form subdivisions of class S, analogous to those of class M, depending on the intensity of the characteristic features, especially of the zirconium bands, and to provide a nomenclature for spectra intermediate between classes M and S; but the detailed discussion of these matters should perhaps await further experience.

TABLE I

STARS OF CLASS S

| Name | H.D. | R.A. 1900 | Dec. 1900 | Mag. | Spect. | Period, Days |
|---|---|---|---|---|---|---|
| X Androm...... | 1167 | $0^h10^m9$ | $+46^\circ 27'$ | 8.1–14.2 | Se | 346.5 |
| R Androm...... | 1967 | 0 18.8 | +38 1 | 5.6–14.0 | Se | 410.7 |
| U Cassiop...... | 4350 | 0 40.8 | +47 43 | 8.0–16 | Se | 276.0 |
| W Cassiop...... | 5235 | 0 49.0 | +58 1 | 8.4–12.2 | (Se) | 403.5 |
| S Cassiop....... | 7769 | 1 12.3 | +72 5 | 7.6–14.5 | Se | 609.5 |
| Boss 826........ | 22649 | 3 33.5 | +62 54 | 5.3 | S | ........... |
| T Camelop...... | 29147 | 4 30.3 | +65 57 | 7.0–13.5 | Se | 370 |
| R Orionis....... | 31798 | 4 53.6 | + 7 59 | 8.7–13.5 | (Se) | 378.5 |
| | 35155 | 5 17.6 | − 8 45 | 7.0 | S | ........... |
| R Lyncis....... | 51610 | 6 53.0 | +55 27 | 7.0–13.8 | Se | 379.2 |
| R Gemin....... | 53791 | 7 1.3 | +22 52 | 6.4–13.8 | Se | 370 |
| R Can. Min..... | 54300 | 7 3.2 | +10 11 | 7.2–10.0 | (Se) | 337.7 |
| | 58881 | 7 22.4 | −11 31 | 9.0 | S | ........... |
| | 62164 | 7 37.5 | −10 39 | Var. | S | ........... |
| T Gemin........ | 63334 | 7 43.3 | +23 59 | 8.0–13.5 | Se | 288.1 |
| | 63733 | 7 45.3 | −18 45 | 8.5 | S | ........... |
| | 64332 | 7 48.3 | −11 22 | 8 1 | S | ........... |
| V Cancri....... | 70276 | 8 16.0 | +17 36 | 7.5–13.0 | Se | 272.1 |
| S Urs. Maj..... | 110813 | 12 39.6 | +61 38 | 7.3–12.5 | Se | 226.5 |
| | 121447 | 13 50.3 | −17 45 | 8.1 | S | ........... |
| R Camelop..... | 127226 | 14 25.1 | +84 17 | 7.9–13.7 | Se | 269.5 |
| RW Librae..... | 136734 | 15 17.2 | −23 42 | 8.6–11.7 | (Se) | 490 (about) |
| | 156957 | 17 15.3 | −41 39 | 8.4 | S | ........... |
| | 172804 | 18 37.1 | + 6 43 | 9.1 | S | ........... |
| | 177175 | 18 58.5 | +12 7 | 8.7 | S | ........... |
| T Sagittarii..... | 180196 | 19 10.5 | −17 19 | 7.2–<13.1 | Se | 381.3 |
| R Cygni........ | 185456 | 19 34.1 | +49 59 | 6.6–13.9 | Se | 425.9 |
| AA Cygni...... | 190629 | 20 0.8 | +36 32 | 8.4– 9.2 | S | Unknown |
| S Cygni........ | ........ | 20 3.4 | +57 42 | 9.2–<14.7 | Se | 323 |
| Z Delphini...... | 195763 | 20 28.1 | +17 7 | 8.2–14.0 | Se | 303.4 |
| $\pi^1$ Gruis........ | 212087 | 22 16.6 | −46 27 | 6.6 | S | ........... |

The journal of observations and certain data concerning the individual spectrograms are given in Table II. The meaning of the letters preceding the plate numbers in the first column is as follows:

C—One-prism spectrograph, attached at the Cassegrain focus of the 100-inch Hooker telescope. Two camera lenses were employed with focal lengths of 10 and 18 inches, and dispersions at $H\gamma$ of 75 and 40 A per mm, respectively.

$\gamma$—One-prism spectrograph, attached at the Cassegrain focus of the 60-inch telescope. Nearly all the plates were taken with the 18-inch camera, having a dispersion at $H\gamma$ of 34 A per mm.

H—Small ultra-violet spectrograph, attached at the Newtonian focus of the 100-inch telescope. Dispersion at $H\gamma$, 95 A per mm.

G—Plane-grating spectrograph for the yellow and red regions, attached at the Cassegrain focus of the 100-inch telescope. Dispersion, 66 A per mm.

R—Three-prism spectrograph for the yellow and red regions, attached at the Cassegrain focus of the 100-inch telescope. Average dispersion from λ 5900 to λ 6700, 40 A per mm.

The source for plate numbers without prefix is indicated in the notes following the table.

The column headed "Phase" gives the number of days before (−) or after (+) the nearest maximum. Most of the photometric data were supplied by the Harvard College Observatory through the courtesy of Dr. Shapley and Mr. Campbell. I wish to thank these gentlemen for their continued co-operation in furnishing data concerning variable stars.

The intensities of the bright hydrogen lines are estimates of the strength of the lines on the negatives, no allowance having been made for instrumental or other observational effects. The $H\beta$ line is often overexposed, and in these cases (say intensity greater than 10) the estimates of this line are doubtless only rough approximations. The estimated intensities of the absorption bands of zirconium oxide and titanium oxide are given next. The figures for the titanium bands denote the subdivision of class M to which the intensity of the bands corresponds. Subdivisions of class S have not yet been formed, but the estimates of the zirconium bands have been made on somewhat the same basis. These estimates may be interpreted as follows: 0, not seen; 1, weak; 2, medium intensity; 3, strong; 4, very strong; "pr," present; "tr," trace. Parentheses indicate uncertainty.

Notes in the last column indicate the portion of the spectrum shown by each spectrogram, if it is other than the usual blue-violet region. Remarks concerning the effective exposure refer to the region from λ 4600 to λ 4800, unless another portion of the spectrum is mentioned.

## TABLE II
### Journal of Observations

| Plate | Date | J.D. 242 | Vis. Mag. | Phase | Intensity Emission Lines | | | Intensity Absorption Bands | | Continuous Spectrum |
|---|---|---|---|---|---|---|---|---|---|---|
| | | | | | $H\beta$ | $H\gamma$ | $H\delta$ | $ZrO_2$ | $TiO_2$ | |
| **X Andromedae** | | | | | | | | | | |
| C 1454.. | 1921 Nov. 13 | 3007 | 9.5 | − 16 | 12 | 2 | .... | 2 | 0 | |
| C 1462.. | Nov. 14 | 3008 | 9.5 | − 15 | 4 | 0.5 | .... | pr | 0 | Trace |
| C 1943.. | 1922 Oct. 8 | 3336 | 9.3 | − 24 | 4 | .... | .... | pr! | 0 | Green to red |
| C 2408.. | 1923 Aug. 29 | 3661 | 11.1 | − 45 | 4 | .... | .... | (2) | 0 | Underexp. |
| C 2468.. | Sept. 30 | 3693 | 9.8 | − 13 | 3 | .... | .... | .... | .... | Not seen |
| γ 12176. | Oct. 3 | 3696 | 9.7 | − 10 | 8 | 0.5 | .... | (2) | 0 | Underexp. |
| C 2511.. | Oct. 26 | 3719 | 9.5 | + 13 | 20 | 6 | 1 | 2 | 0 | |
| C 2566.. | Nov. 28 | 3752 | 10.2 | + 46 | 20 | 5 | tr | (3) | 0 | |
| C 2888.. | 1924 July 18 | 3985 | 11.8 | − 55 | 2 | .... | .... | tr | 0 | Underexp. |
| C 3015.. | Sept. 15 | 4044 | 8.8 | + 4 | 30 | 10 | 2 | 2 | 0 | |
| **R Andromedae** | | | | | | | | | | |
| 3238.. | 1915 May 30 | 0648 | 7.3 | + 5 | 1.5 | tr | tr | pr | .... | Trace |
| 3291.. | July 5 | 0684 | 8.5 | + 41 | 1.5 | tr | tr | pr | .... | Trace |
| γ 8725.. | 1919 Oct. 3 | 2235 | 7.5 | − 25 | 5 | 2 | 1 | 3 | 1 | |
| C 130... | Oct. 15 | 2247 | 7.5 | − 13 | 4 | 2 | 2 | 2 | 1 | |
| C 137... | Oct. 16 | 2248 | 7.5 | − 12 | 6 | 3 | 3 | 2 | 1 | |
| C 1499.. | 1921 Dec. 15 | 3039 | 7.5 | − 16 | 12 | 5 | 5 | 2 | (0) | Violet to yellow; overexp. |
| C 3389.. | 1925 July 7 | 4339 | 9.0 | + 39 | 7 | 2 | 2 | (4) | (3) | Underexp. |
| C 3495.. | Sept. 3 | 4397 | 10.5 | + 97 | 3 | 0.5 | 0.5 | (3) | (4) | Underexp. |
| **U Cassiopeiae** | | | | | | | | | | |
| C 1338.. | 1921 Sept. 21 | 2954 | 10.8 | − 56 | .... | .... | .... | .... | (4) | Trace |
| C 1449.. | Nov. 12 | 3006 | 8.2 | − 4 | 8 | 4 | 4 | 2 | 2 | |
| C 1455.. | Nov. 13 | 3007 | 8.2 | − 3 | 9 | 4 | 3 | 2 | 2 | |
| C 1873.. | 1922 Sept. 8 | 3306 | 9.3 | + 19 | 3 | 2 | 4 | 3 | 5 | |
| C 2363.. | 1923 July 27 | 3628 | 11.5 | + 67 | 1 | 0.5 | .... | .... | (4) | Trace |
| C 3074.. | 1924 Nov. 10 | 4100 | 7.4 | − 11 | 12 | 7 | 6 | 2 | 2 | |
| C 3096.. | Dec. 13 | 4133 | 8.1 | + 22 | 12 | 9 | 6 | (2) | 2 | Overexp. |
| C 3113.. | 1925 Jan. 6 | 4157 | 9.2 | + 46 | 10 | 9 | 6 | 3 | 3 | Overexp. |
| C 3494.. | Sept. 2 | 4396 | 8.9 | − 6 | 2 | 1 | 3 | 3 | 4 | |
| C 3538.. | Sept. 30 | 4424 | 9.0 | + 22 | 3 | 2 | 4 | 4 | 5 | |
| **W Cassiopeiae** | | | | | | | | | | |
| C 3918.. | 1926 July 26 | 4723 | 8.2 | − 18 | 8 | 4 | .... | (0) | 0 | |
| C 3927.. | Aug. 10 | 4738 | 8.0 | − 3 | 12 | 7 | 1 | 0 | 0 | |
| **S Cassiopeiae** | | | | | | | | | | |
| γ 10755. | 1922 Jan. 13 | 3068 | 8.9 | + 22 | 6 | 2 | tr | .... | .... | Trace |
| γ 11985. | 1923 July 29 | 3630 | 7.7 | − 1 | 12 | 4 | 1 | 2 | 1 | |
| γ 12100. | Sept. 2 | 3665 | 8.4 | + 34 | 10 | 3 | 0.5 | 2 | 2 | |

TABLE II—*Continued*

| PLATE | DATE | J.D. 242 | VIS. MAG. | PHASE | INTENSITY EMISSION LINES | | | INTENSITY ABSORPTION BANDS | | CONTINUOUS SPECTRUM |
|---|---|---|---|---|---|---|---|---|---|---|
| | | | | | $H\beta$ | $H\gamma$ | $H\delta$ | $ZrO_2$ | $TiO_2$ | |
| | | | | | H.D. 22649 | | | | | |
| γ 7471.. | 1918 Oct. 20 | 1887 | 5.3 | ..... | .... | .... | .... | 1 | 3 | |
| γ 7838.. | 1919 Jan. 22 | 1981 | ...... | ..... | .... | .... | .... | 1 | 3 | |
| γ 8896.. | Dec. 8 | 2301 | ...... | ..... | .... | .... | .... | 1 | 3 | |
| C 1934.. | 1922 Oct. 7 | 3335 | ...... | ..... | .... | .... | .... | pr | 3 | Blue to red |
| C 2071.. | 1923 Jan. 8 | 3428 | ...... | ..... | .... | .... | .... | pr | pr | Green to red |
| | | | | | T Camelopardalis | | | | | |
| γ 11245. | 1922 Aug. 9 | 3276 | 9.0 | + 59 | 5 | 2 | .... | 3 | 1 | Underexp. |
| | | | | | R Orionis | | | | | |
| C 2409.. | 1923 Aug. 29 | 3661 | 9.3 | + 11 | 10 | 5 | 0.5 | 0 | 0 | Red |
| C 2424.. | Sept. 1 | 3664 | 9.3 | + 14 | 1 | 0.4 | .... | 0 | 0 | |
| C 3017.. | 1924 Sept. 15 | 4044 | 10.0 | − 10 | 10 | 5 | 0.5 | 0 | 0 | |
| | | | | | H.D. 35155 | | | | | |
| C 672... | 1920 Sept. 26 | 2594 | 7.0 | ..... | .... | .... | .... | 1 | 3 | |
| C 2065.. | 1923 Jan. 7 | 3427 | ...... | ..... | .... | .... | .... | pr | pr | Green to red |
| | | | | | R Lyncis | | | | | |
| 3122.. | 1915 Feb. 28 | 0557 | 8.2 | − 4 | 8 | 3 | 1 | 2 | 0 | |
| 3123.. | Feb. 28 | 0557 | 8.2 | − 4 | 7 | 3.5 | 1 | 2 | 0 | |
| 3140.. | Mar. 12 | 0569 | 8.1 | + 8 | 5.5 | 3 | 0.5 | 2 | 0 | |
| 3160.. | Mar. 28 | 0585 | 8.3 | + 24 | 3 | 2 | .... | .... | .... | Not seen |
| C 2512.. | 1923 Oct. 26 | 3719 | 11.3 | +124 | 3 | 0.5 | .... | (3) | 0 | |
| C 3539.. | 1925 Sept. 30 | 4424 | 9.9 | + 62 | 10 | 4 | 1 | 3 | 1 | |
| | | | | | R Geminorum | | | | | |
| γ 8727.. | 1919 Oct. 3 | 2235 | 7.4 | − 27 | 8 | 3 | 0.5 | 2 | 0 | |
| C 127... | Oct. 14 | 2246 | 7.0 | − 16 | 10 | 5 | 2 | 2 | 0 | |
| C 133... | Oct. 15 | 2247 | 7.0 | − 15 | 12 | 6 | 2 | 2 | 0 | |
| C 144... | Oct. 17 | 2249 | 7.0 | − 13 | 12 | 6 | 2 | 2 | 0 | |
| C 238... | 1920 Jan. 9 | 2333 | 8.7 | + 75 | 0.5 | tr | .... | .... | .... | Not seen |
| C 681... | Sept. 28 | 2596 | 7.2 | − 30 | 8 | 3 | .... | 3 | 0 | |
| C 821... | Dec. 27 | 2686 | 8.3 | + 60 | 10 | 4 | 0.5 | 3 | 0 | |
| C 1339.. | 1921 Sept. 21 | 2954 | 8.1 | − 50 | 4 | 0.5 | .... | 2 | 0 | |
| γ 10524. | Oct. 10 | 2973 | 7.2 | − 31 | 12 | 5 | 1 | 2 | 0 | |
| C 1402.. | Oct. 13 | 2976 | 7.1 | − 28 | .... | .... | .... | pr | 0 | Green to red |
| C 1408.. | Oct. 14 | 2977 | 7.1 | − 27 | .... | .... | .... | pr | 0 | Green to red |
| C 1456.. | Nov. 13 | 3007 | 7.2 | + 3 | 15 | 7 | 2 | 2 | 0 | |
| C 1501.. | Dec. 15 | 3039 | 7.3 | + 35 | 12 | 7 | 2 | 3 | 0 | |
| C 1502.. | Dec. 15 | 3039 | 7.3 | + 35 | 7 | 3 | tr | 2 | 0 | Blue to yellow |
| C 2003.. | 1922 Nov. 6 | 3365 | 6.6 | + 10 | 25 | 15 | 7 | (2) | (0) | Overexp. |

TABLE II—*Continued*

| PLATE | DATE | J.D. 242 | VIS. MAG. | PHASE | INTENSITY EMISSION LINES | | | INTENSITY ABSORPTION BANDS | | CONTINUOUS SPECTRUM |
|---|---|---|---|---|---|---|---|---|---|---|
| | | | | | $H\beta$ | $H\gamma$ | $H\delta$ | $ZrO_2$ | $TiO_2$ | |
| R Geminorum—*Continued* | | | | | | | | | | |
| C 2062.. | 1923 Jan. 6 | 3426 | 7.6 | + 71 | 10 | 6 | 1.5 | 3 | 0 | |
| C 2480.. | Oct. 3 | 3696 | 9.1 | − 58 | 3 | 1 | .... | 3 | 0 | |
| C 2515.. | Oct. 27 | 3720 | 7.8 | − 34 | 5 | 2 | .... | 3 | 0 | |
| C 2519.. | Oct. 28 | 3721 | 7.8 | − 33 | 6 | 1 | .... | 3 | 0 | |
| C 2563.. | Nov. 27 | 3751 | 7.3 | − 3 | 8 | 2 | .... | 3 | 0 | |
| C 2701.. | 1924 Feb. 21 | 3837 | 9.2 | + 83 | 12 | 4 | tr | 3 | 0 | |
| γ 13098. | Nov. 11 | 4101 | 6.8 | − 9 | 16 | 8 | 2 | 2 | 0 | |
| C 3097.. | Dec. 13 | 4133 | 7.0 | + 23 | 25 | 12 | 6 | 2 | 0 | Overexp. |
| C 3574.. | 1925 Oct. 30 | 4454 | 6.8 | − 27 | 20 | 10 | 2 | 2 | 0 | |
| H 57.... | Nov. 16 | 4471 | 6.8 | − 10 | 15 | 7 | 2 | pr | (0) | |
| H 61.... | Nov. 17 | 4472 | 6.8 | − 9 | 30 | 16 | 5 | pr | (0) | Overexp. |
| C 3623.. | Dec. 26 | 4511 | 7.1 | + 30 | 24 | 11 | 5 | 2 | 0 | |
| C 3647.. | 1926 Jan. 4 | 4520 | 7.2 | + 39 | 14 | 7 | 3 | 3 | 0 | Violet to red |
| C 3671.. | Jan. 25 | 4541 | 7.7 | + 60 | 16 | 8 | 4 | 2 | 0 | |
| C 3694.. | Feb. 21 | 4568 | 9.0 | + 87 | 15 | 7 | 3 | 2 | 0 | |
| R Canis Minoris | | | | | | | | | | |
| C 294... | 1920 Mar. 3 | 2387 | 8.0 | − 10 | 15 | 5 | 0.5 | 0 | 0 | |
| C 299... | Mar. 4 | 2388 | 8.0 | − 9 | 15 | 5 | 0.5 | 0 | 0 | |
| γ 9047.. | Mar. 7 | 2391 | 8.0 | − 6 | 8 | 3 | .... | .... | 0 | Trace |
| C 909... | 1921 Feb. 25 | 2746 | 8.3 | + 20 | 15 | 7 | 2 | 0 | 0 | |
| γ 9990.. | Feb. 28 | 2749 | 8.3 | + 23 | .... | .... | .... | .... | .... | Red; trace |
| C 958... | Mar. 26 | 2775 | 8.4 | + 49 | 1 | 0.5 | .... | .... | .... | Not seen |
| C 1522.. | 1922 Jan. 12 | 3067 | 8.5 | − 33 | 6 | 3 | .... | .... | .... | Underexp. |
| C 2015.. | Dec. 8 | 3397 | 8.1 | − 42 | 12 | 5 | 0.5 | 0 | 0 | |
| C 2067.. | 1923 Jan. 7 | 3427 | 8.1 | − 12 | 4 | .... | .... | 0 | 0 | Yellow to red |
| C 2157.. | Mar. 8 | 3487 | 8.4 | + 48 | 1 | tr | .... | .... | .... | Not seen |
| H 5..... | Mar. 23 | 3502 | 8.9 | + 63 | 1 | 0.5 | .... | ? | 0 | |
| C 2520.. | Oct. 28 | 3721 | 9.4 | − 77 | 0.5 | .... | .... | .... | .... | Not seen |
| C 2568.. | Nov. 28 | 3752 | 8.3 | − 46 | tr | .... | .... | 0 | 0 | Red |
| C 3573.. | 1925 Oct. 30 | 4454 | 7.6 | − 4 | 14 | 7 | 1 | 0 | 0 | |
| H 58.... | Nov. 16 | 4471 | 7.6 | + 13 | 14 | 6 | 1 | ? | 0 | |
| C 3615.. | Dec. 24 | 4509 | 8.2 | + 51 | 2 | 1 | .... | 0 | 0 | Yellow to red |
| H.D. 58881 | | | | | | | | | | |
| C 2191.. | 1923 Apr. 3 | 3513 | 9.0 | ..... | .... | .... | .... | 2 | 0 | |
| H.D. 62164 | | | | | | | | | | |
| C 3175.. | 1925 Feb. 11 | 4193 | (8.5) | ..... | .... | .... | .... | 2 | 0 | |
| T Geminorum | | | | | | | | | | |
| C 968... | 1921 Mar. 28 | 2777 | 9.1 | − 23 | 2 | 0.5 | 0.5 | (3) | 3 | Underexp. |
| C 1009.. | Apr. 29 | 2809 | 8.6 | + 9 | 10 | 5 | 3 | 2 | 1 | |
| C 2072.. | 1923 Jan. 8 | 3428 | 9.9 | + 65 | 1 | 0.5 | .... | 3 | 3 | |
| C 2516.. | Oct. 27 | 3720 | 9.9 | + 60 | 3 | 2 | 1 | 3 | 5 | |

TABLE II—*Continued*

| PLATE | DATE | J.D. 242 | VIS. MAG. | PHASE | INTENSITY EMISSION LINES | | | INTENSITY ABSORPTION BANDS | | CONTINUOUS SPECTRUM |
|---|---|---|---|---|---|---|---|---|---|---|
| | | | | | $H\beta$ | $H\gamma$ | $H\delta$ | $ZrO_2$ | $TiO_2$ | |
| T Geminorum—*Continued* | | | | | | | | | | |
| C 2747.. | 1924 Apr. 17 | 3893 | 10.6 | − 68 | .... | .... | tr | pr | (4) | Trace |
| C 3171.. | 1925 Feb. 10 | 4192 | 10.2 | − 68 | .... | .... | .... | 3 | 6 | |
| C 3186.. | Mar. 3 | 4213 | 9.4 | − 47 | 0.5 | tr | 2 | 3 | 6 | |
| C 3240.. | Apr. 9 | 4250 | 8.9 | − 10 | 7 | 4 | 3 | 2 | 3 | |
| C 3279.. | May 5 | 4276 | 8.9 | + 16 | 6 | 3 | 2 | 2 | 3 | |
| C 3620.. | Dec. 25 | 4510 | 9.0 | − 40 | 1 | 0.5 | 1 | pr! | (3) | Blue to red |
| C 3672.. | 1926 Jan. 25 | 4541 | 8.7 | − 9 | 16 | 9 | 6 | 2 | 2 | Overexp. |
| γ 14019. | Jan. 28 | 4544 | 8.7 | − 6 | 7 | 4 | 2 | 2 | 2 | |
| γ 14024. | Feb. 18 | 4565 | 8.9 | + 15 | 13 | 7 | 4 | 2 | 2 | |
| H.D. 63733 | | | | | | | | | | |
| C 1464.. | 1921 Nov. 14 | 3008 | 8.5 | ..... | .... | .... | .... | 1 | 2 | |
| H.D. 64332 | | | | | | | | | | |
| γ 9847.. | 1920 Dec. 29 | 2688 | 8.1 | ..... | .... | .... | .... | 2 | 4 | |
| V Cancri | | | | | | | | | | |
| C 194... | 1919 Nov. 9 | 2272 | 8.0 | + 10 | 15 | 7 | 2 | tr | 0 | |
| γ 8875.. | Nov. 13 | 2276 | 8.0 | + 14 | 7 | 3 | 1 | tr | 0 | |
| γ 8883.. | Nov. 14 | 2277 | 8.0 | + 15 | 6 | 3 | 0.7 | tr | 0 | Underexp. |
| γ 10132. | 1921 Apr. 27 | 2807 | 7.9 | − 3 | 10 | 5 | 0.7 | tr | 0 | |
| γ 10757. | 1922 Jan. 13 | 3068 | 7.9 | − 12 | 9 | 5 | 0.7 | tr | 0 | |
| C 1552.. | Feb. 11 | 3097 | 7.8 | + 17 | 15 | 8 | 3 | tr | 0 | |
| C 2743.. | 1924 Apr. 16 | 3892 | 8.0 | + 15 | 18 | 9 | 2 | tr | 0 | |
| C 3117.. | 1925 Jan. 6 | 4157 | 8.1 | − 14 | 5 | 3 | tr | pr | 0 | Blue to red |
| C 3673.. | 1926 Jan. 25 | 4541 | 12.0 | + 99 | a | ? | a | 0 | 0 | |
| S Ursae Majoris | | | | | | | | | | |
| 3193.. | 1915 Apr. 25 | 0613 | 8.5 | − 55 | tr | .... | .... | .... | .... | Not seen |
| 3200.. | May 7 | 0625 | 8.5 | − 43 | tr | .... | .... | .... | .... | Not seen |
| 3254.. | June 11 | 0660 | 8.1 | − 8 | 2 | 2− | .... | pr | (0) | Underexp. |
| 3271.. | June 25 | 0674 | 7.8 | + 6 | 3 | 4 | .... | pr | (0) | Underexp. |
| C 369... | 1920 Apr. 8 | 2423 | 8.5 | − 31 | 7 | 3 | .... | 2 | 0 | |
| C 373... | Apr. 10 | 2425 | 8.5 | − 29 | 11 | 5 | .... | 2 | 0 | |
| γ 9252.. | June 3 | 2479 | 8.2 | + 25 | 6 | 3 | .... | 2 | 0 | |
| γ 9848.. | Dec. 29 | 2688 | 8.4 | + 18 | 6 | 4 | 1 | 2 | 0 | |
| C 866... | 1921 Jan. 28 | 2718 | 8.7 | + 48 | 4 | 2 | .... | 3 | 0 | |
| C 926... | Feb. 27 | 2748 | 10.0 | + 78 | tr | .... | .... | (3) | 0 | Underexp. |
| C 1169.. | July 23 | 2894 | 8.1 | − 3 | 9 | 4 | 1 | 1 | 0 | |
| C 1553.. | 1922 Feb. 11 | 3097 | 8.5 | − 43 | 7 | 3 | .... | 2 | 0 | |
| C 1626.. | Mar. 19 | 3133 | 7.6 | − 7 | 9 | 6 | 1 | 1 | 0 | |
| C 2068.. | 1923 Jan. 7 | 3427 | 10.3 | + 65 | .... | .... | .... | pr! | 0 | Red |
| γ 11744. | May 1 | 3541 | 8.5 | − 42 | 10 | 4 | .... | (2) | 0 | |
| C 2286.. | June 4 | 3575 | 8.0 | − 8 | 11 | 5 | 1 | 1 | 0 | |

### TABLE II—*Continued*

| PLATE | DATE | J.D. 242 | VIS. MAG. | PHASE | INTENSITY EMISSION LINES | | | INTENSITY ABSORPTION BANDS | | CONTINUOUS SPECTRUM |
|---|---|---|---|---|---|---|---|---|---|---|
| | | | | | $H\beta$ | $H\gamma$ | $H\delta$ | $ZrO_2$ | $TiO_2$ | |
| S Ursae Majoris—*Continued* | | | | | | | | | | |
| C 2340.. | July 3 | 3604 | 8.1 | +21 | 12 | 6 | 2 | 1 | 0 | |
| C 2648.. | 1924 Jan. 22 | 3807 | 8.0 | −19 | 12 | 6 | 1 | 2 | 0 | |
| C 2702.. | Feb. 21 | 3837 | 8.2 | +11 | 10 | 5 | 1 | 2 | 0 | |
| C 2748.. | Apr. 17 | 3893 | 10.0 | +67 | tr | .... | .... | 3 | 0 | |
| C 2816.. | June 12 | 3949 | 11.0 | −94 | .... | .... | .... | pr | 0 | |
| C 3118.. | 1925 Jan. 6 | 4157 | 11.2 | +114 | .... | .... | .... | pr | .... | Red; under-exp. |
| C 3172.. | Feb. 11 | 4193 | 10.3 | −73 | .... | .... | .... | (3) | 0 | |
| C 3187.. | Mar. 3 | 4213 | 8.5 | −53 | 9 | 4 | .... | 3 | 0 | |
| H.D. 121447 | | | | | | | | | | |
| C 1706.. | 1922 May 16 | 3191 | 8.1 | ..... | .... | .... | .... | 1 | 0 | |
| γ 11842. | 1923 June 5 | 3576 | ...... | ..... | .... | .... | .... | .... | 0 | Blue to yellow; poor |
| C 2745.. | 1924 Apr. 16 | 3892 | ...... | ..... | .... | .... | .... | 0 | 0 | |
| C 2823.. | June 14 | 3951. | ...... | ..... | .... | .... | .... | 1 | 0 | |
| R Camelopardalis | | | | | | | | | | |
| γ 8266.. | 1919 June 9 | 2119 | 8.2 | +7 | 4 | 2 | .... | .... | .... | Not seen |
| γ 8272.. | June 10 | 2120 | 8.2 | +8 | 2− | 1 | .... | .... | .... | Not seen |
| γ 8345.. | July 8 | 2148 | 8.9 | +36 | 2 | 1 | .... | pr | (2) | Trace |
| γ 11077. | 1922 May 17 | 3192 | 8.2 | −18 | 4 | 2 | 0.4 | pr | .... | Trace |
| γ 11603. | 1923 Feb. 5 | 3456 | 8.6 | −23 | 2 | 1 | .... | 2 | 2 | Underexp. |
| γ 11702. | Apr. 7 | 3517 | 8.6 | +38 | 2 | 1 | tr | 2 | 3 | Underexp. |
| RW Librae | | | | | | | | | | |
| C 2649.. | 1924 Jan. 22 | 3807 | (8.5) | ..... | 12 | 8 | 3 | ? | 1 | |
| C 3188.. | 1925 Mar. 3 | 4213 | (9.5) | ..... | tr | 4 | 2 | ? | 5 | |
| C 3242.. | Apr. 9 | 4250 | (9.3) | ..... | 1 | 4 | 3 | 0 | 5 | |
| C 3281.. | May 5 | 4276 | (10.0) | ..... | .... | tr | .... | .... | pr | Trace |
| C 3375.. | July 5 | 4337 | (10.0) | ..... | .... | .... | .... | .... | .... | Trace |
| C 3780.. | 1926 Apr. 30 | 4636 | (8.5) | ..... | 4 | 3 | 1 | 0 | 2 | |
| H.D. 156957 | | | | | | | | | | |
| C 1130.. | 1921 July 14 | 2885 | 8.4 | ..... | .... | .... | .... | (3) | 4 | |
| C 2878.. | 1924 July 16 | 3983 | ...... | ..... | .... | .... | .... | 3 | 4 | |
| H.D. 172804 | | | | | | | | | | |
| C 472... | 1920 June 6 | 2482 | 9.1 | ..... | .... | .... | .... | 3 | 1 | |
| H.D. 177175 | | | | | | | | | | |
| C 3491.. | 1925 Sept. 2 | 4396 | 8.7 | ..... | .... | .... | .... | 2 | 5 | |

TABLE II—*Continued*

| PLATE | DATE | J.D. 242 | VIS. MAG. | PHASE | INTENSITY EMISSION LINES | | | INTENSITY ABSORPTION BANDS | | CONTINUOUS SPECTRUM |
|---|---|---|---|---|---|---|---|---|---|---|
| | | | | | $H\beta$ | $H\gamma$ | $H\delta$ | $ZrO_2$ | $TiO_2$ | |
| | | | | | T Sagittarii | | | | | |
| C 1059.. | 1921 June 20 | 2861 | (8.5) | + 39 | 7 | 3 | 1 | pr | .... | Trace |
| C 1792.. | 1922 July 13 | 3249 | 9.1 | + 65 | 6 | 2 | .... | pr | (0) | Trace |
| C 2365.. | 1923 July 28 | 3629 | 8.9 | + 47 | 4 | 1 | tr | pr | .... | Trace |
| C 2410.. | Aug. 30 | 3662 | 9.8 | + 80 | 5 | 1 | .... | (2) | 0 | Underexp. |
| C 2817.. | 1924 June 12 | 3949 | 9.0 | − 41 | 2 | .... | .... | 4 | 1 | |
| C 2887.. | July 18 | 3985 | 8.1 | − 5 | 20 | 8 | 3 | 3 | 1 | |
| | | | | | R Cygni | | | | | |
| 345... | 1911 Dec. 5 | 9376 | 6.7 | + 5 | 8 | 3 | tr | (3) | 0 | |
| 349... | Dec. 11 | 9382 | 6.8 | + 11 | pr | .... | .... | pr! | 0 | Blue to red |
| | 1912 Jan. 13 | 9415 | 7.8 | + 44 | 8 | 3 | 2 | .... | .... | |
| C 961... | 1921 Mar. 26 | 2775 | 7.2 | + 30 | 15 | 6 | 3 | 3 | 0 | |
| C 965... | Mar. 27 | 2776 | 7.3 | + 31 | 15 | 6 | 2 | 3 | 0 | |
| C 966... | Mar. 27 | 2776 | 7.3 | + 31 | .... | .... | .... | pr | .... | Red; underexp. |
| C 1007.. | Apr. 28 | 2808 | 8.9 | + 63 | 15 | 5 | 2 | 4 | 1 | |
| C 1038.. | May 26 | 2836 | 9.2 | + 91 | 15 | 5 | 2 | 4 | 0 | |
| C 1055.. | June 19 | 2860 | 9.7 | +115 | 20 | 7 | 2 | 3 | 0 | |
| C 1171.. | July 23 | 2894 | 10.6 | +149 | 7 | 2 | tr | 3 | 0 | |
| γ 11079. | 1922 May 17 | 3192 | 6.8 | + 4 | 10 | 4 | 1 | 4 | 0 | |
| γ 11117. | June 14 | 3220 | 8.0 | + 32 | 15 | 5 | 2 | 4 | 0 | |
| C 1784.. | July 11 | 3247 | 8.9 | + 59 | 15 | 6 | 2 | 4 | 1 | |
| C 1948.. | Oct. 9 | 3337 | 11.5 | +149 | .... | .... | .... | pr! | 0 | Red |
| γ 11746. | 1923 May 1 | 3541 | 8.8 | − 47 | 4 | .... | .... | (3) | 0 | |
| C 2245.. | May 5 | 3545 | 8.5 | − 43 | 9 | 1 | tr | 4 | 0 | |
| R 5..... | June 2 | 3573 | 6.5 | − 15 | .... | .... | .... | pr! | 0 | Red |
| γ 11843. | June 5 | 3576 | 6.4 | − 12 | 18 | 10 | 5 | 3 | 0 | |
| γ 11912. | June 30 | 3601 | 6.5 | + 13 | 20 | 10 | 6 | 3 | 0 | |
| R 12.... | July 1 | 3602 | 6.6 | + 14 | .... | .... | .... | pr! | 0 | Red |
| R 14.... | July 2 | 3603 | 6.6 | + 15 | .... | .... | .... | pr! | 0 | Yellow to red |
| C 2411.. | Aug. 30 | 3662 | 8.5 | + 74 | 20 | 10 | 4 | 3 | 0 | |
| C 2474.. | Oct. 2 | 3695 | 9.8 | +107 | 10 | 4 | 1 | 3 | 0 | |
| C 2510.. | Oct. 26 | 3719 | 10.3 | +131 | 7 | 2 | tr | 3 | 0 | |
| C 2820.. | 1924 June 13 | 3950 | 11.9 | − 80 | 1 | .... | .... | (4) | 0 | |
| C 2886.. | July 18 | 3985 | 9.5 | − 45 | 10 | 3 | tr | 3 | 0 | |
| C 2918.. | Aug. 9 | 4007 | 7.8 | − 23 | 9 | 3 | 0.5 | 3 | 0 | |
| C 3019.. | Sept. 16 | 4045 | 8.2 | + 15 | 15 | 6 | 2 | 3 | 0 | |
| G 25.... | Oct. 4 | 4063 | 8.5 | + 33 | .... | .... | .... | pr! | 0 | Red |
| C 3492.. | 1925 Sept. 2 | 4396 | 9.6 | − 61 | 5 | tr | .... | 4 | 0 | |
| C 3536.. | Sept. 30 | 4424 | 7.4 | − 33 | 12 | 4 | 2 | 3 | 0 | |
| C 3572.. | Oct. 30 | 4454 | 6.8 | − 3 | 15 | 6 | 2 | 3 | 0 | |
| H 59.... | Nov. 17 | 4472 | 6.9 | + 15 | 16 | 8 | 3 | pr | (0) | |
| | | | | | AA Cygni | | | | | |
| C 3013.. | 1924 Sept. 15 | 4044 | (8.5) | ..... | .... | .... | .... | 3 | 4 | |
| C 3377.. | 1925 July 5 | 4337 | (9.0) | ..... | .... | .... | .... | 4 | 5 | |

TABLE II—*Continued*

| Plate | Date | J.D. 242 | Vis. Mag. | Phase | Intensity Emission Lines | | | Intensity Absorption Bands | | Continuous Spectrum |
|---|---|---|---|---|---|---|---|---|---|---|
| | | | | | $H\beta$ | $H\gamma$ | $H\delta$ | $ZrO_2$ | $TiO_2$ | |
| S Cygni | | | | | | | | | | |
| C 458... | 1920 June 2 | 2478 | 8.9 | − 2 | 2 | 2 | 1 | .... | .... | Trace |
| C 3926.. | 1926 Aug. 10 | 4738 | 10.0 | − 1 | 6 | 5 | 3 | 1 | 3 | |
| Z Delphini | | | | | | | | | | |
| C 2565.. | 1923 Nov. 28 | 3752 | 8.6 | − 12 | 11 | 9 | 7 | 1 | 3 | |
| C 3493.. | 1925 Sept. 2 | 4396 | 8.9 | + 21 | 10 | 9 | 6 | 1 | 3 | |
| C 3537.. | Sept. 30 | 4424 | 10.4 | + 49 | 4 | 5 | 3 | tr? | 5 | |
| $\pi^1$ Gruis | | | | | | | | | | |
| 6425 I... | 1915 July 17 | 0696 | 6.6 | ..... | .... | .... | .... | 4 | 3 | |

## NOTES ON INDIVIDUAL STARS

### X ANDROMEDAE

$H\alpha$ is a strong emission line on Plate C 1943.

### R ANDROMEDAE

The first two plates were taken with the 37½-inch reflector at Ann Arbor.[1] $H\zeta$ is present as a bright line on Plates C 137 and C 1499. $H\epsilon$ is not seen on any of the plates.

The bright lines λ 4308 and λ 4571 are present on Plate C 3495.

The zirconium bands, at least certain features of them, are stronger than in R Geminorum. The titanium bands are faintly present near maximum and develop to considerable strength as the light decreases. In R Geminorum, on the other hand, they do not appear on any of my spectrograms. The enhanced barium absorption line λ 4554 is weaker than in the spectrum of R Geminorum. These facts probably indicate a cooler reversing layer than that of R Geminorum.

Plate C 137 is reproduced in Plate XII *a*, *Mt. Wilson Contr.*, No. 252; *Astrophysical Journal*, **56**, 457, 1922.

### U CASSIOPEIAE

Bright $H\zeta$ is present on nearly all of the plates, but $H\epsilon$ is seen on C 3113 only. $H\epsilon$ evidently increased considerably in relative intensity in the interval from December 13, 1924, to January 6, 1925, because $H\zeta$ is a well-marked line on both dates, but $H\epsilon$ is not certainly seen on Plate C 3096, taken on the first date, whereas it is approximately as intense as $H\zeta$ on C 3113 taken on the second date.[2] Several other features increased in intensity during this interval of twenty-four days, notably the titanium bands and a bright line at λ 4215.

---

[1] *Publications of the Astronomical Observatory, University of Michigan*, **2**, 45, 1916.

[2] The increase in the relative intensity of $H\epsilon$ after maximum light has been observed in Me variables also. See *Mt. Wilson Contr.*, No. 200; *Astrophysical Journal*, **53**, 185, 1921; also Mr. Joy's observations of *o* Ceti, *Mt. Wilson Contr.*, No. 311; *Astrophysical Journal*, **63**, 281, 1926. The phenomenon is probably connected with the decrease in effective absorption of the line H of calcium.

The following bright lines, in addition to those of hydrogen, were measured on Plate C 3113: λλ 4138, 4178, 4202, 4215, 4308, 4521. There is a trace of a bright line at λ 4571. The absorption lines on this plate show little contrast with the continuous spectrum. Weak bright lines are seen at λ 4202 and λ 4308 on Plate C 3096.

Plate XVII *c* illustrates the change in intensity of the titanium bands.

### W CASSIOPEIAE

Remark in *H.D.:* "The spectrum is peculiar in the distribution of its light. Nearly all of the brightness is between $H\beta$ and $H\gamma$." Remark by Miss Cannon in *Harvard College Observatory Circular*, No. 221: "The continuous spectrum is faint, but it is not of class M. It appears to resemble the spectrum of R Andromedae, which is peculiar." On the Mount Wilson plates the spectrum closely resembles that of R Canis Minoris.

### S CASSIOPEIAE

The bright enhanced iron lines λλ 4583, 4923, and 5018 are prominent on the second plate. They are slightly less intense on the third plate.

### R ORIONIS

$H\alpha$ is a very intense emission line on Plate C 2424.

The type is not well marked. The spectrum appears to resemble that of R Canis Minoris.

### H.D. 35155

This spectrum, from the violet to the red, closely resembles that of H.D. 22649, Boss 826. Plate C 672 is reproduced in Plate XII *d*, *Mt. Wilson Contr.*, No. 252; *Astrophysical Journal*, **56**, 457, 1922.

### R LYNCIS

The first four plates were taken with the 37½-inch reflector at Ann Arbor.[1]

The bright lines λ 4308 and λ 4571 are present on Plate C 2512. Traces of them are visible also on C 3539.

### R GEMINORUM

*Hydrogen lines.*—$H\alpha$ is a strong emission line on Plates C 1402, C 1408, and C 3647. The plates listed in Table III show one or more hydrogen emission lines of shorter wave-length than $H\delta$.

The ratio of the intensity of $H\epsilon$ to that of $H\zeta$ is considerably greater on the last plate than on the preceding one (see discussion on p. 11 of similar behavior of the bright $H\epsilon$ line in the spectrum of U Cassiopeiae).

On Plates C 1339 and C 2480, taken fifty and fifty-eight days, respectively, before maximum, the hydrogen lines are comparatively weak; but the relative intensities of $H\beta$ and $H\gamma$ are approximately the same as on the other plates. From about phase $-40$ toward maximum the hydrogen lines brighten rapidly. Their intensities, however, do not closely follow the light-curve, but are greater after maximum than at the same number of days before maximum, and at a given magnitude the intensities are greater after maximum than before. In other words, there is a time lag in the behavior of the bright hydrogen lines compared with the total light.

---

[1] *Loc. cit.*

*Miscellaneous bright lines.*—λ 4521 appears as a bright line at about phase −30 and continues to +87 or longer. λ 4511 appears about −10, grows stronger, and becomes equal to λ 4521 at about +50. It is stronger than λ 4521 from then until +87, when both lines are weak.

λ 4308 appears as a bright line on practically all plates taken after maximum. λ 4202 also appears on the stronger plates. Both lines increase in intensity with phase, but λ 4202 is the weaker throughout. On Plate C 3694, phase +87, λ 4571 is a well-marked emission line. Bright lines were measured at λ 4215 and λ 4376 on the last two plates.

*Absorption lines.*—Very few absorption lines are well shown by the spectrograms, except near maximum. The continuous spectrum decreases in intensity so rapidly toward the violet that the region of satisfactory exposure is surprisingly short. Moreover, the lines have a tendency to become weak and indefinite when the star is faint. Thus it happens that on the present plates only a very few of the strongest lines can be followed for more than a few weeks at maximum. λλ 4535, 4554, and 4607 lie in a favorable region and are seen on practically all the spectrograms. λ 4335 is a blend of zirconium, titanium, and perhaps other lines; λ 4554 is the strongest ultimate line of the ionized barium atom; and λ 4607 is the well-known low-temperature line of strontium. λ 4554 remains throughout about twice as strong as λ 4535, but both are more intense near maximum. λ 4607, on the other hand, is decidedly weaker near maximum. The ratio λ 4607 : λ 4554 shows a close correlation with the visual magnitude. Observations before maximum yield about the same curve as those after maximum. According to estimates with a low-power microscope, these two lines are equal when the magnitude is 7.8.

TABLE III

INTENSITIES OF BRIGHT HYDROGEN LINES

| Plate | $H\beta$ | $H\gamma$ | $H\delta$ | $H\epsilon$ | $H\zeta$ | $H\eta$ | $H\theta$ | $H\iota$ | $H\kappa$ |
|---|---|---|---|---|---|---|---|---|---|
| C 2003 | 25 | 15 | 7 | ...... | 2 | ...... | ...... | ...... | ...... |
| C 3097 | 25 | 12 | 6 | ...... | 2 | ...... | ...... | ...... | ...... |
| H 57 | 15 | 7 | 2 | ...... | 1 | ...... | ...... | ...... | ...... |
| H 61 | 30 | 15 | 6 | ...... | 3 | 2 | 1 | 1 | ...... |
| C 3623 | 24 | 11 | 5 | ...... | 1 | ...... | ...... | ...... | ...... |
| C 3647 | 14 | 7 | 3 | ...... | 0.5 | ...... | ...... | ...... | ...... |
| C 3671 | 16 | 8 | 4 | tr | 1 | ...... | ...... | ...... | ...... |
| C 3694 | 15 | 7 | 3 | tr | tr | ...... | ...... | ...... | ...... |

Plate C 133 is reproduced in Plate XII *b*, *Mt. Wilson Contr.*, No. 252; *Astrophysical Journal*, **56**, 457, 1922.

### R CANIS MINORIS

$H\alpha$ is an intense emission line on Plates C 2067, C 2568, and C 3615; it is visible on $\gamma$ 9990 also, although this plate is under-exposed.

This is not a typical spectrum of class S, and there may be some doubt whether or not the resemblance is sufficiently close to warrant its inclusion in this class. The chief objection is that the plates now available do not definitely show the zirconium bands in any portion of the spectrum. Were these bands present there would be no hesitation concerning its classification, as several other features of the spectrum have the same characteristics as in class S. The spectrum of V Cancri closely resembles that of R Canis Minoris in the blue-violet portion, but in the red the zirconium bands are well marked. This circumstance favors including R Canis Minoris in class S. Comparison with UV Aurigae, 051532, on the other hand, is unfavorable to this classification, for the spectrum of this star at one time resembled that of R Canis Minoris, but at two other times appeared to be related to class N.

### H.D. 62164

Remark in *H.D.:* "On an ordinary plate the spectrum consists of dark bands and is seen only in the region between $H\beta$ and $H\gamma$. On a plate stained with pinacyanol, the region of greater wave-length resembles class Mc. Perhaps the spectrum varies."

### T GEMINORUM

*Hydrogen lines.*—The $H\alpha$ line is very weak or absent on C 3620. On Plate C 3672 the bright hydrogen lines have the following intensities: $H\beta$ 16, $H\gamma$ 9, $H\delta$ 6, $H\epsilon$ —, $H\zeta$ 2, $H\eta$ 0.5, $H\theta$ —.

*Absorption lines.*—λ 4535 has one-half or two-thirds the intensity of λ 4554. Near maximum, λ 4607 is about one-fourth as intense as λ 4554, but on Plates C 2072, C 2516, C 3171, and C 3186, taken about two months from maximum, it is nearly as strong as λ 4554. It is estimated that these lines become of equal intensity at mag. 10.0. All three lines appear weaker in this star than in R Geminorum.

*Bands.*—On Plate C 3620 the zirconium bands are strong in the red region; titanium bands are present but are less conspicuous. The titanium bands show a decided dependence upon phase, being much weaker at maximum than when the star is fainter. The zirconium bands show the same behavior to a lesser degree. Plate XVII *d* illustrates the change in the intensity of the bands.

### H.D. 64332

Remark in *H.D.:* "The spectrum shows some resemblance to that of $\pi^1$ Gruis, R.A. $22^{h}16^{m}6$, Dec. $-46°27'$, in the region between $H\beta$ and $H\gamma$. It appears to combine characteristics of classes M and R. Classified Ma on I 38629, on which it is very faint."

### V CANCRI

$H\alpha$ is a strong emission line on Plate C 3117.

The appearance of the spectrum on C 3673 is very different from that on the other plates. The intensity decreases toward the violet less rapidly than on C 2743, for example. From λ 4400 to $H\beta$ the spectrum is nearly continuous. All the lines are weak and have a curious blurred appearance. There are absorption lines in the position of $H\beta$ and $H\delta$. A defect in the emulsion makes the nature of $H\gamma$ indeterminate. *Ca* 4227 is a fairly narrow dark line.

Near time of maximum the spectrum in the blue and violet resembles that of R Canis Minoris, but in the red the zirconium bands are well marked, whereas in R Canis Minoris they are absent or very weak.

### S URSAE MAJORIS

The first four plates were taken with the $37\frac{1}{2}$-inch reflector at Ann Arbor.[1]

*Hydrogen lines.*—$H\alpha$ is a bright line of moderate intensity on Plate C 2068, but is

---

[1] *Loc. cit.*

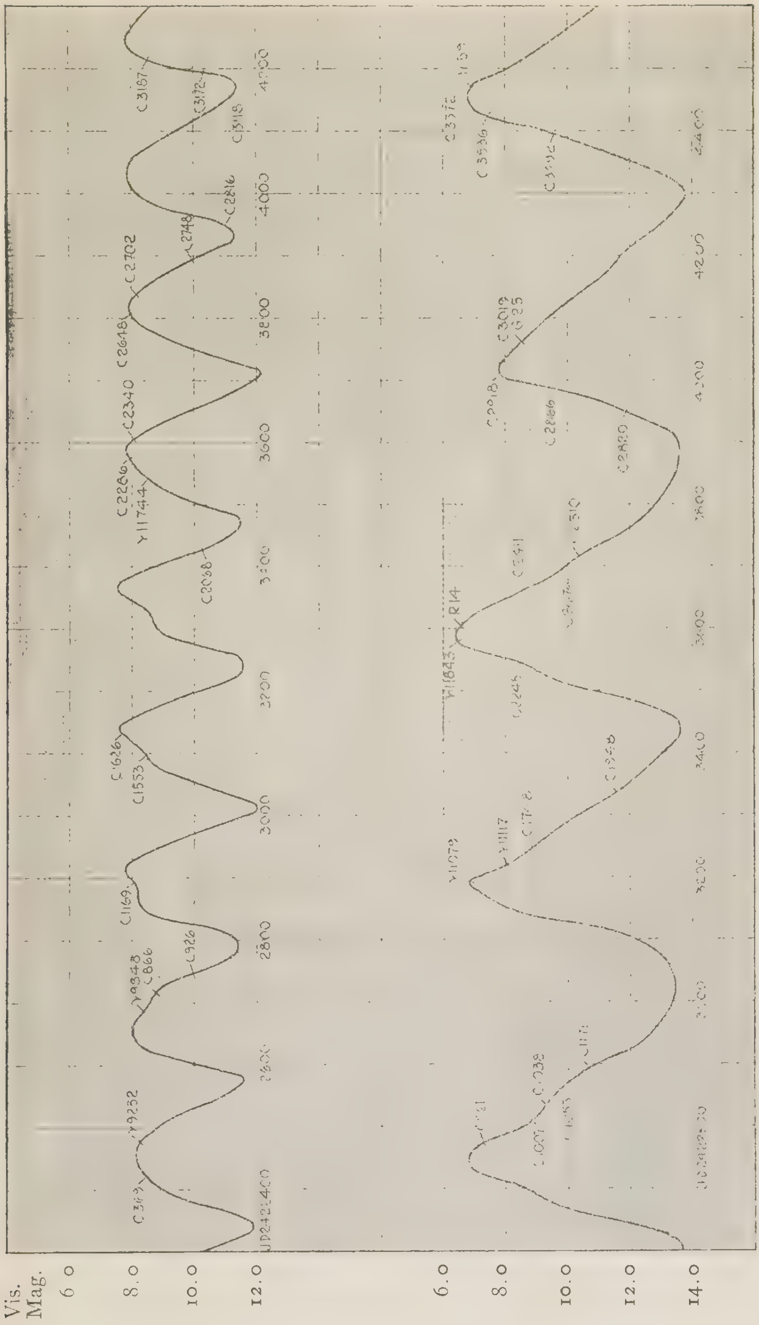

FIG. 1—Light-curves of S Ursae Majoris (above), and R Cygni (below)

not clearly seen on C 3118, although there is weak continuous spectrum in its vicinity. No hydrogen lines of shorter wave-length than *Hδ* are visible on any of the plates. The bright hydrogen lines are absent at minimum, appear about phase −60, and increase in intensity rapidly toward maximum. After maximum they become less intense until at +70 they are again very feeble. They are probably present for a somewhat longer interval and to a slightly fainter magnitude after maximum than before, but the lag is not very marked. As shown by Table II, the relative intensities of the hydrogen lines are nearly the same on all plates except those taken in June, 1915, on which *Hγ* was evidently unusually strong.

*Bands.*—The zirconium bands are present throughout the light-cycle but are less intense at maximum than at other phases.

Figure 1 (upper curve) shows the light-curve of this variable and the distribution of my spectroscopic observations.

Plate C 373 is reproduced in Plate XII *c*, *Mt. Wilson Contr.*, No. 252; *Astrophysical Journal*, **56**, 457, 1922.

### H.D. 121447

The band structure is slightly peculiar, not being identical with that in R Geminorum. This probably accounts for the zero estimate of the intensity of the zirconium bands on the third plate.

This spectrum resembles that of R Canis Minoris.

### RW LIBRAE

The S-type features are not well marked, and the classification is uncertain. The spectrum changes.

### H.D. 156957

Remark in *H.D.:* "This spectrum appears to resemble those of $\pi^1$ Gruis and T Camelopardalis."

The Mount Wilson spectrograms were obtained by Mr. Sanford. See *Publications of the Astronomical Society of the Pacific*, **36**, 353, 1924.

### H.D. 172804

The spectrogram was taken by Mr. Sanford. See *Mt. Wilson Contr.*, No. 276; *Astrophysical Journal*, **59**, 339, 1924.

### R CYGNI

The first three plates were taken by Wright with the 36-inch refractor at the Lick Observatory.[1]

*Hydrogen lines.*—*Hα* is bright on all plates which show the red region. Bright *Hζ* is seen on two plates and has the following intensities: γ 11843, tr; H 59, 1. The bright hydrogen lines are very weak at phase −80, but strengthen rapidly toward maximum, after which they decrease in intensity. They are still of moderate intensity, however, at phase +149. Their behavior is thus unsymmetrical with respect to maximum. In this connection it must be borne in mind that the ascending branch of the light-curve is steeper than the descending. It is probable, however, that the bright hydrogen lines persist to a slightly fainter magnitude after maximum than before, but further observations are needed to determine definitely the characteristic times and magnitudes of appearance and disappearance.

---

[1] *Monthly Notices*, **72**, 548, 1912.

*Miscellaneous bright lines.*—λ 4521 appears in the spectrum about phase −45, followed twenty or thirty days later by λ 4511. λ 4511 slowly gains in relative intensity until it equals λ 4521 about phase +70. It is the stronger from that phase to +150 when both lines are weak.

The enhanced lines of iron, which are present in most Se spectra, are especially strong in R Cygni and persist throughout a considerable portion of the light-cycle. λ 4583 is, in fact, visible on practically all the Mount Wilson spectrograms having the proper exposure for this region. These extend from phase −80 to +149. On many plates λ 4583 is a conspicuous feature, while λλ 4549, 4924, 5018 are present with lower intensities. λ 4233 is faintly visible on two plates.

λ 4308 appears as an emission line on nearly all the plates taken after maximum, and λ 4202 on those taken after phase +60, but the intensity of λ 4202 does not exceed approximately one-half that of λ 4308 on any of my plates. The relative behavior is thus at variance with that in Me variables.[1] λ 4571 appears in emission at about +60 and soon becomes as intense as λ 4308. The following additional lines which have been observed in emission in Me variables have been measured as bright lines on two or more plates of R Cygni: λλ 4139, 4179, 4215, 4352, 4373, 4376, 4427, 4461. As far as may be judged from the small number of observations, their behavior is nearly the same as in the Me variables.

A curious phenomenon is the presence on the same plate of λ 4571 *Mg* and λ 4583 *Fe*+ as conspicuous bright lines. At about phase +100 they are of nearly equal intensity, λ 4571 being weaker before this epoch and stronger after it. λ 4571 is an extreme low-temperature line, while λ 4583 is a well-known spark line requiring high excitation for its production in the laboratory. The simultaneous occurrence of these two lines in a stellar spectrum is very puzzling. If they actually arise from the same region of the star, the physical conditions must differ in some important particular from those within the range of laboratory experience. It may be, however, that they come from different regions of the star, with low excitation for the magnesium line and high excitation for the iron line.

*Absorption lines.*—λ 4535 and λ 4554 appear more nearly equal than in R Geminorum, but prior to phase +30, λ 4554 is somewhat more intense. λ 4607 is much stronger than either of these lines except when the star is brighter than 7.4 mag.; it is estimated that λ 4607 and λ 4554 are of equal intensity at this magnitude, both before and after maximum.

Figure 1 (lower curve) shows the light-curve of this variable and the distribution of my spectroscopic observations. Plates γ 11117, C 1055, C 3492, and C 3572 are reproduced in Plate XVII.

*Earlier observations.*—In *Monthly Notices*, **72**, 546, 1912, Espin has given a summary of the early spectroscopic observations of R Cygni. The spectrum was generally assigned to Secchi's third type, and $H\beta$ was usually seen as a bright line. The Harvard observers noted that "the spectrum is peculiar, and shows changes on the various photographs." Espin's own observations during the autumn and winter of 1911 are quoted in detail. When the star was very faint, its spectrum was "apparently continuous," but when the magnitude reached 8.7, the bands were quite clear. Toward maximum the bands seemed less distinct. The Mount Wilson spectrograms do not afford indubitable evidence of systematic changes in the intensities of the bands, but they suggest, in harmony with

---

[1] *Mt. Wilson Contr.*, No. 200; *Astrophysical Journal*, **53**, 185, 1921.

Espin's observations, that the bands are slightly weakened when the star is brightest. Espin and one or two other observers thought the spectrum to be of type III (class M), but this is not surprising because the zirconium bands and the titanium bands present the same general appearance in the yellow and red. Espin saw the bright $H\beta$ line on several dates and thought it to be most conspicuous about two weeks before maximum. In the pages of the *Monthly Notices* following Espin's article, Wright gives an account of three spectrograms obtained at Lick Observatory shortly after the maximum observed by Espin. The spectrum seems to have been much the same as that shown by the Mount Wilson plates at the same phase.

### AA Cygni

Remark in *H.D.:* "The spectrum is faint, and it is uncertain whether it belongs to Class N or Class S."

On the Mount Wilson plates this spectrum offers a fine example of the presence of both titanium and zirconium bands in considerable intensity. Both sets of bands appear slightly stronger on the second plate, which is reproduced in Plate XVII *b*. A spectrum of class M5e (RS Ursae Majoris, 1925, April 9) is placed beside it for comparison. Notice the difference in structure near λ 4620.

### Z Delphini

Remark in *H.D.:* "On a photograph taken November 20, 1903, the line $H\gamma$ is twice as bright as $H\delta$. The class of spectrum is not well defined. The brightest portion is between $H\beta$ and $H\gamma$."

A feeble bright $H\zeta$ line is present on Plate C 3493. $H\epsilon$ is not seen.

### $\pi^1$ Gruis

The spectrogram was taken at the Chile station of the Lick Observatory and loaned to me through the kindness of Dr. Campbell and Dr. Moore.

Additional notes on the spectra of most of these stars will be found in *Mt. Wilson Contr.*, No. 252; *Astrophysical Journal*, **56**, 457, 1922.

## SUMMARY OF OBSERVATIONS

*Zirconium bands.*—The intensity of these bands is quite different in various S-type stars. In the variables they are present during all or most of the light-cycle, being slightly weaker near maximum. Their intensity is perhaps more closely correlated with magnitude than with the interval from maximum. In S Ursae Majoris they persist throughout the light-cycle, but in V Cancri they apparently disappear during the decreasing phase. More observations will be required to determine the characteristic behavior near minimum.

*Titanium bands.*—The intensity of these bands is widely different in various S-type stars. In about half of the variables they are absent or extremely weak at maximum and throughout the observed phases, which in S Ursae Majoris include the entire light-cycle. In other variables they are present on all plates, but are fainter near maximum than at other times. In some stars the changes in intensity are very marked (see Plate XVII). In R Andromedae the titanium bands are weak or absent near maximum, but are strong when the variable is fainter.

The observations show very clearly that zirconium and titanium bands can exist simultaneously in a stellar spectrum. The significance of the relative behavior of these two groups of bands will be discussed below. One interesting observational feature which plays an important part in the recognition of the zirconium bands may be mentioned here. The titanium bands exercise a marked effect on a large portion of the spectrum, and, when strongly developed, practically obliterate the characteristic S-type structure between λ 4626 and λ 4700. A superficial inspection of the spectrograms might suggest that the zirconium bands disappear when those of titanium become strong, but a closer examination shows that in many cases the titanium band head at λ 4626 is apparently displaced about 6 A toward the violet from its normal position. This is caused by the fortunate circumstance that a zirconium band head occurs at about λ 4620.[1] It is this feature, illustrated in the spectrum of AA Cygni, Plate XVII *b*, which permits the detection of zirconium oxide when the titanium oxide bands are strong.

*Hydrogen lines.*—In non-variable S-type stars the Balmer lines are dark and of moderate intensity. The variable stars, with one exception, have exhibited very conspicuous bright lines near the maximum phase. The exception, AA Cygni, is a variable of class III with a small range and apparently irregular variation. Bright lines are not visible on the two Mount Wilson spectrograms and are not mentioned in the *Henry Draper Catalogue*. This star may thus be analogous to those irregular variables of class M, such as R Lyrae and α Herculis, whose spectra do not contain bright lines.

In the spectra of the long-period S-type variables, emission lines of hydrogen appear during the time of increasing light at about one-fifth of the period before maximum. The variable at this time may be about midway between minimum and maximum on the ascending branch of the light-curve. The intensities increase rapidly so that at maximum the lines are very strong. They decrease again after maximum, but the interval of their visibility is greater than that before maximum, and the magnitude at which they finally disappear is probably slightly lower than at the time of their appearance before maximum. In these respects the bright hydrogen lines behave much as they do in Me variables.[1] One slight difference is that the phase displacement or time lag after maximum seems to be smaller in the S-type variables.

---

[1] The identification is substantiated by unpublished laboratory observations by Dr. Kiess, of the Bureau of Standards, and by Dr. King, of the Mount Wilson Observatory. I am indebted to these gentlemen for the communication of their results in advance of publication.

In spectra in which the titanium bands are absent, the intensities of the bright hydrogen lines decrease rapidly from $H\beta$ to $H\delta$ and the relative intensities remain about the same throughout the observed portion of the light-period. $H\alpha$ is a very strong line, probably stronger than $H\beta$. $H\zeta$ is frequently seen on strongly exposed plates, but $H\epsilon$ is usually absent or very weak. In U Cassiopeiae and R Geminorum, $H\epsilon$ has been observed to increase in relative intensity during decreasing light, due possibly to the diminishing absorption of the H line of calcium. Similar behavior of $H\epsilon$ is known in Me variables. In R Geminorum the regular decrease of intensity of the successive members of the Balmer series in the ultra-violet is interrupted by $H\iota$ which, as in class Me, is strong compared to $H\theta$ and $H\kappa$.

When titanium bands are present in the spectrum, the decrease from $H\beta$ to $H\delta$ is less rapid. $H\delta$ may equal or even exceed $H\gamma$ when the bands are strong.

*Bright enhanced iron lines.*—Several bright lines of ionized iron, particularly λλ 4583, 4924, and 5018, are present with various intensities in the spectra of nearly all Se variables. They are especially prominent in S Cassiopeiae and R Cygni. They are probably strongest near maximum, but their characteristic variation with phase is not clearly brought out by the present spectrograms. In the spectrum of R Cygni they persist through a considerable portion of the light-cycle. A remarkable fact is that at about phase +100, when the extreme low-temperature magnesium line λ 4571 has attained considerable strength, λ 4583 still remains a prominent feature of the spectrum. This is an interesting anomaly.

---

[1] *Mt. Wilson Contr.*, Nos. 200 and 311; *Astrophysical Journal*, **53**, 185, 1921, and **63**, 281, 1926.

*Miscellaneous bright lines.*—The following bright lines, in addition to those of hydrogen and enhanced iron, have been observed in the spectra of one or more Se variables: λλ 4138, 4178, 4202*, 4215, 4308*, 4352, 4373, 4376, 4427, 4461, 4511*, 4521*, 4571*. All these lines are known in Me variables.[1] Those most frequently observed in the present investigation are marked by an asterisk and will be described in the following paragraphs. The general features of the behavior of the other lines, as far as they can be determined from the meager material, are about the same as in the Me variables. The line at λ 4215 seems to have a shorter wave-length than that measured by Joy at λ 4216.19 in *o* Ceti and may have a different origin.

λ 4308 appears at maximum, or soon after, and strengthens gradually as the light decreases. λ 4571 appears at one-tenth to one-fifth of the period after maximum and later becomes stronger than λ 4308. λ 4202 behaves about the same as λ 4308, but is less intense at all phases. λ 4308 makes its appearance rather earlier in the light-cycle in the Se variables than in those of class Me, and this is perhaps true of λ 4571 also. λ 4202, on the other hand, seems to come later, and is never so prominent as in Me variables shortly after maximum. The intensity of these three lines is not the same in all Se variables. They are weak, for example, in the spectrum of S Ursae Majoris.

The lines λ 4511 and λ 4521 have various intensities in different stars. They are fairly strong in the spectra of R Geminorum and of R Cygni, and weak in that of S Ursae Majoris. λ 4521 appears about one-tenth of the period before maximum (phase $-0.1p$). λ 4511 is first visible about $-0.04p$ and increases in relative intensity, becoming equal to λ 4521 at about phase $+0.15p$. It is the stronger from then on to $+0.3p$, when both lines are again weak. The behavior of these lines is thus much the same as in *o* Ceti,[2] except that in the Se variables they both appear somewhat earlier in the light-cycle. The fact that λ 4511 has its maximum intensity at a later phase than λ 4521 probably indicates that the excitation most favorable for its production is lower than that for λ 4521.

---

[1] *Mt. Wilson Contr.*, Nos. 200, 265, and 311; *Astrophysical Journal*, **53**, 185, 1921, **58**, 195, 1923, and **63**, 281, 1926.

[2] Joy, *Mt. Wilson Contr.*, No. 311; *Astrophysical Journal*, **63**, 281, 1926.

*Absorption lines.*—The notes concerning the absorption spectrum of R Geminorum on page 13 apply to the other Se variables as well and explain why it is difficult to follow most of the absorption lines through any considerable portion of the light-cycle. Three lines only, λλ 4535, 4554, and 4607, have been selected for discussion in the following paragraphs. The probable identifications of these lines are stated on page 13.

The ratio of the intensity of λ 4535 to that of λ 4554 ranges, in different stars, from about 0.3 to 1.0. In the variables this ratio does not change markedly during the observed portion of the light-cycle, although in some cases it may decrease slightly near maximum.

The strontium line λ 4607 is generally one-half or two-thirds as intense as λ 4554 in the spectra of the non-variable S-type stars. In the variables its intensity varies with phase in a striking manner. At maximum it is much weaker than λ 4554 (in some instances only one-fifth as intense), but as the star becomes faint it develops rapidly and may become six to eight times as strong as λ 4554. It is also strong before maximum. In fact, as far as the present data go, the relation of the magnitude of the variable and the relative intensity of λ 4607 and λ 4554 seem to be the same for the ascending and the descending branches of the light-curve. Estimates of the magnitude at which λ 4554 and λ 4607 have equal intensities have been made in the case of four variables as follows:

| | Mag. When λ 4554=λ 4607 | Max. Mag. | Mag. Difference |
|---|---|---|---|
| R Gem......... | 7.8 | 6.9 | 0.9 |
| T Gem......... | 10.0 | 8.6 | 1.4 |
| S Urs. Maj...... | 8.7 | 7.9 | 0.8 |
| R Cygni........ | 7.4 | 7.0 | 0.4 |

The maximum magnitude in the third column is the mean of the magnitudes at the maxima which occurred during the period of my spectroscopic observations.

## DISCUSSION

The present observations fully support the previous conclusion that S-type spectra are closely related to those of giant stars of class M.[1] In investigating the physical conditions prevailing in S stars it will therefore be natural to study the relationship between the two types of spectra.

The first thing to notice is the relative behavior of the zirconium and titanium bands. In the ordinary M-type spectra, titanium bands alone are seen; in some S-type spectra we find only the zirconium bands; while in certain other spectra both kinds of bands are present. The behavior of the bands in variable S-type stars is outlined on pages 18 and 19.

The stellar observations indicate that in general the temperature range for the production of the zirconium bands is higher than that for the titanium bands, and this is borne out by King's experiments with the electric furnace, which showed that "the zirconium bands belong to the oxide and their presence indicates a distinctly higher temperature stage than that required for the bands of titanium oxide."[2] The laboratory work does not give a definite upper limit for the production of the bands, but it is probably higher for zirconium than for titanium.

The temperatures of the reversing layers of most S-type stars seem to be near the upper limit for the production of titanium bands. Under the prevailing conditions these bands evidently strengthen rapidly with comparatively small decreases in temperature, and we may therefore arrange the stars in a sequence of decreasing temperature according to the intensity of the titanium bands. Such an arrangement implies that the titanium-band intensity is a function of temperature alone, and, while this may not be strictly true, the evidence indicates that it is at least approximately so. The changing temperatures of several variable stars and the relationships to the titanium bands are shown diagrammatically in Figure 2.

For estimating the relative temperatures of M- and S-type stars the following means are available: (1) color; (2) heat index from measurements of total radiation; (3) absorption-line spectrum;

---

[1] If dwarf stars of class S exist, they are not yet known.

[2] *Publications of the Astronomical Society of the Pacific*, **36**, 140, 1924.

(4) bands, especially those of titanium; (5) behavior of bright lines in variable stars. These indicate that the temperatures of various S-type stars cover a range which overlaps that of the M-type stars, and it thus seems clear that the difference between the two types is not solely one of temperature.

Three important factors, other than temperature, in which stars may differ are mass, density, and chemical composition. Difference in mass between M- and S-type stars is possible, but we have no direct means of establishing it or of proving that it would produce the observed spectral differences. The meager evidence available suggests equal or larger masses for the S-type stars. S-type stars may contain more zirconium and barium than those of class M, but this possibility should be appealed to only as a last resort, because we are not now prepared to deal effectively with the only problems which it suggests. We are left, then, with difference in density as the most promising subject of inquiry, and here a positive result seems attainable.

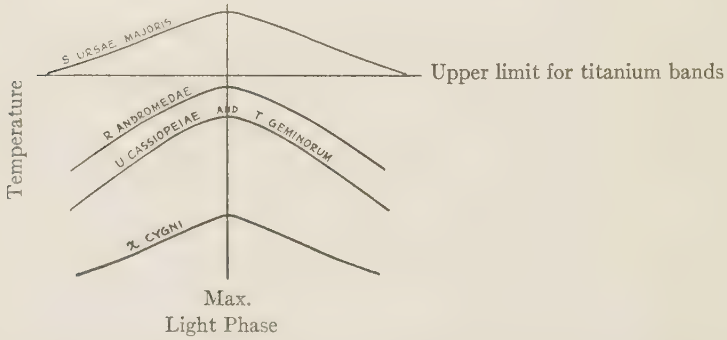

FIG. 2.—Diagram illustrating behavior of titanium bands in S-type variables

A lower density for S-type stars is indicated by the greater intensity of enhanced lines. The most outstanding cases in the absorption spectrum are the strontium lines λ 4077 and λ 4215. The H and K lines of calcium are, I think, stronger in S-type spectra. Barium λ 4554 is much stronger in class S, but this line may possibly be weakened in class M by some cause not directly connected with density. Bright enhanced lines of iron appear in the spectra of most S-type variables. According to a suggestion by King, based on his observations of the high-current arc in vacuum,[1] low density may be an important factor in producing the curious combination of enhanced lines with low-temperature lines in S-type spectra. The general appearance of the typical S-type spectrum is that associated with high luminosity and low density. The S-type stars may bear somewhat the same relationship to those of class M that Cepheids and pseudo-Cepheids do to ordinary F and G stars. The fact that S-type stars exhibit some tendency to congregate near the galactic plane, while the M-types, in general, are practically free from this tendency, is in line with this idea.[2]

The relatively long periods of the S-type variables constitute another strong argument for low density. The temperatures of most S-type stars appear to approximate those of types M1–M3, but the periods correspond to those of variables of types M6–M8, which are generally believed to have lower densities.

A possible additional argument for the low densities of S-type variables lies in the fact that their velocities are about the same as those of classes M6–M8e,[3] the most tenuous of the M-type variables. The relatively small velocities may also indicate higher masses.

No observational fact seems inconsistent with the idea of lower density of S-type stars, and several features strongly favor it. We may therefore accept it as a working hypothesis of the physical difference between the two closely related classes of red stars. It seems possible that the only essential difference between classes M and S is one of density, but judgment must be reserved on this point. It would be extremely interesting if laboratory investigation should show that, in a mixture of titanium oxide and zirconium oxide vapors, low density is relatively favorable to the zirconium bands.

A few remarks concerning certain problems of red stars, suggested by the comparison of S-type spectra with those of class M, will be made in conclusion. Similarities and differences brought out by this comparison have been described in the preceding pages.

---

[1] *Publications of the Astronomical Society of the Pacific*, **38**, 235, 1926.

[2] Adams, Joy, and Humason have recently called attention to a noticeable galactic concentration of supergiant stars of class M (*Mt. Wilson Contr.*, No. 319; *Astrophysical Journal*, **64**, 225, 1926).

[3] Table XII, *Mt. Wilson Contr.*, No. 264; *Astrophysical Journal*, **58**, 215, 1923.

Numerous spectral features common to the two types, or accentuated in the M-types, may be accounted for by low temperature; and certain differences find an explanation in the hypothesis that S-type stars have lower densities than M-type stars at the same temperature.[1] Several remarkable features observed only in long-period variables exhibit similar behavior in classes M and S, and indicate that the circumstances accompanying the variation (and probably its fundamental cause) are the same in both classes. The presence of titanium oxide is evidently not a necessary condition for these phenomena.

Certain other effects, however, seem to be closely correlated with the intensity of the titanium bands. In general, these effects consist of the surprisingly low intensities of certain features which might be expected to be strong. To be specific we may mention (1) weakness of bright $H\alpha$, $H\beta$, and $H\gamma$ in comparison with $H\delta$ and the ultra-violet Balmer lines; (2) weakness of certain ultimate absorption lines, notably $D_1$, $D_2$ of sodium, and λ 4607 of strontium; (3) weakness of the continuous spectrum from λ 4200 toward longer wave-lengths, often made evident by the surprisingly great relative intensity in the region λ 4100 to λ 4200.

Low temperature will not directly account for these peculiarities, and a special cause must be sought. It is perhaps to be found in the absorption of the titanium oxide bands, as in both M- and S-type stars the effects become more marked with increase in intensity of the bands.

The titanium oxide, if responsible for the weakness of the spectral features under discussion, must lie at a higher level than that in which these are produced, and must exert a powerful absorption on the regions of the spectrum in which they are located. If light-pressure is proportional to the amount of radiant energy absorbed, then titanium oxide receives far greater upward impulses than any other substance known in the atmospheres of M- and S-type stars, and may thus exist at a very high level. Moreover, it is reasonable to believe that when the bands appear very strong, the titanium oxide layer is nearly opaque in certain spectral regions (including those of the weakened features under discussion) and practically shuts off radiation from below, the energy which we observe in these regions being largely that emitted by the titanium oxide itself. This would explain how a spectral line can be eliminated from a region in which strong continuous spectrum is still observed.

---

[1] An alternative statement of the hypothesis is that S-type stars have higher temperatures than M-type stars of the same density.

The deletion of the bright $H\epsilon$ line by the absorption of the overlying calcium can be explained in a similar way. It has been difficult to understand how the hydrogen line could suffer greater absorption than the continuous spectrum which can be photographed within the broad H line, but if the calcium is quite opaque in this region, the light observed there being emitted by the calcium itself, this difficulty is overcome.

The attempt to explain the abnormal relative intensities of the bright hydrogen lines in M-type variables by the absorption of titanium oxide will meet serious, but perhaps not insuperable, difficulties. Relative motion of the effective levels of hydrogen emission and titanium absorption may be a part of the explanation. Measurements of the displacements of the bright lines show the hydrogen apparently moving upward with respect to the absorbing materials at the time of maximum. If the effective levels of the hydrogen emission lie partly within the stratum of absorbing titanium oxide, this relative motion may conceivably explain the fact that the weakened lines are stronger after maximum than before.

The value of S-type stars in testing this and other hypotheses concerning red stars lies in the fact that their temperature range overlaps that of the M stars; we are thus offered the opportunity of distinguishing between the general effects of low temperature and special effects such as those of low density or of the absorption of titanium oxide. Class N also may furnish useful comparisons, but its relationship to other classes of red stars is not so close as that between classes M and S.

MOUNT WILSON OBSERVATORY
August 1926

Contributions from the Mount Wilson Observatory, No. 326
Reprinted from the *Astrophysical Journal*, Vol. LXV, pp. 86–107, 1927
Printed in the U.S.A.

# THE ELECTRIC-FURNACE SPECTRA OF YTTRIUM, ZIRCONIUM, AND LANTHANUM

By ARTHUR S. KING and EDNA CARTER

## ABSTRACT

*Furnace spectra of yttrium, λ 2808–λ 7882; zirconium, λ 2792–λ 8305; lanthanum, λ 2799–λ 8347.*—Temperature stages from 2000° to 2800° C. were employed to observe the *initial appearance of lines* and their *rate of increase in intensity*, supplemented by low-temperature absorption spectra in the ultra-violet. A *direct comparison with arc and spark spectra* showed the changes undergone in these sources and served to select the *enhanced lines*. The numbers of lines classified are 451 of yttrium, 858 of zirconium, and 695 of lanthanum. Many enhanced lines of yttrium and lanthanum, and some of those of zirconium, are emitted by the furnace, their intensities in furnace and arc indicating the relative energy-levels of the ionized atom. For zirconium a temperature of about 2400° was required before any considerable number of lines appeared, and for this element a large proportion of lines emitted by the arc are enhanced lines. In the lanthanum spectrum, note is made of the large number of close doublets, and some triplets, all of which have been previously listed as single lines; also of the large proportion of lines relatively stronger in the furnace than in the arc.

From an examination of the furnace, arc, and spark spectra of yttrium, zirconium, and lanthanum in the interval λ 2800 to λ 8400, data have been obtained for a classification of their lines according to the temperature required for initial appearance and the rate of change of line-intensity as the temperature is increased. Not only the lines of the neutral atom, but also, to a considerable extent, those of the ionized atom were treated in this way. The enhanced lines have been selected by a direct comparison of arc and spark spectrograms. For yttrium and lanthanum especially, sufficient ionization is present at the higher furnace temperatures to produce the more sensitive enhanced lines. The degree in which these are radiated by the furnace and by the stronger ionization of the arc should aid in placing the relative energy-levels of ionized lines just as the temperature classification of other elements has served to indicate energy-levels for the neutral atom.

## EXPERIMENTAL METHOD

*Furnace.*—The vacuum furnace previously described[1] was used, the material being vaporized in graphite tubes of the usual dimensions: 12.5 mm bore, 19 mm outside diameter, and 200 mm between the supporting clamps.

---

[1] *Mt. Wilson Contr.*, No. 247; *Astrophysical Journal*, 56, 318, 1922.

*Spectrograph.*—From λ 2800 to λ 5000, the second order of the 15-foot concave-grating spectrograph was employed, the scale of the plates being 1.86 A per millimeter. Beyond λ 5000, the first order of the grating was used.

*Temperatures.*—It was found that for yttrium and lanthanum, a temperature of 1900° C. was required to produce a fair number of lines, and at this temperature the spectrum was faint. About 2000° was therefore regularly used for the low-temperature stage, while 2200°–2300° and 2600°–2800° served for the medium and high temperatures, respectively. Zirconium is more difficult to vaporize, and because of the high temperatures required, only two stages were used —2400° for the low and 2700° for the high temperature.

*Emission and absorption spectra.*—As in the case of spectra previously studied, it was found that low-temperature lines in the ultraviolet appear in absorption at shorter wave-lengths than in emission, on account of the rapid weakening of the furnace emission in this region. To obtain an absorption spectrum, white light from a tungsten lamp provided with a quartz window was passed through the furnace tube while this was heated at the low-temperature stage. The lines which the low-temperature vapor absorbs were thus found, and were used up to the wave-length at which emission spectrograms for the same temperature begin to show lines. By means of the overlapping region, the intensities of the absorption lines were harmonized as well as possible with the emission lines; the emission lines alone were used as the estimation was carried toward longer waves.

*Chemicals.*—Salts of yttrium and lanthanum often contain impurities, especially rare earths, which give many foreign lines, with resulting disturbance by blends. An extensive set of early yttrium spectrograms was rejected on this account. We were assisted in obtaining better yttrium by Dr. W. F. Meggers, who furnished some very pure oxalate prepared by Mr. J. F. T. Berliner, of the Bureau of Chemistry, Department of Agriculture. We are indebted also to Professor B. S. Hopkins, who gave us lanthanum oxide, purified with great care in the chemical laboratory of the University of Illinois.

## TABLE I

### Temperature Classification of Yttrium Lines

| λ (I.A.) | Arc Int. | Furnace Intensities | | | Class |
|---|---|---|---|---|---|
| | | High Temp. | Medium Temp. | Low Temp. | |
| 2807.77..... | 1 | 3 | 1 | ...... | III A |
| 2813.61..... | 8 | 5 | 3 | tr | III |
| 2818.84..... | 3 | 2 | ...... | ...... | IV |
| 2822.55..... | 10 | 3 | tr | ...... | IV |
| 2826.29..... | 1 | 2 | tr | ...... | IV A |
| 2835.78..... | 1 | 1 | ...... | ...... | IV |
| 2854.42..... | 3 | ...... | ...... | ...... | V E |
| 2856.30..... | 1 | ...... | ...... | ...... | V |
| 2886.49..... | 15 | 8 | 3 | ...... | III |
| 2890.39..... | 3 | 1 | ...... | ...... | IV |
| 2897.69..... | 1 | ...... | ...... | ...... | V |
| 2898.85..... | tr | ...... | ...... | ...... | V |
| 2901.46..... | 6 | 5 | 2 | ...... | III |
| 2919.06..... | 20 | 10 | 8 | 4 | II |
| 2948.39..... | 30 | 15r | 12 | 6 | II |
| 2964.96..... | 30 | 15r | 12 | 6 | II |
| 2974.58..... | 35 | 20r | 15 | 9 | II |
| 2980.54..... | 2 | ...... | ...... | ...... | V E |
| 2984.26..... | 50 | 30r | 20 | 12 | II |
| 2995.25..... | 10 | 10 | 10 | 2 | III |
| 2996.93..... | 20 | 12 | 12 | 3 | III |
| 3005.24..... | 12 | 10 | 12 | 2 | III |
| 3018.93*.... | 6 ? | 8 | 3 | ...... | III |
| 3021.70..... | 15 | 20 | 15 | 8 | II |
| 3022.27..... | 12 | 18 | 15 | 6 | II |
| 3038.47..... | 4 | 10 | 7 | tr | III A |
| 3044.83..... | 5 | 5 | 3 | ...... | III |
| 3045.36..... | 20 | 20 | 20 | 12 | II |
| 3047.13..... | 3 | 4 | 2 | ...... | III |
| 3047.38..... | 3 | 3 | 2 | ...... | III |
| 3056.33*.... | 2 ? | 3 ? | 1 ? | —? | III ? |
| 3059.52..... | 4 | 5 | 2 | ...... | III |
| 3072.37..... | 5 | 5 | 2 | ...... | III |
| 3076.50..... | 5 | 5 | 2 | ...... | III |
| 3078.58..... | 2 | ...... | ...... | ...... | V E |
| 3086.86..... | 7 | tr | ...... | ...... | V |
| 3091.70..... | 15 | 10 | 8 | tr ? | III |
| 3095.88..... | 25 | 1 | ...... | ...... | V E |
| 3096.61..... | 3 | 4 | 2 | ...... | III |
| 3103.69..... | 4 | 4 | ...... | ...... | IV |
| 3108.87..... | 5 | 5 | 2 | ...... | III |
| 3111.79..... | 15 | 12 | 10 | ...... | III |
| 3112.02..... | 18 | ...... | ...... | ...... | V E |
| 3114.28..... | 2 | 1 | tr | ...... | III |
| 3128.73..... | 5 | ...... | ...... | ...... | V E |
| 3129.94..... | 10 | ...... | ...... | ...... | V E |
| 3135.18..... | 25 | ...... | ...... | ...... | V E |
| 3152.66..... | 15n | 10 | 4 | ...... | III |
| 3155.62..... | 3 | 12 | 8 | ...... | III A |
| 3171.72..... | 4 | 8 | 4 | ...... | III A |
| 3172.85*.... | 4 | 15 | 12 | tr | III A |
| 3173.07..... | 10 | ...... | ...... | ...... | V E |
| 3179.43..... | 40 | ...... | ...... | ...... | V E |
| 3185.93..... | 2 | 10 | 8 | ...... | III A |
| 3191.28..... | 15 | 15 | 12 | ...... | III |
| 3194.37..... | 6 | 8 | 6 | ...... | III |
| 3195.62..... | 100 | 15 | 10 | ...... | III E |
| 3200.27..... | 100 | 15 | 10 | ...... | III E |
| 3203.33..... | 100 | 15 | 10 | ...... | III E |
| 3209.38..... | 3 | 10 | 10 | ...... | III A |
| 3216.70..... | 150 | 20 | 15 | ...... | III E |
| 3242.29..... | 200 | 25 | 20 | ...... | III E |
| 3252.27..... | 8 | 8 | 6 | ...... | III |
| 3275.56..... | 2 | 2 | tr | ...... | IV |
| 3278.45..... | 5 | 12 | 8 | ...... | III A |
| 3280.94..... | 10 | ...... | ...... | ...... | V E |
| 3287.24..... | 4 | 2 | 1 | ...... | III |
| 3327.88..... | 150 | 20 | 12 | ...... | III E |
| 3330.87..... | 3 | ...... | ...... | ...... | V E |
| 3335.17..... | 8n | ...... | ...... | ...... | V |
| 3340.39..... | 7 | 3 | 2 | ...... | III |
| 3344.54..... | 4n | ...... | ...... | ...... | V |
| 3354.58..... | 10 | {10 ?<br>{5 ? | 5 ?<br>2 ? | ......<br>...... | III<br>III |
| 3358.96..... | 5 | 2 | 1 | ...... | III |
| 3362.00..... | 20 | ...... | ...... | ...... | V E |
| 3364.79..... | 7 | 5 | 3 | ...... | III |
| 3377.67..... | 6 | 2 | 1 ? | ...... | III |
| 3382.82..... | 5 | ...... | ...... | ...... | V |
| 3383.03..... | 7 | ...... | ...... | ...... | V |
| 3388.58..... | 15 | 4 | 2 | ...... | III |
| 3389.87..... | 5 | 1 ? | ...... | ...... | IV ? |
| 3394.97..... | 4 | 3 | 1 | ...... | III |
| 3397.05..... | 15 | 4 | 2 | ...... | III |
| 3412.46..... | 12 | 5 | 3 | ...... | III |
| 3414.5...... | 8n | 4 | 3 | ...... | III |
| 3424.16..... | 7 | 15 | 15 | 1 ? | III A |
| 3431.01..... | 6 | ...... | ...... | ...... | V |
| 3431.67..... | 5 | 6 | 6 | ...... | III |
| 3433.79..... | 6n | 2 | ...... | ...... | IV |
| 3437.98..... | 8n | 3 | tr | ...... | IV |
| 3448.85..... | 35 | 1 ? | ...... | ...... | V E |
| 3450.96..... | 12 | 12 | 8 | tr | III |
| 3461.02*.... | 4 | ? | ? | ...... | V ? |
| 3467.88..... | 20 | 1 | ...... | ...... | V E |
| 3471.77*.... | 10n | 3 ? | 2 ? | ...... | V ? |
| 3473.18..... | 5 | 5 | 3 | ...... | III |
| 3484.05..... | 10 | 15 | 15 | 2 | III |
| 3485.74..... | 40 | 12 | 8 | tr | III |
| 3490.07..... | 150 | 10 | 7 | ...... | III E |
| 3498.90..... | 10n | 3 | 1 | ...... | III |
| 3500.61..... | 7 | 4 | 2 | ...... | III |
| 3501.97..... | 2 | 1 | ...... | ...... | IV |
| 3506.47*d*.... | 6 | 3 | 2 | ...... | III |
| 3510.53..... | 8 | 3 | 2 | ...... | III |
| 3511.17..... | 15 | 6 | 5 | ...... | III |
| 3512.88..... | 20 | 12 | 12 | tr | III |
| 3521.55..... | 6 | 5 | 3 | 1 | III |
| 3549.02..... | 150 | 10 | 6 | ...... | III E |
| 3551.78..... | 8 | ? | ? | ...... | III ? |
| 3552.70..... | 40 | 15 ? | 15 ? | 15 | I |
| 3558.75..... | 5 | 8 ? | 6 ? | 4 | II |
| 3571.45..... | 10 | 8 | 8 | 4 | II |
| 3576.05..... | 12 | 5 | 3 | ...... | III |
| 3584.53..... | 150 | 5 ? | ? | ...... | III ? E |
| 3587.74..... | 20 | 10 | 8 | ...... | III |
| 3589.66..... | 5 ? | ? | ? | ...... | III ? |
| 3592.90..... | 200 | 100R | 50r | 25 | II |
| 3600.77..... | 500 | 20 | 15 | 1 | III E |
| 3601.96..... | 200 | 10 | 8 | ...... | III E |
| 3611.05..... | 400 | 15 | 12 | ...... | III E |
| 3620.95..... | 400 | 200R | 75r | 30 | II |
| 3628.73..... | 150 | 5 | 3 | ...... | III E |
| 3633.13..... | 300 | 10 | 8 | ...... | III E |
| 3664.63..... | 200 | 8 | 6 | ...... | III E |
| 3668.46..... | 3 | ...... | ...... | ...... | V E |
| 3692.57..... | 8 | 2 | 1 | ...... | III |
| 3710.32..... | 800 | 20 | 15 | 1 | III E |
| 3718.14..... | 5 | 2 | ...... | ...... | IV |
| 3738.60..... | 4 | 3 | 1 | ...... | III |

TABLE I—*Continued*

| λ (I.A.) | Arc Int. | Furnace Intensities | | | Class | λ (I.A.) | Arc Int. | Furnace Intensities | | | Class |
|---|---|---|---|---|---|---|---|---|---|---|---|
| | | High Temp. | Medium Temp. | Low Temp. | | | | High Temp. | Medium Temp. | Low Temp. | |
| 3747.57 | 20 | 3 | 1 | ...... | III E | 4366.03 | 10 | 8 | 6 | ...... | III |
| 3774.37 | 200 | 10 | 8 | tr | III E | 4370.98 | 1 | 1 | 1 | ...... | III |
| 3776.57 | 40 | 5 | 3 | ...... | III E | 4374.95 | 300 | 15 | 10 | ...... | III E |
| 3788.73 | 100 | 6 | 4 | ...... | III E | 4375.61 | 8 | 4 | 3 | ...... | III |
| 3818.33 | 20 | 3 | 2 | ...... | III E | 4379.33 | 6 | 8 | 6 | ...... | III |
| 3832.94 | 30 | 4 | 3 | ...... | III E | 4385.49 | 3 | 4 | 2 | ...... | III |
| 3847.87 | 15 | ? | ? | ...... | V(?)E | 4387.71 | 8 | 3 | 1 | ...... | III |
| 3878.33 | 20 | ? | ? | ...... | V(?)E | 4394.03 | 3 | 4 | 2 | ...... | III |
| 3887.75 | 5 | 4 | 2 | tr | III | 4394.68 | 2 | 1 | 1 | ...... | III |
| 3904.58 | 5 | 2 | 2 | tr | III | 4397.79 | 3 | 2 | 1 | ...... | III |
| 3918.25 | 4 | 2 | 1 | ...... | III | 4398.04 | 100 | 5 | 3 | ...... | III E |
| 3930.66 | 10 | ...... | ...... | ...... | V E | 4415.37 | 3 | 2 | 1 | ...... | III |
| 3950.37 | 150 | 8 | 5 | tr | III E | 4417.44 | 2 | 3 | 1 | ...... | III |
| 3951.61 | 8 | ...... | ...... | ...... | V E | 4421.73 | 1 | 1 | ...... | ...... | IV |
| 3955.10 | 5 | 4 | 3 | tr | III | 4422.63 | 80 | 3 | 1 | ...... | III E |
| 3982.64 | 100 | 6 | 4 | tr | III E | 4432.98 | 1 | 1 | ...... | ...... | IV |
| 3987.46 | 4 | 4 | 3 | ...... | III | 4437.32 | 10 | 10 | 6 | ...... | III |
| 4029.84 | 3 | 1 | ...... | ...... | IV | 4443.66 | 15 | 15 | 10 | ...... | III |
| 4039.84 | 60 | 60r | 30 | 20 | II | 4445.25 | 3 | 1 | ...... | ...... | IV |
| 4047.66 | 80 | 80R | 40 | 25 | II | 4446.63 | 15 | 15 | 15 | 1 | III |
| 4077.39 | 300 | 300R | 100R | 60 | II | 4465.29 | 1 | 1 | ...... | ...... | IV |
| 4080.90 | 5 | 2 | 1 | ...... | III | 4472.77 | 2n | tr | ...... | ...... | IV |
| 4081.22 | 9 | 6 | 5 | 3 | II | 4473.89 | 7 | 3 | 1 | ...... | III |
| 4083.72 | 100 | 100R | 40 | 30 | II | 4475.70 | 20 | 12 | 10 | 1 | III |
| 4102.42 | 350 | 350R | 150R | 75 | II | 4476.92 | 25 | 15 | 12 | 2 | III |
| 4110.82 | 5 | 4 | 2 | ...... | III | 4477.41 | 25 | 20r | 15 | 2 | III |
| 4124.95 | 20 | 3 | 3 | tr | III E | 4479.01 | 2 | 1 | ...... | ...... | IV |
| 4128.35 | 300 | 300R | 125R | 70 | II | 4484.45* | 5 | 8 | 8 | 3 ? | II ? |
| 4142.88 | 200 | 200R | 100r | 60 | II | 4487.29 | 20 | 15 | 10 | 1 | III |
| 4157.64 | 6 | 4 | 2 | ...... | III | 4487.48 | 40 | 20 | 20 | 4 | III |
| 4167.57 | 100 | 100R | 50 | 30 | II | 4491.75 | 5 | 4 | 4 | ...... | III |
| 4174.18 | 100 | 100R | 50 | 30 | II | 4492.43 | 4 | 3 | 3 | tr ? | III |
| 4177.58 | 125 | 6 | 4 | tr | III E | 4505.95 | 50 | 25 | 25 | 6 | II |
| 4199.26 | 8 | ...... | ...... | ...... | V E | 4513.57 | 4 | 6 | 6 | 1 | III |
| 4204.72 | 20 | 1 | ...... | ...... | V E | 4514.02 | 8 | 4 | 2 | ...... | III |
| 4213.02 | 6 | 2 | ...... | ...... | IV | 4522.08 | 3 | 2 | 1 | ...... | III |
| 4213.54 | 5 | 4 ? | 2 ? | ...... | III ? | 4527.25 | 80 | 40 | 40 | 15 | II |
| 4217.82 | 10 | 6 | 4 | ...... | III | 4527.81 | 50 | 30 | 30 | 6 | II |
| 4220.62 | 30 | 12 | 6 | ...... | III | 4528.1 | 3 | 1 | tr | ...... | III |
| 4224.27 | 4 | 6 | 4 | 1 | III | 4533.53 | 1 | 1 | ...... | ...... | IV |
| 4229.20 | 2 | 1 | 1 | ...... | III | 4534.12 | 3 | 1 | tr | ...... | III |
| 4232.56 | 1 | 1 | tr | ...... | III | 4537.21 | 2 | 2 | 1 | ...... | III |
| 4235.73 | 40 | 2 | tr | ...... | IV E | 4539.61 | 1 | 1 | 1 | ...... | III |
| 4235.94 | 100 | 100R | 40 | 30 | II | 4544.31 | 10 | 5 | 3 | ...... | III |
| 4249.87 | 1 | 1 | tr | ...... | III | 4554.47 | 2 | 1 | 1 | ...... | III |
| 4250.37 | 1 | 1 | 1 | ...... | III | 4559.37 | 10 | 7 | 5 | 1 | III |
| 4251.17 | 40 | 10 | 8 | tr | III | 4564.41 | 4 | 4 | 3 | ...... | III |
| 4266.89 | 1 | 1 | tr | ...... | III | 4564.94 | 2 | 1 | — ? | ...... | IV ? |
| 4272.14 | 2 | 1 | tr | ...... | III | 4570.71 | 3n | 2 | 1 | ...... | III |
| 4274.18 | 1 | 10 | 8 | 2 | III A | 4573.59 | 10 | 4 | 2 | ...... | III |
| 4291.04 | 2 | 2 | 1 | ...... | III | 4578.86 | 1 | 1 | tr | ...... | III |
| 4300.37 | 2 | 1 | tr | ...... | III | 4581.33 | 6 | 15 | 12 | 4 | II A |
| 4302.29 | 50 | 12 | 10 | 1 | III | 4581.81 | 3 | 10 | 8 | 1 | III A |
| 4309.63 | 125 | 8 | 5 | ...... | III E | 4582.18 | 2 | 1 | 1 | ...... | III |
| 4315.52 | 2 | 1 | tr | ...... | III | 4590.77 | 1 | ...... | ...... | ...... | V |
| 4316.32 | 3 | 3 | 3 | ...... | III | 4594.00* | 15 | 10 | 8 | 6 ? | II ? |
| 4322.32 | 2 | 2 | 3 | ...... | III | 4596.56 | 12 | 5 | 3 | ...... | III |
| 4329.93 | 1 | 1 | tr | ...... | III | 4601.32 | 2 | 1 | tr | ...... | III |
| 4330.76 | 10 | 10 | 8 | 1 | III | 4604.78 | 10 | 4 | 4 | ...... | III |
| 4337.27 | 2 | 1 | 1 | ...... | III | 4613.00 | 4 | 2 | 1 | ...... | III |
| 4344.64 | 4 | 2 | 1 | ...... | III | 4636.50 | 1 | 1 | ...... | ...... | IV |
| 4346.16 | 1 | 1 | 1 | ...... | III | 4643.68 | 150 | 100R | 80 | 80 | I |
| 4348.77 | 60 | 15 | 12 | 1 | III | 4653.79 | 4 | 1 | tr | ...... | III |
| 4352.33 | 5 | 4 | 3 | ...... | III | 4658.31 | 12 | 6 | 3 | ...... | III |
| 4352.68 | 4 | 1 | 1 | ...... | III | 4658.89 | 6 | 2 | 2 | ...... | III |
| 4357.70 | 10 | 4 | 2 | ...... | III | 4666.39 | 3 | 1 | 1 | ...... | III |
| 4358.69 | 50 | 6 | 4 | tr | III E | 4666.85 | 3 | 1 | 1 | ...... | III |

TABLE I—*Continued*

| λ (I.A.) | Arc Int. | Furnace Intensities | | | Class |
|---|---|---|---|---|---|
| | | High Temp. | Medium Temp. | Low Temp. | |
| 4667.47..... | 8 | 4 | 2 | ...... | III |
| 4670.83..... | 4 | 8 | 3 | ...... | III A |
| 4674.85..... | 125 | 70R | 60 | 60 | I |
| 4678.34..... | 3 | 1 | tr | ...... | III |
| 4682.31..... | 20 | ...... | ...... | ...... | V E |
| 4689.76..... | 4 | 3 | 2 | ...... | III |
| 4691.94..... | 1 | 2 | 1 | ...... | III A |
| 4696.79..... | 8 | 5 | 5 | tr | III |
| 4699.24..... | 1 | ? | ? | ...... | III ? |
| 4701.02..... | 2 | ? | 1 | ...... | III |
| 4708.87..... | 3 | ? | ? | ...... | III ? |
| 4725 84 .... | 3 | 1 | tr | ...... | III |
| 4728.50..... | 20 | 8 | ? | ? | III ? |
| 4732.38..... | 3 | 2 | 1 ? | ...... | III ? |
| 4741.42..... | 8 | 4 | 2 | ...... | III |
| 4752.81..... | 12 | 8 | 5 | tr | III |
| 4761.02..... | 40 | 30 | 30 | 30 | I |
| 4780.17..... | 1 | 1 | 1 | ...... | III |
| 4781.06..... | 10 | 12 | 10 | 2 | III |
| 4786.61..... | 10 | 1 | tr | ...... | IV E |
| 4786.90..... | 10 | 8 | 8 | ...... | III |
| 4799.31..... | 15 | 12 | 10 | 3 | III |
| 4804.31..... | 4 | 2 | 1 | ...... | III |
| 4804.81..... | 6 | 3 | 2 | ...... | III |
| 4819.63..... | 10 | 10 | 8 | 2 | III |
| 4821.62..... | 2 | 1 | ...... | ...... | IV |
| 4822.09..... | 8 | 6 | 3 | ...... | III |
| 4823.28..... | 12 | ...... | ...... | ...... | V E |
| 4839.15..... | 3 | 3 | 2 | ...... | III |
| 4839.84..... | 60 | 20 | 20 | 10 | II |
| 4845.67..... | 50 | 15 | 15 | 8 | II |
| 4852.67..... | 50 | 15 | 15 | 8 | II |
| 4854.25..... | 4 | 4 | 2 | ...... | III |
| 4854.89..... | 70 | 1 | ...... | ...... | V E |
| 4856.72..... | 3 | 3 | 2 | ...... | III |
| 4859.82..... | 40 | 15 | 15 | 6 | II |
| 4863.11..... | 1 | 1 | tr | ...... | III |
| 4879.64..... | 4 | 4 | 2 | ...... | III |
| 4883.71..... | 80 | 1 | ...... | ...... | V E |
| 4886.30..... | 4 | 4 | 2 | ...... | III |
| 4886.65..... | 3 | 3 | 1 | ...... | III |
| 4893.42..... | 6 | 12 | 5 | ...... | III A |
| 4900.13..... | 80 | 20 | 10 | 2 | III E |
| 4906.11..... | 6 | 12 | 6 | ...... | III A |
| 4909.00..... | 2 | 3 | 1 | ...... | III |
| 4912.02..... | tr | ? | tr | ...... | III A ? |
| 4921.88..... | 10 | 20 | 10 | 2 | III A |
| 4926.32..... | tr | 1 | tr | ...... | III A |
| 4928.21..... | 1 | 1 | tr | ...... | III |
| 4930.95..... | 2 | 3 | 1 | ...... | III |
| 4948.58..... | tr | tr | ...... | ...... | IV |
| 4950.68..... | 2 | 3 | 1 | ...... | III |
| 4974.31..... | 10 | 4 | ? | ...... | III ? |
| 4982.12..... | 8 | ...... | ...... | ...... | V E |
| 5006.98..... | 10 | 4 | ...... | ...... | IV |
| 5070.18..... | 5 | ...... | ...... | ...... | V |
| 5072.17..... | 5 | 1 | ...... | ...... | IV |
| 5087.43..... | 150 | 4 | ...... | ...... | V E |
| 5088.18..... | 3 | ...... | ? | ...... | V |
| 5119.12..... | 15 | ...... | ...... | ...... | V E |
| 5123.21..... | 40 | ? | ...... | ...... | V E |
| 5135.22*.... | 25 | 10 ? | 6 ? | —? | III |
| 5196.44..... | 2 | ...... | ...... | ...... | V E |
| 5200.43..... | 60 | 3 | ...... | ...... | V E |
| 5205.73..... | 80 | 5 | ...... | ...... | V E |
| 5240.80..... | 15 | 8 | tr | ...... | IV |
| 5289.82..... | 4 | ...... | ...... | ...... | V E |
| 5380.65..... | 15 | 12 | 4 | 1 | III |
| 5402.81..... | 20 | ...... | ...... | ...... | V E |
| 5417.10..... | 3 | 4 ? | ...... | ...... | IV ? |
| 5424.40..... | 20 | 10 | 3 | tr | III |
| 5438.25..... | 50 | 30 | 8 | 4 | II |
| 5466.51..... | 300 | 150 | 100 | 50 | II |
| 5468.48..... | 40 | 10 | 3 | ...... | III |
| 5473.40..... | 10.. | ...... | ...... | ...... | V E |
| 5480.75..... | 8 | ...... | ...... | ...... | V E |
| 5491.48..... | 1 | ...... | ...... | ...... | V |
| 5493.23..... | 15 | 12 | 2 | ...... | III |
| 5495.63..... | 8 | 5 | 1 | ...... | III |
| 5497.43..... | 25 | ...... | ...... | ...... | V E |
| 5503.47d.... | 100 | 5<br>25 | 2<br>8 | ......<br>4 | III<br>II |
| 5509.94..... | 40 | 3 ? | ...... | ...... | V E |
| 5513.66..... | 20 | 10 | 3 | 1 | II |
| 5521.65*.... | 30 | 15 | 5 | 2 | II |
| 5526.73..... | 2 | 2 | ...... | ...... | IV |
| 5527.59..... | 250 | 150 | 80 | 50 | II |
| 5541.65..... | 3 | 3 | 1 | ...... | III |
| 5544.60*.... | 25 | 8 | 2 | ...... | III |
| 5546.03..... | 3 | ...... | ...... | ...... | V E |
| 5556.48..... | 20 | 100 | 200 | 200 | I A |
| 5567.76..... | 15 | 6 | 2 | 1 | II |
| 5577.43..... | 30 | 20 | 6 | 2 | II |
| 5581.09..... | 3 | 1 | ...... | ...... | IV |
| 5581.89..... | 150 | 150 | 80 | 50 | II |
| 5590.96..... | 2 | 2 ? | tr | ...... | IV |
| 5594.13..... | 2 | 2 | tr | ...... | IV |
| 5606.35..... | 20 | 15 | 8 | 5 | II |
| 5630.14..... | 100 | 75 | 50 | 35 | II |
| 5632.25..... | 3 | 8 | 10 | 10 | I A |
| 5644.70..... | 20 | 12 | 8 | 6 | II |
| 5648.49..... | 20 | 7 | 3 | 2 | II |
| 5662.95..... | 50 | tr | ...... | ...... | V |
| 5669.23..... | 1 | 1 | ...... | ...... | IV |
| 5675.30..... | 15 | 10 | 6 | 3 | II |
| 5675.64..... | 1 | ...... | ...... | ...... | V |
| 5686.68..... | 1 | 1 ? | tr ? | ...... | IV ? |
| 5693.64..... | 2 | 5 | 4 | 2 | II A |
| 5706.76..... | 30 | 15 | 12 | 3 | II |
| 5713.85..... | 3n | 1 | ...... | ...... | IV |
| 5714.92..... | 3n | 1 | ...... | ...... | IV |
| 5720.61..... | 3 | 3 | tr | ...... | IV |
| 5723.45..... | 1 | 1 | ...... | ...... | IV |
| 5728.91..... | 3 | ...... | ...... | ...... | V E |
| 5732.08..... | 3 | 4 | 3 | 2 | II |
| 5740.21..... | 1 | 3 | 1 | ...... | III A |
| 5743.87..... | 15 | 6 | 2 | tr | III |
| 5765.67..... | 12 | 4 | 1 | ...... | III |
| 5773.94..... | 4 | 2 | tr | ...... | IV |
| 5781.69..... | 2 | ...... | ...... | ...... | V E |
| 5787.74..... | 1 | tr | ...... | ...... | IV |
| 5797.13..... | 1 | 2 | tr | ...... | IV A |
| 5821.88..... | 4 | 4 | 1 | ...... | III |
| 5832.26..... | 3 | 1 | ...... | ...... | IV |
| 5871.76..... | 2 | 1 | ...... | ...... | IV |
| 5879.95..... | 3 | 1 | ...... | ...... | IV |
| 5902.94..... | 7 | 3 | ...... | ...... | IV |
| 5915.71..... | 6 | 3 ? | —? | ...... | IV |
| 5950.00..... | 5 | 2 | ...... | ...... | IV |
| 6009.20..... | 10 ? | 8 | 1 | ...... | IV |
| 6023.43..... | 20 ? | 200 | 200 | 200 | I A |
| 6024.33..... | ? | 4 | 1 | ...... | III |
| 6135.06..... | ? | 4 | 1 | ...... | III |
| 6138.42..... | 15 ? | 150 | 150 | 150 | I A |

TABLE I—*Continued*

| λ (I.A.) | Arc Int. | Furnace Intensities | | | Class | λ (I.A.) | Arc Int. | Furnace Intensities | | | Class |
|---|---|---|---|---|---|---|---|---|---|---|---|
| | | High Temp. | Medium Temp. | Low Temp. | | | | High Temp. | Medium Temp. | Low Temp. | |
| 6191.72..... | 100 ? | 400 | 400 | 400 | I A | 6815.15..... | 5 | 2 | ...... | ...... | IV |
| 6222.57..... | 50 ? | 250 | 250 | 250 | I A | 6832.47..... | 1 | ...... | ...... | ...... | V E |
| 6338.15..... | 5 | 6 | 10 | 8 | I | 6845.23..... | 10 | 2 | 1 | ...... | III |
| 6402.02..... | 50 | 200 | 200 | 150 | I A | 6858.22..... | 1 | ...... | ...... | ...... | V E |
| 6435.03 .... | 500 | 500 | 500 | 500 | I | 6887.21..... | 8 | 1 | ...... | ...... | IV |
| 6437.17..... | 5 | 1 ? | ...... | ...... | IV ? | 6895.99..... | 3 | ...... | ...... | ...... | V E |
| 6462.58..... | 8 | 3 | 1 | ...... | III | 6908.27..... | 2 | 2 | 1 | ...... | III |
| 6493.77..... | 4 | ...... | ...... | ...... | V | 6933.53..... | 6 | 20 | 15 | 5 | II A |
| 6538.57..... | 35 | 10 | 3 | —? | III | 6950.31..... | 8 | 1 | ...... | ...... | IV |
| 6557.36..... | 30 | 200 | 200 | 150 | I A | 6951.66..... | 1 | ...... | ...... | ...... | V E |
| 6576 86 .... | 6 | 3 | 1 | ...... | III | 6958.01*.... | 4 | 100 | 125 | 100 | I A |
| 6584.88..... | 5 | 40 | 30 | 20 | II A | 6979.86..... | 8 | —? | ...... | ...... | V ? |
| 6613.74..... | 15 | ...... | ...... | ...... | V E | 7008.95..... | 5 | ...... | ...... | ...... | V |
| 6622.51..... | 2 | 1 ? | ...... | ...... | IV ? | 7009.95..... | 4 | ...... | ...... | ...... | V |
| 6636.48..... | 2 | 1 ? | ...... | ...... | IV ? | 7035.19..... | 5 | 1 | ...... | ...... | IV |
| 6650.60..... | 8 | 2 | ...... | ...... | IV | 7052.97..... | 10 | 4 | 2 | ...... | III |
| 6664.38..... | 3 | 1 ? | ...... | ...... | IV ? | 7054.32..... | 4 | ...... | ...... | ...... | V |
| 6687.58..... | 80 | 100 | 100 | 100 | I | 7127.93..... | 2 | 2 ? | 1 ? | ...... | III ? |
| 6691.85..... | 2 | ...... | ...... | ...... | V | 7191.63..... | 10 | 3 | 1 | ...... | III |
| 6694.75..... | 1 | ...... | ...... | ...... | V | 7264.19..... | 8 | 2 | ...... | ...... | IV E |
| 6699.26..... | 3 | 1 | ...... | ...... | IV | 7346.44..... | 10 | 4 | 2 | ...... | III |
| 6700.71..... | 20 | 5 | 2 | ...... | III | 7450.29†.... | 5 | 2 | 1 ? | ...... | III(?)E |
| 6713.20..... | 6 | 2 | 1 | ...... | III | 7563.06..... | 5 | ...... | ...... | ...... | V |
| 6735.99..... | 7 | 2 | 1 | ...... | III | 7719.89..... | 2 | ...... | ...... | ...... | V |
| 6793.69..... | 80 | 100 | 100 | 100 | I | 7724.01..... | 2 | 1 | ...... | ...... | IV |
| 6795.40..... | 15 | ...... | ...... | ...... | V E | 7881.87..... | 10 | ...... | ...... | ...... | V E |
| 6803.15..... | 1 | ...... | ...... | ...... | V | | | | | | |

NOTES—YTTRIUM

| | |
|---|---|
| 3018.93 | Blend *Fe* in arc. |
| 3056.33 | Blend *V*. Probable intensity of *V*-line subtracted. |
| 3172.85 | May be impurity. |
| 3461.02 | Blend *Dy* in furnace. |
| 3471.77 | Furnace line may be *Er*. |
| 4484.45 | May be impurity. |
| 4594.00 | Furnace line may be partly impurity. |
| 5135.22 | Blend with impurity line. |
| 5521.65 | Blend enhanced line. |
| 5544.60 | Blend enhanced line. |
| 6958.01 | Probably impurity, not *La*. |

The limited quantity of these preparations permitted their use, as a rule, only in the arc. For the furnace, which required frequent recharging of the tube during long runs, fairly pure yttrium nitrate and lanthanum chloride were obtained from Eimer and Amend; and, by using only lines which were given by the purer arc material, it is hoped that foreign lines have been largely eliminated. For the zirconium spectrograms, the metal in pulverized or flake form proved satisfactory.

## EXPLANATION OF THE TABLES

Tables I, II, and IV present the intensities in arc and furnace and the resulting classification for lines of yttrium, zirconium, and

## TABLE II

### Temperature Classification of Zirconium Lines

| λ (I.A.) | Arc Int. | Furnace Intensities |  | Class | λ (I.A.) | Arc Int. | Furnace Intensities |  | Class |
|---|---|---|---|---|---|---|---|---|---|
|  |  | High Temp. | Low Temp. |  |  |  | High Temp. | Low Temp. |  |
| 2792.04 | 20 | 8 | ...... | IV | 3233.11 | 5 | ...... | ...... | V |
| 2793.40 | 8 | ...... | ...... | V | 3234.13 | 100 | 100 | 40 | II |
| 2795.13 | 8 | ...... | ...... | V | 3234.80 | 5 | 4 | ...... | III |
| 2806.78 | 12 | 4 | ...... | IV | 3241.05 | 40 | 2 | ...... | IV E |
| 2814.91 | 150 | 12 | ...... | IV | 3243.98 | 8 | ...... | ...... | V |
| 2815.49 | 2 | ...... | ...... | V | 3250.39* | 35 | 25 | 4 | III |
| 2819.56 | 10 | 4 | ...... | IV | 3254.28 | 15 | 1 | ...... | IV |
| 2821.57 | 8 | 3 | ...... | IV | 3260.11 | 40 | 30 | 5 | III |
| 2827.55* | 8 | 2 | ...... | IV | 3269.66 | 40 | 30 | 5 | III |
| 2829.81 | 8 | 1 | ...... | IV | 3272.22 | 40 | 1 | ...... | V E |
| 2836.50 | 4 | ...... | ...... | V | 3273.05 | 150 | 5 | ...... | IV E |
| 2837.23 | 200 | 20 | ...... | IV | 3279.27 | 125 | 4 | ...... | IV E |
| 2848.52 | 150 | 15 | ...... | IV | 3282.73 | 15 | 20 | 6 | II |
| 2857.98 | 2 | ...... | ...... | V | 3284.72 | 80 | 3 | ...... | IV E |
| 2860.85 | 30 | 6 | ...... | IV | 3305.15 | 40 | 1 | ...... | V E |
| 2866.38 | 2 | ...... | ...... | V | 3306.27 | 80 | 3 | ...... | IV E |
| 2875.99 | 200 | 20 | ...... | IV | 3314.50 | 12 | 1 | ...... | IV E |
| 2880.84 | 5 | ...... | ...... | V | 3316.21 | 4 | ...... | ...... | V |
| 2892.27 | 30 | 8 | ...... | IV | 3322.29 | 5 | ...... | ...... | V |
| 2898.26 | 3 | ...... | ...... | V | 3323.00 | 20 | 1 | ...... | IV E |
| 2916.25 | 10 | 4 | ...... | IV | 3333.54 | 4 | 1 ? | ...... | IV ? |
| 2916.49 | 2 | ...... | ...... | V | 3353.65 | 20 | 20 | 6 | II |
| 2923.85 | 10 | 4 | ...... | IV | 3356.09 | 60 | 1 | ...... | V E |
| 2940.77 | 3 | ...... | ...... | V | 3357.27 | 50 | 1 | ...... | V E |
| 2960.87 | 60 | 20 | ...... | IV | 3360.45 | 25 | 15 | 3 | II |
| 2964.85 | 2 | ...... | ...... | V | 3368.61 | 5 | 4 | 1 | II |
| 2969.19 | 40 | 15 | ...... | IV | 3370.71 | 20 | 8 | 1 | III |
| 2985.39 | 200 | 30 | 6 | II | 3379.92 | 10 | 3 | 1 | III |
| 3005.37 | 40 | 8 | ...... | IV | 3385.78 | 5 | ...... | ...... | V |
| 3005.50 | 60 | 6 | ...... | IV | 3387.87 | 40 | 1 | tr | III E |
| 3011.75 | 250 | 40 | 8 | II | 3388.30 | 80 | 2 | 1 | III E |
| 3014.44 | 15 | 10 | ...... | III | 3391.98 | 400 | 6 | 2 | III E |
| 3029.52 | 300 | 50 | 12 | II | 3393.12 | 25 | tr | ...... | V E |
| 3043.26 | 3 | 3 | ...... | III | 3397.92 | 5 | ...... | ...... | V |
| 3045.83 | 10 | 8 | ...... | III | 3401.78 | 3 | ...... | ...... | V |
| 3049.35 | 6 | 6 | ...... | III | 3414.66* | 20 | 8 | 3 | II |
| 3063.59* | 8 | 4 | ...... | III | 3419.66 | 20 | 10 | 4 | II |
| 3072.88 | 3 | ...... | ...... | V | 3430.29 | 8 | 10 | 4 | II |
| 3085.35 | 12 | 12 | ...... | III | 3430.53 | 50 | 1 | ...... | V E |
| 3090.44 | 6 | 5 | ...... | III | 3438.24 | 400 | 12 | 3 | III E |
| 3092.20* | 2 ? | ...... | ...... | V | 3440.44 | 30 | 30 | 15 | II |
| 3093.34* | 2 ? | 2 | ...... | III | 3446.61 | 30 | 15 | 6 | II |
| 3094.80 | 15 | 15 | ...... | III | 3447.37 | 100 | 50 | 40 | II |
| 3095.82 | 12 | 10 | ...... | III | 3449.91 | 6 | 2 | ...... | IV |
| 3099.69 | 2 | ...... | ...... | V | 3455.91 | 30 | 15 | 5 | II |
| 3108.36 | 10 | 8 | ...... | III | 3457.19 | 20 | 10 | 3 | II |
| 3113.50 | 8 | 6 | ...... | III | 3461.09 | 30 | 7 | 2 | II |
| 3120.75 | 125 | 40 | 4 | III | 3465.63 | 10 | 10 | 4 | II |
| 3125.92 | 40 | 1 | ...... | V E | 3469.10 | 4 | 4 | 2 | II |
| 3129.77 | 40 | 1 | ...... | V E | 3471.19* | 100 | 50 | 40 | II |
| 3130.06 | 8 | 5 | ...... | III | 3472.89 | 4 | 1 | ...... | IV |
| 3131.11 | 25 | 15 | ...... | III | 3478.79 | 20 | 10 | ...... | III |
| 3132.06 | 50 | 40 | 3 | III | 3482.81 | 20 | 20 | 1 | III |
| 3133.24 | 20 | 10 | ...... | III | 3483.01 | 15 | 2 | ...... | IV |
| 3136.96 | 30 | 15 | tr | III | 3501.35 | 15 | 15 | ...... | III |
| 3138.68 | 50 | 1 | ...... | V E | 3501.50 | 8 | 1 | ...... | IV |
| 3139.80 | 20 | 12 | ...... | III | 3509.33 | 100 | 100 | 15 | II |
| 3148.81 | 25 | 15 | ...... | III | 3519.61 | 125 | 125 | 30 | II |
| 3157.82 | 50 | 40 | 3 | III | 3530.23 | 15 | 10 | 1 | III |
| 3165.98 | 80 | 3 | ...... | IV E | 3533.23 | 60 | 50 | 3 | III |
| 3191.22 | 100 | 60 | 20 | II | 3535.17 | 20 | 4 | ...... | IV |
| 3191.91 | 10 | tr ? | ...... | V E | 3547.69 | 100 | 60 | 15 | II |
| 3204.90 | 12 | 6 | ...... | III | 3549.74† | 15 | 10 ? | 2 ? | III ? |
| 3212.02 | 100 | 80 | 30 | II | 3550.47 | 30 | 30 | 4 | III |
| 3212.58 | 8 | 3 | ...... | III | 3558.96† | 12 | ? | ...... | IV ? |
| 3231.70 | 70 | 4 | ...... | IV E | 3566.11 | 100 | 100 | 40 | II |

TABLE II—*Continued*

| λ (I.A.) | Arc Int. | Furnace Intensities | | Class | λ (I.A.) | Arc Int. | Furnace Intensities | | Class |
|---|---|---|---|---|---|---|---|---|---|
| | | High Temp. | Low Temp. | | | | High Temp. | Low Temp. | |
| 3568.57†........ | 15 | 3 ? | ...... | IV ? | 4024.92.......... | 40 | 15 | 3 | II |
| 3575.80 ........ | 100 | 50 | 10 | II | 4027.20.......... | 40 | 15 | 5 | II |
| 3577.56†........ | 15 | ? | ...... | IV ? | 4028.95.......... | 15 | 8 | 1 | III |
| 3586.30 ........ | 100 | 50 | 10 | II | 4030.04.......... | 30 | 15 | 3 | II |
| 3591.73 ........ | 2 | 1 | tr | III | 4030.75*......... | 3 | —? | ...... | IV ? |
| 3601.20.......... | 400 | 200 | 60 | II | 4035.89*......... | 40 | 20 | 8 | II |
| 3613.70.......... | 15 | 10 | ...... | III | 4041.64†......... | 5 | —? | ...... | IV |
| 3623.87.......... | 300 | 150 | 30 | II | 4042.22.......... | 10 | 2 | ...... | IV |
| 3634.15.......... | 50 | 50 | 4 | III | 4043.58.......... | 30 | 15 | 6 | II |
| 3638.09.......... | 3 | tr | ...... | IV | 4044.56.......... | 25 | 12 | 3 | II |
| 3656.59.......... | 6 | 3 | ...... | III | 4050.48.......... | 10 | 5 | 2 | II |
| 3661.20 ......... | 30 | 20 | 3 | III | 4054.43.......... | 10 | 7 | 3 | II |
| 3663.65.......... | 300 | 150 | 30 | II | 4055.04.......... | 60 | 30 | 10 | II |
| 3680.38 ......... | 5 | 2 | ...... | III | 4055.71†......... | 20 | 1 ? | ...... | V ? |
| 3706.63.......... | 10 | 5 | tr | III | 4058.63†......... | 3 | 1 ? | ...... | IV ? |
| 3714.13 ......... | 30 | 20 | 2 | III | 4060.08†......... | 2 | ? | ...... | IV ? |
| 3737.40 ......... | 5 | 1 | ...... | IV | 4060.58†......... | 4 | 2 ? | ...... | IV ? |
| 3764.59 ......... | 80 | 50 | 12 | II | 4061.53.......... | 15 | 8 | 2 | II |
| 3766.72 ......... | 60 | 40 | 8 | II | 4064.16.......... | 100 | 50 | 12 | II |
| 3780.54 ......... | 100 | 60 | 15 | II | 4068.73*......... | 4 | 2 | 1 | II |
| 3791.40 ......... | 80 | 40 | 10 | II | 4072.71.......... | 100 | 50 | 15 | II |
| 3822.42 ......... | 40 | 20 | 5 | II | 4074.93.......... | 15 | 8 | 2 | II |
| 3835.97 ......... | 100 | 50 | 15 | II | 4076.53.......... | 10 | 5 | 1 | III |
| 3847.01† ........ | 30 | ? | ? | ? | 4078.31.......... | 12 | 7 | 2 | II |
| 3849.26 ......... | 30 | 15 | 4 | II | 4081.22.......... | 100 | 60 | 20 | II |
| 3863.88 ......... | 100 | 30 | 10 | II | 4082.29.......... | 3 | 2 | 1 | II |
| 3874.34† ........ | 40 | ? | ? | ? | 4083.09.......... | 4 | 2 | 1 | II |
| 3877.60 ......... | 40 | 5 | ...... | IV | 4084.30†......... | 4 | —? | ...... | IV ? |
| 3879.05*......... | 10 | 20 | 10 | I A | 4087.69.......... | 3 | 2 | 1 | II |
| 3885.43 ......... | 100 | 80 | 20 | II | 4090.79.......... | 5 | ...... | ...... | V |
| 3890.32 ......... | 125 | 80 | 25 | II | 4094.27†......... | 3 | —? | 1 | II ? |
| 3891.39 ......... | 100 | 80 | 20 | II | 4099.31.......... | 4 | 4 | 1 | III |
| 3892.03 ......... | 4n | tr | ...... | IV | 4107.50.......... | 8 | ...... | ...... | V |
| 3896.53 ......... | 10 | 10 | 2 | II | 4108.40.......... | 15 | 5 | 1 | III |
| 3897.66 ......... | 3 | ...... | ...... | V | 4121.46.......... | 30 | 10 | 2 | III |
| 3916.64 ......... | 10 | 10 | 2 | II | 4135.68.......... | 10 | 4 | 2 | II |
| 3921.80 ......... | 100 | 50 | 10 | II | 4152.64†......... | 10 | —? | ...... | IV ? |
| 3926.79 ......... | 3n | ...... | ...... | V | 4166.45.......... | 20 | 10 | 3 | II |
| 3929.54.......... | 150 | 80 | 20 | II | 4183.32.......... | 10 | 6 | ...... | III |
| 3933.19.......... | 2 | ...... | ...... | V | 4187.57†......... | 20 | 10 | —? | III |
| 3941.63.......... | 5 | 1 | ...... | IV | 4194.76.......... | 10 | ...... | ...... | V |
| 3963.80 ......... | 2n | ...... | ...... | V | 4199.09†......... | 20 | 10 ? | ? | III ? |
| 3966.67.......... | 50 | 30 | 6 | II | 4201.45.......... | 20 | 10 | 2 | III |
| 3968.26 ......... | 80 | 50 | 15 | II | 4213.86†......... | 15 | 8 ? | ? | III ? |
| 3972.30.......... | 3 | ...... | ...... | V | 4218.44.......... | 6 | 4 | tr | III |
| 3973.51.......... | 60 | 40 | 10 | II | 4220.65.......... | 2 | 1 | ...... | III |
| 3975.30†......... | 15 | 2 ? | ...... | IV | 4222.45.......... | 5n | ...... | ...... | V |
| 3977.33 ......... | 3 | ...... | ...... | V | 4224.69.......... | 2n | ...... | ...... | V |
| 3977.48 ......... | 15 | 5 | 1 | III | 4227.76.......... | 200 | 100 | 40 | II |
| 3978.26 ......... | 2 | ...... | ...... | V | 4234.63.......... | 7 | 5 | 2 | II |
| 3978.74.......... | 30n | 4 | 1 | III | 4236.07.......... | 6 | 2 | tr | III |
| 3981.59.......... | 20n | 2 | ...... | IV | 4237.43.......... | 4 | 1 | ...... | IV |
| 3982.16 ......... | 5 | ...... | ...... | V | 4239.31.......... | 150 | 80 | 30 | II |
| 3984.75* ........ | 20 | 5 | 1 | III | 4240.34.......... | 50 | 25 | 10 | II |
| 3986.80.......... | 5 | ...... | ...... | V | 4241.20*......... | 50 | 15 ? | ? | II ? |
| 3988.68.......... | 10 | 3 | ...... | IV | 4241.69.......... | 80 | 60 | 30 | II |
| 3989.29.......... | 7 | 6 | 1 | III | 4242.02.......... | 2 | 1 | ...... | IV |
| 3989.50 ......... | 12 | ...... | ...... | V | 4253.57.......... | 4 | 1 | ...... | IV |
| 4001.09†......... | 4 | 2 ? | ...... | IV ? | 4256.04.......... | 1 | 1 | ...... | IV |
| 4001.22 ......... | 2 | ...... | ...... | V | 4256.44.......... | 4 | 3 | tr | III |
| 4002.55†......... | 8 | ? | ...... | IV ? | 4261.21.......... | 4 | 2 | ...... | III |
| 4003.10†......... | 12 | ? | ...... | IV ? | 4261.43.......... | 3 | ...... | ...... | V |
| 4004.40†......... | 4 | ? | ...... | IV ? | 4268.02.......... | 20 | 10 | 6 | II |
| 4004.87† ........ | 4n | ? | ...... | IV ? | 4274.76.......... | 5 | 4 | 1 | III |
| 4007.60†......... | 15 | 2 ? | ...... | IV ? | 4276.72.......... | 5 | 4 | ...... | III |
| 4012.25†......... | 12 | ? | ...... | IV ? | 4282.20.......... | 20 | 10 | 7 | II |
| 4017.00†......... | 8 | ? | ...... | IV | 4291.20.......... | 5 | 3 | 1 | II |
| 4023.98 ......... | 30 | 10 | 3 | II | 4291.35.......... | 8 | 4 | 1 | III |

TABLE II—*Continued*

| λ (I.A.) | Arc Int. | Furnace Intensities | | Class | λ (I.A.) | Arc Int. | Furnace Intensities | | Class |
|---|---|---|---|---|---|---|---|---|---|
| | | High Temp. | Low Temp. | | | | High Temp. | Low Temp. | |
| 4294.45 | 2 | tr | ...... | IV | 4667.14 | 4 | 2 | 1 | II |
| 4294.80 | 20 | 10 | 7 | II | 4683.42* | 15 | —? | ...... | V ? |
| 4302.88 | 15 | 7 | 3 | II | 4684.25† | 2 | ? | ...... | V ? |
| 4304.69 | 8 | 4 | 1 | III | 4687.80 | 150 | 20 | 20 | I |
| 4309.82 | 3 | 1 | ...... | IV | 4688.45 | 40 | 15 | 20 | I |
| 4319.05 | 3 | 1 | ...... | IV | 4707.73 | 4 | ...... | ...... | V |
| 4321.17 | 4 | 3 | 2 | II | 4710.08 | 100 | 20 | 15 | I |
| 4324.04 | 4 | 1 | ...... | IV | 4711.91 | 8 | ...... | ...... | V |
| 4325.44 | 15 | 5 | 2 | II | 4713.43† | 2 | ? | ...... | IV ? |
| 4329.57 | 3 | 2 | 1 | II | 4717.62† | 6 | 1 ? | ...... | IV ? |
| 4341.13 | 20 | 5 | 2 | II | 4719.11 | 10 | tr | ...... | V |
| 4343.04 | 4 | 3 | 2 | II | 4732.33† | 15 | 4 ? | 2 ? | III ? |
| 4346.52 | 4 | 1 | ...... | IV | 4739.48 | 100 | 20 | 15 | I |
| 4347.23 | 2 | 1 | ...... | IV | 4751.91* | 2 | 1 ? | ...... | IV ? |
| 4347.90 | 30 | 15 | 8 | II | 4753.05 | 3 | ...... | ...... | V |
| 4348.94 | 2 | 1 | ...... | IV | 4762.77 | 8 | 1 | ...... | IV |
| 4358.75 | 4 | 2 | 1 | II | 4772.32 | 80 | 15 | 12 | I |
| 4360.81 | 15 | 8 | 5 | II | 4784.92 | 12 | 5 | 3 | II |
| 4366.45 | 15 | 2 | 1 | II | 4788.68 | 8 | 3 | 2 | II |
| 4373.07 | 2 | ...... | ...... | V | 4789.12 | 2 | 1 | ...... | III |
| 4394.50 | 2 | 2 | 1 | II | 4805.87 | 15 | 6 | 3 | II |
| 4394.94 | 8 | 1 | ...... | IV | 4809.47 | 8 | 1 | ...... | IV |
| 4395.20* | 6 | ? | ? | ? | 4815.05 | 12 | 5 | 3 | II |
| 4400.24 | 5 | 2 | 1 | II | 4815.63 | 60 | 12 | 10 | I |
| 4402.96 | 4 | 2 | 1 | II | 4824.29 | 12 | 5 | 3 | II |
| 4413.04 | 12 | 2 | 1 | II | 4828.04 | 10 | 4 | 2 | II |
| 4414.14 | 2 | 2 | 1 | II | 4838.78 | 4 | 1 | ...... | IV |
| 4420.46 | 12 | 2 | tr | III | 4838.98 | 2 | ...... | ...... | V |
| 4429.10 | 3 | 2 | ...... | III | 4851.37 | 12 | 5 | 2 | II |
| 4431.48 | 10 | 2 | tr | III | 4866.07 | 5 | 2 | 1 | II |
| 4438.05 | 8 | 3 | 1 | II | 4881.25 | 4 | 2 | tr | III |
| 4444.34 | 2 | ...... | ...... | V | 4883.60 | 5 | 2 | 1 | II |
| 4448.95 | 2 | 1 | ...... | IV | 4893.12 | 2 | tr | ...... | IV |
| 4450.28 | 5 | 1 | ...... | IV | 4933.64 | 3 | ...... | ...... | V |
| 4455.44 | 2 | 1 | ...... | IV | 4948.76 | 2 | ...... | ...... | V |
| 4456.30 | 3 | tr | ...... | IV | 4994.76† | 5 | 2 ? | ...... | IV ? |
| 4459.02* | 2 | 2 | 1 | II | 4996.33 | 2 | ...... | ...... | V |
| 4466.91 | 10 | 3 | 1 | II | 5046.58 | 10 | ...... | ...... | V |
| 4468.78 | 3 | 2 | 1 | II | 5060.39 | 3 | ...... | ...... | V |
| 4470.32 | 5 | 1 | ...... | IV | 5064.90 | 15 | ...... | ...... | V |
| 4470.56 | 15 | 2 | tr | III | 5065.21 | 4 | ...... | ...... | V |
| 4480.77 | 2 | ...... | ...... | V | 5070.25 | 3 | ...... | ...... | V |
| 4482.50 | 2 | ...... | ...... | V | 5073.98 | 2 | ...... | ...... | V |
| 4491.56 | 2 | 1 | ...... | IV | 5078.25† | 20 | ? | ? | V ? |
| 4494.93* | 2 | 1 ? | ...... | IV ? | 5085.26 | 3 | ...... | ...... | V |
| 4507.12 | 30 | 10 | 6 | II | 5115.24 | 5 | ...... | ...... | V |
| 4535.75 | 30 | 10 | 6 | II | 5133.39 | 6 | ...... | ...... | V |
| 4539.98 | 4 | 2 | 1 | II | 5155.45 | 12 | ...... | ...... | V |
| 4542.22 | 20 | 8 | 4 | II | 5158.00 | 7 | ...... | ...... | V |
| 4553.01 | 12 | 4 | 2 | II | 5160.99 | 3 | ...... | ...... | V |
| 4555.13 | 10 | ...... | ...... | V | 5165.94 | 4 | ...... | ...... | V |
| 4555.53 | 8 | ...... | ...... | V | 5183.70 | 6 | 4 | ...... | III |
| 4558.04 | 2 | ...... | ...... | V | 5201.15 | 4 | 4 | ...... | III |
| 4565.46 | 2 | ...... | ...... | V | 5209.30 | 4 | ...... | ...... | V |
| 4575.51 | 40 | 15 | 12 | I | 5224.92 | 6 | 6 | tr | III |
| 4576.21 | 2 | ...... | ...... | V | 5277.39 | 8 | 8 | 1 | III |
| 4582.29 | 3 | ...... | ...... | V | 5280.04 | 2 | ...... | ...... | V |
| 4584.24† | 2 | 1 ? | ...... | IV ? | 5294.82 | 2 | ...... | ...... | V |
| 4590.54 | 6 | 2 | 1 | II | 5296.79 | 5 | 5 | 1 | III |
| 4602.57 | 15 | 2 | ...... | IV | 5311.40 | 6 | 6 | 1 | III |
| 4604.42 | 8 | 4 | 1 | III | 5362.54 | 6 | 4 | ...... | III |
| 4610.10† | 2 | 1 ? | ...... | IV ? | 5385.12 | 40 | 15 | 4 | II |
| 4613.35† | 1 | 1 ? | ...... | IV ? | 5405.11 | 2 | 2 | ...... | III |
| 4626.41† | 12 | 2 ? | ...... | IV ? | 5407.61† | 7 | 5 ? | 2 ? | II ? |
| 4634.02 | 50 | 20 | 20 | I | 5437.74† | 2 | ? | ...... | IV ? |
| 4640.12 | 2 | ...... | ...... | V | 5448.54 | 3 | 2 | ...... | III |
| 4644.83 | 8 | ...... | ...... | V | 5478.31† | 3 | 2 ? | ...... | III ? |
| 4657.64 | 7 | ...... | ...... | V | 5480.81† | 2 | 1 ? | ...... | IV ? |

TABLE II—*Continued*

| λ (I.A.) | Arc Int. | Furnace Intensities | | Class | λ (I.A.) | Arc Int. | Furnace Intensities | | Class |
|---|---|---|---|---|---|---|---|---|---|
| | | High Temp. | Low Temp. | | | | High Temp. | Low Temp. | |
| 5486.08 | 2 | 1 | ...... | IV | 6832.93† | 12 | 5 ? | 1 ? | III ? |
| 5502.13 | 15 | 1 | ...... | V | 6847.06 | 25 | 1 | ...... | V |
| 5517.10 | 2 | ...... | ...... | V | 6849.30 | 4 | ...... | ...... | V |
| 5528.41† | 8 | —? | ...... | V ? | 6888.31 | 20 | 2 | ...... | IV |
| 5537.41 | 2 | ...... | ...... | V | 6900.60 | 2 | 1 | ...... | IV |
| 5545.31 | 3 | ...... | ...... | V | 6904.40 | 2 | 3 | ...... | III |
| 5620.13† | 15 | 2 ? | ...... | IV ? | 6907.41 | 3 | 1 | ...... | IV |
| 5623.52 | 3 | ...... | ...... | V | 6916.97 | 2 | 2 | ...... | III |
| 5664.50 | 25 | 15 | 3 | II | 6932.41 | 2 | ...... | ...... | V |
| 5680.89 | 15 | 8 | 1 | II | 6948.51 | 4 | ...... | ...... | V |
| 5708.85† | 2 | 2 ? | ...... | III ? | 6953.87† | 60 | 10 ? | 1 ? | III ? |
| 5735.68 | 20 | 20 | 2 | II | 6966.49 | 15 | 2 | 1 | III |
| 5797.74 | 25 | 30 | 5 | II | 6990.86 | 50 | 6 | 1 | III |
| 5869.48† | 4 | 2 ? | ...... | IV ? | 6994.39† | 15 | ? | ? | IV ? |
| 5879.77 | 40 | 40 | 8 | II | 7027.41 | 30 | 5 | ...... | III |
| 5885.50 | 8 | 8 | 1 | II | 7057.39 | 3 | ...... | ...... | V |
| 5901.03† | 2 | 2 ? | ...... | III | 7057.99 | 1 | ...... | ...... | V |
| 5925.12† | 12 | 4 ? | 1 ? | III ? | 7087.36 | 20 | 5 | ...... | III |
| 5935.15 | 10 | 12 | 3 | II | 7089.51 | 1 | ...... | ...... | V |
| 5955.34 | 12 | 15 | 3 | II | 7094.63 | 3 | 1 | ...... | IV |
| 5984.22 | 5 | ...... | ...... | V | 7095.67 | 5 | ...... | ...... | V |
| 6032.60† | 5 | 2 ? | ...... | IV ? | 7097.79 | 150 | 30 | 5 | II |
| 6045.88† | 4 | ? | ? | IV ? | 7102.95 | 80 | 25 | 4 | II |
| 6049.24† | 3 | 1 ? | ...... | IV ? | 7103.77† | 40 | —? | —? | II ? |
| 6062.88 | 12 | 10 | 2 | II | 7111.71 | 20 | 5 | 1 | II |
| 6121.87† | 3 | ? | ...... | IV ? | 7112.83† | 4 | ? | ? | IV ? |
| 6121.96† | 20 | 15 | ? | II ? | 7113.55 | 1 | ...... | ...... | V |
| 6124.87† | 5 | 5 ? | ...... | III ? | 7169.15 | 150 | 50 | 20 | II |
| 6127.49 | 200 | 200 | 50 | II | 7201.68 | 4 | ...... | ...... | V |
| 6134.59 | 125 | 125 | 30 | II | 7261.80 | 4 | ...... | ...... | V |
| 6140.59 | 15 | 10 | 3 | II | 7306.24 | 1 | ...... | ...... | V |
| 6143.23 | 150 | 150 | 40 | II | 7311.69 | 2 | ...... | ...... | V |
| 6157.75† | 20 | 2 ? | ...... | IV ? | 7313.73 | 2 | ...... | ...... | V |
| 6192.96† | 5 | 5 ? | ? | III ? | 7318.16† | 8 | 3 ? | 1 ? | III ? |
| 6213.07† | 8 | 3 ? | ...... | IV ? | 7336.04 | 4 | 5 | 1 | II |
| 6214.73 | 6 | ...... | ...... | V | 7344.00† | 4 | —? | ? | III ? |
| 6257.28 | 8 | ...... | ...... | V | 7373.52 | 1 | ...... | ...... | V |
| 6299.73† | 12 | —? | —? | V ? | 7383.66 | 1 | ...... | ...... | V |
| 6313.05† | 50 | —? | ...... | V | 7400.90 | tr | ...... | ...... | V |
| 6321.38 | 2 | ...... | ...... | V | 7439.89 | 10 | 5 | ...... | III |
| 6340.39 | 1 | ...... | ...... | V | 7467.59† | 1 | ? | ...... | V ? |
| 6345.23† | 8 | 5 ? | ...... | IV ? | 7502.91 | 1 | ...... | ...... | V |
| 6346.54 | 2 | ...... | ...... | V E | 7515.80 | 1 | ...... | ...... | V |
| 6407.04 | 4 | ...... | ...... | V | 7540.66 | 1 | ...... | ...... | V |
| 6434.44 | 1 | ...... | ...... | V | 7544.62 | 1 | ...... | ...... | V |
| 6445.75 | 10 | 3 | ...... | IV | 7551.50 | 2 | ...... | ...... | V |
| 6457.55 | 1 | ...... | ...... | V | 7554.73 | 5 | 3 | ...... | III |
| 6470.25 | 15 | 2 | ...... | IV | 7558.47 | 2 | ...... | ...... | V |
| 6489.08 | 25 | 3 | ...... | IV | 7607.19 | 8 | 3 | ...... | III |
| 6493.13† | 1 | —? | ...... | V ? | 7621.17 | 1 | ...... | ...... | V |
| 6503.31† | 5 | 2 ? | ...... | IV ? | 7658.63† | 3 | ? | ...... | IV ? |
| 6506.35† | 6 | 3 ? | ...... | IV ? | 7690.82† | 1 | ? | ...... | V ? |
| 6550.54 | 3 | ...... | ...... | V | 7819.36 | 5 | ...... | ...... | V |
| 6569.43 | 1 | ...... | ...... | V | 7822.97 | 2 | ...... | ...... | V |
| 6576.58 | 1 | ...... | ...... | V | 7826.76 | 2 | ...... | ...... | V |
| 6592.02 | 4 | ...... | ...... | V | 7849.39 | 5 | 3 | ...... | III |
| 6603.27 | 4 | ...... | ...... | V | 7870.01† | 4 | 4 ? | ...... | III |
| 6620.64 | 1 | ...... | ...... | V | 7944.65 | 6 | ...... | ...... | V |
| 6688.19 | 2 | ...... | ...... | V | 7956.69† | 2 | ? | ...... | IV |
| 6702.14 | 1 | ...... | ...... | V | 7960.02 | 2 | ...... | ...... | V |
| 6709.62† | 2 | 2 ? | ...... | IV ? | 8063.11 | 3 | ...... | ...... | V |
| 6717.90† | 3 | 3 ? | 1 ? | III ? | 8070.12 | 20 | 5 | ...... | III |
| 6752.73 | 4 | ...... | ...... | V | 8133.00 | 15 | 5 | ...... | III |
| 6762.39 | 30 | 8 | 1 | III | 8194.67 | 20 | ...... | ...... | V |
| 6769.17 | 40 | 2 | ...... | V | 8194.91 | | ...... | ...... | V |
| 6772.94 | 3 | ...... | ...... | V | 8212.59† | 10 | 4 ? | ...... | III ? |
| 6790.99 | 4 | ...... | ...... | V | 8305.94† | 8 | 2 ? | ...... | III ? |
| 6825.85 | 10 | ...... | ...... | V | | | | | |

TABLE II—*Continued*

NOTES—ZIRCONIUM

| | |
|---|---|
| 2827.55 | Double. Blend with enhanced line. |
| 3063.59 | Enhanced line on red side. |
| 3092.29 | In wing of *Al* line in arc. |
| 3093.34 | |
| 3250.39 | Blend enhanced line. |
| 3414.66 | Blend enhanced line. |
| 3471.19 | Blend enhanced line. |
| 3879.05 | Unusual type. Possibly impurity. |
| 3984.75 | Blend enhanced line. |
| 4030.75 | Blend *Mn*. |
| 4035.89 | Enhanced line on violet side. |
| 4068.73 | Blend with enhanced line λ 4068.63. |
| 4241.20 | Strong line shows here at low temperature, probably due to blend with low-temperature line of unknown origin. |
| 4395.20 | Blend *V* in furnace. |
| 4494.93 | May be impurity. |
| 4683.42 | Faint if present in furnace. |
| 4751.91 | May be band head in furnace. |

lanthanum, respectively. Very faint lines which appear only in the arc are usually not included, unless they have about the same intensity as neighboring lines which appear also in the furnace, so that a comparison may be useful on this account. Enhanced lines are listed when they are of fair intensity in the arc, since many of the enhanced lines of yttrium and lanthanum appear in the furnace, and those which are absent are of interest as requiring a higher excitation than that of the furnace. The case is different with zirconium, where a large proportion of the arc spectrum consists of enhanced lines, very few of which appear in the furnace. To avoid unnecessary length in the furnace tables, these zirconium enhanced lines, with their arc intensities, are listed in Table III. Those which by reason of their presence in the furnace spectrum are classified in Table II are indicated by "f" after the wave-length. Lines not so indicated may be considered as belonging in class VE.

*Wave-lengths.*—The international system is used throughout. Wave-lengths shorter than λ 5500 for yttrium are taken largely from Exner and Haschek,[1] changed to I.A. Use was also made of the tables of Yntema and Hopkins,[2] and of Eder.[3] Zirconium wave-lengths for the same region are chiefly reduced from Vahle,[4] and those of lanthanum from Wolff.[5] Wave-lengths greater than λ 5500

---

[1] *Spektren der Elemente bei normalem Druck*, Leipzig, 1911.

[2] *Journal of the Optical Society of America*, **6**, 121, 1922.

[3] *Sitzungsberichte der Akademie der Wissenschaften in Wien*, II*a*, **125**, 471, 1916.

[4] *Zeitschrift für wissenschaftliche Photographie*, **18**, 84, 1918.

[5] *Ibid.*, **3**, 395, 1905.

## TABLE III

### Zirconium Enhanced Lines

| λ | Arc. Int. | λ | Arc. Int. | λ | Arc. Int. | λ | Arc. Int. |
|---|---|---|---|---|---|---|---|
| 2630.87 | 40 | 2910.25 | 8 | 3165.47 | 10 | 3399.80 | 1 |
| 2639.09 | 30 | 2915.99 | 40 | 3165.98f | 80 | 3402.88 | 6 |
| 2643.41 | 4 | 2916.63 | 8 | 3166.27 | 12 | 3403.69 | 10 |
| 2650.38 | 8 | 2918.26 | 30 | 3178.05 | 10 | 3404.84 | 50 |
| 2667.80 | 20 | 2924.64 | 2 | 3181.56 | 10 | 3408.06 | 8 |
| 2669.46 | 4 | 2925.63 | 2 | 3181.97 | 10 | 3410.27 | 60 |
| 2678.62 | 150 | 2926.99 | 20 | 3182.88 | 60 | 3413.36 | 4 |
| 2681.76 | 2 | 2934.60 | 20 | 3191.91f | 10 | 3414.66* | 6 |
| 2689.45 | 5 | 2936.30 | 20 | 3208.29 | 4 | 3419.10 | 6 |
| 2692.63 | 5 | 2937.74 | 1 | 3212.83 | 8 | 3424.81 | 10 |
| 2693.55 | 30 | 2945.45 | 3 | 3214.18 | 60 | 3430.53f | 50 |
| 2694.06 | 20 | 2948.96 | 20 | 3222.52 | 5 | 3431.60 | 5 |
| 2695.45 | 3 | 2951.48 | 25 | 3228.82 | 15 | 3432.42 | 5 |
| 2699.61 | 15 | 2952.24 | 8 | 3231.70f | 70 | 3433.91 | 4 |
| 2700.12 | 100 | 2955.78 | 15 | 3241.05f | 40 | 3437.13 | 20 |
| 2711.50 | 50 | 2962.70 | 30 | 3242.16 | 2 | 3438.24f | 400 |
| 2712.41 | 25 | 2964.56 | 1 | 3250.41 | 35 | 3443.58 | 3 |
| 2714.25 | 20 | 2968.96 | 30 | 3264.84 | 4 | 3454.56 | 3 |
| 2720.34 | 2 | 2969.64 | 20 | 3271.13 | 8 | 3457.56 | 30 |
| 2722.59 | 150 | 2976.61 | 8 | 3272.22f | 40 | 3458.93 | 10 |
| 2726.50 | 125 | 2978.06 | 40 | 3273.05f | 150 | 3463.01 | 30 |
| 2732.70 | 80 | 2979.18 | 20 | 3275.16 | 2 | 3469.95 | 2 |
| 2734.82 | 150 | 2980.85 | 25 | 3279.27f | 125 | 3471.18 | 100 |
| 2740.36 | 4 | 2987.75 | 40 | 3281.71 | 2 | 3478.30 | 5 |
| 2740.50 | 8 | 2990.14 | 1 | 3282.84 | 4 | 3478.49 | 2 |
| 2741.55 | 15 | 2991.43 | 5 | 3284.72f | 80 | 3479.02 | 10 |
| 2742.55 | 125 | 2998.18 | 1 | 3285.89 | 2 | 3479.39 | 60 |
| 2745.87 | 100 | 3003.76 | 20 | 3287.26 | 2 | 3480.40 | 5 |
| 2750.95 | 3 | 3009.89 | 2 | 3288.79 | 8 | 3481.15 | 80 |
| 2752.22 | 150 | 3012.89 | 1 | 3296.41 | 4 | 3483.53 | 30 |
| 2754.23 | 2 | 3013.33 | 8 | 3302.67 | 4 | 3496.23 | 200 |
| 2758.82 | 80 | 3019.84 | 15 | 3305.15f | 40 | 3499.59 | 6 |
| 2761.91 | 5 | 3020.47 | 30 ? | 3306.27 | 80 | 3505.51 | 10 |
| 2765.76 | 25 | 3025.17 | 1 | 3309.93 | 2 | 3505.68 | 20 |
| 2774.17 | 15 | 3025.61 | 1 | 3311.39 | 4 | 3510.45 | 4 |
| 2783.57 | 4 | 3028.05 | 20 | 3313.71 | 8 | 3525.80 | 10 |
| 2796.91 | 12 | 3030.92 | 15 | 3314.50f | 12 | 3542.60 | 10 |
| 2799.15 | 5 | 3036.39 | 10 | 3318.53 | 6 | 3551.97 | 40 |
| 2808.17 | 2 | 3036.48 | 5 | 3319.04 | 15 | 3556.60 | 60 |
| 2810.94 | 15 | 3044.11 | 1 | 3323.00f | 20 | 3572.45 | 100 |
| 2815.74 | 20 | 3048.26 | 1 | 3326.81 | 10 | 3573.09 | 8 |
| 2825.58 | 30 | 3048.39 | 1 | 3334.24 | 15 | 3576.80 | 40 |
| 2827.54* | 8 | 3052.83 | 2 | 3334.61 | 15 | 3578.21 | 4 |
| 2833.94 | 6 | 3054.86 | 20 | 3337.93 | 1 | 3587.92 | 10 |
| 2834.43 | 3 | 3057.03 | 20 | 3338.41 | 12 | 3607.35 | 5 |
| 2838.04 | 4 | 3057.22 | 2 ? | 3340.58 | 50 | 3611.90 | 8 |
| 2839.35 | 8 | 3060.12 | 4 | 3344.81 | 15 | 3613.11 | 40 |
| 2843.52 | 10 | 3061.34 | 4 | 3354.41 | 10 | 3614.77 | 40 |
| 2844.58 | 50 | 3064.73 | 3 | 3356.09f | 60 | 3630.05 | 10 |
| 2848.16 | 15 | 3065.22 | 3 | 3357.27f | 50 | 3636.42 | 5 |
| 2851.99 | 40 | 3086.45 | 1 | 3360.00 | 10 | 3668.40 | 5 |
| 2854.44 | 3 | 3089.02 | 1 | 3362.73 | 4 | 3671.25 | 10 |
| 2856.07 | 1 | 3095.10 | 25 | 3363.85 | 8 | 3674.69 | 40 |
| 2865.10 | 2 | 3099.27 | 25 | 3367.84 | 7 | 3697.48 | 10 |
| 2865.62 | 8 | 3106.60 | 40 | 3369.30 | 2 | 3698.17 | 40 |
| 2869.82 | 40 | 3110.88 | 20 | 3373.43 | 15 | 3709.26 | 30 |
| 2872.54 | 2 | 3111.18 | 3 | 3374.73 | 30 | 3714.77 | 6 |
| 2877.54 | 10 | 3115.73 | 1 | 3376.28 | 8 | 3731.25 | 10 |
| 2882.11 | 3 | 3125.22 | 5 | 3377.43 | 10 | 3751.64 | 30 |
| 2885.81 | 3 | 3125.92f | 40 | 3378.33 | 4 | 3766.82 | 30 |
| 2888.04 | 6 | 3128.82 | 1 | 3382.92 | 3 | 3915.95 | 15 |
| 2889.42 | 3 | 3129.20 | 25 | 3387.87f | 40 | 3934.12 | 15 |
| 2898.73 | 12 | 3129.77f | 40 | 3388.30f | 80 | 3934.78 | 10 |
| 2901.64 | 4 | 3133.49 | 20 | 3391.98f | 400 | 3936.06 | 2 |
| 2901.84 | 6 | 3134.72 | 1 | 3393.12f | 25 | 3958.19 | 25 |
| 2902.29 | 1 | 3138.68f | 50 | 3394.56 | 2 | 3984.72 | 20 |
| 2904.31 | 1 | 3155.67 | 20 | 3396.34 | 8 | 3991.10 | 30 |
| 2905.24 | 25 | 3157.00 | 15 | 3396.64 | 2 | 3998.94 | 20 |
| 2907.40 | 5 | 3164.32 | 25 | 3399.36 | 40 | 4018.10 | 10 |

* Blend arc line.

TABLE III—*Continued*

| λ | Arc. Int. | λ | Arc. Int. | λ | Arc. Int. | λ | Arc. Int. |
|---|---|---|---|---|---|---|---|
| 4018.35 | 4 | 4208.97 | 20 | 4317.32 | 3 | 4494.42 | 2 |
| 4023.30 | 2 | 4211.90 | 10 | 4333.29 | 1 | 4495.48 | 1 |
| 4024.42 | 5 | 4224.25 | 2 | 4337.64 | 1 | 4496.96 | 15 |
| 4029.66 | 15 | 4230.17 | 1 | 4339.54 | 1 | 4553.96 | 1 |
| 4034.09 | 2 | 4231.63 | 2 | 4342.24 | 1 | 4574.48 | 1 |
| 4040.25 | 2 | 4236.55 | 3 | 4345.55 | 1 | 4613.98 | 2 |
| 4045.63 | 10 | 4258.06 | 10 | 4359.74 | 8 | 4629.07 | 1 |
| 4048.65 | 15 | 4264.89 | 1 | 4370.97 | 6 | 4661.81 | 1 |
| 4050.36 | 15 | 4266.74 | 5 | 4379.74 | 8 | 4685.22 | 1 |
| 4071.10 | 2 | 4273.53 | 2 | 4403.33 | 3 | 4703.07 | 1 |
| 4085.68 | 5 | 4277.36 | 1 | 4414.53 | 5 | 5112.27 | 5 |
| 4090.54 | 5 | 4286.51 | 1 | 4440.43 | 5 | 5191.58 | 15 |
| 4096.62 | 2 | 4293.15 | 1 | 4442.50 | 1 | 5311.76 | 1 |
| 4149.20 | 50 | 4296.76 | 1 | 4443.00 | 12 | 5350.07 | 6 |
| 4151.02 | 8 | 4301.84 | 1 | 4454.80 | 8 | 5350.34 | 6 |
| 4156.24 | 15 | 4308.95 | 1 | 4457.41 | 10 | | |
| 4161.24 | 15 | 4312.24 | 1 | 4461.20 | 5 | | |

are those of Kiess,[1] who kindly furnished an advance list of zirconium wave-lengths to supplement those published for yttrium and lanthanum.

*Intensities and classes.*—The intensity estimates are in accordance with the procedure followed in previous papers, a line distinctly outlined in the negative being given intensity "1." The large range of line-intensities found in these spectra requires high values for many of the stronger lines, and it is doubtful if high enough values have been assigned to some of the strongest. The relative strength of the ionized lines with respect to those of the neutral atom is controlled by arc conditions which vary for different exposures, so that a fair degree of consistency among the line-intensities for each set is all that can be attained.

*Classes.*—In the final column, the usual method of classification is followed. Lines in classes I and II appear at low temperature. Those of class I show a slower change from low to high temperature than those of class II, and as a rule are less conspicuous in the arc. Lines of class III are usually well developed at medium temperature, while lines clearly associated with high temperatures are placed in classes IV and V, those of class V being absent or very faint in the furnace spectrum.

For zirconium the initial temperature required for the appearance of lines in the furnace is so high that only two stages could be

---

[1] *Scientific Papers of the Bureau of Standards*, **17**, 317 (No. 421), 1921.

## TABLE IV

### TEMPERATURE CLASSIFICATION OF LANTHANUM LINES

| λ (I.A.) | Arc Int. | Furnace Intensities | | | Class |
|---|---|---|---|---|---|
| | | High Temp. | Medium Temp. | Low Temp. | |
| 2798.54 | 1 | ...... | ...... | ...... | V E |
| 2808.36 | 10 | ...... | ...... | ...... | V E |
| 2855.89 | 1 | ...... | ...... | ...... | V E |
| 2862.95 | 1 | ...... | ...... | ...... | V E |
| 2880.63 | 3 | ...... | ...... | ...... | V E |
| 2885.14 | 4 | ...... | ...... | ...... | V E |
| 2893.08 | 4 | ...... | ...... | ...... | V E |
| 2950.51 | 2 | ...... | ...... | ...... | V E |
| 3010.80* | 2 | 8 | ...... | ...... | IV A |
| 3096.00 | 10 | 20 | 5 | 4 | II A |
| 3104.58 | 60 | 10 | ...... | ...... | IV E |
| 3108.45 | 5 | 1 | ...... | ...... | IV E |
| 3109.42 | 12 | 50 | 6 | 2 | II A |
| 3142.75 | 50 | 8 | ...... | ...... | IV E |
| 3148.52 | 4 | 20 | 3 | tr | III A |
| 3171.66* | ...... | ...... | ...... | ...... | V E |
| 3175.96 | 15 | 50 | 5 | 2 | II A |
| 3179.76 | 8 | 30 | 4 | tr | III A |
| 3193.00* | 15 ? | 3 ? | ...... | ...... | IV E |
| | 10 ? | 2 ? | ...... | ...... | IV E |
| 3215.80 | 15 | 50 | 10 | 3 | II A |
| 3235.63 | 5 | 30 | 5 | ...... | III A |
| 3245.12 | 200 | 40 | 6 | ...... | III E |
| 3247.03 | 8 | 20 | 8 | 2 | II A |
| 3249.35 | 100 | 20 | 6 | ...... | III E |
| 3265.65d | 150 | 50 | 15 | ...... | III E |
| 3303.10d | 200 | 70 | 20 | ...... | III E |
| 3306.98 | 10 | 1 | ...... | ...... | IV E |
| 3337.47 | 500 | 50 | 15 | ...... | III E |
| 3342.22 | 20 | 50 | 15 | 6 | II A |
| 3344.54 | 300 | 30 | 10 | ...... | III E |
| 3349.81 | 3 | 15 | 4 | ...... | III A |
| 3357.46 | 7 | 20 | 10 | 1 | III A |
| 3362.03 | 12 | 25 | 12 | 2 | III A |
| 3376.31 | 40 | 8 | 2 | ...... | III E |
| 3380.88 | 400 | 50 | 20 | ...... | III E |
| 3381.42 | 15 | 30 | 10 | 3 | II A |
| 3388.60 | 12 | 20 | 8 | 2 | II A |
| 3397.74 | 4 | ...... | ...... | ...... | V E |
| 3404.51 | 15 | 30 | 10 | 2 | III A |
| 3450.65 | 12 | 30 | 10 | 1 | III A |
| 3452.20d | 50 | 10 | 3 | ...... | III E |
| 3453.16* | 70 | 8 | 2 | ...... | III E |
| 3461.18 | 25 | 50 | 20 | 2 | III A |
| 3480.60 | 8 | 30 | 10 | 1 | III A |
| 3509.98 | 25 | 4 | ...... | ...... | IV E |
| 3512.91 | 25 | 3 | ...... | ...... | IV E |
| 3514.06 | 20 | 40 | 15 | 5 | II A |
| 3517.11* | ...... | ...... | ...... | ...... | V E |
| 3530.66† | 20 | — ? | ...... | ...... | V (?) E |
| 3550.81† | 15 | 10 ? | ...... | ...... | IV (?) E |
| 3557.25† | 20 | 5 ? | ...... | ...... | IV (?) E |
| 3574.41* | 50 | ? | 20 | 10 | II |
| 3593.29 | 2 | ...... | ...... | ...... | V E |
| 3601.05 | 15 | 1 | ...... | ...... | V E |
| 3612.35 | 8 | ...... | ...... | ...... | V E |
| 3613.10 | 30 | 30r | 10 | 5 | II |
| 3621.74 | 4 | ...... | ...... | ...... | V E |
| 3628.83 | 125 | 8 | 1 | ...... | IV E |
| 3636.67 | 40 | 25 | 10 | 1 | III |
| 3637.15d | 50 | 1 | ...... | ...... | V E |
| 3641.53* | 100 | 50r | 15 | 8 | II |
| 3645.41 | 400 | 15 | 2 | ...... | IV E |
| 3649.51 | 40 | 30r | 8 | 5 | II |
| 3650.18 | 125 | 12 | 1 | ...... | IV E |
| 3662.07 | 50 | 5 | ...... | ...... | IV E |
| 3672.01 | 30 | 25 | 10 | 2 | III |
| 3699.53 | 12 | 20 | 8 | ...... | III A |
| 3701.80 | 4 | ...... | ...... | ...... | V E |
| 3704.51 | 40 | 30 | 10 | 5 | II |
| 3705.82d | 125 | 2 | ...... | ...... | V E |
| 3713.55 | 300 | 20 | 1 | ...... | IV E |
| 3714.86 | 60 | 2 | ...... | ...... | V E |
| 3715.53 | 80 | 8 | tr | ...... | IV E |
| 3724.77 | 2 | ...... | ...... | ...... | V |
| 3725.05 | 40 | 4 | ...... | ...... | IV E |
| 3735.84 | 20 | 2 | ...... | ...... | IV E |
| 3759.08 | 600 | 25 | 8 | ...... | III E |
| 3780.67 | 50 | 1 | ...... | ...... | V E |
| 3784.80 | 20 | 1 | ...... | ...... | V E |
| 3790.82 | 600 | 25 | 10 | ...... | III E |
| 3794.78 | 600 | 20 | 8 | ...... | III E |
| 3835.09 | 20 | ...... | ...... | ...... | V E |
| 3840.68† | 50 | ? | ...... | ...... | V (?) E |
| 3846.00† | 20 | ? | — ? | ...... | V (?) E |
| 3849.02† | 200 | ? | ? | ...... | III (?) E |
| 3871.61† | 300 | 10 ? | 6 ? | ...... | III (?) E |
| 3886.31 | 400 | 12 | 4 | ...... | III E |
| 3895.65* | 8 ? | 2 ? | ...... | ...... | IV |
| 3898.59 | 40 | 25 | 20 | 10 | II |
| 3902.57 | 20 | 20 | 20 | 6 | II |
| 3910.80* | 15 | 2 ? | ...... | ...... | IV (?) E |
| 3916.04d | 400 | 30 | 5 | ...... | III E |
| 3921.53 | 300 | 30 | 4 | ...... | III E |
| 3927.56 | 80 | 60r | 40 | 40 | I |
| 3929.21 | 500 | 40 | 8 | ...... | III E |
| 3936.22 | 60 | 8 | 1 | ...... | IV E |
| 3949.09d | 1000 | 60 | 15 | ...... | III E |
| 3953.68 | 40 | 30 | 25 | 10 | II |
| 3988.52d | 800 | 40 | 8 | ...... | III E |
| 3995.76 | 600 | 40 | 8 | ...... | III E |
| 4015.41 | 50 | 50r | 40 | 40 | I |
| 4023.58d | 15 | 2 | ...... | ...... | IV E |
| 4025.89 | 40 | 5 | ...... | ...... | IV E |
| 4031.70 | 300 | 20 | 5 | ...... | III E |
| 4036.60 | 8 | ...... | ...... | ...... | V E |
| 4037.22 | 50 | 60r | 50 | 50 | I |
| 4042.92 | 300 | 15 | 2 | ...... | IV E |
| 4050.09 | 60 | ...... | ...... | ...... | V E |
| 4060.33 | 60 | 40r | 40 | 20 | II |
| 4064.79 | 50 | 30 | 30 | 15 | II |
| 4065.58 | 30 | 25 | 25 | 12 | II |
| 4067.40 | 125 | 12 | 1 | ...... | IV E |
| 4076.70 | 30 | 3 | ...... | ...... | IV E |
| 4077.34d | 400 | 40 | 8 | ...... | III E |
| 4079.18 | 40 | 40r | 40 | 35 | I |
| 4086.72 | 400 | 25 | 15 | 1 | III E |
| 4089.62 | 50 | 35 | 35 | 20 | I |
| 4099.55 | 60 | ...... | ...... | ...... | V E |
| 4104.88 | 60 | 30 | 30 | 25 | I |
| 4109.49 | 15 | 30 | 25 | 5 | II A |
| 4109.82 | 20 | 40 | 30 | 20 | I A |
| 4117.69 | 20 | 20 | 5 | ...... | III |
| 4123.23 | 600 | 25 | 10 | ...... | III E |
| 4137.03 | 40 | 40 | 40 | 35 | I |

TABLE IV—*Continued*

| λ (I.A.) | Arc Int. | Furnace Intensities | | | Class | λ (I.A.) | Arc Int. | Furnace Intensities | | | Class |
|---|---|---|---|---|---|---|---|---|---|---|---|
| | | High Temp. | Medium Temp. | Low Temp. | | | | High Temp. | Medium Temp. | Low Temp. | |
| 4141.72d.. | 80 ?<br>40 ? | 8 | ...... | ...... | IV E | 4443.95d.. | 10 | 15 | 10 | 8 | I |
| | | | | | | 4445.12... | 2 | 4 | 2 | ...... | III A |
| 4143.95*.. | 12 | 25 | 15 | 3 | III A | 4452.17... | 30 | 20 | 15 | 5 | II |
| 4151.95d.. | 300 | 20 | 4 | ...... | III E | 4453.85... | 2 | 6 | ...... | ...... | IV A |
| 4152.76†.. | 40 | 2 ? | ...... | ...... | IV (?) E | 4455.23... | 10 | 20 | 15 | 8 | II A |
| 4157.49... | 10 | 20 | 20 | 8 | II A | 4455.82... | 25 | 1 | ...... | ...... | V E |
| 4160.25... | 30 | 30 | 25 | 20 | I | 4468.97... | 25 | 30 | 25 | 10 | II |
| 4163.30... | 8 | 25 | 20 | 2 | III A | 4474.55... | 5 | 10 | 3 | ...... | III A |
| 4171.10... | 8 | 20 | 10 | 1 | III A | 4479.82d.. | 15 | 30 | 30 | 10 | II A |
| 4172.31... | 10 | 20 | 15 | 2 | III A | 4486.07... | 20 | 20 | 6 | 2 | III |
| 4177.47... | 30 | 30 | 25 | 20 | I | 4491.78d.. | 15 | 20 | 6 | 1 | III |
| 4187.31... | 125 | 125R | 100 | 100 | I | 4493.14... | 25 | 30 | 25 | 20 | I |
| 4192.35d.. | 80 | ...... | ...... | ...... | V E | 4493.82... | 10 | 20 | 10 | 8 | I A |
| 4196.55... | 300 | 15 | 6 | ...... | III E | 4494.70... | 30 | 25 | 20 | 15 | I |
| 4204.04... | 100 | 2 | ...... | ...... | V E | 4499.07d.. | 10 | 15 | 5 | ...... | III |
| 4217.56d.. | 80 | ...... | ...... | ...... | V E | 4500.24... | 40 | 30 | 20 | 6 | II |
| 4230.96... | 30 | ...... | ...... | ...... | V E | 4501.59... | 10 | 20 | 8 | 4 | II A |
| 4238.40d.. | 400 | 30 | 4 | ...... | III E | 4522.38... | 500 | 10 | 3 | ...... | III E |
| 4238.61*.. | 10 | 20 | 15 | 3 | III A | 4525.31d.. | 20 | ...... | ...... | ...... | V E |
| 4250.01d.. | 25 | ...... | ...... | ...... | V E | 4526.12... | 200 | 6 | 2 | ...... | III E |
| 4256.93... | 6 | 20 | 8 | ...... | III A | 4530.59... | 2 | ...... | ...... | ...... | V E |
| 4262.35... | 15 | 30 | 30 | 10 | II A | 4541.78d.. | 15 | 15 | 8 | 2 | III |
| 4263.59d.. | 100 | ...... | ...... | ...... | V E | 4549.51... | 50 | 20 | 20 | 20 | I |
| 4269.50d.. | 150 | 1 | ...... | ...... | V E | 4550.16... | 5 | 10 | 6 | 2 | III A |
| 4275.64... | 60 | 8 | 1 | ...... | IV E | 4550.78d.. | 10 | 20 | 6 | 1 | III A |
| 4280.27... | 100 | 100R | 80 | 80 | I | 4552.50... | 8 | 15 | 5 | 2 | II A |
| 4286.98d.. | 150 | tr | ...... | ...... | V E | 4558.47... | 250 | 12 | 3 | ...... | III E |
| 4296.05... | 200 | 15 | 1 | ...... | IV E | 4559.29... | 50 | 1 | ...... | ...... | V E |
| 4300.45... | 30 | 6 | tr | ...... | IV E | 4564.84... | 12 | 20 | 15 | 4 | III |
| 4306.00... | 6 | 20 | 8 | 4 | II A | 4567.92... | 200 | 50 | 50 | 50 | I |
| 4311.74d.. | 4 | 15 | 6 | tr | III A | 4570.03... | 250 | 60 | 60 | 60 | I |
| 4315.91d.. | 12 | tr | ...... | ...... | V E | 4570.96... | 8 | ...... | ...... | ...... | V E |
| 4322.51... | 150 | 15 | 5 | ...... | III E | 4574.89d.. | 300 | 10 | 4 | ...... | III E |
| 4333.77... | 600 | 30 | 20 | 1 | III E | 4580.07... | 100 | 2 | ...... | ...... | V E |
| 4334.98... | 60 | 2 | ...... | ...... | V E | 4581.20d.. | 12 | 12 | 6 | 1 | III |
| 4339.95... | 6 | 20 | 30 | 4 | III A | 4596.17... | 10 | 8 | 10 | 10 | I |
| 4340.74... | 15 | 15 | 15 | tr | III | 4602.03d.. | 20 | 15 | 8 | 1 | III |
| 4354.40... | 80 | 3 | ...... | ...... | IV E | 4604.23... | 10 | 6 | 2 | ...... | III |
| 4354.80... | 25 | 30 | 20 | 2 | III | 4605.09... | 10 | 6 | 2 | ...... | III |
| 4357.92... | 2 | 12 | 4 | ...... | III A | 4605.78... | 50 | ...... | ...... | ...... | V E |
| 4360.48... | 2 | 8 | 2 | ...... | III A | 4613.40*.. | 200 | — ? | ...... | ...... | V E |
| 4360.85... | 2 | 6 | 2 | ...... | III A | 4615.06d.. | 15 | 8 | 3 | 1 | III |
| 4363.07... | 4 | ...... | ...... | ...... | V E | 4619.88... | 150 | ...... | ...... | ...... | V E |
| 4364.68... | 30 | 2 | ...... | ...... | IV E | 4636.42... | 4 | ...... | ...... | ...... | V E |
| 4378.11d.. | 15 | 1 | ...... | ...... | IV E | 4643.12... | 5 | 4 | 2 | ...... | III |
| 4380.55... | 12 | 20 | 30 | 6 | II A | 4645.31... | 40 | ...... | ...... | ...... | V E |
| 4383.46... | 25 | ...... | ...... | ...... | V E | 4646.36... | 12 | 5 | 2 | ...... | III |
| 4385.21... | 20 | ...... | ...... | ...... | V E | 4647.49d.. | 8 | ...... | ...... | ...... | V E |
| 4389.89... | 15 | 10 | 4 | ...... | III | 4648.66... | 40 | 15 | 15 | 15 | I |
| 4393.61d.. | 4 | 3<br>3 | 2 | ...... | III | 4650.35... | 15 | 6 | 6 | 4 | I |
| | | | | | | 4652.11†.. | 20 | 8 ? | 5 | 4 | I |
| 4396.31... | 2 | 1 | ...... | ...... | IV | 4655.53d.. | 150 | ...... | ...... | ...... | V E |
| 4396.79d.. | 4 | 6 | 1 | ...... | IV A | 4660.73... | 8 | 5 | 3 | 1 | III |
| 4397.04... | 2 | 2 | ...... | ...... | IV A | 4662.54... | 200 | 6 | 2 | ...... | III E |
| 4402.66... | 15 | 15 | 8 | 1 | III | 4663.79d.. | 50 | ...... | ...... | ...... | V E |
| 4403.03d?. | 8 | 15 | 8 | 1 | III A | 4668.92*.. | 50 | ...... | ...... | ...... | V E |
| 4411.21... | 2 | ...... | ...... | ...... | V E | 4671.83*.. | 40 | ...... | ...... | ...... | V E |
| 4413.44... | 2 | 6 | 3 | tr | III A | 4688.66... | 2 | ...... | ...... | ...... | V E |
| 4417.11... | 6n | 6 | 3 | tr | III | 4691.16d.. | 30 | ...... | ...... | ...... | V E |
| 4419.16... | 6 | ...... | ...... | ...... | V E | 4692.50d.. | 50 | ...... | ...... | ...... | V E |
| 4423.91... | 30 | 20 | 20 | 4 | II | 4699.62*.. | 20 | ...... | ...... | ...... | V E |
| 4427.58d.. | 40 | ...... | ...... | ...... | V E | 4700.27†d. | 8 | 6 ? | 3 ? | ...... | III ? |
| 4429.89d.. | 500 | 50 | 40 | ...... | III E | 4702.63... | 10 | 8 | 8 | 5 | I |
| 4435.84... | 6 | 2 | ...... | ...... | IV E | 4703.27*.. | 20 | ...... | ...... | ...... | V E |
| 4442.67... | 12 | 15 | 15 | 4 | II | 4708.17†d. | 8 | ? | 2 ? | ...... | III ? |

TABLE IV—*Continued*

| λ (I.A.) | Arc Int. | Furnace Intensities | | | Class | λ (I.A.) | Arc Int. | Furnace Intensities | | | Class |
|---|---|---|---|---|---|---|---|---|---|---|---|
| | | High Temp | Medium Temp. | Low Temp. | | | | High Temp. | Medium Temp. | Low Temp. | |
| 4712.90d.. | 12 | ..... | ...... | ...... | V E | 4968.58... | 2 | ..... | ...... | ...... | V |
| 4714.13... | 5 | 5 | 5 | 4 | I | | | 4 | 1 | ...... | III A |
| 4716.41d.. | 25 | ..... | ...... | ...... | V E | 4970.37... | 100 | 4 | 1 | ...... | III E |
| 4717.56... | 4 | ..... | ...... | ...... | V E | 4977.92... | 8 | 20 | 20 | 5 | II A |
| 4719.90... | 15 | ..... | ...... | ...... | V E | 4984.91†.. | 2 | 1 ? | ...... | ...... | IV ? |
| 4723.68... | 3 | 5 | 4 | 2 | II | 4986.81d.. | 100 | 8 | 2 | ...... | III E |
| 4724.39.. | 6 | ..... | ...... | ...... | V E | 4991.26d.. | 20 | 1 | ...... | ...... | IV E |
| 4728.38†d | 80 | ? | ...... | ...... | V (?) E | 4993.84... | 20 | 25 | 30 | 15 | II |
| 4729.00.. | 1 | ..... | ...... | ...... | V | 4994.64... | 1 | 3 | 1 | ...... | III A |
| 4733.80†d | 4 | — ? | ...... | ...... | V ? | 4996.70*.. | 2 | ..... | ...... | ...... | V E |
| 4739.78.. | 2 | ..... | ...... | ...... | V E | 4999.46*.. | 200 | 10 | 2 | ...... | III E |
| 4740.23.. | 150 | 6 | 3 | ...... | III E | 5001.78d.. | 10 | 20 | 10 | ...... | III A |
| 4743.08d. | 100 | ..... | ...... | ...... | V E | 5002.10*.. | 3 | ..... | ...... | ...... | V E |
| 4748.72... | 100 | 1 | ...... | ...... | V E | 5019.51... | 8 | 4 | 1 | ...... | III |
| 4750.41... | 15 | 8 | 4 | 1 | III | 5046.86d.. | 60 | 30 | 20 | 4 | III |
| 4752.38... | 3 | 3 | 2 | 1 | III | 5048.00... | 1 | ..... | ...... | ...... | V E |
| 4753.13d. | 1 | tr | ...... | ...... | IV | 5050.56... | 80 | 20 | 20 | 10 | II |
| 4756.07... | 1 | ..... | ...... | ...... | V | 5056.45... | 80 | 20 | 20 | 8 | II |
| 4757.10d | 2 | 1 | ...... | ...... | IV | 5062.89... | 4 | ..... | ...... | ...... | V E |
| 4759.71†d | 2 | 2 | ? | ...... | IV? | 5067.86d.. | 15 | 20 | 10 | 1 | III |
| 4766.91... | 100 | 50 | 50 | 60 | I | 5072.12... | 1 | 4 | 2 | ...... | III A |
| 4770.45.. | 15 | 6 | 4 | 2 | II | 5078.94*.. | 2 | ? | ...... | ...... | V ? |
| 4775.10d | 2 | ..... | ...... | ...... | V | 5079.37... | 5 | 2 | tr | ...... | IV |
| 4779.00... | 4 | 5 | 4 | 2 | II | 5080.20*.. | 1 | ..... | ...... | ...... | V E |
| 4780.55d. | 1 | ..... | ...... | ...... | V | 5090.55*.. | tr | ..... | ...... | ...... | V E |
| 4791.39... | 5 | 6 | 8 | 4 | II | 5096.62†.. | 1 | ? | ? | ...... | IV ? |
| 4792.40.. | tr | 2 | 1 | ...... | III A | 5103.13... | 2 | 2 | 1 | ...... | III |
| 4794.57*.. | 2 | ..... | ...... | ...... | V E | 5106.23†d. | 150 | 100 ? | 100 | 50 | II |
| 4796.68... | 4 | ..... | ...... | ...... | V E | 5109.11†.. | 2 | 5 ? | 3 | ...... | III A |
| 4800.00... | 8 | 4 | 3 | tr | III | 5114.55†d | 150 | ? | ? | ...... | III (?) E |
| 4800.25... | 8 | 6 | 5 | 1 | III | 5120.86... | 10 | 5 | 3 | ...... | III |
| 4804.04.. | 50 | 2 | ...... | ...... | V E | 5122.98... | 150 | 3 | 1 | ...... | III E |
| 4809.00.. | 80 | 2 | ...... | ...... | V E | 5135.45... | 2 | ..... | ...... | ...... | V |
| 4817.15*.. | 4 | 4 | ? | ...... | IV ? | 5145.42... | 200 | 125 | 125 | 60 | II |
| 4824.04.. | 80 | 2 | 1 | ...... | III E | 5156.74... | 30 | ..... | ...... | ...... | V E |
| 4826.85... | 4 | ..... | ...... | ...... | V E | 5157.44*.. | 15 | ..... | ...... | ...... | V E |
| 4830.50... | 1 | ..... | ...... | ...... | V E | 5158.69... | 80 | 60 ? | 60 | 50 | I |
| 4839.51... | 25 | 10 | 10 | 6 | II | 5163.62†.. | 20 | ? | ...... | ...... | V (?) E |
| 4840.00... | 10 | ..... | ...... | ...... | V E | 5164.03†.. | 1 | —? | ...... | ...... | V ? |
| 4843.27... | 1 | ..... | ...... | ...... | V | 5167.78... | 20 | 10 | 10 | 2 | III |
| 4850.56... | 5 | ..... | ...... | ...... | V E | 5172.90*.. | 1 | ..... | ...... | ...... | V E |
| 4850.80.. | 20 | 20 | 20 | 30 | I | 5173.85*.. | 10 | ? | ? | ...... | IV (?) E |
| 4854.93... | 8 | 6 | 6 | 1 | III | 5177.30d.. | 300 | 200 | 200 | 100 | II |
| 4860.88... | 100 | 6 | 3 | ...... | III E | 5179.11... | 2 | 2 | 1 | ...... | III |
| 4868.90†. | 2 | 2 ? | ...... | ...... | IV ? | 5183.41*.. | 400 | 5 | 2 | ...... | III E |
| 4870.55.. | 5 | 5 | 4 | 1 | III | 5183.89... | 20 | 20 | 20 | 10 | II |
| 4878.84.. | 15 | 10 | 10 | 2 | III | 5188.20*.. | 25 | ..... | ...... | ...... | V E |
| 4886.81... | 2 | 2 ? | ...... | ...... | IV | 5204.15*.. | 12 | ..... | ...... | ...... | V E |
| 4887.60... | 5 | 8 | 4 | tr | III | 5211.87d.. | 300 | 250 | 250 | 60 | II |
| 4894.23... | 1 | 1 | tr | ...... | III | 5226.19*.. | 1 | ..... | ...... | ...... | V E |
| 4899.91... | 300 | 20 | 10 | ...... | III E | 5234.28d.. | 300 | 250 | 250 | 50 | II |
| 4901.86... | 25 | 30 | 20 | 20 | I | 5239.55... | 4 | 4 | 3 | ...... | III |
| 4905.11... | 4 | 8 | 4 | tr | III A | 5240.81... | 2 | tr | tr | ...... | III |
| 4916.60†.. | 1 | 2 | ? | ...... | III (?) A | 5253.45... | 100 | 50 | 50 | 50 | I |
| 4920.95... | 400 | 15 | 12 | ...... | III E | 5257.85... | 3 | 1 | tr | ...... | III |
| 4921.77.. | 400 | 15 | 10 | ...... | III E | 5259.38... | 40 | 1 | tr | ...... | III E |
| 4925.37.. | 2 | 2 | ...... | ...... | IV | 5271.19... | 150 | 100 | 100 | 80 | I |
| 4934.82... | 20 | 1 | ...... | ...... | V E | 5276.42... | 10 | 6 | 5 | ...... | III |
| 4935.59... | 2 | ..... | ...... | ...... | V E | 5279.13... | 2 | ..... | ...... | ...... | V E |
| 4945.82... | 5 | 12 | 7 | ...... | III A | 5287.43... | 1 | ..... | ...... | ...... | V |
| 4946.42*d | 20 | ? | ? | ...... | IV (?) E | 5290.84... | 60 | 2 | 1 | ...... | III E |
| 4949.76... | 200 | 100r | 100 | 100 | I | 5301.98d.. | 200 | 10 | 10 | tr | III E |
| 4952.03*.. | 5 | ..... | ...... | ...... | V E | 5302.63*.. | 40 | ..... | ...... | ...... | V E |
| 4956.05... | 1 | ..... | ...... | ...... | V | 5303.55... | 100 | 1 | 1 | ...... | III E |
| 4964.80... | 4 | 15 | 8 | ...... | III A | 5304.01... | 30 | 10 | 10 | tr | III |

TABLE IV—*Continued*

| λ (I.A.) | Arc Int. | Furnace Intensities | | | Class |
|---|---|---|---|---|---|
| | | High Temp. | Medium Temp. | Low Temp. | |
| 5307.54... | 3 | 1 | tr | ...... | III |
| 5320.16... | 3 | 5 | 5 | tr | III |
| 5323.57... | 3 | 2 | 2 | ...... | III |
| 5340.69*.. | 40 | 8 | 8 | tr | III E |
| 5357.87... | 60 | 15 | 15 | 2 | III |
| 5359.72... | 2 | 5 | 4 | ...... | III A |
| 5365.89... | 8 | 6 | 5 | ...... | III |
| 5377.09*.. | 2 | ...... | ...... | ...... | V E |
| 5380.01... | 5 | 3 | 3 | ...... | III |
| 5380.99.. | 80 | tr | ...... | ...... | V E |
| 5381.90*.. | 15 | ...... | ...... | ...... | V E |
| 5415.66... | 8 | 6 | 4 | ...... | III |
| 5422.10... | 3 | 6 | 4 | tr | III A |
| 5429.91... | 15 | 10 | 8 | 1 | III |
| 5437.54... | 5 | 4 | 3 | ...... | III |
| 5455.13... | 400 | 200 | 200 | 150 | I |
| 5458.67d.. | 20 | ...... | ...... | ...... | V E |
| 5464.36... | 25 | ...... | ...... | ...... | V E |
| 5466.90... | 3 | 5 | 3 | ...... | III |
| 5475.15d.. | 15 | 10 | 6 | tr | III |
| 5480.71... | 1 | ...... | ...... | ...... | V E |
| 5482.26... | 50 | ...... | ...... | ...... | V E |
| 5486.80... | 3 | ...... | ...... | ...... | V |
| 5491.04... | 8 | 8 | 6 | 1 | III |
| 5493.44... | 20 | ...... | ...... | ...... | V E |
| 5498.70... | 2n | 1 | tr | ...... | III |
| 5501.35... | 300 | 150 | 150 | 125 | I |
| 5502.23... | 4 | 2 | 2 | ...... | III |
| 5502.66... | 10 | 10 | 8 | 2 | III |
| 5503.86... | 80 | 40 | 50 | 6 | III |
| 5506.07... | 40 | 50 | 75 | 20 | II |
| 5507.33... | 2 | 1 | 1 | ...... | III |
| 5515.32d.. | 10 | 8 | 8 | tr | III |
| 5517.39d.. | 30 | 8 | 8 | tr | III |
| 5524.40... | 1 | ...... | ...... | ...... | V |
| 5526.51... | 2 | ...... | ...... | ...... | V |
| 5529.90... | 3 | 2 | 2 | ...... | III |
| 5532.07... | 3 | 4 | 4 | 1 | III |
| 5535.67... | 15 | ...... | ...... | ...... | V E |
| 5541.28d.. | 20 | 8 | 8 | 1 | III |
| 5544.92... | 6 | 2 | 2 | ...... | III |
| 5562.54†.. | 2 | 1 | 1 ? | ...... | III ? |
| 5565.40d.. | 20 | 10 | 10 | 1 | III |
| 5565.74... | 20 | 15 | 15 | 5 | II |
| 5566.94*. | 2 | ...... | ...... | ...... | V E |
| 5568.48... | 50 | 30 | 40 | 12 | II |
| 5570.39... | 5 | 12 | 12 | 4 | II A |
| 5588.35... | 80 | 40 | 60 | 20 | II |
| 5631.22... | 100 | 20 | 20 | 20 | I |
| 5632.06... | 25 | 10 | 5 | 2 | II |
| 5639.30d?. | 5 | 10 | 6 | 1 | III A |
| 5648.26d.. | 80 | 80 | 20 | 2 | III |
| 5654.84d.. | 3 | 15 | 4 | 1 | III A |
| 5656.57... | 1 | 12 | 2 | ...... | III A |
| 5657.74d?. | 50 | 60 | 80 | 25 | II |
| 5661.37d.. | 1 | 5 | 2 | ...... | III A |
| 5669.97... | 1 | 1 | ...... | ...... | IV |
| 5671.56... | 8 | ...... | ...... | ...... | V E |
| 5696.19... | 40 | 40 | 40 | 40 | I |
| 5699.38... | 5 | 6 | 6 | 1 | III |
| 5700.25... | 3 | 3 | 3 | ...... | III |
| 5701.15... | 1 | 1 | 1 | ...... | III |
| 5702.57... | 2 | 2 | 2 | ...... | III |
| 5703.29... | 10 | 15 | 15 | 3 | III |
| 5710.81... | 2 | 1 | 1 | ...... | III |
| 5712.41d.. | 20 | 1 | 1 | ...... | III E ? |
| 5714.02... | 5 | 10 | 10 | 1 | III A |
| 5714.55d.. | 1 | 2 | 1 | ...... | III A |
| 5720.03d?. | 10 | 40 | 30 | 4 | III A |
| 5727.30... | 4 | ...... | ...... | ...... | V E |
| 5734.95... | 5 | 10 | 7 | ...... | III A |
| 5740.65... | 100 | 80 | 80 | 80 | I |
| 5742.95d.. | 2 | 8 | 6 | tr | III A |
| 5744.42d.. | 80 | 60 | 40 | 4 | III |
| 5761.84... | 60 | 60 | 60 | 50 | I |
| 5769.07... | 50 | ...... | ...... | ...... | V E |
| 5769.37... | 80 | 80 | 70 | 60 | I |
| 5769.99... | 25 | 70 | 40 | 8 | III A |
| 5789.23d?. | 250 | 200 | 200 | 150 | I |
| 5791.33d?. | 400 | 400 | 400 | 250 | I |
| 5797.59... | 50 | 10 | 3 | ...... | III E |
| 5802.08d . | 1 | 4 | 2 | ...... | III A |
| 5805.77... | 50 | 10 | 3 | ...... | III E |
| 5808.29*.. | 15 | 2 ? | tr ? | ...... | IV ? |
| 5813.39... | 1 | 3 | 1 | ...... | III A |
| 5822.00... | 30 | 50 | 30 | 3 | III |
| 5823.83... | 10 | 30 | 15 | 2 | III A |
| 5827.55d.. | 3 | 10 | 6 | 1 | III A |
| 5829.73d.. | 10 | 50 | 30 | 4 | III A |
| 5839.79... | 2 | 20 | 12 | 5 | II A |
| 5845.02... | 6 | 50 | 50 | 20 | II A |
| 5848.36d . | 8 | 15 | 6 | 1 | III A |
| 5852.27... | 2 | 15 | 6 | 1 | III A |
| 5855.58... | 15 | 40 | 40 | 20 | II A |
| 5863.68... | 20 | tr | ...... | ...... | V E |
| 5869.97... | 1 | 6 | 3 | ...... | III A |
| 5873.99... | 3 | tr | ...... | ...... | IV |
| 5874.73... | 8 | 15 | 12 | 3 | III A |
| 5877.63... | 2 | 15 | 12 | 4 | III A |
| 5877.98... | 1 | 4 | 3 | ...... | III A |
| 5880.62... | 30 | 2 | 1 | ...... | III E ? |
| 5892.66... | 1 | ...... | ...... | ...... | V |
| 5894.83d.. | 8 | 20 | 15 | 3 | III A |
| 5900.72d.. | 1 | 4 | 2 | ...... | III A |
| 5901.96... | 2 | tr | ...... | ...... | IV E |
| 5904.30... | 2 | 10 | 6 | ...... | III A |
| 5917.62... | 15 | 40 | 40 | 25 | II A |
| 5928.50... | 4 | 12 | 6 | 1 | III A |
| 5930.60... | 400 | 400 | 400 | 300 | I |
| 5935.26... | 15 | 40 | 40 | 20 | II A |
| 5936.22... | 12 | 1 | ...... | ...... | V E |
| 5940.84d.. | 1 | 4 | 3 | ...... | III A |
| 5960.58... | 3 | 8 | 5 | tr | III A |
| 5962.58... | 1 | 4 | 2 | ...... | III A |
| 5965.33... | 1 | 1 | 1 | ...... | III |
| 5973.51... | 5 | ...... | ...... | ...... | V E |
| 5975.79d?. | 3 | 12 | 7 | 1 | III A |
| 5982.34... | 5 | 20 | 20 | 6 | III A |
| 5992.38d.. | 2 | 8 | 5 | ...... | III A |
| 6007.37... | 50 | 200 | 150 | 15 | III A |
| 6017.22... | 1 | 4 | 2 | ...... | III A |
| 6025.11†.. | 1 | ? | ...... | ...... | IV ? |
| 6031.49†.. | 3n | ? | ...... | ...... | IV ? |
| 6034.55... | 3 | ...... | ...... | ...... | V |
| 6035.12... | 2 | ...... | ...... | ...... | V |
| 6038.60... | 25 | 50 | 20 | 4 | III A |
| 6041.59... | 2 | 2 | 1 | ...... | III |
| 6044.85... | 2 | 4 | 1 | ...... | III A |
| 6046.05†.. | 1 | 1 ? | ...... | ...... | IV ? |
| 6061.43†.. | 2 | — ? | ...... | ...... | V ? |

TABLE IV—*Continued*

| λ (I.A.) | Arc Int. | Furnace Intensities | | | Class |
|---|---|---|---|---|---|
| | | High Temp. | Medium Temp. | Low Temp. | |
| 6067.15† | 1 | — ? | ...... | ...... | V ? |
| 6068.70d | 30 | 50 | 20 | 4 | III |
| 6072.06 | 4 | 10 | 3 | 1 | III A |
| 6074.01 | 1 | 4 | 1 | ...... | III A |
| 6075.24 | 1 | 4 | 1 | ...... | III A |
| 6084.93 | 8 | 6 | 1 | ...... | III |
| 6085.46 | 1n | ...... | ...... | ...... | V |
| 6087.95 | 1n | 1 | ...... | ...... | IV |
| 6092.27 | 1 | 3 | 1 | ...... | III A |
| 6100.36 | 10 | ...... | ...... | ...... | V |
| 6107.27 | 12 | 60 | 40 | 10 | II A |
| 6108.50 | 60 | 80 | 40 | 8 | II |
| 6111.73 | 30 | 50 | 15 | 5 | II |
| 6120.34 | 1 | 1 | ...... | ...... | IV |
| 6121.27 | 1 | 1 | ...... | ...... | IV |
| 6123.81 | 2 | 1 | ...... | ...... | IV |
| 6126.08† | 10 | — ? | ...... | ...... | V ? |
| 6127.05 | 12 | 40 | 10 | 2 | III A |
| 6129.55† | 15 | 1 ? | ...... | ...... | IV ? |
| 6134.40d | 30 | 50 | 25 | 6 | III |
| 6136.53 | 2 | 6 | 2 | 1 | II A |
| 6143.99d | 10 | 12 | 2 | ...... | III |
| 6145.34 | 3 | 4 | 1 | ...... | III |
| 6146.55 | 5 | 1 | ...... | ...... | IV |
| 6165.04 | 2 | 3 | tr | ...... | IV |
| 6165.72 | 40 | 60 | 40 | 10 | II |
| 6172.73† | 5 | — ? | ...... | ...... | V |
| 6173.74* | 1 | 3 | tr | ...... | IV A |
| 6174.19 | 1 | ...... | ...... | ...... | V |
| 6188.11† | 1 | — ? | ...... | ...... | V |
| 6203.54† | 2 | — ? | ...... | ...... | V |
| 6218.22 | 7 | 10 | 2 | ...... | III |
| 6219.52 | 2 | ...... | ...... | ...... | V |
| 6233.52 | 15 | 50 | 12 | 2 | III A |
| 6234.84d | 15 | 40 | 10 | 2 | III A |
| 6236.23 | 12 | 6 | 1 | ...... | IV |
| 6236.78d | 10 | 25 | 8 | 2 | III A |
| 6238.59 | 15 | 60 | 15 | 2 | III A |
| 6249.92 | 500 | 300 | 500 | 400 | I |
| 6262.30* | 50 ?<br>30 ? | 8 ?<br>4 ? | 2 | ...... | III |
| 6266.03d | 60 | 100 | 20 | 2 | III |
| 6273.78* | 2n | 2 ? | 1 ? | ...... | III ? |
| 6287.75d | 8 | 15 | 3 | tr | III A |
| 6288.58 | 7 | 15 | 3 | ...... | III A |
| 6293.57 | 80 | 200 | 200 | 50 | II A |
| 6296.10 | 50 | 3 | ...... | ...... | IV E |
| 6305.46 | 5 | 5 | 1 | ...... | IV |
| 6307.27 | tr | tr | ...... | ...... | IV |
| 6308.27 | 3 | 4 | 1 | ...... | III |
| 6308.99 | 2 | 3 | ...... | ...... | III |
| 6310.22 | 12 | 10 | ...... | ...... | IV |
| 6310.94 | 4 | ...... | ...... | ...... | V E |
| 6315.82 | 1 | ...... | ...... | ...... | V |
| 6318.29 | 12 | 40 | 10 | 2 | III A |
| 6320.39 | 80 | 20 | 3 | ...... | III |
| 6325.92 | 150 | 100 | 250 | 200 | I |
| 6330.48 | 2 | 10 | 3 | tr | III A |
| 6333.22† | 2 | 1 ? | 1 ? | ...... | III ? |
| 6333.83† | 2 | 2 ? | ...... | ...... | IV ? |
| 6337.92 | 1 | ...... | ...... | ...... | V |
| 6339.25† | 2 | 10 ? | 3 | 1 | III A |
| 6356.44 | 4 | 8 | 2 | ...... | III A |
| 6358.13 | 5 | 1 | ...... | ...... | IV |
| 6360.24 | 30 | 30 | 10 | 4 | II |
| 6374.14 | 1 | ...... | ...... | ...... | V |
| 6375.11 | 2 | ...... | ...... | ...... | V |
| 6380.56 | 1 | ...... | ...... | ...... | V |
| 6390.45 | 80 | 20 | 4 | ...... | III |
| 6394.24 | 600 | 400 | 500 | 500 | I |
| 6299.06† | 10 | — ? | — ? | ...... | V (?) E |
| 6410.98 | 300 | 200 | 250 | 200 | I |
| 6417.22† | 3 | 10 ? | 2 ? | 1 | III (?) A |
| 6443.09 | 1 | ...... | ...... | ...... | V |
| 6446.62 | 5 | ...... | ...... | ...... | V E |
| 6448.15* | 50 ?<br>10 ? | 100 ?<br>30 ? | 75 ?<br>25 ? | 30 ?<br>10 ? | II A<br>II A |
| 6450.33 | 8 | 20 | 4 | 2 | II A |
| 6454.51d | 200 | 200 | 200 | 200 | I |
| 6455.98 | 300 | 200 | 250 | 250 | I |
| 6468.44d | 8 | 20 | 5 | 2 | II A |
| 6485.54d | 20 | 40 | 10 | 5 | II A |
| 6492.90 | 5 | ...... | ...... | ...... | V |
| 6498.19† | 7 | 1 ? | ...... | ...... | IV (?) E |
| 6506.27 | 6 | 6 | 1 | ...... | IV |
| 6519.33 | 4 | 3 | ...... | ...... | IV |
| 6520.77 | 20 | 6 | 1 | ...... | IV |
| 6523.90† | 2 | 10 ? | 3 ? | 1 ? | III A ? |
| 6526.98d | 100 | 20 | 2 | 1 | III E |
| 6529.76†d | 4 | ? | ? | ...... | III ? |
| 6543.15d | 500 | 400 | 500 | 500 | I |
| 6549.19† | 2n | 5 ? | 1 ? | ...... | III ? |
| 6554.14 | 1 | ...... | ...... | ...... | V |
| 6555.05 | 1 | ...... | ...... | ...... | V |
| 6555.95 | 3 | 10 | 3 | 1 | III A |
| 6565.42 | 40 | 80 | 80 | 80 | I A |
| 6570.94 | 2n | 2 | 1 | ...... | III |
| 6578.52 | 400 | 300 | 400 | 400 | I |
| 6582.21 | 6 | 6 | 1 | ...... | IV |
| 6593.46 | 60 | 80 | 80 | 60 | I |
| 6599.48 | tr | 1 | ...... | ...... | IV A |
| 6600.17 | 50 | 100 | 100 | 50 | II A |
| 6607.68 | 3 | 1 | ...... | ...... | IV |
| 6608.25 | 40 | 40 | 12 | 5 | II |
| 6616.59 | 80 | 125 | 125 | 100 | I |
| 6628.39 | 1 | 2 | ...... | ...... | IV A |
| 6631.22† | 3 | — ? | ...... | ...... | V ? |
| 6636.52 | 1 | ...... | ...... | ...... | V |
| 6642.78 | 3 | ...... | ...... | ...... | V E |
| 6644.39d? | 40 | 125 | 150 | 125 | I A |
| 6645.19 | 8 | 8 | tr | ...... | IV |
| 6650.80 | 100 | 200 | 300 | 300 | I A |
| 6661.41d? | 80 | 150 | 150 | 125 | I A |
| 6671.40†d | 6 | 1 ? | ...... | ...... | IV (?) E |
| 6692.88 | 30 | 60 | 60 | 40 | I A |
| 6699.24† | 2 | 1 ? | 1 ? | ...... | III ? |
| 6699.84 | 4 | 8 | 2 | tr | III A |
| 6709.50 | 200 | 150 | 200 | 200 | I |
| 6714.09 | 2 | ...... | ...... | ...... | V E |
| 6716.01† | 1 | 3 ? | ...... | ...... | IV A ? |
| 6718.66 | tr | ...... | ...... | ...... | V E |
| 6732.79 | 1 | ...... | ...... | ...... | V E |
| 6748.13 | 10 | 20 | 5 | 3 | II A |
| 6753.04 | 50 | 100 | 150 | 150 | I A |
| 6774.27d? | 30 | 12 | 2 | 1 | III E |
| 6776.79 | 1 | 6 | 1 | ...... | III A |
| 6778.24 | tr | ...... | ...... | ...... | V |
| 6783.50 | tr | 1 | ...... | ...... | IV A |
| 6796.71 | 4 | 40 | 15 | 12 | II A |
| 6808.85d | 6 | 3 | ...... | ...... | IV |

TABLE IV—*Continued*

| λ (I.A.) | Arc Int. | Furnace Intensities | | | Class | λ (I.A.) | Arc Int. | Furnace Intensities | | | Class |
|---|---|---|---|---|---|---|---|---|---|---|---|
| | | High Temp. | Medium Temp. | Low Temp. | | | | High Temp. | Medium Temp. | Low Temp. | |
| 6813.66†.. | 1 | — ? | ...... | ...... | V (?) E | 7149.70... | 2 | 2 | 2 | ...... | III |
| 6816.29†.. | 1n | — ? | ...... | ...... | V ? | 7158.06d.. | 50 | 100 | 100 | 30 | II A |
| 6821.53... | 3n | ...... | ...... | ...... | V | 7161.19... | 50 | 50 | 25 | 5 | III |
| 6823.79... | 15 | 30 | 12 | 10 | II A | 7219.88... | 15 | 30 | 15 | 6 | II A |
| 6830.82*.. | tr | ...... | ...... | ...... | V E | 7270.08... | 10 | 5 | 3 | ...... | III |
| 6834.06†.. | 4 | 3 ? | ...... | ...... | IV (?) E | | 5 | 15 | 10 | 6 | II A |
| 6837.91†.. | 3 | 2 ? | ...... | ...... | IV (?) E | 7282.32*.. | 100 | 10 | 2 | ...... | III E |
| 6859.04... | tr | ...... | ...... | ...... | V | 7334.15d.. | 60 | 100 | 100 | 50 | II |
| 6898.41... | tr | ...... | ...... | ...... | V | 7345.31d.. | 20 | 40 | 10 | 1 | III A |
| 6899.55... | tr | ...... | ...... | ...... | V | 7379.71... | 10 | 20 | 3 | ...... | III A |
| 6902.12... | 1 | 1 | tr | ...... | III | 7382.67... | 5 | 10 | 2 | ...... | III A |
| 6903.07... | 1 | 4 | 1 | ...... | III A | 7463.08d.. | 10 | 15 | 4 | ...... | III |
| 6917.24... | 10 | 20 | 10 | 2 | III A | 7483.45*.. | 20 | 5 | ...... | ...... | IV E |
| 6918.27... | 8 | 40 | 20 | 4 | III A | 7498.76... | 5 | 10 | 2 | ...... | III A |
| 6925.24... | 100 | 30 | 15 | 4 | III | 7539.20... | 15 | 20 | 20 | 10 | II |
| 6934.98... | 50 | 60 | 30 | 8 | III | 7664.33*.. | ? | 15 | 5 | ...... | III |
| 6952.50d?* | 2 | 2 | ...... | ...... | IV | 7841.86... | 2 | 8 | 4 | ...... | III A |
| 6954.51d.. | 8 | 4 | tr | ...... | IV | 7947.92d.. | 10 | 15 | 10 | ...... | III |
| 6958.09... | 20 | 3 | ...... | ...... | IV E | 7964.83... | 6 | 10 | 8 | ...... | III |
| 6968.72... | tr | ...... | ...... | ...... | V E | 8001.96... | 4 | 10 | 8 | ...... | III A |
| 6976.84... | 3 | 2 | tr | ...... | III | 8051 36d.. | 10 | 15 | 5 | ...... | III |
| 7023.63d?. | 150 | 100 | 25 | 2 | III | 8086.07... | 15 | 15 | 10 | ...... | III |
| 7032.01... | 15 | 10 | 5 | ...... | III | 8247.48... | 10 | 10 | 5 | ...... | III |
| 7045.93d?. | 300 | 200 | 200 | 80 | II | 8316.03... | 2 | 5 | ...... | ...... | IV A |
| 7066.19d?. | 400 | 10 | 2 | ...... | III E | 8324.69... | 15 | 10 | 5 | ...... | III |
| 7068.32... | 100 | 80 | 80 | 40 | II | 8346.55... | 12 | 8 | 5 | ...... | III |
| 7076.37... | 3 | 3 | 3 | tr | III | | | | | | |

## NOTES—LANTHANUM

| | |
|---|---|
| 3010.80 | Low-temperature spectrum fades out, and class may be too high. |
| 3171.66 | Strongest spark line in this region. |
| 3193.00 | Doublet. Not fully resolved. |
| 3453.16 | Probably triple. |
| 3517.11 | Very strong spark line. Cf. λ 3171.66. |
| 3574.41 | Reversed at high temperature. Obscured by cyanogen band. |
| 3641.53 | Enhanced line on red side. |
| 3895.65 | Blend *Fe*. |
| 3910.80 | Furnace line may be impurity. |
| 4143.95 | May be impurity. |
| 4238.61 | Measured by writers. |
| 4613.40 | Faint if present in furnace. |
| 4668.92 | Probably triple. |
| 4671.83 | Triple, violet member just resolved. |
| 4699.62 | Probably triple. |
| 4703.27 | Probably triple. |
| 4794.57 | Widens to violet in spark. |
| 4817.15 | Probably triple. |
| 4946.42 | Blend impurity line. |
| 4952.03<br>4996.79 | Much enhanced |
| 4999.46 | Triple. |
| 5002.10 | Much enhanced. |
| 5078.94 | Furnace line may be impurity. |
| 5080.20<br>5090.55<br>5157.44<br>5172.90 | Much enhanced. |
| 5173.85 | Blend *Ti* in furnace. |
| 5183.41 | Triple. |
| 5188.20<br>5204.15<br>5226.19<br>5302.63 | Much enhanced. |
| 5340.69 | Much enhanced. Probably coincides with arc line. |

TABLE IV—*Continued*

| | |
|---|---|
| 5377.09<br>5381.90<br>5566.94 | Much enhanced. |
| 5808.29 | Blend with line to violet. |
| 6173.74 | Measured by writers. |
| 6262.30 | Not fully resolved. |
| 6273.78 | Furnace line may be impurity. |
| 6448.15 | Not fully resolved. |
| 6830.82 | Measured by writers. |
| 6952.50 | May be triple. |
| 7282.32 | Triple. Red component strongest. |
| 7483.45 | Triple. |
| 7664.33 | Blend potassium line in arc. |

obtained whose difference was large enough to be significant. In order to retain a consistent classification, the lack of a medium temperature was allowed for as far as possible. This resulted in placing in class III those lines which are strong at high temperature but much weaker at low temperature, while lines which retain considerable strength at low temperature are assigned to class II or class I.

*Symbols.*—The significance of the symbols and abbreviations found in the tables is as follows: * refers to a note at the end of the table; † indicates disturbance by a band spectrum, usually that of carbon, which causes some of the intensities to be questioned; "d," after the wave-length, indicates an unresolved doublet; "tr," a line showing as trace, less than intensity 1; "r," "R," partial or complete self-reversal; "n," "N," degrees of diffuseness in arc lines; "A," after the class number, a line relatively stronger in the furnace than in the arc; "E," after the class number, an enhanced line.

## DISCUSSION

A summary of the types of the 2005 lines classified in this paper is given in Table V. Multiplets corresponding to low energy-levels will normally be found in the low-temperature groups, but may include a few lines which are placed in higher temperature classes on account of faintness, which prevents their appearing on low-temperature spectrograms of ordinary exposure, or which are uncertain on account of blends. The lines which appear with considerable strength at low temperature include from 15 to 30 per cent of the neutral-atom lines listed for these elements.

A large proportion of the lines which appear in the arc spectra of these three elements are enhanced lines, those having sufficient strength to be listed in the tables numbering 85, 342, and 230 for yttrium, zirconium, and lanthanum, respectively. Of these, more than half appear in the furnace for yttrium and lanthanum, but only a small proportion (all of wave-length shorter than λ3450) in the case of zirconium. The lists are by no means complete for the enhanced lines, as many additional ones are given by a strong spark. We have, however, segregated the enhanced lines by this means into two groups requiring different stages of excitation, which correspond in some degree with the low- and high-temperature lines of the neutral atom. Enhanced lines which appear in the furnace, especially those distinct at medium temperature, may be expected to arise from low energy-levels of the ionized atom, while those requiring the arc excitation should belong to higher levels. A third group of still more refractory enhanced lines, possibly in some cases belonging to the second ionization, would contain those lines which are absent from the arc but appear in a highly condensed spark. For both yttrium and lanthanum, many strong enhanced lines in the short wave-length region persist in the furnace at 2100° C.

TABLE V

DISTRIBUTION OF ARC AND ENHANCED LINES ACCORDING TO LOW AND HIGH EXCITATION

| | *Y* | *Zr* | *La* |
|---|---|---|---|
| Low-temperature lines (classes I and II) | 69 | 142 | 145 |
| High-temperature arc lines (in some cases uncertain through faintness) | 305 | 375 | 320 |
| Enhanced lines appearing in furnace | 47 | 22 | 128 |
| Enhanced lines in arc but not in furnace | 38 | 320 | 102 |

The very frequent occurrence of doublets, among both arc and enhanced lines, is a notable feature of the lanthanum spectrum. Those thus designated in Table IV number 127, or 18 per cent of the lanthanum lines listed, and the actual number is probably greater, as the first-order dispersion used beyond λ 5000 was not always sufficient to show the doublet character. The wave-length tables available give these lines as single. The separation of the components is probably always less than 0.08 A, as in only a few cases were they resolved enough in the vacuum furnace to give a rough estimate of the separate intensities. Some of these imperfectly resolved lines are clearly triple and are so noted in the remarks at the end of Table IV; it is probable that other triplets occur among the lines marked as double.

Lines relatively stronger in the furnace than in the arc, indicated by "A" after the class number, are in about the usual proportion in the yttrium list, while the high temperatures required for zirconium make the spectrum difficult for the furnace and only one line is thus designated. For lanthanum the proportion is unusually large, 127 such lines being found. While the number of these lines is regulated by the average strength of lines in the arc spectrograms selected for comparison with those of the furnace, it is significant in the case of lanthanum, because a large proportion of the lines strong in the arc are enhanced lines, while the furnace is highly effective in giving the lines of the neutral atom.

MOUNT WILSON OBSERVATORY AND VASSAR COLLEGE
September 1926

END OF VOLUME XIV

# INDEX TO VOLUME XIV

Nos. 304 to 326

---

## AUTHORS

PAGE

ADAMS, WALTER S., ALFRED H. JOY, AND M. L. HUMASON—The Absolute Magnitudes and Parallaxes of 410 Stars of Type M . . . . . 307

ADAMS, WALTER S., AND CHARLES E. ST. JOHN—An Attempt to Detect Water-Vapor and Oxygen Lines in the Spectrum of Mars with the Registering Microphotometer . . . . . . . . . . 53

ANDERSON, J. A., AND SINCLAIR SMITH—General Characteristics of Electrically Exploded Wires . . . . . . . . . . 359

BJERKNES, V.—Solar Hydrodynamics . . . . . . . . . . 185

CARTER, EDNA. *See* King, Arthur S.

HUBBLE, EDWIN—
  Extra-Galactic Nebulae . . . . . . . . . . . . . 379
  N.G.C. 6822, a Remote Stellar Cluster . . . . . . . . 1
  A Spiral Nebula as a Stellar System: Messier 33 . . . . . . 83

HUMASON, M. L. *See* Adams, Walter S.

JOY, ALFRED H.—
  Provisional Elements and Dimensions of S Antliae Considered as an Eclipsing Binary . . . . . . . . . . . . . 351
  A Spectrographic Study of Mira Ceti . . . . . . . . . 123

JOY, ALFRED H., AND ROSCOE F. SANFORD—The Dwarf Companion to Castor as a Spectroscopic Binary and Eclipsing Variable . . . . 325

JOY, ALFRED H. *See* Adams, Walter S.

JOYNER, MARY C. *See* Seares, Frederick H.

KING, ARTHUR S., AND EDNA CARTER—The Electric-Furnace Spectra of Yttrium, Zirconium, and Lanthanum . . . . . . . . . 457

LUNDMARK, KNUT—Internal Motions of Messier 33 . . . . . . 59

MERRILL, PAUL W.—
  Notes on Lines in the Spectra of Red Stars . . . . . . . 45
  Stellar Spectra of Class S. II. Changes in Spectra of Long-Period Variable Stars . . . . . . . . . . . . . 429

NICHOLSON, SETH B. *See* Pettit, Edison

PETTIT, EDISON, AND SETH B. NICHOLSON—On the Theory of the Continuous Spectrum of the Corona . . . . . . . . . . 241

PAGE

Rosseland, Svein—
  On the Origin of Bright Lines in Stellar Spectra . . . . . . 65
  On the Transmission of Radiation through an Absorbing Medium in Motion, with Applications to the Theory of Sun-Spots and Solar Rotation . . . . . . . . . . . . 215
Russell, Henry Norris—Multiplets in the Spark Spectrum of Iron . 297
St. John, Charles E. *See* Adams, Walter S.
Sanford, Roscoe F.—On the Orbits of Four Spectroscopic Binaries . 275
Sanford, Roscoe F. *See* Joy, Alfred H.
Schilt, J.—
  Remarks on Various Statistical Properties of Galactic Cepheids Having Periods Longer than One Day . . . . . . . 247
  Two New Variable Stars of the Type of W Ursae Majoris . . . 265
Seares, Frederick H., and Mary C. Joyner—Reduction of Thirty-Nine Astrographic Zones to the International Photographic Scale . 27
Smith, Sinclair. *See* Anderson, J. A.
Van Maanen, Adriaan—The Photographic Determination of Stellar Parallaxes with the 60- and 100-Inch Reflectors. Ninth Series . . 333

## SUBJECTS

Absolute magnitudes, of M-type stars, 307
S Antliae, as eclipsing binary, elements and dimensions, 351
Astrographic zones, reduction to international photographic scale, 27
Binaries, eclipsing, elements and dimensions of S Antliae, 351
———, spectroscopic, dwarf companion to Castor, 325
———, spectroscopic, orbits of $\eta$ Orionis A, $\epsilon$ Hydrae C, Boss 4247, B.D.$+57°2309$; 275
Bright lines, origin in stellar spectra, 65
Castor, dwarf companion, as spectroscopic binary and eclipsing variable, 325
Corona, continuous spectrum, 241
Electric-furnace spectra of yttrium, zirconium, and lanthanum, 457
Iron, multiplets in spark spectrum, 297
Lanthanum, electric-furnace spectra, 457
Lines, bright, origin in stellar spectra, 65
———, in spectra of red stars, 45
———, water-vapor and oxygen, detection with registering microphotometer in spectrum of Mars, 53
Magnitude, absolute, of M-type stars, 307
Mars, detection of water-vapor and oxygen lines in spectrum, 53
Messier 33, as a stellar system, 83
———, internal motions, 59
Microphotometer, registering, use in detecting water-vapor and oxygen lines in the spectrum of Mars, 53
Mira Ceti, a spectrographic study, 123
Motions, internal, of Messier 33; 59
Multiplets, in spark spectrum of iron, 297
N.G.C. 6822, a remote stellar system, 1
Nebula, spiral, as stellar system, 83
Nebulae, extra-galactic, 379
———, N.G.C. 6822; 1
Oxygen lines, in spectrum of Mars, 53
Parallaxes, of M-type stars, 307
———, stellar, photographic determination with 60- and 100-inch telescopes, 333
Radiation, transmission through absorbing medium in motion, with application to theory of sun-spots and solar rotation, 215
Spectra, electric-furnace, of yttrium, zirconium, and lanthanum, 457
———, stellar, and the origin of bright lines, 65
———, ———, of class S, 429
Spectral lines, in red stars, 45

Spectroscopic binaries, orbits of $\eta$ Orionis A, $\epsilon$ Hydrae C, Boss 4247, B.D.+57°2309; 275
Spectrum, continuous, of corona, 241
Stars, eclipsing variable, dwarf companion to Castor, 325
———, M-type, absolute magnitudes and parallaxes, 307
———, parallaxes, determination with 60-inch and 100-inch telescopes, 333
———, red, spectral lines, 45
———, S-type, spectra, 429
———, variable, changes in spectra, 429
———, ———, of the type of W Ursae Majoris, 44*i* Boötis, B.D.+75°752; 247
———, ———, Mira Ceti, 123
———, ———, statistical properties of galactic Cepheids having periods longer than one day, 247
Sun, hydrodynamics, 185
———, rotation, 215
Sun-spots, theory, 215
Water-vapor lines, in spectrum of Mars, 53
Wires, electrically exploded, 359
Yttrium, electric-furnace spectra, 457
Zirconium, electric-furnace spectra, 457

522.19 C28 V14

522 19 C28 V14
MOUNT WILSON OBSERVATORY CONTRIBUTION

INSERT BOOK
MASTER CARD
FACE UP IN
FRONT SLOT
OF S.R PUNCH

ESTABLISHED 1885

UNIVERSITY OF ARIZO
LIBRARY

MASTER CARD

GLOBE 901144-0